2012

Morphological development of reef islands on Tarawa Atoll, Kiribati

Naomi Biribo
University of Wollongong

UNIVERSITY OF WOLLONGONG

MORPHOLOGICAL DEVELOPMENT OF REEF ISLANDS ON TARAWA ATOLL, KIRIBATI

A thesis submitted in fulfilment of the requirements
for the award of the degree of

DOCTOR OF PHILOSOPHY

from the
University of Wollongong

By

Naomi Biribo

School of Earth and Environmental Sciences

October 2012

CERTIFICATION

I, Naomi Biribo, declare that this thesis, submitted in fulfilment of the requirements of the award of **Doctor of Philosophy**, in the **School of Earth and Environmental Science, University of Wollongong**, is wholly my own work unless otherwise referenced or acknowledged. The document has not been submitted for qualifications at any other academic institution.

Naomi Biribo

DEDICATION

I dedicate this thesis to my loving mother, Bweneamakin Biribo and my two brothers Taam and Konene who passed away during the course of my study. Mama, this is for your support and encouragement, that I pursue further studies. Your constant love and care has moulded me to whom I have become, which I am so forever grateful for. Taam Biribo, this is for your fatherly advice, guidance and confidence in me over the years. Konene Biribo, this is in remembrance of your interesting stories and brotherly love. I miss you all dearly. May your souls rest in peace.

ABSTRACT

Low-lying reef islands formed on the rim of atolls in Kiribati appear threatened by the impacts of anticipated sea-level rise. The reef islands around Tarawa Atoll are composed of unconsolidated carbonate sediments, particularly the tests of benthic foraminifera. This thesis aims to examine the morphological development of these reef islands over a range of time scales. To achieve this aim, the following tasks were carried out: investigation of the topography and the accumulated volumes of sediment sequestered on the reef islands, reconstruction of the evolution of selected reef islands and determination of whether or not rates of sediment supply have been reduced and, examination of historical shoreline changes.

The topography of the reef islands was described, based on a digital terrain model (DTM) derived from photogrammetry. Using geographical information systems (GIS), it is estimated that approximately 60 million m^3 of sediment has accumulated on the reef islands since the mid Holocene. Most reef islands show a morphology that comprises an oceanward ridge that is generally 2 to 3 m, and in some places greater than 4 m, above mean sea level (MSL). Many reef islands have a low-lying central depression. More than 50% of the land area lies below 2.4 m above MSL. The lagoonward ridge is generally 1.5 to 2.0 m above MSL. Based on the distribution of elevation classes, the hypsometry of reef islands has been examined. Most reef islands (24 of 36) show an S-shaped form with a large proportion of the reef island being in the lowest elevation range. Ten reef islands, typically the smallest are classified as platforms, with little variation in elevation across them. Only two reef islands show a more concave form with a significant proportion of low-lying areas.

The evolution of three reef islands was investigated by dating individual foraminifera, *Amphistegina*, using radiocarbon dating by Accelerator Mass Spectrometry (AMS). A program of paired AMS and amino-acid racemisation (AAR) dating was initiated to determine whether this technique could be used to augment radiocarbon analysis. The reef islands appear to commence formation about 4,500 years BP with the oldest radiocarbon ages located about three quarters of the width across reef islands of Tabiteuea and Marenanuka from the ocean side.

Fossil ages from Tabiteuea, Marenanuka and Notoue becoming progressively younger towards the ocean side indicate a pattern of oceanward accretion. More recent accretion has occurred locally, particularly on the ends of the reef islands and in small embayments.

Estimated AAR ages of individual *Amphistegina* show a range that is broadly consistent with the AMS age trend. Decreasing order of relative fossil ages is as follows: a cluster of fossils obtained from on land pits, lagoon beaches, ocean beaches and younger ages for live foraminifera. Fossils obtained from beaches of reef islands show mixed ages. South Tarawa fossils appear relatively old as they are continuously reworked. Live foraminifera are found on the ocean reef flats of North Tarawa but appear scarce in South Tarawa. It seems likely that the supply of modern foraminifera will continue in North Tarawa, however, it appears limited in South Tarawa.

Historical changes to reef-island morphology were determined on a majority of reef islands. Reef-island area and shoreline changes were examined over 30 years by comparing the shoreline positions derived from 1968 and 1998 aerial photography using the Digital Shoreline Analysis System. Analysis of the area change shows that Tarawa Atoll has substantially increased in size by more than 450 ha, largely driven by development pressures and increasing population on South Tarawa. Reclamations have been directly associated with this net increase, contributing a significant amount of more than 360 ha. Widespread erosion and high average accretion rates appear to be related to numerous reclamations of varying sizes spread along South Tarawa's shorelines. Conversely, reef islands in North Tarawa appear to be predominantly stable with localised shoreline changes observed in areas such as embayments, sand spits, beaches close to blocked channels and beaches facing inter-island channels. Factors affecting changes on North and South Tarawa differ. Shoreline changes on North Tarawa are largely driven by natural factors, whereas shorelines in South Tarawa are predominantly influenced by human activity and seasonal variability associated with El Niño Southern Oscillation (ENSO), which affects the longshore sediment transport.

In the future, reef islands of North Tarawa are anticipated to be stable and more resilient to sea-level rise unless population density increases and conditions do not favour the growth of foraminifera. However, serious concerns are raised for the future of South Tarawa reef islands, as evidence shows that widespread erosion along the ocean and lagoon shorelines is primarily related to the modification of shorelines due to increasing development and population pressures. With sediment supply appearing to be limited due to the scarcity of live foraminifera, it is anticipated that these reef islands will experience increased erosion and be at risk from inundation.

ACKNOWLEDGEMENTS

I acknowledge the invaluable support that both my supervisor Professor Colin Woodroffe and co-supervisor Professor Colin Murray Wallace have tirelessly given to me during the course of my study. The advice, knowledge and constructive criticism have improved my understanding in many ways.

To our Father, God in heaven. Who has given me strength to continue pursuing this task during challenging times, I thank Thee.

My heartfelt appreciation goes to my dear cousin Tafeanga Baakai Teraaka who has tirelessly taken care of my children, Nuea, Tiaon and Christopher. Without your kind heart, assistance and understanding I would not have been able to pursue this degree. To my three beautiful children, Nuea, Tiaon and Christopher, for your patience and understanding in your young age, that I am your mother but also a student. To my husband, Ataata Atauea for your love and being by my side even during hardships. To Baba, my dad, for your guidance, love, care and nurture over the years, I shall always love and remember you! To my dear sister Tinia and husband Barate Teuriaria, for your continued words of encouragement and being there for me when times were difficult as well as your continuous assistance to me and my children. To my sisters-in-law, Matarena and Kamwea, nieces, nephews and cousins and a special mention of Aribo Tabanga, Maria Taniera and Kaboterenga Terite, Kalei Morris and her husband Walter Morris and to my brother in law Timau Atauea and his wife Tetawa, Kareke and Kiaria Benson and family, thank you all so much for helping me and my young family in so many ways.

My sincere appreciation goes to the Australian Agency for International Development (AusAID) for funding this scholarship. Without your support, this study would never have been possible. My thanks to the AusAID staff at the University of Wollongong, Debby Porter and Nhan Nguyen, your assistance in so many ways has made a UOW a better place to be in. A special thank you to Natalie Corriea, you are a wonderful and extraordinary lady whom I shall never forget! You have shared my grief, pain and joy. Your words of encouragement to take this as an experience and outlook for a brighter future motivated me to persist in my studies. To Dr Jocelyn Harper, thank you for sharing with me your precious time and skills to enable me to cope through tough times.

The radiocarbon analysis for this research was made possible by Australian Nuclear Science and Technology Organisation (ANSTO) under its Australian Institute of Nuclear Science and Engineering (AINSE) grant AINGRA10073. I acknowledge the assistance of Dr Quan Hua, in carrying out the analysis.

To my friends at UOW and those who have assisted in different ways, I am indebted to you all for your kind assistance: Michael Stevens, Heidi Brown, Deirdre Ryan, Dr Javier Leon, Dr Sarah Hamlyton, Dr Hannah Power, Jose Abrantes, Dr Pam Abuodha, Dr Terry Lachlan, Dr William Nicholas, Dr Megan Williams, Dr Helen McGregor, Professor John Morrison, Penny Williamson, Professor Brian Jones, Dr Solomon Buckman, Wendy Weeks, Denise Alsop, Brent Peterson, Sandra Chapman

and David Wheeler. To my office mates, Kahlid Albarhi, Mutassam Hassan and Thang Thi Xuan Nguyen, thank you for sharing with me. Thanks also go to Dr Jessica Carilli for sharing her views.

To my friends and their families in New South Wales, my sincere appreciation to you all in the various ways you have assisted my family over these years: Kaibwa, Timetaake T. Eritai and family; Mark, Judith Hurley and family; Mark, Bessie Bowry and family; Itinikua, Tracey Kauabanga and family, Kibamoa, Vanessa Teaatu and family, Christopher Swales, Makiro Tetinako and family and Ietaake Reebo. To the NSW I-Kiribati community you have created a mini Kiribati community where I have enjoyed dancing, sharing jokes and laughter over the past few years, and made me miss home even less.

To the Catholic Diocese and Saint Brigid Primary School, my sincere thanks for allowing my children to experience Australian life and participate in the many events related with Kiribati and Climate Change.

To Mary Sparks and fellow senior residents, Pam, Than, Michael, Rebecca, Chulantha, Nadeesha, Hanh thank you for your support and friendship over the years.

To my Pacific sister, Josie Tamate. I will treasure your companionship. I have enjoyed our long walks and talks. To my friends Tererei Abete Reema and Tebao Awira, I will never forget your words of encouragement throughout my studies.

To my colleagues and friends in Kiribati who have assisted me with my data collection, thank you so much for giving me your precious time and making it possible to undertake this research. To name them, Farran Redfern, Romano Reo, Boata Iabeta, Titeem Auatabu, Tion Uriam, Ribanataake and Teaoto Awira, Tiuere Torua, Kintoba Tearo, Beero Tioti, Teurakai Teaoti, Tentao Takaaio, Maria Redfern and family, Kaiaua and Geradine Tiban and their Catholic group in Abaokoro, Catholic sisters in Immaculate Heart College in Taborio and not forgetting Iranimwemwe Tiengia who unfortunately passed away during one of my field visits. You will be sadly missed. To the Ministry of Fisheries and Marine Resources Development, the Ministry of Home Affairs and Rural Development, the Lands Division and Environment Division of the Ministry of Environment, Agricultural and Lands Development, my sincere appreciation for providing me assistance, and also to the Eutan Tarawa Urban Council for allowing me to undertake field work in North Tarawa.

To all of you mentioned above and those whom have assisted me in any way during my studies, *Au bwai ma ngkami Te Mauri, Te Raoi, ao Te Tabomoa n taainako. Kam bati n rabwa.* (May the blessing of Kiribati be bestowed on us all always which is Health, Peace and Prosperity. Thank you very much).

TABLE OF CONTENTS

LIST OF FIGURES

LIST OF TABLES

ACROYNMS

Asp	Aspartic acid
BB	Base of beach
BP	Before Present
BOM	Bureau of Meteorology
CSIRO	Commonwealth Scientific and Industrial Research Organisation
DSAS	Digital Shoreline Analysis System
DTM	Digital Terrain Model
ENSO	El Niño Southern Oscillation
ESAT	Environmentally Safe Aggregate Tarawa
IDW	Inverse Distance Weighting
IPCC	Intergovernmental Panel on Climate Change
IPO	Interdecadal Pacific Oscillation
ITCZ	Inter Tropical Convergence Zone
GIA	Glacial Isostatic Adjustment
GIS	Geographical Information System
Glu	Glutamic acid
KAP	Kiribati Adaptation Project
MHWN	Mean High Water Neap
MHWS	Mean High Water Spring
MHWSP	Mean High Water Perigean Spring
MSL	Mean Sea Level
MLOS	Mean Level Of the Sea
NTFA	National Tidal Facility, Australia
SAM	Sediment Allocation Model
SOI	Southern Oscillation Index
SOPAC	Pacific Applied Geoscience Commission
SPC	South Pacific Commission
SPSLCMP	South Pacific Sea Level and Climate Monitoring Project
SEAFRAME	Sea Level Fine Resolution Acoustic Measuring Equipment
TGZ	Tide Gauge Zero
UH	University of Hawaii Tide Gauge
ΔR	Marine Reservoir effect (Delta R)
^{14}C	Radiocarbon
VL	Vegetation Line

Units	
cal yrs	Calendar year
cm	centimetre
ha	hectare
ka	Thousands of years
m	metre
m^2	square metre
m^3	cubic metre
mm	millimetre
mm/yr	millimetre per year
persons/ha	persons per hectare
yr	year
%	percentage

1. CHAPTER ONE: INTRODUCTION

1.1 Impacts of climate change on reef islands

Low-lying reef islands on atolls, such as those in Kiribati, have captured considerable political and media attention, as they may be threatened by impacts of anticipated sea-level rise. The Fourth Assessment Report (AR4) of the Intergovernmental Panel on Climate Change (IPCC, 2007) indicated that global climate change is a critical issue. Low-lying reef islands barely 2 m above mean sea level (MSL) are increasingly at risk from, impacts of climate change as indicated in Chapter 16 of AR4 (Mimura *et al.*, 2007). Based on a significant body of scientific assessments, several climate change drivers are likely to have a range of impacts on these reef islands, such as sea-level rise, increased sea surface temperature, and greater frequencies and intensities of storms (Nicholls *et al.*, 2007). Sea-level rise is anticipated to accelerate, although rates of change remain uncertain (IPCC, 2007).

Average global sea-level rise is estimated to range from 0.18 m to 0.59 m by 2090 to 2099 based on Global Climate Models (GCM) (IPCC, 2007). Future inter-decadal variability of sea surface height near the equator will be influenced by El Niño Southern Oscillation (ENSO) (Australian Bureau of Meteorology and CSIRO, 2011). In the western Pacific, sea level has been rising by +1.8 mm/yr on average over the past 60 years (Becker *et al.*, 2012). A significant body of scientific evidence at this time suggests that sea level will continue to rise even if emissions are stabilised (IPCC, 2007). The projected sea-level rise is causing a widespread concern about the future of small low-lying reef islands as they appear particularly sensitive to these changes (Mimura *et al.*, 2007; Nicholls *et al.*, 2007; Australian Bureau of Meteorology and CSIRO, 2011), and will affect their populace and economies (Roy and Connell, 1991). The sensitivity of reef islands to sea-level rise is largely influenced by their physical characteristics such as their small size and low elevations (Harvey and Kench, 2003; Yamano *et al.*, 2007; Woodroffe, 2008).

The three principal impacts anticipated on reef islands as a result of sea-level rise are a) inundation and flooding; b) increased coastal erosion; and c) saltwater intrusion

into groundwater (Mimura *et al.*, 2007). Coastal erosion on many reef islands in the Pacific is not caused by sea-level rise alone, but is also affected by the seasonal variability of sea level associated with ENSO (Gillie, 1994; Gillie, 1997; Solomon and Forbes, 1999; Donner, 2012). The effects of erosion can be exacerbated by human activities which lower the beach elevations such as beach sand mining (Xue, 1996; Xue, 2001; Peletikoti, 2007), poorly-engineered coastal structures (SOPAC, 1993; Kench, 2005), and coastal structures blocking longshore sediment transport (Forbes and Hosoi, 1995; Solomon and Forbes, 1999; Ford, 2012). In most situations, the combined effect of the natural variability of sea level and human activities appear to create more coastal problems than sea-level rise alone (Gillie, 1994; Solomon and Forbes, 1999; Donner, 2012).

Despite the growing global concern for the future of reef islands, there are relatively few studies examining their morphological responses to anticipated sea-level rise. There is general agreement that the impact of sea-level rise on these reef islands will be largely negative (Mimura *et al.*, 2007). Despite this, past and future responses of reef islands to changing sea level are poorly understood (Roy and Connell, 1991). One approach to determine how these reef islands will respond to future sea-level rise is to examine their past behaviour. This involves investigating their geomorphological response over different time scales (from millennia to decades) (Kench and Cowell, 2002; Masselink and Hughes, 2003; Samosorn, 2006; Woodroffe, 2008).

A limited number of studies have examined the morphological evolution of reef islands by studying their past behaviour. As a result, conclusions about the likely response of reef islands to accelerated sea-level rise vary. There is, however, a general agreement that reef islands are geologically young formed during the Holocene epoch and have grown through the accumulation of biogenic sediment (Woodroffe *et al.*, 1999; Woodroffe and Morrison, 2001; Dickinson, 2004; Kench *et al.*, 2005; Woodroffe, 2008; Kench *et al.*, 2012). There are several ways in which reef islands may have formed. Initially, 27 accretion modes were suggested by Woodroffe *et al*. (1999), illustrated by the pattern of likely time of deposition (isochrons). A simplified version showing nine major accretion patterns is shown in

Figure 1.1. From these proposed nine patterns of accretion, two patterns have been identified from radiocarbon ages of fossil sediments on reef islands. Oceanward accretion was found to be the predominant mode of reef-island accretion in the Cocos (Keeling) Islands (Woodroffe *et al.*, 1999). This pattern was also inferred from radiocarbon ages from Makin, Kiribati, where the reef island developed from a central core, prograding oceanward at a decelerating rate (Woodroffe and Morrison, 2001). On Warraber in Torres Strait, the radiocarbon ages indicate an incremental growth pattern of the sand cay on the leeward end of the reef platform under conditions of sufficient sediment supply (Woodroffe *et al.*, 2007). The other pattern, a single episode was suggested to be the mode of accretion for Bewick Cay, Great Barrier Reef, Australia indicating that this reef island evolved very rapidly in a single episode (Kench *et al.*, 2012). The last two examples are not reef islands on atolls, however, they contribute to an understanding of the differences in how reef islands form.

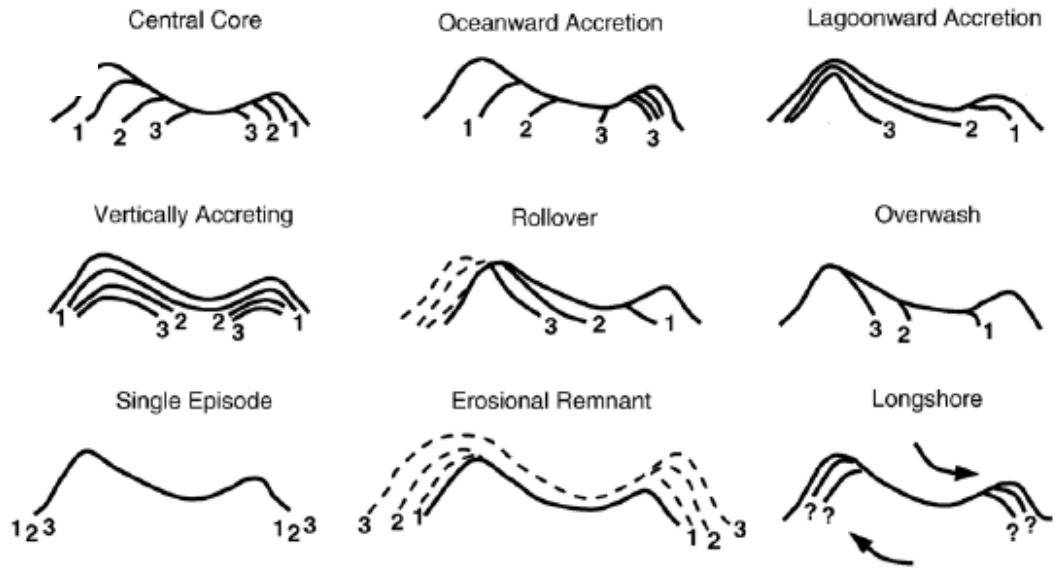

Figure 1.1. Schematic diagram of cross island profiles illustrating the revised nine major reef island scenarios as indicated by the isochrones of deposition marked 1, 2 and 3 in thousands of years (ka). The ocean is on the left and the lagoon is on the right (source: Woodroffe, 2000).

Several studies investigating the responses of reef islands to anticipated sea-level rise indicate that reef islands will experience increased erosion whereas others predict continued accretion. Sheppard *et al.* (2005) suggests that reef islands will reduce in size as a result of wave erosion. They observed massive coral loss from the seaward reef rim on Seychelles, Indian Ocean, related to the 1982 El Niño event, which has

allowed more wave energy to reach the shorelines, thus leading to increased coastal erosion. Other researchers propose that reef islands may grow naturally in response to accelerated sea-level rise conditions (Kinsey and Hopley, 1991; Rankey, 2010). Under conditions of warmer temperatures and increased wave energy, it is suggested that reef islands will receive more sediment due to the combined effect of prolific coral growth and increased sediment transport (Kinsey and Hopley, 1991). Long-term shoreline changes on Maiana Atoll, Kiribati over a period of 40 years (1969 to 2009) show that the atoll has grown naturally at a slow accretion rate of 0.2 m/yr (Rankey, 2010). Seasonal variability in the climate, such as El Niño, however, influences predominant longshore sediment transport, altering its direction and in turn affecting the shorelines (Solomon and Forbes, 1999). Shoreline changes show that reef islands on Majuro Atoll, in the central Pacific are growing, but anthropogenic influences, through widespread reclamations have contributed significantly to the increase in size of reef islands (Ford, 2012). Other studies suggest that reef islands are resilient to sea-level rise (Kench *et al.*, 2005; Kench *et al.*, 2006). Reef islands that respond by eroding imply that sediment supply is insufficient limiting the ability of the reef islands to maintain their state of dynamic equilibrium (Solomon, 1997; Woodroffe *et al.*, 2007; Woodroffe, 2008). The behaviour of reef islands appears to differ between atolls and seems to vary as a consequence of sediment supply and the processes that control sediment transport.

Another study investigating the morphological behaviour of reef islands proposes that they will grow to a certain physical limit. Barry *et al*. (2007) investigated the morphological behaviour of reef islands using a numerical model known as the Sediment Allocation Model (SAM) tested with field data obtained from reef islands in the Cocos (Keeling) Islands (Woodroffe *et al.*, 1999) and Makin, Kiribati (Woodroffe and Morrison, 2001). The results of this study led Barry *et al*. (2007) to suggest that the growth of these reef islands are determined by accommodation space. The magnitude of the accommodation space is related to the reef surface area that the sequestered sediment occupies on the reef flat. The proposed view is based on the assumption that reef islands grow towards equilibrium whereby they will continue growing until they reach maximum accommodation space where no more sediment

can be sequestered on the reef islands. The reef islands will continue to maintain equilibrium under conditions of sufficient sediment supply.

The topography of reef islands also contributes to their susceptibility to sea-level rise. A review of reef islands in the western Pacific Ocean and eastern Indian Ocean showed that reef islands are low-lying, with on average only a small proportion of their surface area above 2 m above MSL (Woodroffe, 2008). Additionally Woodroffe (2008) also showed that $\leq$ 8% of the reef islands area is above 3 m above MSL, signifying how susceptible these reef islands are to projected sea level rises. Reef islands typically have prominent ocean ridges that protect the low-lying areas facing the ocean from highest astronomical tides (HAT) and storm surges. The lagoon ridges, barely 1-2 m in height, shelter the low-lying areas behind them from HAT (Woodroffe, 2008). This clearly indicates that building and maintenance of these ridges is very crucial as they protect a significant proportion of the reef island from present high water levels. These ridges are even more important in light of anticipated increases in sea level.

1.2 Definitions

The two terms atoll and reef island have been used throughout this thesis and need to be clarified as their definitions vary. For the purpose of this thesis, a clear definition of the terminology in the context of Kiribati is necessary.

The term atoll is derived from a Maldivian word *atolu*. Atolls may vary in shape and thus have been defined differently. This thesis defines an atoll as annular reefs with a rim enclosing a central lagoon and occurring in mid ocean (Woodroffe and Biribo, 2011). Atolls occur in linear chain groups known as archipelagos such as the three that make up Kiribati: the Gilbert Group, the Line Islands and the Phoenix Islands.

Reef islands are defined as small low-lying landforms that are accumulations entirely composed of biogenic sediments, situated on the reef rim of atolls. Reef islands may vary in shape and are generally accepted to have formed during the Holocene epoch. Table reefs are one variant of atolls forming as a single reef island on a reef platform

and may have a swampy central depression (Tayama, 1952). In this thesis, this is also considered as a reef island, with Tarawa Atoll consisting of 59 reef islands.

1.3 Significance of reef islands on Tarawa Atoll

Reef islands are important, providing home to citizens of small atoll nations in the Pacific and Indian oceans such as Kiribati, the Marshall Islands, Tuvalu and the Maldives. The reef islands of the main atoll of Kiribati, Tarawa are home to a population of more than 56,000, which makes up 55% of the country's population (Ministry of Finance, 2010). As Tarawa Atoll is the capital of Kiribati, urbanisation has largely focussed on the reef islands of that atoll, especially those in South Tarawa. This has resulted in a lot of internal migration from the outer reef islands of Kiribati by those who seek better opportunities such as employment and higher education. The increase in migration has resulted in most of the reef islands in South Tarawa being densely populated, with a population density of 2,558 persons per km^2 recorded in the 2005 census. Betio, a major port and administration centre, has a very high population density of 10,400 persons per km^2, double the population density of Hong Kong which is one of the most densely populated cities (Haberkorn, 2007). This has led to serious overcrowding issues. In order to increase their land space, people are forced to build out towards the sea, living in areas that are already at risk from high tides (Solomon and Forbes, 1999). These challenges may very soon increase twofold, as it is estimated that within 20 years time, the population of urban Tarawa Atoll will double (Haberkorn, 2008). Any morphological changes on these low-lying small reef islands especially in areas where population density is high, will affect a significant proportion of the country's population as well as its economy.

1.4 The need to investigate the morphological development of reef islands, Tarawa Atoll

The projections by IPCC (2007) that sea level will continue rising during the 21^{st} century suggest that inundation is inevitable for these low-lying reef islands. Reef islands on atolls especially those in Kiribati have been identified to be potentially at higher risk to anticipated sea-level rise (Elrick and Kay, 2009). This is especially the

case of reef islands of Tarawa Atoll as they serve as the capital of Kiribati and accommodate more than half of the country's population. In addition Tarawa is considered to be one of the most densely populated islands of the Pacific (Haberkorn, 2007). To develop appropriate coastal management plans for Tarawa Atoll, it is considered essential to assess the past morphological changes of the reef islands in order to better understand how they may respond to the anticipated sea-level rise. Only Tarawa Atoll has available datasets to enable this study to progress. The information gained from this study is significant as it will contribute to a better understanding of the physical responses of reef islands to climate change and sea-level rise. The results of the study will have implications for future coastal management.

Coastal studies carried out on Tarawa Atoll have largely focussed on urban South Tarawa with less studies investigating North Tarawa (Woodroffe and McLean, 1992; Gillie, 1993; Forbes and Hosoi, 1995; Solomon, 1997; Solomon and Forbes, 1999; He, 2001; Webb, 2005; Elrick and Kay, 2009). This study will build on the existing information to understand the sediment dynamics and gain an insight into what may occur in the future in both North and South Tarawa.

1.5 Research Aims and Objectives

This thesis aims to examine the morphological development of these reef islands on Tarawa Atoll over different time scales (millennial to decadal). The three specific objectives of this study are to:

a) Examine the topography of reef islands on Tarawa atoll and consider the implications of extreme sea levels; as well as calculate the first-order estimate of the sediment volume sequestered on the reef islands.
b) Establish the pattern of reef-island accretion and determine whether or not there is a supply of sediment that is still available to the reef islands.
c) Examine the historical changes that have occurred to reef island shorelines.

To achieve these objectives, this study follows the approach proposed by Woodroffe (2008) whereby studies of different temporal scales can be combined to better understand the past behaviour of reef islands. The study uses the following

information gained from i) construction of a digital terrain model (DTM) for the atoll using available Geographical Information Systems (GIS) data; ii) detailed radiocarbon and amino acid racemisation dating of constituent sediment grains; and iii) comprehensive mapping of shoreline changes across individual reef islands.

1.6 Organisation of this thesis

This thesis contains seven chapters and has been organised as follows:

- Chapter Two describes Tarawa Atoll and its geological setting.
- Chapter Three discusses the physical and social characteristics of the reef islands of Tarawa Atoll.
- Chapter Four uses available GIS data to construct a DTM examining the elevation variation; and, in addition, determines the first-order sediment volume of the reef islands around Tarawa Atoll.
- Chapter Five examines the morphological evolution of reef islands by radiocarbon dating individual foraminifera from sequences of samples across three reef islands. The modern sediment supply is also investigated using paired Accelerated Mass Spectrometry (AMS) and Amino Acid Racemisation (AAR) dates.
- Chapter Six investigates the area changes over the past 30 years on Tarawa Atoll reef islands. The short-term shoreline changes over 30 years for both the ocean and lagoon shorelines are examined using Digital Shoreline Analysis System (DSAS) and are compared with shoreline changes over 64 years on selected reef islands
- Chapter Seven discusses the main findings of the thesis highlighting the implications for coastal management. In addition, the chapter outlines directions for future research.

2 CHAPTER TWO: PHYSICAL AND SOCIAL SETTING

2.1 Aims

The aim of this chapter is to describe the physical and geological setting of Tarawa Atoll. The implications of current and projected sea-level trends are also introduced, both in a global and local context. This will be carried out by reviewing the following:

a) The Quaternary evolution of Tarawa Atoll
b) The present surface morphology of Tarawa Atoll, in particular the outer reef, reef rim and lagoon.
c) The climate of Tarawa Atoll and factors that influence climatic variability.
d) Historical sea-level changes and future sea-level predictions with an emphasis on the Pacific region.

2.2 Introduction

Atolls are annular reefs with a rim that encloses a central lagoon. On these reef rims are low-lying reef islands composed of unconsolidated carbonate sediment derived from the surrounding coral reefs. It is widely accepted that reef islands are dependent on biogenic materials for their formation and that evolution of these reef islands is strongly influenced by changing sea levels. Concern about the future of these low-lying atolls, in the face of predicted sea-level rise, has captured the attention of the global community. It is therefore very important to understand the relationship between reef islands on atolls and sea level, as well as the factors that influence sea level, in order to determine how atolls may be affected in the future.

2.3 Geographical location of Tarawa Atoll

The Republic of Kiribati lies in the central Pacific Ocean located between the longitudes 169^{o} to 177^{o} E and between latitudes 4^{o} North and South of the equator (Figure 2.1). The country comprises 33 coral atolls grouped into three main island groups spread across the equator, namely the Gilbert, Phoenix and Line islands (west to east). The Gilbert Group consists of 11 low lying atolls and 5 reef islands with the

exception of Banaba, a raised coral atoll. Tarawa Atoll, the capital of Kiribati is part of the Gilbert Group and is located at 1°30'N, 173°00'E (Figure 2.2).

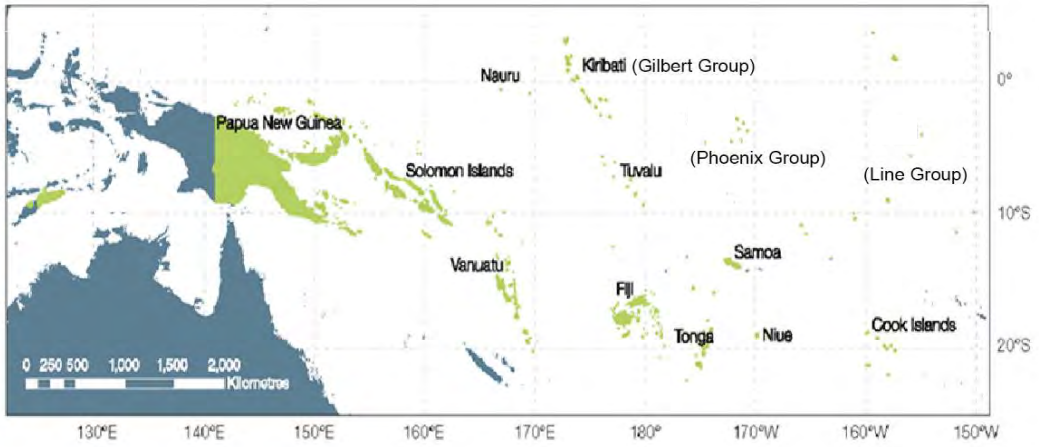

Figure 2.1. Map of the Pacific showing the location of Kiribati in respect to other neighbouring Pacific countries (source: Meteorology and CSIRO, 2011 p 8).

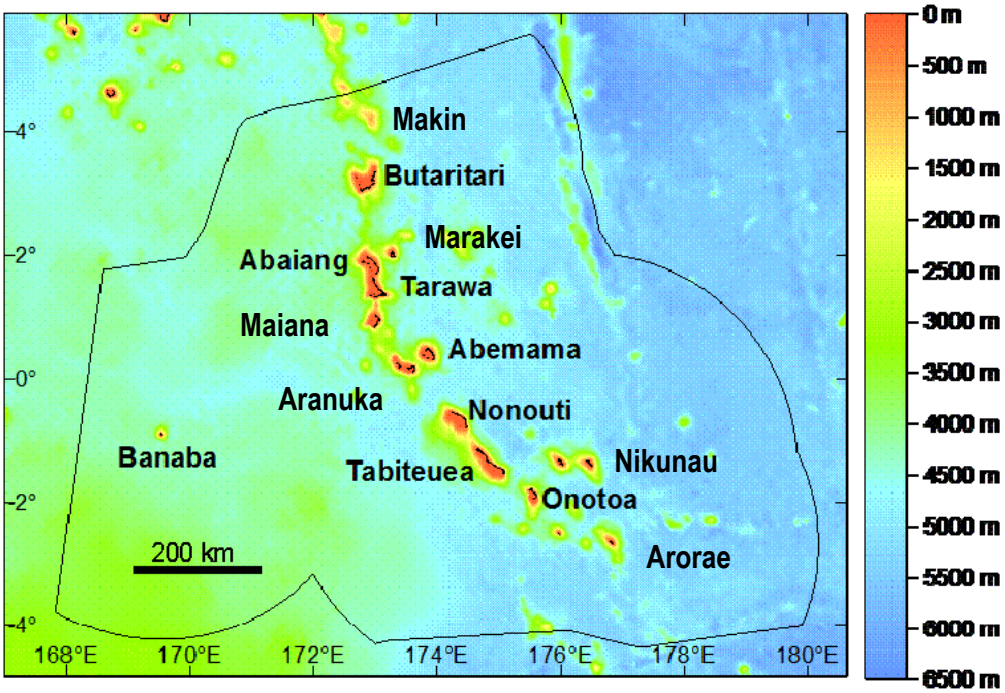

Figure 2.2. Map of the Gilbert Island Group showing the locations Tarawa in relation to the others (source: Smith and Sandwell, 1997).

Tarawa Atoll is triangular in shape; it has a length of 40 km and maximum width of 25 km. In the centre of Tarawa Atoll lies a shallow lagoon with a maximum depth of 24 m. The western submerged reef allows unrestricted exchange between lagoon and open ocean waters. The lagoon is partially enclosed by a chain of small complex reef islands lying on the northeast (NE) and southern rim of the atoll (Figure 2.3).

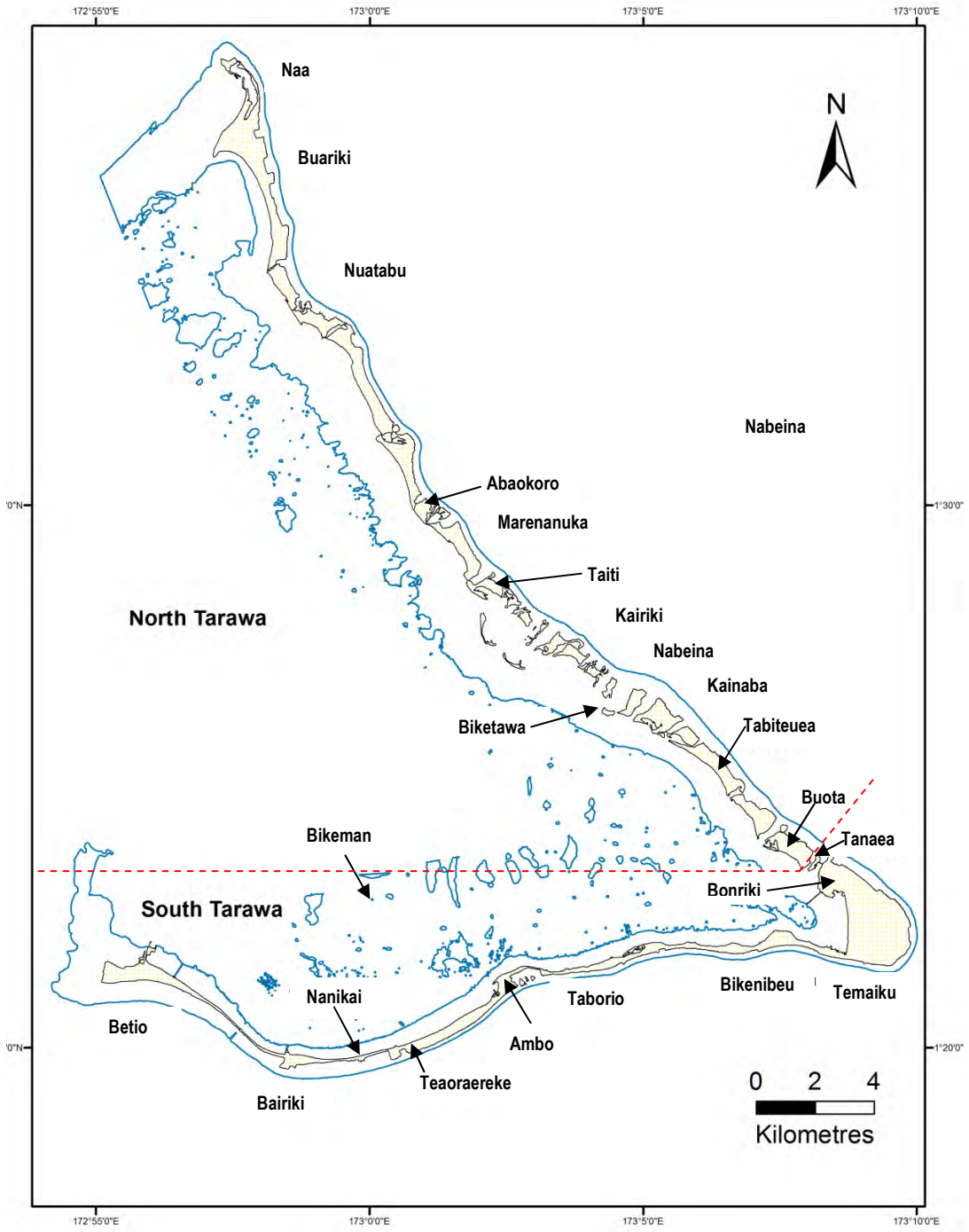

Figure 2.3. Tarawa Atoll showing the administrative regions of North Tarawa and South Tarawa (marked by the red dashed line). North Tarawa region covers Naa to Buota, whereas South Tarawa covers Tanaea to Betio.

The NE section stretches from Naa in the north to Tanaea in the southeastern corner. The southern arm consists of Bonriki in the southeastern corner and extends to Betio in the far west. The reef islands on the NE section are directly exposed to the easterly trade winds. However reef islands on the southern part are less exposed as they lie parallel to the trade winds. The atoll is administratively divided into two

parts: North (rural) and South Tarawa (urban) (Figure 2.3). The administrative boundary separating North and South Tarawa lies between Buota and Tanaea reef islands on the southeastern corner (Figure 2.3). Most of the reef islands are located on the windward (NE) side of the atoll. Reef islands are rarely more than 100 to 400 m wide. They are separated by inter-island reef channels allowing ocean water to flow into the lagoon.

Passages between reef islands located in the central part of the northern section extending from the south of Taiti to the north of Buota reef island are all open (Figure 2.4). The remaining passages have been closed by solid causeways constructed in the early 1960's (Hydraulics Research Station, 1979). The reef islands in the southern part have all been artificially connected to each other by structures mainly causeways, many of which are solid but some have culverts to allow tidal access. The Nippon Causeway and Baileys Bridge are the only two structures that allow ocean water to flow into the lagoon (Figure 2.4). The Fisheries Channel is located in the Nippon Causeway that connects the reef islands of Bairiki and Betio and is a 5% opening reducing the water flow by 95 to 97% (Zann, 1982). The causeway was built in 1987 and is the longest in Tarawa Atoll, measuring 3 km. The Baileys Bridge links Tanaea to Buota on the southeastern (SE) end of the Atoll. The bridge is open allowing ocean water to flow freely through.

2.4 Quaternary evolution of Tarawa Atoll

The evolution of atolls is generally explained by Darwin's (1842) subsidence theory of coral reef development. Darwin hypothesised that atolls evolved as a result of the subsidence of a mid-ocean volcano and simultaneous upward growth of a reef surrounding it. This model of atoll evolution is divided into three progressive stages (Figure 2.5). The first is a fringing reef, which later becomes a barrier reef in the second stage. The final stage is an atoll with a lagoon and a surrounding reef, which is reached through continued volcanic subsidence and reef growth. This theory was widely accepted after Darwin proposed it, but was not verified until many decades later after deep drilling tests on Funafuti (Tuvalu), Enewetak (Marshall Islands) and other atolls supported it (Guilcher, 1988).

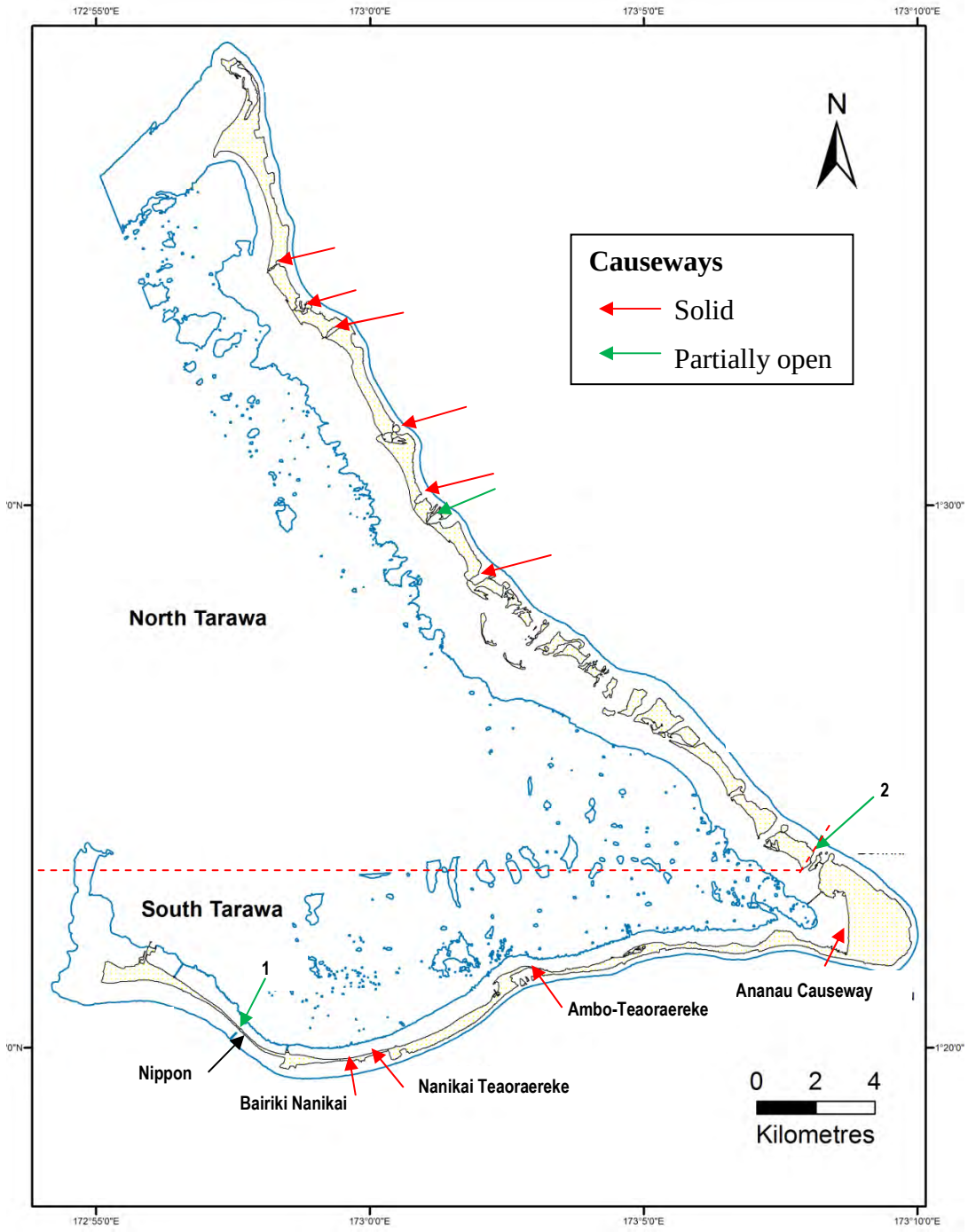

Figure 2.4. Tarawa Atoll showing the causeway locality and status (partially open or solid). Fisheries channel is marked by 1 and the Baileys Bridge is marked by 2.

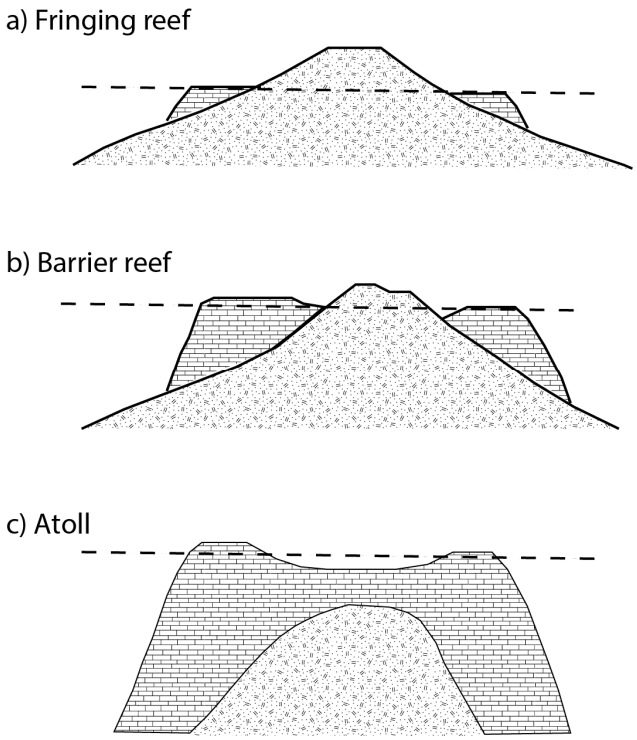

Figure 2.5. A schematic diagram illustrating an atoll's progressive stage proposed by Charles Darwin (source: (Woodroffe, 2003), p 10).

In Tarawa Atoll, no deep drilling has been performed, however, studies of neighbouring atolls in the Marshall Islands (Ladd *et al.*, 1953) and Tuvalu (Hinde, 1904) suggest that atolls along this chain have formed close to, or at, sea level on a volcanic basement that has now subsided to several hundred metres below sea level. Deep drilling in Tuvalu demonstrated that limestone is still present at 300 m depth (Hinde, 1904). Drilling in Enewetak Atoll, indicated that basalt was present beneath 1300 m of limestone (Ladd *et al.*, 1953). The 1300 m thickness of limestone contained fossils of organisms that live in shallow water depths. This supports the occurrence of two processes: subsidence of the capped volcanic rock and upward growth of reef limestone, which must have occurred simultaneously as proposed in Darwin's theory.

Shallow drilling on Tarawa Atoll has provided an insight into the Quaternary evolution of the atoll. The drilling that has been conducted consisted of ten boreholes drilled to a depth of up to 30m (Marshall and Jacobson, 1985). In ascending order, the four lithologies observed were: 1) basal, leached limestone, 2) a poorly consolidated coral unit, 3) unconsolidated sediment and, 4) cemented

conglomerate or cay rock. The leached limestone unit was encountered at depths of 11 to 30 m. The calcite fraction, which increased with depth, indicates that vadose and phreatic freshwater diagenesis has occurred indicating that the limestone material has been subaerially exposed. The presence of voids within the limestone structure indicates that these changes have taken place within the vadose zone, a subsurface layer present between the surface and the water table whereby groundwater and air have filled the voids. A sample collected of this limestone unit from Bonriki was dated using uranium series dating and showed an age of 125,000 ± 9000 yr (Marshall and Jacobson, 1985), indicating that the reef developed during the last interglacial.

A solution unconformity, a boundary separating two different aged units was observed between the older basal leached limestone unit and overlying coral unit (Marshall and Jacobson, 1985) has also been identified on other atolls such as Bikini (Ladd and Tracey, 1948) and Enewetak in the Marshall Islands (Ladd *et al.*, 1953).

This unconformity delineates the Pleistocene reef limestone and the Holocene reef and is consistent with the Darwinian theory of coral reef development. Daly (1915) contested Darwin's theory and tried to explain coral reef development based primarily on sea-level fluctuations. Studies building on the work of Daly suggested that modern reefs were veneers of growth over older reef forms (Asano, 1942; Yabe, 1942). This idea was later further developed by Tayama (1952) proposing that some of the larger atolls may have maintained their original form with younger reefs overlying older reefs which had been exposed during lower sea levels.

The glacial control theory developed by Daly (1915) was later refined by Weins (1959). He proposed that during the extended Pleistocene glaciation period, when sea level was low, the exposed coral reef platform was completely truncated. This would imply that the Pleistocene limestone does not provide a foundation for Holocene reefs to grow on. However, evidence from several atolls within the Indo-Pacific, including Tarawa Atoll and Christmas Reef island, Kiribati, indicate that this has not occurred, with Pleistocene limestone at the surface on Christmas Reef island and at ~10 m depth on Tarawa Atoll (Figure 2.6; (Marshall and Jacobson, 1985;

McLean and Woodroffe, 1994). This shows that Pleistocene limestone can provide a foundation over which the Holocene reefs can grow (McLean and Woodroffe, 1994).

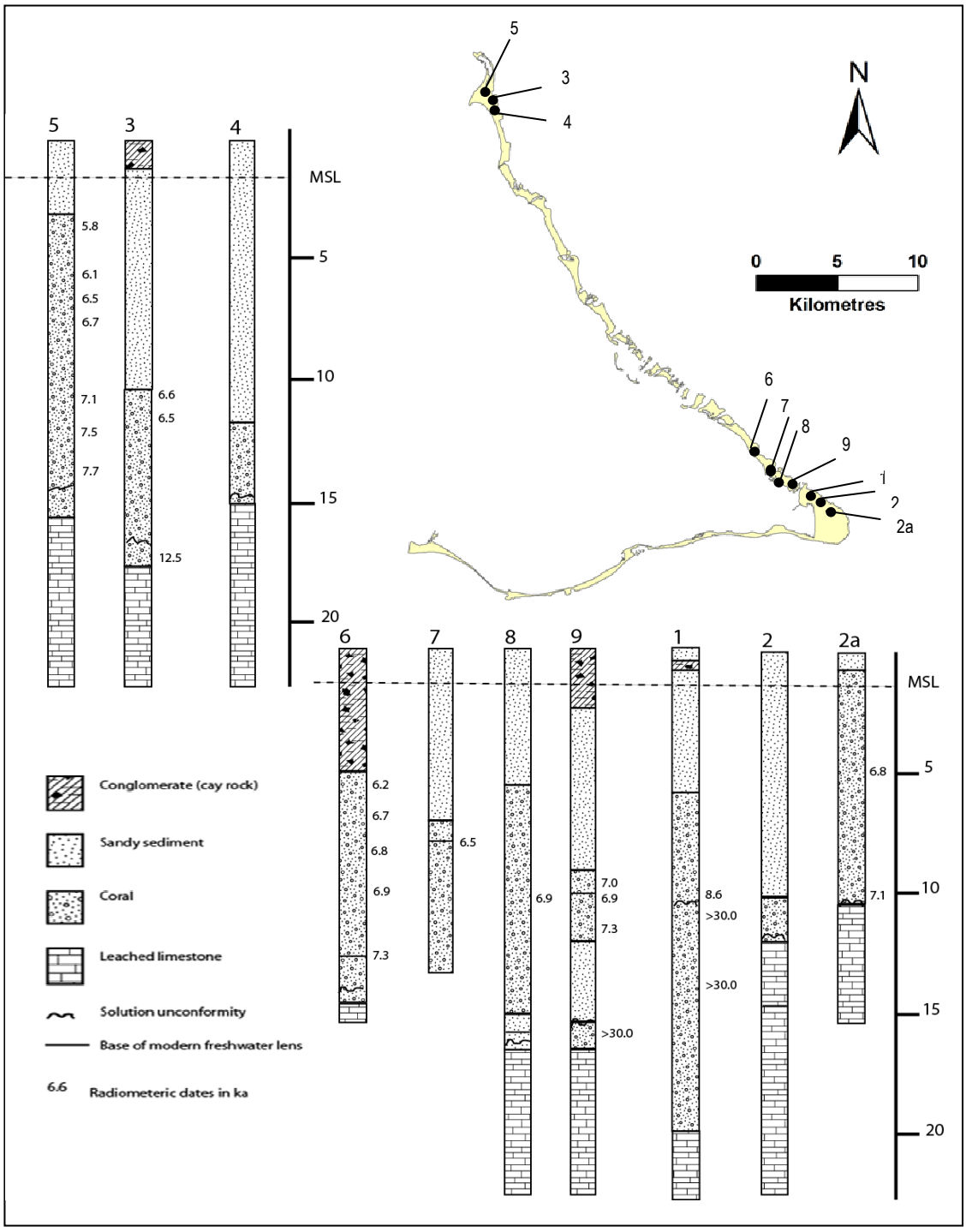

Figure 2.6. Map of Tarawa Atoll showing the locations of each drill core and the stratigraphy in each core (modified from Marshall and Jacobson, 1985).

The development of mid oceanic atolls such as Tarawa Atoll can be incorporated into a plate-tectonic understanding of the Pacific Plate. Volcanic reef islands undergo

subsidence as a result of gradual plate migration (Scott and Retondo, 1993). For most coral atolls, a reef platform existed approximately 120,000 years ago when sea level was high during the Last Interglacial. This reef platform was later exposed to surface erosion for a considerable length of time when sea level was lower during the glacial period. Mid-oceanic atolls such as Tarawa and Enewetak, in the Marshall Reef islands (Szabo *et al.*, 1985), followed the Darwinian sequence, whereby the limestone gradually subsided with the volcano providing both a platform and accommodation space for the vertical growth of Holocene coral. For a few atolls, Pleistocene limestone is exposed at the surface indicating they have not subsided. Christmas Reef island is an example of one of these atolls as emergent outcrops of Last Interglacial reef limestone are still exposed at the surface (Woodroffe and McLean, 1998). Some reef islands in the Phoenix Group also have outcropping reef limestone from the last interglacial (Tracey, 1972).

2.4.1 Holocene coral reef growth

The growth of the Holocene coral reef on Tarawa Atoll commenced around 8,000 years BP., after continental ice sheets from the Last Glacial Maximum melted adding significant volumes of water to the oceans which led to the inundation of the Pleistocene limestone reef. Drill cores, dated using radiocarbon dating, have shown the presence of a Holocene coral unit 8-11 m thick established over the Pleistocene (Last Interglacial) limestone reef. The growth rate of this coral unit was shown to be up to 8 mm/yr (Marshall and Jacobson, 1985) which is comparable to reef growth rates reported for the Great Barrier Reef (Marshall and Davies, 1982; Hopley *et al.*, 2007). This rapid reef growth indicates two things: first, a rapid sea-level rise occurred during the past 8,000 years similar to that observed in Tuvalu (Ohde *et al.*, 2002); and second, as a result of this rapid sea-level rise, coral growth lagged behind sea level for some time, but later caught up as sea level stabilised in the mid-Holocene (Marshall and Jacobson, 1985; Falkland *et al.*, 2004; Woodroffe, 2008). The composition of catch-up reefs is generally observed to be dominated by massive corals (Neumann and Macintyre, 1985). This is supported by the general description of the Holocene unit at Tarawa Atoll which is comprised of coral heads with diameters up to 0.8 m (Marshall and Jacobson, 1985). In a recent coral survey, massive *Porites* corals were shown to be predominantly found on the windward areas

of Tarawa Atoll (Lovell, 2000). However, branching *Heliopora* coral is characteristic of sheltered areas, such as Teaoraereke and the north west (NW) reef area (Lovell, 2000; Donner *et al.*, 2010).

2.5 Atoll surface morphology

The perimeter of an atoll can be divided into three zones: the outer reef, the reef crest and the reef rim (Wiens, 1962, see Figure 2.7). The reef rim is largely dominated by the reef flat but also includes reef islands grading into the lagoon. The important features of a typical transect on Tarawa Atoll were described by Zann (1982) using the area around Betio reef island which he examined by snorkelling and scuba diving. Richmond (1993) also examined the morphology and sedimentology of Tarawa Atoll and other atolls of the Gilbert Group by identifying the important features on vertical aerial photography followed by photography. Donner *et al* (2010) investigated and described the reef morphology of several sites around Tarawa Atoll.

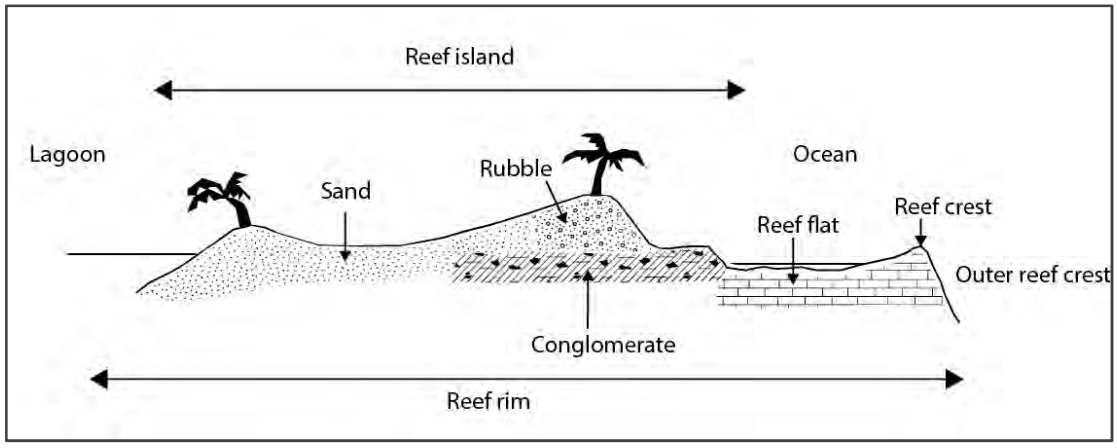

Figure 2.7. Typical cross section of an atoll showing the main features: outer reef crest, reef flat, reef island and lagoon (modified from Woodroffe, 2008 p. 80)

The reef rises from deep ocean floor depths of 4000 m to 6000 m. The submarine morphology at 500 to 1500 m depth shows variability, characterised by scarps, canyons and channels (Sharma and Kruger, 2008). Three ridges (described as saddles) with widths ranging from 2 to 2.5 km, and at depths of 250 to 300 m are present at the North, SE and SW corners of Tarawa Atoll (Figure 2.8). The northern ridge connects Tarawa Atoll to Abaiang, further north (Zann, 1982; Richmond,

1993). The reefs on the southern part of the atoll are wider than in other regions. This can be seen in the submarine morphology map (Figure 2.8) which was produced from a high resolution bathymetric survey taken 3 km offshore of the atoll to a depth of up to 1300 m (Sharma and Kruger, 2008). The reef front of eastern Tarawa Atoll is steep with slopes up to 70^{o} on the NE and SE sides of the atoll (Sharma and Kruger, 2008). The southern section has a gradual slope ranging from 5 to 15^{o} (Donner *et al*, 2010). Descriptions of the seabed morphology by Sharma and Kruger (2008) show that the slope of the reef front increases with depth; from 30 to 40^{o} at 50 m, and from 40 to 60^{o} at 250 to 450 m water depths. The upper outer reef slope is relatively steep with an angle of 45^{o}, as in the case of the reef platform between Betio and Bairiki (Figure 2.8) (Zann, 1982).

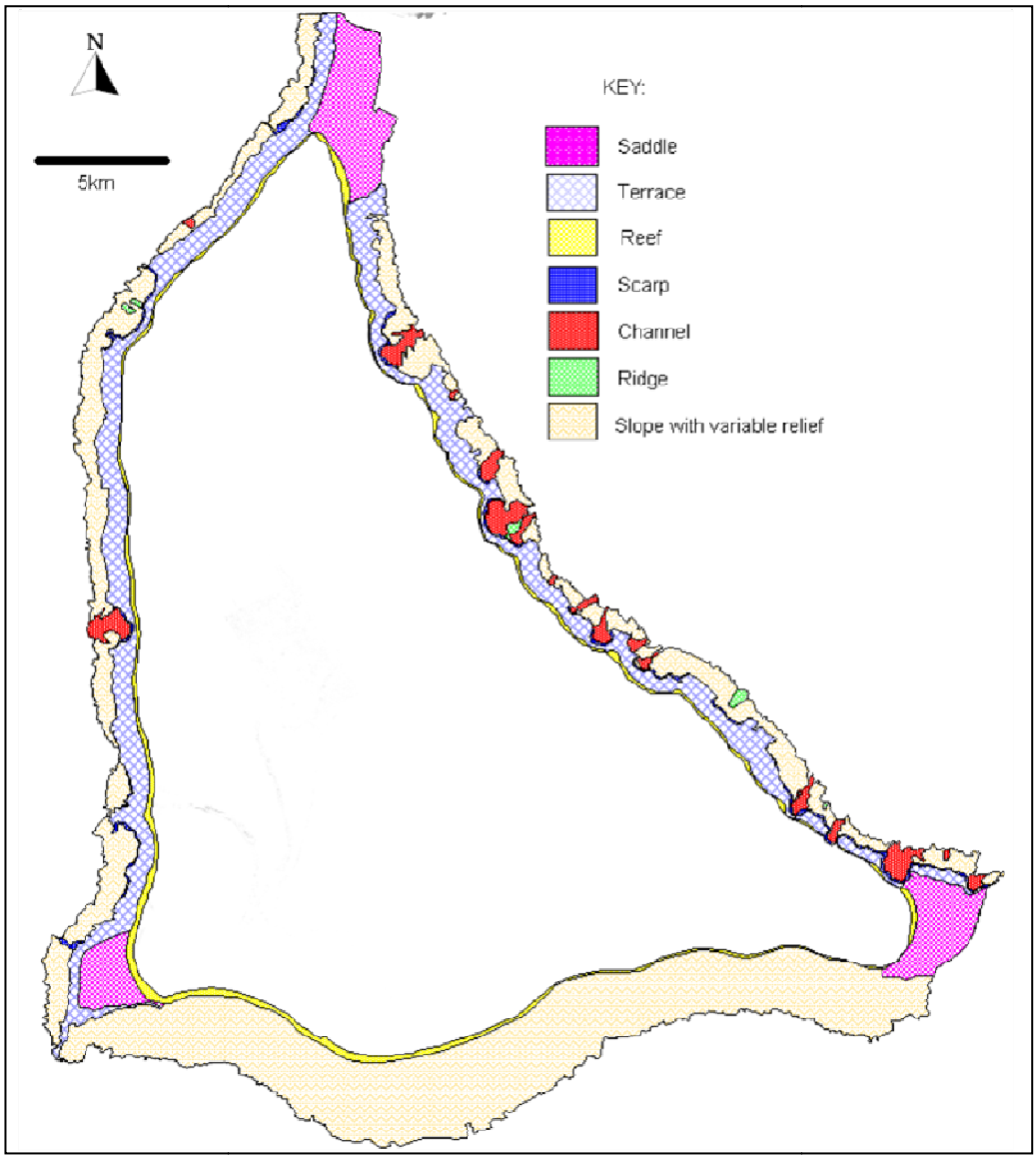

Figure 2.8. Submarine morphology of Tarawa Atoll (source: Sharma and Kruger, 2008 p 15).

The terrace at Betio has a distinctive spur and groove morphology indicative of high energy environments (Figure 2.9) (Zann, 1982; Woodroffe and Biribo, 2011). These spur and grooves are considered very important as they cause waves to dissipate before they reach the reef rim (Tracey *et al.*, 1948; Kench *et al.*, 2006). The spurs are mainly comprised of algal encrusted corals with 20 to 30% living coral cover as reef-forming corals are restricted to depths of 40 - 50 m (Zann, 1982). The grooves are deep channels, 2-6 m in height and width. They are possibly formed by waves constantly moving the sand and rubble on the bed of the groove as observations suggest that the mobility of the material on the floor of the channel is high (Zann, 1982). In deeper areas off the Betio and Bairiki reef platform, the spur and groove morphology differs from the rest of Betio reef island with more widely spaced spurs and grooves, possibly as a result of lower wave energy. In some areas adjacent to channels formed across the length of the reef platform, large deposits of fine silty sand were found, indicating that these originated from the lagoon, transported across the reef flat through channels and lost to the system (Zann, 1982).

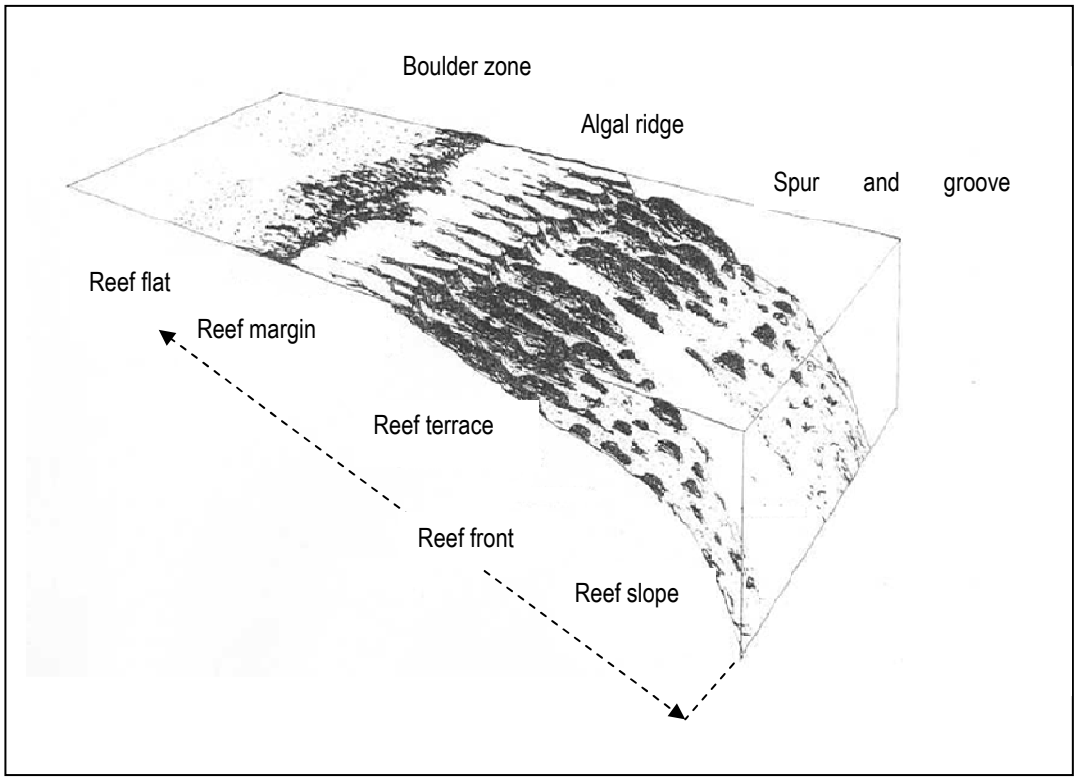

Figure 2.9. Cross section of the reef platform between Betio and Bairiki showing the morphology of the reef flat to the outer reef (modified from Zann, 1982 p 14).

2.5.1 Reef crest

The reef crest is a prominent ridge and is the upper portion of the spur and groove, delineating the seaward edge of the reef platform (Zann, 1982) (Figure 2.7 and Figure 2.10). The ridge is encrusted and maintained by crustose coralline algae (Newell, 1956; Dawson, 1961; Litter, 1973). The algae develop well in inter-tidal areas that are constantly exposed to water surges and sprays, dissipating wave energy (Litter, 1973). The reef crest is a highly productive zone of algae providing food for reef grazers, both at low and high tides. Behind the reef crest, lies the reef flat also referred to as the back-reef zone. Tarawa Atoll's outer windward reef crest is exposed to ocean swells breaking on the reef crest (Richmond, 1993). The reef crest is a continuous feature on the southern and eastern margin. In contrast, the leeward outer reef is discontinuous due to the submerged western reef connecting the ocean and the lagoon.

Figure 2.10. Waves breaking on the reef crest east of Tabiteuea, North Tarawa.

2.5.2 Reef rim

The reef rim extends from the reef crest to the lagoon (Figure 2.7) (Woodroffe and Biribo, 2011). In Tarawa Atoll, reef rims are broad solid reef flats that are generally exposed during very low tides (Zann, 1982; Richmond, 1992). The reef flats on the ocean side are wider than those on the lagoon side. These solid features, often with a veneer of coralline algae or thin sediment cover, appear to be non-depositional or erosional surfaces (Richmond, 1992). Reef flats located on the windward side are

bare or have a thin veneer of sediments, as most sediment is transported ashore or into the lagoon (Figure 2.11). Reef flats are important as they provide an accommodation space on which sediments can accumulate to form reef islands as well as being the most important source for reef islands sediments. Reef islands can form directly on the reef flat, but in many places are perched on outcrops of conglomerate. Reef islands will be discussed in more detail in Chapter 3.

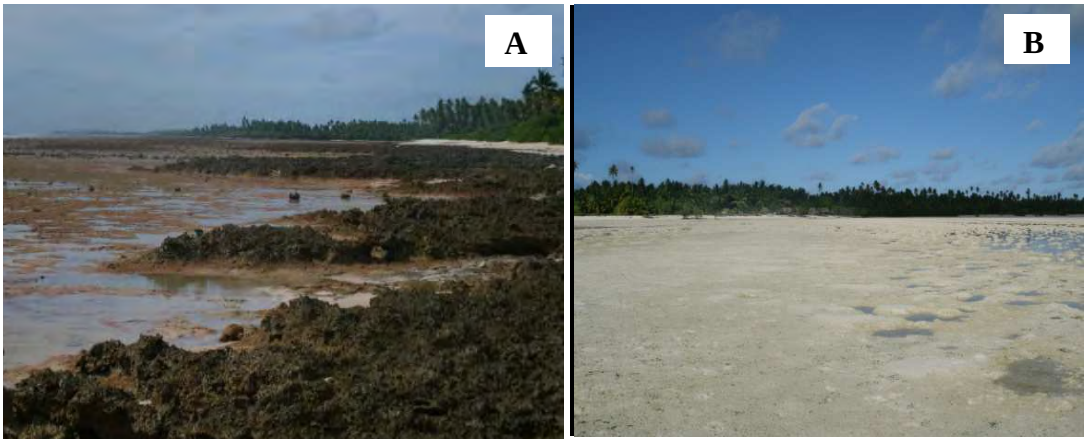

Figure 2.11. Reef flat morphology. A) ocean reef flat east of Tabiteuea and B) the extensive lagoon flat west of Notoue.

Behind the reef crest on the reef flat there are often eroded low-lying areas which have numerous pools at low tides allowing some corals to live but not thrive well (Figure 2.11A). Despite the lack of coral, many calcareous organisms can be found on the reef flat and contribute significantly to the reef island sediments. For example, benthic foraminifera occur behind the reef crest and are often found attached to the underside of the coral rubble (Collen and Garton, 2004). A slightly elevated discontinuous ridge of algal-cemented coral rubble lies at the back of this eroded zone (Zann, 1982). This ridge runs parallel to the reef crest and is comprised of storm debris, detached coral heads, reef limestone fragments and branches of coral fragments covered with blue-green algae (Figure 2.13).

Figure 2.12. Eroded areas on the ocean reef flat east of Bonriki indicating isolated pools during low tides, with little habitat suitable for coral growth.

Figure 2.13. Storm debris on the ocean reef flat of Tabiteuea.

Reef flats located on the lagoon side of reef islands are markedly different from ocean reef flats (Figure 2.11B). In Tarawa Atoll, these depositional surfaces are generally covered with fine sand particles (Zann, 1982) (Figure 2.11B). As a result, it is important to understand how sediment produced on the reef crest and ocean reef flat is transported to the reef islands or into the lagoon. In North Tarawa, the main exchange of water is over the reef flat in a lagoonward direction. This was observed through field measurements of current velocities and direction in three representative channels in North Tarawa which showed that 98% of the current flow was directed

towards the lagoon (Damalmian, 2008). This suggests that sediments derived from the productive reef crest and back reef environments may be transported directly onshore to ocean beaches or moved through inter-island channels to the lagoon beaches and reef flats. A comprehensive study carried out across Tarawa Atoll supported these patterns of sediment transport through studies of foraminifera test concentrations collected from different depositional environments (Ebrahim, 1999).

Sediments deposited on the lagoon flat close to passages can form sand spits. These sand spits form in sheltered areas that are protected from the direct impact of waves and provide a habitat for mangroves to grow. Mangrove species commonly found in Tarawa Atoll are *Bruguiera gymnorrhiza*, *Lumnitzera littorea*, *Rhizophora mucronata* or *Rhizophora stylosa* and *Sonneratia alba* (FAO, 2007).

2.5.3 Conglomerate outcrops

Conglomerate underlies the ocean shore of many reef islands in Tarawa Atoll. It often outcrops extending across the ocean reef flats in shore-parallel or long, prominent shore-normal groyne-like features (Richmond, 1993) (Figure 2.14). The long shore-normal conglomerates have widths of ~10 m and lengths of >100 m, whereas the shore-parallel conglomerates have widths of >100 m and lengths of ~10 m. Extensive shore-normal conglomerates occur at the ends of several reef islands on the eastern side of Tarawa Atoll augmenting the resilience of reef islands (Woodroffe, 2008). Conglomerates can be exposed in the centre of reef islands, and also extend into the subsurface, as observed in some cores (Marshall and Jacobson, 1985). In some places the conglomerate is composed of two units (Figure 2.15). The solid bottom unit contains coral in growth position, particularly *Heliopora*, that has grown slightly higher than its modern counterparts (Falkland and Woodroffe, 1997). The upper unit of the conglomerate is composed of coral rubble debris and modern material deposited after storm events (Ladd *et al.*, 1950) (Figure 2.15).

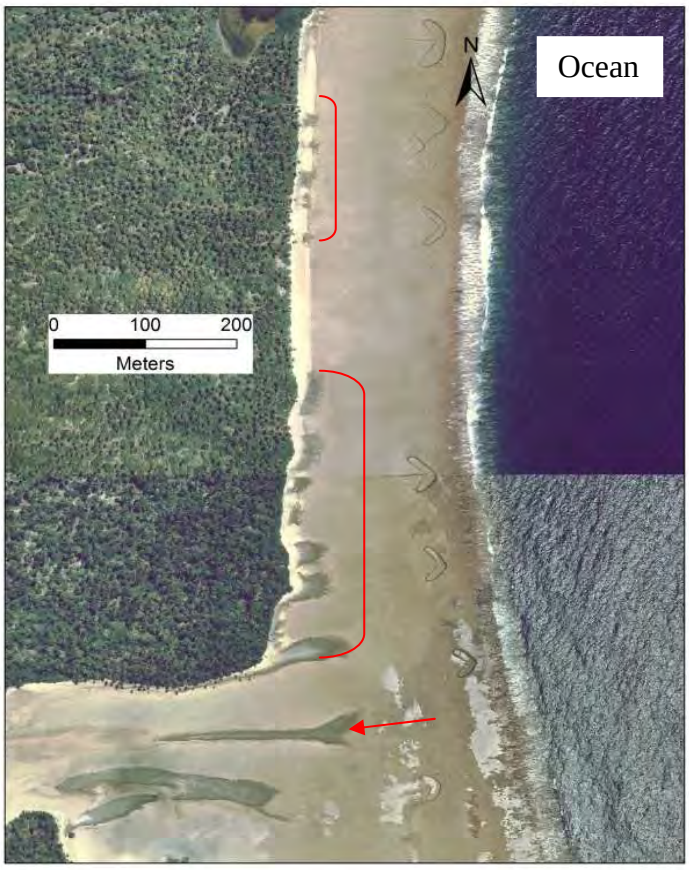

Figure 2.14. Examples of conglomerate outcrops. Long shore-normal conglomerate marked by an arrow, and shore-parallel are marked by brackets.

Figure 2.15. Conglomerate platform is made up of two units; an in-situ *Heliopora* coral unit (marked in green) overlain by cemented storm debris unit (red).

2.5.4 Lagoon

Tarawa Atoll lagoon is a shallow lagoon with a mean depth of 6 m and a maximum depth of 24 m (Damalmian, 2008). This distinguishes it from the lagoons in neighbouring atolls such as Abaiang which have depths greater than 30 m (Smith, 1999). The lagoon is partially enclosed except on the western side where the outer reef is submerged. On the eastern and southern reef rim exchange of ocean water with the lagoon is limited by the near continuous chain of reef islands and because the channels are blocked by solid causeways on the southern side. The poor connection between the lagoon water and the ocean makes the SE corner very turbid with the presence of fine grain sediment (Weber and Woodhead, 1972). The lagoon is sheltered from the NE trade winds, but is exposed to the SW winds.

Numerous patch reefs, some living and some dead, are scattered throughout the lagoon, but mainly occur near the submerged western reef. Zann (1982) established that the coral diversity and coverage of these patch reefs increased with distance away from reef islands, and he inferred that anthropogenic activities affect reef growth and diversity. Also present in the lagoon are scattered shoals that lie between Bikeman and the main reef islands.

Sediment composition varies greatly within the lagoon. On the western more exposed margin, the sediment is coarser compared to the fine muddy texture present in the sheltered southeastern corner (Weber and Woodhead, 1972). The principal sediment components tend to be foraminifera, *Halimeda* and molluscs which are present in the deeper parts of the lagoon (Weber and Woodhead, 1972; Ebrahim, 2000; Paulay, 2000). A detailed description of the variation within the lagoon is provided in Chapter 3.

The development of the lagoon has been linked to periods of low sea level (MacNeil, 1954). It has been proposed that during these conditions, solution of the soluble exposed coral limestone resulted in the development of a karst topography. This theory is supported by echo-sounding profiles and observations taken during diving across the lagoons of the Marshall and Caroline Islands (Shepard, 1970). Another theory is that lagoon morphology appears to have been developed largely by solution

rather than by subsidence (Purdy and Winterer, 2001; Purdy and Winterer, 2006). This currently remains an issue of debate.

Atoll lagoons are gradually filling up with sediments generated from within the lagoon itself and from the windward and leeward reef rims. An "empty bucket" theory has been proposed by Purdy and Gischler (2005) to explain the infilling of lagoons using examples from Indian, Pacific and Atlantic Ocean atolls. They apply the "empty bucket" analogy by likening the narrow reefs to the bucket rim and the lagoon to the interior of the bucket and propose that under conditions of low sea level during glaciations, the lagoon was dry. Under conditions of high sea level, the surrounding reef rims begin to grow again. As they catch up to the sea level, sediment around the atoll margin can once again be transported into the lagoon. Most importantly as Purdy and Gischler (2005) also recognise, the infilling of the lagoon depends on its geometry, and sand transported by ocean currents may "leak" through passages on the reef flat and be lost from the system.

2.6 Climate of Tarawa Atoll

Located within 5^{o} N and S of the equator, the reef islands of the Gilbert Group are exposed to easterly trade winds. The average air temperature of Tarawa Atoll is approximately 28^{o} C, and is similar to the average sea surface temperature (Australian Bureau of Meteorology and CSIRO, 2011). BOM and CSIRO (2011) also show that there is a strong relationship between the atmosphere and the oceans in the Pacific region. This is based on the analysis of data from several sources such as local meteorological stations recording wind, rainfall and temperature extending back to 1949, satellite altimetry data since 1993 and sea surface temperature (HadiSST dataset) from the Meteorological Office Hadley Centre.

The climate of the Gilbert Group is governed by several features including the Inter-tropical Convergence Zone (ITCZ), the South Pacific Convergence Zone (SPCZ) and the trade winds (Burgess, 1987; Australian Bureau of Meteorology and CSIRO, 2011). The ITCZ is a narrow convergence zone lying at about 5^{o} N, where winds from the northern and southern hemispheres meet (Burgess, 1987). The zone is

characterised by low wind, cloudiness and high rainfall (Burgess, 1987; Australian Bureau of Meteorology and CSIRO, 2011). The SPCZ is a broader convergence zone where winds meet (Burgess, 1987). The zone is orientated in a north-west and south-east fashion, extending from near the Solomon islands down to 30^{o} S, meeting up with the ITCZ around 170^{o} E (Australian Bureau of Meteorology and CSIRO, 2011). Seasonal fluctuations in winds appear related to the shifting of these two zones. A wet season, which occurs during November to April, develops when the ITCZ moves closer to the Gilbert Group. It is characterised by heavy rainfall and variable winds predominantly from the northeast. A dry season occurs in the months of June to November when both zones move further north of the Gilbert Group. This season is characterised by low rainfall, fine weather and winds blowing from the southeast.

El Niño Southern Oscillation (ENSO) significantly influences the climate of Kiribati by causing inter-annual variability. Analyses of the climate data of Tarawa Atoll using rainfall data (1950 to 2008), and temperature data (1947 to 2008) show that during El Niño conditions, increased sea surface temperatures raise the air temperatures above average, and the reef islands experience higher than average rainfall of more than 4000 mm (Australian Bureau of Meteorology and CSIRO, 2011). The opposite occurs during La Niña conditions. The sea surface temperature around the reef islands is cooler lowering the air temperature below average with a lower than average rainfall of less than 150 mm (Australian Bureau of Meteorology and CSIRO, 2011).

2.6.1 Wind

Lying in the equatorial region, dominant moderate winds blow from the northeast and southeast. During the months of June to August, and December to February, an irregular but strong wind pattern blows from the northwest and southeast (Burgess, 1987). In the middle of the year, the mean speed of the westerly wind is only 5 – 7 knots, but the strength increases from 7 to 10 knots from the months of December to February. Kiribati is located in an area that does not experience tropical cyclones, however strong west to northwest winds generated from cyclones do occur. Wind variability and duration depend on ENSO conditions (see 2.5.2).

2.7 Past sea-level changes

Past sea-level changes and trends are very important in understanding what the possible future trends may be, especially in relation to the future of low-lying atolls. However historical sea-level data in the Pacific region is sparse making it difficult to determine the sea-level pattern and the factors controlling these changes.

Sea level stabilised around 6,000 years ago across much of the Pacific region as shown by the record from coastal deposits in eastern Australia (Thom and Chappell, 1975). Around this time, polar ice ceased melting, with little further addition of water to the ocean (Woodroffe and Biribo, 2010). Relative sea-level changes have been geographically variable, depending on hydro-isostatic adjustments related to the limits of the former ice sheets; classified as near, ice margin, intermediate and far field (Lambeck, 1993). The Indo-Pacific region is a far field site, as it lies well beyond the former ice sheet limits. Drilling and dating of cores from the rim of Tarawa Atoll indicate that reef growth lagged behind sea level and only reached modern level between 4,000 and 5,000 years BP (Marshall and Jacobson, 1985) (Figure 2.16).

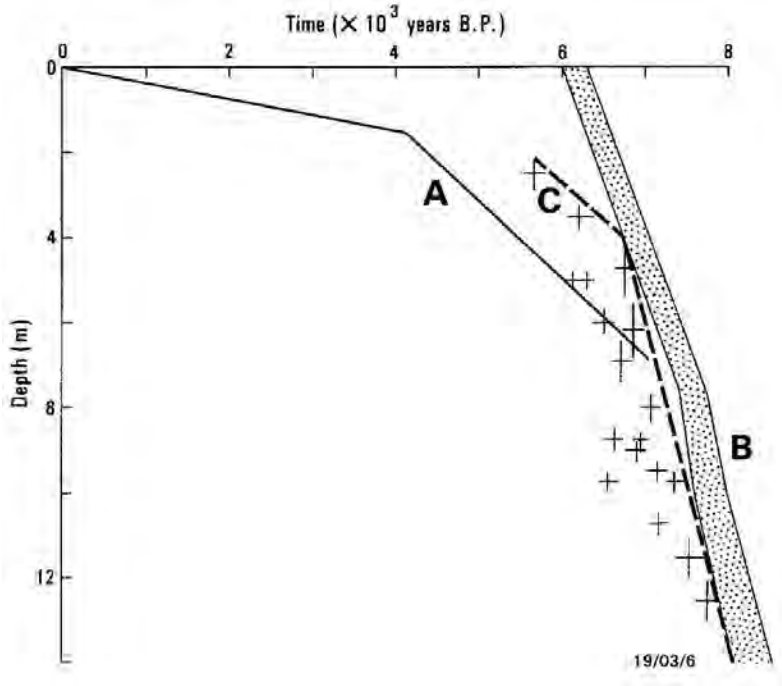

Figure 2.16. Comparison of sea-level curves developed from coral position and age obtained from A) Micronesia (Bloom, 1970); B) Eastern Australia (Thom and Chappell, 1975) and C) Tarawa Atoll, Kiribati (Marshall and Jacobsen, 1985) (source: Marshall and Jacobsen 1985 p 16).

Outcrops of cemented conglomerate rock occur on several of the reef islands around Tarawa Atoll (Figures 2.14 and 2.15). These are very important as their formation has been considered evidence of a mid-Holocene sea-level highstand. The presence of a higher mid-Holocene sea-level highstand in the Pacific is a controversial issue that has been widely debated. A comprehensive review of studies carried out in the Pacific Islands including those on Tarawa Atoll which will be discussed later generally supports the presence of a mid-Holocene highstand of a few centimetres above present sea level across the wider Pacific between 5000 and 1500 years (Grossman *et al.*, 1998). A conglomerate outcrop located in Bikenibeu village, from which in-situ corals and *Tridacna* yielded ages of 2760±70 yrs BP was considered evidence of highstand by Schofield (1977). But his claims were rebutted by Marshall and Jacobson (1985), as the upper layer of the conglomerate platform was composed of materials that appeared to be storm debris. Fossils of blue coral *Heliopora* in growth position present beneath conglomerate platforms have been described from Abemama, Maiana and Kuria in Kiribati and also occur on Tarawa Atoll (Falkland and Woodroffe, 1997), (Figure 2.15). The coral forms the base of the conglomerate platform (green in Figure 2.15) on which storm debris later accumulates. The growth of the *Heliopora* was restricted to a height of 0.7-0.8 m above their modern counterparts which could only occur if there was a sea-level highstand. An in-situ *Heliopora* coral, 0.4 m higher than its modern counterpart with a radiocarbon age of 2400±80 yrs BP was found at the base of a conglomerate outcrop in Makin, the northernmost reef island of the Gilbert Group (Woodroffe and Morrison, 2001). This evidence supports the presence of a mid Holocene sea-level highstand on Tarawa Atoll and elsewhere in the Gilbert Group.

However, in Christmas Island, there is no evidence of a Holocene sea-level high stand. Radiometric ages of over 100 fossil microatolls collected from the reef flat and interior of Christmas Island show no evidence of a highstand, but that sea level has been within a few tens of centimetres of its present level over the past 5000 yrs (Woodroffe *et al.*, 2012). Christmas Island is an example of a far field site which has not experienced sea-level oscillations of a metre or more as suggested for other Pacific Islands. This new evidence further suggests that there is greater variation within the wider Pacific than earlier considered.

2.7.1 Measurements of sea level in the Pacific

A series of sea-level stations were installed in the Pacific as part of the Tropical Ocean-Global Atmosphere (TOGA) program (Wyrtki and Mitchum, 1990). One important factor to consider when installing tide gauges is that the observations they record need to be related to land elevations. To ensure this, tide gauges need to be levelled to a fixed land benchmark so that any vertical movements of the land can be eliminated. At the initiation of the TOGA program, determination of land movements was considered to be an expensive exercise and was not accounted for, therefore any reported sea level from this program will incorporate land movements (Wyrtki, 1990). In Kiribati, as part of the program, a tide gauge was installed at Tarawa Atoll (University of Hawaii), and the existing stations at Christmas Island, Kanton Island and Fanning Island; in eastern Kiribati were incorporated into the program. The tide gauge at Tarawa Atoll is discussed further in Section 2.5.3. Wyrtki (1990) reviewed data from six monitoring tide gauges from Pacific countries including those at Christmas Island and Kanton Island, eastern Kiribati. This showed that there was no sea-level rise for eastern Kiribati but at other locations, such as Pago Pago Samoa, sea level had risen by 1.6 mm/yr for the 40 years from 1948 to 1987 (Wyrtki, 1990). However, the records did show the influence of El Niño periods raising the sea level around Christmas Island and Kanton Island up to 30 cm and 15 cm respectively during the 1982 - 1983 El Niño episodes. The influence of the El Niño is discussed further in Section 2.7.2.

The sea-level trend for this vast region remains uncertain as the number of tide gauges is limited and the tide gauge records are short. To address the issue of limited data, Church *et al*. (2006) reconstructed global mean sea levels from satellite altimetry data together with the reconstructed sea-level time series from tide gauges. The analysis showed that the average sea level in the Indo-Pacific region has been rising relative to land by +1.4 mm/yr since 1950. It also showed that sea-level variability in the Indo-Pacific region is predominantly influenced by ENSO. To compare this average sea-level rise of 1.4 mm/yr with the global average rate of sea-level rise, a correction was applied which involved the Glacial Isostatic Adjustment (GIA) and atmospheric pressure effects. As a result, an average rate of sea-level rise of +2.0 mm/yr was calculated, which was similar to the global average rate of

+1.8±0.18 mm/yr over 51 years (1950 to 2000) (Church *et al.*, 2004). The above studies show that over the past 60 years, mean sea level has been rising in the Pacific region and the globe. This indicates that sea level poses a major threat to low-lying atolls of the Pacific Ocean.

2.7.2 Influence of ENSO on sea level

ENSO is a phenomenon that influences the sea level and climate of the equatorial Pacific Ocean (Church *et al.*, 2006; Ramsay *et al.*, 2010; Australian Bureau of Meteorology and CSIRO, 2011; Becker *et al.*, 2012; Donner, 2012). And especially the climate of those reef islands that lie within 10^{o} of the equator such as Tarawa Atoll (Australian Bureau of Meteorology and CSIRO, 2012). It is widely accepted that the ENSO is a quasi-cyclic phenomenon recurring on average about 2 to 7 years, and influencing the climate of much of the Pacific Ocean and beyond.

This climatic phenomena was first recognised in the eastern tropical Pacific by the fishermen of Peru (Wang and Fiedler, 2006). They observed that at Christmas, the cold ocean conditions changed to warm conditions. During warm phases of ENSO (El Niño), a warm pool of water (which has been likened to a tongue) forms near Peru and moves eastwards to the equator driven by the difference in trade wind strengths, and warms up the oceans. The wind variations in direction and strength in the tropics are correlated with the Southern Oscillation Index (SOI). This index reflects the difference in atmospheric pressure between Darwin and Tahiti; a positive SOI is associated with La Niña, a constant negative SOI is associated with El Niño and a neutral SOI value is associated with normal conditions (Trenberth, 2001). This warm phase, El Niño, is characteristic of higher sea surface temperatures, low atmospheric conditions and weakening of trade winds leading to the strengthening of the westerly winds in the eastern Pacific. In Tarawa Atoll, the El Niño phase is characterised of westerly winds, high rainfall (Burgess, 1987), high sea surface temperature and upwelling (Australian Bureau of Meteorology and CSIRO, 2011). At the onset of El Niño conditions, the level of the sea is initially raised reaching a maximum of 30 cm and then lowered throughout the duration of the episode (Becker *et al*., 2012; Church *et al*., 2010). This large but temporary rise in the sea surface felt

across the equator appears to be related to the generation of the westerly winds (Bureau of Meteorology, 2010).

Conversely La Niña phase is characterised by lower sea surface temperatures, higher atmospheric pressures, strengthening of the easterly trade winds and less rainfall. In Tarawa Atoll, it is associated with strong easterly winds and less rainfall (Burgess, 1987). The level of the sea around Tarawa Atoll during these conditions is raised as the strengthened easterly trade winds tend to push more water across towards the west (Australian Bureau of Meteorology and CSIRO, 2011). These anomalies vary in intensities and durations influencing the wind and oceanographic conditions giving rise to seasonal variations in sea level.

Results from global sea level models show that during El Niño, rates of sea-level rise in the eastern Pacific are higher, 33 mm/yr, whereas in the central Pacific lower rates are observed, >1.5 mm/yr (Church *et al.*, 2004). A short satellite altimetry data set (1992 to 2002) and geoid model support this, adding that across the equator during El Niño conditions, the sea level in the eastern Pacific is 50 cm higher than the western Pacific (Maximenko *et al.*, 2009).

A recent study of the sea level in the tropical western Pacific by Becker *et al.* (2012) supports the theory that sea level has been rising, and that variability in the region is strongly associated with ENSO. The authors reconstructed a 60-year mean sea level record from 1950 to 2009, using the data: records from 91 tide gauges, satellite altimetry, GPS data and an ocean circulation model. The analysis showed that mean sea level has risen by 1.8±0.5 mm/yr since 1950. The results also showed that ENSO causes sea level to vary by up to 20 to 30 cm in this region supporting earlier findings by Wrytiki (1990) (see Section 2.6.2). In addition, the study reveals that Tarawa Atoll and the rest of the Gilbert Group, lying west of the dateline experience sea levels higher than average during La Niña conditions and lower than average sea levels during El Niño conditions. Christmas Island and the remaining reef islands of the Line and Phoenix Group lying east of the dateline experience the opposite, with sea levels lower than average during La Niña, and higher than average during El Niño.

2.7.3 Measurements of sea level at Tarawa Atoll

Historic sea level data for Tarawa Atoll has been recorded over the past 35 years and interpreted from data obtained from two tide gauges installed on Betio. It is important to understand how the tide gauge is related to land elevation as well as the history of the tide gauge, as it has been moved several times, affecting the monitoring of the sea level. Solomon (1997) relates the University of Hawaii (UH) tide gauge datum to a network of land elevations on South Tarawa measured in a 1972 land survey. The land elevations are related to the Cox datum which lies 0.107 m above the UH tide gauge zero (Figure 2.17). This relationship between the network of land elevations and Cox datum allowed the elevations of the network of beach profiles obtained in 1982 to be related to MSL (Howorth, 1985; Solomon, 1997).

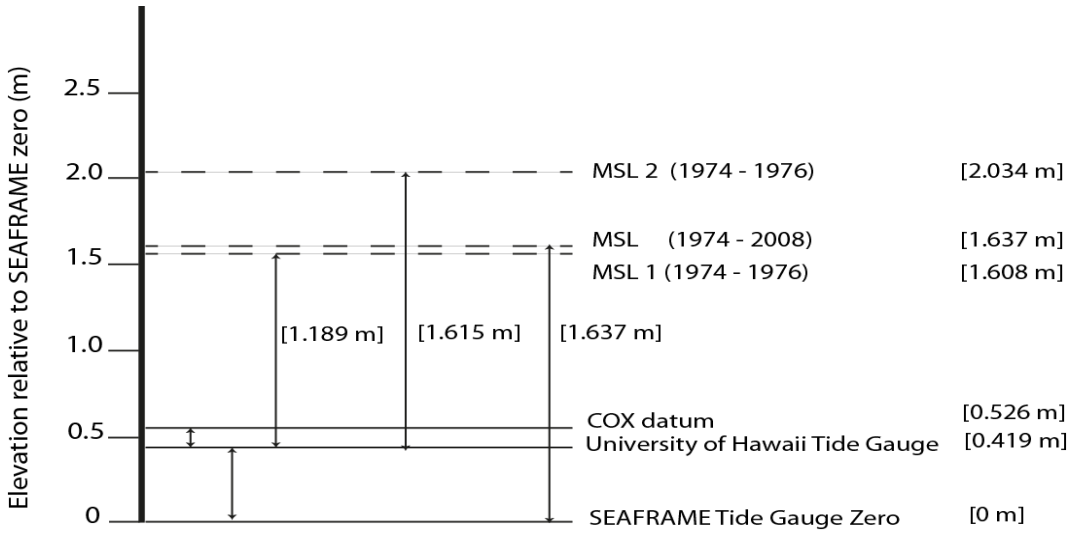

Figure 2.17. Heights of tide gauges used as vertical reference points in relation to differing MSL reported by Howorth (1983), Solomon (1999) and Ramsay *et al*., (2010). This also shows the relationship between the tide gauges (modified from Howorth, 1985 p 2).

The history of the tide gauge has been well described by Solomon (1997) and Ramsay *et al*. (2010) (Table 2.1). The first tide gauge was installed on the 31st May, 1974 by the UH which recorded nine years of data (Wrytiki, 1990; Solomon, 1997). Another station was installed in Bairiki as there were some vertical datum difficulties. This was installed in 17th of May 1983 and recorded another 5 years data, before it was turned off on the 10th of May, 1998. Another tide gauge was

established in Betio and started monitoring on the 20th of January 1998. The monitoring efforts on sea level continued until the 31st December, 1997.

Table 2.1. Sea level data, tidal stations and sources used to determine the Tarawa Atoll sea level. Note that the tidal stations have been referenced from the SEAFRAME datum. (modified from Ramsay *et al*., 2010).

Organisation	Location	Start Date	End date	Datum shift (mm)	Source
University of Hawaii (UH)	Betio	31May 1974	31Dec, 1983	+ 419	Howorth, 1983
University of Hawaii (UH)	Bairiki	17 May, 1983	10 May, 1988	+23	Solomon, 1997
University of Hawaii (UH)	Betio	20 January, 1988	31 Dec 1997	+23	Solomon, 1997
NTF, Flinders University, Australia	Betio	2 December, 1992	31 Dec, 2008 till present	0	AMSAT *et al*. 2004

The second and current tidal station, Sea Level Fine Resolution Acoustic Measuring Equipment (SEAFRAME) gauge or KIR 1, was installed at Betio on 2nd December, 1992 by the National Tidal Facility, Australia (NTFA) (Bureau of Meteorology, 2007) (Figure 2.18). This was part of a regional initiative by the Pacific Forum Leaders, to improve the understanding of the sea-level changes in the Pacific region by having accurate long-term sea-level records. As part of this initiative, the Australian Government funded a regional project titled South Pacific Sea Level and Climate Monitoring (SPSLCMP) which installed a network of SEAFRAME stations including that at Betio. These stations were initially monitored by National Tidal Facility of Australia (NTFA), which is now known as the National Tidal Centre (NTC) after it was absorbed into the Australian Bureau of Meteorology (BOM). Each station undergoes annual quality control checks carried out by BOM in close collaboration with Applied Geoscience and Technology Division (SOPAC) of the South Pacific Commission (SPC). Since 2010, 12 checks have been performed, and they show that the tide gauge does not appear to have moved relative to the land implying that tide gauge foundation is stable (Bureau of Meteorology, 2010).

Figure 2.18. SEAFRAME station in Port Betio, Tarawa Atoll.

The SEAFRAME station was installed such that it could be directly related to the UH tide gauge. However, in 2008, consultants from the National Institute of Water and Atmospheric Research (NIWA) in New Zealand who were tasked to carry out analysis of the tide data by the Kiribati Adaptation Programme (KAP) 'an adaptation programme initiated by the Kiribati Government aimed at addressing potential climate change risks' observed that there was a difference of 419 mm in height between the two tide datums (Stephens and Ramsey, 2008). In a draft discussion paper, they highlighted that the SEAFRAME gauge had been established at a height of 419 mm lower than the UH Gauge Zero datum. This means that any reported readings from the SEAFRAME gauge should be corrected by adding an additional +0.419 m. For example the MSL measured for 1974 to 2007 is 1.637 m above SEAFRAME gauge and 1.218 m above the UH.

The observation by NIWA that there was a difference between the tide datums was later confirmed by a consultant tasked by KAP to acquire accurate heights for seawalls to be constructed as climate change options for Kiribati Government Assets. To prevent overtopping of seawalls, the heights of the seawalls must be related to sea level, which necessitated the extension of the three benchmarks established by

SPSLCMP to cover Bonriki using the correct tide datum (Office of the Beretitenti, 2011). To test this, an exercise involving surveying observations of the low and high tides over a period of more than 12 hours was carried out. The exercise proved that NIWA's observation was accurate. In addition it established 31 new benchmarks and verified that the SOPAC network of benchmarks for beach profiling was related to the SEAFRAME gauge. The above shows the complexity of the history of the tide gauges in Tarawa Atoll. In this thesis, the SEAFRAME gauge will be referred to as SEAFRAME whilst the University of Hawaii tide gauge will be referred to as the University of Hawaii (UH).

2.7.4 Historical sea-level pattern for Tarawa Atoll

Several analyses of the sea-level data for Tarawa Atoll since 1974 have been undertaken. The first analysis was performed by Howorth in 1985 in order to relate the elevations of the beaches measured from the beach profiles to MSL. As discussed earlier in Section 2.3.7, MSL at this time was based on the Cox datum. Using the UH tide gauge data from 1974 to 1976, MSL was calculated to be 1.082 m above Cox datum which is expressed as 1.189 m above UH tide gauge zero (Howorth, 1985) (Table 2.2) (Figure 2.17).

Table 2.2. MSL values from Tarawa Atoll tidal records and their characteristics

MSL	Heights (m)	Heights (m) above SEAFRAME datum	Period	Source
MSL 1	1.189 above UH	1.608	1974 - 1976	Howorth, 1985
MSL 2	1.615 above UH	2.034	1980 - 1999	Solomon, 1997
MSL 3 or MSL	1.637 above SEAFRAME	1.637	1974 - 2008	Ramsay *et al*. 2010

The second analysis of the sea-level data for Tarawa Atoll since 1974 covering 23 years shows an average rise of +0.078 m (Solomon, 1997) (Tables 2.2 and 2.3). However, the calculated rate of sea-level rise over that period seems abnormally high at a rate of 33 mm/yr, which Solomon suggests maybe attributed to uncertainty surrounding the vertical datum as it moved several times. Based on the data, Solomon proposes that the sea-level pattern shows a rise, but the rate is uncertain. Contributing towards this uncertainty is the 0.419 m difference between the tide datums, which was later discovered in 2011. Another aspect of sea level calculated

from this analysis is the MSL, which is reported to be +1.615 m above UH datum in 1980. In Table 2.2 and Figure 2.17, this is referred to as MSL 2.

Table 2.3. Calculated rates of sea-level rise around Tarawa Atoll from tide records and their characteristics

Rate	Tide datum	Dates (period)	Source
33 mm/yr	UH	23 yrs (1974 to 1997)	Solomon, 1997
2.9 mm/yr	SEAFRAME	17 yrs (1993 to 2010)	Bureau of Meteorology, 2010
1.7 mm/yr	UH	9 yrs (1988 to 1997)	Becker *et al*. 2012
2.2 mm/yr	UH	22 yrs (1988 to 2009)	Becker *et al*. 2012
1.8 mm/yr	SEAFRAME	35 yrs (1974 to 2008)	Ramsay *et al*. 2010

A third, and more recent, analysis calculated the average sea-level rise for Tarawa Atoll to be 2.2 mm/yr (Becker *et al.*, 2012). This analysis involved two datasets: 1) a 9 year tide record (1998–1997) when the UH tide gauge was reinstalled in Betio but excluding the SEAFRAME data, and 2) satellite altimetry data covering 13 years (1997-2009). The average sea-level rise calculated from the tide gauge record shows a rise of 1.7 mm/yr. Analysis of the longest sea-level records for Tarawa Atoll shows MSL of 1.637 (Table 2.2, Figure 2.17) and a linear rise of 1.8 mm/yr over the past 35 years since 1974 (Ramsay *et al.*, 2010). The two rates are comparable even though one is derived from much shorter records. The difference between the rates of sea level rise presented in Table 2.3 is associated with the large effect of ENSO and the duration of the data records. In the case of the research by Becker *et al*. (2012), the inclusion of the satellite altimetry data may have contributed to the large increase in sea level, as measurements were obtained from a wider grid. The other common factor of the studies by Solomon, Becker and Bureau of Meteorology, is that they all fall short of the required 25 years to remove any noise associated with ENSO and the Interdecadal Pacific oscillation (IPO) (Ramsay *et al.*, 2010). The enormous difference in rates of sea-level rise observed by Solomon (33 mm/yr) and Ramsay (1.8 mm/yr) may be associated with differences in tide gauge datums and non- adjustment of the historical data to SEAFRAME datum making the results obtained from Solomon unreliable. The average rate provided by Ramsay incorporates these factors and is reported relative to SEAFRAME datum.

The rate of sea-level rise of 1.8 mm/yr obtained from Ramsay *et al*.(2010) is comparable to other global rates (Church, 2006), including that of the western Pacific

(Becker *et al*., 2012) but higher than the regional rate of +1.4 mm/yr (Church *et al.*, 2006). The reason for this is that the local average sea level is derived from site-specific data located close to the equator where the influences of ENSO are greater, whereas the regional average is obtained from a larger area spread across the Indo-Pacific region (Ramsay *et al.*, 2010). The study by Ramsay shows that with longer trends, the pattern of sea-level rise, the variability, and the factors that control it may be estimated.

Sea level in Tarawa Atoll and the Gilbert Group is influenced by several other variables including astronomical tides and storm surges (Figure 2.19). These factors have been discussed by Ramsay *et al*. (2010). The astronomical tide in Tarawa Atoll is semi-diurnal i.e. that there are two high tides and two low tides each day. These tides result from the gravitational effects of the moon and the sun on the earth and can be classified as Mean High Water Perigean Spring (MHWPS), Mean High Water Spring (MHWS) and Mean High Water Neap (MHWN). The effect of astronomical tides especially MHWPS which is also known as King tides can be devastating on low-lying areas along South Tarawa, particularly so if they coincide with strong wind conditions. This scenario occurred in February, 2005 and several assets on South Tarawa such as causeways and Betio Hospital were threatened by a king tide and strong winds (Donner, 2012). Finally, sea level is affected by storm surges caused by low barometric pressure and wind set-up.

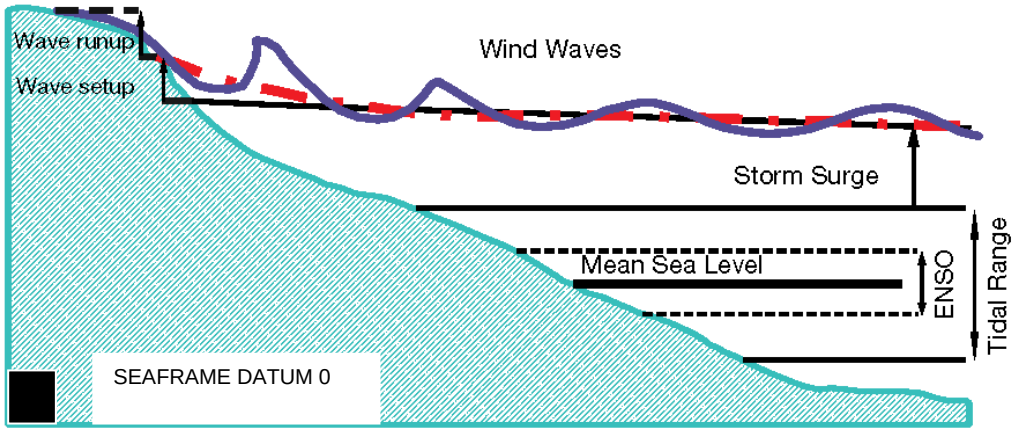

Figure 2.19. Magnitude of influences on the mean sea level (MSL) (modified from Meteorology and CSIRO, 2011, p 48).

As Tarawa Atoll lies outside the cyclone belt, sea level is rarely affected by intense storms and cyclones. Storm surge is the difference between observed still water level at a tide gauge, (not including setup and runup) and predicted (tidal) water level (Ramsay *et al.*, 2010). Storm surges of less than 0.15 m primarily affects the ocean shorelines for a short length of time (maximum 3 days) (Ramsay *et al.*, 2010). But compared to the effects of wave setup caused by waves breaking on the seaward edge of the reef flat raising the water levels up to 1 m this is very minimal.

Mean sea level varies constantly. In order to capture that variability Ramsay *et al*. (2010) considered it is best reported as Mean Level Of the Sea (MLOS). They define MLOS, as the average level of the sea over a certain period of interest; for example the MLOS in Ramsay *et al*. study is the average level of the sea from 1974 to 2007. The tide gauge data over the past 33 years show that the MLOS is 1.637 m (1974 – 2007). The MLOS reaches a maximum value of more than 1.72 m and a minimum of about 1.45 m. For the 33 years from 1974 to 2007, the heights of the astronomical tides are as follows, MHWPS is 2.641m, MHWS is 2.528 m and MHWN is 1.930 m (Table 2.4). The total sea level range in relation to SEAFRAME datum is 3.0 m. The factors that vary sea level in descending order of contribution are: a) astronomical tides (with a maximum range of 2.25 m); b) long-term fluctuations in MLOS due to factors such as ENSO and c) storm surges (0.32 m) (Figure 2.20). Storm tide is the temporary increase in water level which develops offshore beyond the wave breaker. The storm tides are a combined effect of MLOS, astronomical tides and storm surge height (Ramsay *et al.*, 2010).

Table 2.4. Tide elevations in relation to MLOS based on the 33 year tide data relative to SEAFRAME datum (source: Ramsay *et al*. 2010).

MHWPS (m) above MLOS relative to SEAFRAME	MHWS (m) above MLOS relative to SEAFRAME	MHWN (m) above MLOS relative to SEAFRAME
1.004	0.891	0.293

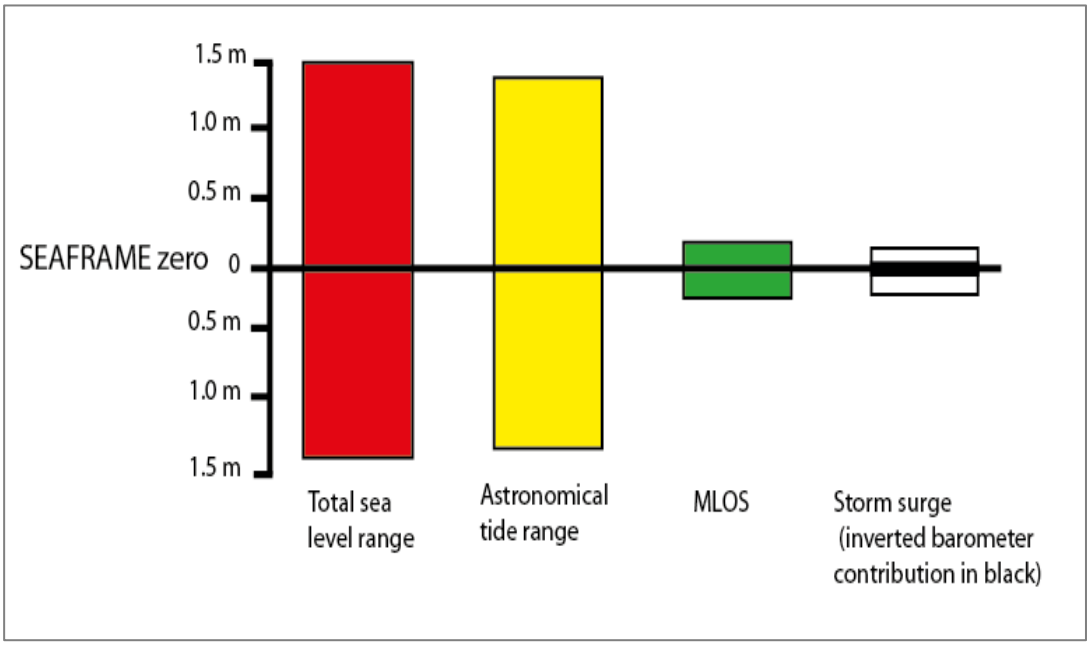

Figure 2.20. The contribution of various variables to sea level analysed from the 33 year tide gauge data from Betio (source: Ramsay *et al*., 2010, p 14).

2.8 Future sea-level changes

2.8.1 Future global average sea-level changes

The Fourth Assessment Report (AR4) of the Intergovernmental Panel on Climate Change (IPCC, 2007) states that there is high confidence that ocean waters are warming and expanding due to the increase in global ocean temperatures. Based on a 42 year global data set (1961 to 2003), evidence shows that the global ocean temperature has risen by 0.10^{o} C and that this extends to a water depth of 700 m (Bindoff *et al.*, 2007). AR4 estimates that the projected average global sea-level rise is 0.18 m to 0.59 m by 2090 to 2099 relative to 1980 - 1999.

To make predictions for future global climate, AR4 coupled 17 of 24 existing global climate models (GCM) to develop multi-model data (MMD) and presented six scenarios from the Special Report on Emissions Scenarios. Applications of these scenarios show that during 2000 to 2020, there are no significant differences between the scenarios with all six giving a global projected rate of rise as 1.3±0.7 mm/yr. In the case of 2080 to 2100 there are large differences giving a projected sea level rise of 1.9±1.0 mm/yr for scenario B1; 2.9±1.4 mm/yr for scenario A1B; and 3.8 ±1.3 mm/yr for scenario A2. MMD shows that sea level is projected to rise at an

increasing rate in the 21st century due to global warming. It will vary geographically due to variations in temperature, salinity and ocean circulation with different models showing different patterns (Meehl *et al.*, 2007).

The sea-level ranges provided by AR4 are narrower than the Third Assessment Report (TAR) models results. This means that there is more information known about factors influencing sea level now thus lowering the range. However, the existence of a range of predicted sea levels indicates that some uncertainty still exists about some factors such as the carbon cycle feedbacks and dynamic drawdown of major ice sheets (IPCC, 2007). As more information becomes known about certain factors, the range will reduce. Models show that sea level will continue to rise for another century and beyond even as a result of the already high concentrations in the system and the slow response of the ocean. It should be noted that these projections of sea levels predicted by the AR4 do not incorporate changes related to the potential accelerated dynamic drawdown of the major Antarctic and Greenland ice sheets.

Other global models indicate that ice melt from Antarctica and Greenland will increase but slowly within the millennia and that this will have a significant contribution to sea-level rise (IPCC, 2007). Recent findings after the publication of the AR4 support these claims and show that ice melting from these two areas has increased over the past decade (Cogley, 2009; Velicogna, 2009). The debate on the contribution of ice melt to sea level still remains as there are major concerns that the current sea-level projections, underestimating the rates by not including accelerated ice drawdown from Antarctica.

As sea-level rise in the Pacific region is influenced by ENSO (see Section 2.7.2), an understanding of the future changes of ENSO is also important. Based on all global models available, results of the AR4 show that future sea-level inter-annual variability will be influenced by ENSO. However out of the 19 models utilised, only six realistic ones showed no clear indication of any future change in ENSO amplitude or frequency indicating that ENSO modelling is poor (Meehl *et al.*, 2007). The differences between models imply that there is no confidence in any particular model and that uncertainties still exist about ENSO.

2.8.2 Future local astronomical tide level and extreme water levels

Projected water levels for Tarawa Atoll were generated using a coastal calculator developed by NIWA. The Microsoft Excel spreadsheet based tool was developed using recent information from IPCC AR4, physical coastal parameters of Tarawa Atoll predicted wave data from a hydrodynamic model of Tarawa lagoon, and recorded sea-level and wave data from Betio tide gauges for the years 1974 to 2007 (Elrick and Kay, 2009; Ramsay *et al.*, 2010). The objective of the tool was to generate projections of potential astronomical tide levels and extreme water levels (such as storm tides and storm surges) in Tarawa Atoll that would feed into the Kiribati Adaptation Programme (KAP) risk assessment of coastal areas around South Tarawa (Elrick and Kay, 2009). On the scenario page, the coastal calculator allows the user to change the following parameters: climate change scenarios, timeframe, baseline information and the datum (Ramsay *et al.*, 2010). The Tarawa Atoll page generates the extreme water levels and joint probabilities which account for the frequency of that event occurring within a year (i.e. 10%, 2% and 1%) (Figure 2.21). The water levels have been pre-calculated for the ocean and lagoon shorelines along Tarawa Atoll or the user has the option of determining water levels for a specific area. With the latter choice, the user can input specific parameters involving reef flat, shoreline, beachrock and seawall characteristics. The tool also considers the different levels that extreme sea levels would reach on the ocean and lagoon shorelines.

The climate change scenarios that are used in the coastal calculator were established by I-Kiribati Government officials in a KAP workshop held in 2008 (Kay, 2008). Following the IPCC AR4, the officials decided to apply three emission scenarios and include an allowance for the ice sheet melt. The AR4 report discusses the contribution of ice melt to sea-level rise, but does not include accelerated ice dynamics when considering global climate change scenarios, as there is still no consensus on the issue (see Section 2.8.1). Although there is no consensus, it was considered appropriate to include the potential known contribution of this uncertainty in future planning for the coastal areas of Tarawa Atoll as this low-lying atoll is particularly sensitive to any sea-level changes (Kay, 2008; Ramsay *et al.*, 2010). The modified scenarios to suit the Kiribati context are outlined in Table 2.5.

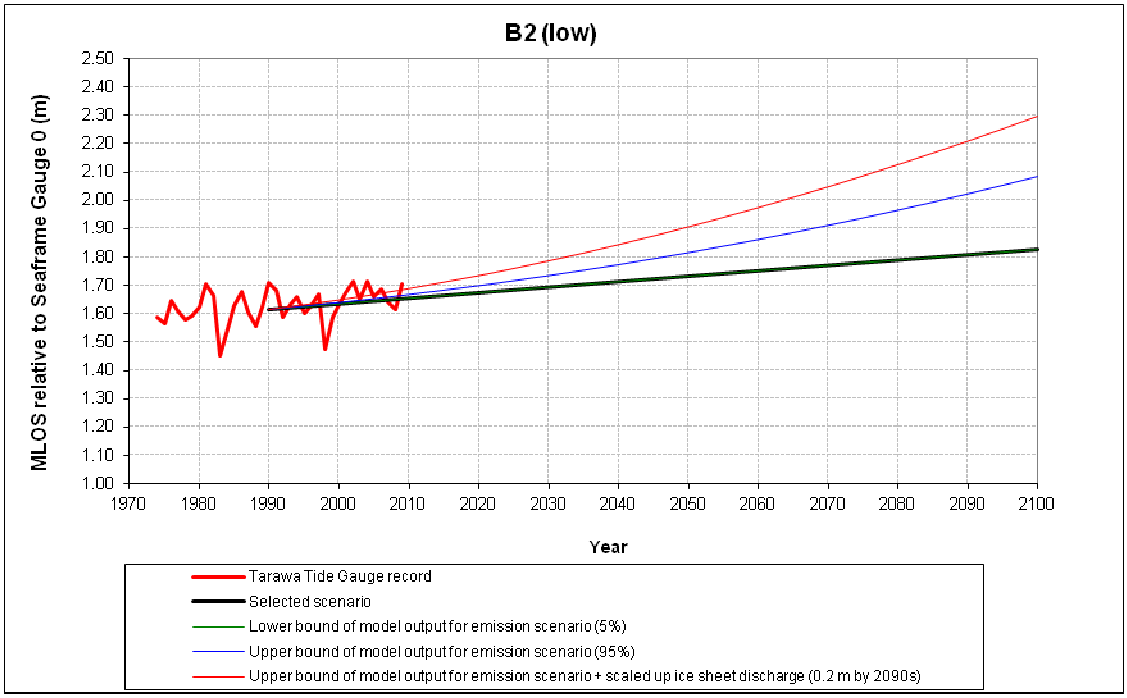

Figure 2.21. Projected mean sea-level rise scenarios for Tarawa using MLOS measured for 1974 – 2007, timeframe and low emission scenario B2. The green and blue line show the lower (5%) and upper (95%) limit respectively. The red line indicates the upper limit of the emission scenario including an additional discharge of the ice melt (source: Ramsay *et al*., 2010).

Table 2.5. I-Kiribati Climate Change Scenarios (source: Ramsay *et al*., 2010)

Scenario	Description
Low: IPCC Scenario B2	Low range of model output (5%) + no scaled –up ice sheet component by 2090
Intermediate: IPCC Scenario A2	Mid range of model output (50%) +10 cm scaled up ice sheet component by 2090.
High: IPCC Scenario A1FI	Upper range of model output (95%) + 20 cm scaled up ice sheet component by 2090

The timeframes of the climate change scenarios were also adapted to suit the Kiribati context commencing in 2012 to coincide with the presidential election (Elrick and Kay, 2009). A time step of 24 years was selected which would relate to the two office terms that two Kiribati Presidents could serve. By constitution, a Kiribati president can be re-elected into position for three consecutive terms equating to 12 years. This is also based on the fact that former Kiribati Presidents have normally completed their office term. The established three 24 year timeframes were given local names such as *Tibu* (grand children) 2012 – 2036; *Tibu-toru* (great-grand-children) 2036 – 2060 and *Tibu-mwamwanu* (great-great-grand-children) 2060 – 2084 Table 2.6). The advantage of naming these timeframes with local terms allows I-Kiribati people to easily relate to this new concept of climate change.

Table 2.6. I-Kiribati timeframes for general climate change assessments (source: Kay, 2008).

Time frame Name	Timeframe Name (Kiribati)	Time frame (period)
Grand children	*Te Tibu*	2012 – 2036
Great-grand children	*Tibu-toru*	2036 – 2060
Great-great grand children	*Tibu-mwamwanu*	2060 - 2084

The coastal calculator tidal information is based on the analysis of the 33 year tidal dataset (1974 to 2007) recorded from the Betio tide gauges (see Section 2.7.3) (Ramsay *et al.*, 2010). Results show that the MLOS has been varying due to the combination of contributing factors including ENSO and astronomical tides, which can give rise to extreme water levels.

Investigations on the variation of high astronomical tide levels and extreme storm tide levels were performed using a hydrodynamic model that SOPAC developed for the Tarawa Atoll lagoon. The model was developed from using multi-beam bathymetric data and calibrated using field observations such as water circulation patterns, current speeds and directions and water surface elevations from the SEAFRAME datum (Damalmian, 2008). Extreme water levels were simulated using the TAR sea-level scenario of 0.48 m and a 0.79 m.

Analysis of the 33 year tidal data set showed the spatial variation of levels across Tarawa Atoll. Results showed a 0.01 m higher mean water level for the southern eastern end of the lagoon compared to the northern and western corner of the atoll (Ramsay *et al.*, 2010). Storm tides can cause a difference of up to 0.1 to 0.2 m between different locations with the highest storm tide level occurring in the region from Eita to Tabiteuea in North Tarawa measuring 3.07 m, whereas the lowest is around Notoue to Buariki with 3.05 m. The difference between the lagoon and the ocean shorelines is that the latter are affected by wave set-up resulting from offshore waves breaking onto the solid reef flat. The effect of these offshore waves depends on the magnitude of the water level increase on the reef flat as this will result in waves with larger wave heights reaching the shores (Gourlay, 1988; SOPAC, 1993). The model predicts a difference between 0.03 to 0.14 m between the ocean shorelines on the northeast, south and west coast with magnitudes of 3.28 m, 3.17 m

and 3.14 m respectively relative to SEAFRAME datum as a result of the effect of the wave set up. This will be discussed in more detail in Section 4.2.7. Further simulation from the model involving potential wave set up and wave height were performed following Gourlay's approach (1996; 1997). The model shows that the impact of the wave set up decreases as sea level increases (Ramsay et al., 2010).

2.8.3 Future regional sea-level changes

Multi-model data from 16 Atmosphere Ocean General Circulation Model (AOGCM) incorporating both ocean density and circulation changes predict that sea level will rise in the Pacific region, but that the rises will not be uniform (Meehl *et al.*, 2007) (Figure 2.22). This variation may be attributed to variables such as enhanced eddy activities (Suzuki *et al.*, 2005), wind stress (Landerer *et al.*, 2007) or low thermal expansivity (Lowe and Gregory, 2006). The AOGCM projections share many similar aspects with observed patterns of sea-level rise such as a narrow, well defined band of sea-level rise, in the Southern Pacific (Meehl *et al.*, 2007). According to Meehl *et al*. (2007) the model's low resolution is due to the existence of large deviations which indicates no confidence in the models and calls for longer term data.

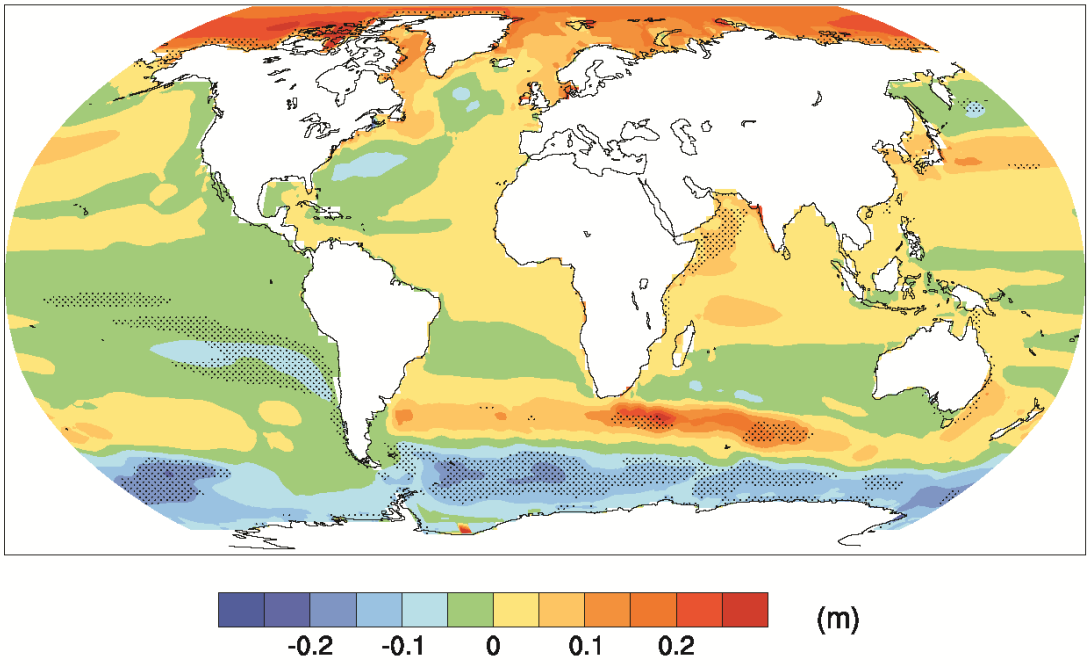

Figure 2.22. The irregular local sea-level change using ocean density and circulation change data derived from 16 AOGCMs forced with the SRES A1B scenario (source: Meehl *et al*., 2007 p. 813).

A recent report carried out by the Bureau of Meteorology and CSIRO (2011) suggests that sea level within this century will continue to rise in the Pacific. This study builds on the AR4 by providing climate change projections specifically for the Pacific region, as the AR4 highlights that global models are unsuitable for predicting finer resolution in climate change and variability. Climate change scenario projections were developed for the region by collating all existing climate data (both available in digital and paper format) for 14 Pacific countries which covered 92 years. With the information gained from weather, ocean observing stations and satellites, climate change scenarios B1, A1B1 and A2 were developed using 18 global models with a smaller period of 20 years to suit the dataset. The time periods of 20 years were established in order to suit the dataset i.e. 2030, 2055 and 2090. In the case of sea level, the total regional sea-level change was used to estimate only for the A1B (medium) for a 2080 - 2100 relative to 1980 – 1999. The estimates were determined by using the global average sea-level projections and regional changes due to ocean dynamics and mass distribution but not GIA (Australian Bureau of Meteorology and CSIRO, 2011). A distinctive narrow zone of 0.39 m sea level rise by 2100 is present within 5^{o} N and 5^{o} S of the equator, i.e., where Kiribati lies. The highest value of sea-level rise lies at higher latitudes beyond 20^{o} N and 20^{o} S.

There is high confidence that mean sea level around Kiribati will continue to rise (Australian Bureau of Meteorology and CSIRO, 2011). The existing data presented here suggests that there has been a mean sea-level rise for Tarawa Atoll that appears to be 2.2 mm/yr over the past 60 years (Becker *et al.*, 2012). In addition, the sea-level rise data from other regions of Kiribati show that sea level has also been rising; for example in Kanton over the past 69 years (1950 to 2009) sea level has risen by 2.1 mm/yr; in Fanning over 15 year period (1973 to 1987) sea-level rise by 1.5 mm/yr and in Christmas Island over the past 36 years (1974 to 2009) sea-level has risen by 1.8 mm/yr (Becker *et al.*, 2012). The range of sea-level rise obtained from these different studies are all comparable to global estimates for the same period (1.9 to 3.8 mm/yr) and all these studies project that in the next century, both globally and regionally, mean sea level will continue to rise.

2.9 Summary

This chapter has reviewed the physical and geological setting of Tarawa Atoll. It shows that the evolution of Tarawa Atoll is closely related to Quaternary sea-level patterns. The development of the surficial features of the atoll is also associated with Holocene sea-level variations, signifying the importance of sea level in determining the future changes on Tarawa Atoll.

Sea level is rising and will continue to rise. Global data and models have high confidence that sea level has been rising over the past 50 years and will continue to rise; however, there are still doubts about the robustness of these projections as the dynamics of accelerated dynamic drawdown have not been included, which may causes projections to be underestimated. In the Indo-Pacific region, modelling of satellite and tide gauge data also shows that sea level is rising at an average rate of 1.4 mm/yr (Church *et al.*, 2004). In the western Pacific, modelling of tide gauge data extended with satellite data over the past 60 years shows that mean sea level has risen by 1.8 mm/yr (Becker *et al.*, 2012). In Tarawa Atoll, sea level has also been rising at an average rate of 1.8 mm/yr, which is higher than that of the Indo-Pacific region but similar to that of the western Pacific (Ramsay *et al.*, 2010). Both the regional and local sea-level variations are strongly influenced by ENSO (Australian Bureau of Meteorology and CSIRO, 2011). The regional data show a west to east gradient of sea-level in the Pacific, however there are still some uncertainties surrounding its future magnitude and trend (Australian Bureau of Meteorology and CSIRO, 2011). Sea-level variations still remain a subject of debate and revision, especially in the Pacific where measurements are not yet sufficient to capture the long-term trend. A longer-term dataset is required to gain a better understanding of the sea-level trend and variation in the Pacific region and, at a local scale, in Tarawa Atoll.

3 CHAPTER THREE: PHYSICAL AND SOCIAL SETTING OF THE REEF ISLANDS OF TARAWA ATOLL

3.1 Aims of the chapter

The aim of this chapter is to examine the physical characteristics of the reef islands around Tarawa Atoll including the population distribution and the anthropogenic impacts on the coastline. This chapter will review the following:

a) The classification of reef islands
b) The sediment composition of different depositional environments.
c) The inapplicability of the Bruun Rule to determine reef-island shoreline responses to future sea-level rise.

In addition this chapter will:

d) Describe the physical dimensions of these reef islands.
e) Examine the beach sediment composition.
f) Outline the population distribution and discuss its influence.

3.2 Introduction

Atolls comprise an annular mid-ocean reef surrounding a central lagoon. The reef rim of atolls may consist of individual or near-continuous reef islands of varying shapes and sizes. Reef islands are small, low-lying landforms that are accumulations of sediments that are entirely biogenic in origin. On average the majority of the land area is below 2 m above MSL (Woodroffe, 2008). These physical characteristics make reef islands fragile and expose them to the impacts of climate change and the associated sea-level rise. This has raised widespread concern in both the global and scientific communities about the future of reef islands on atolls (IPCC, 2004). An understanding of reef-island responses to sea-level rise requires an understanding of their physical characteristics. These characteristics, which can vary from one reef island to another, include reef-island geomorphology, substrate characteristics and the morphology and sediment composition of beaches. The physical ability of reef islands to respond to sea-level rise is likely to be impaired by population growth and by unsustainable urban development (Elrick and Kay, 2009). Therefore it is also

important to consider the distribution of the population and the impact that human activities have on the coastlines of these reef islands.

3.3 Background

3.3.1 Global distribution of atolls

Byran (1953) complied a global list of atolls and identified 425 atolls distributed as follows: 334 in the Pacific Ocean, 68 in the Indian Ocean, 26 in the Caribbean Sea and only one in the Atlantic. More atolls have been subsequently identified, increasing the number to over 525 (Purdy and Winterer, 2001) (Figure 3.1). Each individual atoll contains reef islands around its perimeter, and these can vary significantly in number and morphology. Weins (1962), in a comprehensive book titled *Atoll environment and ecology*, showed that there was a westward decrease in reef island number and area on atolls across the Pacific extending from the Tuamotu archipelago in the eastern Pacific to the Caroline Islands on the west.

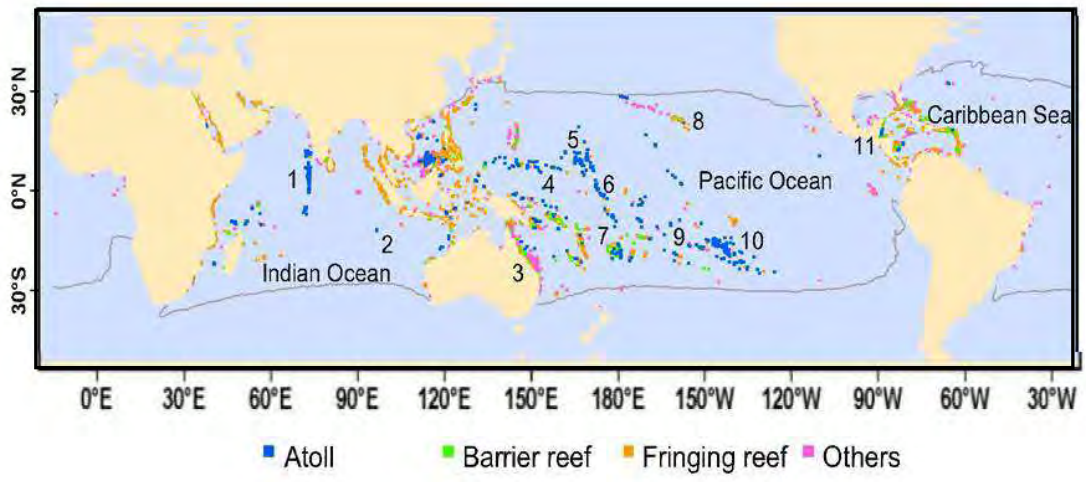

Figure 3.1. Global distribution of atolls centred in the Pacific Ocean, Indian Ocean and Caribbean Sea. The areas marked in the map are: 1. Maldives; 2. Cocos (Keeling); 3. Great Barrier Reef; 4. Caroline Islands; 5. Marshall Islands; 6. Kiribati; 7. Tuvalu; 8. Hawaii; 9. Northern Cook Islands; 10. Tuamotu Archipelago; French Polynesia and 11. Belize (source: Yamano *et al*. 2005, p. 10).

3.3.2 Reef island classification

Despite the diversity in the different types of reef islands (Ladd *et al.*, 1950), it is possible to classify them into several types. The first classification attempt was carried out by Steers (1937) as part of an expedition to the Great Barrier Reef. Steers

divided the reef islands visited into three groups: shingle reef islands, sandy reef islands and low wooded reef islands.

This classification was later extended by MacNeil (1972) to include the reef islands of atolls in the Marshall Islands, Pacific Ocean. He based his classification on the formation and sediment origin of reef islands using those situated in the northern part of the Marshalls Group. MacNeil defined three classes, describing them as follows:

a) Rocky islands are reef islands that have formed on reef platforms or on eroded remnants of a raised reef.
b) Rubbly reef islands are reef islands formed from rubble tracts or conglomerate platforms derived from storm deposits.
c) Sandy reef islands (also known as cays) are reef islands that have formed from sand bars.

Reef islands are generally thought to occur as a result of the interplay of various physical processes at different locations on the reef flat (Stoddart and Steers, 1977). Richmond (1992) extended MacNeil's classification to embrace the wider Pacific region. Richmond used a larger sample of 14 atolls, predominantly from western Kiribati, but also from Tuvalu and the Cook Islands to modify MacNeil's (1972) classification to increase the understanding of reef-island development. The sample population of atolls involved a wide variety of different shaped reef islands including those from Tarawa Atoll. His approach focused on several physical characteristics of the reef island, such as reef island morphology, its position on the reef rim, the dominant sediment composition and rock characteristics. These factors gave rise to an additional reef-island type and his classification comprising sand cays, complex and small reef islands, elongated and U-shaped reef islands is described below:

a) *Sand cays* are small reef islands that are predominantly sandy in composition (Figure 3.2A). The shapes of these cays range from symmetrical to oval. Generally cays are situated on the sheltered side of the atoll. In some instances, they are located within the lagoon on patch reefs. The shorelines of these reef islands are predominantly composed of sand. Beachrock may occur but conglomerates are seldom found.

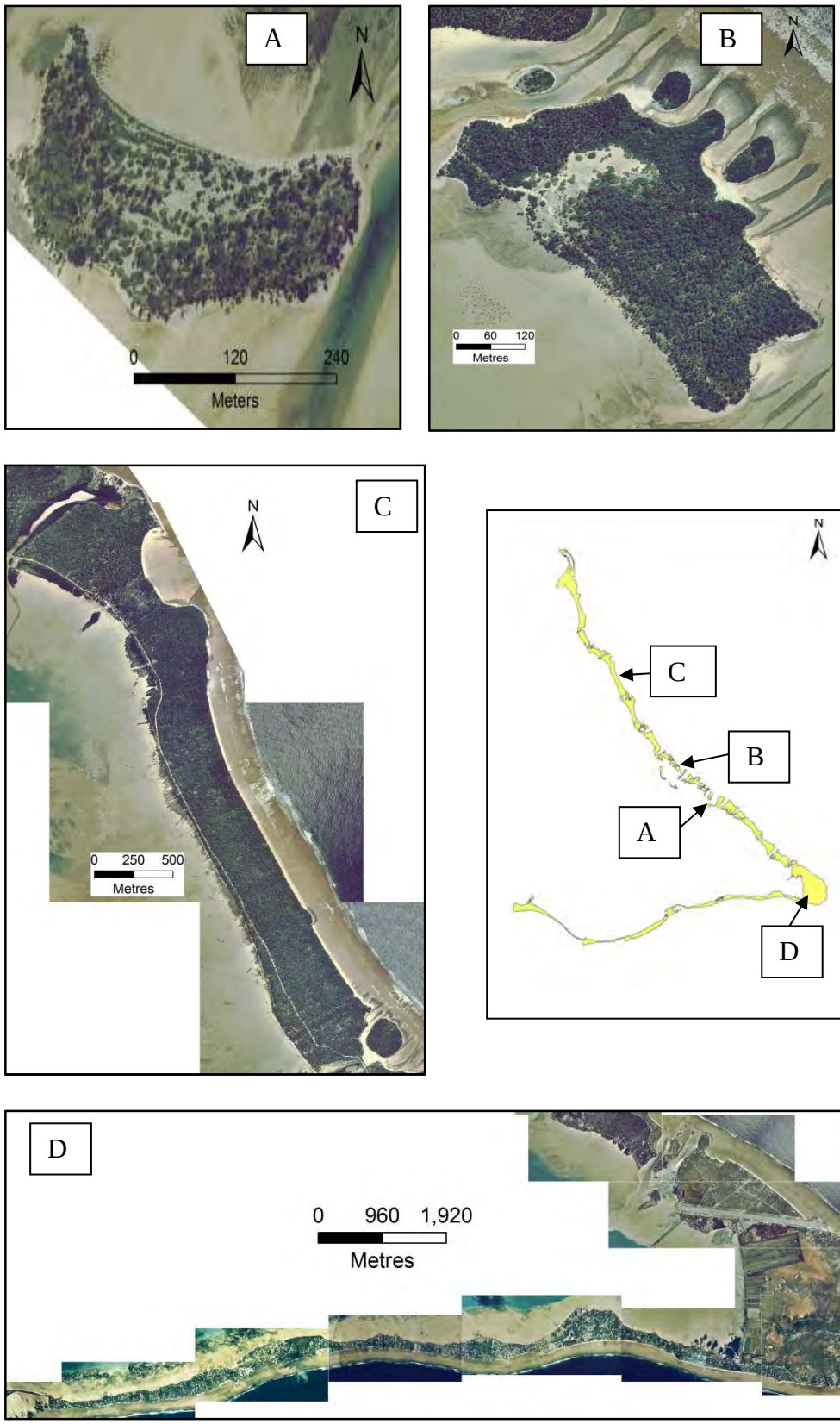

Figure 3.2. Examples of reef islands following Richmond's (1992) classification. The insert shows the locations of the reef islands on Tarawa Atoll. A: Sandy cay, Biketawa located in the lagoon on the northern section, B: A small complex reef island located in North Tarawa, C: An elongate reef island, Tabiteuea located on the northern section of Tarawa Atoll and, D: The only U-shaped reef island, in Tarawa Atoll, Bonriki-Taborio in the south-eastern corner of Tarawa Atoll.

b) *Complex and small* reef islands consist of complex landforms that have developed around cemented rubble and reef-flat deposits (Figure 3.2B). They predominantly occur on the windward sides of atolls. The cross section of these reef islands is similar to that of U-shaped and elongated reef islands, however, in some cases, they lack central depressions. Exposed beachrock and conglomerates occur around the shores. Conglomerate outcrops are very important features protecting the shorelines on these reef islands from erosion. This last group is derived by combining MacNeil's (1972) sand cays and U-shaped reef islands.

c) *Elongated* and gently curved or sinuous shaped reef islands have a cross-island profile similar to U-shaped reef islands (Figure 3.2C). The reef islands form on the straight portion of the reef rim and are composed of multiple parallel ridges occurring on both sides of the reef island separated by a central depression. Beachrock and conglomerate platforms are usually present around the reef islands with sand spits occurring at the ends.

d) *U- or boomerang-shaped reef islands* are a group of reef islands that form around the atoll rim, at the point where both the rim changes direction and it is exposed to high wave energy (Figure 3.2D)(Richmond, 1992; McLean, 2011). Cross-island transects show that the exposed ocean side has beaches that are generally steeper whilst the sheltered lagoon side has beaches that have a more gradual slope. The ocean and lagoon ridges are usually separated by a central depression which is typically a low-lying swamp. Re-curved sand spits occur at the tips of these reef islands.

This classification shows that reef island types present on North Tarawa are sandy cays, elongated reef islands and complex reef islands. On the other hand in South Tarawa the reef island types present are elongated, complex and small reef islands. Not all reef islands are present in the two sections. The classification does not provide a useful basis to differentiate reef islands from North Tarawa from those in South Tarawa and therefore the reef islands are classified into two categories showing North (reef islands that are rural) and South (reef islands that are urban).

3.3.3 Reef-island beaches

Ocean and lagoon beaches on reef islands differ. Beach profiles measured on Bairiki and Betio reef islands showed that ocean beaches have an average slope of 10^{o} whereas lagoon beaches have more gradual gradients of 6-7^{o} (Howorth *et al.*, 1986). A combination of several factors drive this variability including sediment composition, sediment grain size, and exposure to wind and wave energy.

Beach slopes vary depending on reef island types. Reconnaissance field mapping and analysis of aerial photographs of selected reef islands from the Pacific, including Tarawa Atoll, showed that exposed ocean beaches of boomerang-shaped reef islands have very steep slopes reaching 40^{o} (Richmond, 1992), whereas lagoon beaches had more gradual slopes of 3-5^{o} lower than that of small and complex reef islands.

3.4 Carbonate sediments and component composition around Tarawa Atoll

Studies of reef islands in the Pacific have shown that the sediment is generally composed of corals, coralline algae, molluscs and, in some cases, there is a major contribution from foraminifera. The composition of the sediments provides important information about their origin and the processes of sediment delivery. A global review to determine the major constituent of beach materials from 17 atolls, two platform reef islands and one reef island found that corals and foraminifera are the dominant grain type (Yamano *et al.*, 2005). Another study examined compositional grain analysis of 93 samples collected from various environments around Fongafale, Funafuti Atoll, Tuvalu, and showed that in order of decreasing abundance the sediment was composed of foraminifera (41%), *Halimeda* (24%), coral/calcareous red algae (23%), molluscs (9%), echinoids (1.5%) and other other/unidentified, sources (1.5%) (Collen and Garton, 2004). On Makin, the northernmost atoll with reef islands in Kiribati the sediment composition comprised coral (30%), foraminifera (30%), other/unidentified sources (30%), molluscs (8%) and coralline algae (2%) (Woodroffe and Morrison, 2001). Analysis of sediment samples obtained from eight traverses laid across the reef flat of Heron Island, Great Barrier Reef, Australia showed that the sediment composition was mainly coral and algal detritus (Maxwell *et al.*, 1961). Also present, but with insignificant

contributions, were foraminifera, molluscs, bryozoans and echinoderms. Atolls with lagoons have an additional carbonate material source from *Halimeda* (Yamano *et al.*, 2005). It is clear from these studies that reef islands depend entirely on biogenic sediments for their formation and stability.

Sediment grain analysis can be used to establish the origin of skeletal components, the productivity of each responsible carbonate organism and the local sediment distribution patterns from different depositional environments within atolls (Weber and Woodhead, 1972; Ebrahim, 1999; Collen and Garton, 2004). The sediment composition of Tarawa Atoll has been examined in several studies. The locations of these studies are provided in a map showing that the majority of the locations of sediment samples are concentrated in South Tarawa (Figure 3.3). Although different approaches were adopted, the results of these studies have been compiled with a map showing the variation of sediment composition for Tarawa Atoll (Figure 3.4).

Sediment composition analyses (Weber and Woodhead, 1972; Ebrahim, 1999) and benthic ecological studies (Zann, 1982; Paulay, 2000) carried out in Tarawa Atoll have contributed to the understanding of the origins of the material, mechanical breakdown and patterns of sediment transport. These studies have concentrated on South Tarawa and had different objectives, study areas and sampling methods, so they are not directly comparable. The studies will be discussed separately below.

Weber and Woodhead (1972) collected 69 spot samples, 57 of which were lagoon samples and 12 were from South Tarawa's reef flat to compare variations in lagoon carbonate sediments with other neighbouring atolls. They concluded that the principal contributors to lagoon sediments were *Halimeda* and molluscs, which increased in proportion towards the sheltered eastern part of the lagoon. The contribution of corals showed an inverse trend, representing a greater proportion on the western reef crest and gradually decreasing towards the east.

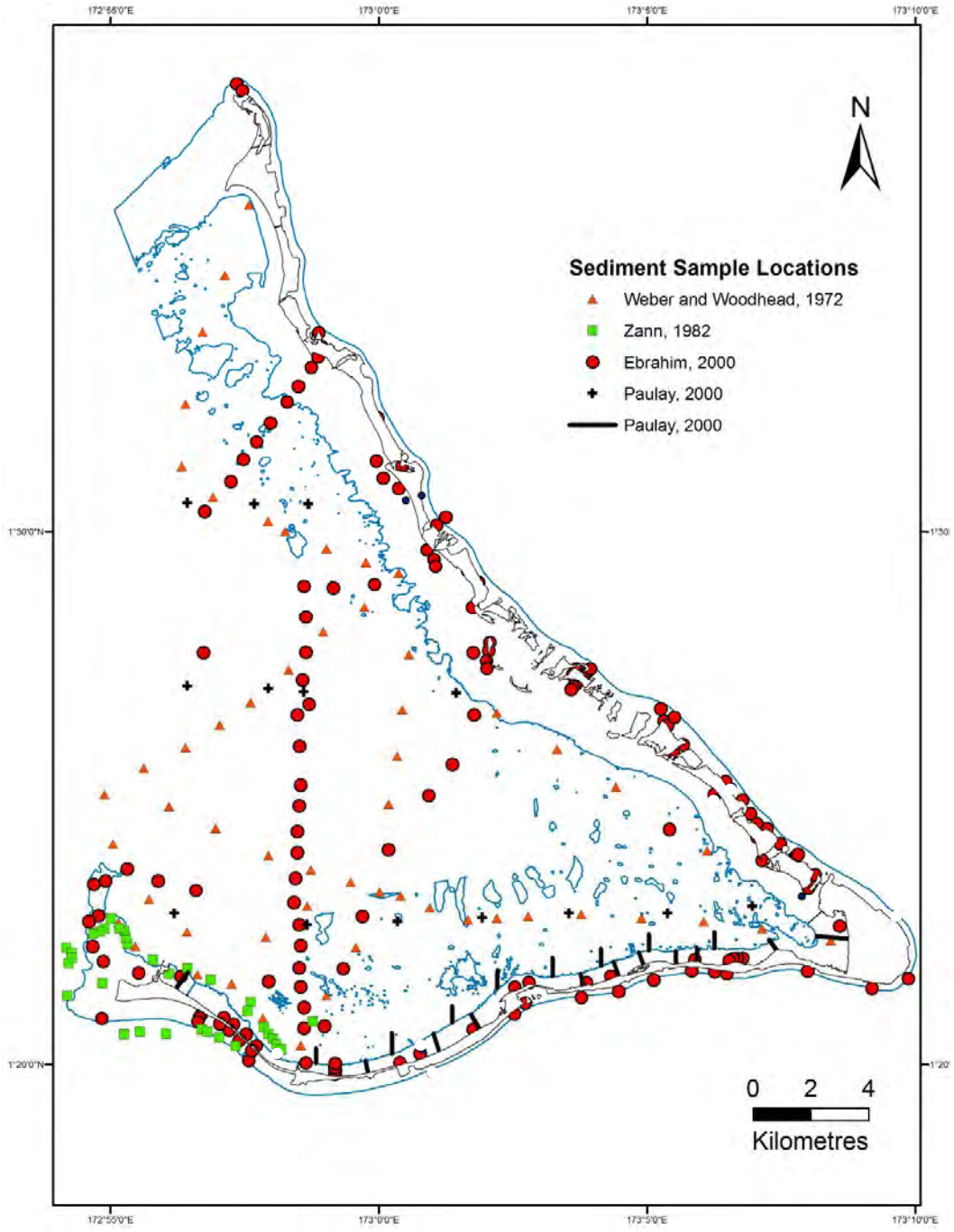

Figure 3.3. Locations of sediment samples collected for sediment composition studies by Weber and Woodhead, (1972); Zann, (1982); Ebrahim, (1999) and Paulay, (2000).

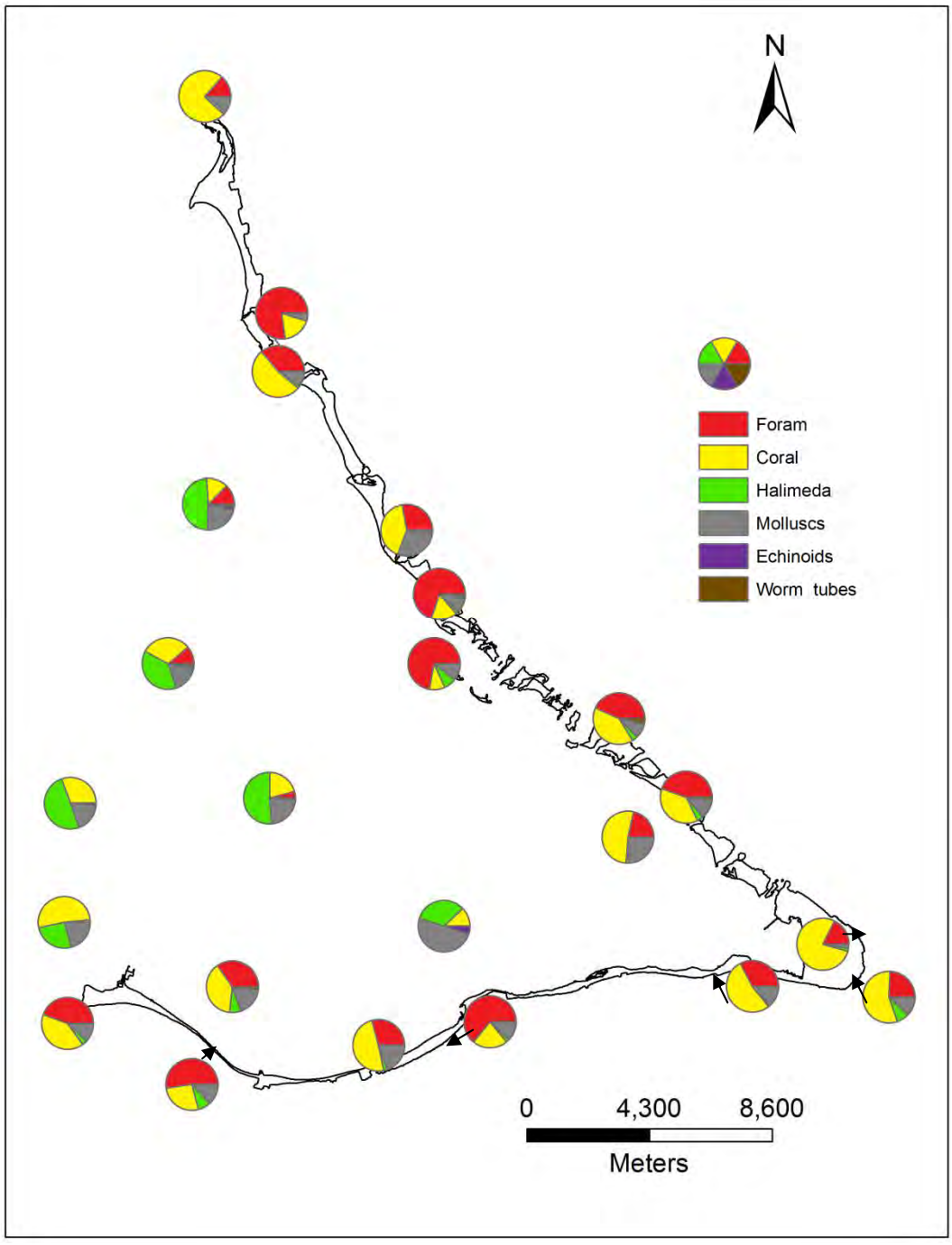

Figure 3.4. Generalised sediment composition map of Tarawa Atoll showing compositional differences between environments and organism abundance. The data is compiled from the following studies: Weber and Woodhead, (1972); Zann, (1982) Ebrahim, (1999) and Paulay, (2000).

In 1982, Zann carried out a study on the ecological status of Betio and Bairiki prior to the establishment of the Nippon Causeway. He described the marine ecology of Betio and of the platform between the two reef islands recording percentage cover for 134 transects and stations. Both living and dead coral were present in most

locations around Betio. Zann observed that the sediment composition of Betio reef island is largely dominated by sand and coral rubble, especially on the western side. *Halimeda* dominates in the lagoon, particularly on the northern end of the reef island. Gastropods are also present but only occur in patches on the sandy lagoon reef flats. Zann forecast that the coral communities within the area would be affected by dredging.

In 1999, as part of his PhD thesis, Ebrahim carried out a comprehensive study to determine the natural and human-induced processes controlling carbonate sedimentation. He collected 170 mostly surficial sediment samples from the following environments: the ocean reef flat, ocean beaches, on land, in channels, the lagoon reef flat, lagoon beaches and the lagoon floor. The sediment grains that were greater or equal to 0.25 mm in diameter were identified. From 161 samples, he identified more than 200,000 individual grains and concluded that Tarawa Atoll's sediments were predominantly composed of coral, foraminifera, molluscs, *Halimeda* and algal debris. Present, but occurring in lower quantities, were crustacea, echinoids, ostracods, worm tubes, beachrock and bryozoan fragments. The remaining nine samples collected from the lagoon reef flat were not included as they had grains less than 0.25 mm in diameter.

In 2000, Paulay carried out a quantitative study of molluscs in order to manage South Tarawa's shellfish resources, as shellfish are one of the major sources of protein in the local diet. Fifteen transects were laid perpendicular to the shore at regular interval spacing covering the full length of South Tarawa. On each transect, nine stations were established which covered the following benthic habitats: the beach slope, the sand flat and seagrass beds. At each station, 0.25 m^2 paired quadrats were used to mark sample areas. Sediment material was collected from surface up to a depth of 0.2 m or until bedrock was reached. Live molluscs and echinoids were collected after sieving the sediment using a 2 mm mesh screen. The total number of samples collected was 130 including samples from the lagoon. No shellfish were collected from 5 stations and Paulay (2000) suggests that this a reflection of the lack of shellfish in the station areas due to hard substrata.

The above studies have enabled a summary of the geographic variation of the contribution of each component to the sediments of Tarawa Atoll to be complied (Figure 3.4). Based on the work by Weber and Woodhead (1972) and Ebrahim (1999) the principal contributors are corals, foraminifera, molluscs and *Halimeda*. Over the atoll as a whole the average composition of all clasts is coral (41.0%), foraminifera (27.2%), molluscs (17.9%) and *Halimeda* (9.4%) (Ebrahim, 1999). Corals and foraminifera are predominantly located on the reef rims. *Halimeda* is largely found in the lagoon and is particularly predominant in the SE corner of the lagoon. Molluscs are located in the lagoon and also present in lower quantities on the ocean side. Echinoids are found in the lagoon in very small amounts.

3.4.1 Foraminifera

Foraminifera are single-celled marine animals called protozoans that are major contributors to reef island sediments, in particular large benthic foraminifera from the Family Rotalidae, primarily *Amphistegina*, *Baculogypsina* and *Calcarina*. Factors that the control global distribution of large benthic foraminifera are water temperature, nutrient content, light intensity and hydrodynamic energy. These organisms are generally found between 42^{o}N and 40^{o}S (Belasky, 1996).

Foraminifera are generally abundant in warm areas such as the Indian and Pacific Oceans (Cushman, 1959). Low energy areas are ideal habitats for foraminifera. On the reef flat they are present on hard substrates (epifaunal), seagrass and calcareous algae (epiphytic). In the Pacific, *Amphistegina* is found on reefal and sandy substrates (Hohengeger, 1994). At shallow water depths of less than 30 m, they tend to grow faster, with a generation time of 3 -6 months (Hallock, 1981; Hallock *et al*., 1986b), however, during storms they are either washed ashore or removed offshore into the deep ocean. For example when Hurricane Bebe struck Funafuti, Tuvalu, in 1972, the reef habitat was destroyed and foraminifera became scarce (Collen, 1996). Several years later rapid re-colonisation was observed.

Large benthic foraminifera have been shown to be one of the principal contributors to reef-island sediments on many reef islands and Pacific atolls, including Tarawa Atoll (Ebrahim, 1999), Fongafale, Tuvalu, (Collen and Garton, 2004), Majuro,

Marshall Islands, (Fujita *et al.*, 2009), Makin, Kiribati, (Woodroffe and Morrison, 2001), and Onotoa, Kiribati (Todd, 1961). Compositional analyses of carbonate sediments on Tarawa Atoll reef islands show that large foraminifera are a primary component of the sediment contributing more than 50% (Ebrahim, 1999). Further analysis of the size fractions shows that they contribute 40% (1-0.5 mm) and 27% (2-1 mm) to the sand-sized fractions.

On the ocean-facing shores and the lagoon beaches of Tarawa Atoll, the sand size particles are predominantly foraminifera (Weber and Woodhead, 1972). Modern beach sands from Makin, Kiribati show that foraminifera contribute an even greater percentage (70%) to the medium size sands when compared with Tarawa Atoll (Woodroffe and Morrison, 2001). This may be related to the difference in exposure to high wave energy. Evidence shows that the percentage of observations of wind speeds higher than 1.8 m/s is greater for Butaritari (south of Makin) than Tarawa Atoll for the period 1970 to 1974 and may have influenced the difference in wave energy (Holmes, 1979).

On lagoon and ocean-facing reef flats foraminiferal tests contribute only 27% and 18% to the sediment composition respectively (Ebrahim, 1999) (Figure 3.5). The difference in energy exposure between these environments as well as the distance from the source of foraminifera are suggested to be the driving forces responsible for this low percentage (Weber and Woodhead, 1972; Ebrahim, 1999). As ocean-facing reef flats are exposed to higher energy, most of the tests within the coarse fraction are transported onshore, however in lagoon reef-flat and beach environments that are sheltered from the wind, foraminifera that are deposited are mainly sourced from the ocean reef flats which shows that they can be moved great distances (Ebrahim, 1999). The higher percentage of foraminifera observed on the lagoon reef flat compared to the ocean reef flat led Ebrahim to suggest that lagoon sources of foraminifera are also contributing to the sediment.

The average contribution of foraminiferal tests to different environments in descending order is as follows: land (50%), ocean beaches (37%), lagoon beaches (35%), inter-island channels (30%), lagoon reef flat (27%), ocean reef flat (18%),

lagoon reef flat (27%) and lagoon (10%) (Figure 3.5) (Ebrahim, 1999). The higher percentage of foraminifera on the ocean beaches and reef islands and exposed to predominant easterly winds led Ebrahim to suggest that an onshore movement of foraminiferal test sources from the ocean reef flats to the ocean beaches and land. The high percentage of foraminifera observed on the inter-island channel beaches and the predominant easterly trade winds blowing to the west indicates that foraminifera are transported from the ocean reef flats across to the lagoonside via the channels (Ebrahim, 1999).

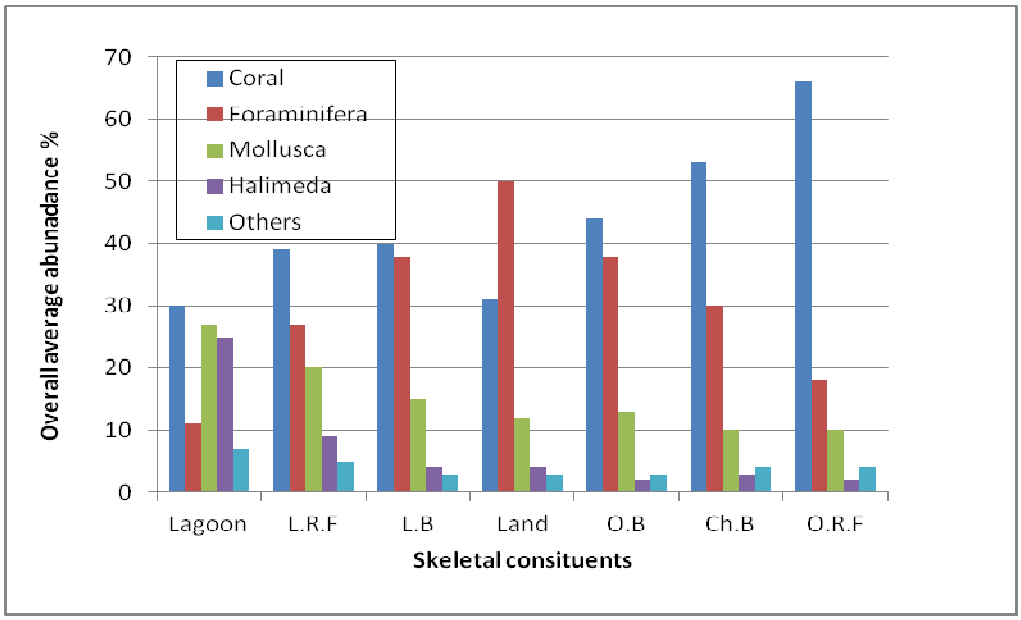

Figure 3.5. Average abundance of various carbonate organisms across the different depositional environments on Tarawa Atoll. L.R.F - Lagoon Reef Flat; LB - Lagoon beach; O.B - Ocean Beach; Ch.B - Channel (inter-island) beach and O.R.F - Ocean Reef Flat (source: Ebrahim, 1999, p. 97).

3.4.2 Corals

Coral skeletons form the framework of reefs. They require certain conditions for growth which include sufficient light, water temperatures ranging from 23 to 30^{o}C and salinity within the range 32-40‰ (Tucker and Wright, 1990). Coral genera that have been identified around Tarawa Atoll include *Acropora*, *Heliopora*, *Pocillopora*, *Favites* and *Porites* (Zann and Bolton, 1985; Lovell, 2000; Donner *et al.*, 2010). In Tarawa Atoll, corals are more abundant in quieter areas and shallow depths where currents are slower but water circulation is present to provide food and oxygen (Lovell, 2000). In the partially enclosed lagoon at Tarawa Atoll, corals do not thrive, and are limited to patch reefs (Lovell, 2000; Donner *et al.*, 2010). On the ocean side,

however, where they are exposed to currents and water circulation, corals are abundant (Lovell, 2000; Donner *et al.*, 2010). Investigation on an ocean site at different depths showed that coral cover increases with depth (Lovell, 2000). Lovell suggests that the drivers for this variation are water depth and wave energy. Other factors such as the influence of sewerage outfall contribute to the variation in coral but at specific sites as observed in the case of Bikenibeu village with the presence of the local sewerage outfall in the vicinity (Lovell, 2000).

Corals can be damaged by changes to environmental conditions such as increased sea surface temperatures as a result of El Niño events. Coral bleaching was initially observed on the atolls of Tarawa and Abaiang during a South Pacific Commission (SPC) Fisheries Assessment course in 2004 (Donner *et al.*, 2010). Investigations to assess the effects of the 2004 El Niño event on the Tarawa and Abaiang corals were carried out in early 2005. The surveys were repeated again in mid 2009 and results showed a significant decrease in live coral to more than 10% in some areas such as Teaoraereke and Naa (Donner *et al.*, 2010). In contrast, some coral species such as *Porites* increased their percentage coral cover up to 18% after the bleaching event, which implies they preferred warmer conditions. The survey showed that only one site located on the ocean side of Bikenibeu out of the three selected sites in Tarawa Atoll recovered from the bleaching event. However, all three sites monitored in Abaiang located on the leeward side of the atoll significantly recovered from the bleaching event as they were less exposed to the influence of humans and wave activity. The bleaching of corals may reduce the ability of the reefs to withstand storms (Donner *et al.*, 2010). In addition, anthropogenic influences such as increased nutrients levels as a result of sewage outfalls can adversely affect the growth of corals (Lovell, 2000). The factors that control the spatial recovery pattern of corals include anthropogenic, hydrodynamic and wave action (Donner *et al.*, 2010).

The broken remains of coral are one of the major contributors to both the unconsolidated sediment on reef islands and the lagoon sediments of Tarawa Atoll. The average contribution of corals to reef islands varies from as low as 15% to as high as 77.5% (Ebrahim, 1999). In Makin, results of sediment composition studies are consistent with those from Tarawa Atoll with corals contributing about 30% of

the reef-island sediment (Woodroffe and Morrison, 2001). On modern beaches in Tarawa Atoll, coral contributes slightly more on average to the ocean beaches (45%) than to the lagoon beaches (40%) (Figure 3.5). The average contribution of corals to ocean and lagoon reef flats is 67% and 38% respectively (Ebrahim, 1999). These differences may be attributed to factors such as exposure to wind or wave energy. For example, in the case of the outer margin of the south eastern corner, the contribution of coral is 60% (Ebrahim, 1999), as it is directly exposed to the easterly trade winds. At this location at 3 m depth, Lovell (2000) found limited coral cover leading him to propose that strong wave action had caused corals from deeper depths to be detached and washed ashore. In North Tarawa, the highest coral concentrations in sediments range from 69.5% to 96% and are found on ocean reef flats (Ebrahim, 1999). These observations show that areas directly exposed to the easterly trade winds and with corals present at shallower depths receive larger amounts of corals compared to those facing away from the wind. The composition of coral shows a progressive decrease in concentration onshore: ocean reef flat (67%), channels (53%), ocean beach (43%), land (32%), lagoon beach (40%), lagoon reef flat (37%) and lagoon (30%).

3.4.3 Molluscs

Tarawa Atoll is home to a wide variety of mollusc species consisting of bivalves and gastropods ranging from 50 to 150 species (Ebrahim, 1999). The habitats of molluscs are wide ranging with bivalves found buried in sediment, while gastropods prefer hard reef substrates. Molluscs are an important source of protein to the local population and are collected at low tides on sand flats. They are becoming scarce and are now often sourced from deeper areas in the lagoon due to the harvesting pressures as a result of population increase on South Tarawa.

Molluscs contribute relatively small volumes of sediment to the depositional areas of Tarawa Atoll (Ebrahim, 1999). They contribute only less than 12% to the average reef islands sediment composition. Their contribution increases significantly in larger sediment fraction, from 2 mm to ≥4 mm. The average contribution of molluscs to the depositional environments of Tarawa Atoll is as follows: lagoon

(28%), lagoon reef flat (21%), lagoon beach (18%), land (12%), ocean beach (13%), channels (10%) and ocean reef flats (10%) (Ebrahim, 1999).

3.4.4 *Halimeda*

Halimeda is a calcareous green alga present in many tropical reef environments. It prefers shallow, sheltered areas and lagoons with water depths less than 15 m (Tucker and Wright, 1990). The alga uses rhizoids to anchor itself to sand and hard substrates such as dead corals (Walters and Smith, 1994). In stressful environments with high temperatures and excessive light, these calcified plants adapt fast by regenerating, and becoming more compacted (Hay, 1981).

This alga is considered to be an important contributor to Pacific lagoon sediments (Weber and Woodhead, 1972; Ebrahim, 1999). The studies by Weber and Woodhead (1972) and Ebrahim (1999) found that the percentage of *Halimeda* is highest in the sheltered south eastern corner of the atoll. The lagoon beach, reef islands, the ocean beach and ocean reef flat have similar proportions of *Halimeda* in their sediment (Ebrahim, 1999). The percentage of *Halimeda* on the lagoon reef flats is four times the value of that found on the ocean side. The decreasing order of abundance on difference environments is as follows: lagoon (25%), lagoon reef flat (8%), lagoon beach (3%), land (3%), channels (2%) ocean beach (2%) and ocean reef flat (2%) (Ebrahim, 1999). The pattern of distribution is similar to that of molluscs but with significantly lower proportions.

3.5 Bruun Rule: Response of shorelines to sea-level rise

There is concern as to how shorelines of reef islands will respond to future sea-level rise. A conceptual model developed by Bruun (1954) has provided a foundation for many contemporary shoreline management applications (Figure 3.6). The model represents how shorelines may respond to rising sea level, proposing that they react by maintaining an equilibrium profile (Bruun, 1962). This concept was initially tested on shorelines in Denmark and California. The concave equilibrium shape of the profile is explained using a parabolic equation outlined in Equation 1:

$h = Ax^{2/3}$……..…..Equation 1

Where h = water depth, x is the horizontal distance between the shoreline and the offshore area; A represents the sediment characteristics and *2/3* is an exponent.

The rule implies that when sea level rises; shorelines maintain equilibrium by retreating uniformly causing the upper part of the profile to be eroded away and the sand deposited on the lower part of the profile (Figure 3.6). This is illustrated in Equation 2:

$R = S\,(L/(B+h)) = (S)\,1/\tan Ø$……..…Equation 2

L is the length of the profile, *Ø* is the profile angle, *B* is berm height and *h* is the closure depth. Simply the equation means that when sea level rises by an amount *S*, the profile will be displaced landward by an amount *R* (Bruun, 1988). In other words, when sea level rises by a certain amount, the shore profile responds by eroding the upper part of the profile, which ends up on the nearshore to maintain equilibrium. Erosion rates differ depending on the slope of the profile. Low gentle sloped profiles will have low erosion rates; whereas steep ones will have high erosion rates.

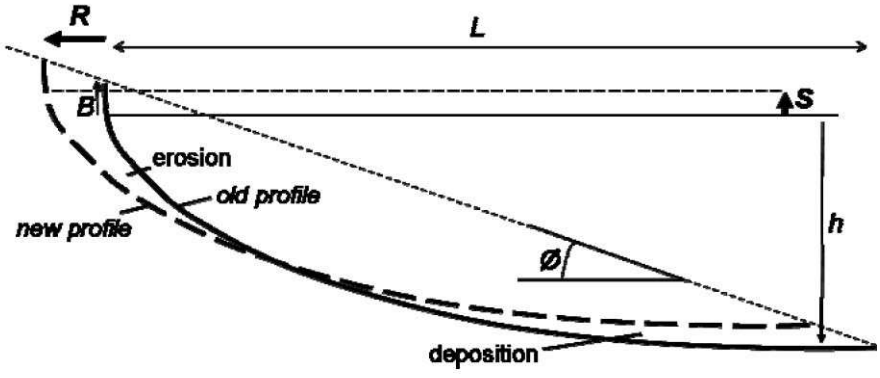

Figure 3.6. Schematic diagram illustrating the Bruun Rule of shoreline erosion (source Abuodha and Woodroffe,(2010).

As with all models, the Bruun Rule is based on several assumptions of which the three principal ones are: (1) the profile is a closed two-dimensional system, between the beach and closure depth, depth beyond which waves do not move sediment (Cooper and Pilkey, 2004); (2) the profile maintains equilibrium over a long-term

under rising sea level conditions; and, (3) it is unaffected by other constraints, for example rock outcrops (Bruun, 1988).

The Bruun Rule has been widely criticised (Cooper and Pilkey, (2004); Komar, 1988). The criticism is that the assumptions are too restrictive, disregarding many important variables that determine the movement of sediment grain. Another point raised is that the Bruun Rule is considered to be inappropriate to all shorefaces. In nature, the nearshore is more complex and can rarely be considered a closed system (Cooper and Pilkey, 2004). In addition, studies have shown that during stormy conditions, new materials get moved onshore or lost offshore beyond the closure depth. For it to be considered as a closed system requires cell boundaries with consideration of sediment transport pathways and sediment budget approaches (Cowell, *et.al.*, 2006). Additionally other variables such as geology and bathymetry have impacts on shoreface responses to sea-level rise which need to be considered as well. Overall, the Bruun Rule does not work in sedimentary environments that are highly complex, where factors such as sediment supply, wave conditions, coastal erosion rates and geology vary (Cooper and Pilkey, 2004).

The Bruun Rule is also considered inappropriate for reef islands of Kiribati. This was indicated by the results of a study carried out in several reef islands of Tarawa Atoll and atolls of Kiribati. The study applied the Common Methodology developed by IPCC which involved the application of the Bruun Rule to assess the coastal vulnerability to sea-level rise. The shore-normal profiles of reef islands generally end abruptly at the point where the sand meets the hard reef-flat surface (Figure 3.7). Under conditions of sea-level rise, beaches on reef islands undergo erosion, but not all the material is lost as some is deposited to build up the beach ridge (Woodroffe and McLean, 1992). However, with rapid sea-level rise and abnormal storm surges, Woodroffe and McLean (1992) propose that the reef islands may be overwashed and severely eroded as the beaches may not have time to equilibrate.

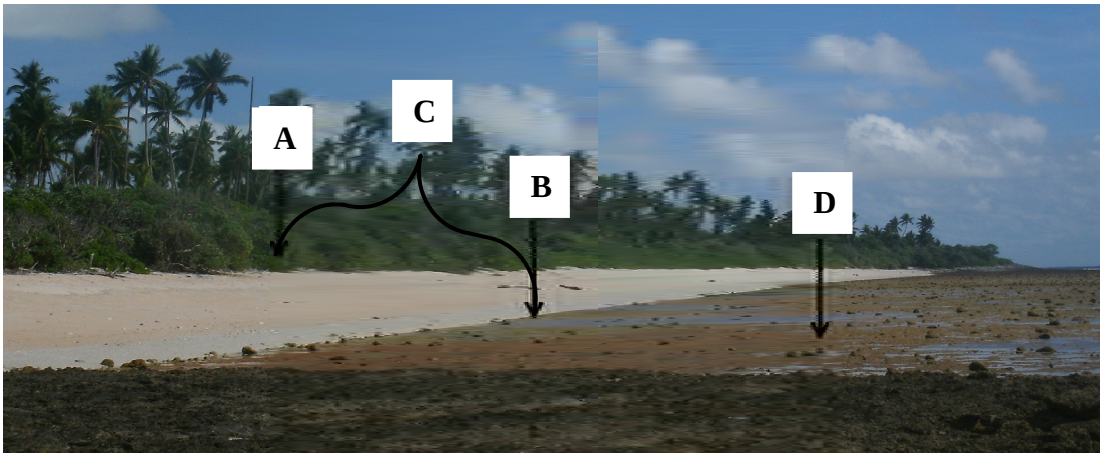

Figure 3.7. Ocean reef flat and beach on Tarawa Atoll demonstrating the in-appropriateness of the Bruun Rule for use on atolls. The upper limit of the beach profile is marked by A. B shows the abrupt break in beach profile due to the contact between the beach and the hard reef surface. C shows the extent of the beach profile which does not continue onto the non-erodible reef flat as marked by D. The non-erodible reef flat on atolls does not allow eroded sand from the beach (A) to be deposited on the lower part of the profile as proposed under the Bruun Rule. Note that hardly any sand is present on the reef flat.

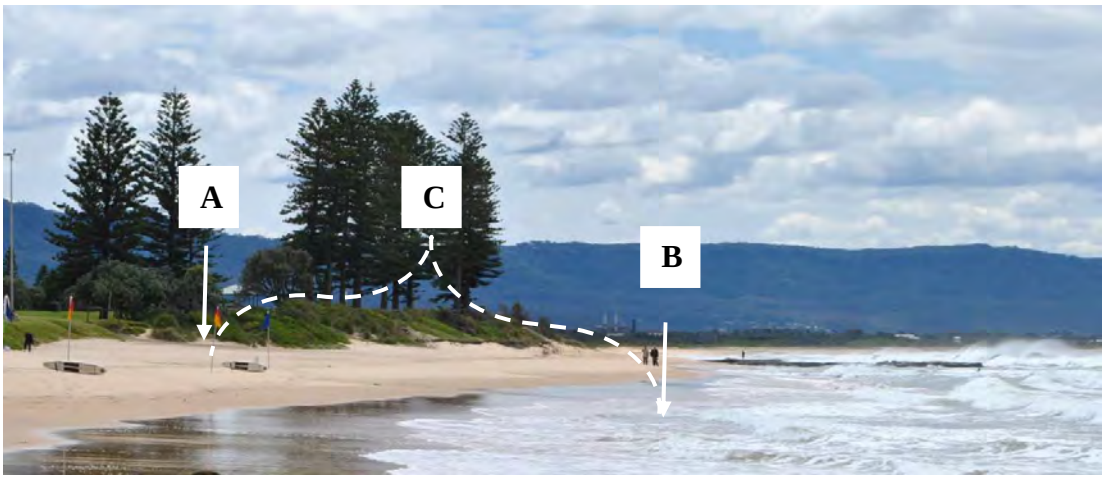

Figure 3.8. A cross-section of North Wollongong beach in Wollongong showing the applicability of Bruun Rule for areas with true continental shelves. The upper limit of the shoreface is marked by A. B shows the lower profile area and nearshore region where sand can be deposited can continue out beyond B up to 30 m which may be a number of kilometres offshore. C indicates the possible extent of the profile where sand can be removed from A under conditions of sea-level rise.

Another study undertaken to assess the vulnerability of Betio to sea-level rise, following the IPCC Common Methodology involved the application of the Bruun Rule. This study also found that it was inappropriate to apply the Bruun Rule as the shoreline has been accreting in response to past sea-level rise (Solomon, 1997). The solid reef flat on reef islands does not allow for the lower beach profile to adjust,

therefore identification of a closure depth is inappropriate or impossible (Woodroffe, 2008) (Figure 3.7). This is in contrast to other areas with a true continental shelf such as those in Denmark and California (Figure 3.8). According to the Bruun Rule, sediments would be displaced and appear on the reef flat, however, this is unlikely as reef flats are generally observed to be "clean" or have only a thin veneer of sediment as waves effectively transport sand from the reef flat onto the beaches (Richmond, 1993; Kench and Brander, 2006). Eroded sediments from the upper part of the profile may be transported longshore or offshore into the ocean (Harper, 1989; Forbes and Hosoi, 1995; Solomon and Forbes, 1999) whilst some may be deposited on the reef island to build up the beach ridge (Woodroffe and McLean, 1992).

3.6 Anthropogenic impacts on coastal areas.

Tarawa Atoll is the capital of Kiribati, with South Tarawa as the centre of government, development, economics and population. South Tarawa has a high population density ranging from 19 to 75 persons per ha (Ministry of Finance, 2007). This is a result from increased migration as people move from Kiribati's rural areas to South Tarawa in search of better opportunities, such as work and education. One of the main consequences of the increasing population is the reduction in land space forcing people to reside on unsuitable land such as low-lying land, or land close to, and on beach berms. Increasing development places more pressure on building materials that are always sourced from beaches. These human-induced activities have brought about changes to the coastal areas.

Anthropogenic impacts on the coastal areas are generally negative rather than positive. These can compound the effects of physical change for reef islands. The concentration of the population and government activities in Betio and Bairiki results in unequal distribution of the population and intensifies the anthropogenic impacts. Densely populated areas are more likely to be vulnerable to impacts of sea-level rise compared to less populated areas. As a result, many studies in the Pacific region have focussed primarily on developed areas where anthropogenic activities have adversely affected the coast. Urban South Tarawa is no exception (Gillie, 1993; Forbes and Hosoi, 1995; Solomon and Forbes, 1999).

Anthropogenic impacts can be classified into internal and external impacts. Although these impacts are classified differently, they have the potential to exacerbate impacts of each other. For example internal activities such as pollution have potential to exacerbate impacts of external activities such as greenhouse gas emissions and accelerated sea level rise to increase vulnerability. These impacts are defined below:

Internal impacts are impacts resulting from human actions carried out within the atoll at a local scale. These activities cause direct damage to the coastal area of Tarawa Atoll.

External impacts are a result of large scale anthropogenic developments outside Kiribati, particularly in developed countries. These impacts are considered to be more threatening although they affect Tarawa Atoll indirectly.

3.6.1 Internal impacts

Internal human-induced changes on atolls, in particular Tarawa Atoll, result from the following activities.

Lagoon and ocean pollution in South Tarawa has resulted from domestic waste dumping and sewage outfalls into both the lagoon and ocean contaminating the seawater. This is further exacerbated where reef islands are connected by causeways such as in South Tarawa as these block ocean water circulation. Reports have shown that Tarawa Atoll lagoon is contaminated with high nutrient levels due to human waste (Kelly, 1994; Loran, 1994; Ebrahim, 2000).

Studies carried out in the Pacific on Fongafale, Tuvalu and Majuro, Marshall Islands show that living foraminifera are becoming scarce around populated areas implying that human activities are adversely affecting their populations (Collen and Garton, 2004; Fujita *et al.*, 2009).

An extensive program carried out by Ebrahim (1999) to determine the distribution of live foraminifera around Tarawa Atoll confirmed that foraminifera were scarce on

South Tarawa's ocean reef flats. This is in agreement with Collen's (1995) earlier findings. Ebrahim (2000) showed that only live but deformed specimens of the foraminifera *Baculogypsina sphaerulata* and *Calcarina spengeleri* were found on the ocean reef flat of Temaiku in the southeastern corner of Tarawa Atoll. In North Tarawa, field observations showed that live foraminifera were only discovered on the ocean-facing reef flats of Nuatabu and Kainaba. The Rose Bengal stain a standard method applied to establish whether foraminifera are alive was performed on all samples collected indicated that only samples from ocean beaches, reef flats and shallow and deep lagoonal areas in North Tarawa appeared alive; however, the test results appeared to be limited as the stain medium also stained other proteins beside protoplasm (Ebrahim, 1999). The scarcity of live foraminifera in disturbed areas as a result of human-induced activities (Collen, 1995; Ebrahim, 1999; Ebrahim, 2000) raises serious concerns, as the reef islands and beaches of Tarawa Atoll need to have continuous sediment supply in order to maintain a state of dynamic equilibrium.

Extraction of aggregate resources is the removal of material from the beach for construction purposes. Beach mining is increasing, as more demand is placed on construction materials to meet the growing development needs. A key finding of a household demand study carried out in South Tarawa by Peletikoti (2007) shows that a large proportion of households (38%), principally located in Bonriki and Temaiku villages, depend on beach mining as their main source of income. This implies that beach mining will continue to be an issue. Within a one year period, 280 households mined approximately 4,700 m^3 of aggregate from local beaches for use as raw construction materials. This is more than the volume of sediment that has taken 20 years to accumulate beside the Nanikai-Teaoraereke Causeway (4,300 m^3) (Forbes and Biribo, 1996). This suggests that the rate of extraction by household beach mining alone far exceeds the rate of sediment accumulation. These beach mining activities appear to have contributed significantly to the increasingly widespread coastal erosion and instability that can be observed around South Tarawa (Forbes and Hosoi, 1995; Solomon, 1997; Webb, 2005). The miners extract the material directly from the beaches into empty rice bags (about 20 kg) and sell them for $2.00 per bag (Peletikoti, 2007; Leney, 2012).

The current aggregate demand for South Tarawa is estimated to be 82, 500 m^3 per year (Geer Consulting Services, 2007) (Table 3.1). This value was obtained by combining (a) household extraction of 70,000 m^3 which was estimated by extrapolating the results of the household survey at South Tarawa, (b) Government requirements of 5,000 m^3 sourced by the Ministry of Public Works and Utility (MPWU) for their maintenance and project needs; (c) imports of overseas aggregates of 5,000 m^3 and (d) finally the commercial sector with a demand of 2,500 m^3(Geer Consulting Services, 2007). Future increases in demand per year from all sources were estimated to be +5% except for imports which will increase by 7% (Geer Consulting Services, 2007). It should be noted there is no complete record of annual aggregate extraction and so most of the values stated here have been estimated, however, these estimates do not include significant fluctuations in demand that occur when major Government aid funded construction projects are implemented, such as the new hospital complex at Bikenibeu constructed in 1992 and 1993 which significantly raised demand for aggregate (Biribo and Smith, 1994).

Table 3.1. Current and future estimates of aggregate for South Tarawa (source: Geer Consulting Services, 2007).

Source of aggregate	Current demand (m^3)	Future increase per year	Source
Household extraction	70,000	+ 5%	Peletikoti, 2007
MPWU maintenance/projects	5,000	+ 5%	Geer (consultant) estimate, 2007
Importation	5,000	+ 7%	Geer (consultant) estimate, 2007
Commercial sector	2,500	+ 5%	Geer (consultant) estimate, 2007
Total	82,500		

Concerns are raised about the sustainability of coastal areas around South Tarawa due to the low rate of sediment replenishment and the escalating demand on coastal resources. To address this issue, a bilateral (European Union and Kiribati Government) project known as the Environmentally Safe Aggregate Tarawa (ESAT) managed by SOPAC with a budget of 3.2 million Euros recently established a state owned enterprise (SOE) The Atinimarawa Company Ltd (ACL) to provide an alternative mining area that would supply cheap aggregate sourced offshore in Tarawa Atoll's lagoon encouraging people to stop mining from beaches at the household level (project here) (Kiribati Government and South Pacific Applied Geoscience Commission, 2008; Leney, 2012). This resource site known as the

Vinstra Shoal in the lagoon located close to Betio was identified during a joint exercise in 1994 between SOPAC and the Government of Kiribati collecting 10 km of high resolution seismic data and 70 km of bathymetric data (Smith and Biribo, 1995). During the same exercise, the extent of the resource site was determined (Figure 3.9). The sediment characteristics such as composition, distribution and grain size were determined from 29 jet probe holes taken within the resource area. Based on the jet probe information, the resource site comprises about 76% of sand gravel, 17% of gravel and 7% of gravelly sand based on the Folk grain size classification (Folk, 1968). The volume of the resource was estimated to be approximately 5.2 million m^3 (Smith and Biribo, 1995). The ESAT managed by SOPAC with a staff present within the Mineral Unit of the Kiribati Government proposes to allow those currently selling beach aggregate to become retailers for the company in order to maintain their source of income (Leney, 2012). A Community Participation Programme (CPP) developed in 2011 and is currently implemented by Foundations of the Peoples of the South Pacific (FSPK) and ThEcoCare (TEC) aimed at increasing the awareness of the community by engaging them in understanding the projects objective (Leney, 2012). The overall aim of the ESAT is to reduce the direct mining effects on beaches by focussing mining in one area, the Vinstra Shoal thus reducing coastal vulnerability and possibly allowing the beaches to regenerate (Kiribati Government and South Pacific Applied Geoscience Commission, 2008).

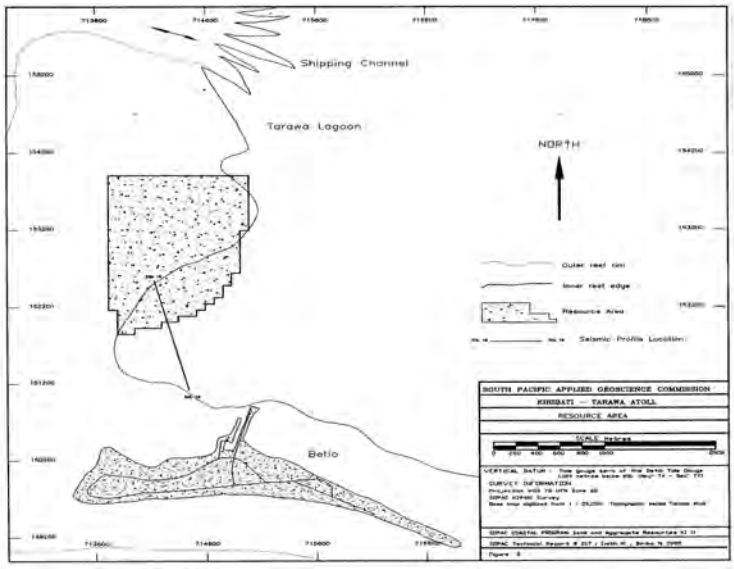

Figure 3.9. Map of Betio showing the location of the resource area Vinstra Shoal lying further north of Betio reef island (source: Smith and Biribo, 1995 p. 25).

Coastal structures are man-made structures extending onto the active beach that are built for various reasons ranging from protection purposes and creation of better tidal access channels, to the expansion of habitable land to accommodate the growing population (Figure 3.15). Coastal structures include boat channels, groynes, reclamations, seawalls, jetties and causeways. These permanent or temporary structures are rarely maintained well due to limited resources (Kench, 2005). This is a common issue for other South Pacific countries (Byrne *et al.*, 1994).

Studies carried out on South Tarawa show that the impacts of these artificial coastal structures are wide ranging. For example, groynes and other coastal structures can block longshore sediment transport causing erosion on the down-drift side of the structure (Harper, 1989; Gillie, 1994; Forbes and Hosoi, 1995; Webb, 2005). Solid causeways obstruct water exchange between the ocean and lagoon areas and enhance the longshore sediment transport along the coast (Zann, 1982; Harper, 1989). The vertical design of coastal seawalls and reclamations reflects wave energy causing scouring at the foot of the structure and forcing sediment on the beach offshore. Excavations of the reef flat commencing at the foot of the beach and extending to the edge of the reef flat also disrupt longshore sediment. These channels create a passage for the displacement of sediments from beaches to offshore areas (Kench, 2005).

Figure 3.10. Aerial photo and satellite image from Google Earth showing how densely populated A: Betio and B: Bikenibeu village in Bonriki-Taborio are (source: 2011 Google Earth image GEBCO Image © 2011 DigitalGlobe).

3.6.2 External impacts

Climate change and its range of projected impacts, such as sea-level rise and increased sea surface temperatures in coastal areas, are very likely to be human induced (IPCC, 2007). Industrial and agricultural developments have substantially increased global atmospheric concentrations of gases such as carbon dioxide, methane and nitrous oxide. These significant increases have already adversely affected the climate system causing global warming. The vulnerability of coastal areas, especially of low-lying atolls such as Tarawa Atoll, is very likely to increase as a result of impacts of climate change and sea-level rise (Nicholls *et al.*, 2007) (see Section 2.8 for a more detailed discussion).

3.7 Geographical Information Systems Data

The availability of recently acquired aerial photography, satellite imagery, and digital terrain data enables a considerably more sophisticated analysis than was possible using the previous Overseas Departmental Agency (ODA) maps based on the 1968 aerial photographs. The dataset utilised in the following sections was acquired by Schlencker Mapping Pty Ltd. This study also uses this data in combination with Geographic Information Systems (GIS) to develop the Digital Elevation Model and determine sediment volume (Chapter 4) and shoreline changes (Chapter 6) for each individual reef island.

In 1998, Kiribati Lands Division commissioned Schlencker Mapping Pty Ltd to carry out mapping of Tarawa Atoll, and to transform the Tarawa Local Grid system to the WGS84 datum. This procedure was carried out using differential GPS, whereby benchmarks throughout Tarawa Atoll were related to the Betio Trigonometric Station using a photo control point at Otintaai Hotel, Bikenibeu, and a known control point, KWJ1, on Kwajalein Atoll, Marshall Islands (Schlencker Mapping Pty Ltd, 1998).

A set of 45 aerial photographs was acquired by Schlencker Mapping in 1998 and has been used in this study. The established WGS84 datum on the Betio Trig station allowed the photographs to be vertically tied to the University of Hawaii tide gauge datum in Betio, Tarawa Atoll; allowing land heights to be related to M.S.L (see

Section 2.7.4). The data set has a scale of 1:2,500, colour imagery and associated GIS vector files such as spot heights and one metre spacing contours, making it a highly valuable dataset.

In 2009, the Kiribati Adaptation Project (KAP) commissioned Schlencker Mapping Pty Ltd to produce, from the same data, contours with 0.1 m vertical spacing in order to determine the potential risk of inundation for low-lying areas of South Tarawa and its villages (Elrick and Kay, 2009). The availability of these photographs and data enables investigations into sediment volume and the determination of areas likely to be inundated due to a rise in sea level. This is completed in Chapter 4. In addition, this dataset also permits analysis of shoreline changes by comparing this aerial photography with images acquired at other dates (see Chapter 6).

The base map (1998 aerial photograph) provided by Schlencker was geo-referenced to the Tarawa Local Grid (Table 3.2). To transform this image to Universe Transverse Mercator (UTM) Zone 59N and to correct for a 400 m offset all images and associated vector files had to be transformed, redefining their new coordinate system to the new Tarawa Local Grid. After this transformation was complete, all files were re-projected to UTM59N.

The shoreline for each individual reef island was digitised from the 1998 aerial photograph. For the purpose of this chapter, the shoreline used is the base of the beach (BB) and has been mapped as a polygon in GIS to show the area of each individual reef island. The base of the beach is defined as the point where the beach meets the ocean reef flat (see point B in Figure 3.7). The selection of other shorelines used will be discussed in further detail in Chapter 6. The landward extent of mangroves and the seaward extent of artificial structures are included in this shoreline, which forms the basis of analysis later in this thesis (Chapter 6). The polygon obtained for each individual reef island enabled their areas to be calculated.

The population of each individual reef island was sourced from the Kiribati census conducted in 2007. The population density was calculated using these population

data and the reef island areas obtained as described above. Using these results, a distribution map was developed.

Table 3.2. Characteristics of the 1998 aerial photograph

Image	1998 Aerial photo (new projection)
Spatial Reference	Transverse Mercator
Linear Unit (meter)	Meter (1.00000)
Angular Unit	Degree (0.017453292519943299)
False Easting	40000
False Northing	0
Central Meridian	173.033300
Scale Factor	1
Longitude of Origin	0
Datum	D_WGS_84

Field surveying was conducted which involved ground-truthing a range of aspects of reef-island morphology, sediment composition and slopes of various beaches around the atoll. The slopes of the beaches were measured using a clinometer placed in the middle portion of the beach.

3.8 Results

3.8.1 Number and physical features of Tarawa Atoll reef islands.

Tarawa Atoll has 59 reef islands present on the atoll (Figure 3.11). Each of these reef islands has been assigned an individual identification number, but local names have been utilised for the bigger reef islands, for example, Buariki (Table 3.3). Lying on the north-eastern arm of the atoll, the North Tarawa section has 51 reef islands starting from Buariki in the north, to the small islet (51) close to Tanaea in the southeast corner. The central part of North Tarawa has predominantly small reef islands (Figure 3.11see insert). This region also has three sand cays located lagoonward of the inter-island channels, Bikenamori, Biketawa and Bikenubati sheltered from the direct exposure of the winds. On the southern arm of the atoll, South Tarawa has 8 reef islands in total, commencing from Bonriki-Taborio in the south-eastern corner extending to Betio in the far west.

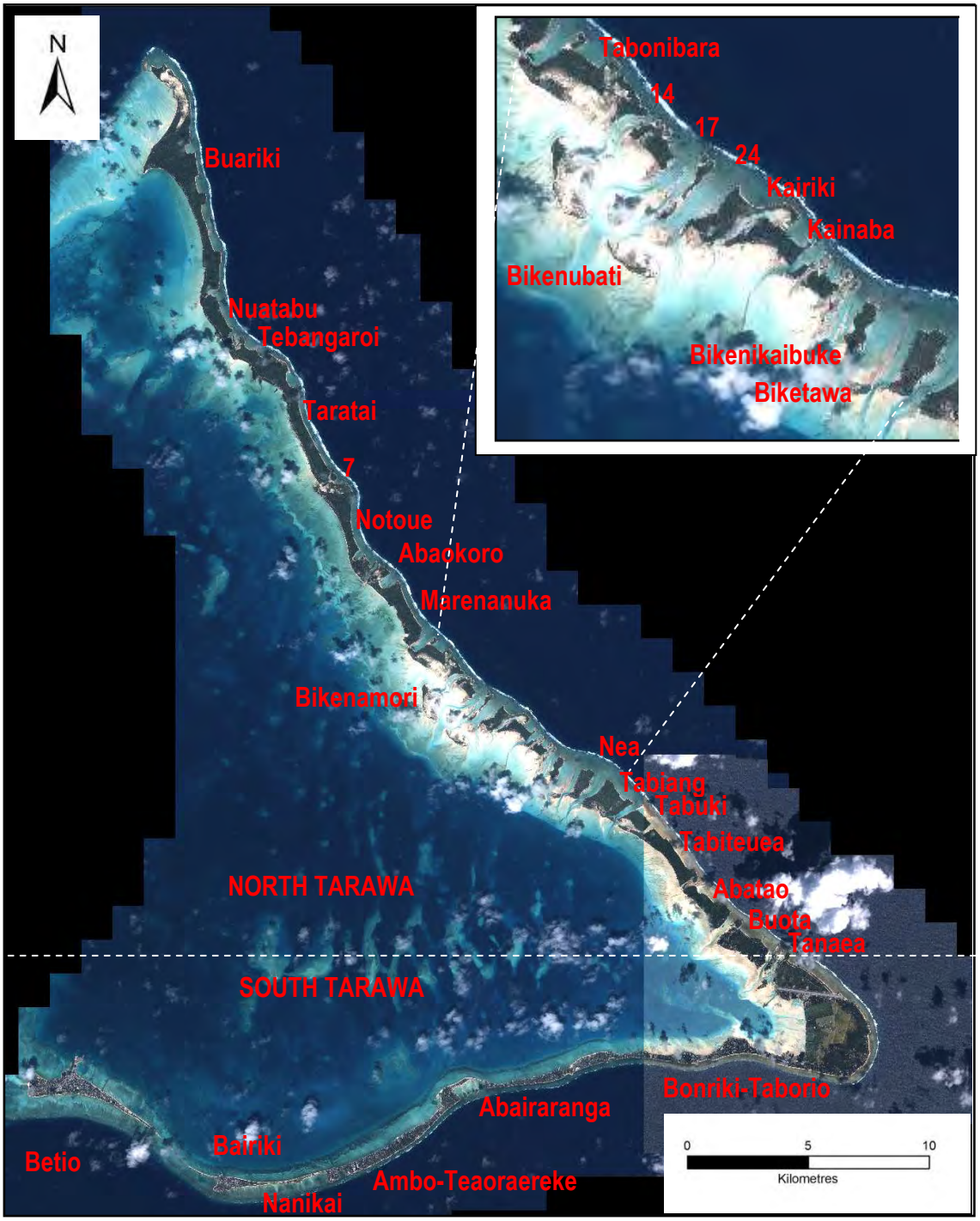

Figure 3.11. An IKONOS satellite image of Tarawa Atoll showing the study area. Insert shows the reef islands lying in the central portion of North Tarawa.

The physical characteristics of Tarawa Atoll reef islands vary (Table 3.3). The length of the reef islands ranges from 17.8 m (40) to 12,524.0 m (Bonriki-Taborio) with an average length of 1,214.5 m. The length of Bonriki-Taborio is measured from the far south eastern corner to the far western end of the reef island. The width of the reef islands ranges from 14.1 m (40) to 2,047.5 m (Bonriki-Taborio) with an average width of 343.2 m. The area of the reef islands ranges from 0.02 ha (40) to 863.19 ha (Bonriki-Taborio) with a mean area of 486 ha. The results show that these reef islands are typically small.

Table 3.3. Physical and social characteristics of Tarawa Atoll reef islands

ID	Name	North/South	Length (m)	Width (m)	1998 Area (ha)	Population	Population density (persons/ha)
1	Buariki	N	7534.00	1722.87	390.36	1000	3
2	Nuatabu	N	1562.8	545.1	67.04	197	3
3		N	244.3	78.8	1.54	0	0
4		N	34.3	26.5	0.10	0	0
5	Tebangaroi	N	1259.3	731.5	70.87	40	1
6	Taratai	N	3928.1	735.0	177.62	151	1
7		N	226.4	227.0	4.71	0	0
8	Notoue	N	2419.3	872.8	119.96	814	7
9	Abaokoro	N	491.3	497.2	32.64	262	8
10		N	399.8	326.7	8.90	0	0
11	Marenanuka	N	2156.4	686.7	103.07	101	1
12	Tabonibara	N	857.1	324.4	44.00	363	8
13		N	96.8	128.3	2.30	0	0
14		N	652.3	485.6	14.90	0	0
15		N	53.7	54.2	0.20	0	0
16		N	61.2	56.7	0.3	0	0
17		N	575.0	293.6	17.4	0	0
18		N	63.2	53.3	0.50	0	0
19	Bikenamori	N	1402.0	182.6	10.3	0	0
20		N	161.2	30.3	0.30	0	0
21		N	57.6	26.6	0.1	0	0
22		N	32.8	21.8	0.04	0	0
23		N	96.8	84.2	1.02	0	0
24		N	689.2	156.2	5.36	0	0
25		N	351.7	127.5	1.94	0	0
26	Bikenikaibuke	N	955.6	108.2	6.60	0	0
27	Kairiki	N	1588.0	370.7	35.24	0	0
28	Kainaba	N	1188.9	378.7	28.53	266	9
29		N	436.8	184.8	3.44	0	0
30		N	79.9	28.9	0.17	0	0
31		N	89.2	44.2	0.31	0	0
32		N	111.5	37.1	0.38	0	0
33	Bikenubati	N	553.2	277.8	11.35	0	0

Table 3.4 cont. Physical and social characteristics of Tarawa Atoll reef islands

ID	Name	North/South	Length (m)	Width (m)	1998 Area (ha)	Population	Population density (persons/ha)
34		N	120.1	57.3	0.60	0	0
35		N	65.9	43.9	0.22	0	0
36		N	163.2	37.5	0.40	0	0
37		N	66.9	42.6	0.17	0	0
38		N	320.1	104.9	1.73	0	0
39		N	185.9	38.4	0.73	0	0
40		N	17.8	14.1	0.02	0	0
41	Nea	N	685.3	273.2	14.27	0	0
42	Biketawa	N	410.5	173.7	6.28	0	0
43	Nabeina	N	1106.4	430.7	36.25	435	12
44	Tabiang	N	1593.4	1061.8	85.26	0	0
45	Tabuki	N	712.0	439.2	31.24	0	0
46	Tabiteuea	N	2972.2	634.9	104.49	505	5
47	Abatao	N	1568.7	875.1	80.19	499	6
48	Naninimai	N	230.9	222.6	4.65	0	0
49	Buota	N	1474.7	658.9	88.18	1469	17
50	Tanaea	N	733.7	194.6	8.22	279	34
51		N	86.0	55.7	0.33	0	0
52	Bonriki-Taborio	S	12524.0	2047.5	863.19	20209	23
53	Abairaranga	S	137.2	130.3	1.28	0	0
54	Tebwe	S	177.5	58.3	0.64	0	0
55	Abaokoro-South	S	263.7	174.7	2.99	0	0
56	Ambo-Teaoraereke	S	5154.1	622.2	181.44	9427	52
57	Nanikai	S	1663.3	216.6	15.32	988	64
58	Bairiki	S	3685.0	538.5	59.22	3524	60
59	Betio	S	5127.1	1193.8	166.76	15755	94
	Average		**1214.5**	**343.2**	**486.00**		
	Total				**2,915.54**	**56,284**	

3.8.2 Ocean beach geomorphology

Ocean and lagoon beaches across Tarawa Atoll generally vary in response to factors such as exposure to direct trade winds, sediment composition and human activities. Exposed to wind and high energy waves, ocean beaches are generally steeper than lagoon beaches (Figure 3.12). Beach slopes lower than 12° were considered low whilst slopes above that were considered high. Measured beach angle slopes ranged from 8° to as high as 16° (Table 3.5).

3.8.3 Lagoon beach geomorphology

Located on the leeward side of the atoll, lagoon beaches are generally sheltered making them depositional areas (Figure 3.12). The beaches typically have gentle slopes ranging from 4° to 11° (Table 3.5). Generally sediment composition is finer and less sorted than that of

Figure 3.12. Study beaches showing the variation of beach slopes across ocean and lagoon including North and South. A and B: Notoue, North Tarawa, C and D: Tabiteuea, North Tarawa, E and F: Bairiki, South Tarawa and G and H: Betio, South Tarawa.

ocean beaches (Figure 3.13 B, D and F). These sheltered environments provide a good habitat for burrowing animals and organisms.

Table 3.5. Beach angle measurements of modern ocean and lagoon sites from several reef islands across the atoll.

Reef island	Modern beach Location		Angle	
	Ocean	Lagoon	Ocean	Lagoon
Notoue	N01.52169, E173.00187	N01.52159, E173.00177	9°	11°
Abaokoro	N01.29.156, E173.01611	N01.29.806, E173.00893	8°	6°
Tabiteuea	N01.25498, E173.06200	N01.25.317, E173.05951	11	5°
Taratai	N01.33052, E172.59652	N01.32968, E172.59697	10°	6°
Bonriki-Taborio	N01.36269, E173.12039	N01.36280, E173.12050	11°	6°
Bonriki-Taborio	N01.36315, E173.12012	N01.36410, E173.12052	16°	5°
Ambo-Teaoraereke	N01.19961, E173.00864	N01.20125, E173.00807	15°	5°
Bairiki	N01.32856, E172.98227	N01.20.034, E172.05797	11°	5°
Bairiki	N01.32846, E172.98247	N01.20.125, E172.00807	10°	4°

3.8.4 Ocean beach sediment composition

Sediments on ocean beaches are generally well sorted medium sand to gravel (Figures 3.13 A, C and E). In descending order of abundance are coral fragments, foraminifera and molluscs. North Tarawa samples show that foraminifera sediment grains appear lustrous and are generally intact with spines present on *Baculogypsina* and *Calcarina* (Figure 3.13 A and C) implying that they have not travelled very far from their source. Coral fragments on the other hand appear more rounded, as the corals may have undergone more abrasion due to their larger size.

3.8.5 Lagoon beach sediment composition

Sediments from several lagoon beaches across Tarawa Atoll show that foraminifera are present in all depositional environments investigated, and thus play a significant role in the maintenance of these beaches (Figure 3.13 B, D and E). The sediment samples collected from the lagoon beaches are mainly well sorted medium sand to gravel and generally appear abraded implying that these materials are far from their source or have undergone bioturbation (Figures 3.13 B and F). Causeways on South Tarawa closing the inter-island channels may have prevented fresh material from reaching the lagoon side therefore the lagoonal material becomes more abraded travelling long distances as it is transported by predominant longshore sediment transport along the shorelines of South Tarawa. In Buota lagoon channel adjacent to Tanaea, high bioturbation in the area may have abraded a large proportion of the

samples; however, on Notoue lagoon beach, samples appeared to retain their spines, implying that these samples have not moved very far from their origin (Figure 3.13 D). It is anticipated that samples obtained from Buota lagoon channel will be similar to that of Teaoraereke lagoon beach (Figure 3.13 F) as the inter-island channel on both ends of the reef island is closed, preventing ocean-reef sources of foraminifera to be transported across.

3.8.6 Population distribution

Tarawa Atoll has a population of 56,284, accounting for more than half of Kiribati's population of 103,058 (Statistics, 2010). Only 19 of the 59 reef islands are inhabited; this includes all the elongated reef islands as they are larger and therefore provide more space (Table 3.3; Figure 3.14Figure 3.14). The reef islands that are uninhabited are mainly located in the central part of North Tarawa. They are not occupied primarily because they are too small or they are situated close to the reef edge. The distribution of population across the two sections of Tarawa Atoll is unequal, with higher population density in the southern section than that of the northern section. North Tarawa people live on the sheltered, lagoon-facing side of the reef islands away from the trade winds, as is normal for people in Kiribati.

In contrast, people on the southern arm tend to occupy both sides of the reef islands as they are not directly exposed to the northeasterly trade winds. In South Tarawa, population density increases towards the west. Three reef islands, Betio, Bairiki and Nanikai, have population densities ≥60 persons per hectare (Table 3.3, Figure 3.14). These reef islands are the main administration centres for Tarawa Atoll. People who reside on these reef islands live on the remaining land on that is not occupied by Government Infrastructure. Reef islands with population densities <60 but >10 persons per hectare in descending order are as follows Ambo-Teaoraereke (52) and Bonriki-Taborio (23), (Table 3.3, Figure 3.14). In North Tarawa, reef islands with high population densities of ≥5 persons per hectare are Tanaea (34) Buota (17), Nabeina (12), Kainaba (9), Tabonibara (8) Abaokoro (8), Notoue (7) and Abatao (6) (Table 3.3).

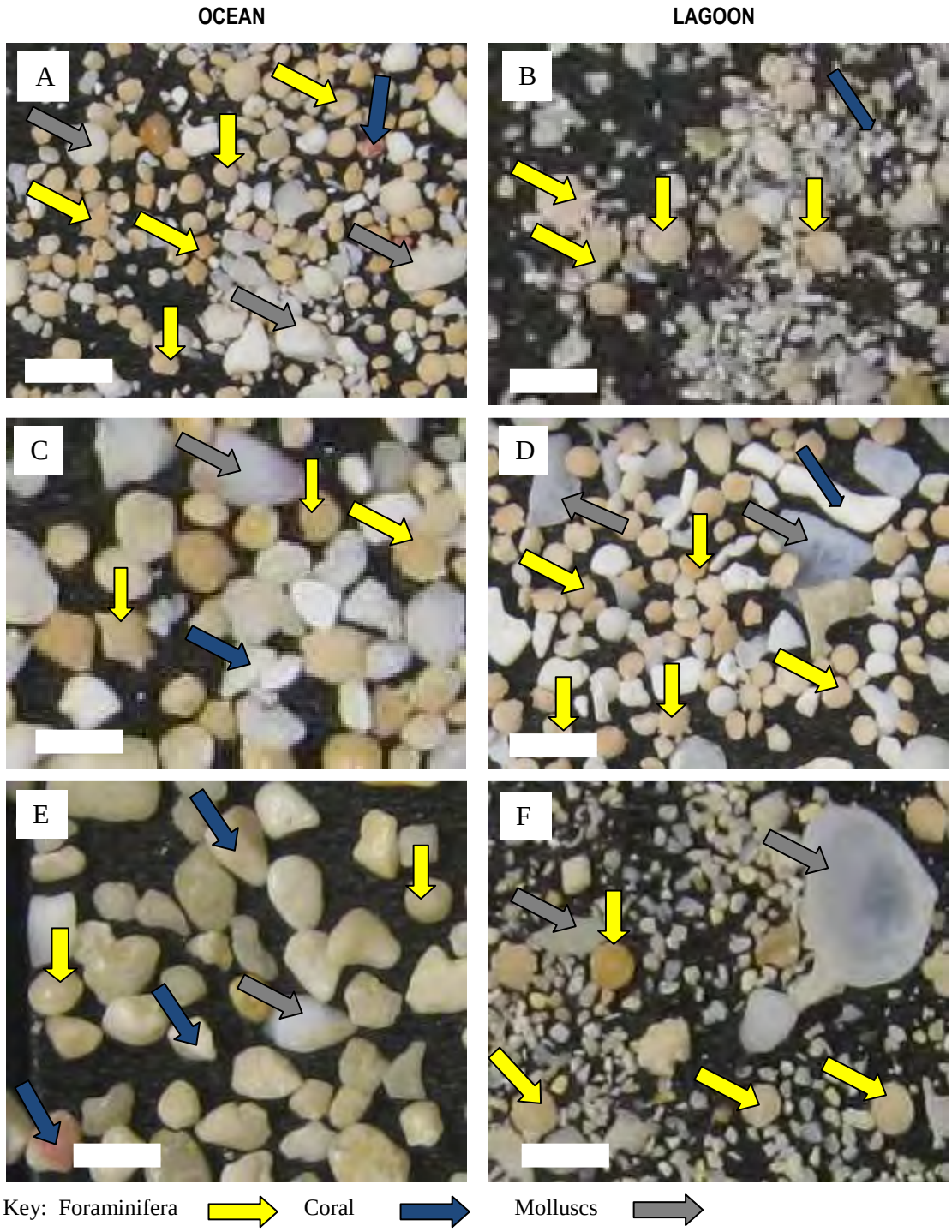

Figure 3.13. Sediment composition of selected ocean and lagoon beach locations. A: Tabiteuea ocean, B: Buota lagoon channel, C: Notoue ocean, D: Notoue lagoon, E: Teaoraereke ocean and F: Teaoraereke lagoon. Note that foraminifera are abundant and present in all photos indicating their importance to reef island sediment composition. Corals are next in abundance whilst molluscs are of minority proportion.

Some of these places are close to South Tarawa (Buota and Abatao), where access is available by causeways, bridges, or even by canoes. Abaokoro is the administration

centre of North Tarawa hosting the hospital, government and secondary schools. Reef islands located in North Tarawa with population densities <5 persons per hectare are Tabiteuea (5), Nuatabu (3), Buariki (3), Marenanuka (1), Taratai (1) and Tebangaroi (1) (Table 3.3, Figure 3.14). The smaller reef islands located in the central part of North Tarawa are uninhabited.

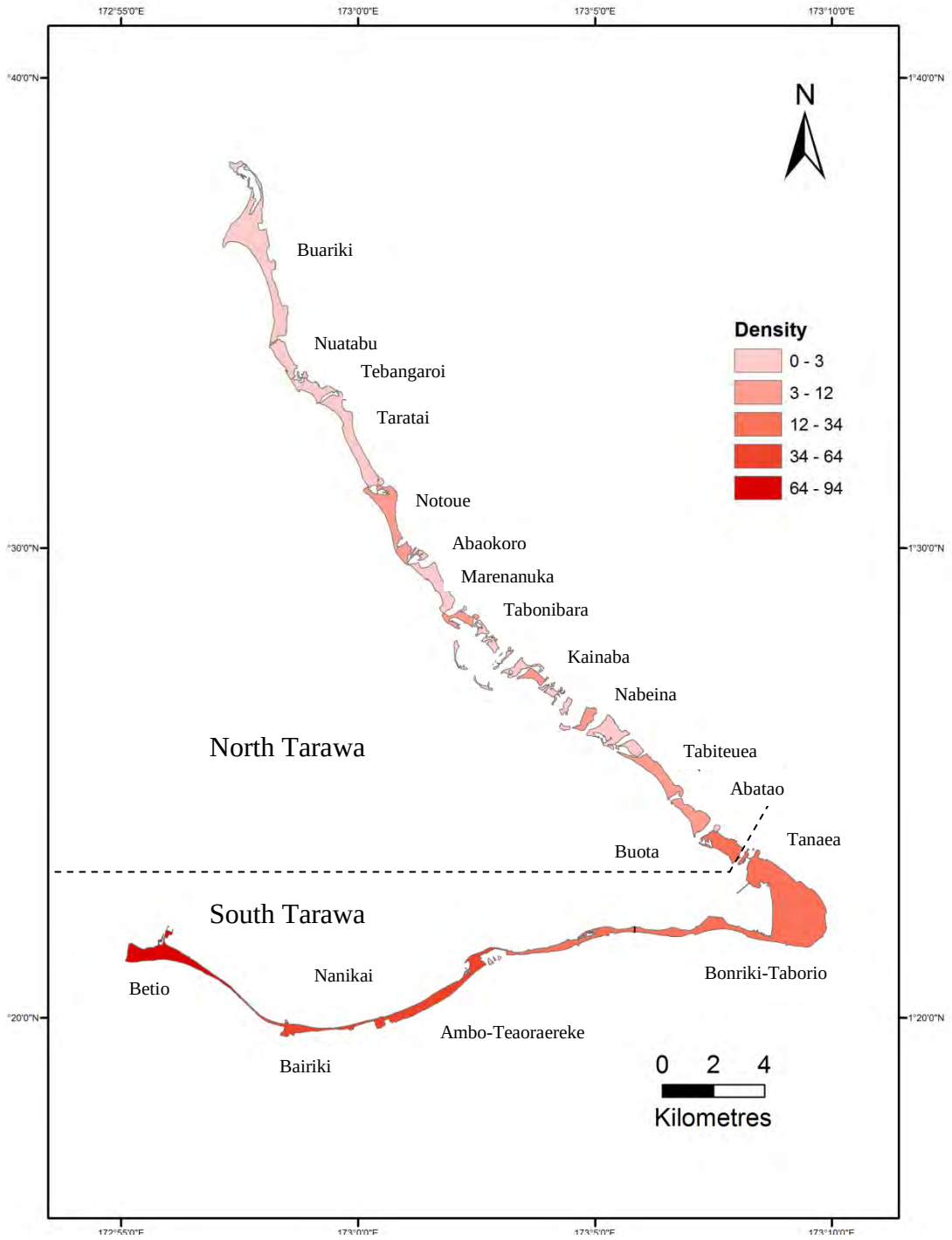

Figure 3.14. Population density (persons per ha) distribution across reef islands of Tarawa Atoll. Distribution of population is unequal with a greater population density in South Tarawa.

New residents to North Tarawa are mainly retired Government workers who do not wish to return to the outer reef islands. In the case of Tabiteuea, many residents are people who are still working but prefer to live in a rural setting and commute to work on Bairiki, Betio or Bonriki-Taborio by sea. This suggests that there is internal migration from South Tarawa to North Tarawa due to issues of living space.

Population increase has led to issues of overcrowding. This has forced people residing in Betio, Bairiki, Nanikai and Bonriki-Taborio reef islands to live in vulnerable areas such as on dynamic sand spits, active beach berms and in low lying areas. In North Tarawa, with low population densities, space is not an issue so people do not reside on newly accreted areas as the locals understand that they are dynamic. Locals tend to develop these areas by planting coconut trees to stablise the mobile sand.

Space becomes a serious issue in South Tarawa with the growing population, as more local residents encroach onto the dynamic beach. As assets are placed close to the active beach berm, the risk from high tides and storm events increases, and eventually leads to the construction of a coastal structure. These structures serve two purposes: the first is to protect the assets at risk, and the second is to reclaim more land to address the space pressure. Individuals and religious groups have constructed reclamations of varying sizes, shapes and designs around South Tarawa. These developments make the shorelines appear abnormally straight with 90^{o} corners when viewed on aerial photos (Figure 3.10B).

In order to build a coastal structure, approval from the Lands and Foreshore Committee (LFC) responsible for these areas is required. In addition, approval also needs to be obtained from the Environment Division in line with the recent Environment Act. However, as was noted in an inventory survey carried out by the Lands Management Division in 2000, this is not normally done. Many seawalls and reclamations have been erected without prior approval from the LFC.

The LFC generally approves seawall applications of I-Kiribati people wishing to construct a seawall for the purpose of protecting assets; however, the committee does

not usually approve reclamations as they are extensions of land, and disrupt longshore sediment transport. Therefore when most applications for seawalls are approved, they are built as reclamations (Figure 3.15 B). Examples of approved reclamation applications are those built in front of mangroves on the lagoon side as these appear to have a minimal detrimental impact on the sediment transport (Figure 3.15G). Most of these structures lack engineering design and are generally vertical. A large proportion of these structures are temporary as shown in Figure 3.15 (A, C, D, E, F, G and H). These structures are frequently built from logs, coral boulders, and cement bricks backfilled with rubbish, sand or a mixture of both. Others appear more permanent with cement added to bind the structure.

Figure 3.15 illustrates the various types of seawall designs that are present throughout South Tarawa. A significant proportion of these coastal structures depend on construction material sourced locally from the surrounding reefs and beaches such as coral rocks, conglomerate, gravel and sand. This contributes to the removal of material from beaches (see Section 3.6.1). Most of these developments are owned by individuals, whilst some are public structures created by religious groups, schools or the Government. Engineer designed structures such as jetties, ports and causeways are Government assets.

3.9 Discussion

An understanding of the current physical and social situation on reef islands is important in order to recognise how they may respond to anticipated sea-level rise. Information regarding the sediment composition and the natural processes that transport sediment around the reef islands, as well as the physical conditions of coastal areas and changes to these areas by humans, provides a better understanding of the perceived morphological responses under conditions of anticipated sea level rise. In this discussion, the current physical conditions, the population density and their impacts will be discussed and compared with examples from other Pacific reef islands. The population density will be compared with those highly populated places such as Hong Kong and Singapore.

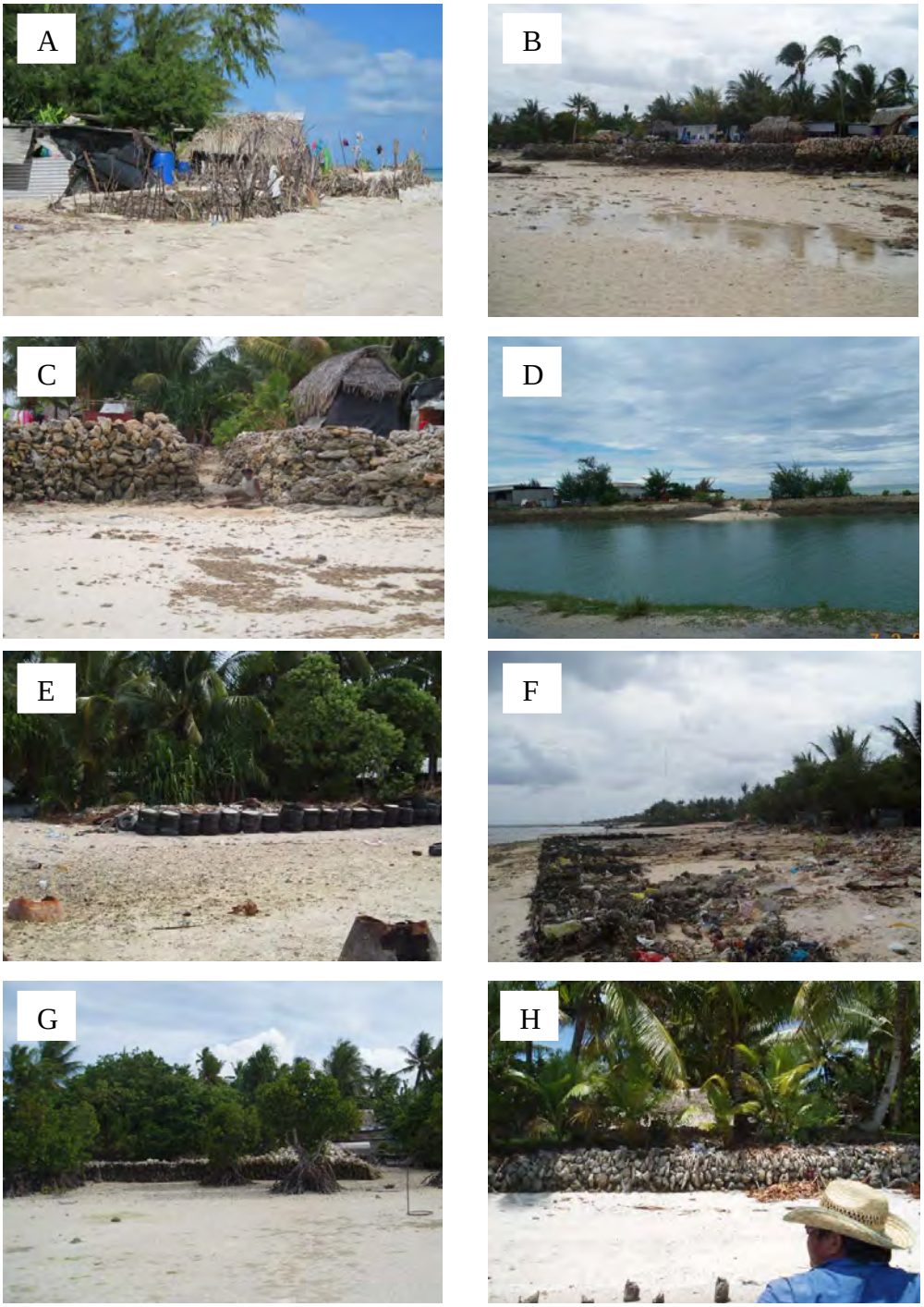

Figure 3.15. The typical vertical seawalls found along Tarawa shorelines. Note that seawalls A – C and E - G are located at a distance from the shoreline to serve two purposes: to; reclaim land and to protect the land. A: loose logs placed vertically, B: coral rocks vertically stacked and cemented to strengthen the structure, and C: loosely stacked coral rocks and boulders, D: a Government owned sand bag seawall, E: private seawall made out of drums filled with cemented sand, F: a failed Government owned seawall made out of gabion baskets filled with loose sharp coral rocks, G: local reclamation in a mangrove area, and H: a typical outer island design of a vertical seawall interlocked to provide a sturdy structure. Note that there are two owners to the seawall shown in C as seen by the gaps in the wall, which may lead to erosion issues. Also note the difference between structures that are placed close to the land to protect the affected area (H) and those that are used to reclaim land (A, B, C, D, E and G).

The reef islands of Tarawa Atoll are dependent on biogenic carbonate organisms mainly foraminifera for their composition. The reef islands also possess physical characteristics that make them susceptible to sea-level changes. Most of these reef islands are located on the windward side of the atoll and are directly exposed to the influence of trade winds as also is the case in other atolls within the Gilbert Islands (Richmond, 1992), in Marshall Islands (MacNeil, 1972), the Caroline Islands, the Tuamotu Archipelago and many other central Pacific atolls (Wiens, 1962; Richmond, 1992). Reef islands of Tarawa Atoll are characteristically small and complex (Table 3.3). The longest reef island, Bonriki-Taborio, is not a typical elongated reef island as it appears to be joined with two other elongated reef islands. Evidence from historical aerial photos suggest the existence of a channel in the villages of Bikenibeu and Abarao, which are on this reef island (Byrne, 1991). In Bikenibeu, the channel is assumed by Byrne to lie on the western side of Bikenibeu village, however, a 1945 aerial photograph shows signs of a channel infilling from the ocean side, further eastward (Figure 3.16) (Biribo, 2008).

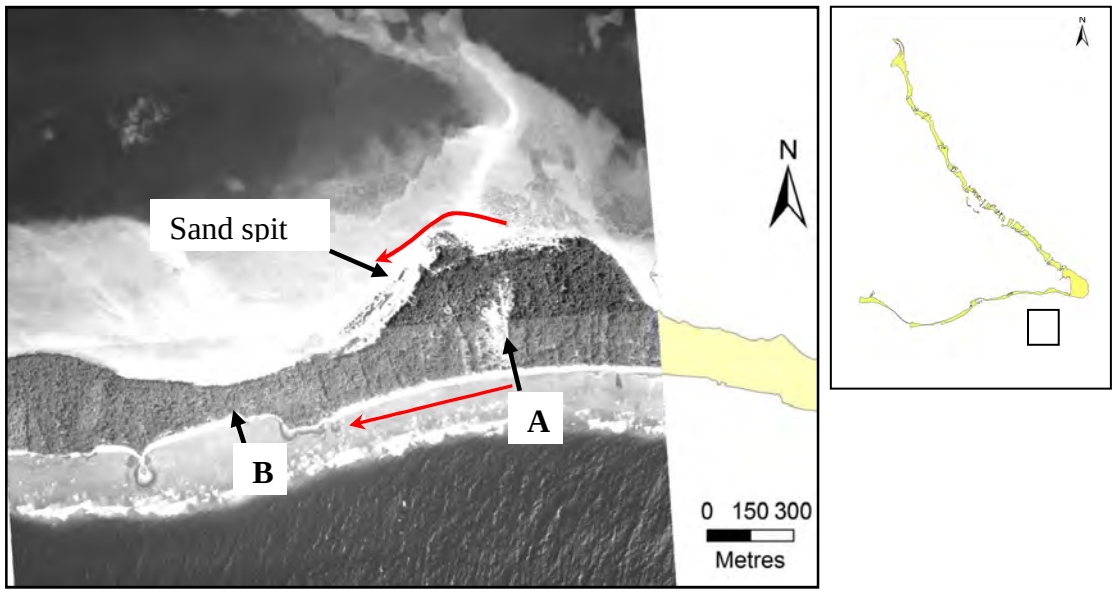

Figure 3.16. An aerial photograph from 1943 shows the location of the channel (A) east indicated by the presence of white sand in the middle of the island. B is the assumed location reported by Byrne (1991). Red arrows show the predominant direction of the longshore sediment transport. Insert shows the location of site on Tarawa Atoll.

Morphological changes to these reef islands will be compounded by increasing population density leading to increased human activity in the coastal area. Census

shows that a small proportion of reef islands are sparsely inhabited, especially in the northern arm, and that the residents of these reef islands do not face any issues with space. Conversely, in urban South Tarawa, where development has been focussed, people have relocated to the South Tarawa reef islands from the outer reef islands in Kiribati, leading to densely populated reef islands. This serious issue of overcrowding has forced residents to build closer to beach berms and to the active beach. Residents construct temporary vertical structures close to the beach berm or on newly accreted areas to serve two purposes; (a) protect their assets from high spring tides, and (b) provide more space. This has lead to the widespread construction of structures along the shorelines of South Tarawa and, in addition, has resulted in increased removal of building material from the beaches or the reef flat. The same situation has also been observed in some urban areas of the Marshall Islands (Maragos, 1993) and the Maldives (Turner *et al.*, 1996) where population density is also increasingly forcing people to expand seaward and therefore placing them in vulnerable situations. With increasing population, in South Tarawa, it is anticipated that more coastal structures of varying sizes will be built. As a result, the shoreline of South Tarawa is expected to become increasingly artificial with vertically designed temporary reclamations or seawalls laid next to or linked to one another (e.g. Figure 3.15 C). The construction of these structures will increase the amount of material directly removed from the beaches. These activities will lead to alteration and disruption of the natural coastal processes and will adversely affect the reef island shorelines.

The population density of Betio is not as high as earlier reported. The reported population density for Betio being 10,400 persons per km^2 by Haberkorn (2007) was calculated using the last 2005 census figures and a land area estimated to be 1.2 km^2 using the reef islands maximum length and width. However, this value underestimates the actual land area for Betio which can be derived by digitising the base of the beach around the reef island showing that it is greater than 10 km^2 (Table 3.3). The calculated population density using these figures should be more than 900 persons per km^2 and is similar to that obtained using recent figures of reef island area and population density. This demonstrates that the population density of Betio is much lower than that for Hong Kong, Singapore and Kawajalein on Ebye, Marshall

Islands but still faces challenges given a high population occupying a small land area.

3.10 Summary

This chapter describes the current physical and social situation in Tarawa Atoll. It highlights some of the physical characteristics of the reef islands including their sediment composition, and the influence of unequal population distribution on shorelines. This chapter also shows that the reef islands depend entirely on biogenic sediments mainly foraminifera. There are 59 reef islands in Tarawa Atoll that are predominantly small in size with an average length and width of less than 2000 m and 400 m respectively. The mean area of the reef islands is more than 50 ha. The beaches of these reef islands vary in slope with ocean beaches generally steeper than the lagoon beaches.

Human activities also contribute to the variation of beach geomorphology, in both North and South Tarawa. Increased urbanisation, centred on the reef islands of South Tarawa, has lead to unequal distribution of population, thus causing serious overcrowding issues. This has forced residents on South Tarawa to expand shorelines seaward, and a major consequence of this is the widespread construction of temporary vertical structures along South Tarawa's shorelines. This in turn has placed more pressure on building materials which are locally sourced from beaches. Conversely, North Tarawa residents, with their low population density, do not face overcrowding issues and rarely create seawalls; however when seawalls are constructed in North Tarawa, they are generally built close to the affected areas so as not to block the coastal processes. This may change in coming years, as more retired Government workers migrate to these areas.

The GIS data developed and cited in this chapter, including the classification of reef island types, population densities and shoreline geomorphologies will be used in the following chapters.

4 CHAPTER FOUR: REEF-ISLAND ELEVATION AND SEDIMENT VOLUME

4.1 Aims of the chapter

The main objective of this chapter is to investigate the topography of the reef islands of Tarawa Atoll and to consider the implications of extreme sea levels for these reef islands. Another objective of this chapter is to calculate the volume of sediment that has been deposited in these reef islands over the past millennia since their formation. This involves the construction of a Digital Terrain Model (DTM) using the elevation-topography data set derived photogrammetrically by Schlencker (Schlencker Mapping Pty Ltd, 1998). Specifically, this chapter will:

a) Examine the distribution of elevation and its variability across the different reef islands.
b) Create a DTM and use this model to construct cross-island transects to show the variation in elevation.
c) Determine risks of lagoon and ocean inundation due to high tides and extreme water levels.
d) Calculate and compare first-order estimates of sediment volume for individual reef islands around the atoll.

4.2 Introduction

Reef islands on atolls, such as Tarawa Atoll, are composed of unconsolidated sediment that has been deposited over time. The topography derived from the accumulation of sediment is generally low-lying, with elevations typically less than 2 m above MSL (Woodroffe, 2008). This makes these low-relief reef islands particularly threatened in light of anticipated sea-level rise (IPCC, 2007). The impacts of rising sea level on these reef islands are increased inundation and erosion, which raises global concern for their future (IPCC, 2007). The generally low topography and elevation variability contributes to the risk to reef islands from high tides and extreme water levels.

A comprehensive review of reef islands situated on the rim of an atoll from the eastern Indian Ocean and western Pacific Ocean identified that many reef islands

showed a similar morphology to those of Tarawa Atoll (Woodroffe, 2008). A series of cross-island profiles covering reef islands from the Gilbert Group, Kiribati, the Cocos (Keeling) Islands, the Maldives and the Chagos Archipelago show that a major proportion of the reef islands have elevations lower than 2 m above MSL (Table 4.1). This study showed that the proportion of Marakei, Kiribati with elevations less than 2 m above MSL is greater than 60% (Woodroffe, 2008). This is also the case for the remaining islands in the Gilbert Island chain.

Table 4.1. Proportion of reef islands at elevations above MSL based on surveyed cross sections (source: Woodroffe, 2008).

Atoll or archipelago	% above 2 m above MSL	% above 3 m above MSL
Gilbert chain/Tuvalu	34	7
Marakei	32	8
Cocos (Keeling) Islands	33	8
Chagos	18	7
Maldives	4	1

Cross-island profiles show that many reef islands consist of a prominent ocean ridge and a lower lagoon ridge separated by a central depression (Woodroffe, 2008). Prominent oceanward ridges are generally 3 - 4 m above MSL. Lagoonward ridges rarely exceed 1 - 2 m above MSL. Some reef islands, however, such as Betio appear relatively flat with no distinctive ridges (Woodroffe and McLean, 1992; Solomon, 1997). Profiles show that morphology may vary within a group of reef islands and also along the length of a reef island.

Several factors influence reef island elevation such as energy exposure, sediment availability, and ENSO conditions (Forbes and Hosoi, 1995; Gillie, 1997). Energy exposure is considered to be the driving factor responsible for other variations in relation to reef island morphology such as sediment distribution (Emery and Tracey, 1954; McLean and Stoddart, 1978; Richmond, 1992) and ridge heights (McLean and Hoskings, 1991; Woodroffe and Morrison, 2001).

Oceanward ridge elevations are influenced by various factors but are considered to demonstrate low variability (Woodroffe, 2008). Located in relatively calm conditions outside the cyclone belt, the islands of the Gilbert Group, Kiribati have no

storm ridges (Forbes and Hosoi, 1995; Woodroffe and Morrison, 2001). But the ridge heights experiences some variability in relation to ENSO events and energy exposure (Burgess, 1987; Australian Bureau of Meteorology and CSIRO, 2011). A time-series of two shoreline positions from 1969 and 1992 including beach profiles taken in 1995 at the new Hospital on South Tarawa showed that elevations of oceanward ridge changes during normal and ENSO conditions. Under normal conditions, the oceanward ridges reached 3 to 3.5 m above MSL (Forbes and Hosoi, 1995). During El Niño periods, predominant longshore sediment transport is reversed the site undergoes erosion, and this results in the oceanward ridge experiencing a slight reduction in elevation. A cross-island transect on Buota shows that the ocean ridges are the highest feature on the reef island reaching above 3.5 m above reef flat (Woodroffe and McLean, 1992). Further north, cross-island transects show that Marakei's ocean ridges, which are exposed to the easterly trade winds, are 3 m above MSL (Woodroffe, 2008).

Lagoonward ridges have lower elevations and show greater variability in topography than oceanward ridges (Harper, 1989). Even though they are sheltered from the wind, these areas are influenced by the size of the lagoon and water depth (Woodroffe, 2008). Tarawa Atoll's shallow lagoon depth and locally-generated wind waves both contribute to the variability in elevation and morphology of the lagoonward ridge which can be seen in the seven year beach profile dataset for Betio and Bairiki reef islands (Harper, 1989) (Figure 2.2). Tarawa Atoll's lagoon is well connected to the open ocean on its western side which consists of a submerged reef rim (Zann, 1982). Water levels are therefore likely to be similar to open ocean water levels. This contrasts with lagoons with no passages which often have water levels that are perched above ocean water level at all stages of the tide (Callaghan *et al.*, 2006). Tarawa Atoll's shallow lagoon depth and locally-generated wind waves all contribute to the variability and magnitude of the lagoonward ridge morphology recorded on the 7-year beach profile data for Betio and Bairiki reef islands (Harper, 1989) (Figure 2.2). An example of this is Marakei Atoll which has a nearly enclosed lagoon and shows little variability in lagoon water levels (Woodroffe, 2008).

The central depressions of reef islands occur at various elevations. Some of these areas are natural whereas others have been modified by human activities particularly the excavation of pits for the cultivation of taro plants. It is presumed that these natural depressions result from the formation of ocean and lagoon ridges. In Kiribati, man-made pits are generally excavated in the central parts of the reef islands for the cultivation of *babai*, a type of taro. These excavated large pits reach freshwater lens to ensure that *babai* crops have access to water. The banks of pits where spoils have been deposited are frequently the highest points on reef islands. In some cases the central depression is connected to the ocean or lagoon through a lower part of the ridge or a passage, as in Fongafale, Funafuti Atoll, Tuvalu (Yamano *et al.*, 2007). Low relief areas, immediately backshore of low ridges are vulnerable to overwash. For example, in Ukiangang and Keuea, Butaritari Atoll, Kiribati, low relief areas such as backshore *babai* pits located immediately landward of the ocean ridges have been inundated by saltwater overwash during stormy conditions approximately every 3 to 4 years (Gillie, 1994).

Variability in topography has also been investigated by extracting profiles from a DTM for a low-lying reef island on Funafuti in Tuvalu (Yamano *et al.*, 2007). A study in Funafuti, Tuvalu, investigated why a low-lying area situated in the central portion of the island was at risk to flooding by high spring tides despite being protected by a high storm ridge and a beach ridge (Yamano *et al.*, 2007). Results from the DTM, cross-island profiles and evidence from maps and aerial photographs showed that a region of the island originally contained a mangrove swamp and seawater had penetrated into this region through a storm ridge. Now reclaimed and raised, this region is still at risk from spring tide flooding as other human-induced changes have contributed to a lowering of the permeable storm ridge (Yamano *et al.*, 2007). The spatial extent of the low-lying area as well as significant elevation changes was determined from the DTM and survey transects thus providing a better understanding of the variation in elevation.

The variability in elevation of some reef islands in Tarawa Atoll has been examined to assess their vulnerability to anticipated sea-level rise; however, the approaches that have been taken vary (Woodroffe and McLean, 1992; Solomon, 1997; He, 2001;

Elrick and Kay, 2009). A preliminary study on Betio, Buota and Buariki examined the elevations of certain features above present high water levels and observed a difference between a reef island (Buota) exposed to the trade winds and one that was less exposed to the trade winds (Betio) (Woodroffe and McLean, 1992). A cross-island transect of Buota showed that the ocean ridge is >3.5 m relative to the reef flat and extreme water levels can approach 3.5 m, however, the reef island does not appear to have been overtopped at any time. Conversely, Betio, with a large percentage of its shoreline modified by vertical seawalls, appeared to be at a greater risk from flooding. Another study carried out on Betio measured the elevations of beach crests and seawalls, and compared them to present day extreme water levels allowing identification of four areas at risk located in eastern and northern Betio (Solomon, 1997). However, when Solomon (1997) modelled the potential risks using the First Assessment Report IPCC projection of 0.5 m sea-level rise by 2100 with constant beach crest elevations, the results showed that many areas in Betio will be overtopped or flooded.

He (2001) conducted inundation modelling for Bairiki and the village of Bikenibeu under the 2100 IPCC forecasts coinciding with a spring tide and a 1 in 14 year storm event. This study used an average elevation for the reef island of 2.64 m above MSL, and average elevations for the ocean and lagoon ridges of 3.25 m and 2.38 m above MSL respectively. The results showed the lagoon side of the reef island to be more vulnerable to sea level rise and overtopping compared to the ocean side. In this study He (2001) rounded the still water level of 1.073 m above Cox datum (1.18 m above UH – Table 2.2) to 1.5 m using Solomon's (1997) analysis of the tidal data from 1992 to 1997. This still water results from the addition of the maximum anticipated high tide level of 1.22 m and the maximum observed residual water of 0.27 m. To this new still water level of 1.5 m he added the 2100 IPCC projected sea level rises of 0.3, 0.5 and 0.95 m. Applying the highest scenario of 0.95 m sea-level rise by 2100 gave a projected sea level rise of 2.45 m during a spring tide. Combining this with the elevations of beach ridges, coastal structures such as seawalls and reclamations and areas on the reef island, He (2001) established that the western part of Bairiki and a large proportion of Bikenibeu village would be flooded from the lagoon side. Under the same scenario, combined with the effects of a 14

year return period storm event and wave set up on the ocean side, He determined that the whole of Bairiki and the village of Bikenibeu would be totally overwashed.

A recent study on South Tarawa used the Coastal Calculator tool developed by Ramsay *et al*., (2012) to create hazard maps for 2070 showing the extent of areas at risk from inundation from MHWS and extreme water levels under the A1FI scenario (Figure 4.1) (Elrick and Kay, 2009). The maps were developed using 0.1 m island elevation contours, MHWS water levels (2.09 to 2.61 m) and storm events (2.6 m to 3.1 m) in order to show levels of risk ranging from low to extreme at a village level (Figure 4.1).

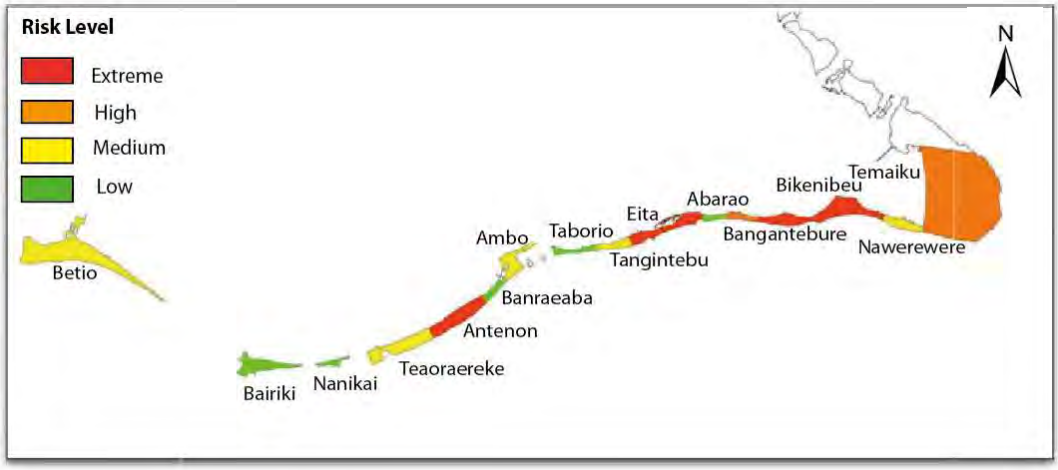

Figure 4.1. Map showing the extent of hazards at the village level on South Tarawa (source: Elrick and Kay, 2009, p. 19).

The above studies show that the risk of reef islands from inundation or overtopping from sea-level rise is primarily related to the elevation of beach ridges and the stability of shorelines (Solomon, 1997; He, 2001). Shorelines that continue to accrete will raise the elevations of the ridges, reducing the possibility of the risk. The studies also show that with differing sea level scenarios, the results would differ greatly and reef islands with modified shorelines appear to be placed at greater risk compared to those without.

Another objective of this study is to determine the volume of sediment that has accumulated on each individual reef island since the reef islands began forming around 4,000 years ago. Reef islands are primarily the net result of wave action that deposits sediment (Kench *et al.*, 2005; Woodroffe *et al.*, 2007; Barry *et al.*, 2008;

Kench *et al.*, 2012). It has been suggested that with sufficient sediment supply reef islands may accrete and are likely to be more resilient against anticipated sea-level rise (Solomon, 1997; Woodroffe *et al.*, 2007; Woodroffe, 2008).

Most studies investigating sediment volumes of reef islands are based on two-dimensional (2D) analysis determined by using cross-sectional profiles and maps of areas in order to estimate volumes (Harper, 1989; Gillie, 1993; Forbes and Biribo, 1996). For example, beach profiles established around Betio measured beach heights and distances but for volumetric analysis assumed that the sand accumulated to a height of 1 m above the reef flat (Harper, 1989). This approach allows the calculation of volumes for a particular section of the beach, but is limited as it does not have continuous surface for determining the volume of an entire reef island. Another study applied a time-series of shoreline positions, whereby the area changes of the island were established. The volume changes were calculated based on the assumption that the beach thickness was 2 m (Gillie, 1993). An alternative approach to determine volume is to use Digital Terrain Models (DTM's), however, this has rarely been applied to reef islands. The term digital terrain model (DTM) is a broad term including both digital elevation models of regular gridded points (DEM) and triangulated irregular networks (TIN). A DTM is a representation of the surface topography created by interpolating a continuous surface from spot heights. The limiting factor is the high cost of data acquisition that can prevent wide coverage and/or capture of high density data. An example of a successful application of DEMs in determining the accumulated volume of sediment on reef flats is a study conducted in Torres Strait in northern Australia (Leon, 2010).

The total sediment volume of sand on the reef island of Warraber in the central Torres Strait was determined using a photogrammetrically-derived DTM (Samosorn, 2006). The surface of the reef flat derived from surveys and spot heights showed height variation: a lower elevated western part of the reef island and an elevated eastern part rising 2 m above the Lowest Astronomical Tide (LAT) level. The topography of the sand cay, illustrated by a Triangulated Irregular Network (TIN) model, showed several beach ridges. The beach ridges have prograded to the southeast as determined by radiocarbon ages on both bulk carbonate samples

collected on the ridges, and individual shells, establishing 5 growth phases (Woodroffe *et al.*, 2007). The growth phases, combined with a beach slope and the reef-flat surface, established a total sediment volume of 2,611,206 m^3 and an average rate of accumulation about 900 m^3/yr.

In summary, this chapter will discuss reef-island topography to determine the total sediment volume of reef islands in Tarawa Atoll. The variability and distribution of elevation will be examined by using a DTM constructed from high density data to provide greater detail. This will enable a better understanding of the distribution of elevation classes across each individual reef island and their risks from extreme water levels.

4.3 Background

4.3.1 Elevation measurements

Measurements of elevations of reef-island surfaces with high spatial densities can be extracted from aerial photographs using a stereo-plotter, which uses a method known as digital photogrammetry (Yamano *et al.*, 2006). Aerial photography is carried out when cloud cover is absent to reduce the visual obstruction of features by clouds. Aerial photos are also generally captured during low spring tides in order to capture as much of the reef islands as possible, including the beaches and lagoon flats. The quality of the elevation datasets extracted from aerial photographs can be assessed in terms the datasets accuracy and the density and distribution of the points (Li *et al.*, 2005).

Elevations can also be obtained from beach profile data. In South Tarawa a beach profiling program established in 1982 which covers Betio, Bairiki and later the Nippon causeway has measured the heights of the beach, reef heights and distances from a vertical datum tied to the UH tide gauge (Howorth, 1983).

A spot height has three coordinates: an *x* and a *y* coordinate locating its position in latitude and longitude, and its elevation, *z*. Spot heights need to be measured in relation to a reference point in order to determine an elevation. In this thesis, heights

are measured from the UH datum and then converted to SEAFRAME datum to relate them to MSL and to tidal information (see Chapter 2).

Contours are isolines connecting areas on maps with the same height (Longley *et al.*, 2005). Reef-island surfaces are generally low gradient, with small changes in elevation and are represented by well-spaced contours (e.g., Figure 4.2). Closely spaced contours indicate a rapid rise or fall in surface elevations for example an eroded beach face or steep oceanward ridge (e.g., Figure 4.2). In GIS, contours are represented using poly-lines with their elevations stored in the attribute table.

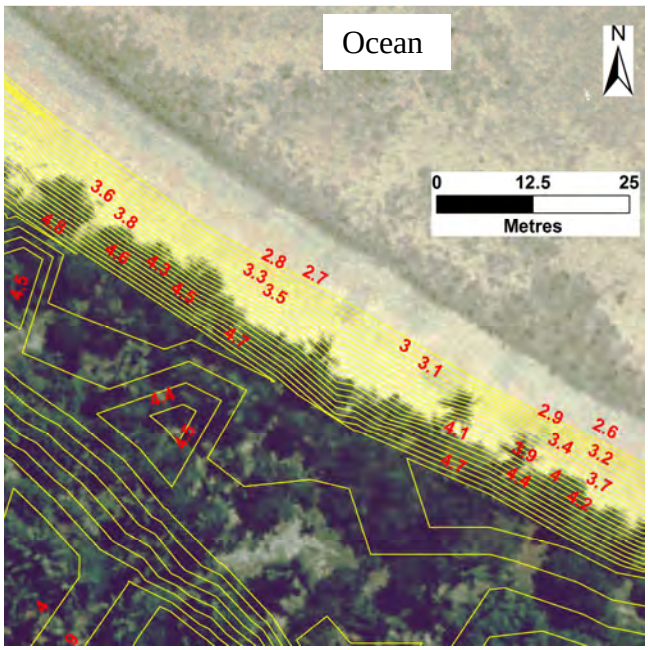

Figure 4.2. Example of reef-island topography with 0.1 m contours. Closely spaced contours facing the ocean show an area of steep gradient on an oceanward ridge. Contours spaced out indicate relatively flat terrain such as that located behind the beach ridge. The sharp edges of the contours are artefacts, a result of determining elevations from a generally flat area.

4.3.2 Digital Terrain Models

DTMs with adequate detail can show the variability in topography across a surface. DTMs should characterize a complete continuous land surface for a given area, and permit calculations of heights from any given point (Hengl and Evans, 2009). The most common method used for creating DTMs is to use high-density elevation points extracted from aerial photographs (Nelson *et al.*, 2009).

A DTM may have break-lines which are features that illustrate the change in surface slope (Longley *et al.*, 2005). These features can either contain irregularly spaced

points with elevation information. In this study, the breakline is the polyline at the base of the beach that defines the sharp discontinuity present between the foot of the beach and the reef flat. The height of the base of the beach is assumed to be 1.166 m above SEAFRAME datum.

There are many advantages to constructing DTMs for reef islands. Within an atoll, it may be difficult to access all the reef islands and carry out fieldwork, thus limiting observations of the topography of all the reef islands. By constructing a terrain model of the reef islands more information can be made available and generally at a larger scale. For example, a DTM of Fongafale, Funafuti, Tuvalu, was used to portray topography in great detail and show areas that may be affected by sea-level rise (Yamano *et al.*, 2006). This was made possible by extracting cross-island transects from the DTM to show the variable morphology. The extent to which topographical features of an area can be determined depends on the resolution of a DTM; the higher the resolution, the greater the detail, whereas the lower the resolution, the less detail it provides.

In choosing an appropriate DTM format, several factors need to be considered such as the task objective and the spread of data points. Triangular based DTM (TINs) can be applied in any given situation (Yanalak and Baykal, 2003), however raster grid based DTMs are only suitable for regularly distributed elevation points (Hengl and Reuter, 2009) Spatial analysis works well with raster formats, as each elevation point is stored as one node/cell, making it easier to perform investigations (Longley *et al.*, 2005). The grid or cell size of raster formats depends on the average distance between data points (Chow and Hodgson, 2008). In TINs, spatial analysis is more complex, as this format manages the information for a single node as well as for its neighbours. Another disadvantage of TINs is that these models require more computer memory to store large datasets, and therefore it takes more time to carry out analysis. One of the advantages it has over other raster formats, however, is its greater capability to present detailed information when surface relief is irregular (Yanalak and Baykal, 2003).

In all DTM's spatial interpolation fills in the missing gaps required to create a continuous surface (Longley *et al.*, 2005). Interpolation methods work by approximating the elevation of an interpolated point using the known values of neighbouring points that are distributed around the point within a given area (Yanalak and Baykal, 2003). In GIS, spatial interpolations are based on Tobler's (1970, p. 236) First Law of Geography that states "everything is related to everything else, but near things are more related than distant things". Currently there is a range of spatial interpolation methods available that can be applied to predict an unknown elevation value. This study will only discuss the two interpolation methods Inverse Distance Weighted (IDW) and Delaunay triangulation methods. TINs are derived from the latter interpolation method.

The IDW method uses mathematical algorithms and neighbouring points to estimate the elevations (z) at unknown locations (x_0) (Burrough and McDonnell, 1998; Longley *et al.*, 2005). This is a simple and commonly applied interpolation method that predicts the elevation of an unknown location based on the elevations of, and the distance to, surrounding measured values (Longley *et al.*, 2005; Hengl and Reuter, 2009). Applying Tobler's First Law, IDW estimates the interpolated value by obtaining the mean value of its close neighbours. The neighbours closer to the position of the unknown location have more weight in the estimation compared to those located at a further distance (Longley *et al.*, 2005). This interpolation method was considered appropriate for this study for two reasons. The dataset was dense and the interpolated height values fell within the range of the measured values. However, this is not the case with some interpolation methods, such as spline. The requirement of the spline method is that the interpolation passes exactly through all input data points predicting heights above and below the points creating a smooth surface (Longley *et al.*, 2005).

The Delaunay triangulation method interpolates elevation data following the Delaunay criterion which does not allow any data to be placed within the circumcircle of any triangle (Hengl and Reuter, 2009). This method has been applied in this study to develop a TIN from many single elevation points referred to

as mass points converted from contours to provide a detailed topography across reef islands.

The quality of a model cannot be determined by its visual appearance alone, but must be tested using either quantitative or qualitative methods (Burrough and McDonnell, 1998). One quantitative approach to assess the quality of a model would be to verify the uncertainties and errors within the dataset. However, sometimes surfaces that are statistically accurate do not represent the topography of a given area, therefore the best method to apply is that which best represents the true surface (Yang and Holder, 2000). The best way to determine the quality of a model is to assess if it meets both the study's objectives and portrays a true surface of the study site, which can be defined simply by the term "fitness for use" (Fisher and Tate, 2006).

TIN models can be converted to grid formats by using GIS. By using GIS, it is possible to perform analysis on a selected format that suits the dataset, and also this selected format can then be converted to another format to meet the objective of the study (Hengl and Reuter, 2009). In this chapter, the two DTM formats are utilised. Firstly, the raster grid format is used to create a DEM to enable calculations of reef island volumes. Secondly, the DEM is converted to a TIN format to show differences in elevations between the reef islands. This is visually compared with the other TIN model developed from denser mass elevation points derived from contours.

4.3.3 Distribution of elevation classes

Hypsometric analysis is a method which focuses on the distribution of elevation classes (Strahler, 1952). A hypsometric curve is a cumulative distribution curve of elevations in an area that is constructed by calculating the percentage area that lies within each elevation class. Normalisation of this curve allows comparative measures to be obtained between areas of varying sizes and with different elevations (Gordon *et al.*, 2004). This approach has been widely applied in river catchment studies to characterise the distribution of elevation or geomorphic forms (Willgoose and Hancock, 1998; Gordon *et al.*, 2004). It has also been applied to other situations,

such as in the description of the morphology of submerged coral reefs (Harris *et al.*, 2008).

Three forms of hypsometric curves have been identified based on river and mountain studies. These have been classified as convex (Strahler, 1952), concave (also referred to as monadnock) and S-shaped (Summerfield, 1991; Hiroo, 1993) (Figure 4.3). The curves have been interpreted as an indication of landscape age in the context of catchment topography. Convex represents youthful stages whereas both concave and S-shaped correspond to maturity. In this study, hypsometry has been applied to show the distribution of elevation across an entire reef island. The hypsometric curve shows the relative distribution of elevations across the reef island, and is constructed by determining the surface area at each successive contour interval. Normalising the area as a percentage of the total reef-island area shows the distribution of elevation across an individual reef island, allowing for comparison with other reef islands and to MSL and extreme water levels.

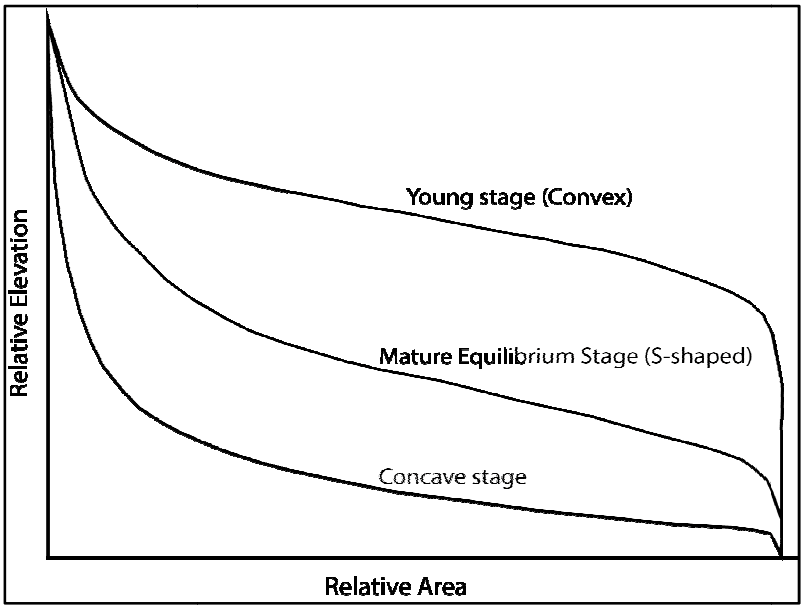

Figure 4.3. Hypsometric curves showing the three common forms: convex (young stage), S-shaped (mature) and concave (source: Willgoose and Hancock, 1998).

4.3.4 Sediment volume calculations of reef islands

Surveyors and engineers calculate volumes using a topographical surface, a horizontal reference and area (Yanalak and Baykal, 2003). This approach can be applied when calculating sediment volumes of reef islands. A lower surface is required and the solid reef flat on which the reef islands have accumulated can be

used for this (Samosorn, 2006; Leon, 2010). This assumes that the horizontal surface of the reef flat extends beneath the entire reef island (Harper, 1989; Gillie, 1993; Woodroffe and Morrison, 2001; Barry *et al.*, 2007). The extent of the reef island can be determined by using the polygon that represents high water level (HWL) or some other measure of reef-island perimeter. Sediment volume in successive elevation slices of a reef island can be calculated by establishing the respective surface areas of each contour and multiplying it by the elevation interval (Leon, 2010). It is well established that the determination of accuracy for volume calculations derived from DTMs depends on the spread and density of data including the applied method of calculation (Yanalak and Baykal, 2003).

4.1 Study sites

There are 59 reef islands on the north and south margins of Tarawa Atoll (Figure 3.11), however only 36 reef islands were analysed hypsometrically. The remaining 23 are particularly small reef islands that have areas ranging from 0.02 ha to 4.65 ha totalling 16 ha. Those reef islands had only a number of spot heights ranging from 1 to 6 spot heights, which did not meet the requirement of a minimum of 12 spot heights to interpolate an unknown cell and create a continuous surface.

4.2 Materials and method

4.2.1 Sources of elevation data

In 1998, Schlencker Mapping Pty Ltd captured overlapping colour aerial photographs of Tarawa at a scale of 1:2,500. Using photogrammetric techniques, spot heights were extracted from areas not covered with vegetation. The aerial photos were vertically tied to the Betio Trigonometric Station and related to the UH datum, located in Betio, allowing the spot heights derived from these photos to be related to MSL. One-metre contours were developed from these spot heights by Schlencker using a photogrammetric program that allows the operator to identify the spot heights of a given elevation by viewing the scanned aerial photographs on a computer screen using stereo glasses (Falkner, 1995; Schlencker Mapping, 2012). From these spot heights, the operator was able to interpolate the contours. As described in Chapter 3, the Kiribati Adaptation Project (KAP) commissioned Schlencker Mapping Pty Ltd to subsequently develop 0.1 m contours from the

original one metre contours with a vertical error of ±0.05 m (Elrick and Kay, 2009) (Table 4.2). This provided a higher resolution elevation dataset enabling the derivation of surface areas and sediment volumes across Tarawa Atoll from these 0.1 m contour intervals.

Table 4.2. Data information sourced from Schlencker Mapping, Australia.

Elevation data	Scale Accuracy	Year	Holdings Location
Spot heights (50m spacing), contour (1 m spacing)	1:2,500 ±0.5 m	1998	Kiribati Lands Division
Contour (0.1m spacing)	0.1 ±0.05 m (vertical error)	2009	Kiribati Adaptation Project

Elevation data from North and South Tarawa were provided by Schlencker Mapping as two separate vector shapefiles (Tara_Topo_Spot_hts_point.shp and Tar_Topo_Spots_Hts_fonts.shp). The different sources of elevation data were added to the vector files prior to analysis. The spot height initially reported relative to the UH were converted to the SEAFRAME datum allowing comparison with calculated MSL. The two shapefiles were merged as one (and named MasterHts_1998) using the data management tool box. Visual analysis was performed to remove points located on mangroves, reef flats and conglomerates. The total number of spot heights observed on reef islands was 5158 with an average spacing of 50 m.

4.2.2 Reef-flat elevations

In order to use the reef-flat surface as a lower boundary for each island, its elevation needed to be determined. Reef-flat elevations were selected from points that were visually located on the reef flat. This produced 132 reef-flat elevations distributed randomly across the atoll. The entire reef flat was not covered. There was no data coverage for the southern end of central North Tarawa, or the western end of South Tarawa, from Bairiki west. There was a bias towards the ocean reef-flat elevations as most of the lagoon spots located in the middle of the extensive sandy or muddy flats were deleted as they were not near the horizontal reef flat. In North Tarawa, the retained spot elevations on the lagoon reef-flat were those close to the base of the beach as field observations showed that the sediment thickness on the reef flat increased towards the lagoon. Data were available on the northern tip of Buariki and the northeastern corner of the Bonriki-Taborio reef island. There was no data coverage for the Betio reef flat, on the far western corner.

The missing reef-flat data for Betio was filled in using information obtained from the beach profile program established for Betio and Bairiki. The Beach Level Profiles (BLP) that were used were BLP 13 (formerly 1), BLP20 (formerly 8), BLP22 (formerly 10), BLP23 (formerly 11) and BLP26 (Table 4.3). The elevation of the reef flat is a single elevation measurement obtained from the beach profiling data provided by Harper (1989). This beach profiling dataset was reported in heights above MSL (MSL 1 see Table 2.2) which is 1.189 m above UH datum (Howorth, 1985). Adjustments need to be made so that this beach profiling data can be related to the current MSL (1.637 m relative to SEAFRAME datum).

Table 4.3. Information of Betio reef-flat elevation derived from beach profiling data.

Former BLP	New BLP	Reef flat height (m)	Survey date	Horizontal distance from benchmark (m)	Relative to UH (m)	Relative to SEAFRAME (m)	Relative to MSL (2007)
1	13	-0.37	Jan, 1982	30	0.819	1.238	-0.399
8	20	-0.59	Jan, 1982	50	0.599	1.018	-0.619
10	22	-0.61	Jan, 1982	50	0.579	0.998	-0.639
11	23	-0.58	Jan, 1982	50	0.609	1.028	-0.609
-	26	-0.06	Jun, 1987	60	1.129	1.548	-0.089

The reef-flat elevation based on the spot heights obtained from the photogrammetric data ranges from 0.639 m to 2.239 m in relation to SEAFRAME datum (Figure 4.4). The reef flat varies across the atoll; in central North Tarawa it has a height of 1.805 m in relation to the SEAFRAME datum (Table 4.4). Comparison of the three corners of Tarawa Atoll shows that the southeastern ocean corner reef flat is higher, with an average value of 1.706 m, than the north and western corners, with average values of 0.910 m (Naa-Northern corner) and 1.166 m (Betio-SW corner) above SEAFRAME datum. This varying reef-flat elevation implies that the reef has grown to different heights. This also indicates that the ocean reef flats of Betio and Naa must be covered for more of the tidal cycle than those of Temaiku and the central part of North Tarawa.

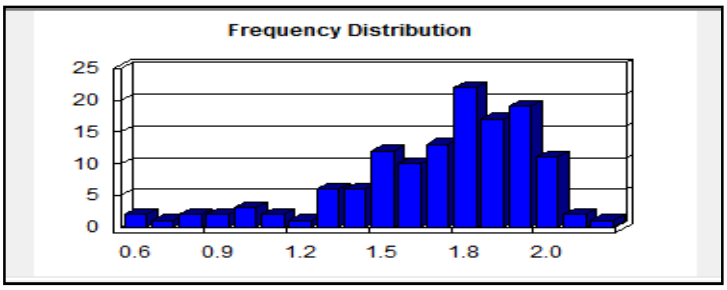

Figure 4.4. Reef-flat elevation statistics of Tarawa Atoll. Reef elevations is in metres relative to SEAFRAME datum.

Table 4.4. Reef-flat spot heights across Tarawa Atoll

Location	N (number of spot heights)	Average elevation of reef flat in relation to UH (m)	Average elevation of reef flat in relation to SEAFRAME datum (m)	Elevation of reef flat in relation to MSL (m).
Central North Tarawa Arm	5	1.386	1.805	0.16 8 m above MSL
SE corner	15	1.287	1.706	0.069 m above MSL
SW corner	5	0.747	1.166	0.471 m below MSL
North corner	9	0.491	0.910	0.73 m below MSL
Reef flat height of Tarawa Atoll	132	1.2825	1.701	0.06 m above MSL

The reef-flat elevation was calculated by averaging all 132 spot height data. The average height of Tarawa Atoll reef flat is +1.282 m above UH and 1.701 m above SEAFRAME datum, lying higher than MSL by +0.06 m (Table 4.4). This average reef-flat elevation of 1.701 m above SEAFRAME datum appears to be very high, and all spot heights were checked again to ensure that they were not located on conglomerate platforms; however, they were not. Therefore it was decided that the average reef-flat elevation of Betio (SW corner) would be used to represent the atoll for two reasons: firstly, sea level is recorded by the tide gauge installed in Betio, and secondly, the average elevation of 0.747 m above UH (1.166 m above SEAFRAME datum) would include other low-lying areas in the North Corner (Naa) and SW (Betio) (Table 4.4). This average reef-flat elevation value of 0.747 m in relation to UH datum falls in the elevation range of 0.6 to 1.0 m suggested by Solomon (1997). It is also relatively close to the 0.81 m used by Ramsay *et al*. (2010) when developing the coastal calculator tool to generate water levels for Tarawa (see Chapter 2). In this situation, where the reef flat varies, the average height cannot be used to represent its elevation because it would not include low-lying reef flat areas.

4.2.3 Base of the beach

The base of the beach (BB) marks the extent of the reef islands overlying the reef flat surface. For individual reef islands, this feature was obtained from the 1998 aerial photographs, digitised as poly-lines (for further detail see Chapter 5). The BB was identified by the contact point between the beach and the reef flat. On the ocean side, this was easily distinguished; conversely, on the lagoon side this was not so distinguishable due to the gradual beach slope and transition into the mud present on the reef flat. These poly-lines were then converted to polygons (MasterBeachReef_Project).

4.2.4 Reef-island elevations across Tarawa Atoll

Elevation data statistics for the 5158 spot heights acquired for Tarawa Atoll show that reef-island elevations range from 0.419 m to 6.689 m in relation to SEAFRAME datum (Figure 4.5). The mean elevation of the reef islands is 3.74 m relative to the SEAFRAME datum and this can also be expressed as 2.09 m above MSL. The bi-modal distribution indicates that elevation varies across the atoll with greater frequencies of reef-island elevations between 3.6 m and 4.3 m above SEAFRAME datum followed by elevations between 2.7 m to 3.6 m and those between 4.3 m and 4.9 m above SEAFRAME datum (Figure 4.5). On the other hand, elevations between 0.4 m to 2.7 m, and greater than 4.9 m above SEAFRAME datum are rare.

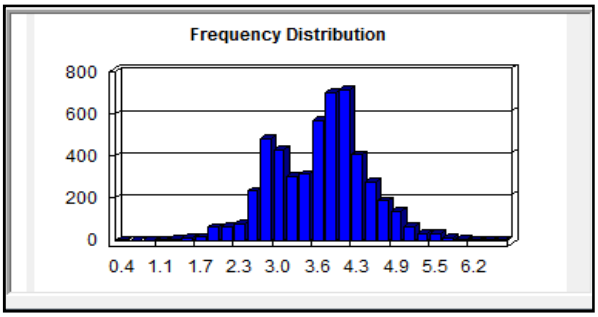

Figure 4.5. Reef-island spot height statistics relative to SEAFRAME datum. Elevations are in metres relative to the SEAFRAME datum.

The Inverse Distance Weighted (IDW) was used to interpolate missing data, and to produce a continuous surface as it provided estimates within ranges of the measured spot heights based on the accuracy test briefly discussed in Section 4.3.1. First, a raster grid model with a cell size of 50 m by 50 m was developed based on the average separation between the spot heights, and an interpolation method IDW was

applied using a total of 12 spot height points to calculate the unknown cell. The polygon (MasterBeachReef_Project) was used as to cut away the hard edges based on the reef island polygon shape (Figure 4.6).

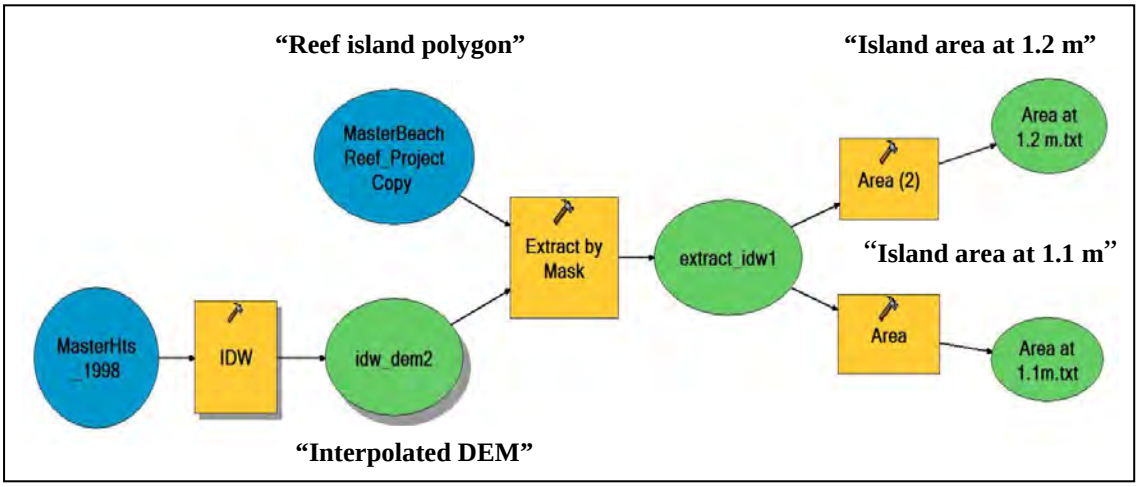

Figure 4.6. The steps taken to calculate the area between two contours, 1.1 m (reef flat) and 1.2 m of an individual reef island.

4.2.5 Area and volume at different elevations

Area and volumes are determined using the Model Builder in ArcGIS and by applying the IDW method to develop a raster grid model (Figure 4.6). The Model Builder is a toolbox that guides and simplifies analysis especially when large datasets are involved requiring multiple steps to be repeated numerous times. The raster grid model, with a continuous surface and cell size of 50 m, was developed by interpolating the spot heights using the IDW method. The missing gaps or unknown grid cells in the raster grid model were calculated by using a total of 12 spot height points (Figure 4.6). Calculations of areas were performed to determine the area at each individual cell between each 0.1 m contour. The raster grid model and individual reef-island polygons provide the topographical surface and bounded area respectively. The reef-island area within two contour intervals was calculated using an ArcGIS difference tool for TINs.

To determine the volume of sediment between contours 1.1 and 1.2 m contour, the area between 1.1 m contour was added to the area of the 1.2 m contour and divided by 2, times 0.1 m. The formula is as follows:

$$\text{Volume between 1.1 m and 1.2 m} = (A_{(1.1)} + A_{(1.2)}) /2 \times 0.1 \text{ m}$$

The total volume of sediment that has accumulated for an individual reef island can be obtained by adding all the volumes at each successive contour height. The individual reef-island sediment volumes are then added to provide the total volume of sediment that has been sequestered on the reef islands of Tarawa Atoll only.

4.2.6 Interpolation of mass points (contours) to create a continuous surface

To gain an understanding of the reef-island morphology, a series of transects across the reef island were derived from the constructed DTM. The profiles extracted did not provide much elevation detail therefore a second TIN model was constructed by converting the 0.1 m contours to mass elevation points. Visual analysis of the 0.1 m contour dataset in some low-gradient areas showed that contours were jagged introducing "stepping" artefacts developed during their generation (Smith and Clark, 2005). The 1 m contours did not show these issues as they were spaced further apart producing a smoother surface. In some areas, the contours did not match the spot heights as shown in Figure 4.7.

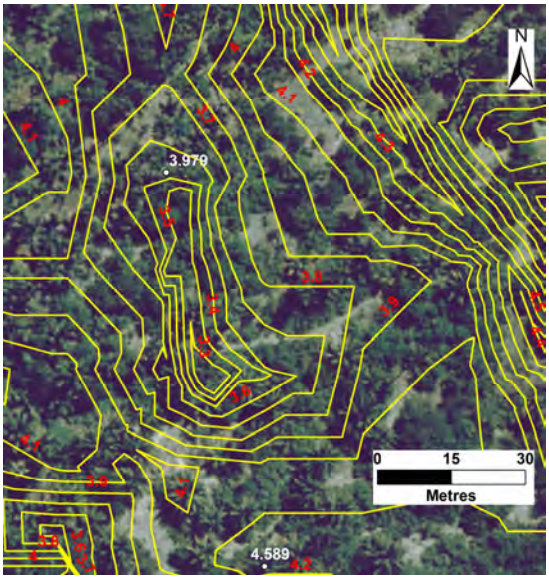

Figure 4.7. Example of a rare situation where contours (yellow) do not match the spot height (white). Also note the jaggedness of the contours which is an artefact of the generation of contours.

The area where the foot of the beach meets the solid reef flat was obtained by using the 1998 base of the beach (BB). The beach meets the reef flat, and it was assumed that the elevation was 1.166 m above SEAFRAME datum, similar to that of the reef flat (see 4.2.2 for more details).

Using the ArcToolbox, the TIN model features were edited. This was done by adding mass points developed from contour and the base of the beach data. The model shows elevation variation in greater detail compared to the constructed DTM. This TIN model has been used to show the elevation across the reef islands as well as showing the risks to extreme water levels.

4.2.7 Future tidal and extreme water levels

The projected tidal and extreme water levels, which can result in inundation and flooding, depend on the selected emission scenario (Cyan *et al*., 2008; Ramsay *et al*., 2010). To develop extreme water level projections would require the selection of a timeframe and a Climate Change Scenario that would be realistic for Tarawa's situation. The probability that the Low IPCC Scenario B2 will occur within the timeframe *Te Tibu* (2012-2036) is almost certain, compared to the *Te Tibu-mwamwanu* (2060-2084) and higher emission scenario (A1FI) as applied by Elrick and Kay (2009), as it is closer to the average sea-level record of 33 years provided by Ramsay *et al*. (2010). Extreme water levels rarely occur and vary in their frequency. The Annual Exceedance Probability (AEP) is defined as the probability that a given extreme water level is exceeded within a year (Ramsay *et al.*, 2010). These are provided as 10%, 2% and 1%, with 10% having a higher occurrence probability. Based on these assumptions and the likelihood that these events would occur, extreme water levels were generated from the coastal calculator using the *Te Tibu* timeframe (2012 – 2036), emission scenario B2 and a 1980-1999 average of level of the sea for present day as the baseline year relative to the SEAFRAME datum. This is the average level of the sea water that has been measured during the period 1980 to 1999. The generated tidal and extreme water levels for Tarawa are shown in Table 4.5.

Tables 4.5 and 4.6 show that elevation of extreme water levels does not vary significantly around the atoll. The magnitudes of extreme water levels (storm surge) in descending order occur on the ocean beaches in the northern part of the atoll (3.28 m) followed by south ocean beaches (3.17 m) and finally the ocean beaches on the western end of the atoll (3.14 m). The ocean areas facing the east experience waves that are 0.9 m higher than those on the southern area, and 0.14 m higher than those

on the western end. This difference is related to the exposure of the areas to the trade winds, and in order of decreasing exposure is the ocean area of North Tarawa (east), which is directly exposed, followed by the southern end and lastly the western end. Table 4.6 shows the insignificant differences in the storm tides for different locations on the lagoon side ranging from 3.09 m to 3.10 m. The storm tide levels, in descending order, are as follows: Eita to Tabiteuea (3.10 m), Betio to Eita and Abaokoro to Buariki (3.09 m). The results show a slight difference of 0.01 m between those three corners of the atoll which is within the error of analysis and is probably related to the changes in tide and storm surge characteristics (Ramsay *et al.*, 2010).

Table 4.5. Generated tidal and extreme water levels relative to SEAFRAME datum for Tarawa Atoll developed from the Te Tibu (2012 – 2036) and low emission scenario B2.

Water Levels relative to SEAFRAME datum (m)	Lagoon (m)	Ocean North (east) coast (m)	Ocean South coast (m)	Ocean West coast (m)
Mean Level of the Sea	1.70	1.70	1.70	1.70
Mean High Water Spring (MHWS)	2.58	2.58	2.58	2.58
Mean High Water Perigean Spring (MHWPS)	2.71	2.71	2.71	2.71
Storm Tides (10% AEP)	3.09	3.09	3.09	3.09
Storm surges (Storm tides and wave set up (10% AEP)		3.28	3.17	3.14

Table 4.6. Generated tidal and extreme water levels for Tarawa Atoll lagoon shores relative to SEAFRAME datum developed from the *Te Tibu* (2012 – 2036) and low emission scenario B2.

Water Levels relative to SEAFRAME datum (m)	Betio-Eita (west)	Eita (central) - Tabiteuea	Abaokoro - Buariki
Storm Tides (10% AEP)	3.09	3.10	3.09

A high tide exceedance curve has been generated for the next 100 yrs (by 2090) to show the frequency in which each astronomical tide is exceeded (Figure 4.8). The figure shows four curves representing the simulated MLOS relative to present day MLOS, using three different scenarios of sea-level rise: 0.18 m, 0.58 m and 0.78 m. Percentage exceedance of a present day MHWSP (2.71 m) was calculated to be 29% and 96% of all high tides for sea level rises of 0.18 m and 0.78 m respectively (Ramsay *et al*., 2012). This demonstrates that the Higher Astronomical Tides (HAT)

at present day will be exceeded by high tides under differing projected sea-level rise within the next 100 yrs.

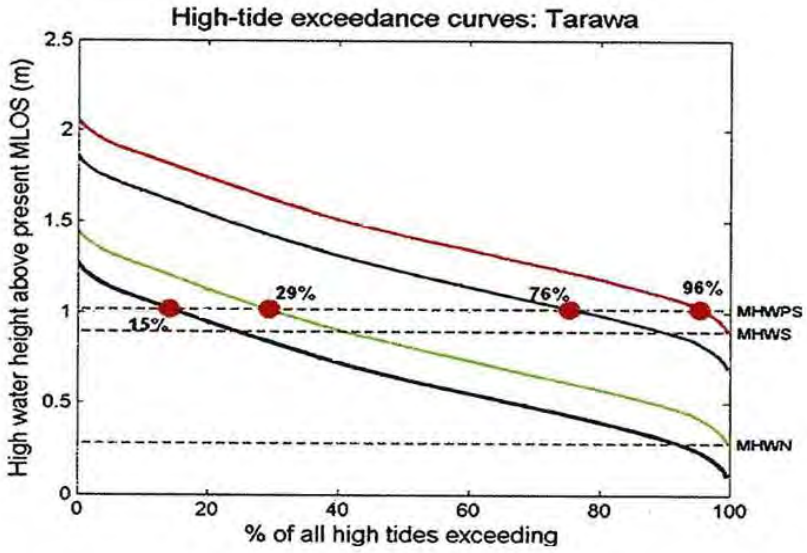

Figure 4.8. A high tide exceedance curve simulated from tide predictions for Tarawa Atoll for the next 100 years (by 2090). The dotted black lines represent the mean Higher Astronomical Tides relative to MLOS. In ascending order the dotted black lines represent MHWN, MHWS and MHWPS. The solid black curve shows the MLOS at present day. The other curves running parallel to this curve show the high tide exceedance for different sea level rises of 0.18 m (green), 0.59 m (blue) and 0.79 m (red). The red solid dots show the frequency to which the present day is exceeded MHPWS is exceeded under different sea level rises, for example, under a sea-level rise of 0.79 m, the MHWPS will be exceeded by 96% of all high tides (source: Ramsay *et al*. 2010, p. 34).

To determine what elevations on land these extreme water levels may reach, transects were extracted from the TIN model and plotted with the different extreme water levels. Three reef islands were selected on the basis that they have a high percentage of low-lying areas, < 2 m above MSL, and that they are inhabited; those with higher population densities were considered a priority, as the risk from extreme water levels would be greater. Reef islands that were uninhabited (see Table 3.3) were not used in this part of the study. The reef islands selected for this analysis are:

a) Bonriki-Taborio with 78% of its area low-lying (Table 4.9) and a population density of 23 persons/ha (Table 3.3),
b) Betio with 25% of its area low-lying (Table 4.8) and a population density of 94 person/ha (Table 3.3), and
c) Taratai with 81% of its area low-lying (Table 4.8) and a population density of 1 persons/ha (Table 3.3).

4.3 Results

4.3.1 Accuracy test

The accuracy of a DTM depends on the quality of the elevation data, the spread of points and the interpolation methods applied (Reuter *et al.*, 2009). An accuracy test was performed on the spot height data used to develop the Tarawa Atoll DTM. The accuracy test involves selecting random spot heights from the spot height dataset and subdividing it into two subsets; training and a test. The training subset comprises 75% of the spot heights whilst the test subset comprises only 25%. The training subset becomes the reference dataset whereas the spot heights in the test subset undergo interpolation. The vertical accuracy or Root Mean Square Error (RMSE) was determined which does not give an indication of the error spread (Li, 1992). The formula for RMSE is as follows:

$$RMSE = sqrt[\Sigma(Zdem - Zref)^2/n]$$

Whereby the following are:

Zdem represents the elevation derived from the raster grid;

Zref is the elevation from the reference (test);

n is the number of samples utilised.

The calculated RMSE was 0.25 m. The spread of elevation data was not evenly distributed as there were more data points on South Tarawa reef islands compared to North Tarawa reef islands (Figure 4.9). The IDW approach appears to be the most suitable interpolation method to model the reef islands of Tarawa Atoll and determine the volumes based on the low RMSE value which indicates less than a sub-meter vertical accuracy and interpolated elevation values falling in the range of the measured data.

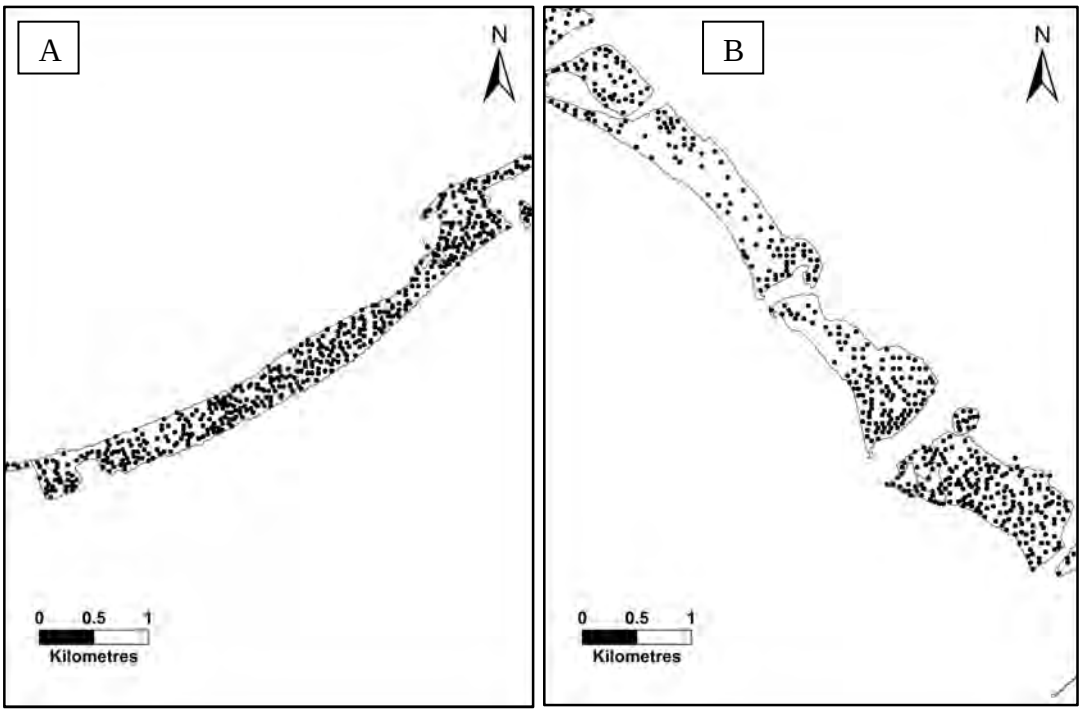

Figure 4.9. Spread of spot heights across A: South Tarawa and B: North Tarawa, note that South Tarawa has more data points (coverage) compared to North Tarawa.

4.3.2 Distribution of elevation

Elevation varies across the atoll with higher elevations generally occurring on the ocean side and lower elevations on the lagoon side (Figures 4.10 and 4.11). Results show that the elevation of the reef islands range from 0.419 m to 6.689 m relative to SEAFRAME datum (Figure 4.5). The highest elevation of 6.689 m relative to UH is found in the middle of the reef island, in Eita village of Bonriki-Taborio reef island. Eita village is one of the places where a lot of *babai* pits are present. The excavated material has been deposited on the banks of the pit raising the level of the ground artificially. The lowest elevations of 0.419 m relative to SEAFRAME datum are found in three different areas in pits. Two near the lagoon sides of Buariki (Figure 4.10 A) and Nuatabu, whilst the last is situated on the southern end of Abatao. Figure 4.10 to 4.13 show the elevation distribution relative to MSL across selected reef islands: Buariki, Abaokoro, Biketawa, Bonriki-Taborio, Ambo-Teaoraereke and Betio. The distribution of elevation is categorised into 5 classes with elevations ranging from < MSL, MSL+1.3 m to 1.8 m, MSL+1.8 m to 2.3 m, MSL +2.3 to 2.7 m and > MSL+ 2.7.

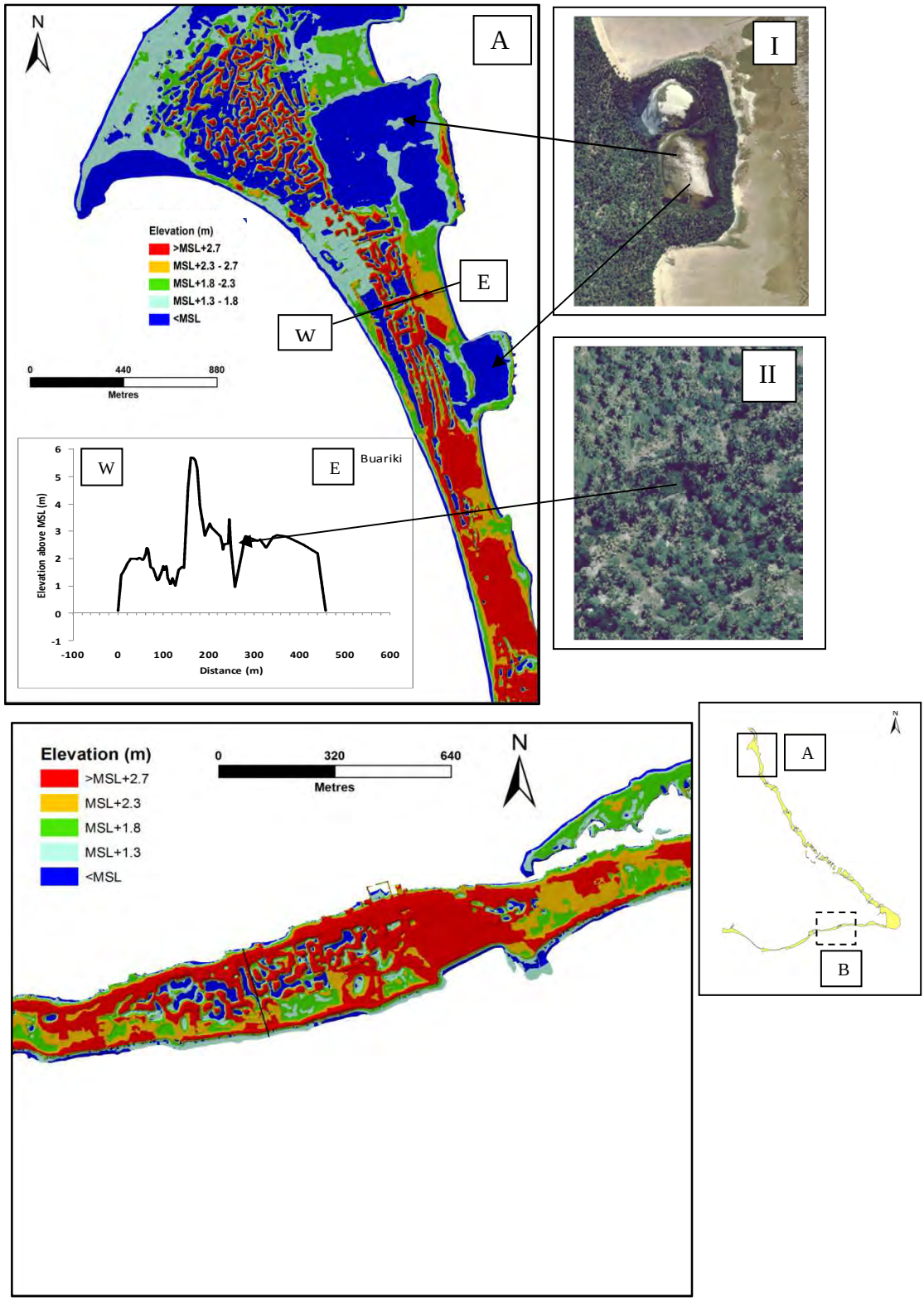

Figure 4.10. DTM showing the distribution of various elevation classes across A: Buariki and B: Bonriki-Taborio profile of the cross-island transect profile of the cross-island transect with locations in relation to the other islands illustrated in the Tarawa outline insert. The profile shows the prominent ocean ridge and a lower lagoon ridge separated by a central depression. Note the presence of a high ocean ridge only covering the lower portion of the island. The inserts on A show low-lying areas such as I: open water ponds and II: babai pits.

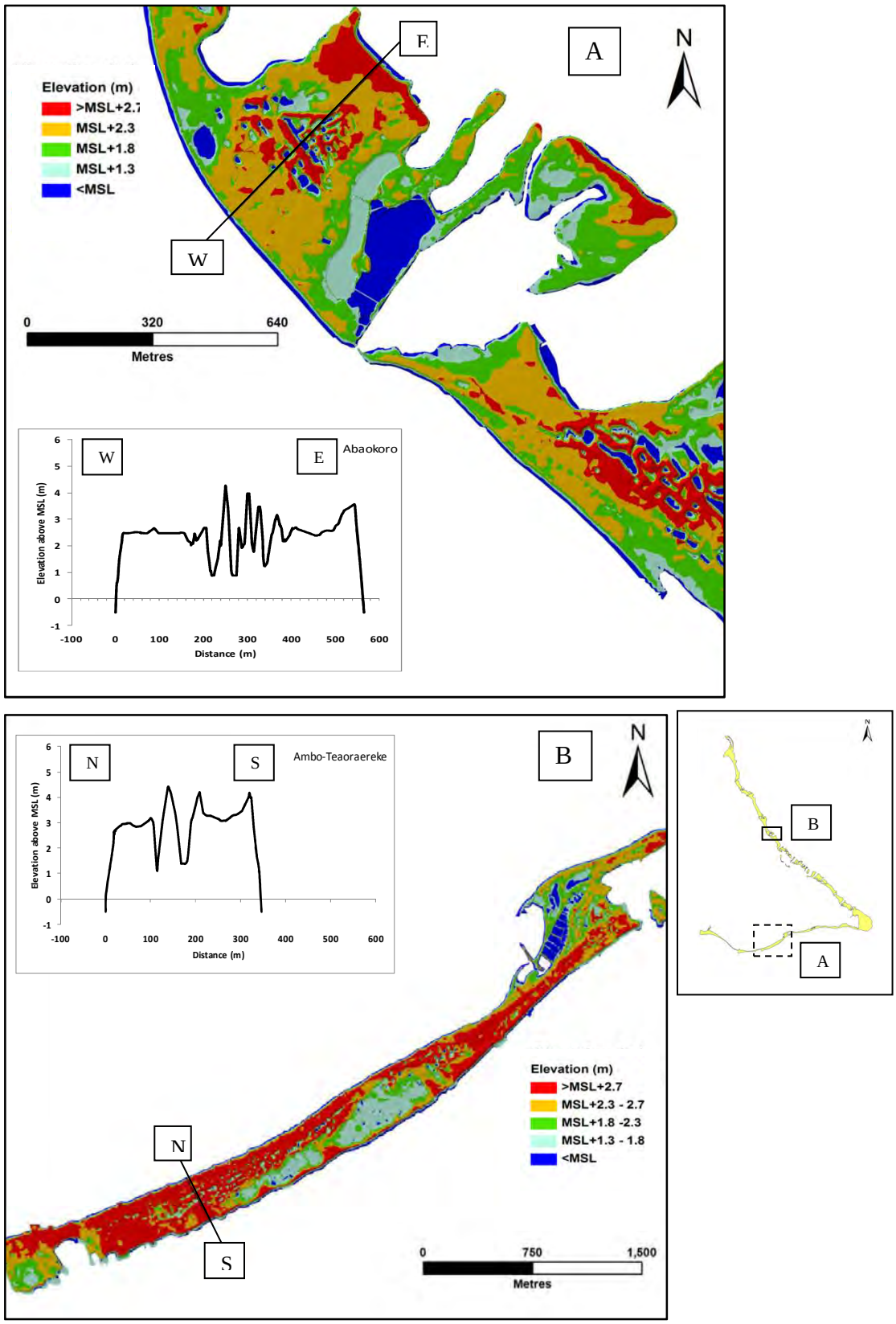

Figure 4.11. The cross island transects across Abaokoro (A) and Ambo-Teaoraereke (B) with locations in relation to other reef islands as illustrated in the Tarawa Atoll outline insert. Both possess a high ocean ridge and a lower lagoon ridge which are separated by a central depression. But the difference is that the ridges on Abaokoro, appear to be on broader area and narrower on Ambo-Teaoraereke.

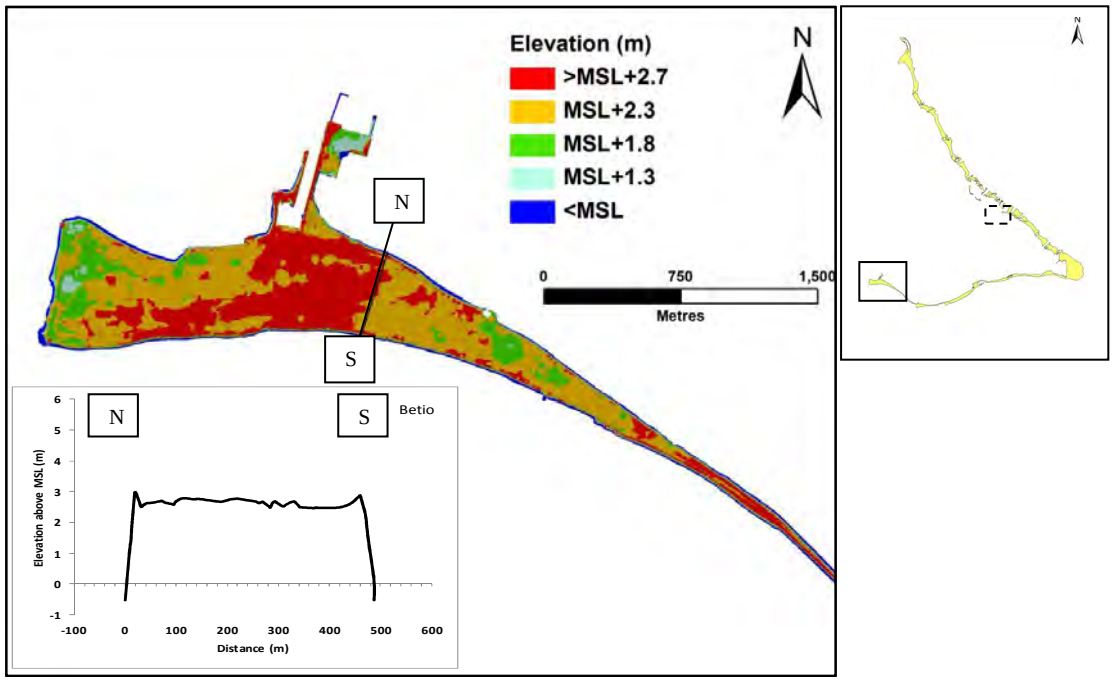

Figure 4.12. The cross island transects across Betio showing elevation variability. Location of Betio is marked as a solid square on the Tarawa outline insert. Note that Betio appears flat, as both ridges do not appear distinctive. This is most likely to occur as Betio is not directly facing the trade winds, as those reef islands in North Tarawa.

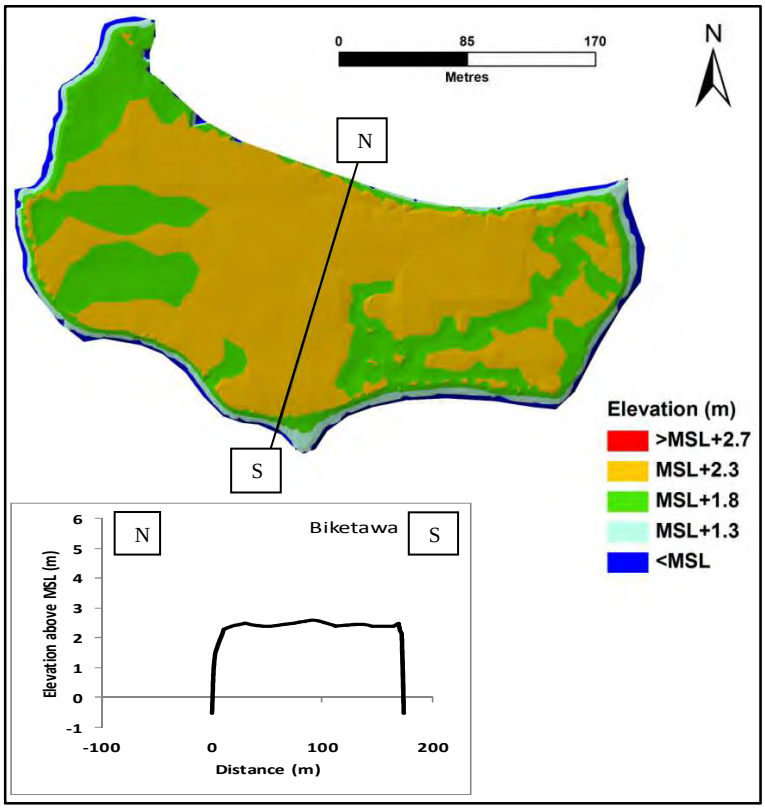

Figure 4.13. The cross island transects across Biketawa, marked as dashed outline in Tarawa Atoll outline insert. Note that the reef island appears flat with no distinctive ocean or lagoon ridge.

Analysis of spot heights shows that varying proportions lie above and below MSL (Table 4.7). The reef-island spot heights show that the proportion of points at different elevations decreases as elevation increases. The summarised data show that 93.6% of spot height points lie above 1 m above MSL, 58.4% lie above 2 m above MSL, and 10.4% lie above 3 m above MSL. The percentage significantly decreases to 0.7% with heights above 4 m above MSL and < 0.1% above 5 m above MSL. These results show that 89.6% of the area of the reef islands lies below 3 m above MSL.

Table 4.7. Summary of reef island spot heights at different elevations below and above MSL

Elevation (m) relative to SEAFRAME datum	% at different elevations
Above 1 m above MSL	93.6
Above 2 m above MSL	58.4
Above 3 m above MSL	10.4
Above 4 m above MSL	0.7
Above 5 m above MSL	<0.1

A typical profile across elongate reef islands shows the presence of two parallel shoreline ridges separated by a low-relief central area (Figure 4.10 and 4.11). The lower interior is formed naturally but can be disturbed by excavation of *babai* pits (Figure 4.10 insert I). In some cases, spoil heaps placed on the banks of *babai* pits have artificially raised the elevation of the land surface higher than the ocean ridges reaching more than 5 m above MSL (Figure 4.11 A). Reef-island transects also show that excavated pits have low-lying areas reaching MSL as the *babai* plants require water for growth. Open water ponds are also low-lying and occur backshore of the ocean ridges as illustrated in Figure 4.10A insert I. Twenty-six other reef islands also possess this type of profile: Buariki, Bonriki-Taborio, Ambo-Teaoraereke, Betio, and reef islands numbered 2, 5, 6, 8, 9, 11, 12, 14, 17, 24, 27, 28, 33, 41, 43, 44, 46, 47, 49, 50, 57, and 58. Betio has been included in this group as it does possess an ocean and lagoon ridge but they are not as prominent as the rest of the group. In addition, the central part of Betio is not as low-lying as the others as illustrated in Figure 4.12. This was also observed by Woodroffe and McLean (1992) and Solomon (1997). The remaining ten reef islands do not have a low-lying central

area. These reef islands are Biketawa, and reef islands numbered 7, 10, 13, 19, 26, 29, 45, 53, and 55 (Figure 4.13).

Less than 0.1% of the reef islands on the atoll are higher than 5.0 m above MSL (Table 4.7). These are scattered across the atoll and are only present on eight reef islands: Buariki, Bonriki-Taborio, Ambo-Teaoraereke, and the reef islands numbered 8, 11, 28, 46 and 49. These areas are located on the ocean ridges and the edges of the *babai* pits (Figure 4.11B).

Ocean ridges generally reach up to 2 to 3 m and in some places to greater than 4 m above MSL as shown by the DTM (Figure 4.11). Ocean ridges on atolls are built as a result of a combination of factors which include exposure to wind and extreme wave events (McLean, 2011). The only two reef islands in the far western end of Tarawa, Betio and Bairiki do not have ocean ridges higher than 2 m above MSL. This may be related to a combination of factors involving their location away from the high energy areas in the east and the fact that most of the ridges have been with buildings for decades. In some areas, the ocean ridges extend almost the length of the reef island, such as in Tabiteuea where the ocean ridge covers about 90% of the reef islands length of 2900 m (Tables 3.3 and 4.9). This high and extensive ocean ridge is very important as it protects the reef island from high-energy waves. However, not all reef islands have these extensive high ocean ridges. An example of these reef islands not having an extensive high ocean ridge is Buariki (Figure 4.10A).

In the centre of some reef islands, spoil materials removed to create pits for *babai* cultivation are dumped on the banks of the pits raising the level of land artificially such that it reaches 4 m above MSL or higher (Figure 4.10A, Figure 4.11 and Figure 4.15B). In Ambo-Teaoraereke, on South Tarawa, numerous *babai* pits are present making areas within this central part of this reef island abnormally high (Figure 4.14A and Figure 4.15A). Some of these places are situated close to the lagoon are higher than the ocean ridge as shown in Figure 4.10B. The highest spot on Tarawa Atoll is situated on this reef island facing the lagoon side is also a result of this human activity (Figure 4.10B) with evidence of this abnormality shown on the DTM (Figure 4.10B).

Figure 4.14. Examples of low-lying areas below 2 m above MSL. A: Lagoon beach on Notoue. B: A depressed area located on the centre of Bonriki-Taborio reef island. Note the bus on an elevated area on the lagoon side due to human-induced changes.

Figure 4.15. Examples of elevated areas above 3 m above MSL. A: Ridges on the ocean side of Tabiteuea show that high. B: Spoils deposited on the banks of pits raising the land artificially in the background and around an area on Bonriki-Taborio.

4.3.3 Hypsometric curves

Table 4.8 summarises the elevation results for the 36 reef islands studied (See Appendix A-1 for the distribution of elevation for individual reef islands). The elevations for the remaining 23 reef islands cannot be determined, as the reef islands have no or low coverage of spot heights. All of these reef islands are small with areas ranging from 0.02 ha to 4.65 ha. Predominantly reef islands of Tarawa Atoll are lower than 2 m above MSL and rarely reach above 5 m above MSL (Table 4.9). It was not possible to capture the highest spot height of 5.05 m above MSL (6.687 m above SEAFRAME datum) largely due to the limitation of the interpolation method, as high elevations are only represented by single spot heights.

There are two reasons why this occurs: the first is that the grid cell has been set at 50 m by 50 m, and the second is that the IDW method interpolates the unknown value of this grid cell using the 12 closest neighbours. The highest elevation reported is surrounded by spot heights of lower elevations predominantly 4 m above MSL. The

application of the IDW calculates an elevation for the grid cell that is an average of these 12 spot heights. This issue is a common artefact in the generation of DTMs and is known as a padi-terrace, where the highest points are cut off in areas where data density is low (Reuter *et al.*, 2009). One way of addressing this is to increase the density of spot heights within this data poor area when a resurveying opportunity arises (Leon, 2010). Another way is to include breaklines that would show this feature in more detail. Breaklines for example waterlines can be considered as contours as they successfully indicated emerged parts of the reef flat such as palaeo reef flat, cemented rubble/pavement and a prominent high ridge (Yamano, 2007). These features extracted from synthetic aperture radar (SAR) sensor data and other satellite imagery were used to provide additional data in which the topography of reef platforms could be constructed (Yamano *et al.*, 2006; Yamano, 2007).

The average proportion of reef islands above 2 m above MSL is 77% (Table 4.9). There is only one reef island that does not reach above 2 m above MSL and that is reef island number 7. There are 23 reef islands which have more than 50% of their elevations reaching above 2 m above MSL. These reef islands are Betio, Bairiki, Abairaranga, and Tanaea, South Tarawa, and Taratai, Abaokoro, Tabonibara, and reef island numbers 13, 17, 19, 24, 26, 27, 28, 29, 33, 42, 43, 44, 45, 46, 47, and 49 from North Tarawa. Seven reef islands, namely 13, 19, 26, 29, 33, 42 and 53, are all above 2 m above MSL. These reef islands are small, mainly located in the North Tarawa and are uninhabited (Table 3.3).

There are six reef islands that have elevations above 4 m above MSL comprising Buariki, Marenanuka, Tabiteuea, Buota, Bonriki-Taborio and Ambo-Teaoraereke (Table 4.9). The average proportion of elevations of reef islands above 4 m above MSL is less than 0.1%. Buota, located on North Tarawa with 0.1% has the highest proportion above 4 m above MSL, but this may be related to the spoils of the numerous *babai* pits present on the reef island (Table 4.9). No elevations on the reef islands appeared higher than 4.4 m above MSL (Table 4.9). This is due to the low density of spot heights with higher elevations as they were averaged out in the making of the DTM (Table 4.9). This is a limitation of the interpolation method as higher elevations are generally only represented by single spot heights.

Table 4.8. Reef island characteristics with hypsometric curves including areas and individual volumes based on hypsometry derived from raster DTM. Elevation is relative to MSL (m)

ID	Name	Location (N/S)	Inhabited (Y/N)	Hypsometric curve	Highest elevation) (m)	Lowest elevation (m)	Area (ha)	Volume (m^3)
1	Buariki	N	Y	Concave	4.1	0.2	390	6,182,723
2	Nuatabu	N	Y	S	3.4	-0.1	67	1,292,381
5	Tebangaroi	N	Y	S	3.2	1.0	71	1,318,216
6	Taratai	N	Y	S	3.7	0.6	178	3,576,720
7		N	N	Platform	2	1.6	5	45,834
8	Notoue	N	Y	S	3.9	1.3	120	2,626,344
9	Abaokoro	N	Y	S	3.6	1.9	33	612,436
10		N	N	Platform	2.7	1.5	9	91,713
11	Marenanuka	N	Y	S	3.9	0.7	103	2,181,883
12	Tabonibara	N	Y	S	3.7	1.8	45	821,331
13		N	N	Platform	2.7	2.2	2	14,920
14		N	N	S	3.1	1.0	15	168,862
17		N	N	S	3.4	1.7	17	255,944
19	Bikenamori	N	N	Platform	2.6	2.1	10	85,566
24		N	N	S	2.9	1.7	5	42,922
26	Bikenikaibuke	N	N	Platform	2.7	2.2	7	15,127
27	Kairiki	N	N	S	3.4	1.5	35	563,691
28	Kainaba	N	Y	S	3.7	1.9	29	649,033
29		N	N	Platform	3.0	2.2	3	15,413
33	Bikenubati	N	N	S	3.6	2.2	11	203,793
41	Nea	N	N	S	2.8	1.0	14	203,218
42	Biketawa	N	N	Platform	2.7	2.0	6	101,072
43	Nabeina	N	Y	S	4.0	1.8	36	827,487
44	Tabiang	N	N	S	3.6	1.3	85	1,936,045
45	Tabuki	N	N	Platform	3.0	1.9	31	671,298
46	Tabiteuea	N	Y	S	4.1	1.3	104	2,446,393
47	Abatao	N	Y	S	3.2	1.2	80	1,721,155
49	Buota	N	Y	S	4.1	1.2	88	2,070,865
50	Tanaea	N	Y	S	3.0	1.2	8	127,410
52	Bonriki-Taborio	S	Y	Concave	4.4	0.8	863	17,841,469
53	Abairaranga	S	N	Platform	2.4	2.3	1	6,875
55	Abaokoro	S	N	Platform	2.4	1.5	3	25,486
56	Ambo-Teaoraereke	S	Y	S	4.4	1.3	181	3,813,413
57	Nanikai	S	Y	S	2.7	0.8	15	112,322
58	Bairiki	S	Y	S	3.4	0.7	59	1,036,478
59	Betio	S	Y	S	3.5	1.8	167	3,875,979
							2900	**57,561,625**

Table 4.9. Proportion of elevations across Tarawa Atoll above MSL based on hypsometry derived from the DTM.

ID	Reef Island	% of areas above MSL (m)										
		1	1.2	1.4	1.6	1.8	2	2.2	2.4	2.6	2.8	3
1	Buariki	69	60	51	40	31	25	19	13	10	7	5
2	Nuatabu	95	91	85	75	63	51	38	18	6	3	1
5	Tebangaraoi	100	97	91	80	68	54	37	17	5	2	0.3
6	Taratai	96	92	85	74	62	45	30	19	10	4	2
7		100	100	100	100	43	0	-	-	-	-	-
8	Notoue	100	100	99	95	84	71	60	41	21	11	7
9	Abaokoro	100	100	100	100	100	97	89	61	18	6	4
10		100	100	100	99	88	58	43	23	1	0	
11	Marenanuka	99	97	92	84	75	64	47	31	21	9	5
12	Tabonibara	100	100	100	100	100	97	93	78	53	29	10
13		100	100	100	100	100	100	100	77	12	0	-
14		100	99	97	91	69	34	9	4	2	1	0
17		100	100	100	100	99	93	71	30	16	7	3
19		100	100	100	100	100	100	97	30	0	-	-
24		100	100	100	100	99	95	87	36	14	2	0
26		100	100	100	100	100	100	100	82	33	0	-
27	Kairiki	100	100	100	99	97	95	86	63	38	17	7
28	Kainaba	100	100	100	100	100	99	98	95	85	72	50
29		100	100	100	100	100	100	100	81	46	12	0
33	Bikenubati	100	100	100	100	100	100	100	76	51	26	12
41	Nea	100	98	95	81	70	47	23	14	5	0	-
42	Biketawa	100	100	100	100	100	100	77	58	1	0	-
43	Nabeina	100	100	100	100	100	96	90	79	69	29	15
44	Tabiang	100	100	99	97	94	90	80	58	42	26	15
45	Tabuki	100	100	100	100	100	98	82	61	31	3	0
46	Tabiteuea	100	100	99	98	96	88	77	60	36	25	14
47	Abatao	100	100	95	87	81	71	55	28	8	2	0.3
49	Buota	100	100	98	92	83	71	55	43	34	28	22
50	Tanaea	100	100	98	95	91	85	77	60	9	2	0
52	Bonriki-Taborio	98	91	75	63	54	42	32	22	13	8	5
53	Abairaranga	100	100	100	100	100	100	100	100	100	-	-
55	Abakoro	100	100	100	99	89	68	18	0	-	-	-
56	Ambo-Teaoraereke	100	100	99	93	87	78	67	55	43	26	13
57	Nanikai	99	98	97	91	77	55	27	3	0	0	-
58	Bairiki	99	98	98	97	95	90	84	64	45	8	1
59	Betio	100	100	100	100	100	98	93	75	43	16	2
	Average	**99**	**98**	**96**	**93**	**86**	**77**	**67**	**47**	**27**	**12**	**7**

Table 4.9 continued. Proportion of elevations across Tarawa Atoll above MSL based on hypsometry derived from the DTM.

ID	Reef Island	% of areas above MSL (m)						
		3.2	3.4	3.6	3.8	4.0	4.2	4.4
1	Buariki	2	0	0	0	0	-	-
2	Nuatabu	0	0	-	-	-	-	--
5	Tebangaraoi	0	0	-	-	-	-	-
6	Taratai	1	0	0	-	-	-	-
7		-	-	-	-	-	-	-
8	Notoue	3	1	1	0	-	-	-
9	Abaokoro	2	0	0	-	-	-	-
10		-	-	-	-	-	-	-
11	Marenanuka	3	2	1	0	0	-	-
12	Tabonibara	4	1	0	-	-	-	-
13		-	-	-	-	-	-	-
14		0	-	-	-	-	-	-
17		1	0	-	-	-	-	-
19		-	-	-	-	-	-	-
24		-	-	-	-	-	-	-
26		-	-	-	-	-	-	-
27	Kairiki	2	0	-	-	-	-	-
28	Kainaba	24	5	2	0	-	-	-
29		-	-	-	-	-	-	-
33	Bikenubati	2	0	0				
41	Nea	-	-	-	-	-	-	-
42	Biketawa	-	-	-	-	-	-	-
43	Nabeina	8	4	1	0	0	-	-
44	Tabiang	5	1	0	-	--	-	-
45	Tabuki	-	-	-	-	-	-	-
46	Tabiteuea	7	3	1	0	0	0	
47	Abatao	0	0	-	-	-	-	-
49	Buota	17	11	6	3	0	0	-
50	Tanaea	0	-	-	-	-	-	-
52	Bonriki-Taborio	3	1	1	0	0	0	0
53	Abairaranga	-	-	-	-	-	-	-
55	Abakoro	-	-	-	-	-	-	-
56	Ambo-Teaoraereke	5	1	0	0	0	0	0
57	Nanikai	-	-	-	-	-	-	-
58	Bairiki	1	0	-	-	-	-	-
59	Betio	0	0	0	-	-	-	-
	Average	**4**	**1**	**1**	**>0.1**	**>0.1**	**>0.1**	**>0.1**

Examination of the distribution of elevation across each individual reef island shows that there are three types of hypsometric curve (Appendix A-2 which shows the hypsometric forms of each individual reef island). These curves have been classified as concave, S (which looks "S" shaped) and platform are explained below (Figure 4.16). The concave curve defines reef islands with high elevation variability and where a significant percentage of the reef island is low-lying. The S curve defines reef islands that have a significant proportion of low-lying areas but lower than the concave curve. This curve shows that elevation variability is high, with a large proportion of low-lying areas, and small proportion of elevated areas. The platform curve defines reef islands with flat surfaces.

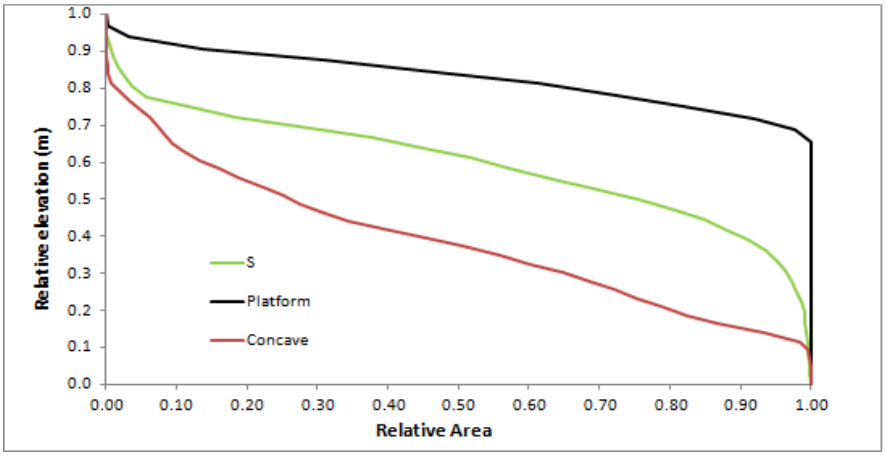

Figure 4.16. Hypsometric curves illustrating distribution of area for reef islands of Tarawa Atoll. The different forms are representative examples of each type: "S" (Nuatabu), platform (Tabuki) and concave (Buariki).

The majority of the reef islands show the S hypsometric form (Figure 4.17, Figure 4.18 A). This group comprises 24 (67%) reef islands, namely Betio, Bairiki, Nanikai, Ambo-Teaoraereke, Tanaea, Marenanuka, Tabiteuea, Abatao, Buota, Nuatabu and the reef islands numbered 5, 6, 8, 9, 12, 14, 17, 24, 27, 28, 33, 41, 43 and 44 (Table 4.8). The lower part of the S curve for each reef island has values that range from 0.1 m below MSL (Nuatabu) to 2.2 m above MSL (Bikenubati) (Table 4.8), indicating that some of these reef islands are at greater risk from sea-level rise than others. The maximum elevation ranges from 2.7 m (Nanikai) to 4.4 m (Ambo-Teaoraereke) above MSL (Table 4.8).

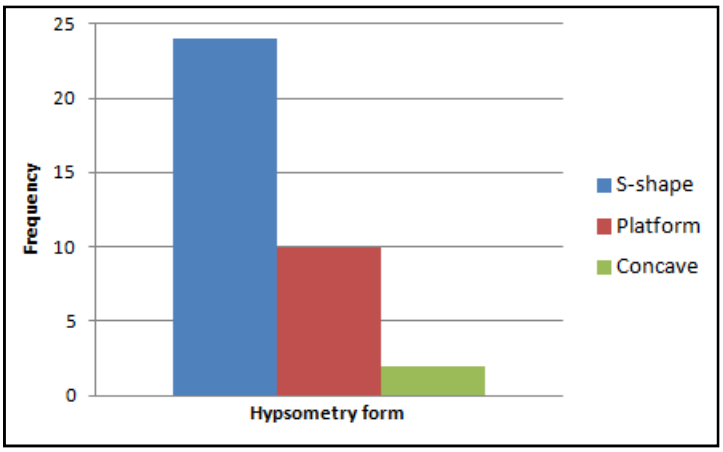

Figure 4.17. Frequency histogram of the hypsometry types

The next most common hypsometric form is the platform shape comprising 10 (28%) of the reef islands studied (Figure 4.17, Figure 4.18B). This includes Abaokoro in South Tarawa and reef islands numbered 7, 10, 13, 19, 26, 29, 42, 45 and 53 in North Tarawa (Table 4.8). All of these reef islands including Abaokoro in South Tarawa are uninhabited (Table 3.3). The majority of these reef islands (91%) are located in central North Tarawa. The lower elevations for these reef islands range from 1.5 m (Abaokoro and reef islands numbered 10) to 2.3 m (Abairaranga) above MSL. The maximum elevation ranges from 2.0 m (Abaokoro-South Tarawa and reef islands 7) to 3.0 m (reef islands numbered 29 and 45) above MSL. These results show that the variability in elevation is low for these types of reef islands. The platform shape of these reef islands indicates that there are no natural low-lying areas or *babai* pits present. These reef islands are too small to have depressed central areas with lengths and widths less than 600 m and 300 m respectively (Table 3.3). Reef islands are required to have more than 100 m in width for the formation of a freshwater lens, which will support *babai* cultivation (Whitehead and Jones, 1969). In this situation, the reef islands may be too small to support a community or in the case of *babai* cultivation, too rocky for excavation.

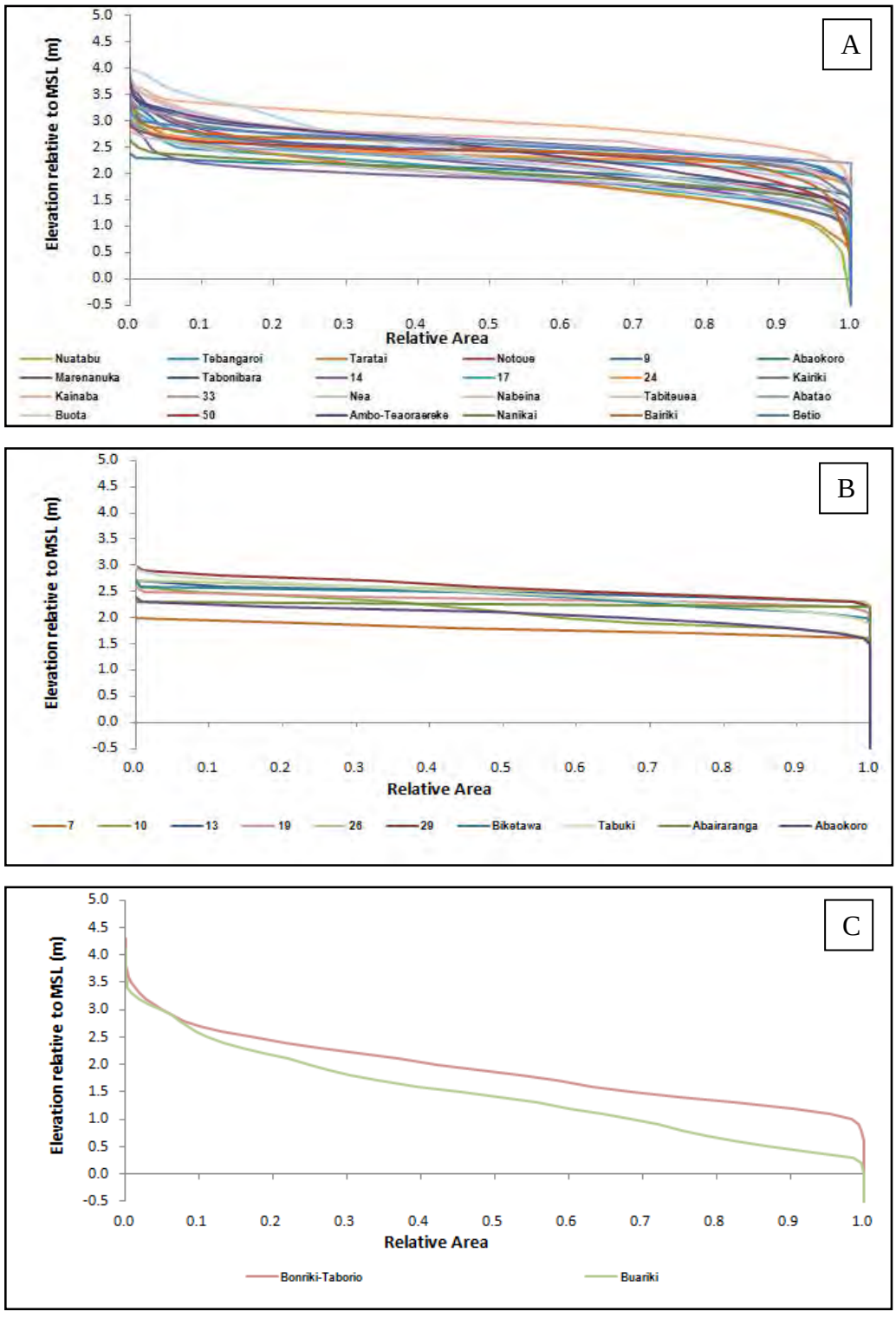

Figure 4.18. Graphs showing the three different hypsometric forms. A represents the S-shaped reef islands, B the platform reef islands and C the concave forms.

The least common form is the concave (Figure 4.17, Figure 4.18C). This group consists of only two reef islands (5%) but these reef islands are the longest and widest reef islands: Buariki and Bonriki-Taborio (Table 4.8). The elevation ranges from 0.2 m above MSL (Buariki) to as high as 4.4 m above MSL (Bonriki-Taborio).

The lower elevation ranges from 0.2 m (Buariki) to 0.8 m (Bonriki-Taborio) above MSL (Table 4.8). This low elevation indicates that the reef islands have many low-lying areas that are below or slightly above MSL. In Buariki, these areas include the *babai* pits, the pond, the low-lying spit on the northern tip of the reef island facing the ocean and the open water pond located close to the ocean beach (Figure 4.11A, insert I). These open water ponds are also found in some other reef islands. In Bonriki-Taborio, these areas include the swampy reclaimed area on the reef islands eastern end. The highest elevation ranges from 4.1 m (Buariki) to 4.4 m above MSL (Bonriki-Taborio) (Table 4.8). The low proportion of high elevations is related to the ocean ridges and pit spoils dumped on the ground artificially raising the elevation. Both reef islands are located at the corner of the atoll so they are wider (Richmond, 1993).

4.3.1 Sediment volume

Table 4.8 summaries the first-order estimate of sediment volume for the 36 individual reef islands studied (See Appendix A-2 for sediment volumes at different elevations). These volumes show the available sediment present down to the base of the beach as of 1998, including the reclamations that may extend beyond the base of the beach. The total sediment that has accumulated on the reef flat based on these 36 reef islands is 57,581,124 m^3. The total sediment volume is slightly higher than what would have been calculated as the elevation of the reef flat is not established at 1.166 m but at 1.19 m above SEAFRAME (0.77 m above UH datum) as the contours are provided in 0.1 m intervals. As this is a first-order estimate and given that the reef flat varies in elevation, this volume is considered to be appropriate. The reef islands that are not included are the small reef islands close to the reef rim including those on North Tarawa's central rim. They would have slightly increased the volume as they contribute a total area of 16 ha which is 0.56% of the total area of the reef islands of Tarawa Atoll. The volume of individual reef islands ranges from as low as 6,875 m^3 (Abairaranga) to as high as 17, 841,469 m^3 (Bonriki-Taborio) with a mean volume of 1,599,476 m^3 per reef island. The contribution of reef islands located in the northern (n=29) and southern sections (n=7) is 54% and 46% respectively.

To investigate the relationship between area (y) and volumes (x), and how it relates to the different hypsometry form, a plot is developed of the area (Table 3.3) and

volumes of each reef island (Table 4.9). A linear relationship expressed as y = 49.3x exists between the area (y) and volume (x) of each reef island. This suggests that for the volume (x) is 49.3 times that of the area (y) (Figure 4.19). The high R^2 value of 0.99 indicates that a strong relationship exists between the area and volume of each individual reef island. Another plot of reef islands, excluding the large reef islands of Buariki and Bonriki-Taborio has been developed (Figure 4.20).

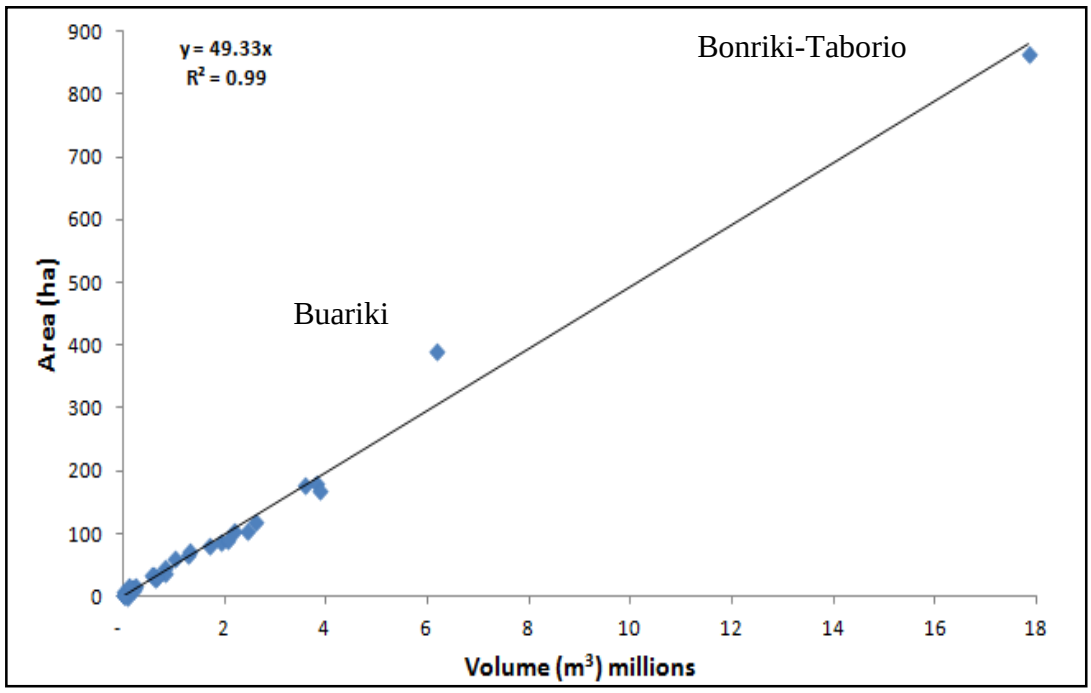

Figure 4.19. Graph plotting the volume of reef islands against the area shows a linear relationship y = 49.3x. Buariki lies well above the line whilst Bonriki-Taborio lies below the line.

According to the different hypsometric forms, eleven S-shaped reef islands lie above the line and they are Nuatabu, Tebangaroi, Tabonibara, Nanikai, Bairiki and the reef islands 14, 17, 24, 33, 41 and 50). Another ten lie below the line and they are Notoue, Abaokoro, Ambo-Teaoraereke and the reef islands numbered 11, 28, 43, 44, 46, 47 and 49. The remaining three, Betio, Taratai and Kairiki lie close to the line. For the platform reef islands, eight reef islands lie above the line and they are Abaokoro (South Tarawa), Bikenamori and the reef islands numbered 7, 13, 19, 26, 29 and 45). Platform reef island Abairaranga lies above the line, whereas reef island number 7 lies below the line. Figure 4.19 shows that the concave reef islands Bonriki-Taborio and Buariki vary. Buariki lies well above the line, whereas Bonriki-Taborio lies below. The results show that there is variation with hypsometry forms

as predominantly platform reef islands lie above the line whilst S-shaped and concave reef islands vary.

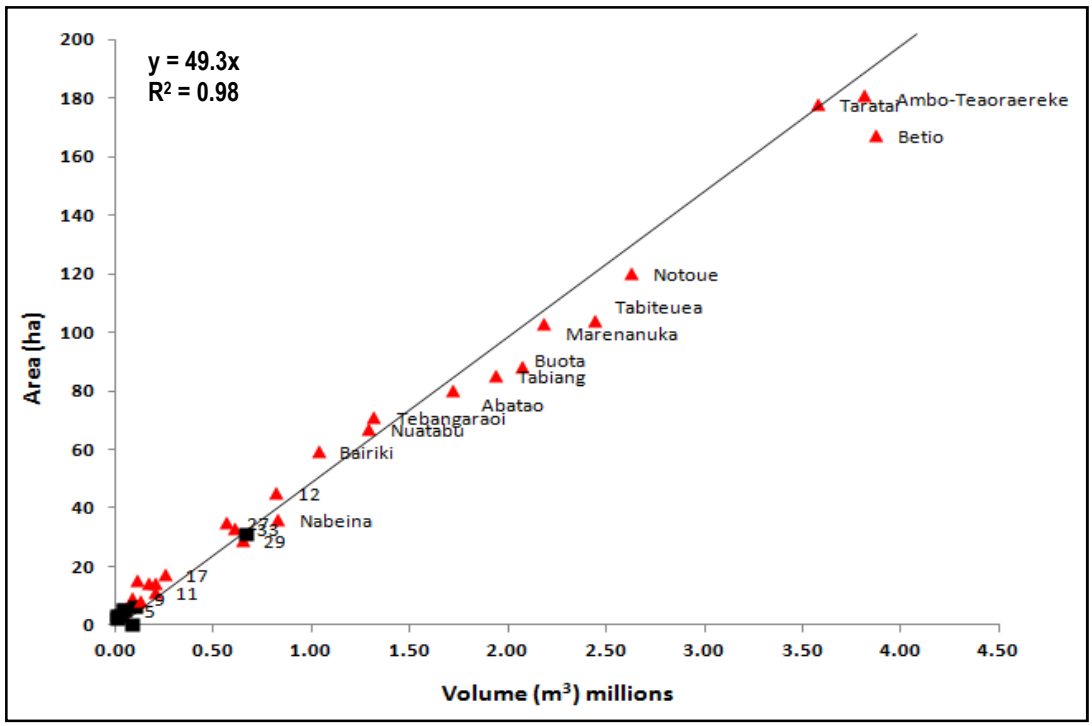

Figure 4.20. The relationship between area and volumes of different reef islands based on hypsometry. S-shaped reef islands are represented by red triangles and platform reef islands are represented by black squares.

Figure 4.21 illustrates the three hypsometric forms plotted with lagoonal extreme water levels generated from a low emission scenario B2 from IPCC AR4 (IPCC, 2007) and a 1980-1990 baseline year average of the IPCC relative to SEAFRAME datum (Table 4.5) (see Appendices A-2 for each individual reef island). The lagoonal extreme water levels have been applied to demonstrate the proportion of areas at risk within each hypsometric form. The results show that low-lying areas below 0.891 m and 1.004 m above MSL are at risk from these extreme water levels. The concave forms (Figure 4.21C) and the S-shaped (Figure 4.21A) are at greater risk compared to the platform shape (Figure 4.21B). However this approach is limited in showing the location of the low-lying areas within the reef-island and whether or not they are directly connected to the water levels on the ocean and lagoon sides (Figure 4.21).

4.3.2 Areas at risk from extreme water levels

It is important to understand that extreme water levels that have been used in this report are averages of the 33-year tidal record. This means that the extreme water

levels plotted on the cross-island transect do not show the highest and lowest water levels but the mean and the elevations on land that they reach.

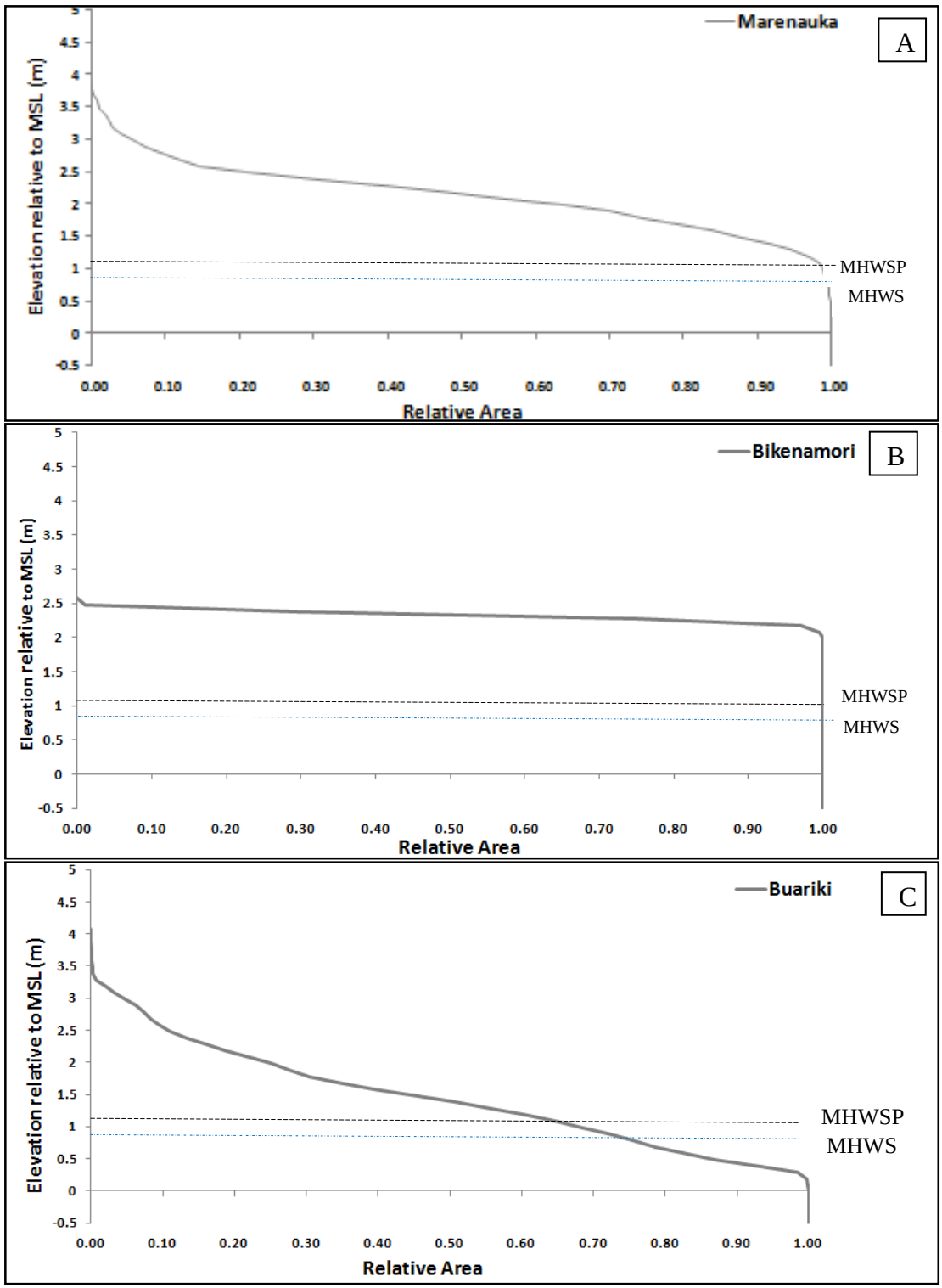

Figure 4.21. Different hypsometric forms plotted with extreme lagoonal water levels of Mean High Water Spring (MHWS) and Mean High Water Spring Perigean (MHWSP) generated from emission scenario B2 and a 1980-1990 baseline year average of the IPCC relative to SEAFRAME datum. A: An "S" curve; B: platform shape representing a reef island with no low-lying areas and; C: concave curve.

The selection of reef islands to be examined is based on the three hypsometry forms. The cross-island transects of these selected reef islands are plotted with the projected extreme water levels showing the heights of these water levels in relation to each different reef-island type (Figure 4.22). The cross-island transect of Bonriki-Taborio reef island on its far eastern side shows that a large proportion of the land is low-lying below the projected MHWS, 0.891 m above MSL (equivalent of 2.528 m above SEAFRAME datum) (Figure 4.22A). This is based on the cross-island transect taken across the widest part of the reef island on its far eastern side which accommodates a large population as well as Government assets. There are current plans to develop this area to house more Government employees. The transect shows that these low-lying areas located in the middle of the reef island are protected from flooding and inundation by a narrow strip of land on the lagoon side. Lagoonward areas are generally low and directly connected to the lagoon water making them vulnerable to sea-level rise. This indicates that location and connectivity to water can increase the risk from inundation.

The reef islands of Taratai and Betio (S-type) show that a larger proportion of the reef islands are above the level of projected storm tides and surges (Figure 4.22B and C). The cross-island transects show that Taratai has broader ridges on the lagoon sides protecting the low-lying areas from inundation and flooding. Betio, on the other hand, has less distinctive ocean and lagoon ridges. Both these reef islands appear to be at lower risk from these projected extreme water levels; however, it is anticipated that with future sea level rise, many areas on Betio will be at risk from flooding and overtopping due to the increasing development and population pressures modifying the coastal areas, and in turn reducing the elevation of the beach ridge.

These results reinforce the significant role that ocean and lagoon ridges play in protecting the reef island interior from extreme water levels. The ocean ridges are created by high water events, and are higher in North Tarawa as it is more exposed to the wind and to storm surges compared to the western end. The elevation of the ridge is very important in relation to waves and water levels. The lower the elevation of the ridge is, the greater the risk of areas behind it being flooded or inundated. Conversely, the higher the ridge, the lower the risk to other areas on the reef island

from flooding or overwash. Only two reef-islands (Bonriki-Taborio and Taratai) have high ocean ridges protecting the reef islands from wave impacts. The lagoon ridge of Bonriki-Taborio appears to be at risk of inundation from storm tides and MHWSP. With projected extreme water levels, low-lying lagoon areas are shown to be at greater risk (Figure 4.22A and B). Another factor that needs to be considered is that some ridges are very narrow and can be at risk from erosion, which would allow water to flood low-lying areas within the reef island and affect the ground water. This emphasizes the importance of maintaining the ocean and lagoon ridges, especially where beaches are narrow, so that these reef islands can be protected from projected increases in sea level. As people prefer to live in these sheltered areas away from the easterly trade winds they are therefore placed at greater risk.

4.4 Discussion

The DTM has met the objective of the study by allowing the distribution and variability of elevation to be examined as well as determining the volume of sand sequestered on the individual reef islands by slicing the reef island area at an interval of 0.1 m and obtaining nearly 60 million m^3 of sediment. Based on the fitness for use concept (Fisher and Tate, 2006), the model has demonstrated that it has achieved that, however it does have some limitations such as not being able to capture the highest points on the reef island. But this can be improved in the future by collecting more spot heights thus increasing the density of data within the poor data area.

The cross-island transects of the reef islands of Tarawa Atoll show a general morphology comprising of an ocean ridge and a lagoon ridge with a central depressed area. Twenty five reef islands out of the 36 studied in detail possess a prominent oceanward ridge and a low-lying lagoon ridge separated by a central depression, similar to other atoll reef islands in the Pacific and Indian Oceans. Betio, a densely populated reef island, which is included in this group, has less distinctive ocean and lagoon ridges. Ocean ridges have elevations between 2 to 3 m and in some places greater than 4 m above MSL. These ocean ridges are lower than those reported by Woodroffe (2008) in Tuvalu and most of the Indian Ocean reef islands with the exception of the Maldives.

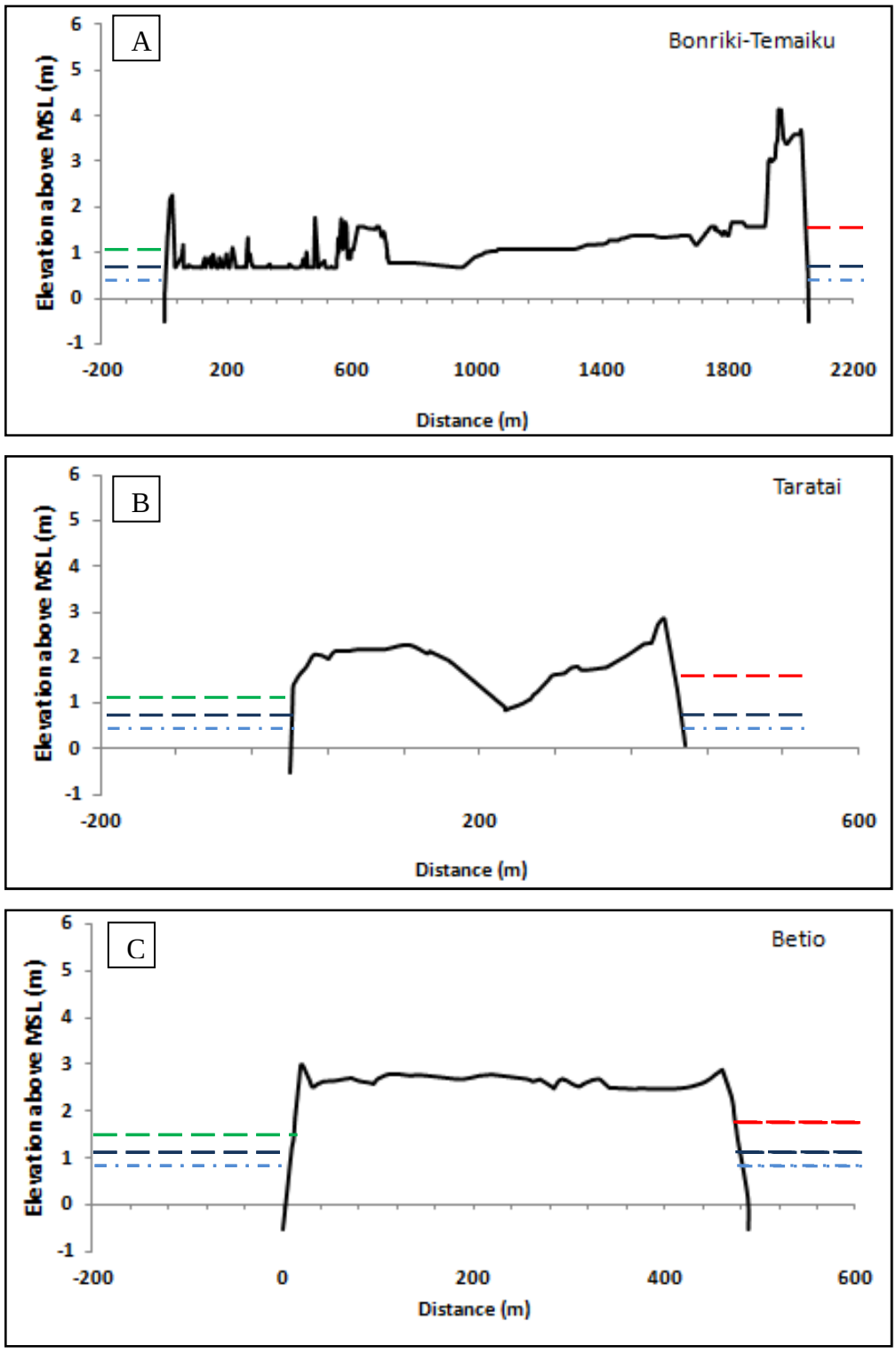

Figure 4.22. Examples of concave (Bonriki-Taborio (A)), S (B-Taratai (B)and Betio (C) forms plotted with water levels applying the climate change scenario using the timeframe Tibu (2012-2036) and low emission scenario B2. The elevation heights (m) are relative to MSL.

The difference in the elevation of the ocean ridges on Tarawa Atoll compared to those investigated by Woodroffe (2008) is that Tarawa Atoll does not lie within the cyclone belt where greater wave energy is largely responsible for the higher ocean ridges (Forbes and Hosoi, 1995). The elevations of the lagoonward ridges facing away from the wind are generally 1.5 to 3 m above MSL. *Babai* pits on some reef islands generate the lowest elevations reaching below MSL similar to that observed in Tuvalu and earlier studies on Tarawa Atoll (Yamano *et al.*, 2007; Woodroffe, 2008). The spoil heaps dumped beside the pits are the highest points on many reef islands reaching up to 5 m above MSL, which has also been observed in Tuvalu (Yamano *et al.*, 2007). The remaining 10 reef islands appear flat and are uninhabited. These reef islands have elevations ranging from 1.5 m to 2.6 m above MSL, which suggests they are at less risk from inundation and flooding when compared to S-shaped and concave reef islands.

Based on the distribution of elevation across all reef islands, the proportion of land area above 2 m above MSL is 77%. This value is greater than the 34% indicated by Woodroffe (2008) for the Gilbert chain and Tuvalu reef islands (Table 4.1). The percentage of reef island area 3 m above MSL is only 7%, similar to the reported values for all studied reef islands from Pacific and Indian Ocean atolls that range from 1 to 8%. It should be noted that percentages presented by Woodroffe (2008) are an average of elevations taken from either a single profile or several profiles across reef islands. This study represents an improvement on that approach as it captures elevation classes across 36 reef islands rather than basing the elevation distribution on a single cross-island transect. However, it is limited in capturing the highest elevation, as this only occurs at a few spot heights.

Two approaches have been taken to examine the topography of the reef islands, one investigates the distribution of elevation classes across individual reef islands (hypsometry), and the second extracts cross-island transects from a DTM. The hypsometric approach uses a visual summary permitting the entire reef island topography to be assessed using a cumulative elevation-area curve, which provides an estimate of the proportion of an area above and below certain water levels. This approach shows three different categories of reef islands: S-shaped, platform and

concave. Reef islands that are flat are portrayed as platforms and do not have low-lying areas, whereas the S-shaped and concave forms do, and may be at greater risk from high tide levels and other extreme water levels. However, this approach is limited in showing how vulnerable these low-lying areas are for two reasons. The first is that the results show the distribution of elevation classes, but do not show where the low-lying areas are situated within the reef island, and whether or not they are directly connected to water. In some cases, low-lying areas are situated in the centre of the reef islands and are protected by ocean or lagoonward ridges, which make them less vulnerable to sea-level rise. As sea level rises, however, the ground water table may be shifted closer to or above the surface creating an open pool at the ground surface (Burns, 2000) and eventually turning these low-lying areas to swamps. The second reason is that the coastal calculator developed for Tarawa shows that there is a difference between the lagoon and ocean extreme water levels, and therefore one single extreme water level cannot be applied directly to each hypsometric curve. In addition, variability in both lagoon and ocean side due to storm tides as well as variability in the ocean side due to storm surges only makes it difficult to model this directly onto the different curves. However, the hypsometry classification provides a good way to classify the reef islands based on the distribution of elevation. This can also be used as a means to select reef islands with high elevations and those with low elevations when investigating the reef islands risks of inundation from extreme water levels.

The benefit of this approach is that the percentages of areas that are above and below different elevations can be represented visually. In contrast, the cross-island transects provide more detailed information with regards to the different elevations and the level on land that extreme water levels can reach. With this approach, different water levels can be applied depending on where the reef island is located on the atoll. In some cases, the profiles show that low-lying areas within the reef island or those that are immediately backshore from ridges are protected from wave impacts by ocean and lagoon ridges. This reaffirms the importance of these ridges, however, in some instances these ridges are narrow increasing the vulnerability of areas immediately backshore of the ridges to overwash.

Elevations of ocean and lagoon ridges appear to vary across the atoll. In North Tarawa Atoll the ridges appear to be on broad areas compared to those on South Tarawa which could be a result of the wind and wave activity. North Tarawa ocean ridges are directly facing the trade winds, and are exposed to higher wave setup which occurs in storms that generate waves of 0.9 m higher compared to those on the southern coast and 0.14 m higher than those on the western coast of the atoll as shown by the coastal calculator (Ramsay *et al.*, 2010). In South Tarawa, these ridges appear to be narrower. As activities such as beach mining removing large volumes of sediment directly from the beaches is anticipated to increase in the future, the elevations of these ridges will be lowered increasing the risk of low-lying areas present behind these ridges from overwash and inundation. With the current significant removal of sediment from beaches in South Tarawa to meet the growing demand for aggregate for use in development (Geer Consulting Services, 2007; Peletikoti, 2007) it is more than likely that this will result in a reduction of the elevation of the ocean and lagoon ridge. This suggests that anthropogenic modification of the shoreline also contributes to the increasing risk of overwash and inundation in low-lying areas.

4.5 Summary

The chapter has examined the morphology of 36 reef islands in Tarawa Atoll using digital terrain analysis. The total volume of sediment that has accumulated to form these reef islands is nearly 60, 000, 000 m^3. The distribution of elevation shows that a significant proportion (77%) of the land on these reef islands lies above 2.0 m above MSL. On average, less than 10% of the reef island lies above 3 m above MSL, much of which is located on artificially raised grounds (*babai* spoils) and on the ocean beach ridges. The proportion of land above 4 m above MSL is less than 0.1%. With present Higher Astronomical Tide water levels, the low areas that are directly connected to the lagoon and those located behind narrow ridges are already at risk. In South Tarawa, low-lying areas will be placed at greater risk from wave impacts and inundation as the removal of sediment directly from beaches is anticipated to increase in the future to meet the growing demand for construction material. This activity should be stopped immediately as it will have an adverse impact on the reef islands, increasing the risk of inundation of low-lying areas

directly connected to the water or those behind the ridges as a result of high tides and extreme water levels. The cross-island transects show that ocean and lagoon ridges protect interior areas from wave impacts; however, not all reef islands are protected by elevated ocean ridges and those that are not are more likely to be at risk from wave impacts. Ocean ridges, especially those in urban areas, that have been modified by human activity have lower elevations making them more susceptible to high tides and even more so to anticipated sea-level rise.

The DTM for Tarawa Atoll enables area and volume estimates for each individual reef island. The TIN converted from mass elevation points derived from contour offers more detailed elevation information across the reef islands than the TIN constructed from spot heights. The TIN model shows that 25 reef islands have a prominent oceanward ridge, low-lying lagoon ridge, and a depressed central area. Betio varies slightly from this form with less distinctive ocean and lagoon ridges and a flat central area. But not all reef islands possess this profile, as 10 reef islands are relatively flat. The hypsometry approach is useful in providing a generalisation of the distribution of elevations across an entire reef island allowing comparisons across different reef islands. The application of this approach to reef islands offers a better understanding of the distribution of elevation in relation to MSL.

The three different hypsometric forms are affected differently by high tides and the extreme water levels that are described by the B2 emission scenario. The factors affecting risk from inundation are whether or not there is a direct connection to ocean or lagoon water and the elevations of lagoon and ocean ridges. Concerns have been raised as some low-lying areas that are at risk to sea-level rise currently accommodate large populations and, in addition to this, there are plans to further develop some of these areas to provide more housing such as in reclaimed area on the eastern end of Bonriki-Taborio reef island.

The distribution and variability of elevation and estimated volumes will be used in Chapter 7 to discuss the morphological changes of Tarawa Atoll to anticipated sea-level rise.

5 CHAPTER FIVE: PATTERN OF REEF ISLAND DEVELOPMENT AND SUPPLY OF MODERN BEACH SEDIMENT

5.1 Aims of the chapter

This chapter examines the mode of reef-island formation and establishes whether or not sediment supply is still available to reef-island shorelines. The specific aims of this chapter are to:

a) Establish the pattern of reef-island formation using Radiocarbon dating by Accelerator Mass Spectrometry (AMS) for three reef islands: Tabiteuea, Notoue and Marenanuka.
b) Investigate the effectiveness of amino acid racemisation (AAR) dating on single foraminifera by comparing the ages yielded from this method to paired AMS radiocarbon ages in order to establish the pattern of deposition on Tabiteuea and Notoue reef islands, and selected modern beaches.
c) Determine the vulnerability of modern ocean and lagoon beaches by comparing relative ages of foraminifera to establish whether they are continuing to be replenished with recently dead foraminifera.
d) Investigate whether foraminifera are still living on ocean reef flats around Tarawa Atoll

5.2 Introduction

Reef islands on atolls, such as Tarawa Atoll, appear to be threatened by the impact of climate change and its associated impacts of sea-level rise and coral bleaching. This is a result of their characteristically low elevation, small size, and high reliance on reefal sediments (IPCC, 2007). Reef islands such as Makin, Kiribati, and the Cocos (Keeling) Islands have poorly consolidated or unlithfied sediments that were deposited during the late Holocene, over the past 4000 yrs (Woodroffe and McLean, 1994, Woodroffe and Morrison, 2001, Dickinson, 2004, Kench *et al*., 2005, Hopley *et al*., 2007). Due to the growing global concern about the vulnerability of these reef islands, several studies on their morphological evolution have been carried out to determine how they have developed. The diversity of reef islands in terms of shapes, sizes and orientation led Stoddart *et al*., (1978) to suggest that they may have been formed differently. But a consensus on reef-island evolution has not yet been

reached as these studies are too limited and have conflicting views. However, it is generally accepted that late Holocene sea-level change plays a large role on reef-island development (Stoddart and Steers, 1977). An understanding of how reef islands on Tarawa Atoll have accreted in the past and whether they will continue to receive modern sediment is important for future management in light of anticipated sea-level rise and increasing human impacts. Such insights will assist in forecasting reef-island responses to sea-level rise, and in turn support identification of appropriate management measures to reduce their vulnerability.

Reef islands have formed over the past 4000 years (Woodroffe *et al.*, 1999; Woodroffe and Morrison, 2001; Dickinson, 2004; Kench *et al.*, 2005; Woodroffe, 2008; Kench *et al.*, 2012). The geological time scales concerned do not allow physical processes involved in the formation of these reef islands to be observed. Therefore, conceptual models have been useful in suggesting how they have formed. For example, a detailed mapping of the geomorphological changes on reef islands of Ontong Java Atoll, Solomon Islands, led Bayliss-Smith (1988) to propose that hurricanes have a significant influence on the formation of these landforms. On a long-term scale storms are constructive whilst on a short-term scale they are destructive. From three Pacific countries, Kiribati, Tuvalu and Cook Islands, Richmond (1992) selected a wide variety of reef islands in order to determine their evolution. He proposed a relationship between the morphology and location of reef islands on the reef-flat with the formation and maintenance processes of the reef island.

There are several proposed concepts for the morphological evolution of reef islands which suggest that modes of evolution vary. A chronological investigation of the Cocos (Keeling) islands led Woodroffe *et al*. (1999) to suggest that if the reef islands have developed on a reef-flat or conglomerate platform, there are several ways in which they might have formed and as a result, they proposed nine major accretion scenarios (Figure 1.1). The difference between the patterns of accretion is due to varying accretion rates, which depend on other variables including the frequency of events such as storms which can trigger deposition. These result in different volumes of sediment being deposited on the reef islands. The proposed modes of

accretion are: (a) regular from a central core, (b) oceanward accretion, (c) lagoonward accretion, (d) vertically accreting, (e) rollover, (f) overwash, (g) single episode, (h) erosional remnant, and (i) longshore (Figure 1.1). The first three modes assume predominantly horizontal accretion. Commencing from the central core, accretion can occur at the same rate on both sides, or be oceanward dominated, e.g., Makin, Kiribati, (Woodroffe and Morrison, 2001), or lagoonward dominated. The fourth mode, assumes vertical accretion whereby sediment is added to the whole reef-island surface as seen in South Maalhosmadulu Atoll, the Maldives (Kench *et al.*, 2005). The fifth and sixth modes are associated with rollover and overwash. These modes are similar, involving the erosion of the ocean shore face with this material transported across to the lagoon side and deposited on the lagoon beach. The single episodic mode involves deposition of sand that may have been generated by a storm or change in sea level causing enormous volumes of sediment to be transported onto the reef platform and deposited, as in the case of Bewick Cay, Great Barrier Reef, Australia (Kench *et al.*, 2012). The erosional remnant mode is where the surface of the reef island is eroded. The last is the longshore sediment mode, where the reef island undergoes erosional and accretional changes due to longshore sediment transport moving sediment to one end of the reef island and back again with changing directions of transport during seasonal changes.

An alternative model proposes that reef islands evolve through a combination of lateral and vertical accretion (Barry *et al.*, 2007). This numerical model, known as the Sediment Allocation Model (SAM), is based on morphological concepts and was tested with field data obtained from the Cocos (Keeling) Islands (Woodroffe *et al.*, 1999) and Makin, Kiribati (Woodroffe and Morrison, 2001). The model proposes that the reef islands can grow to a certain physical limit known as the maximum accommodation space at which point reef islands would not be able to accommodate any more new sediment (Barry *et al.*, 2007). Assuming that reef islands grow towards this equilibrium, SAM proposes a combination of lateral and vertical accretion where the reef islands continue to accrete by receiving sediment from the surrounding areas. This can be interpreted to mean that reef islands that accrete are those that still have available accommodation space thus allowing sediment deposition; those that are stable have filled their accommodation space such that

there is no more room available for deposition. These reef islands still maintain equilibrium as the sediment supply still exists. However, the model is limited in assuming that the only mode of change that takes place on these reef islands is accretion, as there are also other changes that may take place such as longshore sediment transport.

These two conceptual models were descriptive models based on results of radiometric ages of sediment samples collected from pits on-land, which were used to establish the sequence of reef island development. These models, proposed by Woodroffe *et al*. (1999) and Kench *et al*., (2005), both advocate that reef islands have grown through the accumulation of biogenic sediments but with varying patterns.

Reef islands and beaches are accumulations of sediment derived from only a few calcareous organisms such as foraminifera, molluscs and corals (Weber and Woodhead, 1972; Ebrahim, 1999). On some atolls, such as Tarawa or Makin, Kiribati, and Majuro, Marshall Islands, sediment composition is largely dominated by foraminifera (Ebrahim, 1999; Woodroffe and Morrison, 2001; Fujita *et al.*, 2009). Thus investigations into reef-island morphological development need to focus on these calcareous organisms. In addition, the vulnerability of beaches depends on the supply or continuous replenishment of recently dead foraminifera. For densely populated areas, such as South Tarawa, Kiribati and Majuro Atoll, Marshall Islands, concerns have been raised that no live foraminifera have been observed on the reef flats due to the effects of eutrophication (Collen, 1995; Ebrahim, 1999). This may have also contributed to the limited occurrences of foraminifera in North Tarawa as well as the deformed foraminifera observed on Temaiku's ocean reef flat on South Tarawa .(Ebrahim, 1999)

Various IPCC assessment reports have emphasized that small island nations will be among the most vulnerable to the anticipated impacts of sea-level rise but there are few studies that establish this. For instance, for some decades, focus on radiometric age control of reef-island development has been very limited and the need has become urgent to assess the times of deposition on these reef islands (Stoddart, 1969;

Roy and Connell, 1991; Woodroffe *et al.*, 1999). The difficulty that arises when applying radiocarbon dating is that it provides an estimate of the time of death but not the time of deposition of the skeletal sand grains (Woodroffe *et al.*, 1999; Kench *et al.*, 2005). Radiocarbon dating measures the cessation of ^{14}C uptake which, in short-lived organisms, may be regarded as corresponding with the time of death. Recent findings have suggested that there is an indeterminate period of transport, breakdown and mixing occurring prior to sediment deposition (Roy, 1991; Kench *et al.*, 2005; Woodroffe *et al.*, 2007). Bulk samples have been used in many studies to determine ages of reef islands such as in the Maldives (Woodroffe *et al.*, 1999; Kench *et al.*, 2005), Warraber, Australia (Samosorn, 2006; Woodroffe *et al.*, 2007), and Bewick Cay, Great Barrier Reef, Australia (Kench *et al.*, 2012). However, the study on Warraber Island established that bulk samples comprising different skeletal organisms, such as coral, coralline algae, foraminifera or molluscs, provided different ages thus indicating a different mode of accretion compared to the utilisation of component specific skeletal organisms (Woodroffe *et al.*, 2007). Based on this, it is considered best to use young and fresh individual samples of the same organism to determine ages of reef islands (Woodroffe *et al.*, 2007) especially from those that contribute largely to the sediment composition of the reef island (Yamano *et al.*, 2000).

Beaches can be composed of carbonate sediment material such as foraminifera of mixed ages (Roy, 1991). The selection of robust and well preserved fossils with the least physical alteration for age determination can minimise the time between death and deposition and may provide a better indication of recently deposited sediments on the beaches. However, there are certain issues when using radiocarbon dating. For instance it is not possible to establish the radiocarbon age of beach carbonate material beyond the limits of radiocarbon dating (Libby, 1955). Additionally, to use radiocarbon dating to analyse a sample size representative of a study area composed of individual foraminifera would be a very expensive exercise (Goodfriend and Stanley, 1996).

Amino acid racemisation (AAR) is a method that dates the cessation of amino acid synthesis which, for short-lived organisms, may be taken as corresponding to the

time of death. This method offers the opportunity to determine the ages of foraminifera younger than AD1950. AAR is based on protein decomposition (Hare and Abelson, 1968) and was first discovered by Abelson (1954) who noted the presence of residual protein in fossil carbonates and suggested it could be used as a dating technique. An advantage of AAR is that it is less costly and uses milligram quantities of samples (Kaufman and Manley, 1998), thus allowing more samples to be analysed and therefore cover a wider study area. However, AAR has a lower age resolving power and, with the complexities of racemisation kinetics, the method requires calibration with an independent method such as radiocarbon dating.

This chapter examines the Holocene chronology of reef-island formation on Tarawa Atoll using radiocarbon ages of single foraminifera from selected reef islands of Tabiteuea, Notoue and Marenanuka. With detailed paired radiocarbon dating and AAR records from individual *Amphistegina* fossils, trials have been undertaken to determine if AAR can establish if a true modern population exists within the "modern" sand beaches across Tarawa Atoll. This is important for future management of reef islands. Rose Bengal, a stain used to establish whether foraminifera are alive is used to investigate the presence of live foraminifera on the ocean reef-flats and "modern" beaches to indicate that sediment supply still exists.

5.3 Background

5.3.1 Foraminifera

Studies carried out across many Pacific reef islands and atolls such as Fongafale, Tuvalu (Collen and Garton, 2004) Majuro, the Marshall Islands (Fujita *et al.*, 2009), and Makin (Woodroffe and Morrison, 2001), Onotoa (Todd, 1961), and Tarawa Atoll, Kiribati (Ebrahim, 1999) show that foraminifera are the main sediment contributor. Foraminifera contributes 50% to the average sediment composition on reef islands of Tarawa Atoll signifying its importance for their development (Ebrahim, 1999).

Compositional analyses of reef islands on Tarawa Atoll (Ebrahim, 1999) and Onotoa (Todd, 1961) show that dominant genera are *Amphistegina*, *Baculogypsina* and *Calcarina* (see Chapter 3 for more detail). In Tarawa Atoll, *Calcarina* and

Baculogypsina contribute more than *Amphistegina* (Ebrahim, 1999), however tests of dead *Calcarina* and *Baculogypsina* undergo physical alteration where their spines break off or tests are abraded, or altered allowing materials to contaminate them (Lobegeier, 2002; Collen and Garton, 2004). This may affect calculated numerical ages when analysed by AAR resulting in an incorrect apparent age. In contrast, the solid test of *Amphistegina*, is more robust appearing polished, and is less prone to contamination (Collen and Garton, 2004). This would make *Amphistegina* a better choice for reef-island development studies.

Foraminifera can be classified on the basis of test characteristics according to Loeblich and Tappan's classification (Gupta, 1999). Characteristics focus on the chemistry, mineralogy and structure of the test walls, including chamber arrangements, aperture shapes and positions of aperture. *Amphistegina* has two tests: an outer and an inner test. The outer calcareous test covers the mass of protoplasm (Hansen, 1999), which is a thin transparent chitinous layer responsible for the brown colour noted in live *Amphistegina* (Cushman, 1959).

5.3.2 Habitat and distribution of live *Amphistegina*

Amphistegina are symbiotic bearing foraminifera, with test sizes greater than 2 mm (Hallock, 1999; Murray, 2006). As a result of the symbiotic microalgae, they are restricted to live in oligotropic areas with water temperatures >20^{o}C (Langer and Hottinger, 2000). Several other factors control the distribution and abundance of these organisms such as light, temperature, water energy and water quality type (Hohenegger, 2004). Geographic and latitudinal distribution is determined primarily by temperature.

Studies in the Indo-Pacific show that the depth distribution of *Amphistegina* is zoned, and test shape is closely related to depth (Larsen and Drooger, 1977). Test shapes of foraminifera have been measured as ratios of thickness to diameter (t/d). *Amphistegina* that occupy shallow water environments with depths less than 10 m and those that are more exposed to wave motion possess thick, robust tests with $t/d >$ 0.6. These foraminifera are generally located on substrates in back-reef and reef-margin environments (Larsen and Drooger, 1977; Hohenegger, 1994). Some

environments on Pacific islands allow *A. lobifera* and *A. lessoni* to flourish such that they dominate the beach sediment composition (Hallock, 1981). Hallock (1981) found that *Amphistegina* with *t*/*d* ratios < 0.6 are present in deeper waters of 10 - 30 m. They can also live water up to 130 m, if light is sufficient (Hottinger, 1983). Generally the maximum depth at which foraminifera can grow is controlled by the lower limit of the euphotic zone which can be as deep as 100 - 150 m in the Pacific region (Murray, 2006). At water depths of less than 30 m, the life span of *A. lessoni* is 3 to 6 months (Hallock, 1981). However, *A. lobifera* tend to live longer, from 6 to 12 months. *Amphistegina* are also present in shallow shelf coral reefs and lagoon environments. Those living on the outer coral reef crest are found attached to the underside of substrates or onto algae present in eroded low-lying areas on the reef flat forming shallow pools during low tides (see Figure 2.11) (Hallock, 1981; Ebrahim, 2000; Fujita *et al.*, 2009). Those in the lagoon are epifaunal, living on the surface of lagoon sediments.

A study on the distribution of living foraminifera in Majuro, the Marshall Islands discovered that *Amphistegina* preferred areas where water is calmer such as small pools where macroalgae are present (Fujita *et al.*, 2009). Experiments have shown that *Amphistegina* with weak pseudopodials are protected from being transported away by filaments of macroalgae (Rottger and Kruger, 1990). Based on these studies, Fujita (2009) suggests that *Amphistegina* prefer areas where water flow is moderate but avoid high energy areas as they may be washed away.

5.3.3 *Amphistegina* test shape

Two different test morphologies of *Amphistegina* spp. are found in Tarawa Atoll as a result of the presence of two different species (Ebrahim, 1999). Even though they differ, Ebrahim reported them as one category. He found that *A. lobifera* were typically orange in colour with intermediate sphericity and were restricted to shallow areas and reef flats. This has been attributed to their requirement for higher light intensity for reproduction (Hallock, (1981). On the other hand, *A. lessoni* were white in colour, had a lower sphericity, and were present in deeper areas. Live *A. lessoni* were also found in 5-7 m water depths around the fore-reefs of South Tarawa (J.

Carill, pers. comm., 2010). Increasing water depth reduces the thickness of the lamellar or carbonate walls of *Amphistegina* (Hallock and Hansen, 1979).

The test of *Amphistegina* is trochospiral in shape with numerous chambers and a lobed suture (Gupta, 1999). The Rotalidae family, which includes *Amphistegina*, is characterised by bilamellar wall, referring to the last chamber having two carbonate walls, and an outer and an inner lamellar separated by organic matter. As the *Amphistegina* grows, it keeps on adding new and larger chambers (Hansen, 1999). A study by Hansen (1999) found that as chambers are added, the new shell material covers the existing chambers thus thickening the walls An outer calcite test covers the whole foraminifer, once all chambers have been built. In addition Hansen (1999) also discovered that the lamellar walls comprise calcite platelets assembled in stacks with similar orientation. In the case of *Amphistegina*, they possess very thin organic layers that separate these platelets. These organic layers are lined with organic tubules that are further divided by organic plates.

5.3.4 Transport and redistribution of dead foraminifera tests

When foraminifera die, their empty tests are very robust and resistant to physical alteration, such as breakage and abrasion (Martin and Liddell, 1991; Kolter, 1992; Kotler *et al.*, 1992; Ebrahim, 1999), and to a lesser degree to dissolution and bioerosion (Martin and Liddell, 1991). The extent of both dissolution and bioerosion varies depending on certain variables such as foraminifera genera, microorganisms present and environments.

Transport and redistribution of foraminiferal tests are influenced by human activities such as construction of causeways. In Sesoko, Japan, activities such as reclamations extending onto the reef flat and the dredging of the reef flat interrupted the transport of foraminifera from the ocean reef flat to the reef islands (Hohenegger, 1994). The study of foraminifera in sediments on Tarawa Atoll by Ebrahim (1999) shows that construction of causeways closes or reduces inter-island channels which affects the distribution of foraminifera and also their *post mortem* transport. Solid causeways close the inter-island channels blocking ocean-lagoon water circulation and sediment transport. Additionally, in South Tarawa, causeways enhance predominant

longshore sediment transport, the direction of which is seasonally affected by ENSO (see Section 6.3.1)(Harper, 1989; Solomon and Forbes, 1999).

Fossil foraminifera deposited on land or beaches may have been reworked, or re-deposited. The sediment dynamics may be inferred by examining the taphonomy of the fossils. Taphonomy is important using information lost from carbonate fossils to inform an understanding of past chemical and physical processes that have acted on them (Behrensmeyer and Kidwell, 1985). As time of death for a carbonate organism is often considered to be close to the time of deposition, fossil tests that appear to be well preserved and robust, indicate that they have not travelled far from their source, and that there is little reworking within the beach sediments. In contrast, tests of fossils that have undergone physical alteration, such as dissolution or abrasion indicate reworking or re-incorporation of the sediments which suggests they are older, and have been deposited earlier than the well preserved tests (Wehmiller *et al.*, 1995).

To gain a better understanding of fossil reworking, recent studies have used taphonomic characteristics of shells calibrated against amino acid D/L ratios (Powell and Davies, 1990; Wehmiller *et al.*, 1995; Murray-Wallace *et al.*, 2005). The D/L ratio of amino acid indicates the inter-conversion of the two forms in which amino acids can occur, from L (*laevorotatory* – left handed) to D (*dextroratory* – right handed) forms, which takes place after the death of an organism (Murray-Wallace, 1995). However, the taphonomy of fossil buried within sediments on sheltered environments, such as lagoons maybe influenced by other variables, such as bioturbation (Berkeley *et al.*, 2009), making it difficult to determine whether the fossil was originally living in this site or has been incorporated here. Bioturbators or burrowers mix the surface sediments (Martin *et al.*, 1995). By doing so, they alter the preserved taphonomy and may also introduce fossils from other sites. This stratigraphic disorder and incompleteness of the geological record due to selective dissolution or other factors is known as time-averaging (Kowalewski, 1996). The phenomenon can either assist or cause confusion in the interpretation of buried fossils and, therefore, the sediment dynamics of the materials deposited on the beaches. The fossil materials on beaches may appear old but may largely be

composed of buried fossil materials now deposited at the surface, material washed ashore by currents or even recently relict material depending on the durability of the fossil test (Ford, 2010).

5.3.5 Radiocarbon dating

Radiocarbon dating is a well established method for aging sediments and fossils and was initially developed by Libby (1949). It measures the radioisotope carbon-14 (^{14}C), a radioactive element present in the Earth's atmosphere that is produced by cosmic rays. ^{14}C rapidly oxidises to form carbon dioxide and is present in the atmosphere, biosphere and ocean. ^{14}C contributes $1x10^{-10}$ % of the atmospheric gases and decays with a half life of 5730 yrs, i.e., for every 5730 yrs, 50% of the original amount of radiocarbon present is lost (Arnold, 1995; Trumbore, 2000). Marine organisms absorb carbon dioxide from the oceans to produce their carbonate shells and tests. After death, intake of carbon ceases, and radioactive decay of ^{14}C commences. By measuring the proportion of ^{14}C per gram of carbon the time of death of the organism can be determined.

^{14}C in atmospheric CO_2 was originally considered to be constant. Tree ring studies have shown that this is not the case, confirming that ^{14}C concentration has varied due to natural and human-induced factors (Burr and Scott, 2007). Natural factors include solar activity, geomagnetic field strength, and uptake and release of $^{14}CO_2$ by the Earth's reservoirs, in particular the ocean (Arnold, 1995; Trumbore, 2000). The human factors involve pre-industrial fossil fuel burning and bomb testing. The atomic bomb activities approximately doubled the ^{14}C concentration in atmospheric CO_2, while fossil fuel use involved burning of ^{14}C-free material for energy use. This required a calibration of the ^{14}C timescale to determine its relationship with historical time. The significantly altered proportion of atmospheric ^{14}C as a result of bomb testing after 1950 means that 1950 is used as the benchmark for dating i.e. dates are reported as yrs BP (before present) where 0 yrs BP corresponds to 1950 (Mook and Van der Plicht, 1999).

The maximum limit of radiocarbon dating is achieved after approximately ten half-lives whereby the low concentrations of ^{14}C remaining in the material are close to the

limit of detection. In radiocarbon years this is between 40 to 50 ka BP depending on the background level attained by a specific laboratory (Arnold, 1995; Trumbore, 2000). On the other hand, fossils younger than 300 yrs cannot be measured accurately using radiocarbon dating because it is not possible to distinguish the ^{14}C concentration in the fossil from modern levels. Challenges arise from the enormous volumes of CO_2 produced as a result of the human activities and from the calibration of conventional radiocarbon ages to sidereal or calendar years (Arnold, 1995).

Conventional radiocarbon dating involved measurement of ^{14}C liquid scintillation or gas proportional counting of CO_2. ^{14}C can also be measured using Accelerator Mass Spectrometry (AMS), which has been the most powerful method since its development in 1977 (Linick *et al.*, 1989; Donahue, 1995). The fundamental difference between conventional radiocarbon dating and AMS lies in the measurement. Radiocarbon dating measures the decay of ^{14}C atoms whilst AMS measures the number of ^{14}C atoms relative to ^{13}C atoms (Linick *et al.*, 1989; Donahue, 1995; Cook *et al.*, 2007). Benefits of AMS include greater precision and a requirement of only milligrams of sample therefore requiring less measurement time (Linick *et al.*, 1989).

5.3.6 Marine reservoir influence on radiocarbon ages

Benthic foraminifera fossils found in Tarawa Atoll originate from the atoll's surrounding shallow reef areas (Ebrahim, 1999); they uptake marine waters through symbionts that live within them, to develop their calcareous tests. In order to determine the age of a carbonate fossil originating from marine environments, it is important to consider the marine reservoir effect (ΔR), as oceans act as reservoirs for carbon. This phenomenon occurs from the ocean surface to depths of 200 m of the global ocean (Petchey *et al.*, 2008). At some stage, the ocean surface waters sink to deeper depths of up to 200 m, when its carbon concentration partially equilibrates with the atmospheric conditions (Stuiver and Reimer, 1986; Arnold, 1995). Carbon has a longer residence time in ocean waters as a result of two processes: slow exchange of ^{14}C between the atmosphere and ocean, and mixing of surface waters with upwelled waters from deeper depths (Stuiver *et al.*, 1986; Petchey *et al.*, 2008). The process of exchanging newly produced atmospheric ^{14}C to the ocean takes about

400 years and fluctuates with time (Stuiver et al., 1986). When carbon resurfaces through upwelling, its radiocarbon concentration is comparatively less than the surrounding carbon of atmospheric origin due to radioactive decay. The radiocarbon age of materials in the equatorial ocean is approximately 400 to 500 year older than that of associated material of atmospheric origin (Stuvier and Polach, 1977). As a result, the age of the fossil must be adjusted to remove the marine reservoir effect, which differs geographically (Stuvier and Polach, 1977).

The marine reservoir value used for Tarawa Atoll is an average of three Christmas Island, Kiribati, marine specimens obtained from the Bishop Museum: a shell and two corals collected alive in 1924 AD. Analyses of these specimens by ANSTO in 2009 provided an average value of 39 ± 56 yr (Q. Hua, pers. comm., 2009) similar to ΔR values obtained from nearby islands in the Pacific. The ΔR value for the Marshall Islands (ΔR = 33 ± 33 yr) was obtained from a single paired measurement by applying both Uranium/Thorium dating (at The University of Queensland) and ^{14}C dating (at ANSTO) on a coral that was growing in 1870 AD (Q. Hua, pers. comm., 2009). A correction for the Northern Solomon Islands gave an average ΔR value of 66 ± 31yrs, which was obtained from five samples collected prior to 1950 (Petchey *et al.*, 2008).

Radiocarbon ages presented as conventional ages (BP) have not been corrected for marine reservoir effect. The removal of the marine reservoir effect is undertaken by processing the radiocarbon ages using the CALIB ^{14}C Calibration program (Stuiver, 1993; Stuiver *et al.,* 2005). This can be used to eliminate the marine reservoir effect for Tarawa Atoll ocean surface waters by using the value obtained for Christmas Island, Kiribati (ΔR = 39 ± 56 yrs). This program also converts the radiocarbon ages to calibrated or sidereal years expressed as cal yr BP. This allows samples from different parts of the world with known radiocarbon ages that have been corrected for the marine reservoir effect to be compared (Stuvier and Polach, 1977; Stuiver and Reimer, 1986; Stuiver, 1993; Stuiver *et al.*, 2005).

5.3.7 The AAR method

Amino acid racemisation (AAR) is a geochronological tool that has been used to determine fossil age estimates of carbonate materials such as bones, teeth, mollusc shells and foraminifera. The method was first developed by Hare and Abelson in 1962 extending Abelson's work in 1954, which showed that proteins present within fossils can be separated into different amino acids (Hare and Abelson, 1968). The age of fossils is obtained from the extent of the amino acid racemisation reaction with respect to time.

The method has been widely reviewed (Schroeder and Bada, 1976; Bada, 1985; Miller and Brigham-Grette, 1989; Rutter and Blackwell, 1995; Wehmiller and Miller, 2000). Broader applications of the technique involve an understanding of Quaternary chronology and solving of regional and local stratigraphic variations. Recent applications of AAR dating have focussed on Holocene chronologies, however, the limitation of AAR to resolve differences less than 10-15% of the sample age highlight the tool's low resolution (Wehmiller and Miller, 2000). Studies also highlight recent efforts to increase the utility of the method to include: studies of Holocene series of alluvial deposits (Goodfriend and Stanley, 1996; Murray-Wallace and Colley, 1997; Sloss *et al.*, 2004), use of sub-milligrams of samples (Kaufman and Manley, 1998), and the use of various marine carbonate samples (Cann and Murray-Wallace, 1986; Wehmiller *et al.*, 1995). These studies demonstrate this methods capability to determine ages of carbonate fossils beyond the limits of radiocarbon dating. Thus AAR can be used as a relative dating method, to extend the geochronology of a given area provided that an independent method such as AMS radiocarbon dating is used to calibrate the ages. Direct calibration studies have used individual molluscs (Goodfriend, 1992; Goodfriend and Stanley, 1996; Sloss *et al.*, 2004) and gastropods (Murray-Wallace and Colley, 1997) to achieve this. No study has yet performed direct calibration of AAR using AMS radiocarbon dating on individual foraminifera involving sub-milligram quantities. This study aims to trial this application with a view to examining the dynamics of reef sedimentation.

5.3.8 Basic principles of amino acid racemisation

Proteins are fundamental to life. They comprise amino acids linked via peptide bonds. The significant role they play in organisms makes it possible to apply geochemical methods to determine the ages of these organisms (Wehmiller and Miller, 2000). Proteins assist with the calcification process of shells and tests and are stored in the shells and tests in trace amounts. In the case of foraminifera, for example, they are either located between the calcite mineral crystals (inter-crystalline) or within the crystals themselves (intra-crystalline) (Hansen, 1999). For molluscs, organic materials can be preserved for a long period of time. Studies on mollusc shells show that inter-crystalline fractions racemise faster than the intra-crystalline fraction (Penkman *et al.*, 2008). Additionally, intra-crystalline amino acids are resistant to prolonged application of chemical oxidation, which can be isolated by extensive bleach treatment (Sykes *et al.*, 1995; Penkman *et al.*, 2008). These examples indicate that amino acids are well preserved within the carbonate tests.

Protein formation within tests terminates when carbonate organisms die. After death, peptide bonds break creating smaller polypeptide chains. These bonds can further degenerate to release individual amino acids into solution (Bada, 1985; Miller and Brigham-Grette, 1989). About ten of the twenty protein amino acids commonly present in fossils can be utilised for geochronological applications (Miller and Brigham-Grette, 1989; Wehmiller and Miller, 2000). Amino acids have characteristic rates of racemisation allowing direct comparison of two individual amino acids (Miller and Brigham-Grette, 1989). The comparison of these two amino acids can also act as a way of validating the results (Miller and Brigham-Grette, 1989). The advantage of this method is that different amino acids can be applied to investigate different time scales. For example Aspartic acid, a fast racemising amino acid has been widely used in studies of Holocene fossils (Bada and Schroeder, 1975; Goodfriend, 1992; Goodfriend and Stanley, 1996; Murray-Wallace and Colley, 1997; Sloss *et al.*, 2004). This enables direct comparison of characteristic racemisation rates of individual amino acids to determine relative and numeric ages of fossil materials. The other amino acid used in this study is Glutamic acid which has a

relatively slower racemisation rate compared to Aspartic acid (Murray Wallace and Belperio, 1994; Hearty *et al.*, 2004).

5.3.9 Amino acid racemisation reaction

An amino acid's basic structure comprises three main groups: amine (NH_2), carboxylic acid (COOH) and an R group also known as a side chain. All amino acids with the exception of glycine, possess this form, with one asymmetrical central carbon atom, known as the α-amino derivate of carboxylic acid (Rutter and Blackwell, 1995). The asymmetrical formation allows amino acids to exist as mirror images or optical isomers of each other (Miller and Brigham-Grette, 1989; Rutter and Blackwell, 1995).

Amino acids can exist in two forms. One form is the L (*laevorotatory* – left handed) isomer and the second is the D (*dextroratory* – right handed) isomer. Living organisms are entirely comprised of L-isomer amino acids. After death, proteins degrade via breaking of peptide bonds; a slow process enabling the racemisation reaction to occur which involves the inter-conversion of the L-isomer to a corresponding D-isomer. This change in form is termed racemisation; and is a time-dependent process (Figure 5.1). This allows the time since death to be calculated using a D/L ratio which acts like a geological clock that starts after the death of an organism (Murray-Wallace, 1995). The clock stops when the D/L ratio reaches an equilibrium value of 1 i.e. 50% of L isomers and 50% of D isomers. For most amino acids, the conversion reaction can take up to thousands or millions of years, however isoleucine is an exception having two centres of asymmetry and equilibrates at approximately 1.3 (Wehmiller and Miller, 2000).

The general AAR reaction can be expressed as follows:

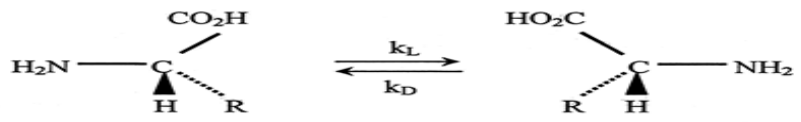

L-Aspartic Acid D-Aspartic Acid

k_D and k_L represent the reversible first order constant for conversions of an L to D form.

Figure 5.1. Acid racemisation reaction of Aspartic acid, where the L isomer converts to a D isomer (source: Sloss, (2005)).

To model diagenetic racemisation reactions that occur over lengthy time intervals such as 10 to 100 ka, pyrolysis experiments have commonly been undertaken at a constant temperature of 110°C (Kaufman and Manley, 1998). This time-dependent reaction permits relative rates of racemisation between fossil genera to be determined.

Amino acid racemisation was originally considered to be a first-order reaction, but is now understood to occur in two stages due to kinetic differences as heating continues (Goodfriend and Meyer, 1991). Initial heating causes a rapid linear reaction whereas continued heating leads to a more gradual one that markedly flattens off, as there is significant reduction in racemisation rate of about 10% of the initial apparent linear stage (Kriausakul and Mitterer, 1978; Wehimiller, 1980). The following processes contributed to this non-linear kinetic process:

a) The initial heating of the amino acids causes a rapid rate of reaction. Continued heating is indicated by a distinctive flattening off of the kinetic curve largely due a significant reduction in racemisation rate as the rate of hydrolysis slows down as well as a reduction in the availability of individual amino acids to undergo racemisation; and
b) In solution the amino acids are available in various forms, such as proteins, polypeptides, and free amino acids which all have their own characteristic rate of racemisation (Kvenvolden and Peterson, 1976).

This non-linear process can be demonstrated with the application of a logarithmic or apparent parabolic equation (Mitterer and Kriausakul, 1989). The equation can be determined by graphing a sample's amino acid D/L ratio against the square root of its radiocarbon age. The parabolic curve developed by using paired AMS and AAR dates will provide calibration of the AAR ages, therefore allowing the extension of the single foraminifera dating, within the calibrated line limits (Sloss *et al.*, 2004).

To replicate a natural system, experimental racemisation uses higher temperatures to speed up this process. For instance, the analysis of Holocene samples use temperatures of 110°C (Hare and Abelson, 1968). There is a series of assumptions that AAR is based on and they are as follows:

a) Fossil tests have acted as “closed systems” whereby there has not been any contamination or loss of amino acids by or to the surrounding environment enabling interpretation of fossil burial (Collins and Riley, 2000).
b) Amino acids in a solution behave in a predictable way during diagenesis, where peptide chains are reduced due to heat breaking peptide bonds (Mitterer and Kriausakul, 1989).
c) As racemisation is temperature-dependent, it is assumed that samples collected within a restricted region have been exposed to the same diagenetic temperature, which means that the region’s climate has been the same. Rates of AAR, and hence ages of samples depend on the temperature history of a given area provided they have been deeply buried.

As racemisation is a chemical reaction, the measured extent of racemisation within fossils will be influenced by several factors such as diagenetic temperature, free or bound amino acids and genus effect (Wehmiller and Miller, 2000). This can inform which genus to select, the depths at which to collect the fossil and the amino acid to test. These are explained in more detail below:

- **Diagenetic temperature**

Tarawa Atoll located on the equator is exposed to warm air temperatures. Determination of numeric ages of benthic foraminifera fossil that are exposed to warm conditions may be affected, as racemisation reactions are primarily influenced by temperature. The relationship between rate of racemisation and temperature is described as an exponential one (Miller and Hare, 1980). Therefore for every 1°C increase in temperature, it is predicted that the rate of racemisation will correspondingly increase by 18%. Based on that relationship, it has been demonstrated empirically that with every 5°C, the rate of racemisation approximately doubles (Miller and Brigham-Grette, 1989; Murray-Wallace, 1995). Hence temperature variations can cause serious issues when determining numeric ages of fossil foraminifera if adequate control is not exercised in sampling (e.g. analysing surface samples that have been subaerially exposed for several thousand years or the majority of the diagenetic history of the fossil).

Samples of known ages obtained from low temperature areas such as the deep ocean (1 to 4°C) or high latitudes (-20 to -10°C) take a longer time to achieve equilibrium (Wehmiller and Miller, 2000). The duration could be from 1 to 5 million years respectively. In warm regions, the rate of racemisation will reach equilibrium significantly faster. In a study on the Huon Peninsula, Papua New Guinea, using *Tridacna* shells obtained from coral reef terraces, Hearty and Aharon (1988) found that samples of ages 125 ka were closely approaching equilibrium. Therefore rates of racemisation vary with location. Assumptions are made that samples in a region have been exposed to the same temperature; however, a study by Wehmiller *et al*. (2000) showed that some regions experience temperature variability, leading to different rates of racemisation. Wehmiller and Miller (2000) showed that, under varying temperature conditions, a single amino acid D/L value can yield a wide range of ages. This implies that a single D/L ratio for areas with dissimilar temperature histories will give different ages for the fossil investigated.

Large benthic foraminifera fossils found on reef islands of Tarawa Atoll originate from the shallow areas around the atoll. After death they have been transported ashore and may have been exposed to the surface temperature before being buried, however, the length of exposure time is uncertain. As time of deposition has been considered to be close to the time of death, it is important to collect fossils that are less influenced by subaerial exposure, as this affects the rate of racemisation. Samples subaerially exposed for a substantial proportion of their diagenetic history will be affected by surface temperature fluctuations. Those of the same age that were buried shortly after deposition will have less exposure to these variations, particularly the disproportionate effect of higher summer temperatures. Fossils buried at depths of 1 m or greater are considered to be less exposed to seasonal temperature fluctuations where the amplitude of temperature waves is less than 6°C (Wehmiller, 1977; Miller and Brigham-Grette, 1989; Wehmiller and Miller, 2000). Based on the calculations and findings of Norton and Friedman (1981) this amplitude provides an acceptable temperature variation of less than 1°C; a difference between the effective and arithmetic mean temperature. This led to the development of a general rule that samples that are at depths of one or more metres below the ground surface have been buried for most of their depositional history. Following on from

that, samples of the same age, but which were exposed to different lengths of subaerial temperatures will have undergone different rates of racemisation and hence may yield different numeric ages. This also applies to shallow-water environments. 481 mollusc shells from four different taxa collected from sediment cores obtained from the lagoon bed of the Great Barrier Reef, Australia deposited 5000 years ago, showed varying D/L results (Rutter and Blackwell, 1995). The study showed that *Turbo* had higher D/L ratios compared to *Ethalia, Natica*, and *Tellina* due to the difference in temperature exposure as it is not infaunal but prefers hard reef and shallow-water environments. This highlights the importance of understanding the samples diagenetic history prior to any sampling and analysis (Rutter and Blackwell, 1995).

- **Free or bound amino acids in solutions**

During diagenesis, polypeptides are broken into smaller peptides, producing more free amino acids in solution (Rutter and Blackwell, 1995). Locations of amino acids within a polypeptide chain influence the rate of racemisation. Amino acids bound within the protein chain differ from those at the terminal sites and those within the protein chain are generally difficult to detach, having lower rates, and therefore a higher extent of racemisation. Those at the terminal sites are relatively easier to separate and have higher rates and lower extents of racemisation (Bada and Schroeder, 1975). But this is not always true, as amino acids positioned within proteins can also racemise faster (Miller and Brigham-Grette, 1989; Wehmiller and Miller, 2000). Another factor influencing the rate of racemisation is the molecular weight of amino acids. Amino acids with high molecular weights have a lower degree of racemisation (Miller and Brigham-Grette, 1989; Wehmiller and Miller, 2000). Those with lower molecular weights have a higher degree of racemisation.

- **Genus effect**

In Tarawa Atoll, the large benthic foraminifera comprising three main genera *Calcarina, Bacuolgypsina* and *Amphistegina* which appear to have different racemisation rates based on well-established information (Wehmiller and Miller, 2000). This was first observed in samples of fossil foraminifera collected from deep-sea sediments (King and Neville, 1977; Müller, 1984). Planktonic foraminifera

fossils of *Orbulina universa* and *Globortalia tumida-menardii* collected from a sediment core in Sierra Leone Rise, eastern equatorial Atlantic Ocean demonstrate this well. From the two genera, the racemisation of amino acid isoleucine provided two distinct curves indicating two different pathways (Müller, 1984). The same result has also been observed with fossil molluscs (Miller and Brigham-Grette, 1989; Murray-Wallace *et al.*, 1993; Sloss, 2005). Variations at the taxonomic level are attributed to the different protein and polypeptide chemistry, which gives rise to varying rates of racemisation. Based on the above information, *Amphistegina* has been selected for use in this thesis as it can be assumed that it provides a "closed system" as it does not possess any spines that may break during transportation affecting its physical state, as is the case for *Bacuolgypsina* and *Calcarina* (Ford, 2010). This may result in better preservation for *Amphistegina* than the other two foraminifera genus.

5.3.10 AAR Age

Numeric and relative ages are the two ways in which the extent of amino acid racemisation can be applied in geochronology. Both methods allow the determination of ages of fossils from the same genus that have been collected from various sites across a region with the same diagenetic temperature history, however, the difference is that relative age does not involve any assessments of racemisation kinetics, whereas numeric age does, requiring an independent dating method such as radiocarbon dating by AMS to calibrate the rate of racemisation (Murray-Wallace and Bourman, 1990; Wehmiller and Miller, 2000; Sloss, 2005).

In this thesis, direct calibration of both AMS ^{14}C and AAR analyses is carried out on the same individual foraminiferal test to investigate the possibility of using AAR ages. This method enables the extension of dating by offering the potential to determine ages of numerous skeletal sand grains in a sample. A calibration line can be developed by using several paired ages of individual samples, and this can be interpolated beyond the known ages to allow the estimation of an unknown age from an undated sample (Kaufman, 2006). However, in this study the development of the calibration line based on a low number of samples limited the ability to use this age determination approach. As a result, relative ages have been used in this study which

requires two amino acids to be graphed against each other, such as Aspartic acid and Glutamic acid. Plotting these multiple D/L ratios allows them to be organised into aminozones or clusters of D/L ratios (Murray-Wallace and Kimber, 1987; Wehmiller and Miller, 2000). An aminozone is a distinctive cluster of amino acid D/L ratios that represents a defined time and can be compared with other clusters within the same region (Murray-Wallace, 2000). Fossils with low D/L ratios are young, whilst those with high D/L ratios are considered to be older. Assessment of relative age allows for the construction of broad chronologies within a region of similar diagenetic temperatures without involving assessments of racemisation kinetics. Differentiation of these aminozones is made by correlating D/L ratios of an amino acid cluster relative to another cluster, for example such as cluster A is older than cluster B, or cluster A is younger than cluster B (Wehmiller and Miller, 2000). This application of relative ages appears to be more appropriate than numeric ages to Tarawa Atoll whereby replicate individuals have been used to determine ages of a sample and provide comparison with other fossils collected from other areas across the atoll.

In summary, the pre-requisites of fossils for amino acid racemisation dating, include fossils that behave as "closed systems", fossils that have been buried to a depth of more than a metre and are not exposed to seasonal variations in temperature (Miller and Brigham-Grette, 1989) and fossils from a single genus for multiple analyses (Wehmiller and Miller, 2000).

5.3.11 The Rose Bengal stain method

The Rose Bengal stain is a standard method applied to establish whether foraminifera are alive and hence modern. To apply this method, the Rose Bengal powder needs to be dissolved in ethanol to form a solution (Walton, 1952). The solution is applied to samples and left to stain for a period of approximately 8 to 14 hours (Alve and Bernhard, 1995) or up to a week (Rathburn *et al.*, 2000). The protoplasm of live foraminifera are stained red, however, this powder can also stain other materials which limits the ability of the test (Murray, 2000). In this study, the Rose Bengal stain has been applied to determine whether foraminifera collected from the reef flats

are alive and whether the “modern” beach sediments are composed of recently dead foraminifera thus indicating that sediment supply still exists.

5.4 Study sites

To establish the pattern of reef-island growth, three elongated reef islands, Tabiteuea, Marenanuka and Notoue, in North Tarawa were investigated (Figure 5.2). Three criteria were used for the selection of these reef islands. First, the reef islands need to be elongated in shape as this type of reef island appears to be less affected by wind and waves compared with small reef islands. Second, the reef islands should be located in an environment with low anthropogenic disturbances. Finally, the reef islands should be accessible so they can be sampled.

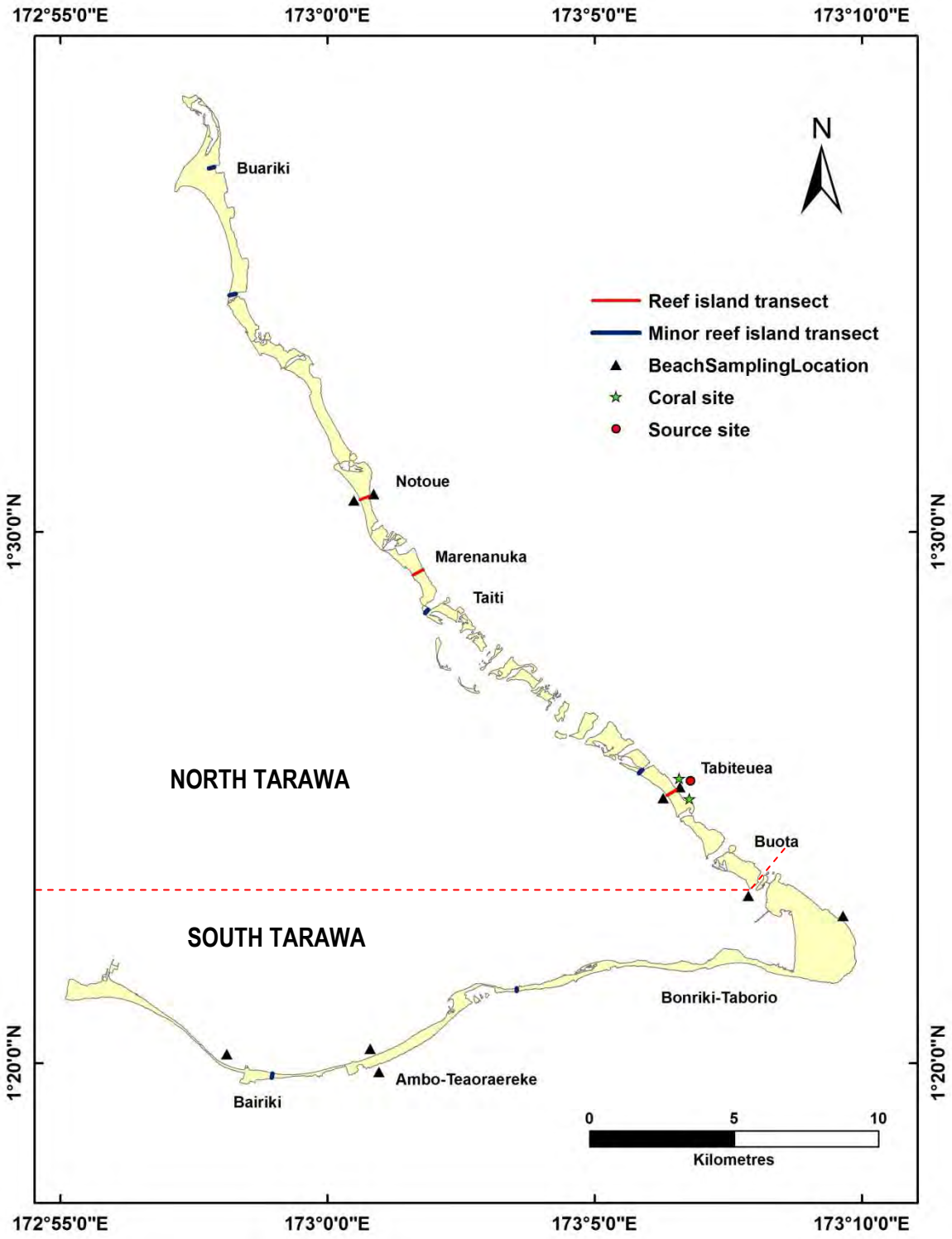

Figure 5.2. Map of Tarawa Atoll showing locations of cross-island transects, beach sample sites and source sites of live foraminifera.

An additional six smaller transects were placed on areas such as sand spits and embayments to increase the number of samples across the atoll to be radiocarbon dated, and thus provide a better control on ages. These smaller transects are located on reef islands of Buariki, Bairiki, Bonriki-Taborio, Tabiteuea and Taiti (Figure 5.2).

To determine whether foraminifera were still alive, two study sites on another atoll were also investigated. Butaritari Atoll, located to the north of Tarawa Atoll was selected as the control site to examine the effects of humans on foraminifera. Two locations on a comparatively rural elongate reef island in the south of the atoll were selected as the study sites: Ukiangang, and Temanokunuea (Figure 5.3).

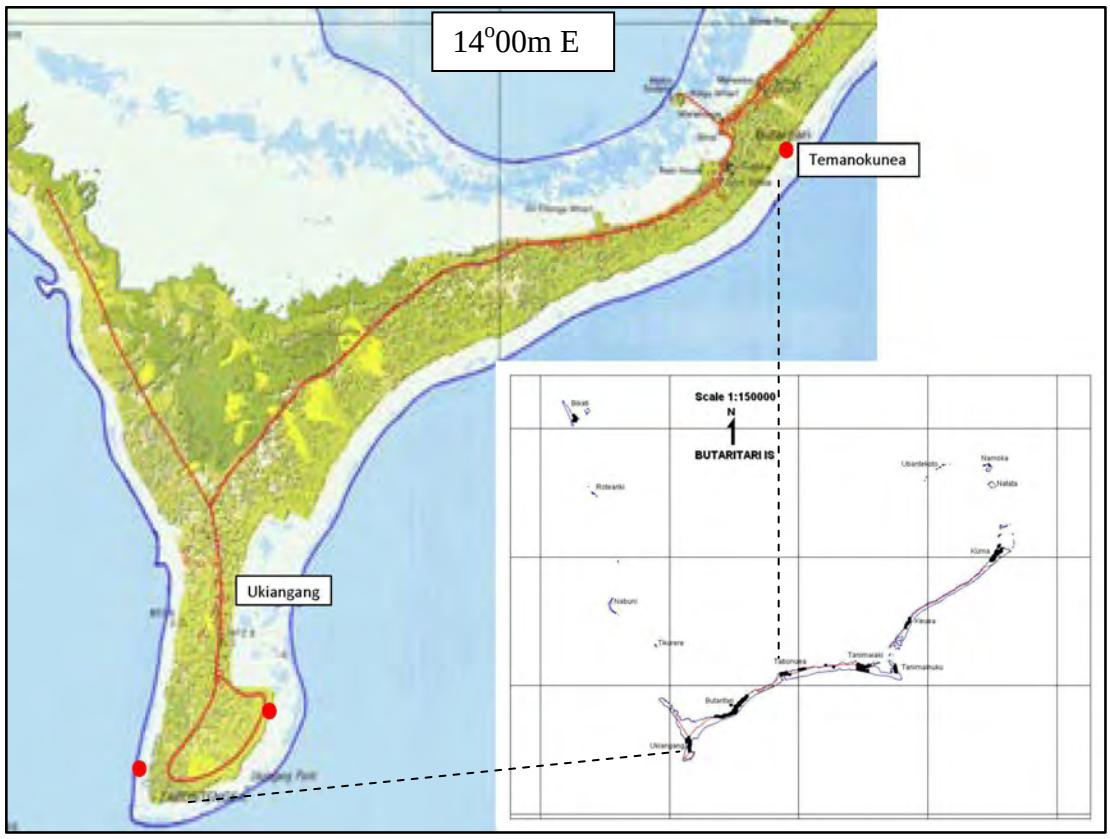

Figure 5.3. Topographical map of Butaritari Atoll showing the sample locations in Ukiangang and Temanokonuea village marked in red. Insert is an outline map of Butaritari Atoll.

5.5 Materials and methods

5.5.1 Field Survey

Transects were surveyed across selected reef islands using a dumpy level. These were all reduced to the 1998 Schlencker ground control mark enabling the surveys to be related to the tidal datum. The survey transects crossed the reef islands in their centres, from the ocean reef flat across to the lagoon sand flat. The transect lengths from Tabiteuea, Notoue and Marenanuka measured 400 m, 330 m and 600 m

respectively. Pits from which samples were obtained were spaced at intervals of 50 m starting from the ocean shoreline. Across Tabiteuea, pits one to four were dug. Pit five utilised an existing *babai* pit, and pit six was a drinking well. In the case of Notoue, pits one to four were sampled, however the remaining two encountered lithified rock at very shallow depths that proved difficult to penetrate. Across Marenanuka, pits one to six were dug, but only samples from pits one, four, five and six were used as funding was a limiting factor. Additional smaller transects were laid across Bairiki, Bonriki-Taborio, Buariki, Tabonibara and Tabiteuea (Figure 5.2). The number of pits dug on each reef island is as follows: Bairiki (n =2), Bonriki-Taborio (n =1), Buariki (n = 5), Tabonibara (n=2) and Tabiteuea (n = 2), a total of 12 pits. All 26 pits were dug to depths of more than one metre and samples were collected from depths of one metre to reduce effects of seasonal temperature changes.

Modern beach samples were collected from central sections of beaches at depths of 2 cm to increase the opportunity of obtaining "modern" recently deposited sediment. All sample locations were recorded with a hand held Geographical Positioning System (GPS).

5.5.2 Beach samples stained with Rose Bengal

Rose Bengal stain was applied to foraminifera and modern beach sediments to establish whether the foraminifera were alive, and if the "modern" beaches were composed of live foraminifera during collection. Foraminifera that have been stained pink after seven days of Rose Bengal staining indicate that they were recently dead when collected. To determine this, half of the samples collected were placed in a sample bag and soaked with Rose Bengal stain for one week. These were then washed and dried.

5.5.3 Laboratory methods

Sediment preparation

Samples were washed, dried and sieved using a >500 µm sieve in order to obtain the medium grain sizes. Sediment grains of >500 µm diameter were collected from which individual *Amphistegina* were selected using an optical microscope with 30x

magnification. Selection of "best preserved" tests was based on a taphonomic classification adapted from W. Nicholas (pers. comm., 2008) developed from Davies *et al*. (1989; 1990). Taphonomic indicators used for classification involve six characteristics which are each ranked from 0-4: (a) completeness (0-4), (b) corrosion (covering dissolution, abrasion and re-crystallisation; 0-4), (c) discolouration (0-4), (d) lustre (0-3), (e) fractures (0-1), and (f) bio-erosion (0-4) (see Appendix B-1). Individuals given a rank of 0 are considered to be that of fresh live foraminifera, whereas 4 represents a highly physically altered fossil.

Single carbonate grain samples collected for age determination were selected based on those with the least physical alteration or those that were youngest looking in order to minimise the time between death and deposition. Wherever possible, samples with the lowest combination of taphonomic indicators were selected. This may provide a better indication of the recently deposited sediments and higher possibility of representing a least reworked fossil (Murray-Wallace, 1995; Ford, 2010). Additionally, this will reduce potential leaching or contamination from foreign material, yielding an apparent age of the fossil as determined from AAR analysis.

AMS 14C dating

Radiocarbon measurements by AMS were carried out on 38 samples collected across Tarawa Atoll. A total of 32 individual foraminiferal samples were selected from pits across Tarawa Atoll. Another four were collected from the "modern" ocean and lagoon beaches. In addition two coral specimens of blue coral octocoral *Heliopora* were submitted for radiocarbon dating obtained from Tabiteuea reef island. One was obtained from a *babai* pit (Pit 5) and the other was an *in situ* coral present within the lower unit of the conglomerate outcrop on the ocean side of Tabiteuea, close to the reef island transect (see Figure 5.3).

AMS 14C measurements were carried out at the Australian Nuclear Science and Technology Organisation (ANSTO), using the Australian National Tandem Research Accelerator (ANTARES) facility. Prior to analyses, samples underwent thorough physical and chemical cleaning following the procedures outlined by Hua *et al*. (2001). After cleaning, the carbon content of samples was converted to carbon

dioxide (CO2) by hydrolysis and then further converted to graphite pellets using the Fe/H2 method (Hua *et al.*, 2001). These graphite pellets were then analysed by AMS. Samples were allocated with a laboratory code OZK, OZN or OZO indicating different batches of analysis. The weak acid residue of 17 selected carbonate samples was sent back to The University of Wollongong (UOW) for AAR analysis. This enabled the same samples dated with AMS to be also dated using AAR. The list of samples used for this paired method is shown in Table 5.2.

Direct calibration on single foraminifera

Direct calibration of AAR ensured that the same individual foraminifera were being analysed by both methods. The weak acid residues of 17 selected carbonate samples of 100 mL were concentrated to remove the water and to increase the amino acid content. Several trials were carried out to concentrate the acid residue prior to the hydrolysis step. The trial that provided the best result was used for the calibration of age is as follows:

a) Two subsamples of 50 mL of the acid residue were transferred to a vial, and left in a desiccator to evaporate to dryness. Once dried, 25 mL of 2 M HCl was added to the vial and shaken for 20 minutes to remove the salts from the sides of the vial. This was then left to dry again in the desiccators. This step was again repeated a second time using 12.5 mL 2 M HCl. At this stage the acid residue is considered to be concentrated. The next steps follow the Kaufman laboratory procedures, with a slight change to the hydrolysis step: adding 5 mL 6 M of HCl to hydrolyse the sample. The change from an 8 M HCl to a less concentrated acid was chosen to allow complete hydrolysis of the low amino acid concentration present in the subsamples (Bada, 1985).

Samples for AAR analyses

A total of 485 single foraminifera were analysed using AAR. These were obtained from both the pits and modern beach samples. From the 26 pit samples, 10 replicates were analysed. Another 25 replicate samples were collected from each ocean and lagoon beach totalling 225. The large sample population (25 replicates) of the same genus was based on the sampling strategies adopted by Murray Wallace and Kimber (1989) which were used to assess ages of Quaternary sediments, in the Perth Basin, Western Australia. To overcome issues of age assessments based on single ages

requires a large population of the same genus and statistical approaches including independent dating techniques. Statistical and chronological significance of results increases with clusters of D/L ratios based on larger populations. In addition larger sample populations improve the understanding of the different processes that affect age mixing (Wehmiller and Miller, 2000) and can also show the spread of relative ages present on these beaches.

AAR analyses were undertaken for the total acid hydrolysate (THAA), a complex mixture of amino acids bound within peptides of varying molecular weight as well as free amino acids. Preparations of samples for AAR analyses followed the laboratory procedures described by Kaufman and Manley (1998) Samples analysed for AAR using the High Performance Liquid Chromatography (HPLC) have been allocated with a laboratory code UWGA-No. The D/L ratios of two amino acids, Aspartic acid and Glutamic acid were calculated using peak areas. These two amino acids were selected as they are fast racemising amino acids and therefore would be best for representing Holocene samples (Goodfriend and Meyer, 1991; Murray-Wallace *et al.*, 1996; Sloss *et al.*, 2006). All D/L ratios have been reported to three significant figures to allow age differentiation (Murray-Wallace and Kimber, 1989).

5.6 Results

Tarawa Atoll Temperature

As temperature primarily affects rates of racemisation, the mean annual air temperature for Tarawa Atoll was determined. This was calculated from daily temperatures collected over a 23 years period from 1977 to 2010 using data obtained from the Kiribati Meteorological Services. The calculated maximum and minimum mean temperatures are 31.25°C and 25.4°C respectively. From those values, the mean temperature is calculated to be 28.3°C. These values indicate that throughout the year, Tarawa Atoll is exposed to fairly constant warm temperatures.

5.6.1 Reef-island chronology based on radiocarbon data

Table 5.1 shows radiometric ages of individual fossil *Amphistegina* and *Heliopora* coral obtained from various sites across Tarawa Atoll (Figure 5.3). The radiocarbon ages have been calibrated to sidereal yrs with reference to the marine reservoir effect using the value obtained from Christmas Island, Kiribati ($\Delta R = 39 \pm 56$ yrs). All the

radiocarbon ages fall within the Holocene epoch, with ages ranging from modern (post 1950 AD) to 5040±215 cal yr BP, and have been reported as a date ± 2σ (where σ is the standard deviation) (Table 5.1). The modes of accretion across Tabiteuea, Marenanuka and Notoue based on the reef island transects are discussed in detail below.

Tabiteuea reef-island pattern

Tabiteuea has a width of 0.6 km and maximum length of 3 km (Figure 5.2) (Table 3.3). It is located on the southern end of North Tarawa's arm. Both ends of the reef island are flanked by open inter-island channels that allow ocean water to flow and transport sediments across into the lagoon. Two sets of radiocarbon dating analysis were performed on Tabiteuea. The results of the first radiocarbon ages obtained from pits across Tabiteuea range from 4165±305 cal yr BP (youngest – OZN134) situated near the ocean beach, to 4505±315 cal yr BP (oldest - OZN137) found in pit 4, about 600 m away from the ocean beach (Table 5.1, Figure 5.4A and 5.5A), however, these ages were not statistically different from each other suggesting that the reef island developed during a single episode. The similar ages of a coral fragment and foraminifera obtained from Pit 5, 4095±195 and 4210±315 cal yr BP respectively, imply that the samples were deposited contemporaneously approximately 4,000 yrs ago.

Table 5.1. Radiocarbon ages of fossils *Amphistegina* (F) and *Heliopora* (C) across Tarawa Atoll expressed both as conventional and calibrated radiocarbon age. *Indicates minor transects. MOB (Modern Ocean Beach), MLB (Modern Lagoon Beach).

ANSTO Lab Code	UWGA No	Fossil	Reef island	Pits	Depth (m)	Conventional radiocarbon age (yr BP)	Calibrated age (cal yr BP)
OZK812		F	Buariki*	Pit 1 (BTP1)	1.50	655±50	255±185
OZK813	8315	F		Pit 5 (BTP5)	1.50	1910±45	1425±150
OZK814		F		Pit 1 (BTP1)	1.50	675±50	265±185
OZK816	8317	F		Pit 5 (BTP5)	1.50	1260±50	780±135
OZL963	7717J	F	Buariki*	Pit 1	1.00	Post 1950 AD	Post 1950 AD
OZL964	7718J	F		Pit 2	1.00	4900±45	5125±210
OZL965	7720J	F		Pit 3	1.00	1015±40	570±95
OZN846	7743Z	F	Notoue	MOB	0.02	Post 1950 AD	Post 1950 AD
OZN847	7744A	F		Pit 1	1.00	1250±70	775±145
OZN848	7745A	F		Pit 2	1.00	1460±60	965±185
OZN849	7746A	F		Pit 3	1.00	1420±60	920±185
OZO295	7747A	F		Pit 4	1.00	1480±60	985±190
OZN850	7748Z	F		MLB	0.02	4350±60	4450±250
OZN851	7754A	F	Marenanuka	Pit 1	1.00	1300±60	805±140
OZN852	7755A	F		Pit 4	1.00	4060±60	4050±240
OZN853	7756A	F		Pit 5	1.00	2710±60	2400±250
OZO296	7757A	F		Pit 6	1.00	1500±50	1010±175
OZL961	7715J	F	Tabonibara*	Pit 2	1.00	965±40	540±105
OZL962	7716J	F		Pit 3	1.00	1320±45	815±135
OZL959	7713J	F	Tabiteuea*	Pit 1	1.00	990±40	555±100
OZL960	7714J	F		Pit 3	1.00	990±40	555±100
OZN844	7731Z	F	Tabiteuea	MOB	0.02	510±60	125±125
OZN134	7732A	F		Pit 1	1.00	4155±100	4165±305
OZO291	7732A	F		Pit 1		4090±80	4100±275
OZN135	7733A	F		Pit 2	1.00	4195±110	4215±340
OZO292	7733A	F		Pit 2		4060±70	4060±260
OZN136	7734A	F		Pit 3	1.00	4290±105	4350±345
OZN137	7735A	F		Pit 4	1.00	4395±110	4505±315
OZO293	7735A	F		Pit 4		4790±60	5040±215
OZN138	7736A	F		Pit 5	1.00	4195±100	4210±315
OZO294	7736A	F		Pit 5		4000±50	3190±200
OZN140	7741	C		Pit 5	1.00	4100±30	4095±195
OZN139	7737A	F		Pit 6	1.00	4300±100	4385±325
OZN845	7738Z	F		MLB	0.02	825±50	400±120
OZN141	7742	C		*Insitu*	0.30	1800±25	1310±135
OZL958	7711J	F	Bonriki-Taborio*	Pit 1	1.00	4055±40	4035±195
OZL956	7709J	F	Bairiki*	Pit 1	1.00	1280±40	790±125
OZL957	7710J	F		Pit 2	1.00	2945±40	2640±190

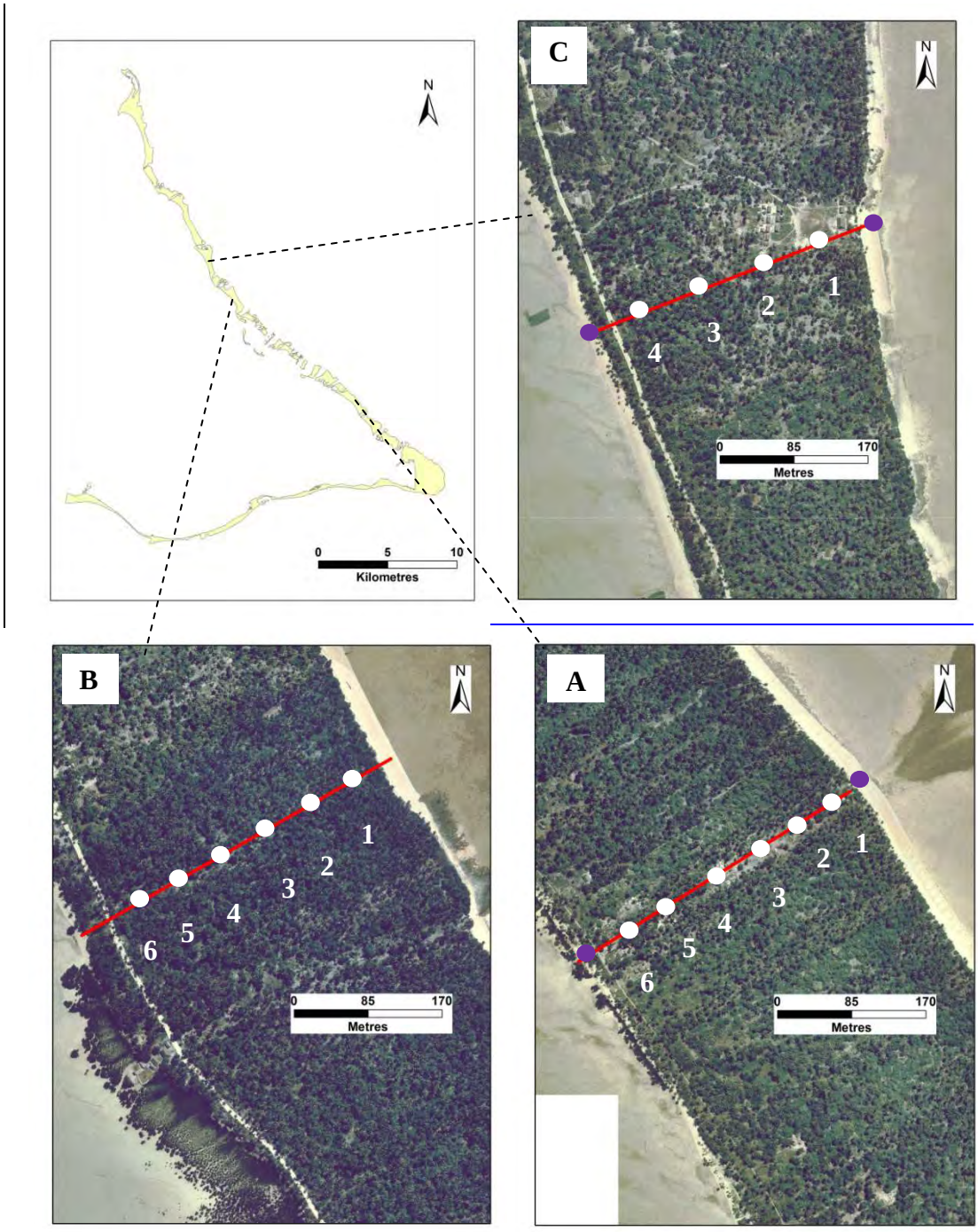

Figure 5.4 Locations of major transects across North Tarawa reef islands with accompanying pits. A: Tabiteuea, B: Marenanuka and C: Notoue. The red line shows the cross-island transect. The white and purple spots mark the locations of the pits and ocean and lagoon sample sites respectively.

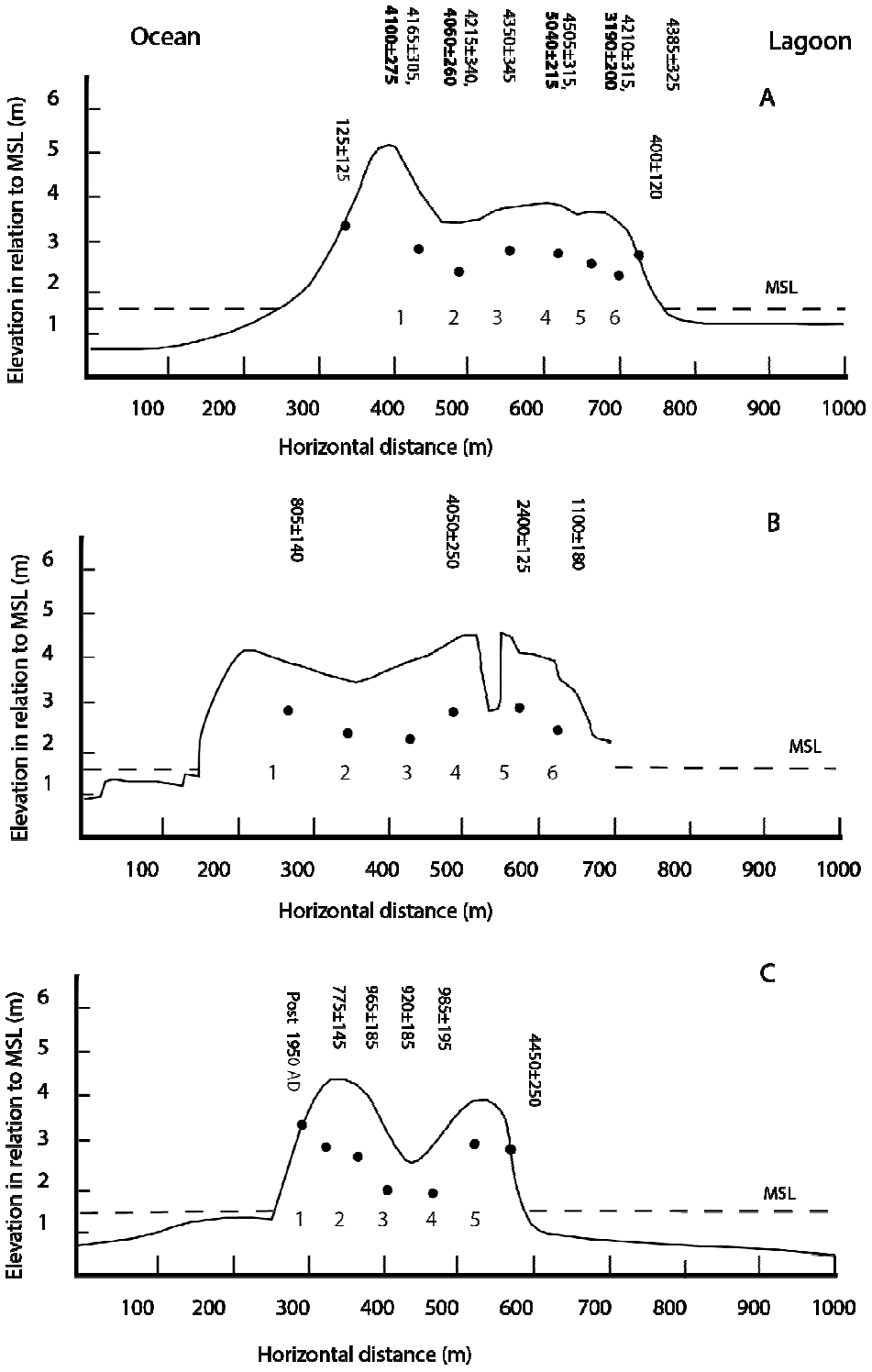

Figure 5.5. Cross island transect with locations of pits across different reef islands; Tabiteuea (A), Marenanuka (B) and Notoue (C). The pits are numbered from the ocean side. Elevation (m) is relative to MSL. Sites where a second set of radiocarbon dates were obtained from Tabiteuea are shown in bold.

To establish if there was any statistical difference between the ages, a *Z* score test was performed on the results. The conventional radiocarbon age of the samples were used as they were reported in ± 1σ (Stuvier and Polach, 1977). A pooled age has

been used to calculate the statistical test as there are more than two radiocarbon ages used. Calculations show that the calculated *Z* value is 3.78, less than that obtained from the Chi-squared table (at 0.05, 5), which is 11.07. This indicates that the ages are not statistically significantly different from each other implying that the sediments on Tabiteuea were deposited in a single episode.

To determine the mode of accretion and whether or not the centre was older, a second set of samples collected from pits 1, 2, 4 and 5 were radiocarbon dated. The ages range from 4100±275 cal yr BP (youngest – OZO291) collected from pit 1 situated near the ocean beach, to 5040±215 cal yr BP (oldest - OZO293) found in pit 4. This sample (OZO293) appears slightly older than sample OZN137, also collected from pit 4, and could indicate that initially there was a slow rate of accretion. The samples collected from pit 5 also show that OZN138 is older than OZO294 (Table 5.1), which may indicate a slower rate of accretion on the lagoon side or reworking.

One possibility is that *Amphistegina* fossils originating from the lagoon side have been added to the reef islands but appear older as they have undergone bioturbation before being deposited on the lagoon beaches. This view is supported by the presence of *Amphistegina* on the lagoon reef flat but in low quantities (Ebrahim, 1999). The results of the second set of ages appeared to be different from each other, and the statistical test on the four ages confirmed this. Results showed that the computed *Z* value of 37.98 is greater than the 5% confidence level indicating the ages are statistically significant from one another. This also confirms that the oldest sample is located in pit 4, close to the lagoon beach, and that sediments on Tabiteuea decrease in age towards the ocean side suggesting oceanward accretion. The ages also decrease from pit 4 towards the lagoon beach as observed in pit 5. The radiocarbon ages on foraminifera suggest that Tabiteuea reef island commenced formation around 4,500 yrs BP, with initial deposition about three quarters of the width of the reef island from the ocean side. The depositional pattern for Tabiteuea as indicated by the radiocarbon ages implies rapid oceanward accretion over a period of around 1,000.

Tabiteuea ocean and lagoon beaches appear to receive young fossils as indicated by the ages of the additional samples collected from the ocean and lagoon beaches. The ocean (OZN844) and lagoon beach samples (OZN845) have ages of 125±125 and 400±120 cal yr BP respectively, both of which are younger than the pit samples close to the beaches. This also suggests that fossils reaching ocean beaches are younger than the lagoon ones. The lagoon samples are relatively young which may indicate that the fossils have originated from the lagoon reef flats.

An *in-situ Heliopora* coral sample obtained from the base of the conglomerate platform on ocean side of Tabiteuea located further south of the transect, shows a coral growing higher than its modern counterparts with an age of 1310±140 cal yr BP (Table 5.1). This indicates a higher sea level at that time as the coral occurs 20 to 35 cm higher than its modern counterparts (Figure 5.7) and is younger than the pit samples. This implies that the conglomerate platform had developed during the late Holocene when sea level was higher than the modern sea level.

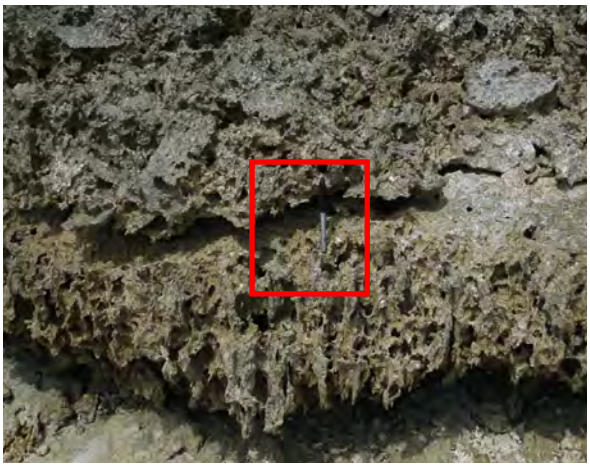

Figure 5.6. Pen located in middle of red square shows the contact point between the cemented storm debris overlying the coral unit. This coral unit is where the *in situ Heliopora* coral (OZN141) was sampled

Marenanuka reef-island pattern

Marenanuka is an elongate reef island with a width and length of 0.7 km and 2 km respectively; and is located further north of Tabiteuea (Figure 5.2) (Table 3.3). Four samples collected from Marenanuka have radiocarbon ages of 805±140 (OZN849-pit 1), 4450±250 (OZN850 – pit 4), 2400±250 (OZN853 – pit 5) and 1100±175 cal yr BP (OZO296 – pit 6) (Table 5.1), Figure 5.5B, Figure 5.6B). A foraminifera collected from pit 1 situated 50 m away from the modern beach is relatively young,

whilst the others located closer to the lagoon beach appear older. The oldest sample (OZN850) obtained from pit 4 may indicate that the reef island initially developed from this point and prograded oceanward as implied by the relatively young age of the sample from pit 1. The reef island also accreted towards the lagoon side as noted by the decreasing age of the fossils towards lagoon beach. The ages suggest that Marenanuka began developing around the same period as Tabiteuea, approximately 4000 years ago. The fossil with the oldest age is located in pit 4 close to the lagoon indicating that the initial deposition of the sediments was similar to that observed for Tabiteuea. The depositional pattern for Marenanuka is similar to that observed on Tabiteuea, however, the sample ages ranging over a period of 3,000 years suggest a slower oceanward and lagoonward build out.

Notoue reef-island pattern

Notoue is located further north of Marenanuka and measures 0.2 km in length (Figure 5.2). The reef island channels either side of Notoue have been closed by solid causeways connecting it to the neighbouring reef islands: Taratai to the north and Marenanuka to the south. Results of radiocarbon dating show that the ages of the four samples obtained from Notoue range from 985±15 (OZO295) to 775±145 cal yr BP (OZN847) (Table 5.1, Figure 5.4C, Figure 5.5C). The youngest sample was collected from pit 1 (OZN847), 50 m away from the modern beach and the oldest (OZO295) from pit 4. The calculated value of Z is 7.29, which is relatively close to the tabulated chi square value of 7.82, therefore the sample ages are statistically different. These results imply that development of the reef island initiated around pit 4 closer to the lagoon side. In pit 5 at 0.3 m depth, limestone was encountered (Figure 5.7). The formation of this less-lithified limestone of about 3-5 cm thickness, known as cay sandstone, appears to be related to the watertable (Woodroffe, 2008; Woodroffe and Biribo, 2011). This prevented the collection of any samples thus limiting an understanding of how the reef island developed in this location. In general the samples appear younger than those of Tabiteuea.

Figure 5.7. Limestone encountered at 0.3 m depth in pit 5 of Notoue reef island.

It is highly likely that the central part of Notoue is not where the reef island initially formed but an area that may have developed afterwards. This is based on two pieces of evidence; one is that the oldest parts of Notoue reef island appears to have ages around 4000 cal yrs BP, and the second is that the young radiocarbon ages on Notoue are similar to those observed on other minor transects. A wider area towards the north of the reef island may possibly be where the reef island initially formed. However, sampling was not carried out in this area as it is very disturbed accommodating the village and a Secondary school.

Notoue ocean beach fossils appear younger than the lagoon beaches fossils. Sample OZN846 obtained from the modern ocean beach has an age of post 1950 AD implying the reef island is still receiving modern fossils. In contrast, OZN850 obtained from the modern lagoon beach is old, with an age of 4450±250 cal yr BP. One possible reason for this is that the lagoon sediments may have undergone bioturbation or reworking as suggested earlier. The relatively old age of this fossil may indicate reworking and taphonomy tends to support this. Taphonomic characteristics of fossil UWGA 7748Z taken from the same sample location show that the test has slightly lost its original pearly lustre and is beginning to show the effects of dissolution, which is consistent with the interpretation that this test may have travelled some distance or that it has been reworked.

Additional samples obtained across Tarawa Atoll

Other samples were collected from the reef islands of Buariki (both within an embayment and further south), Tabonibara, Tabiteuea (on the northwest sand spit), Ambo-Teaoraereke and Bairiki (Figure 5.8). Transects were laid across the reef islands from the ocean to the lagoon side similar to the cross-island transects described previously. Samples were collected from pits at regular intervals of 50 m; with the first sample collected 50 m away from the ocean beach crest.

Buariki is a reef island lying at the northern tip of North Tarawa. It is an elongated reef island measuring 7000 m in length. Two sets of samples were collected from Buariki: one within an embayment and the other located towards the south of the reef island (Figure 5.2, Figure 5.8A). The first set, comprised three samples collected from pits 1 and 5 at depths of 1.5 m from the surface. Sample OZK812 aged 255±185 cal yr BP was collected from pit 1 located 50 m away from the modern beach. Samples OZK813 and OZK816 have ages of 1425±150 and 780±135 cal yr BP respectively and were collected from pit 5, located 180 m inland of the ocean beach. The landward pit yielded much older ages compared with that located close to the beach. This implies that sediment is being added to the ocean beaches at this embayed site, thus filling up the embayment. The foraminifera ages of pit 5 indicate that within the pits, there can be populations with very large age differences suggesting that some populations are reworked.

Samples from the second site on Buariki near the southern end of the reef island (Figure 5.2, Figure 5.8B) are in a sequential order of OZL963 (pit 1), collected 50 m away from the beach crest, OZL964 (pit 2), collected 50 m further inland while OZL965 (pit 3) is located near the middle of the reef-island (Figure 5.8). Radiocarbon results show that OZL963 (pit 1) has a modern age and OZL965 (pit 3) has an age of 570±95 cal yr BP. This indicates that the samples get younger towards the beach (Table 5.1). The only exception was OZL964 (pit 2), obtained from the pit in between the other two, with an age of 5125±210 cal yr BP, which appears to be older and may indicate reworking.

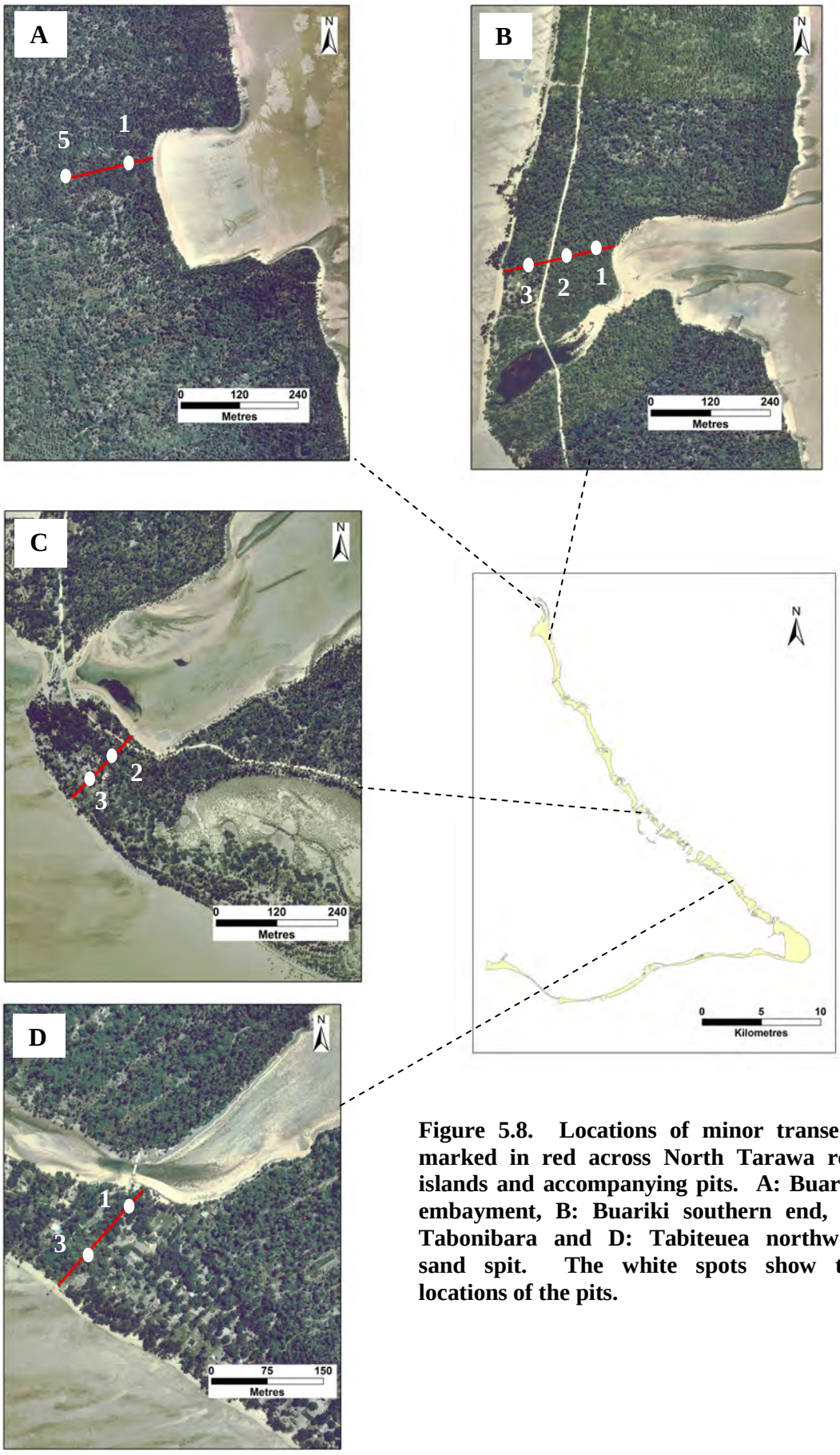

Figure 5.8. Locations of minor transects marked in red across North Tarawa reef islands and accompanying pits. A: Buariki embayment, B: Buariki southern end, C: Tabonibara and D: Tabiteuea northwest sand spit. The white spots show the locations of the pits.

Tabonibara reef island is located in North Tarawa and is 0.9 km in width, and 0.3 km in length. The cross-island transect was located close to the northern end of the reef island in length (Figure 5.2). Samples collected from Tabonibara were located 50 m away from the beach crest on the ocean (OZL961 – pit 2) and lagoon side (OZL962 – pit 3) (Figure 5.8C). The radiocarbon dating yielded ages of 540±105 and 815±135 cal yr BP respectively indicating that this part of the reef island is still developing and that the ocean beach is younger compared to the lagoon beach (Table 5.1).

Two samples were collected from a sand spit on Tabiteuea located to the north of the main cross-island transect discussed earlier (see Section Tabiteuea reef island pattern, Figure 5.2). These samples were obtained from pits situated 50 m away from the beach crest on both the ocean (OZL959 – pit 1) and lagoon sides (OZL960 – pit 3) (Figure 5.8D). Radiocarbon dating shows that these samples have similar ages of 555±100 cal yr BP. This suggests that foraminifera of the same age originating from the ocean reef flat and another from the lagoon reef flat could have been deposited on the ocean beach and lagoon beach at similar times. In addition, the ages of these samples were similar to those obtained from Tabonibara's ocean side (OZL961) (Table 5.1), suggesting that these areas formed around the same time.

On South Tarawa, two sites were selected: Bairiki and Ambo-Teaoraereke (Figure 5.2). Bairiki, a reef island lies east of Betio and has a length of about 4 km (Table 3.3). Ambo-Teaoraereke is an elongated reef island that lies further east of Bairiki and is longer, measuring 6 km (Table 3.3). Samples were collected in sites that appeared to be less disturbed by humans. The pit locations followed the same spacing interval as that of the main transects, with intervals of 50 m starting from the oceanward beach crest. Two samples were collected from Bairiki, one at 50 m from the oceanward beach crest (pit 1) and the next at 100 m (pit 2). Results show that these samples OZL956 (pit 1) and OZL957 (pit 2), are aged 790±125 and 2640±190 cal yr BP respectively (Figure 5.9A) implying that age gets progressively younger towards the ocean beach, and that material has been added to the ocean beach. The age of OZL956 (pit 1) is similar to that of Notoue, OZN847 (pit 1), Marenanuka OZN851 (pit 1) and Buariki OZK816 (pit 5). All three of these sites spread across have relatively young fossils located close to the beach, indicating that these sites

were still receiving young material from the ocean side around 800 yrs BP. This implies that Tarawa Atoll was still receiving sediment from the ocean, 800 years ago. Only one sample was collected from Ambo-Teaoraereke located 50 m away from the ocean beach, and this was dated to 4035±195 cal yr BP (Figure 5.9B). This is similar to samples OZN134 to OZN136 collected from Tabiteuea, and sample OZN852 from Marenanuka. These old sample ages indicate that they represent the oldest parts of the reef islands.

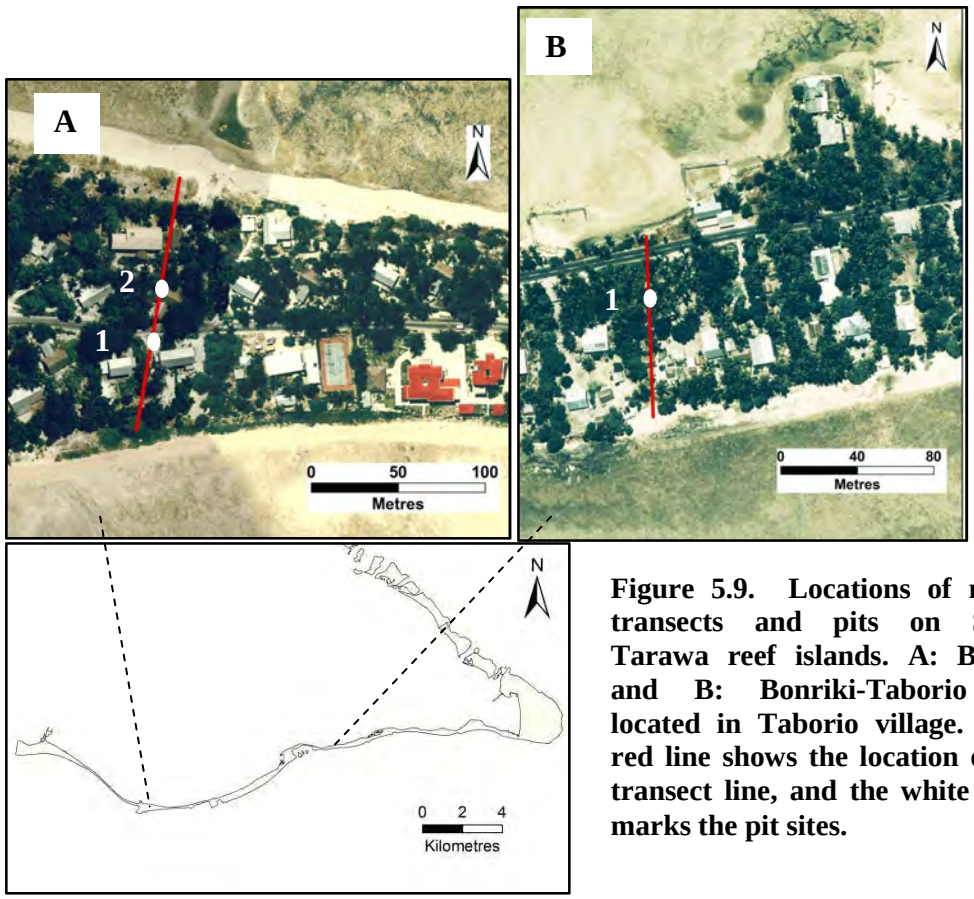

Figure 5.9. Locations of minor transects and pits on South Tarawa reef islands. A: Bairiki and B: Bonriki-Taborio site located in Taborio village. The red line shows the location of the transect line, and the white spots marks the pit sites.

5.6.2 Paired (AMS and AAR) ages of single foraminifera

A trial was undertaken to directly calibrate AMS and AAR ages on single foraminifera. It should be noted that it is very tricky to determine the AMS age of a foraminifera sample that weighs less than a milligram, and it is even more difficult to determine the AAR age on the resultant acid residue from the AMS dating. The first attempt to concentrate the HCl residue yielded only low concentrations of residual proteins. Another attempt was carried out to concentrate the 17 acid residues (Table 5.2) which involved concentrating the dilute acid residues of 1mL prior to AAR analyses in a similar way to that developed by Kaufman and Manley (1999). Ratios

of these amino acids were determined using the peak area on the chromatogram which is a measure of the area covered by the amino acid signal. Using the selection criteria to identify outliers a screening test was applied to these paired (AMS and D/L ratio) results of single foraminifera. The criteria to identify outliers follows those of Kosnik *et al*. (2008) and are a) high serine content greater than 15% indicates contamination, b) D/L ratios higher than 2σ of the group imply reworked samples and, c) samples with greater than 3% covariance between the concentration and D/L values for Aspartic and Glutamic acid indicate samples have been exposed to different environmental conditions. As most of these samples were geologically young (Table 5.1) it was anticipated that the serine content would be high (Kosnik *et al.*, 2008). Using the above selection criterion, five samples that showed very high concentration of serine with a coefficient variation (CV) greater than 15% were eliminated as this was an indication of contamination (Kosnik *et al.*, 2008). Coefficient variation is the uncertainty expressed as a percentage and can be calculated using:

$$CV = ([SD/Mean_{D/L}] \times 100\%)$$, where SD is the standard deviation.

Table 5.2. Paired radiocarbon and amino acid D/L ratios obtained from single foraminifera of fossil *Amphistegina* collected from pits of 1.0 – 1.5 m depths and around Tarawa Atoll. The paired ages marked in # have been used to develop the apparent parabolic model. Reported D/L are mean values except where only one analysis has been undertaken (+). A * indicates D/L values were obtained by peak height.

Radiocarbon Lab Code	UWGA No.	Reef island	Pit	Radiocarbon ages (yrs BP)	Calibrated age (cal yr BP)	Asp	Glu	Ser	CV (%)
OZL964+#	7718J	Buariki	2	4900±45	5125±210	0.35	0.17	0.11*	10
OZN137+#	7735A	Tabiteuea	4	4395±110	4505±315	0.44	0.24	0.17	
OZN139#	7737A	Tabiteuea	6	4300±100	4385±325	0.40	0.18	0.07	5
OZN136	7734A	Tabiteuea	3	4290±105	4350±345	0.39	0.17	0.13	33
OZN135#	7733A	Tabiteuea	2	4195±110	4215±340	0.34	0.15	0.08	4
OZN138	7736A	Tabiteuea	5	4195±100	4210±315	0.42	0.19	0.11	88
OZN134# +	7732A	Tabiteuea	1	4155±100	4165±305	0.37	0.14	0.06	
OZL958	7711J	Bonriki-Taborio	1	4055±40	4035±195	0.30	0.12	0.10	66
OZL957#	7710J	Bairiki	2	2945±40	2640±190	0.34	0.13	0.18	8
OZK813#	8315	Buariki	5	1909±45	1425±150	0.18	0.10	0.07	11
OZL962	7716J	Tabonibara	3	1320±45	815±135	0.17	0.07	0.07	100
OZK816+#	8317	Buariki	5	1260±50	780±135	0.22	0.07	0.07	
OZL965	7720J	Buariki	3	1015±40	570±95	0.17	0.10	0.17	124
OZL959#	7713J	Tabiteuea	1	990±40	555±100	0.22	0.08	0.15	3
OZL960#	7714J	Tabiteuea	3	990±40	555±100	0.24	0.09	0.17	3
OZL961#	7715J	Tabonibara	2	965±40	540±105	0.17	0.06*	0.07	3
OZL963+#	7717J	Buariki	1	Post 1950 AD	Post 1950 AD	0.12	0.05	0.10	

Instead of using peak areas, peak heights for any Aspartic, glutamic or serine were found to be more suitable for subsamples with high CV (>9%). Peak areas are considered to be more susceptible to contamination than peak heights, as they cover a wider area (Wehmiller and Miller, 2000). Out of the 17 samples only 12 passed the selection criteria and could be used to develop a simple linear relationship of amino acid racemisation against radiocarbon age for the same foraminifera (Table 5.2). This enables the degree of racemisation of amino acids to be directly compared with the set of ages provided by the independent AMS radiocarbon dating. There is quite a spread of data, as Aspartic acid ranges from as low as 0.017 to as high as 0.44. A plot of Aspartic or Glutamic acid with depth shows that samples OZL813 and OZK816 have higher D/L ratios for both Aspartic and Glutamic acid compared to other samples as their burial depths were greater, up to 1.5 m (Figure 5.10 A and B). This indicates that these samples are older than the others. To further investigate the spread of data the D/L ratio of Aspartic acid was plotted against the D/L ratio of Glutamic acid for each sample (Figure 5.10). This graph demonstrates that as sample age increases, consistent with age trend, so does the extent of amino acid racemisation for both Aspartic and Glutamic acid. Results show that sample OZL963 has the lowest D/L values whilst OZN137 has the highest ratios of 0.44 (Asp) and 0.17 (Glu).

To determine which amino acid was more suitable for the determination of numeric ages of foraminifera, a comparison between Aspartic and Glutamic acid was made. To accomplish this, the amino acid D/L ratio was plotted against the corrected radiocarbon age (cal yr BP). Figure 5.11A and B and Figure 5.12 A and B show the simple linear model of the amino acids under ambient temperatures. This linear model shows the early stages of diagenesis in terms of the history of the reaction (Clarke and Murray-Wallace, 2006).

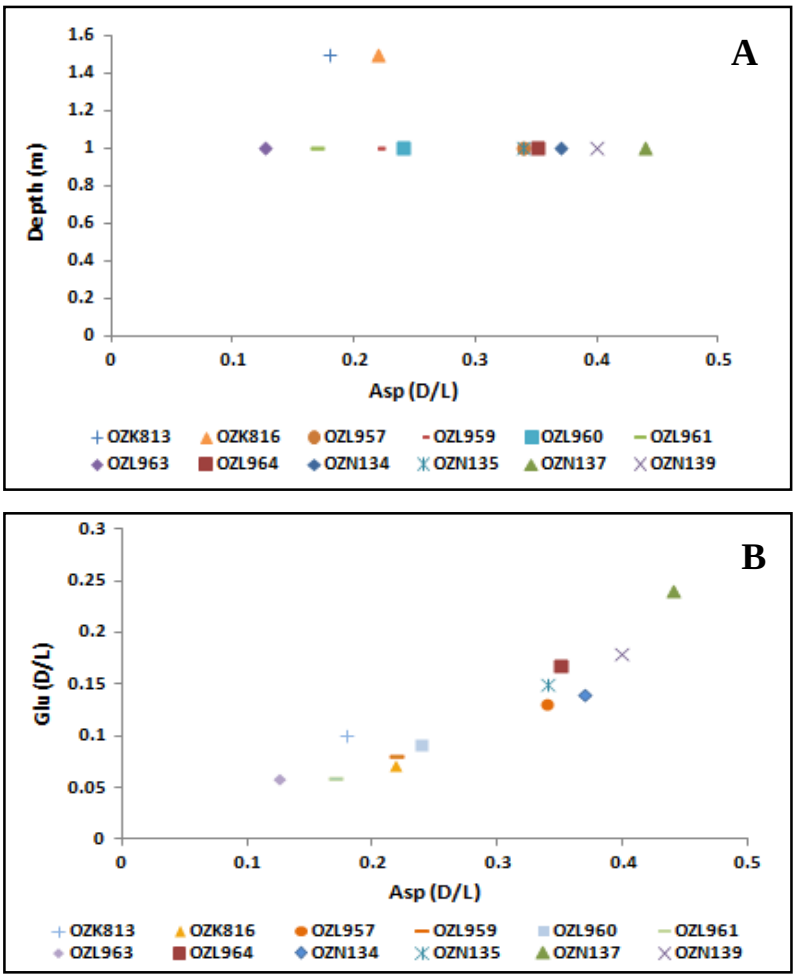

Figure 5.10. A: Plot of depth vs Asp (D/L) shows that OZK813 and OZK816 have higher Asp D/L buried at a depth of 1.5 m; B: shows that D/L ratios increase with age using Aspartic vs Glutamic acid (D/L).

This relationship can be seen by plotting the amino acid D/L versus the square root of the radiocarbon ages as illustrated in Figure 5.12 A and B, whereby the D/L values of live foraminifera have been deducted from the samples. This step takes into consideration any racemisation that takes place prior to diagenesis (Bada and Schroeder, 1972). The y-intercept for the regression line is derived from the D/L ratio of a live collected foraminifera that was obtained from Tabiteuea located under coral rubble in a rock pond (Figure 5.13), following an approach by Kosnik *et al.* (2008). The live specimen had D/L values of 0.028 for Aspartic acid and 0.016 for Glutamic acid (Table 5.3), similar to values obtained from live *Natica* mollusc shells collected from the Great Barrier Reef, Australia (Kosnik *et al.*, 2008). The regression line is based on 70% of the samples and has high R^2 values of 0.83 and 0.79 for both Aspartic acid and Glutamic acid respectively indicating a high degree of correlation between the degree of racemisation and age (Figure 5.12A and B).

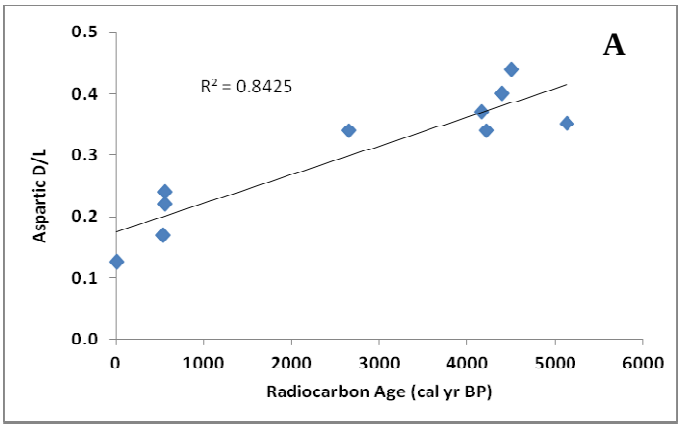

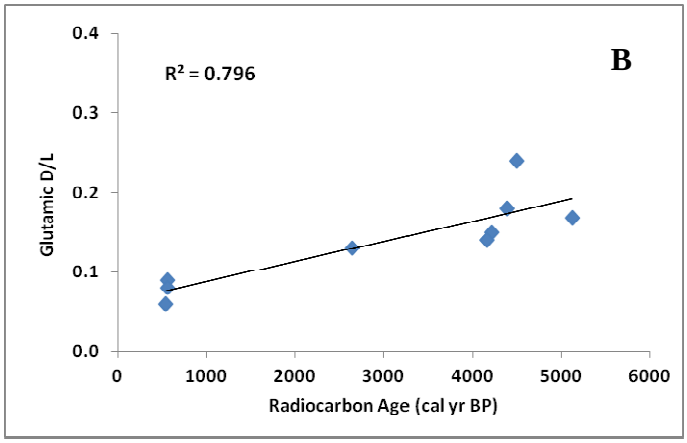

Figure 5.11. Graphs of D/L ratios of Aspartic and Glutamic acids and equivalent radiocarbon ages obtained on *Amphistegina* spp. A: Aspartic D/L ratio versus equivalent radiocarbon ages and B: Glutamic D/L ratio versus equivalent

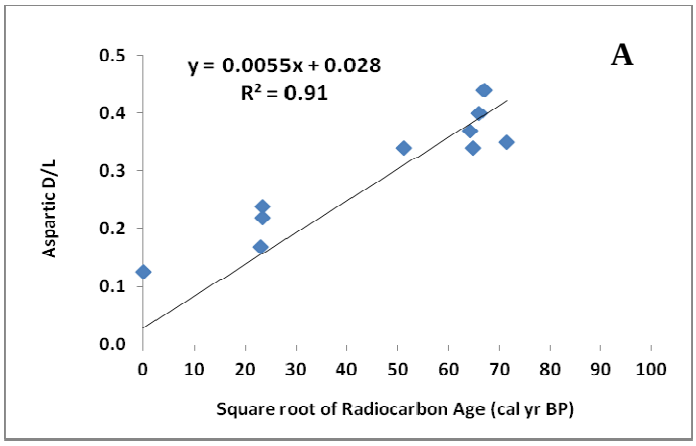

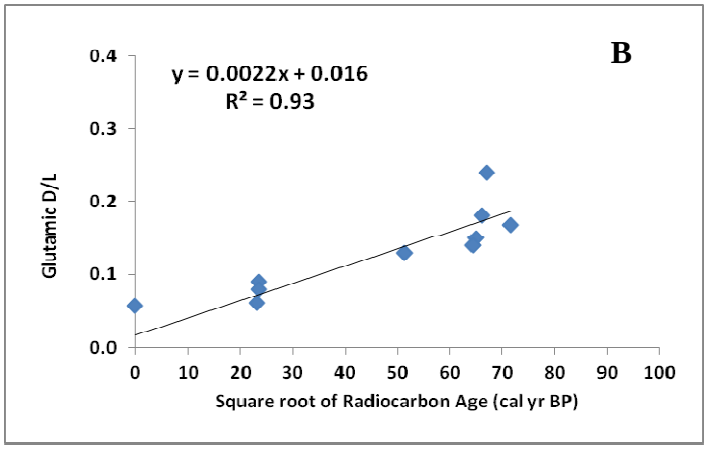

Figure 5.12. Graph of D/L ratio of two amino acids used versus the square root of radiocarbon ages from *Amphistegina* spp. A: Aspartic acid and B: Glutamic acid. The D/L ratio of modern *Amphistegina* has been removed to remove any racemisation that may have

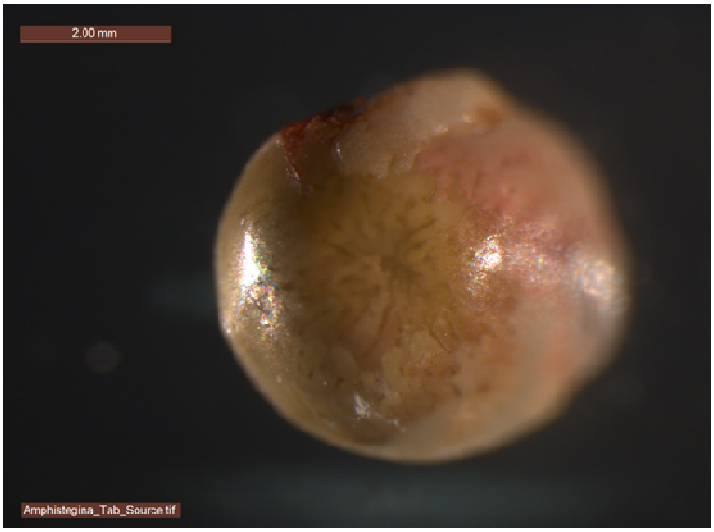

Figure 5.13. Live *Amphistegina* treated with Rose Bengal; note only the outer test is stained. The brown colour indicates the presence of organic material, i.e., protoplasm. Photo taken with Leiza MZ16A polarising microscope.

Although these graphs show high R^2 values, the linear model has not been applied in this study. The reasons for this are: a) the model has been developed based on a limited number of paired samples; and b) the numeric age of the samples when determined will be dependant on the uncertainties involved in the racemisation kinetics, and diagenetic temperature, thus producing apparent ages and radiocarbon dating uncertainties (Murray-Wallace and Kimber, 1989). Therefore relative age dating is selected as the best choice to discuss and compare these ages as there is less uncertainty involved.

Comparison of the two graphs (Figure 5.12A and B) shows that Aspartic acid is a better choice for dating these geologically young fossils for two reasons. The first is that it is a fast racemising acid and has a greater age-resolving power over shorter time periods, and secondly it covered a larger extent of D/L ratios for the fossil samples collected across Tarawa Atoll similar to those observed in a study in south-east Australia (Sloss, 2005).

In order to achieve a single best age for a population, data were screened and outliers identified by applying the criteria developed by Kosnik and Kaufman (2008) as discussed earlier (see Section 5.5.3).

5.6.3 Reef-island development derived from paired AMS radiocarbon and AAR data

By plotting the mean D/L ratios of Aspartic acid against Glutamic acid for different samples across the two reef islands Tabiteuea and Notoue, a broad range of relative ages were derived. The results show that Tabiteuea samples are older than those obtained from Notoue. A pattern is noted: a distinct cluster of old samples with higher D/L ratios from the pits; a relatively younger sample from the modern lagoon and ocean beach and a much younger age for live foraminifera. Samples obtained from Tabiteuea pits have mean Aspartic D/L ratios ranging from 0.226±0.08 (UWGA7731) to 0.473±0.05 (UWGA 7732) (Table 5.3). Those with the lowest D/L are from modern ocean and lagoon beach samples UWGA7731 (0.226±0.08) and UWGA 7738 (0.29±0.06) respectively. This implies that the ocean beach of Tabiteuea receives younger foraminifera compared to its lagoon beach. Samples collected from pits are clustered together and have higher mean Aspartic D/L ratios ranging from 0.424±0.041 (UWGA7737) to 0.473±0.051 (UWGA 7732) indicating that they are older than the other samples collected from the ocean and lagoon beaches (Figure 5.14A). The standard deviations of all reef island samples show that analytical results overlap with each other making it difficult to interpret a mode of reef-island development.

Table 5.3. Mean D/L ratios of Tabiteuea and Notoue reef island and modern ocean and lagoon beach samples. See Appendix B-2 for raw data

Reef island	UOW Lab Code	Mean D/L values		η samples	Standard Deviation (σ1)	
		Asp	Glu		Asp	Glu
Tabiteuea	UWGA7731	0.226	0.110	23	0.08	0.035
	UWGA7732	0.473	0.243	10	0.051	0.047
	UWGA7733	0.451	0.243	11	0.061	0.042
	UWGA7734	0.444	0.208	10	0.032	0.025
	UWGA7735	0.460	0.250	10	0.027	0.04
	UWGA7736	0.429	0.219	11	0.058	0.047
	UWGA 7737	0.419	0.219	11	0.040	0.030
	UWG A7738	0.29	0.156	24	0.06	0.036
	UWGA7752	0.028	0.016	1		
Notoue	UWGA 7743	0.092	0.048	24	0.043	0.026
	UWGA7744	0.310	0.132	9	0.015	0.011
	UWGA7745	0.327	0.131	8	0.026	0.016
	UWGA7746	0.326	0.157	6	0.042	0.041
	UWGA7747	0.354	0.157	9	0.018	0.074
	UWGA7748	0.249	0.145	21	0.061	0.041

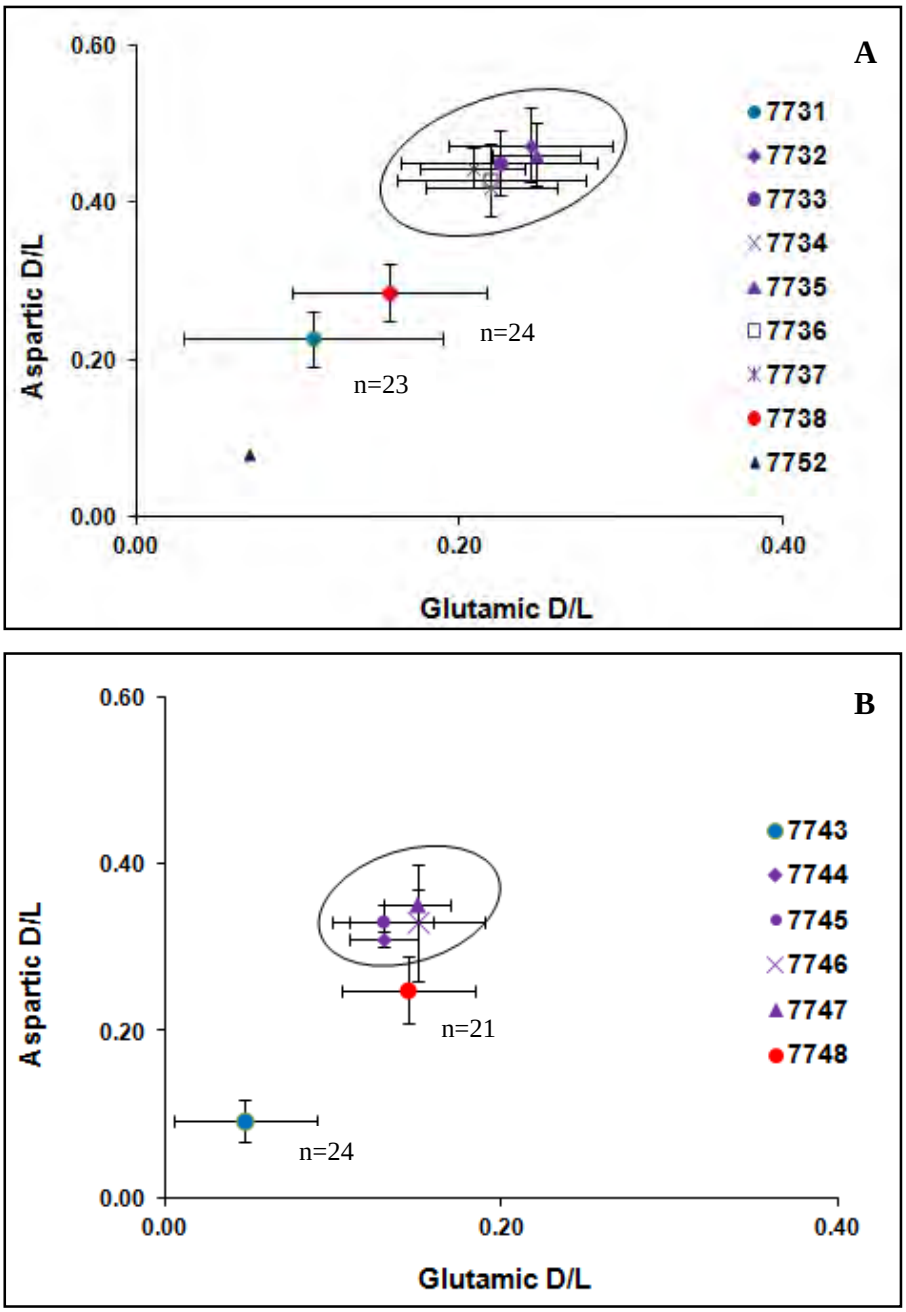

Figure 5.14. D/L ratio of samples obtained from selected sites across A: Tabiteuea reef island and B: Notoue reef island. These sites include pits (purple), the ocean reef flats (solid dark blue triangle), the modern ocean beach (solid blue circles) and the modern lagoon beach (solid red circles). The lines on the samples indicate the uncertainties for Aspartic and Glutamic acid calculated using the standard deviations for the number of samples used represented by n. Note that only sample 7752 is comprised of only one sample.

A similar pattern is observed for Notoue reef island. Mean Aspartic D/L ratios for modern ocean beach samples were 0.092 ±0.043 which were lower than the D/L ratio for the lagoon sample (0.249 ±0.061) (Figure 5.14B). However, in this situation, the lagoon sample is relatively older appearing closer to the pit D/L ratios (Table 5.3).

The samples on the lagoon beaches may have been exposed to bioturbation prior to being deposited on the beaches. The series of pit samples collected from the reef island appear to be relatively older than those from the lagoon and ocean beaches with a mean D/L ratio for Aspartic acid ranging from 0.31±0.132 (7744) to 0.354 ±0.157 (7747). A comparison between mean D/L ratios from reef island samples from Notoue with those from Tabiteuea implies that Notoue is relatively younger. This tends to support the radiocarbon results.

5.6.4 Modern beach trend across Tarawa Atoll

To determine the trend of ages across Tarawa Atoll, the sample populations (pop) within the nine different sites were determined using the extent of racemisation of Aspartic acid. These sites are Notoue (ocean and lagoon beaches), Tabiteuea (ocean and lagoon beaches), Buota (lagoon channel), Bonriki (ocean beach), Teaoraereke (ocean and lagoon beaches) and Bairiki (lagoon beach) (Table 5.4, Figure 5.2). (See Appendix B-2 for raw data).

Table 5.4. Summary of modern populations of age on nine different beaches

"Modern" Beaches									
	Notoue		Tabiteuea		Buota	Bonriki	Teaoraereke		Bairiki
	Ocean	Lagoon	Ocean	Lagoon	Lagoon	Ocean	Ocean	Lagoon	Lagoon
Pop 1	0.29	0.35	0.38	0.4	0.44	0.23	0.35	0.40 ±0.01	0.38
Pop 2	0.1	0.31 ±0.02	0.35	0.36	0.41	0.22	0.31	0.37	0.31
Pop 3	0.09 ±0.01	0.29 ±0.01	0.27	0.33	0.36	0.21 ±0.01	0.30 ±0.01	0.36 ±0.01	0.29
Pop 4	0.07	0.28 ±0.01	0.25 ±0.01	0.31 ±0.01	0.35	0.2	0.29	0.35	0.25 ±0.02
Pop 5	0.06	0.27 ±0.02	0.23 ±0.02	0.28	0.32	0.19	0.27	0.34 ±0.01	0.22
Pop 6	-	0.25	0.19 ±0.02	0.27	0.24 ±0.02	0.18	0.24	0.33	0.18
Pop 7	-	0.24	0.18	0.25 ±0.01	-	0.1	0.22	0.31 ±0.02	-
Pop 8	-	0.22	0.17	0.23	-	0.08	0.21	0.30 ±0.02	-
Pop 9	-	0.2	0.15 ±0.01	0.22	-	-	0.16	0.27	-
Pop 10	-	0.21	0.13 ±0.01	0.21	-	-	0.14	-	-
Pop 11	-	0.15	-	0.2	-	-	-	-	-
Pop 12	-	0.14	-	-	-	-	-	-	-
Pop 13	-	0.13	-	-	-	-	-	-	-
Mean	0.12	0.23	0.23	0.28	0.35	0.18	0.25	0.34	0.27
SD	0.1	0.07	0.08	0.07	0.07	0.06	0.07	0.04	0.07

Notoue ocean beach has only five populations of age with the extent of Aspartic acid D/L ranging from as low as 0.06 to as high as 0.29 (Table 5.4). In order of descending Aspartic acid D/L sample values were 0.29 (pop 1), 0.1 (pop 2), 0.09±0.01 (pop 3), 0.07 (pop 4) and 0.06 (pop 5) (Figure 5.15 A). The D/L ratios indicate that the populations on these beaches are mixed, and appear relative young compared to other beaches.

Notoue lagoon beach indicates that there is a lot of mixing occurring with a large number of age populations present (Table 5.4). The 13 populations have D/L ratios ranging from as low as 0.13 to as high as 0.35. In descending order of extent of racemisation of Aspartic acid, the D/L ratios are; 0.35 (pop 1), 0.31 ±0.01 (pop 2), 0.29 ±0.01 (pop 3), 0.28 ±0.01 (pop 4), 0.27 ±0.02 (pop 5), 0.25 (pop 6), 0.24 (pop 7), 0.22 (pop 8), 0.21 (pop 9), 0.20 (pop 10), 0.15 (pop 11), 0.14 (pop 12) and 0.13 (pop 1) (Figure 5.15 A). The average Aspartic acid D/L ratio for this beach is 0.23±0.07 indicating that the samples are relatively old therefore suggesting reworking.

Tabiteuea ocean beach is composed of 10 populations of age, suggesting that mixing is occurring (Table 5.4). The Aspartic acid D/L ratios range from 0.13±0.01 to as high as 0.38 similar to that of Notoue ocean beach. In descending order, D/L ratios are: 0.38 (pop 1), 0.35 (pop 2), 0.27 (pop 3), 0.25±0.01 (pop 4), 0.23±0.02 (pop 5), 0.19±0.02 (pop 6), 0.18 (pop 7), 0.17 (pop 8), 0.15±0.01 (pop 9), and 0.13±0.01 (pop 10) (Figure 5.15 B). The average D/L ratio for Tabiteuea ocean beach is 0.23±0.08, which is similar to that of Notoue lagoon beach and Tabiteuea lagoon beach. The relatively high D/L ratios suggest that the samples are old and may have been reworked.

Tabiteuea lagoon beach has 11 populations of age suggesting that a lot of mixing is occurring on this beach (Table 5.4). The extent of racemisation of Aspartic acid shows that D/L ratios range from as low as 0.2 to as high as 0.4. In descending order, the D/L ratios are: 0.4 (pop 1), 0.36 (pop 2), 0.33 (pop 3), 0.31±0.01 (pop 4), 0.28 (pop 5), 0.27 (pop 6), 0.25±0.01 (pop 7), 0.23 (pop 8), 0.22 (pop 9), 0.21 (pop 10), and 0.20 (pop 11) (Figure 5.15 B). The average D/L ratio for Tabiteuea lagoon

beach is 0.28±0.07, which is relatively high and indicates that the beach is comprised of reworked sediment grains.

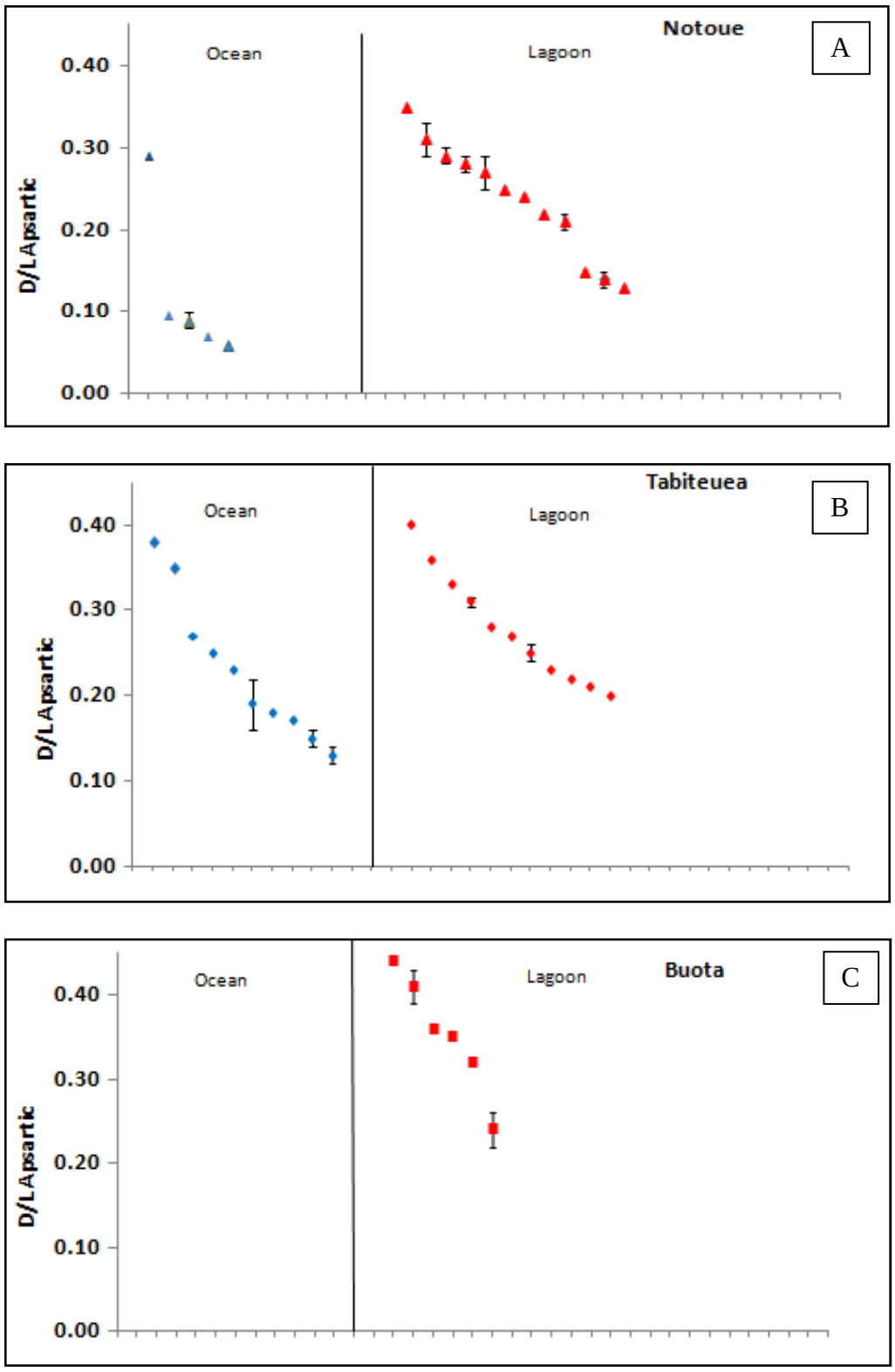

Figure 5.15. Graphs illustrating the extent of racemisation of Aspartic acid in *Amphistegina* tests collected from A: Notoue, B: Tabiteuea and C: Buota ocean and lagoon beaches in North Tarawa. The blue colours indicate ocean samples and the red colours indicate lagoon samples.

Buota lagoon channel beach is composed of only six populations of age (Table 5.4). The extent of racemisation of aspartic acid shows that the D/L ratios range from 0.24 ±0.02 to 0.44 indicating that these samples are relatively old (Figure 5.15 C). In descending order, the D/L ratios are: 0.44 (pop 1), 0.41 (pop 2), 0.36 (pop 3), 0.35 (pop 4), 0.32 (pop 5), and 0.35±0.07. These values are relatively higher than those obtained the Tabiteuea lagoon beach and Notoue lagoon beach but similar to those from Teaoraereke lagoon beach.

Bonriki ocean beach has only eight populations of age indicating that mixing is also occurring on this beach (Table 5.4). The D/L ratios range from as low as 0.08 up to 0.23. The extent of racemisation of aspartic acid in descending order is: 0.23 (pop 1), 0.22 (pop 2), 0.21±0.01 (pop 3), 0.2 (pop 4), 0.19 (pop 5), 0.18 (pop 6), 0.1 (pop 7), and 0.08 (pop 8) (Figure 5.16 A). The mean D/L ratio is 0.18±0.06, which appears to be relatively low, indicating young samples.

Teaoraereke ocean beach has 10 populations of age and is one of the beaches comprising many populations. The large population size indicates that mixing is prevalent on this beach (Table 5.4). The range of D/L ratios is large, from 0.14 to 0.35, which is similar to that of Notoue lagoon (0.13 to 0.35). The extent of racemisation of aspartic acid in descending order is: 0.35 (pop 1), 0.31 (pop 2), 0.30±0.01 (pop 3), 0.29 (pop 4), 0.27 (pop 5), 0.24 (pop 6), 0.22 (pop 7), 0.21 (pop 8), 0.16 (pop 9), and 0.14 (pop 10) (Figure 5.16 B). The mean D/L ratio is 0.25±0.07, which appears to be relatively old indicating reworked samples. The beach showed similar results to that of Bairiki ocean beach, Notoue lagoon beach and Tabiteuea ocean beach.

Teaoraereke lagoon beach has 10 populations of age with many populations (Table 5.4). The large population size as well as the large range in age indicates that mixing is prevalent on this beach. The range of D/L ratios is large, from 0.14 to 0.35, and is similar to that of Notoue lagoon (0.13 to 0.35). The extent of racemisation of aspartic acid in descending order is: 0.35 (pop 1), 0.31 (pop 2), 0.30±0.01 (pop 3), 0.29 (pop 4), 0.27 (pop 5), 0.24 (pop 6), 0.22 (pop 7), 0.21 (pop 8), 0.16 (pop 9), and 0.14 (pop 10) (Figure 5.16 B). The mean D/L ratio is 0.25±0.07, which appears to be

relatively old indicating reworked samples. The beach is similar to that of Bairiki ocean beach, Notoue lagoon beach and Tabiteuea ocean beach.

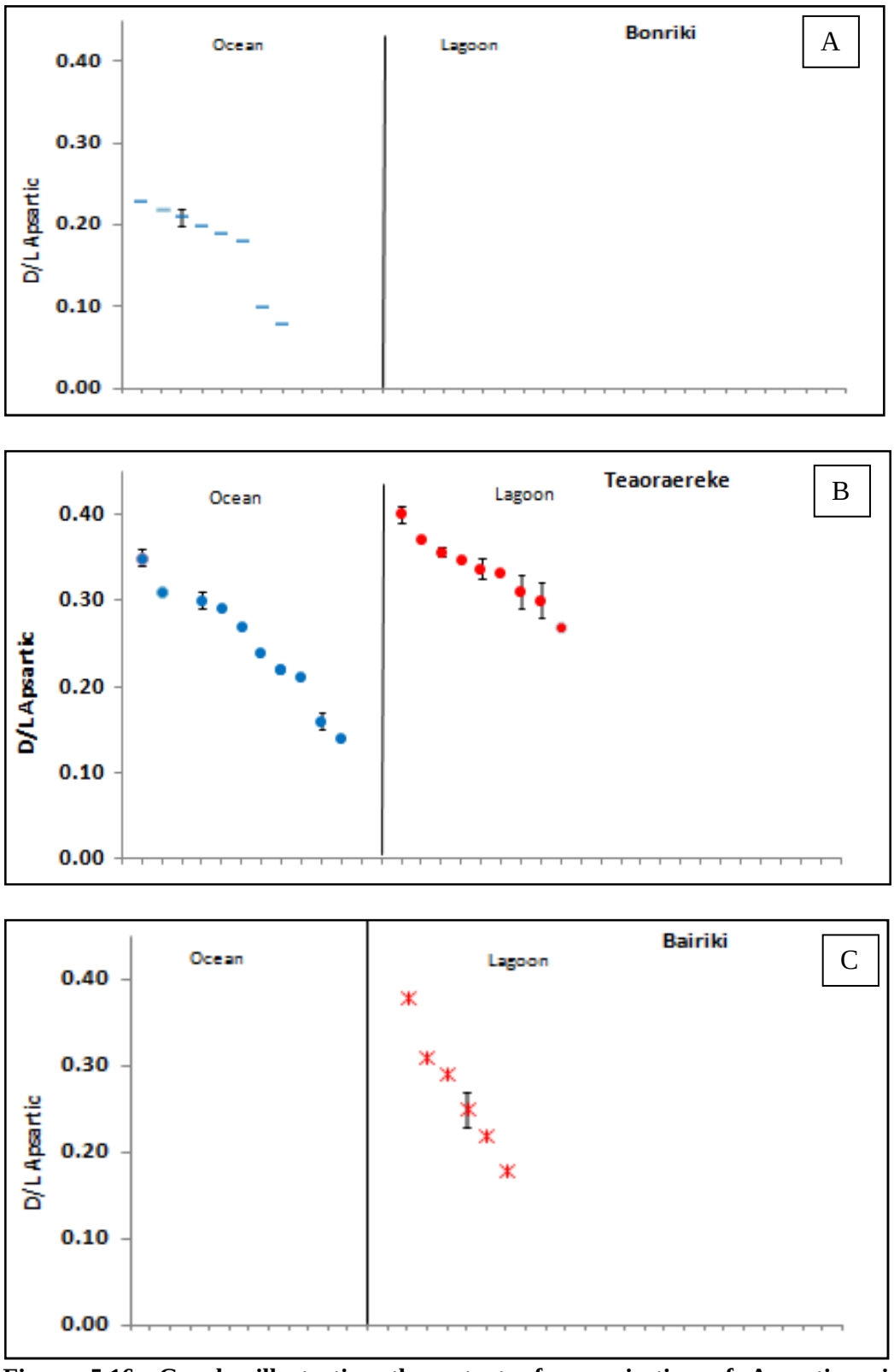

Figure 5.16: Graphs illustrating the extent of racemisation of Aspartic acid in *Amphistegina* tests collected from South Tarawa ocean and lagoon beaches on A: Bonriki, B: Teaoraereke and C: Bairiki. The blue colours indicate ocean samples and the red colours indicate lagoon samples.

Bairiki lagoon beach is composed of only six populations with D/L ratios ranging from as low as 0.18 to as high as 0.38 (Table 5.4). The small population size but large differences in D/L ratios indicate that there is a lot of mixing occurring. In descending order, the D/L ratios are as follows: 0.38 (pop 1), 0.31 (pop 2), 0.29 (pop 3), 0.25±0.02 (pop 4), 0.22 (pop 5), and 0.18 (pop 6) (Figure 5.15 C). The D/L ratios of these samples appear relatively old, indicating reworking and are similar to D/L ratios obtained on Teaoraereke ocean and lagoon beaches, Buota lagoon beach, Tabiteuea ocean and lagoon beaches and Notoue lagoon beach.

Using the average D/L values for each site (Table 5.5), a graph was plotted showing the average D/L ratios for each site (Figure 5.17). Results show the following trends:

a) Average D/L ratio (age) increases from North to South Tarawa, and
b) Ocean beaches have lower D/L ratios (age) compared to lagoon beaches

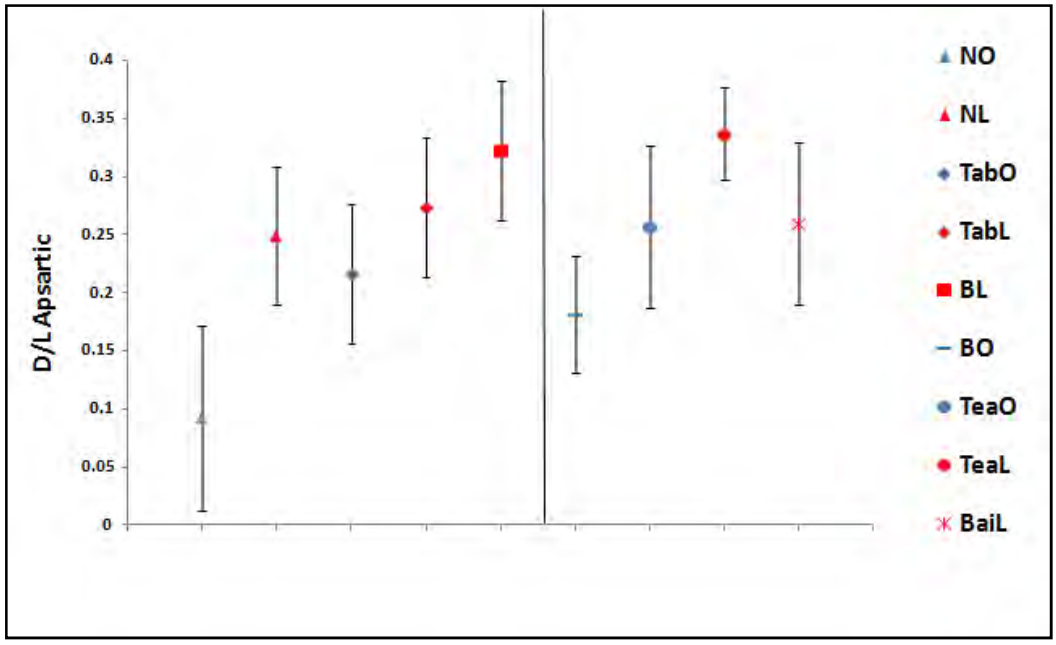

Figure 5.17. Extent of racemisation (total acid hydrolysate) for Aspartic acid from foraminifera *Amphistegina* obtained from "modern" beaches across Tarawa Atoll. Sites are NO: Notoue Ocean, NL: Notoue Lagoon, TabO: Tabiteuea Ocean, TabL: Tabiteuea Lagoon, BL: Buota Lagoon, BO: Bonriki Ocean, TeaO: Teaoraereke Ocean, TeaL: Teaoraereke Lagoon, BaiL: Bairiki Lagoon. The blue colours indicate ocean samples and the red colours indicate lagoon samples. The vertical line in the graph shows the division between North and South Tarawa. Error bars show the standard deviations for each average value.

Results show that extent of racemisation of Aspartic acid increases from North to South Tarawa. Average D/L ratio values from North Tarawa range from 0.092±0.04, Notoue ocean beach to 0.323±0.08, Buota lagoon beach (Table 5.5, Figure 5.17). In

contrast, South Tarawa beaches have slightly higher average D/L ratios ranging from 0.181 ±0.05, Bonriki ocean beach to 0.34±0.04 found on Teaoraereke lagoon beach (Figure 5.17). The spread of average D/L ratios for North Tarawa is greater than South Tarawa beaches.

Table 5.5. Summary of data samples from beaches across Tarawa Atoll with their average D/L rate of racemisation of Aspartic acid. Raw data is provided in Appendix B-2. Key: O = Ocean, L = Lagoon

Reef island	Village	Locality	UWGA Sample No	No. of *Amphistegina* (analysed)	Aspartic Average D/L ratio
North Tarawa					
Notoue		O	7743	25	0.092±0.04
Notoue		L	7748	21	0.249±0.06
Tabiteuea		O	7731	22	0.216±0.06
Tabiteuea		L	7738	19	0.274±0.05
Buota		L	7750	11	0.323±0.08
South Tarawa					
Bonriki-Taborio	Bonriki	O	7751	10	0.181±0.05
Bonriki-Taborio	Teaoraereke	O	7739	15	0.257±0.07
Bonriki-Taborio	Teaoraereke	L	7740	18	0.337±0.07
Bairiki		L	7749	11	0.260±0.06

Results show that extent of Aspartic racemisation for ocean beach samples are lower than lagoon beach samples (Table 5.5, Figure 5.17). From lowest to highest, the average D/L ratio obtained from ocean beach samples is: Notoue (0.092±0.04), Bonriki (0.181±0.05), Tabiteuea (0.216±0.06) and Teaoraereke (0.257±0.07). In the case of lagoon beach samples, the average D/L ratio from lowest to highest is: Notoue (0.249±0.06), Bairiki (0.260±0.06), Tabiteuea (0.274±0.05), Teaoraereke (0.337±0.07) and Buota (0.323±0.08). The spread of D/L values for lagoon beaches is slightly smaller than for ocean beaches.

Beach samples along Tarawa Atoll appeared to be mixed and reworked. A graph showing the average D/L ratio Aspartic acid for each population within a site was plotted including an isochron of 1425 ±150 cal yr BP (based on sample OZK813 – Buariki –pit 5) to illustrate the relative ages of the foraminifera samples collected

(Figure 5.19). Earlier results showed that the sample OZK813 appears to have been reworked but it provides a means to compare whether the samples from the beaches are younger or reworked (see 5.6.1 and Section on Additional samples obtained across Tarawa Atoll). Figure 5.18 illustrates that the spread of ages is large indicating that there is a lot of mixing occurring on these beaches. In addition most of the fossil relative ages were greater than or roughly equal to the isochron, implying that these foraminifera are likely to have been reworked. Only a few samples from beaches such as Notoue ocean and lagoon beaches, Tabiteuea ocean beach, Bonriki ocean beach, and Teaoraereke ocean beach were below the isochron suggesting that they are younger.

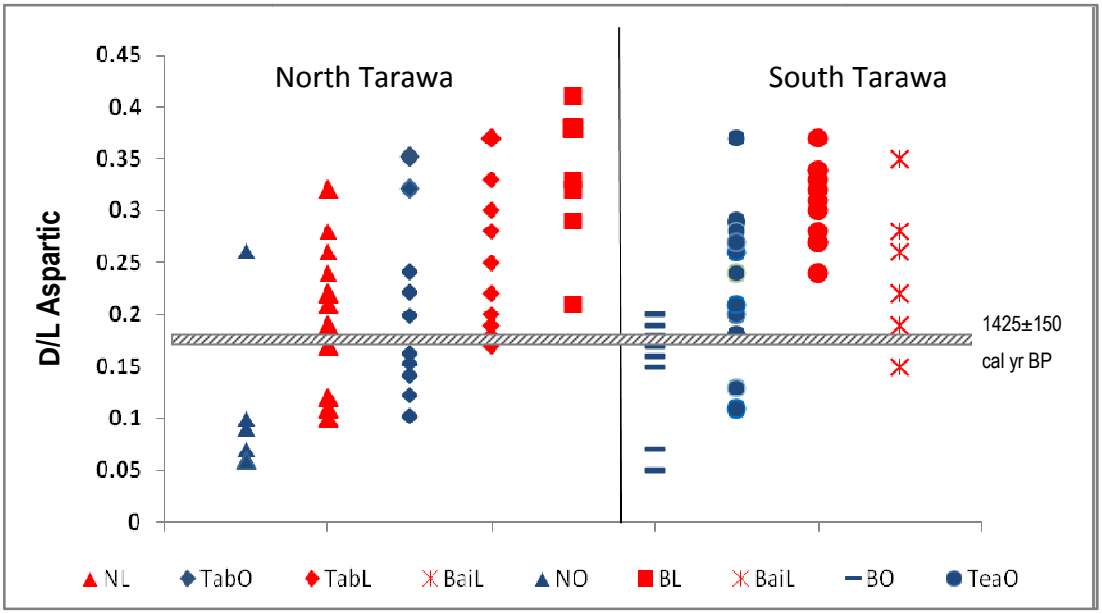

Figure 5.18. Extent of racemisation (total acid hydrolysate) for Aspartic acid from foraminifera Amphistegina obtained from modern beach sediments across Tarawa Atoll. The ischron is based on sample OZK813 which has an Aspartic acid D/L value of 0.18 (Table 5.3). Sites are NO: Notoue Ocean, NL: Notoue Lagoon, TabO: Tabiteuea Ocean, TabL: Tabiteuea Lagoon, BL: Buota Lagoon, BO: Bonriki Ocean, TeaO: Teaoraereke Ocean, TeaL: Teaoraereke Lagoon, and BaiL: Bairiki Lagoon.

Rose Bengal test of live foraminifera

The results of the one hour staining with Rose Bengal on "modern" beach sediments did not establish whether foraminifera were alive when collected or not. All results were negative, even those applied on live foraminifera. Results show that protoplasm was not stained but only the outer test was stained (e.g., Figure 5.13). Another staining trial was undertaken to increase the staining period to seven days

from samples collected from different areas across both Tarawa Atoll and Butaritari Atoll. The Rose Bengal did not show any positive results, again only staining the outer tests.

Live samples collected from the first sampling, undertaken in 2010 were collected from the ocean side of Tabiteuea, located beneath the coral rocks and attached to algae. A visible brown colour within the test indicated the presence of protoplasm (e.g., Figure 5.13). From the second sampling undertaken in August, 2011, live samples were also collected from North Tarawa and Butaritari Atoll from in shallow rock pools where water motion was low.

During collection, live brown foraminifera (*Amphistegina, Calcarina and Baculogypsina*) were observed with the naked eye. Figure 5.20 shows samples collected from various ocean reef flats on Tarawa Atoll and Butaritari Atoll. Live samples of foraminifera, both *Amphistegina* and *Baculogypsina* were collected in Notoue (Figure 5.19A) and Abaokoro (Figure 5.19B) of North Tarawa. In both Ukiangang and Temanokunuea, Butaritari Atoll, *Amphistegina* appeared very brown indicating they were alive when collected even though they did not stain pink (Figure 5.19G and H). The other areas investigated along South Tarawa (Figure 5.19C, D, E and F) did not show any live foraminifera, as they appeared pale yellow. A comparison of the foraminifera using photos showed that live foraminifera were abundant on Butaritari, whilst in the North Tarawa samples, the quantity of live foraminifera was low. Across many South Tarawa ocean reef flats, high concentrations of star fish and algae colonies were sighted supporting earlier observations by Richmond (1993) and Ebrahim (2000). In North Tarawa this was less common. These may signify that seawater in these areas had increased nutrients indicating pollution. This in turn may have affected foraminiferal health leading to its absence (or scarcity) from both North and South Tarawa ocean reef flats.

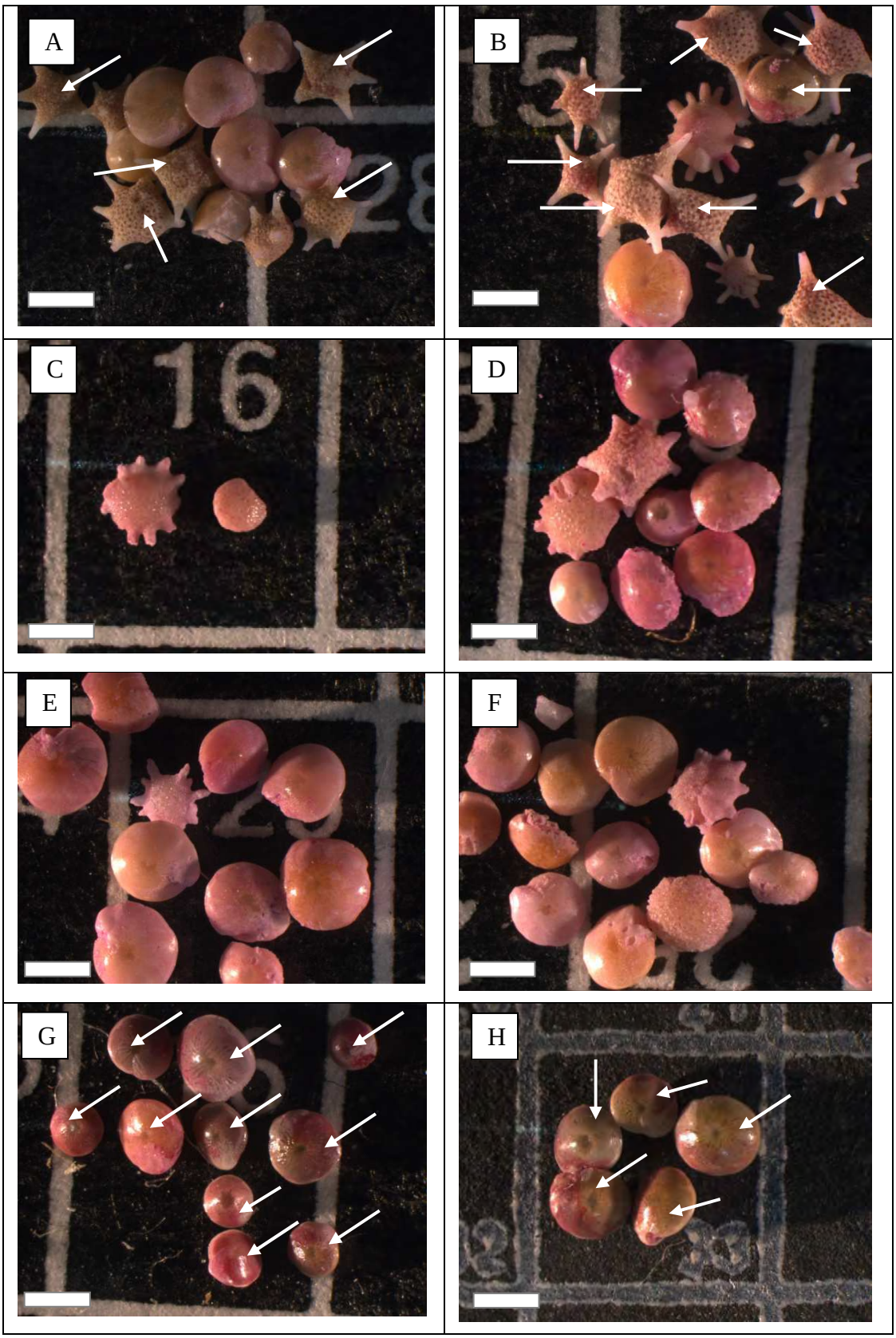

Figure 5.19. Foraminifera collected from ocean reef flats of Tarawa Atoll and Butaritari. A: Notoue, B: Abaokoro, C: Bonriki-Taborio, D: Ambo-Teaoraereke, E: Bairiki, F: Betio, G: Ukiangang and H: Temanokunuea. White arrows indicate live foraminifera based on the brown colour within the tests indicating the presence of protoplasm. Scale is 1 mm.

During short periods of staining, *Amphistegina* pores do not permit Rose Bengal stain to penetrate (Leutenegger and Hansen, 1979). Leutenegger and Hansen (1979) demonstrated that in live foraminifera, the youngest chambers will be stained, whilst the rest remain unstained as chamber pores are impermeable. However, for the samples collected in this study this did not occur. Observations by J. Carilli on stained live foraminifera, showed that as a result of exposure to long staining periods (a week), *Amphistegina* will be stained bright pink (J. Carilli, pers. comm., 2010). However this also did not work in this study and it has been suggested by Martin and Steinker (1973) that apertural blockage of live foraminifera can prevent the stain from reaching the cytoplasm.

5.7 Discussion

The radiocarbon ages of single foraminifera *Amphistegina* indicate that the reef islands began to form about 4,500 years BP. Radiocarbon ages of single foraminifera obtained from pits located closer to the lagoon side on Tabiteuea and Marenanuka indicate that these areas are the oldest parts of the reef islands with ages around 4,500 yrs BP. On Bonriki-Taborio reef island, a foraminiferal fossil of comparable age was obtained in a similar locality, however the foraminifera fossil may have been moved as the reef island has been disturbed by humans.

The depositional pattern of accretion on Tabiteuea, Marenanuka and Notoue was oceanward as indicated by the radiocarbon ages of fossils. With the oldest aged foraminiferal fossils of around 4,500 yrs BP obtained about three quarter of the width of the reef island from the ocean side, and fossil ages progressively getting younger towards the ocean, consistent with an oceanward accretion pattern. On the lagoon side, there was a slower accretion as would be expected under the oceanward accretion pattern proposed by Woodroffe (2000). The results are consistent with reef island formation ages commencing around 5,000 to 4,000 yrs BP which have been identified in other Pacific and Indian Ocean islands including the Cocos Keeling (Woodroffe *et al.*, 1999), South Maalhosmadulu, Maldives (Kench *et al.*, 2005), Warraber island, Australia (Woodroffe *et al.*, 2007) and Bewick Cay, Australia (Kench *et al.*, 2012).

The initial timing of reef-island formation varied. Comparison of the radiocarbon results suggest that Tabiteuea and Marenanuka began forming around 4,500 yrs BP while Notoue, only began to form more recently, around 1,000 yrs BP. The placement of the transect on a narrow part of Notoue, even though it crosses the central part of the reef island, may be the reason why it appears to be younger. Based on two lines of evidence, it is fairly clear that this is not where the reef island initially formed. The first evidence is that the oldest parts of the reef islands appear to have ages of around 4,500 yrs BP. The second piece of evidence is that radiocarbon ages of samples collected from minor transects around the atoll, appear to have the same ages as those observed on Notoue. A transect laid on the widest part of the reef island further north of the chosen transect site which appears to have taken more time to develop may indicate an age similar to that of Marenanuka and Tabiteuea. This suggests that the central part of the reef island in terms of width is not always where the reef island may have initially formed, as reef islands are complex systems where different parts form in different manners. Variables such as sediment supply (Woodroffe *et al.*, 2007), exposure to high energy and environmental conditions (Stoddart *et al.*, 1978) may need to be considered as they appear to control and vary the formation of reef islands.

A model illustrating a possible mode of reef-island development is based on reef islands radiocarbon ages and the Holocene sea-level history for Tarawa Atoll and Micronesia (Bloom, 1970; Marshall and Jacobson, 1985) (Figure 5.20) A mid Holocene sea-level high stand would have allowed the *Heliopora* coral unit collected at the base of the conglomerate platform to grow 0.3 to 0.5 m higher than its modern equivalent. The age of this coral unit was found to be 1800±25 yr BP (or 1310±135 cal yr BP) which appears to fall within this period. Falkland and Woodroffe (1997) reported the same coral species to be in growth position but higher than their modern counterparts on two other reef islands of Kiribati, Abemama and Maiana. A similar height of 0.4 m was reported from a *Heliopora* obtained from the base of a conglomerate platform in Makin, an atoll located further north of Tarawa Atoll (Woodroffe and Morrison, 2001). The radiometric age of this coral dates to the late Holocene implying that sea level was slightly higher than its present level.

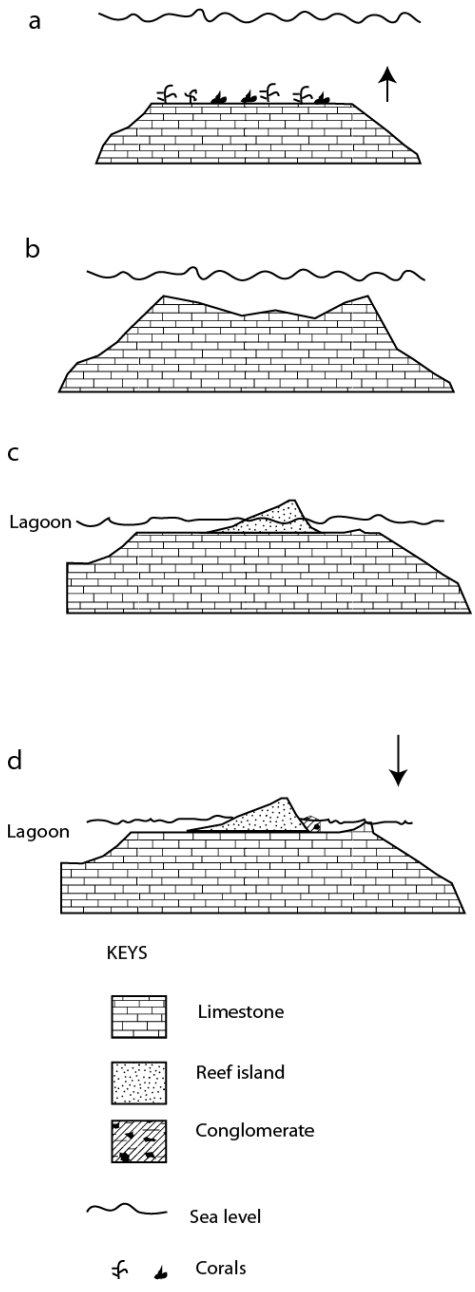

a) 8,000 yrs BP. Corals are catching up to sea-level rise. Evidence from drill cores obtained from several sites around Tarawa shows that Holocene coral growth began around 8,000 yrs BP at varying depths.

b) 6,000 yrs BP. Sea level stabilised. Drill core data from Tarawa shows that reefs grew laterally (Marshall and Jacobson, 1985).

c) 4,000 to 700 yrs BP. Within this period, phases of high energy events caused large volumes of carbonate material such as sand to be deposited on the reef flat. Reef-island initiation and formation varies in time and duration. The islands have been receiving sediment supply mainly from the ocean side. Based on the age of a *Heliopora* coral of about 1,400 yrs BP situated at the base of a conglomerate platform, mid Holocene sea-level reached approximately 0.5 m above modern level.

d) Present. Sea level fell to the modern level. During storms, coral debris collected on the coral unit and cemented together forming the conglomerate platform. At the seaward edge of the reef rim, a ridge is built and maintained by crustose coralline algae by cementing the corals in the area (Newell, 1956; Dawson, 1961). The algae develops well in inter-tidal areas and is exposed to persistent wave conditions (Litter, 1973).

Figure 5.20. Model of reef-island development on Tarawa Atoll reef islands based on radiocarbon ages of pit samples and *insitu* coral obtained from the ocean reef flat including a Holocene sea-level history for the Pacific.

About 4,500 yrs BP, sediment accumulated onto the reef flat possibly under high energy conditions. These conditions may have triggered volumes of sediment to be deposited onto the reef flat. The reef islands continued to develop up to AD 1950, according to the radiocarbon ages of individual foraminiferal grains obtained from pits on the major transects located close to the ocean (Table 5.1). The ocean beaches

appear to be receiving younger material than the lagoon beaches based on radiocarbon ages, and this is supported by the results from the AAR method.

Additionally, the AAR method shows a broad range of relative ages from Tabiteuea and Notoue foraminiferal samples obtained from all land, beach and ocean reef flat samples, and these are consistent with AMS age trend. In decreasing order, the age of fossils is as follows: a distinct cluster of relatively old age fossils collected from pits, fossils collected lagoon beaches, fossils collected from ocean beaches and younger ages for live foraminifera.

The accommodation space on the reef islands appears to be nearly full except for some small areas. This is implied from the distinctive cluster of relatively old age fossils obtained from the reef islands and younger ones on the beaches, which indicates that no younger foraminifera are being added onto the reef islands. The areas that are still receiving sediment are those on the beaches and within embayments, with young to modern radiocarbon ages of foraminifera. In the embayment in Buariki, the radiocarbon ages of the fossils get younger towards the beach.

Whether the beaches are being replenished with recently dead foraminifera still remains uncertain. Both AMS and AAR methods were limited in resolving this issue. In the case of AMS, the method can only measure up to modern age (AD 1950) (Arnold, 1995) but it does show that some of the material reaching the ocean beaches is old such as on Tabiteuea ocean beach with material approximately 130 years old. AAR on the other hand, relies on an independent method to calibrate ages which, in this situation, is AMS. Results show that numeric ages could not be derived for AAR samples, as the apparent parabolic model required more paired AMS and AAR ages to improve the curve. It was not possible to obtain more results for two reasons. The first was that funding was limited and the second was that this was primarily intended as a trial to determine the effectiveness of the model as stated in the objective of the study. However, the broad range of ages yielded by AAR was consistent with the age trend, which indicates that the method is reliable. In order to

determine the numeric age from racemisation kinetics more analysis and samples would be required.

Beaches show a lot of age mixing and reworking of foraminifera indicating that sediment supply may vary along North and South Tarawa. As there are more factors affecting the health and distribution of foraminifera on South Tarawa, this will be discussed separately.

In North Tarawa, the large spread of ages shown by the Aspartic acid D/L ratios ranging from 0.06 to 0.44 indicate that the ages of foraminifera on these beaches are relatively old with lagoon beaches older than ocean beaches. This implies that ocean beaches receive younger foraminiferal tests compared to the lagoon beaches which may be due to bioturbation affecting the ages. Field observations shows that live foraminifera are present on the ocean reef flats in North Tarawa but vary in quantity. In Butaritari, live foraminifera were found in abundance in all the areas visited, suggesting that some environmental factors have affected the health of these foraminifera in North Tarawa; a view also proposed by Ebrahim (2000). The timing when this commenced is uncertain and requires more investigation. The changes may have occurred 50 years ago, as the youngest dated fossils obtained from "modern" beaches of Notoue (OZN846) and Buariki (OZL963) have a radiocarbon modern age (Table 5.1). However, the AMS radiocarbon dating is limited in resolving this requiring another method to determine the absolute age. The evidences indicate that sediment supply is likely to continue but may vary.

In South Tarawa, beaches appear to be reworked with few, if any recently dead foraminifera being added to the reef islands. Field observations on ocean reef flats of South Tarawa showed that live foraminifera were absent on the ocean reef flat confirming the results of Collen (1995) and Ebrahim (2000). Notwithstanding the limitations of the paired dating method, the results from South Tarawa beaches suggest that there is a lot of mixing occurring with ages of the sediments appearing relatively old. This suggests that the beaches are composed of reworked material that has been re-incorporated, which may be a result of predominant longshore sediment transport moving sediment eastward and reversing it back to the west

during El Niño periods, unless it is removed by beach mining. Increasing urbanisation also contributes to the relatively older foraminifera appearing reworked on the beaches. Urbanisation adversely affects the health of foraminifera (Hallock, 1999). Live foraminifera on surrounding reef flats can be deformed as a result of increasing pollution and can be eventually wiped out (Yanko *et al.*, 1999). On South Tarawa this has raised serious concerns (Collen, 1995; Ebrahim, 2000). Live but deformed foraminifera were found in the Temaiku Bight area (Ebrahim, 2000) indicating that this is now occurring in South Tarawa and may possibly wipe out the whole foraminifera population. In South Tarawa the pollution is due to increased faecal coliform counts associated with sewage (Kelly, 1994; Loran, 1994), a decrease in seawater quality (Richmond, 1990) and solid rubbish being dumped in coastal areas, which affects the water quality. The impacts of these activities have made it unsuitable for foraminifera to survive; therefore live foraminifera appear absent from the ocean reef flats. This implies that the sediment supply on South Tarawa is limited.

A similar situation to that of South Tarawa where live foraminifera appear scarce on the ocean reef flats has also been observed in the Marshall Islands where populated areas showed signs of lower foraminiferal abundances (Fujita *et al.*, 2009). Observations by diving have shown the presence of living foraminifera at depths less than 10 m around South Tarawa (J. Carilli. pers. comm., 2010.) where eutrophication effects may be diluted by open ocean water. This observation indicates that live foraminifera are still present around South Tarawa but only in deeper water. Given that this appears to be the situation in urban areas where human activities have adversely affected the health of foraminifera, it is highly likely that the foraminifera present in Temanokunuea village of Butaritari will also be affected if human activities increase. Caution needs to be applied so that other atolls are not affected.

Many factors may have affected the tests and distribution of the *Amphistegina* fossils leading to ocean beaches having younger sediment material compared to the lagoon. One of these factors is the close proximity of ocean beaches to locations where live Foraminifera are present. Several studies have inferred that after the death of *Amphistegina*, tests on the ocean reef flats are transported ashore by waves and

deposited on the ocean beaches (Yamano *et al.*, 2000; Woodroffe and Morrison, 2001; Kench *et al.*, 2005; Woodroffe *et al.*, 2007; Woodroffe, 2008). Although there are live foraminifera in lagoon areas as identified by Ebrahim (1999), he supports the idea that a large proportion of the lagoon composition is sourced from the ocean reef flat (See Section 3.4.1). Human factors such as causeways, may have affected the distribution of foraminifera by blocking the lagoonward sediment transport. In South Tarawa with a long barrier of land of approximately 30 km inclusive of causeways, separating the ocean from the lagoon, the impact may be greater than that in North Tarawa. However, the AMS-AAR dating was limited in showing ages of relict foraminifera.

5.8 Summary

This chapter shows that the reef islands of Tarawa Atoll are geologically young, beginning to form around 4,500 yrs BP. The radiocarbon ages obtained from pits spaced at regular intervals across the central parts of Tabiteuea, Marenanuka and Notoue indicate an oceanward accretion pattern. The radiocarbon age of *in situ Heliopora* fossil coral suggests that the mid Holocene sea-level high stand occurred around 1,400 yrs ago and was approximately 0.5 m higher than the present sea level. The reef islands appear to be full, however, there are still some areas that have space for sediment to deposit such as beaches and ends of the reef islands as indicated by the young to modern radiocarbon ages of fossils. Embayments are also areas where sediment is being deposited as indicated by the radiocarbon ages, which get progressively younger towards the ocean.

Beaches along Tarawa Atoll appear to have mixed ages, with ocean beaches appearing relatively younger than the lagoon beaches. Relative ages of foraminifera on North Tarawa beaches indicate that no recently dead foraminifera have been deposited on the beaches. The presence of live foraminifera but in varying amounts on ocean reef flats of North Tarawa implies that sediment supply varies. These two pieces of evidence indicate that sediment supply is likely to continue but will vary. On the contrary, South Tarawa beaches are evidently at a higher risk of a loss of sediment supply than North Tarawa beaches. Human activities have affected the health and distribution of foraminifera resulting in older fossils on the beaches. The

scarcity of live foraminifera on ocean reef flats and on “modern” ocean beaches implies that new foraminifera are unlikely to be added. The fossils appearing older indicate that sediment is reworked and that the beach sediment supply is limited, raising concerns about the future sustainability of these beaches.

The pattern of reef-island development, including the supply of modern skeletal foraminifera, will be used in Chapter 7 to discuss and forecast the future morphological changes of Tarawa Atoll in response to sea-level rise.

6 CHAPTER SIX: SHORELINE CHANGE ON REEF ISLANDS

6.1 Aims of this chapter

The overall objective of this chapter is to examine the changes that have occurred to reef-island shorelines. This will be carried out by investigating the rates of historic shoreline change on reef islands across Tarawa Atoll. The specific aims of this chapter are to:

a) Determine the area changes on reef islands and examine whether there has been net accretion or erosion.
b) Calculate and compare shoreline change over a period of 30 years, for ocean and lagoonal shoreline changes of reef islands.
c) Calculate and compare rates of shoreline change over a period of 64 years focussing on six selected reef-island shorelines.
d) Compare the trends in shoreline rates of change as shown by two shoreline indicators: base of beach and vegetation line.
e) Compare trends and rates of shoreline change between natural shorelines and those influenced by human activity.

6.2 Introduction

Low-lying reef islands on atolls, such as Tarawa Atoll, are threatened by the impacts of climate change, particularly observed and anticipated sea-level rise (IPCC, 2007). Increased inundation appears inevitable, but there is a widespread perception that reef-island shorelines directly exposed to increased wave action are likely to erode, resulting in a reduction in reef island size (Sheppard *et al.*, 2005). In contrast, an alternative view is that as a result of more prolific coral growth and enhanced sediment transport, shorelines will actually experience net accretion, thus increasing reef island size (Kinsey and Hopley, 1991). Currently there is no scientific consensus on the responses of Pacific reef islands to rising sea level. The number of studies that have investigated the shoreline responses or area changes across all reef islands on an atoll is also limited.

Shorelines of reef islands are dynamic features that are largely dependent on the balance between sediment availability and oceanographic processes (Kench and

Cowell, 2002). A range of factors control spatial and temporal shoreline changes on reef islands and these factors can be grouped into those that are natural and those that are human-induced (SOPAC, 1994). The natural factors include physical characteristics of reef islands, such as size, morphology, location on the reef rim, and their relative exposure to prevailing winds, storms and seasonal variability of the sea level related to ENSO (McLean, 2011). Also important is the availability of sediments to build and maintain the stability of these reef islands, which are derived from either productive oceanward reefs or sources in the sediment-rich lagoon (Ebrahim, 1999; Paulay and Kerr, 2001; Woodroffe and Morrison, 2001). Human factors also influence shoreline changes and these include: reclamations, groynes, seawalls (Gillie, 1993; Gillie, 1994; Ford, 2012), and beach mining (Gillie, 1994; Peletikoti, 2007) .

Natural factors influencing shoreline changes on Pacific atolls vary between reef islands. A study of shoreline changes on 27 Pacific reef islands from four different atolls indicated that a significant percentage of reef islands had either remained stable (43%) or increased in area (43%) (Webb and Kench, 2010). The reef islands that were observed to have accreted the most were on Tarawa Atoll; these reef islands and their increase in area are: Betio (30%), Bairiki (16.3%), Nanikai (12.5%) and Buariki (2.9%) (Table 6.1). The first three are located in urban South Tarawa and represent the most rapidly accreting reef islands in the study. It was inferred that ocean-facing shorelines located on the windward side displayed erosion, but that lagoon beaches facing away from ocean swells primarily responded by net accretion. These reef islands contributed disproportionately to the study's overall conclusion that reef islands have accreted over the past few decades despite an average sea-level rise of +1.8 mm/yr (Church *et al*. (2006). Webb and Kench (2010) implied that reef islands in the central Pacific are naturally growing because of net accretion and, in particular reef islands on Tarawa Atoll are growing faster than average. Although they discuss that the observed shoreline changes on these urban reef islands occurred during a period when human activity was high, their conclusion does not take into account the numerous reclamations. It is also not clear from their study how widespread these responses were, or if the reef islands selected on Tarawa Atoll were representative of other reef islands on the atoll, or on other atolls in the region.

Observations of long-term shoreline changes over 40 years (1969 to 2009) at Maiana Atoll, south of Tarawa Atoll in the Gilbert Group (Figure 2.2), which has had little impact from anthropogenic processes, support the view that growth of reef islands is largely natural with slow accretion rates (Rankey, 2010; Rankey, 2011). Both long and short-term shoreline changes on large reef islands located on the windward side of Maiana and Aranuka, Kiribati (Figure 2.2) indicate that the major changes occurring on the reef island tips are associated with changing wind conditions.

Table 6.1. Summary of changes of reef islands of Tarawa Atoll over a period of 35 and 61 yrs within the years 1943-2004 (source: Webb and Kench, 2010).

Reef islands	Time period	Initial Area (ha)	Final Area (ha)	Net Change (ha)	Rate of change (ha/yr)	% change
Betio	61 yrs (1943 - 2004)	120.03	156.00	36.00	0.5	+30.0
Bairiki	35 yrs (1969 - 2004)	35.46	41.25	5.79	0.2	+16.3
Nanikai	35 yrs (1969 - 2004)	6.40	7.20	0.80	0.02	+12.5
Buariki	61 yrs (1943 - 2004)	338.30	348.40	10.10	0.2	+2.9

Other natural factors such as ENSO are also likely to contribute to shoreline changes by influencing the longshore sediment transport, and these were also discussed to some extent by Webb and Kench (2010). Widespread coastal erosion on many reef islands of the Gilbert Group in 1982 was associated with the occurrence of the strong 1982 to 1983 El Niño event (Gillie, 1994; Gillie, 1997). Increased erosion on the eastern shorelines of Maiana and Aranuka reef islands has been linked to exposure to wind and wave energy during the strong La Niña period of 2005 to 2009 (Rankey, 2010) indicating that oceanographic conditions associated with ENSO can play an important role in explaining reef island behaviour in Kiribati.

Human activities alter, interrupt or block coastal processes which can lead to increased erosion or accretion on shorelines. For instance, coastal structures extending out onto the beach block longshore sediment transport causing the down-drift side to be severely eroded (Harper, 1989; Webb, 2005). In the case of Oahu, Hawaii shoreline changes measured on four beaches over a minimum of 46 years (1949 to 1995) showed that seawalls and revetments placed on eroding beaches as a means to protect them appear to have accelerated beach erosion causing these beaches to become narrower in width (Fletcher *et al.*, 1997). Fletcher *et al*. (1997) also observed that the areas down-drift from these artificial beaches experience

erosion. He discussed that the construction of seawalls or revetments fix the sand on beaches thus reducing its availability for transportation by coastal processes causing down-drift areas to be eroded. Significant erosion observed near major villages on Maiana and Aranuka, Kiribati was possibly related to the modification of the lagoonal shorelines with structures such as groynes causing down-drift areas to erode (Rankey, 2010). Many studies have demonstrated that shoreline changes on populated reef islands, such as Betio, Tarawa Atoll, are largely due to human activity (Burne, 1983; Harper, 1989; Howorth and Radke, 1991; Gillie, 1993; Forbes and Hosoi, 1995; Forbes and Biribo, 1996; Biribo, 2008). Long-term shoreline observations over 34 to 37 years on Majuro Atoll, the Marshall Islands, showed that human activities are largely responsible for the changes observed there (Ford, 2012). Major developments on both the ocean and lagoon shorelines, such as reclamations, have significantly modified the land, with the largest increase having a proportion of 67.5% of the entire reef island size, being associated with construction of the international airport. Erosion of lagoon beaches in rural areas appears to be related to coastal structures in urban areas interrupting the longshore sediment transport (Ford, 2012). This demonstrates that in areas where longshore sediment transport is significant, it is possible that activities in the up-drift coastal areas may affect down-drift coastal areas.

This chapter examines the morphological response of reef islands on Tarawa Atoll. It summarises well-documented changes that have been recorded by successive studies undertaken by SOPAC of the shoreline around the densely populated commercial and administrative reef islands of Betio and Bairiki, which highlight the effects of both ENSO and human activities. The chapter then examines shorelines for the entire atoll over different periods of time, comparing shorelines 30 and 64 years apart over which time there has been a gradual rise in sea level (Church *et al.*, 2006; Ramsay *et al.*, 2010). This involves investigating the historical shoreline and area changes, including their trends, over the past several decades to see how these changes are likely to occur in the future.

6.3 Background

6.3.4 Shoreline changes around Tarawa Atoll

Past shoreline studies of Tarawa Atoll have focussed on the densely populated reef islands of South Tarawa. This has been due to concerns related to population increases, causeway construction and erosion, with results showing that human activities have affected shorelines. Studies have been carried out on the reef islands of Betio, Bairiki and Bonriki-Taborio. Most of these studies were undertaken by SOPAC, a regional body which advises the Kiribati Government on geoscience matters. Since 1982, SOPAC has played a key role in understanding the sediment dynamics of South Tarawa and the potential impacts of proposed developments. The following sections will discuss the movement of sediment around South Tarawa reef islands and the developments that may have influenced shoreline changes around Betio.

The initial SOPAC study intended to determine the effects of a proposed causeway on the sediment dynamics of the reef islands of Betio and Bairiki (Howorth, 1982). The 3.4 km long Nippon causeway was built to improve communications and access between these two major administrative centres. However, there were major concerns that this massive solid structure with only a 10% opening, known as the Fisheries Channel, would significantly reduce water flow and alter sediment transport pathways.

In order to monitor the potential impacts, a beach profiling program was established in 1982 investigating 11 profile lines for Bairiki and 15 for Betio (Howorth, 1982) (Figure 6.1). Later in the year, the vertical datum for these profiles was tied to the UH tide gauge (Howorth, 1983). Monitoring was carried out on a biannual basis in collaboration with the Kiribati Lands Division. An additional set of 10 profiles were established in 1986 prior to the completion of the Nippon causeway in 1987 (Harper, 1989). Some were renumbered so that the profiles would start from the far-east ocean side of Bairiki in a clockwise direction ending on its lagoon side. Analysis of the seven years of beach profiling data demonstrated that ENSO (see Chapter 2) plays a significant role in the sediment dynamics of South Tarawa, and that lagoon shorelines are more dynamic than ocean shorelines (Harper, 1989). The difference

between the dynamics of lagoon and ocean shorelines is possibly related to local generation of waves in the lagoon. The locally-generated waves are more susceptible to changing wind conditions, exposing the lagoon shorelines to greater variation in wave magnitude and direction (Harper, 1989). Harper (1989) also suggests that waves on ocean beaches are less sensitive to changing offshore wave conditions as the swell is filtered by the reef rim and only small waves reach the ocean shorelines.

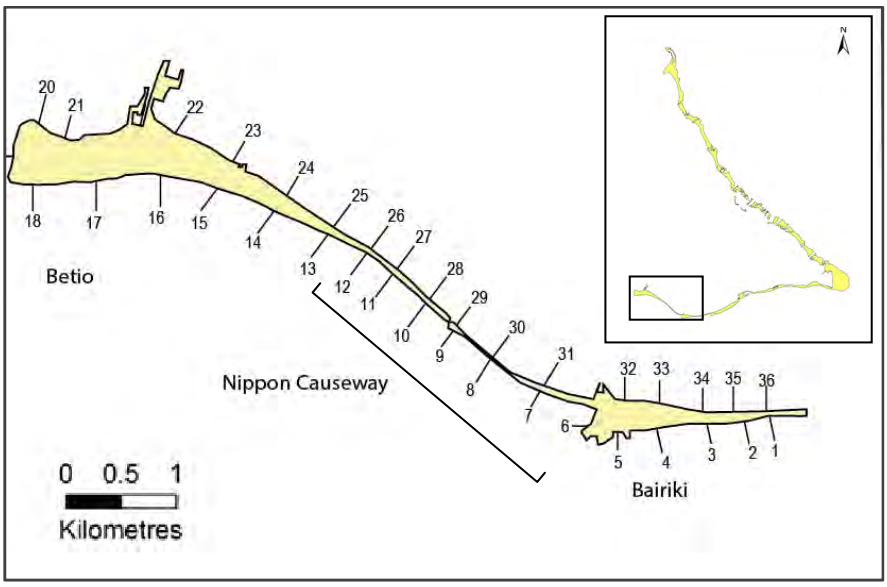

Figure 6.1. Beach profile locations around the reef islands of Betio and Bairiki and along the Nippon Causeway. The bracket shows where Bairiki and Betio reef islands end and where the Nippon Causeway begins.

Sediment transport along the southern part of Tarawa Atoll during normal conditions is predominantly westward resulting from prevailing easterly winds and the associated incident wave climate (Harper, 1989). To better understand sediment dynamics that have shaped this part of the atoll, Byrne (1991) described some key geomorphological features present on aerial photographs and in the field. Of particular importance is the presence of three re-curved spits on the reef islands of Bonriki-Taborio, and Ambo-Teaoraereke. Two re-curved spits occur on Bonriki-Taborio with one at its eastern end and a second in the central part of the reef island. A range of available information, including the wind and current patterns, the morphology of the spits located on Ambo-Teaoraereke and the central part of Bonriki-Taborio reef island, evidence of the possible existence of some old inter-island channels noted on aerial photographs and the direction of spit growth, enabled Byrne to deduce that the predominant longshore sediment transport direction is

westward. Byrne (1991) assumed that the entrance of the channel lay west of the spit and not east suggesting that sediment transport and the growth of the sand spit was different for the eastern end of Bonriki-Taborio. An aerial photograph from 1943 shows that this spit is also moving to the west, while the entrance of the channel from the ocean is actually towards the east and not to the west (Biribo, 2008), as suggested by Byrne (1991) (Figure 3.16). This confirms that longshore sediment transport on South Tarawa is predominantly westward under most conditions except during El Niño.

In South Tarawa, El Niño reverses the direction of the predominant longshore sediment transport from westward to eastward (Harper, 1989). The change in the direction of longshore sediment transport as a result of ENSO is supported by a significant body of evidence resulting from SOPAC's research work on South Tarawa as well as time-series of shoreline positions obtained from aerial photographs (Gillie, 1993; Forbes and Hosoi, 1995) and ground surveys (Forbes and Hosoi, 1995; Solomon and Forbes, 1999). Analysis of beach profile data shows that during El Niño conditions, shoreline changes on the lagoon side appear to be more significant especially in areas where coastal structures block longshore sediment transport (Harper, 1989). For example, an area just east of the Bairiki port undergoes severe erosion during El Niño conditions as the port structure prevents the sediment being transported to the east causing sediment to accumulate on its western side (Harper, 1989; Webb, 2005). This resulted in the loss of several houses built in this area during the El Niño events that occurred in 1982-1983, 1987 and 1996 (Solomon and Forbes, 1999).

All causeways in Tarawa Atoll that have a major influence on sediment movement have closed inter-island channels preventing hydraulic transport from the ocean to the lagoon side (Harper, 1989). The Nippon Causeway is an exception to this as it is not entirely solid but, with only a 10% opening, has dramatically reduced the tidal exchange within the Betio and Bairiki area by 95 - 97% (Zann, 1982). As a result, it has altered the existing natural sediment pathways (Harper, 1989; Gillie, 1997). Significant volumes of sediment have accumulated on the sides of causeways; for example, 43,000 m^3 has built up alongside the Nanikai-Teaoraereke causeway over 20 years (Forbes and Biribo, 1996) and >108,000 m^3 accumulated beside the Nippon

Causeway in an 18 month period (Forbes and Hosoi, 1995). These significant volumes of sediment have accreted besides these two structures at high accumulation rates of 2,150 m^3/yr and 72,000 m^3/yr for the Nanikai-Teaoraereke and Nippon causeways respectively. These high rates indicate that the land beside the causeways will grow accumulate over time if sediment is still available. Most causeways in Tarawa Atoll were built in the early 1960's and, as longshore sediment transport is dominant in South Tarawa, these causeways have contributed to shoreline changes. In addition, these causeways have contributed significantly to the increase in the volume of reef islands adjacent to these structures. The Nippon Causeway, a massive structure covering a larger area and built 20 years later than most causeways, has a greater influence on the sediment patterns.

Case study of Betio

Coastal change on Betio has been extensively studied and has been linked to human development (Howorth and Radke, 1991; Gillie, 1993; Solomon, 1997; Biribo, 2008), although Webb and Kench (2010) did not appear to take these studies into consideration when concluding that atoll reef islands are growing. During World War II, Betio was heavily fortified by the Japanese with bunkers and gun emplacements (Howorth and Radke, 1991). After the war, the Americans cleaned up Betio, by collecting war debris and dumping it on the west coast (Howorth and Radke, 1991). Time series of shoreline positions over a 49 year period, from 1943 to 1992, showed that Betio has accreted by 23 hectares which is a 20% increase of the total reef island area (Gillie, 1993). This is in agreement with the results by Webb and Kench (2010) (Table 6.1) that indicates that Betio reef island has increased in area by 13 ha over a 12 year period (1992 to 2004).

Determination of the factors responsible for changes along the shoreline of Betio was made possible by dividing the reef island into ten sections (Gillie, 1993) (Figure 6.2). The northwest tip where the dump site is located, shows that the rubbish dump has contributed to Betio's increase as the Betio Town Council have continued to use it. In the southwest corner, erosion has occurred as a result of a gun emplacement and a sewage outfall altering the sediment dynamics in the area (Gillie, 1993; Biribo, 2008).

A sand spit on the SE tip has been further developed for the causeway approach between Betio and Bairiki. In late 1978, 44,000 m^3 of sediment was removed from the lagoon mud flat and deposited on the spit to construct this approach (Howorth and Radke, 1991; Gillie, 1993). On the SE lagoon side, the shoreline has extended seaward 30 to 50 m as a result of the port of Betio acting as a massive groyne blocking the predominant westward sediment transport (Gillie, 1993).

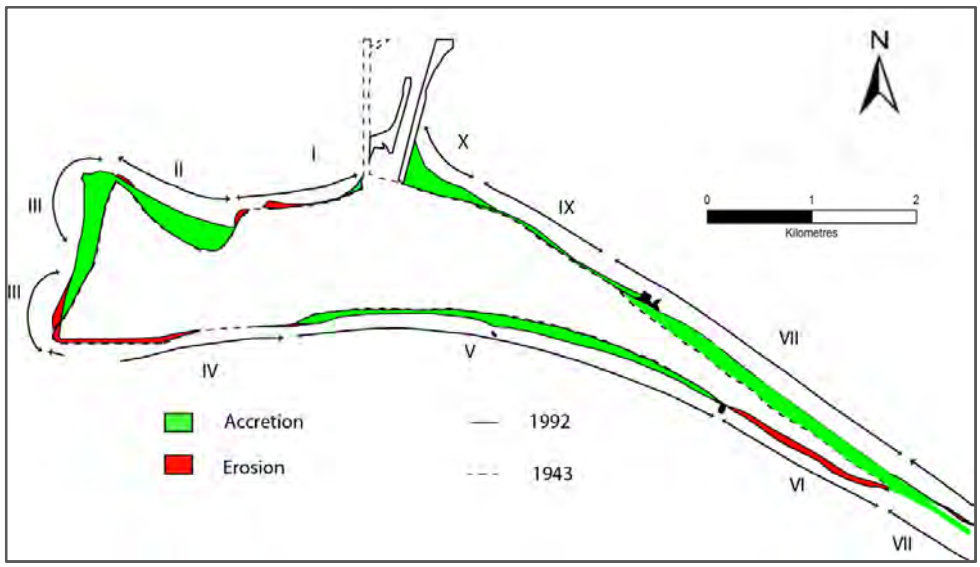

Figure 6.2. Map of Betio highlighting the ten sections identified by Gillie (1993) and the corresponding substantial changes that appear related to human activities. The dotted and solid lines are the shoreline positions.

The presence of this major accretion was observed by comparing aerial photographs taken in 1945 and land maps from 1954 (Howorth, 1982). Howorth (1982) estimated the accretion rate to be 10,000 m^3/yr over the years 1945 to 1954 and; associated its formation to the port and longshore sediment transport. These observations were made by carrying out several beach profiles and taking photos along the shorelines of Betio and Bairiki. Using photographs taken in the field, Byrne (1983) disputed Howorth's (1982) suggestion that longshore transport has contributed to the accumulation of sediment in this area. However, he recognised that the port has acted like a groyne causing sediment to accumulate on the eastern side of the structure. Expanding the time series of shoreline positions from 1968 to 2003, Biribo (2008) noted that the land area for Betio has significantly increased, by 26.7 ha, and 95.9% of the observed increase was associated with major developments such as the construction of the causeway and the upgrading of the Betio port. In some areas,

such as the lagoon shoreline west of the port, the shoreline is stable. A seawall protecting the high population density and assets within the area contributes to this stability (Howorth, 1982).

The Nippon causeway development between Bairiki and Betio had a major impact on the coastal changes in Betio. The causeway was developed from large volumes of materials (230,000 m^3) dredged from four large burrow pits situated on the ocean and lagoon reef flat adjacent to the structure (Forbes and Hosoi, 1995). Beach profiles have shown that over time, mobile sediment has accumulated on the sides of the causeway in large quantities (Harper, 1989). These newly developed lands developed from the sediment accumulating on the side of the causeways are stabilised by trees. A substantial contribution towards these lands is suggested to have come from the sand bars that were present on the reef flat prior to the causeway construction thus further removing mobile sediment (Forbes and Biribo, 1996). These studies highlight that by developing Betio, humans have contributed significantly to its shoreline change primarily by dumping, reclaiming and interrupting sediment movement.

Small private reclamations have also contributed to the coastal change. Betio, a densely populated reef island, has serious problems with overcrowding and a severe shortage of land space. Solomon (1997) reported that many houses and *maneabas* (traditional meeting places) have been built close to the active beach berm, which should have been retained as a buffer zone between the land and the sea. Overcrowding has forced people to occupy newly accreted, but unstable, land for residential purposes; for example, the northwest tip of the reef island is now densely populated. In another attempt to address this overcrowding problem, people have tried to expand seaward by reclaiming land. Solomon (1997) observed large excavations on the beach in front of the reclaimed land where fill material has been sourced for these developments. Reclamations are also observed in other populated areas such as Bairiki (Harper, 1989; He, 2001; Webb, 2005; Office of Te Beretitenti, 2010), Nanikai (Webb, 2005; Office of Te Beretitenti, 2010) and Bonriki-Taborio (Forbes and Hosoi, 1995; He, 2001; Office of Te Beretitenti, 2010). The history of anthropogenic disturbance on Betio over the period observed by Webb and Kench

(2010) indicates that it is likely that the fast growth rate of this reef island is due to anthropogenic influence.

6.3.5 Shoreline indicators

Historical shoreline changes can be measured by comparing shoreline positions derived from aerial photographs and satellite images. To compare shoreline changes, an appropriate shoreline proxy should be selected that can be identified on each aerial photograph or image. A large number of studies have been carried out to monitor shorelines and they revealed that selection of shoreline indicators plays a significant part in the trends detected (Morton *et al.*, 2004; Boak and Turner, 2005; Morton and Miller, 2005; Hapke *et al.*, 2006; Hanslow, 2007). Historical shoreline changes can be measured with tools such as the Digital Shoreline Analysis Systems (DSAS) developed by the United States Geological Survey (USGS) which has been used to standardise national shoreline change analysis (Morton *et al.*, 2004). It is becoming widely used to assess historical shoreline changes, for example, it has been applied in Hawaii (Fletcher *et al.*, 2003) and Majuro (Ford, 2012).

The change of reef-island shorelines can be monitored using shoreline indicators, and which shoreline indicator is chosen largely depends on data availability and resolution. Shoreline indicators should be detectable at different time periods to allow repetition (Crowell *et al.*, 1991). An extensive literature review on available shoreline indicators has classified them into visible, tidal datum or features extracted from digital images (Boak and Turner, 2005). Examples of some of the most commonly used shoreline indicators are the high water line (HWL), the base of the beach (BB), debris lines, the landward edge of coastal protection structures, the mean high water line and the vegetation line (VL). VL is the seaward edge of coastal vegetation (Boak and Turner, 2005). On atolls, it is generally a distinct line of small shrubs, such as *Scaevola* on the ocean side, providing a good indication of the top of the beach. On the other hand, BB is used in this study to indicate the position of the change in beach slope between beach and reef flat (Figure 6.3). This was also used by Rankey (2010) in his study on Aranuka and Maiana atolls in Kiribati. In countries with true continental shelves, where BB has been used, it is the least utilised indicator compared to VL as it is difficult to interpret (Boak and Turner,

2005). On reef-islands, the beach slope changes when the beach meets the hard reef surface, especially at the foot of the ocean beach.

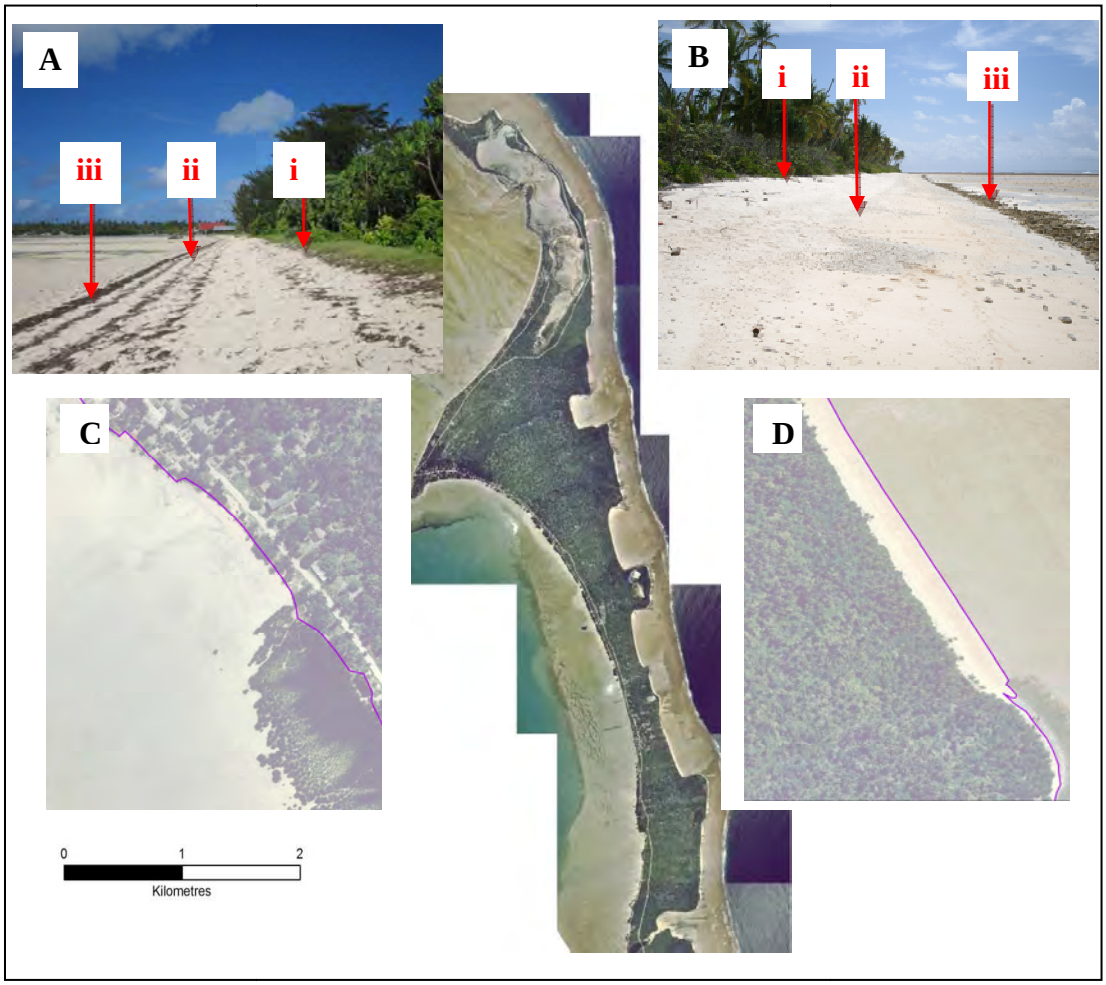

Figure 6.3. The 1998 aerial photograph of Buariki reef island with photographs of lagoon (A) and ocean (B) shorelines showing several of the shoreline indicators recommended by Boak and Turner. The letters stand for the following i: seaward vegetation line; ii: wet line; and iii: base of beach, (C) illustrates the Vegetation Line (VL) (purple line) marking the seaward extent of the coastal vegetation but not including mangroves, (D) ocean base of the beach (BB) (purple line) shows the distinct contact between the beach and reef flat or conglomerates.

6.3.6 Relationship between water levels and shoreline indicators.

The relationship between the two tide gauges installed in Betio by the University of Hawaii and Australian National Tidal Facility, known as the SEAFRAME Gauge is illustrated by Figure 6.4. This figure also shows other additional information such as VL, BB, MSL, MHWS, MHWN and MHWSP to provide a better understanding of the links between the tide gauges, water levels, MSL, reef islands ocean beaches and

shoreline indicators used in this study. The water levels are sourced from Ramsay *et al*. (2010)(see Chapter 2 Table 2.5, for more details).

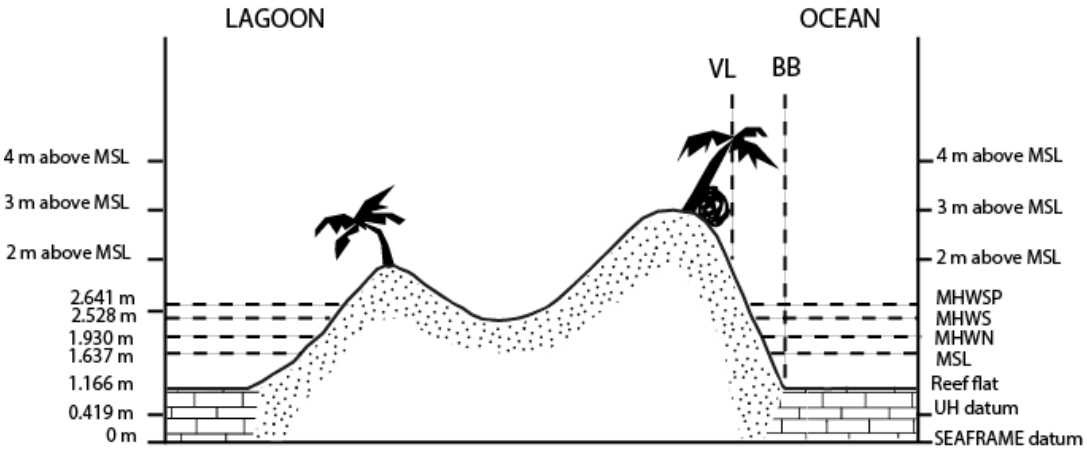

Figure 6.4. Schematic cross section of a reef-island illustrating the relationship between different water levels and shoreline indicators BB and VL. The dotted horizontal lines indicate the MSL, MHWN, MHWS and MHWSP.

At spring low tide, the toe of the beach is uncovered, meaning that the BB shoreline indicator is exposed and can be digitised. The seaward extent of the vegetation line marked as VL lies higher than the MHWS level which is 2.528 m above SEAFRAME datum. But the position of VL can be affected if there are strong winds raising the water level, as waves may reach the vegetation line due to wave set up and wave run-up.

Table 6.2. Water levels for Tarawa Atoll (Modified from Ramsay *et al.* 2010).

Water levels	Relative to SEAFRAME datum (m)	Relative to UH (m)
MSL	1.637	1.218
MHWN	1.930	1.511
MHWS	2.528	2.109
MHWSP	2.641	2.222

6.4 Study sites

Of the 59 reef islands around the northern and southern margins of Tarawa Atoll (Figure 3.17), only 48 were used to investigate area change, as the remaining 11 were not completely covered in the 1968 aerial photography. Six of these 11 reef islands were very small with a maximum area of 0.3 ha. The number of reef islands studied was further reduced to 35 when investigations of shoreline changes on ocean and lagoon beaches were carried out. This was because 12 reef islands were too small

and the number of transects that could be placed on them (2 to 3) was considered too few to provide a realistic rate of change. These 12 reef islands not included in the study are located in the central part of North Tarawa including those situated close to the reef rim (Figure 3.17) and their total area only amounts to 15 ha which is 0.5% of the total reef island area for the entire atoll.

The reef islands selected as study sites for the long-term changes (64 years) were based on the results of the 30 year shoreline change. Five reef islands were selected to be representative of these two groups as they covered the predominant reef island types found on Tarawa Atoll. For North Tarawa the reef islands were Buariki, Nea and Kainaba and for South Tarawa, Bairiki and Abairaranga.

6.5 Materials and method

Scanned aerial photographs from 1968 were prepared for shoreline analysis using DSAS 4.2 following steps described in Section 3.7. Georeferencing was carried out at a scale of 1:1,000. The 2007 Quickbird satellite image also required georeferencing as there was an average shift of about four metres (false easting) between it and the re-projected 1998 aerial photos. A similar shift was also noted when ground truthing Quickbird satellite imagery of the Federated States of Micronesia (Lomani and Tokalauvere, 2008).

Table 6.3. Aerial photo 1998 and pan sharpened Quickbird satellite image projections

Image	**1998 Aerial photo (new projection)**	**Pan-sharpened Quick-bird satellite image**
Spatial Reference	Transverse Mercator	WGS_1984_UTM_Zone 59
Linear Unit (meter)	Meter (1.00000)	Meter (1.00000)
Angular Unit	Degree (0.017453292519943299)	Degree (0.017453292519943299)
False Easting	40000	50000
False Northing	0	0
Central Meridian	173.033300	171.00000
Scale Factor	1	0.9996
Longitude of Origin	0	0
Datum	D_WGS_84	D_WGS_84

Digital images were geo-referenced by selecting a minimum of six to a maximum of 30 ground control points (GCP) on each photo. Points were chosen such that they were well spaced in order to reduce distortion and error as described by Crowell *et*

al. (1991). GCPs are stable physical features for which coordinate positions can be determined. As most historical aerial photography in the Pacific was not taken specifically for coastal monitoring purposes, ground control points are generally limited. This was the case with the 1943 and 1968 aerial photos therefore alternative secondary GCP features had to be selected. These consisted of points that could be identified on two images that appeared persistent and not to have moved such as rock fish traps (Figure 6.5A), conglomerate outcrops edges (Figure 6.5B) and corners of concrete structures. With these characteristics they are dependable control points thus increasing the reliability of shoreline positions selected from multi-temporal images. Although comprehensive GCP's were determined by Schlencker (1998), these were not identifiable in the historical photos due to the low resolution.

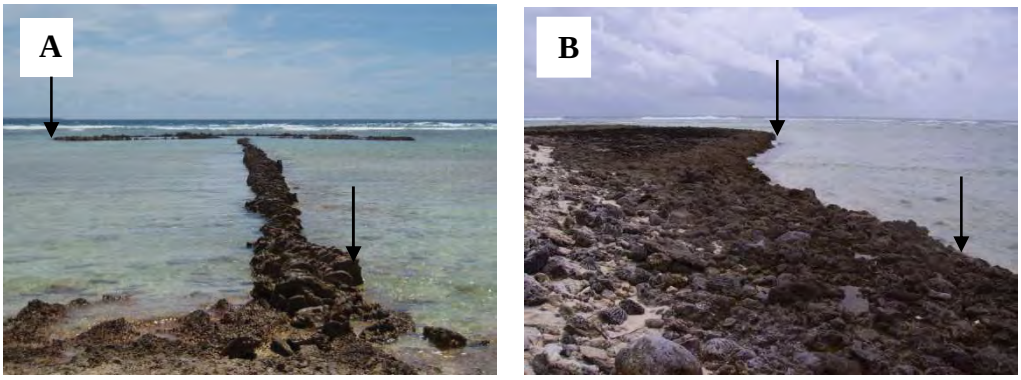

Figure 6.5. Examples of secondary GCP's that are persistent, visible and have not moved over time. For example A: fish trap and B: conglomerate platform. The arrows mark the outline of the features used as GCPs.

Historical aerial photos have issues such as distortion, poor quality or sun glint as they were acquired for other purposes other than coastal monitoring. For example, the 1943 air photos were flown by the United States Government to assist with reconnaissance activities during World War II. Georectification used the spline method in order to reduce distortion; however, spline does not produce any measure of error therefore quality control was performed to ensure that the images were accurate to within +/- 0.5m (1:2500 – base map scale). For any study requiring detection of small changes, such as shoreline positions on atolls, accuracy is critical.

Every effort was made to ensure quality control of the geo-referencing. This was performed by checking the outlines of persistent features such as fish traps and conglomerate outcrops with the base map (Figure 6.5). These features are

considered relatively immobile over time. A fish trap is made out of boulders that have cemented through time. The outlines of these features were then displayed using the 1998 backdrop, and kept within the image error of +/- 0.5 m. The image was geo-rectified again if this level of accuracy was not achieved.

6.5.1 Selection and digitisation of shoreline indicators

Poor resolution of some historical images constrained the selection of shoreline indicators meaning that in some areas it was difficult to determine the position of the shoreline. Shoreline delineation was also limited in some areas due to reflection from sand on beaches, particularly in 1943 and 1968 aerial photos. This made it impossible to determine the shoreline position therefore those areas were left un-digitised. Several shorelines could not be observed in the 2007 Quickbird satellite image due to cloud cover.

The most visible shoreline proxies that could be identified were the base of the beach (BB) and the vegetation line (VL) and these could be repeatedly detected over time. VL has been digitised as the outermost edge of the coastal vegetation above the HWL. Mangroves are an exception to this, as they occur on the lagoon intertidal flats (Figure 6.3 A) lying below the HWL and are therefore excluded from the selection of the VL. In some areas coastal vegetation is not present due to anthropogenic or natural factors, such as storm events. An alternative shoreline indicator, BB, was also used to map the shoreline. BB demarcates the clear contact point between the beach and the reef flat, beachrock or conglomerates (Figure 6.3B). On atolls there is a distinct change in slope where the ocean beach intersects the reef flat. This is far more distinct on atolls than it is for beaches on continental shorelines as shown by authors such as Boak and Turner (2005). On the lagoon beaches, no clear distinction occurs as the beach sand grades more gradually into the muddy sands of the lagoon flat. In situations where there are mangroves, BB is marked as the landward extent of mangrove vegetation.

Figure 6.3D illustrates the BB proxy shoreline on the ocean shore. Where artificial coastal constructions like seawalls or reclamations extend out onto the beach or reef flat, these structures have been included as seaward extents of both BB and VL

indicators. Shorelines have been digitised at a scale of 1:1,000. Once completed, the shoreline indicators, BB and VL were analysed using DSAS to determine the shoreline change and trends, following procedures described in Thieler *et al.* (2009). Figure 6.6 illustrates how geo-rectification can enable images to be projected at the same scale allowing a time series of shoreline positions to be investigated.

6.5.2 Area changes

Area changes for the 30 year period (1968 to 1998) including both accretional and erosional changes on the reef islands have been determined. Area changes were investigated by comparing the 1968 shoreline with the 1998 shoreline. In areas that have accreted, the outermost seaward line is the 1998 shoreline, showing progradation (Figure 6.7). Negative area changes occurred when the 1968 line becomes the outermost seaward line indicating that the area in between these two shorelines has eroded. Stable areas are those where the shorelines of 1968 and 1998 overlap at the level of detection. The 1998 aerial photograph is used as the base map (scale of 1:2500, with +/- 0.5 m). Section 6.5.3 discusses the sources of uncertainty in greater detail.

6.5.3 Digital Shoreline Analysis System

The Digital Shoreline Analysis System (DSAS), a tool developed by USGS, can be applied to establish rates of shoreline changes and trends. It is an extension of ArcGIS. The objective of the development of this tool was to standardise approaches to shoreline studies and to allow comparison. In order to operate the tool the shoreline positions need to be digitised from a series of aerial photographs or satellite images with different dates. Following this, a baseline for the shorelines is defined from which orthogonal transects are generated along the shore at user-defined intervals. The tool offers a range of methods such as Linear Regression Rate (LRR) and Endpoint Rates (EPR) to calculate shoreline changes. These will be discussed further below.

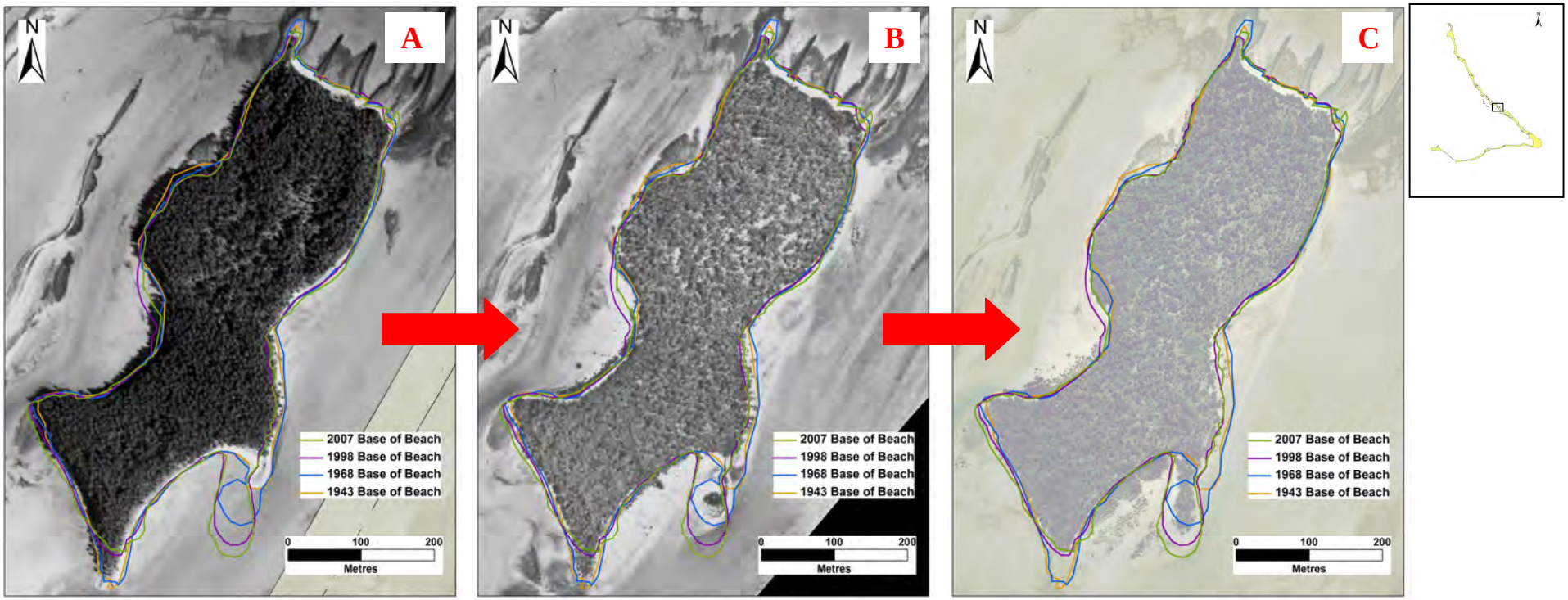

Figure 6.6. The reef island of Nea, North Tarawa illustrating how geo-rectification enables images to be projected at the same scale. This permits delineated shorelines from these georectified images to be overlain on top of each other for comparison purposes. The base of beach shoreline indicator has been utilised in this example. Aerial photos used as backdrops from left to right are A – 1943 (black and white), B - 1968 (black and white) and C – 1998 (colour). Note the persistent conglomerates on the reef-flat on all time series. Such stable features are an example of reliable secondary ground control features making image rectification possible.

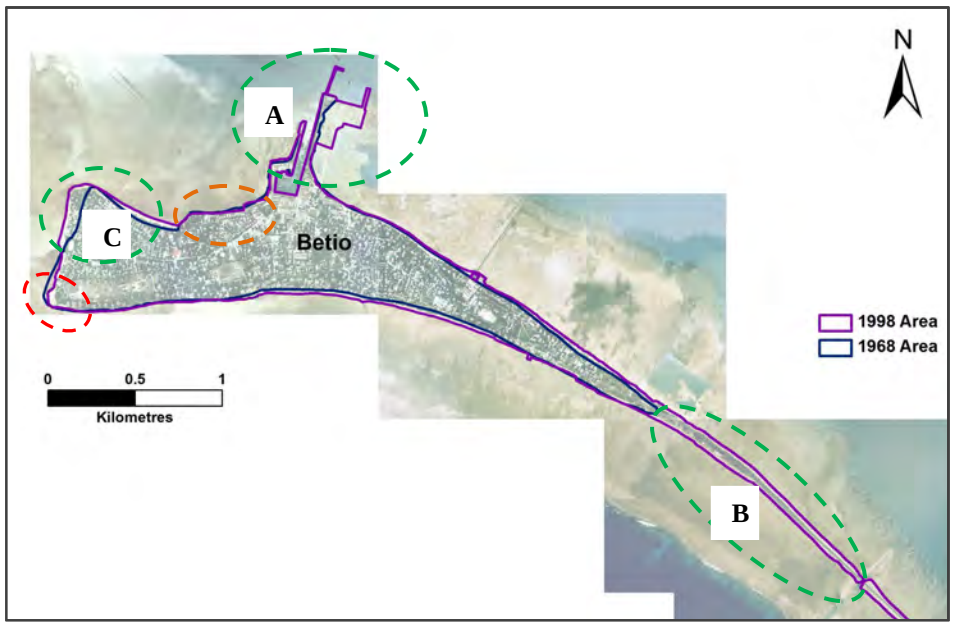

Figure 6.7. Green circles showing areas of accretion on Betio. A: Betio port development, B: Nippon Causeway and C: the rubbish dump. The red circle highlights the eroded site at the west tip of Betio, and the orange circle shows the stable area, where a seawall has been constructed.

Statistical shoreline change rates, LRR, EPR and associated statistics such as confidence intervals (CI), can be calculated with DSAS. Commonly these methods are considered statistically robust when a limited number of shorelines, such as four, are available (Crowell *et al.*, 1997). These two methods are summarised here. LRR is the slope of a best fit regression line drawn for those shorelines that intersect with the placed orthogonal transects. This computation rate of change calculates the slope of that regression line despite any changes in trend. It provides the long-term shoreline trend, but masks the short-term beach behaviour (Thieler *et al.*, 2009) (Figure 6.8A). LRR is applied in this study to measure the change between the period 1943 and 2007 utilising the four time series of 1943, 1968, 1998 and 2007. EPR is the rate of change obtained by dividing the maximum shoreline displacement by the total time period (youngest to oldest date) (Thieler *et al.*, 2009). EPR has been used to calculate the change within the shorter period of 1968 to 1998 (Figure 6.8B) which can be done for 90% of the atoll (in contrast to the 1943 photography which was not available, or suitable, for as much of the atoll). CI measured from the standard error of the slope relate to the standard deviation of a sampling distribution. DSAS provides the user with several CI options ranging from 90% - 99.9%. In this study, a CI of 99% is used. The coefficient of determination (R^2) relates to the linear

relationship between erosion and accretion rates (Abuodha, 2009). A high value of R^2 indicates a linear relationship and points to a dominant trend.

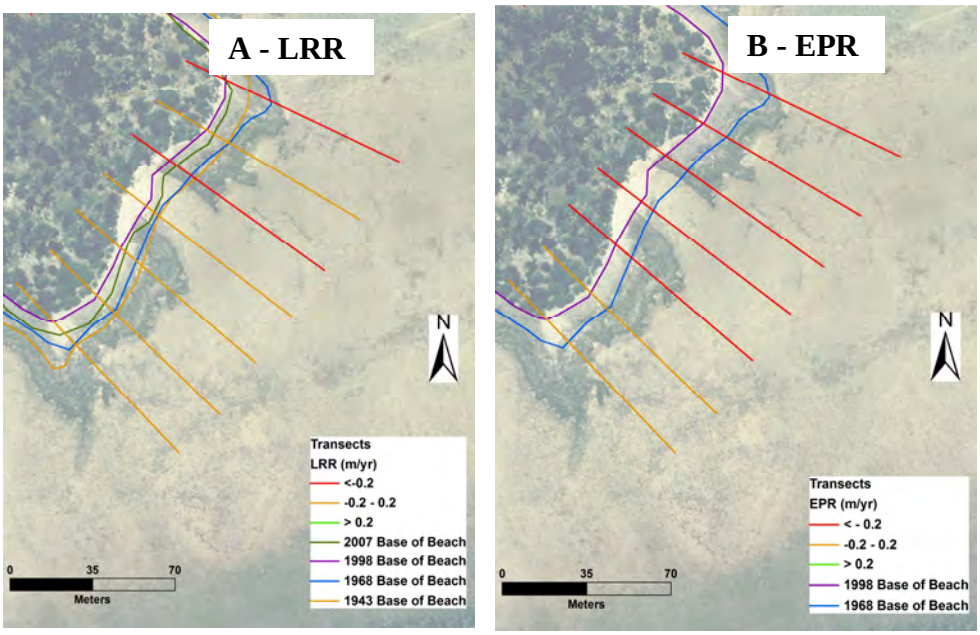

Figure 6.8. Images illustrating the differences between LRR (A) and EPR (B) using an example from Abaiaranga ocean beach applying the BB shoreline indicator. LRR considered changes over three time windows spanning 64 years whereas EPR focuses on one time windows spanning 30 years. The results of LRR shows that the coastline is predominantly stable with more orange transects, while EPR shows predominant erosion (red transects). However, visual analysis of the shorelines in A suggests more shoreline fluctuations than are indicated by the results.

The user can set the number of shorelines that must be intersected allowing DSAS to automatically eliminate transects where data is missing. For example, with LRR for locations where there are less than four shorelines, as is the case on the northern lagoon side of Buariki and in the central portion of Bonriki-Taborio, no statistical shoreline changes have been calculated. Some transects were manually eliminated as they overlapped with other transects. Examples of where this occurs are at corners of embayments, corners of coastal structures, or when transects have been constructed around shoreline bends and coastal re-entrants that are partially enclosed within the land. In cases where shorelines are irregular, such as locations where there are bends, coastal re-entrants and spits, transects have been edited to be perpendicular to the shoreline morphology (Hapke and Reid, 2007). Long-term rates of change over 64 years were calculated at each transect using the LRR method for four shoreline positions (Figure 6.8A). EPR was calculated for the period from 1968 to 1998. Both rates are reported as m/yr (Figure 6.8B). For discussion purposes, the BB shoreline indictor will be used as it is advantageous over VL in that it captures the footprint of

the reef islands enabling an estimation of reef island area. In many continental situations, the BB provides a more distinctive indicator of the shoreline (Boak and Turner, 2005). The same is also noted on reef islands (Rankey, 2010).

The possible sources of uncertainty encountered in shoreline change were discussed by Crowell *et al*. (1991), whilst Moore (2000) reviewed all coastal studies and their methods, discussing all possible measurement error sources. In this study the spline method was applied in the georectification of all images and therefore no measurement of error could be determined, so errors were limited to those estimated in the field and on aerial photos. Transect measurements can show positive (accretion), negative (erosion) or no change (stability) of shorelines. In the field and using aerial photos, areas of accretion and erosion were assessed. It was considered that positions could be measured to within 3 m of the 1998 or 1968 aerial photos so that an overall change of the order of 3 m and a rate of change of the order of 0.1 m/yr could be discriminated. Shoreline changes greater than 0.1 m/yr were considered measurable changes as those of lower magnitude were below the resolution of the data. Based on limits of measurement and the scale of the 1998 aerial photograph measured shoreline changes of between +0.2 m/yr to -0.2 m/yr were considered to reflect stability (at that level of detection) (Figure 6.9). Transects that recorded changes $\geq$+0.2 m/yr indicate accretion and those $\leq$ -0.2 m/yr indicate erosion.

6.6 Results

The results of the area changes of reef islands over a 30 year period will be discussed first. This will be followed by a discussion of the rates and trends of shoreline change on the ocean-facing and lagoon-facing beaches of individual reef islands. Additional analyses were performed to investigate whether factors such as reef-island location (northern or southern sections), beach location, human influences and natural processes have contributed significantly to the shoreline change results.

Figure 6.9. Shoreline changes over past several decades. A: An eroded shoreline resulting in a *Tournefortia* tree becoming isolated on the beach; B: *Scaevola* shrubs in front of the line of coconut trees appearing to be 30 years old indicates accretion.

The total perimeter of the reef islands studied using BB is approximately 236 km. On the ocean beaches, 2966 transects were placed perpendicular to these shorelines at intervals of 20 m for both BB and VL to determine the shoreline change over a 30 year period using the 1968 and 1998 data. On the lagoon beaches, 2918 transects were placed perpendicular to these shorelines using the same spacing of 20 m. Results of the shoreline changes are presented in Figures 6.10 to 6.15. Data from BB indicators are summarised according to beach (ocean or lagoon), location (northern or southern section) and presented as percentages (Figures 6.10 to 6.15 and Tables 6.7, 6.8 and 6.10) under the respective sections describing rates and trends of shoreline changes on North and South Tarawa. The VL indicators are also summarised and presented the same way as BB (Appendices 6.1 to 6.4). The discussion of shoreline change is primarily focussed on BB values for two reasons. The first is that it clearly demarcates the contact point between the beach and the reef flat. The second is that the results show that the correlation between BB and VL appears to be strong in most situations.

6.6.1 Area change and patterns over a period of 30 years

One objective of this study was to determine whether the reef islands are growing at the rapid rates suggested by Webb and Kench (2010) or at slower rates as proposed by Rankey (2010), or eroding over the 30 year period, from 1968 to 1998. Examples of the reef islands investigated using BB are outlined in Figures 6.10 to 6.15. A summary of the area changes obtained using BB are presented in Table 6.4. Results show that the all land area in 1968, not including any major developments such as causeways, reclamations and seawalls, was 2370.68 ha. In 1998, the land area,

including all major developments, had increased to 2819.38 ha, a net increase of 448.70 ha or 19%. However, the increase is dominated by major developments, all in urban South Tarawa, which have built land from materials that have been sourced from the adjacent beach or surrounding nearshore areas. These developments have contributed a significant amount of 363.50 ha towards the 1998 land area. The developments and their contributions are summarised as follows: construction of the *Te Ananau* Causeway on Bonriki-Taborio, which led to the reclamation of the eastern corner of the reef island, contributed 335 ha, the construction of the Nippon Causeway contributed 22.60 ha, the expansions of the Betio Port contributed 4.40 ha and finally reclamation on Ambo-Teaoraereke reef island added an additional 1.50 ha (Table 6.5). Deducting this amount from the net area increase of 448.70 ha, ha, the land increase due to the combined effect of natural processes and "small" developments (e.g., the numerous individual- or family-scale interventions that contribute to the increase, as discussed in more detail below for Bairiki) is estimated to be only 85.20 ha (or 19% of the total) (Table 6.4). This analysis clearly shows that human activities have contributed the vast majority of the net increase of reef island area in Tarawa Atoll including the reef islands that Webb and Kench (2010) used to derive their reported rates of reef island growth in relation to sea-level rise.

Table 6.4. Summary of area changes for the entire atoll over the 30 year period.

Sections	Initial (ha) – 1968	Final (ha) – 1998	Net Area change (ha)	% change	Major reclamations (ha)	Natural changes and small developments (ha)
North Tarawa	1489.42	1528.54	39.13	2.6		39.12
South Tarawa	881.26	1290.84	409.58	46.5	363.50	46.08
Total Change	2370.68	2819.38	448.70	18.9	363.50	85.2

Table 6.5. Contributions of major developments

Development	Reef island	Area (ha)
Temaiku Bight reclamation	Bonriki-Taborio	335.00
Nippon Causeway	Betio and Bairiki	22.60
Betio Port	Betio	4.40
Reclamation	Ambo-Teaoraereke	1.50
Total		363.50

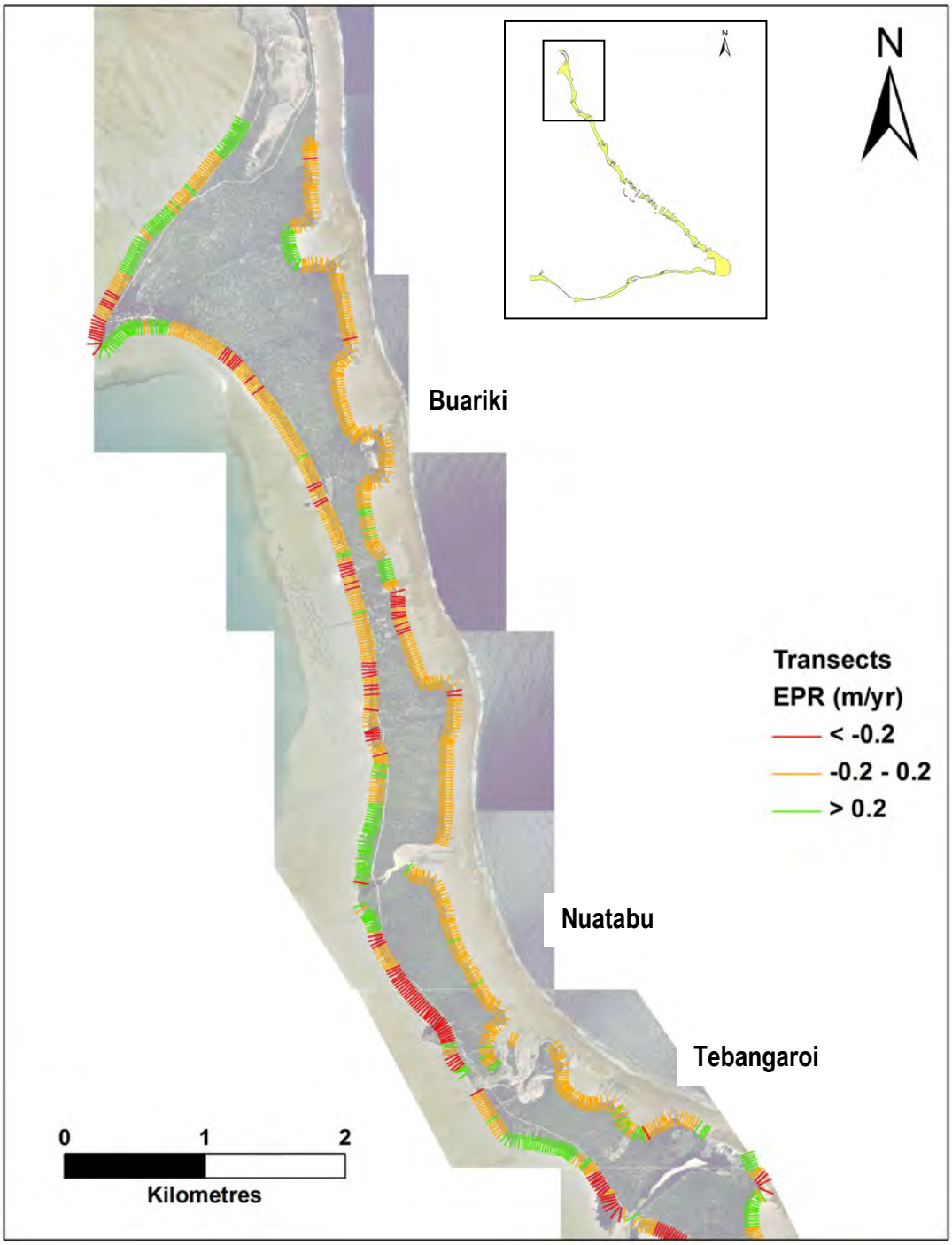

Figure 6.10. Thirty years of shoreline change on Buariki, Nuatabu and Tebangaroi reef islands of North Tarawa. Red lines indicate erosion, green lines indicate accretion and orange lines indicate stability.

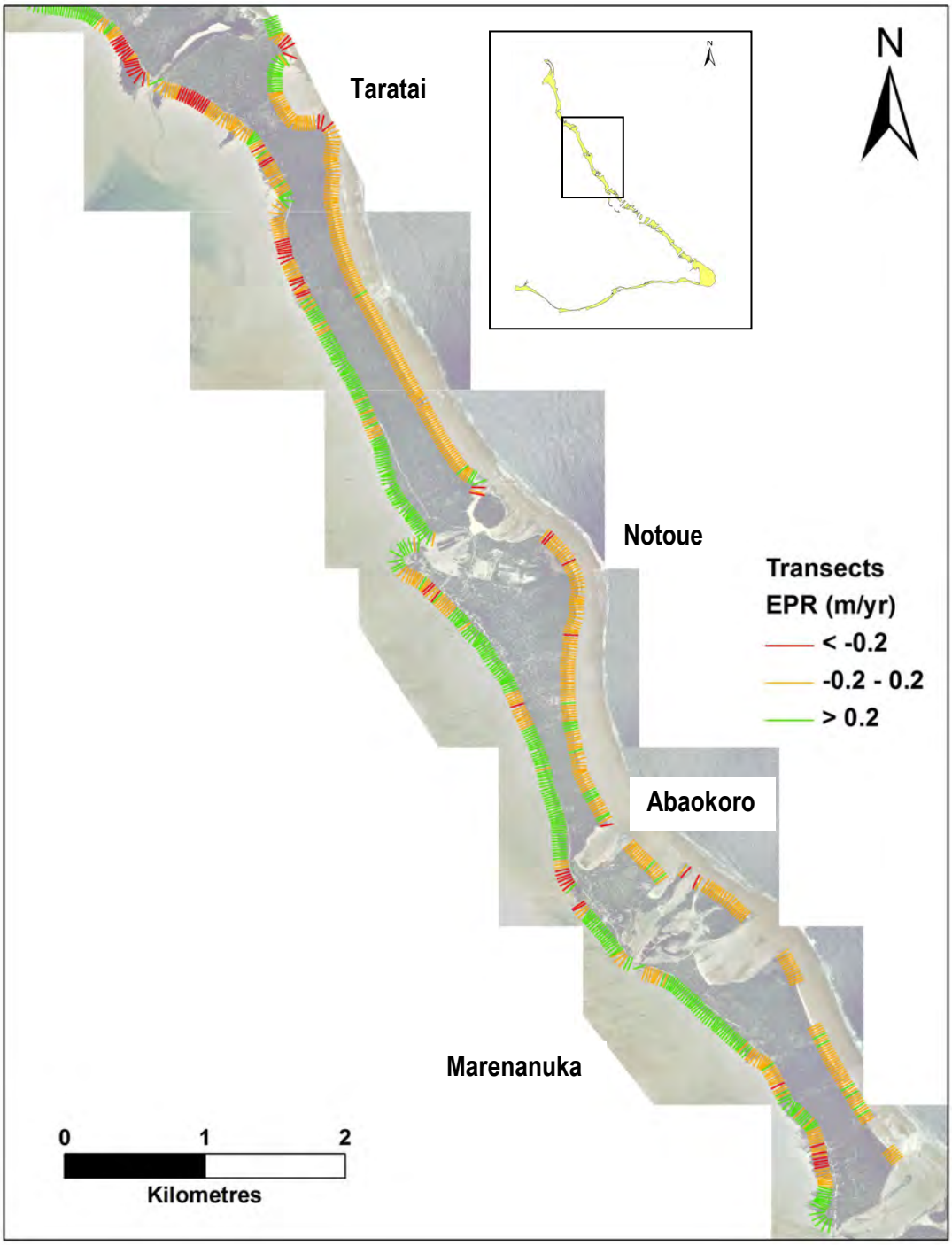

Figure 6.11. Thirty years of shoreline change of Taratai, Notoue, Abaokoro and Marenanuka reef islands, North Tarawa

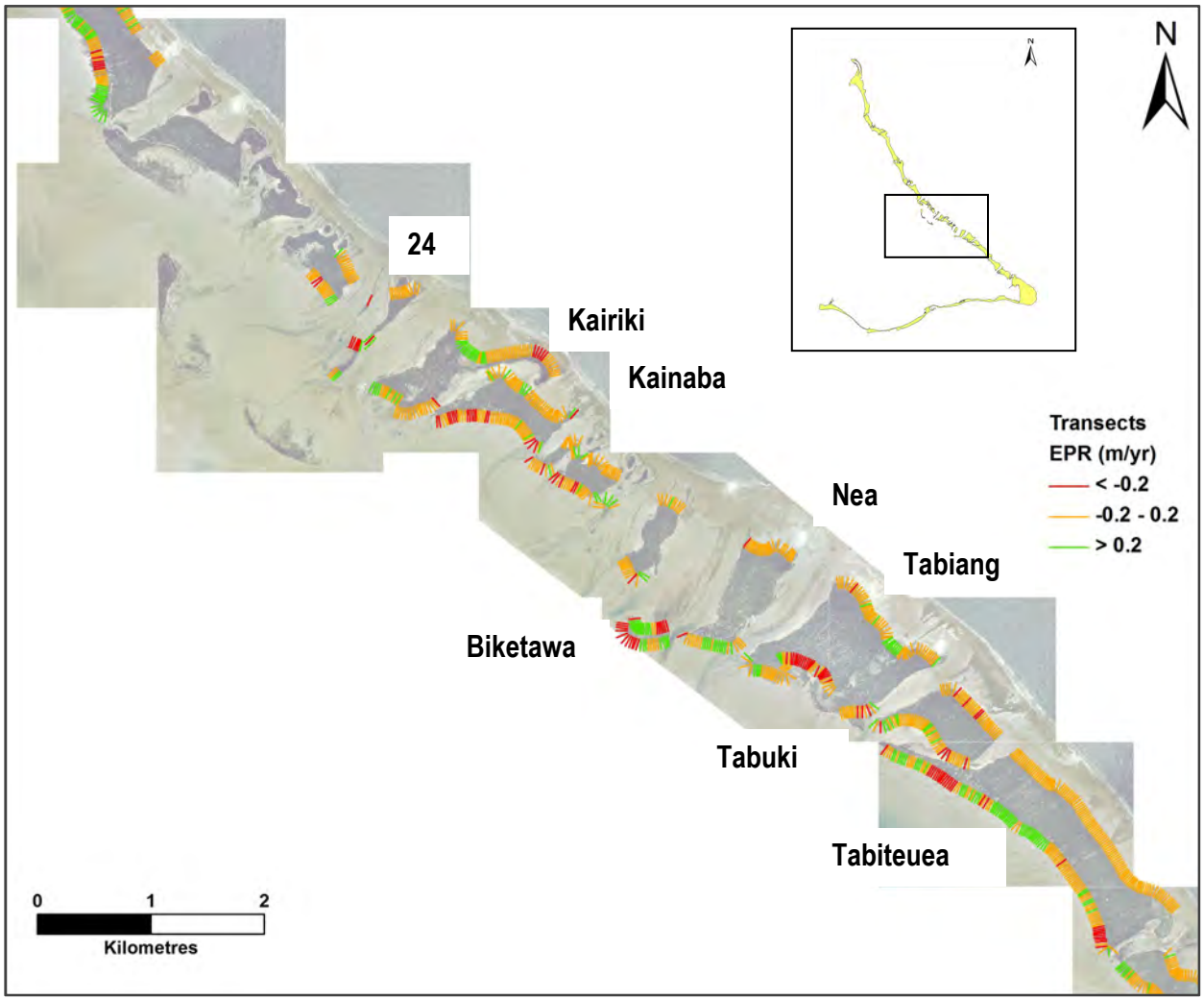

Figure 6.12. Thirty years of shoreline change on the reef islands located on the central part of North Tarawa from 24 to Tabiteuea.

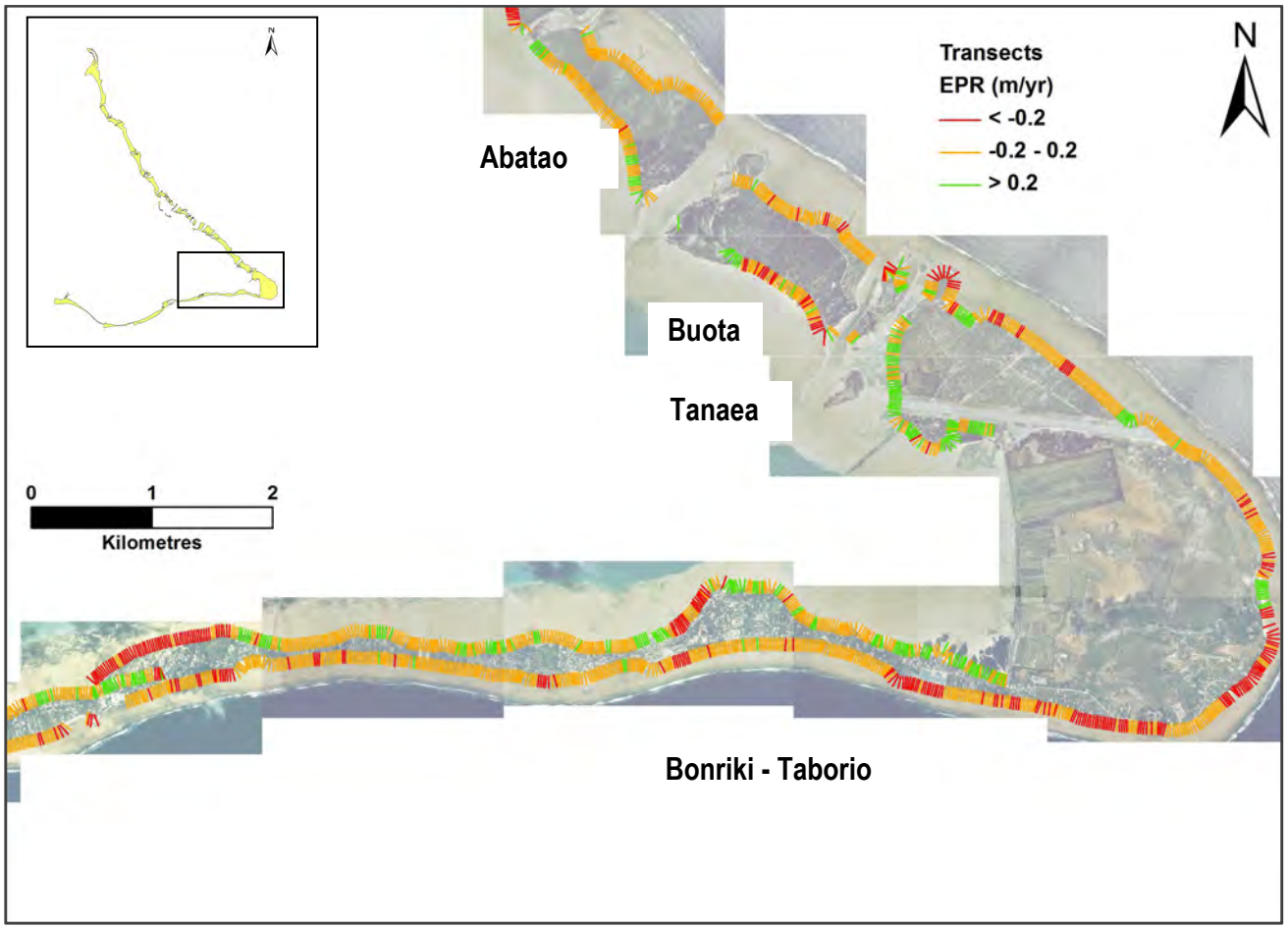

Figure 6.13. Thirty years of shoreline change on Abatao, Buota and the eastern portion of Bonriki-Taborio reef islands.

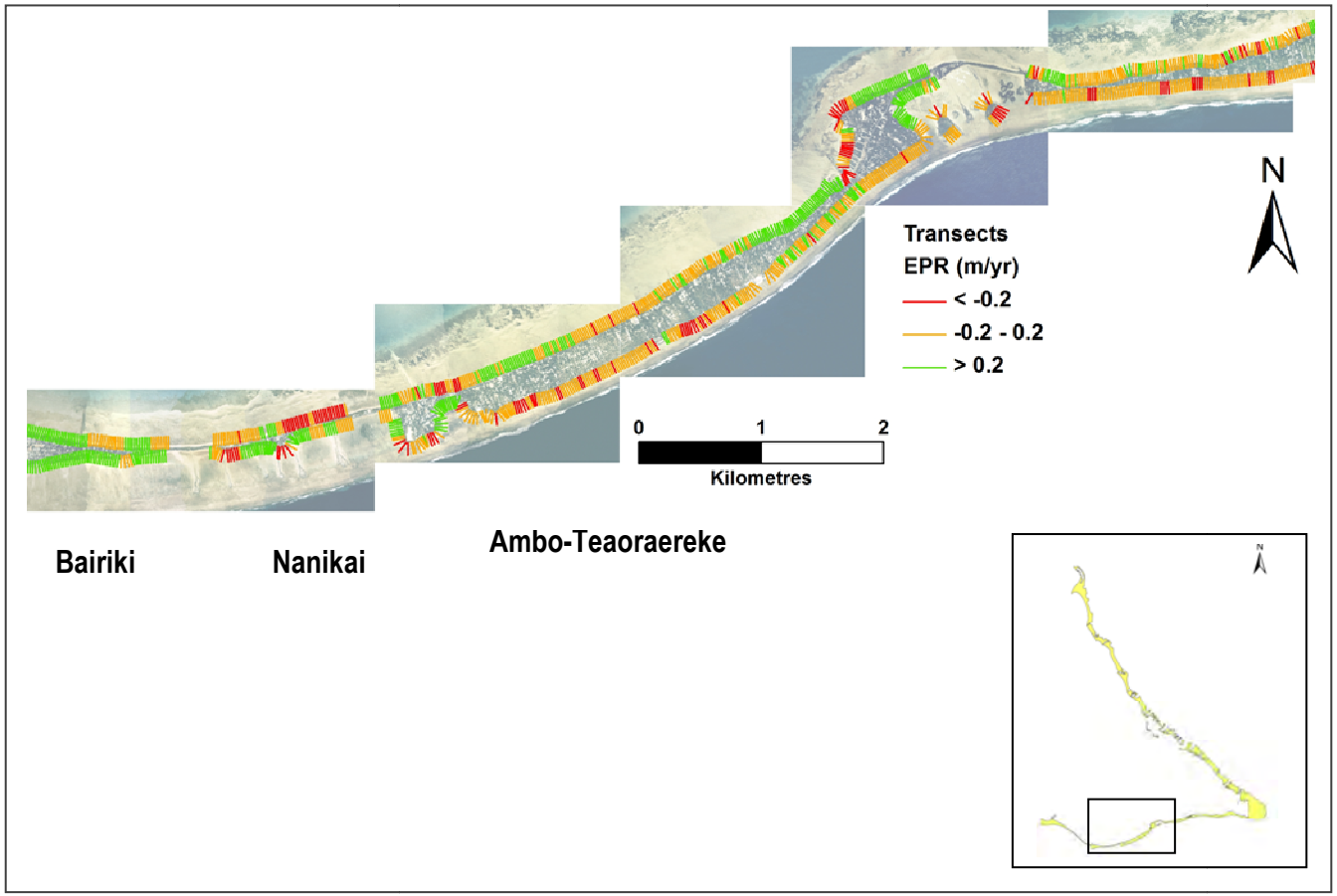

Figure 6.14. Thirty years of shoreline change on the western portion of Ambo-Teaoraereke, Nanikai and the eastern part of Bairiki reef islands, South Tarawa

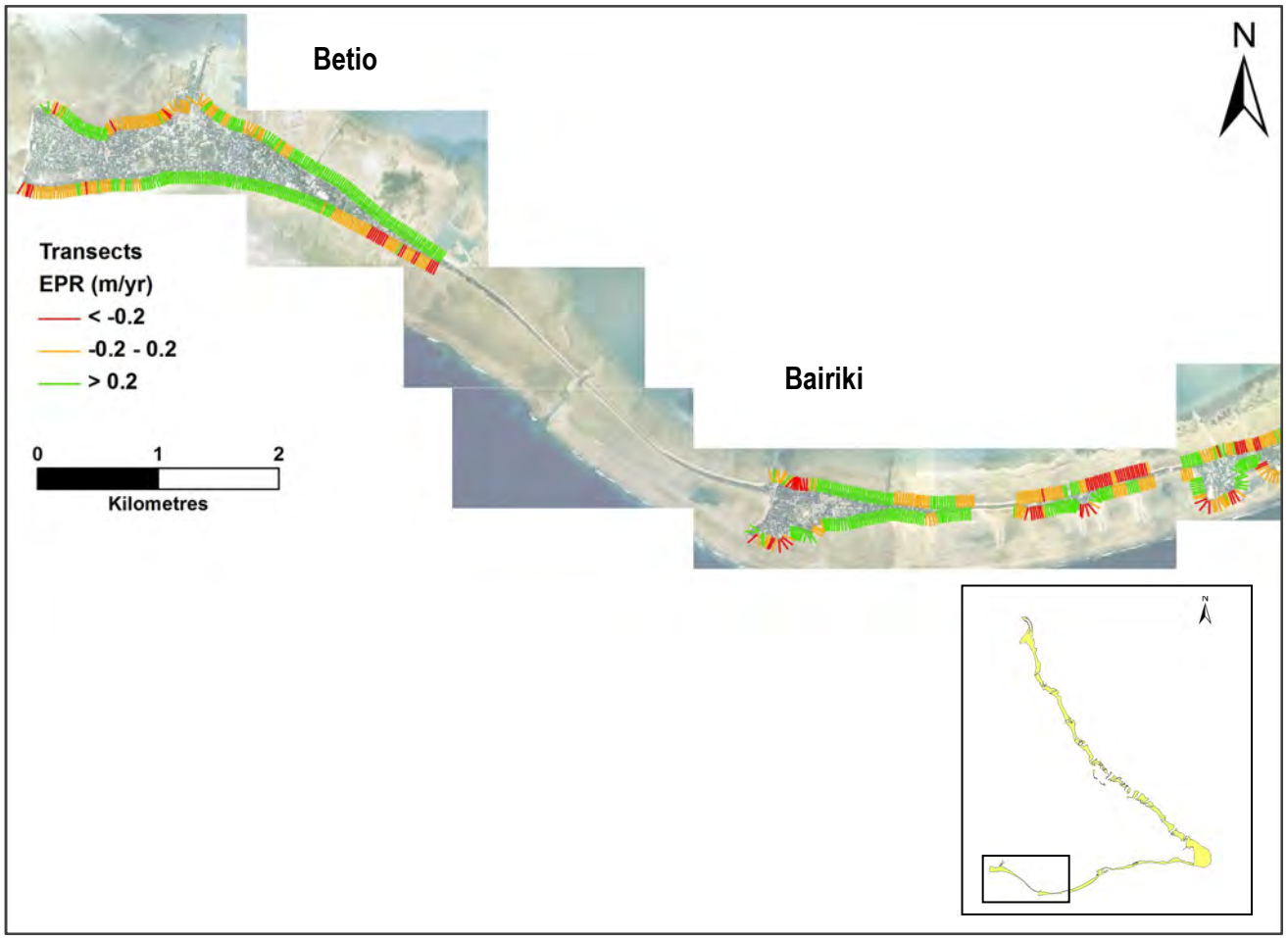

Figure 6.15. Thirty years of shoreline change on Bairiki and Betio reef islands, South Tarawa

Rural North Tarawa area changes

The area changes from 1968 to 1998 on the 40 reef islands located on North Tarawa differ from those observed in South Tarawa as they are relatively smaller with a total net increase of only 39.12 ha (2.6%) (Table 6.6). North Tarawa area results show that stability is the dominant response of area change (n = 25), followed by accretion (n = 13) and lastly erosion (n =2) (Table 6.6). The 25 reef islands showing no significant change are as follows: Nea, Nabeina, Abatao, Buota, Naninimai, Bikenubati, and reef islands numbered 3, 4, 7, 18, 20, 23, 24, 25, 29, 30, 31, 32, 34, 35, 36, 37, 38, 39, and 51 (Figure 6.16). All these reef islands are uninhabited.

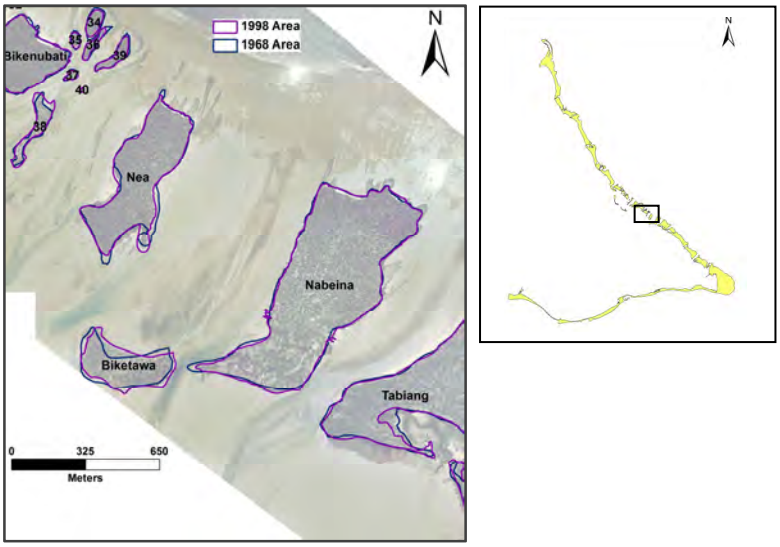

Figure 6.16. Reef islands with no changes on the central rim of North Tarawa. Biketawa located further away from the high energy waves has significantly accreted.

Of the 13 reef islands that showed net accretion, the increase ranges from 0.54 ha to 7.91 ha (Table 6.6). In descending order of area increase is Marenanuka (7.91 ha), Notoue (6.63 ha), Buariki (6.36 ha), Taratai (4.96 ha) and Tebangaroi (4.91 ha) (Figure 6.17) with five reef islands having increases from 0.54 ha to 1.10 ha (namely reef island 10, Tabiteuea, Nuatabu, Kainaba and Biketawa) (Figure 6.16). Buariki has shown a trend of stability with accretion occurring in specific areas (embayments, sand spits and in areas where the channels have been blocked by causeways); however, not all of the reef island was mapped as some aerial photographs were missing from 1968. For the same reef island, Webb and Kench (2010) measured a net change of 10 ha from shoreline changes between 1943 and 2004. To compare these results to the results from this study, the rates of shoreline

change were calculated from both studies using the net area change and both showed similar rates of 0.2 m/yr.

Table 6.6. North Tarawa area changes

ID	Name	Area (ha)		Net Area Change		Contribution to overall increase of atoll (%)	Status
		1968	1998	(ha)	%		
1	Buariki	384.00	390.36	6.36	1.7	1.4	Accretion
2	Nuatabu	66.12	67.04	0.91	1.4	0.2	Accretion
3		1.65	1.54	- 0.11	-6.8	-0.0	Stable
4		0.11	0.10	- 0.02	-15.3	-0.0	Stable
5	Tebangaraoi	65.96	70.87	4.91	7.4	1.1	Accretion
6	Taratai	172.66	177.62	4.96	2.9	1.1	Accretion
7		4.66	4.71	0.05	1.0	0.0	Stable
8	Notoue	113.33	119.96	6.63	5.8	1.5	Accretion
9	Abaokoro	28.26	32.64	4.38	15.5	1.0	Accretion
10		7.80	8.90	1.10	14.0	0.2	Accretion
11	Marenanuka	95.16	103.07	7.91	8.3	1.8	Accretion
18		0.64	0.50	- 0.14	-22.2	- 0.0	Stable
20		0.45	0.30	- 0.14	-32.3	- 0.0	Stable
23		1.10	1.02	- 0.08	-7.3	- 0.0	Stable
24		5.37	5.36	- 0.00	-0.1	- 0.0	Stable
25		2.02	1.94	- 0.07	-3.6	- 0.0	Stable
27	Kairiki	36.13	35.24	-0.89	-2.5	- 0.2	Erosion
28	Kainaba	27.92	28.53	0.61	2.2	0.1	Accretion
29		3.43	3.44	0.01	0.3	0.0	Stable
30		0.23	0.17	- 0.06	-26.6	-0.0	Stable
31		0.37	0.31	- 0.07	-17.5	- 0.0	Stable
32		0.58	0.38	- 0.20	-34.0	- 0.0	Stable
33	Bikenubati	11.48	11.35	-0.13	-1.1	- 0.0	Stable
34		0.79	0.60	- 0.19	-23.8	- 0.0	Stable
36		0.47	0.40	- 0.07	-14.3	- 0.0	Stable
35		0.24	0.22	- 0.02	-8.2	-0.0	Stable
37		0.20	0.17	- 0.03	-13.7	- 0.0	Stable
38		1.36	1.73	0.37	27.0	0.1	Stable
39		0.80	0.73	- 0.07	-9.0	- 0.0	Stable
41	Nea	14.49	14.27	- 0.23	-1.6	- 0.1	Stable
42	Biketawa	5.74	6.28	0.54	9.3	0.1	Accretion
43	Nabeina	36.42	36.25	- 0.17	-0.5	-0.0	Stable
44	Tabiang	84.00	85.26	1.26	1.5	0.3	Accretion
45	Tabuki	32.24	31.24	-1.00	-3.1	-0.2	Erosion
46	Tabiteuea	103.53	104.49	0.96	0.9	0.2	Accretion
47	Abatao	79.83	80.19	0.36	0.5	0.1	Stable
48	Naninimai	4.71	4.65	-0.06	-1.3	- 0.0	Stable
49	Buota	87.83	88.18	0.35	0.4	0.1	Stable
51		0.48	0.33	-0.15	-31.3	-0.0	Stable
50	Tanaea	6.86	8.22	1.36	19.9	0.3	Accretion
40		**1489.42**	**1528.54**	**39.1**	**2.6**	**8.7**	

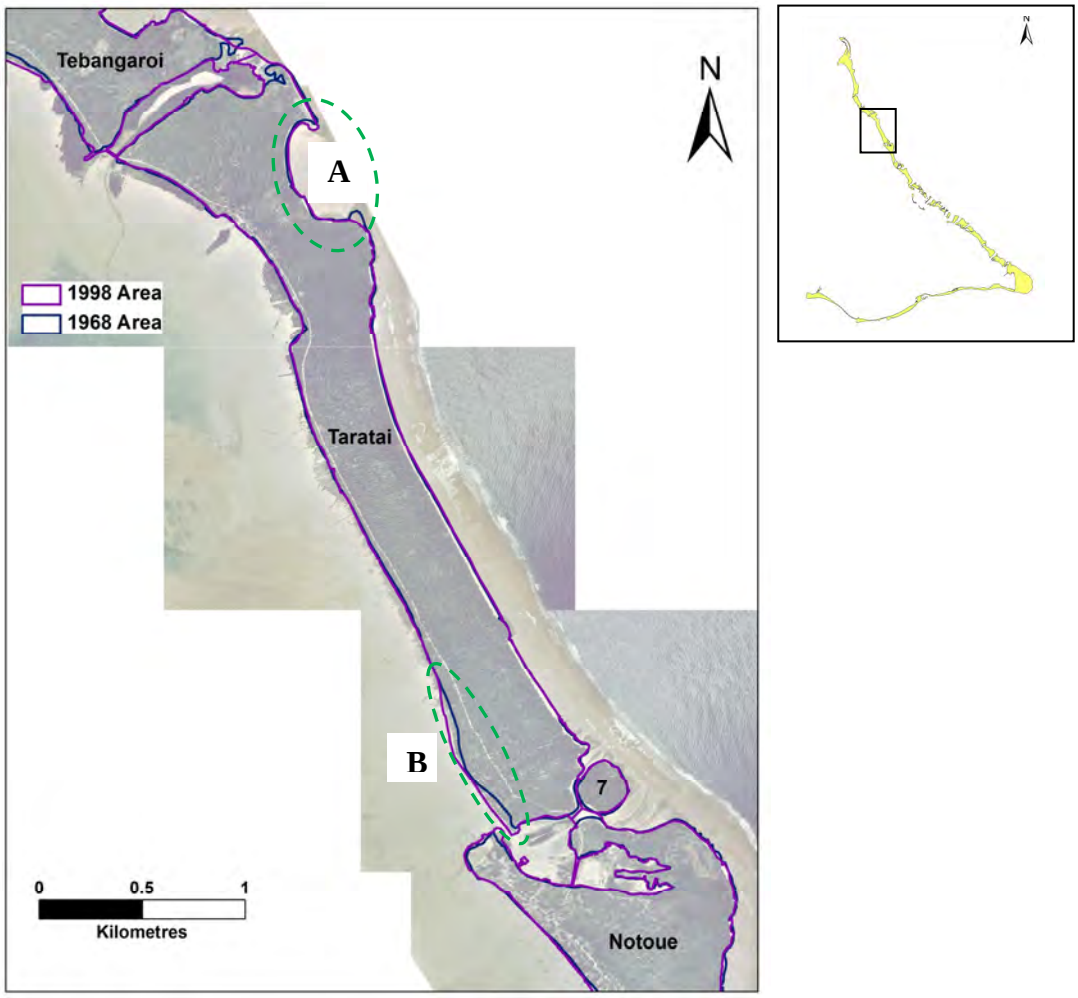

Figure 6.17. Taratai is an example of reef island with minimal changes showing areas of accretion in embayments (A) and beaches close to blocked channels (B).

Erosion was observed only on two reef islands, Tabuki (1 ha) and Kairiki (0.89 ha) (Table 6.6). Tabuki has generally lost sediment from its ocean-facing beaches and those facing the channel on the northern end. In the case of Kairiki, the south-eastern part of the reef island extending out further to the reef rim has been subjected to erosion (Figure 6.18). These two reef islands are both uninhabited.

The changes in area vary from one reef island to another for reef islands that show accretion. The changes in North Tarawa are generally due to natural causes. On elongated reef islands, embayments and ocean beaches have accreted (Figure 6.17A). Accretion is also observed on sand spits, and in areas where channels have been blocked by causeways thus allowing sediment to deposit on adjacent beaches (Figure 6.17B). In other locations, embayments and ocean beaches have accreted. All of

these reef islands, except reef island number 10, are occupied but the population density is generally low suggesting that development of the coastal area is minimal.

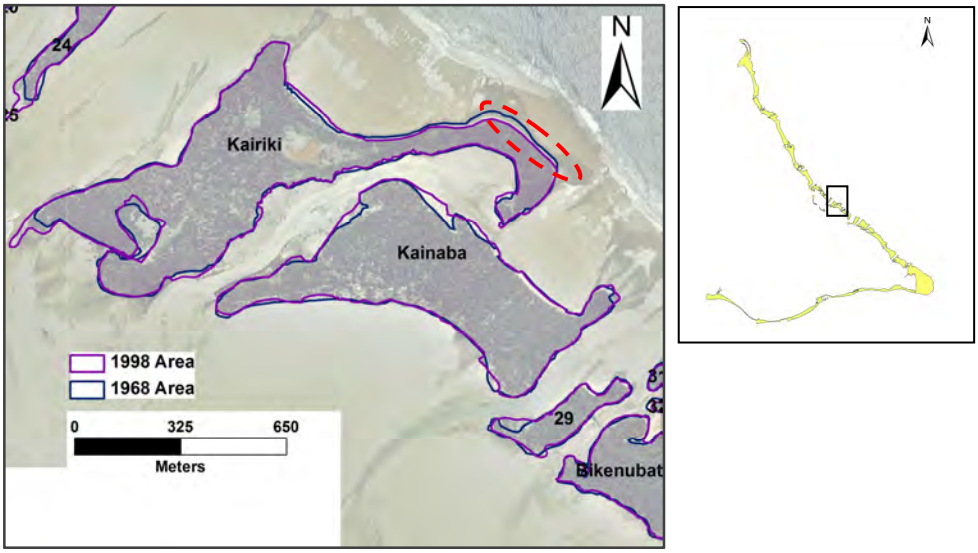

Figure 6.18. Kairiki is an example of a reef island showing erosion. Note the portion of Kairiki exposed to high energy on the ocean side shows significant erosion (circled in red).

Rates and trends of shoreline changes on North Tarawa

This section will discuss the rates and trends of shoreline changes across ocean- and lagoon-facing beaches. The average rates of change on ocean and lagoon beaches are reported in Tables 6.7 and 6.8 respectively for the 25 reef islands situated in North Tarawa. These values are an average of all observed rates of change measured at each transect along the shoreline. It is not a direct measurement of the length of shoreline covered and the number of transects used. This is because transects have been deleted in some situations where they overlap with other transects for example at corners of embayments and coastal structures (see Section 6.5.3). The results will be presented using the BB, however, there is difficulty in detecting the BB on lagoonal beaches leading to greater uncertainty in the results. Results show that the ocean-facing beaches are predominantly stable (n = 24). The remaining two ocean beaches have accreted. The reef islands with no significant changes are Nabeina, Taratai, Bikenubati, Buariki, Kairiki, Tabiteuea, Nuatabu, Abatao, Nea, Buota, Tabuki, Tabiang, Marenanuka, Tebangaroi, Notoue, Kainaba, Abaokoro, Tanaea and reef islands numbered 24, 29, 3, 10, 16, and 25. The reef islands that have accreted are Biketawa (0.5 m/yr) and reef island number 38 (0.4 m/yr).

Table 6.7. Ocean shoreline changes on North Tarawa reef islands

ID	Name	Length (km)	No of transects	Average Rates (m/yr)	Accretion (%)	Erosion (%)	Stable (%)	Status
Base of beach								
1	Buariki	6.3	296	0	10	5	85	Stable
2	Nuatabu	1.8	87	0.1	8	0	92	Stable
3		0.1	3	-0.1	0	100		Stable
5	Tebangaroi	1.5	78	0.1	16	1	83	Stable
6	Taratai	4.1	201	0	13	4	83	Stable
8	Notoue	2.3	111	0	11	5	85	Stable
9	Abaokoro	0.1	41	0	2	93	5	Stable
10		0.4	19	0.1	0	0	100	Stable
11	Marenanuka	1.7	58	0.1	10	0	90	Stable
16		0.3	15	0	7	0	93	Stable
24		0.2	13	0	0	0	100	Stable
25		0.1	6	-0.2	17	66	17	Stable
27	Kairiki	1.2	57	0.1	26	7	67	Stable
28	Kainaba	0.9	43	0.1	12	2	86	Stable
29		0.2	8	0	0	0	100	Stable
33	Bikenubati	0.5	22	0	5	0	95	Stable
38		0.1	6	0.4	50	0	50	Accretion
41	Nea	0.2	10	0.1	0	0	100	Stable
42	Biketawa	0.4	23	0.5	61	26	13	Accretion
43	Nabeina	0.5	26	-0.1	0	0	100	Stable
44	Tabiang	1.2	60	0.1	15	0	85	Stable
45	Tabuki	0.7	32	-0.1	0	3	97	Stable
46	Tabiteuea	2.2	103	0	0	0	100	Stable
47	Abatao	1.7	74	0	0	0	100	Stable
49	Buota	1.5	69	-0.1	1	6	93	Stable
50	Tanaea	0.3	20	0	25	20	55	Stable
26	**Total**	**30.5**	**1481**					

Table 6.8 summarises the results of the shoreline changes on lagoon-facing beaches. The number of lagoon beaches studied was reduced to 23 as two reef islands (9 and 24) do not have lagoon beaches, but only have leeward beaches located on the ocean side (Table 6.7). The third reef island 38 could only have one transect placed on the lagoon side. The lagoon beaches show only two responses, stability and accretion. Nineteen beaches are stable and four beaches are accreting. The reef islands with stable lagoon beaches are Nabeina, Taratai, Bikenubati, Buariki, Kairiki, Biketawa, Tanaea, Tabiteuea, Nuatabu, Abatao, Abaokoro, Nea, Buota, Tabuki, Kainaba, Tabiang, and reef islands numbered 17, 24, and 29. The four reef islands with lagoon beaches that have accreted in descending order of average accretion rate are Marenanuka (0.5 m/yr), Notoue (0.4 m/yr), reef island 25 (0.3 m/yr) and Tebangaroi

(0.3 m/yr). Even though the rates of change appear similar to those on the ocean-facing beaches there is less certainty in the results as the exact location of the base of the beach on the lagoon side was difficult to discern

Table 6.8. Lagoon shoreline changes on North Tarawa reef islands

ID	Name	Length (km)	No of transects	Average Rates (m/yr) (±0.2)	Accretion (%)	Erosion (%)	Stable (%)	Status
Base of beach								
1	Buariki	7.4	360	0.1	27	10	63	Stable
2	Nuatabu	1.6	74	0	22	56	22	Stable
5	Tebangaroi	1.5	72	0.3	40	20	40	Accretion
6	Taratai	4.1	200	0.2	41	9	50	Stable
8	Notoue	3.3	145	0.4	62	32	6	Accretion
9	Abaokoro	0.5	28	0.2	53	4	43	Stable
11	Marenanuka	2.6	125	0.5	55	3	42	Accretion
17		0.4	19	0	11	6	83	Stable
24		0.1	3	0.1	67	33	0	Stable
25		0.1	5	0.3	50	0	50	Accretion
27	Kairiki	0.7	33	0.1	15	3	82	Stable
28	Kainaba	1.0	54	-0.1	4	24	72	Stable
29		0.1	10	0	10	70	20	Stable
33	Bikenubati	0.1	21	0	10	85	5	Stable
41	Nea	0.2	13	0	15	8	77	Stable
42	Biketawa	0.5	24	-0.1	29	46	25	Stable
43	Nabeina	0.4	25	0.1	36	60	4	Stable
44	Tabiang	1.7	74	-0.1	12	69	19	Stable
45	Tabuki	1.0	51	0.1	12	82	6	Stable
46	Tabiteuea	2.8	142	0.1	33	15	52	Stable
47	Abatao	1.7	86	0.1	15	0	85	Stable
49	Buota	1.1	60	-0.1	18	62	20	Stable
50	Tanaea	0.1	4	0.1	0	25	75	Stable
23	**Total**	**33.0**	**1628**					

The above results show that over 30 years, reef islands in North Tarawa are predominantly stable. Results show that 18 reef islands have not changed significantly on either the ocean or lagoon beach. These are Bikenubati, Taratai, Tabiteuea, Buariki, Nabeina, Abatao, Nuatabu, Nea, Kairiki, Tabuki, Abaokoro, Tanaea, Tabiang, Kainaba Buota, and reef islands numbered 12, 24, and 29. The four reef islands that are stable on the ocean and show accretion on the lagoon side are Notoue, Marenanuka, Tebangaroi and 25. The only reef island that has accreted on the ocean side and shows no significant change on the lagoon side is Biketawa.

Urban South Tarawa area changes

South Tarawa's responses have been tabulated differently as human-induced changes have had such a large impact here. The net changes of the reef islands have been calculated to determine the contribution of large reclamations towards the total net change which in most cases is significant.

The area changes over the past 30 years (1968 to 1998) on the eight reef islands of South Tarawa differ significantly from those in North Tarawa, contributing a substantial 409.58 ha to the net accretion of 448.70 ha of all reef islands (Table 6.9). Table 6.9 summarises the area changes that have taken place on urban South Tarawa. Results show that six reef islands have undergone accretion whilst two do not show any significant changes (at the level of detection). In descending order, the individual reef-island contribution to overall accretion is Bonriki-Taborio (348.41 ha), Betio (26.88 ha), Bairiki (17.21 ha), Ambo-Teaoraereke (14.31 ha), Nanikai (2.06 ha) and Abaokoro-South Tarawa (0.61 ha). The first five reef islands have high population densities, only Abaokoro is uninhabited (Table 3.3). Accretion has occurred where human activity, especially reclamation, has taken place increasing the land area from 1968 to the present. The results from Betio, Bairiki and Nanikai differ from Webb and Kench's study. The reason is that the 1998 area for the reef islands calculated from this study includes a larger portion of the attached causeways. In the case of Betio, the reef island includes the length of the Nippon Causeway stretching from the eastern tip of Betio to the Fisheries Channel (Figure 6.7). With Nanikai, the causeways attached to both ends of the reef island have been divided equally with the neighbouring reef islands so that each has relatively equal share of the structure.

The majority of the increase in reef island area on South Tarawa is due to human activity, which contributes 363.50 ha towards the net increase of 448.70 ha (Table 6.4). Large developments have been considered here but not small developments such as private reclamations and seawalls. A minor increase of 46.08 ha appears to relate to the combined contribution of natural reef island processes and minor coastal developments (Table 6.4). This area is obtained by subtracting the land area gained by major developments (363.50 ha) from the net change from urban South Tarawa

reef islands (409.58 ha) (Table 6.4 and Table 6.9). This will be further discussed using an example from Bonriki-Taborio reef island.

On Bonriki-Taborio, the construction of the Ananau Causeway led to a significant reclamation on the eastern end of the reef island (Figure 6.19). This reclaimed area measures 335 ha and accounts for 96.2% of the land increase for this reef island and 74.7% to the total area change for the atoll (Table 6.9). The remaining 13.41 ha from the net area change of the reef island are therefore likely to include small scale reclamations and natural changes. The small-scale human activities include reclamations, seawalls and groynes. The main objective of these developments is to extend land area for the increasing population and this is also the case on other reef islands in South Tarawa with high population densities. Therefore, humans through this major development have contributed significantly to the growth of this reef island, and a very small amount of growth appears to be related to minor developments and natural changes.

Table 6.9. Summary of urban South Tarawa reef island changes

ID	Name	Area (ha)		Net Area change		Net Area change by reclamation		Contribution of reclamation to Atoll's net change	Status
		1968	1998	ha	%	ha	%	%	
52	Bonriki-Taborio	514.78	863.19	348.41	67.7	335.00	96.2	74.7	Accretion
53	Abairaranga	1.54	1.28	-0.26	-16.8		0.0	0.0	Stable
54	Tebwe	0.29	0.64	0.35	122.6		0.0	0.0	Stable
55	Abakoro-South Tarawa	2.38	2.99	0.61	25.8		0.0	0.0	Accretion
56	Ambo-Teaoraereke	167.13	181.44	14.31	8.6	1.50	10.5	0.3	Accretion
57	Nanikai	13.26	15.32	2.06	15.6		0.0	0.0	Accretion
58	Bairiki	42.01	59.22	17.21	41.0	13.00	75.5	2.9	Accretion
59	Betio	139.88	166.76	26.88	19.2	14.00	52.1	3.1	Accretion
8		**881.26**	**1290.84**	**409.58**	**46.5**	**363.50**	**88.7**	**81.0**	

Betio is another example where 14 ha of the reef island's 26.88 ha increase is due to human activities (Table 6.9). This area includes the improvement works on the port (Figure 6.7A), the construction of the Nippon Causeway up to the Fisheries Channel (Figure 6.7B) and the sand accumulating on the western end as a result of the rubbish dump (Figure 6.7C). The remaining 12.88 ha are likely to be related to small coastal

developments and natural changes. In the case of Bairiki, the construction of the Nippon Causeway extending from the western tip of Bairiki towards the Fisheries Channel adds a major contribution of 13 ha to the reef island's net increase of 17.21 ha (Table 6.9). This eastern portion of the Nippon Causeway alone adds nearly the same amount of land area to Bairiki as that gained by Betio from all its major developments, indicating that contribution of developments may vary depending on their physical size. Tebwe and Abaiaranga are the only two reef islands that have shown stability in of the South Tarawa group. These reef islands are both uninhabited.

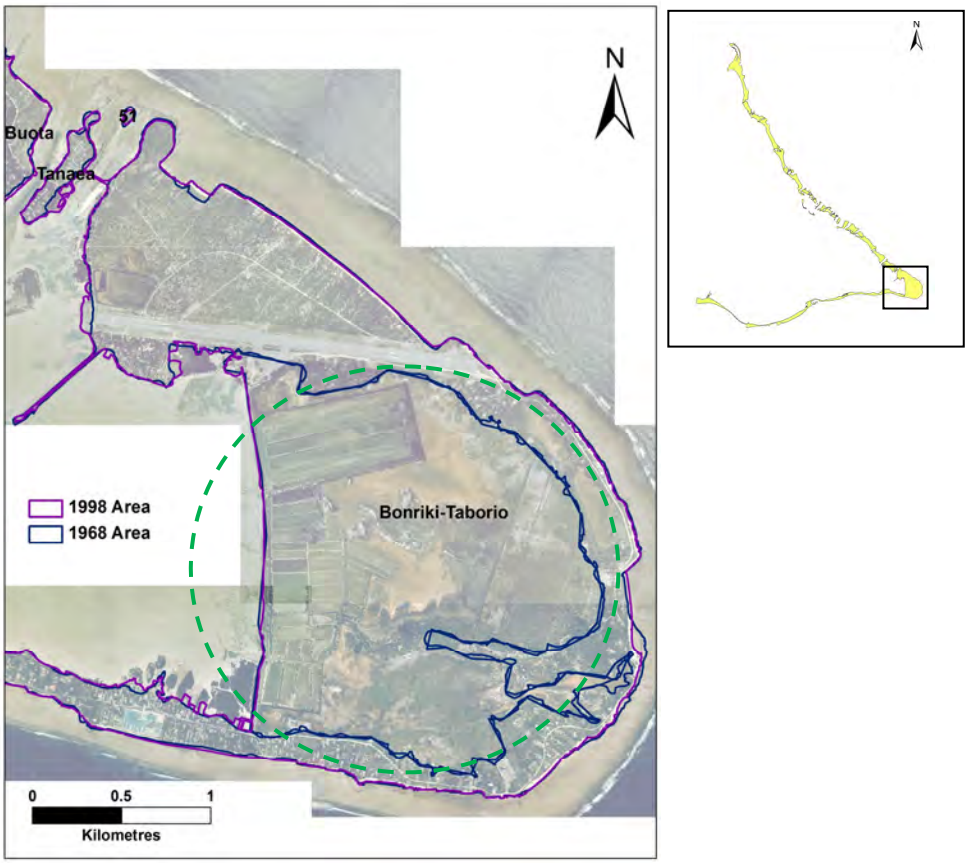

Figure 6.19. The reclamation marked in green on the eastern corner of Bonriki-Taborio reef island contributes nearly 75% to 448.70 ha increase across the whole atoll over the 30 years time period.

Urban South Tarawa shoreline changes

Table 6.10 summarises the rates and trends of ocean and lagoon shoreline changes on the seven reef islands. The reef island of Tebwe is not included in this analysis because of its small size. The results showed that the dominant mode of shoreline change for ocean shorelines in descending order is accretion followed by no

significant change (n=3). The four reef islands showing shoreline accretion in order of descending average rates are Bairiki (0.5 m/yr), Nanikai (0.5 m/yr), Abaokoro-South Tarawa (0.4 m/yr) and Betio (0.3 m/yr). The average accretion rates are relatively high and occur in areas with a strong influence from human activities. The three reef islands showing no significant change are Ambo-Teaoraereke, Bonriki-Taborio and Abairaranga.

Table 6.10. Ocean and lagoon shoreline changes using BB indicator on urban South Tarawa reef islands

ID	Name	Length (km)	No of transects	Average Rates (m/yr)	Accretion (%)	Erosion (%)	Stable (%)	Status
Ocean								
52	Bonriki-Taborio	3.6	857	-0.1	3	17	79	Stable
53	Abairaranga	0.2	7	-0.2	0	14	86	Stable
55	Abaokoro-SouthTarawa	0.2	6	0.4	50	0	50	Accretion
56	Ambo-Teaoraereke	5.2	298	0.1	22	9	69	Stable
57	Nanikai	1.2	62	0.5	10	16	74	Accretion
58	Bairiki	2.6	92	0.5	79	7	14	Accretion
59	Betio	4.3	182	0.3	49	10	41	Accretion
7	**Total**	**17.3**	**1504**					
Lagoon								
52	Bonriki-Taborio	10.7	670	0.2	29	11	60	Stable
53	Abairaranga	0.1	5	-0.1	0	20	80	Stable
55	Abaokoro-SouthTarawa	0.1	5	-0.2	0	20	80	Stable
56	Ambo-Teaoraereke	5.3	279	0.2	44	9	47	Stable
57	Nanikai	1	56	-0.1	11	39	50	Stable
58	Bairiki	1.7	87	0.1	39	18	43	Stable
59	Betio	3.6	180	0.5	64	2	34	Accretion
7	**Total**	**22.5**	**1282**					

The lagoon shorelines differ slightly as these shorelines are predominantly stable (Table 6.10). The reef islands with no significant change are Ambo-Teaoraereke, Bonriki-Taborio, Bairiki, Nanikai, Abairaranga and Abaokoro. Only Betio has shown accretion with an average rate of 0.5 m/yr. It should be noted that the substantial reclamation of Bonriki-Taborio was not included in the analysis as all transects had to be of similar lengths for DSAS so that the average rates of change for each individual reef island could be compared. Another reason was that it would have significantly raised the average rates.

The predominant accreting ocean and stable lagoon shorelines of South Tarawa will be represented using Bairiki reef island. A bar graph showing the shoreline changes using both BB and VL indicators will be used. This will also show whether or not

there is a relationship between the BB and VL shoreline change rates. The changes will be described using the geomorphology of the shoreline from the 1998 colour aerial photograph.

Bairiki

Bairiki has a broad western and elongated eastern end (Figure 6.21). Both ends of the reef island are connected by causeways: the eastern end is connected to Nanikai via the Bairiki Nanikai Causeway completed in 1963 (Hydraulics Research Station, 1979) (Figure 2.4), and western end is connected to Betio via a 3 km long causeway (Nippon Causeway) (Figure 2.4). Prior to its completion in 1987, Carter (1983) predicted that the Nippon Causeway would reduce ocean-lagoon and lagoon-ocean flow causing unstable shorelines. Bairiki's 1.8 km long ocean coastline comprises mainly sandy shores with sections of "seawalls" and conglomerate shorelines to the west. A total of 92 transects were constructed on the reef island shoreline commencing from the eastern tip to the conglomerate at its western corner (Figure 6.20). Bairiki's 1.7 km long lagoon coastline comprises vegetated sandy, open sandy, "seawalls" and beachrock shorelines. The major artificial shoreline lies on the far west, in the Bairiki port with beachrock shores on both sides. There are several small seawalls on the lagoon shoreline in the east with a boat channel cutting across the reef-flat to allow all tide access. Eighty-seven transects were constructed from the east continuing to the west and intersecting with the two time series shorelines.

BB and VL indicator for Bairiki Ocean beach

Table 6.10 shows the average shoreline changes on Bairiki ocean beach. These two shoreline indicators BB and VL are graphed to allow comparison (Figure 6.20). The results show that the pattern of change on the ocean side for both shoreline indicators, BB and VL, is accretion. The average rates of accretion are 0.4 m/yr (BB) and 0.5 m/yr (VL). The 92 transects spaced along the ocean shoreline show that for both BB and VL 79% are stable, 14% are accreting and only 7% display erosion (Table 6.9, Figure 6.20B). This indicates a strong correlation between two shoreline indicators (Figure 6.21B) (Appendix 6.3). Shorelines experiencing accretion are situated on the sandy and artificial shorelines. These extend across the

reef island but are mainly situated in the far eastern end (transect 1) to the east of a conglomerate outcrop that is located approximately 0.6 km from Bairiki's western tip (transect 66). A small area to the west of this conglomerate outcrop is an embayment enclosed by another conglomerate outcrop on its far western end. This embayment (transects 72 to 79) appears to have accreted naturally. Further west, near the western tip, from transects 80 to 87, erosion has occurred possibly related to human activity. There is a good possibility that this is linked to the removal of a conglomerate in the vicinity to enable the placement of a sewage pipe in 1981 (Howorth, 1982). The maximum accretion rates are observed on transect 94 with a rate of 1.6 m/yr (BB) and transect 71 with 1.7 m/yr (VL) (Figure 6.20). The highest erosion of -1.3 m/yr is observed on transect 94 for both BB and VL.

BB and VL indicator for Bairiki Lagoon beach

Table 6.10 shows the average shoreline changes that have occurred on Bairiki lagoon beach. Results show no significant change for BB whereas VL shows accretion. The average rates of accretion are 0.1 m/yr (BB) and 0.4 m/yr (VL). The results from the 87 transects placed from east to west showed that 43% of transects were stable, 39% displayed accretion and 18% displayed erosion for BB (Figure 6.20B). In contrast, VL transects showed 54% of transects accreting, 36% displaying stability and 10% of transects eroding (Appendix 6.3). This strong correlation between BB and VL is shown in Figure 6.21. The accreted portions of the shoreline are observed on sandy beaches and artificial shores (from transects 13 to 16 and from 34 to 64). The eastern end of Bairiki shows lower accretion rates. The maximum accretion of 1.3 m/yr and 1.4 m/yr is detected on transect 50 for BB and transect 47 on VL respectively (Figure 6.20). In contrast, eroded transects (67 to 81 and 84 to 86) are located just east and west of Bairiki port on beachrock and sandy shores. The maximum erosion of -1.8 m/yr (BB) was observed on transect 78 and -1.1 m/yr (VL) on transects 76 and 77 (Figure 6.20). This localised erosion demonstrates the influence of El Niño on Bairiki's shoreline changes, where the Bairiki jetty has acted like a groyne, blocking the eastward longshore sediment transport, thus confirming earlier findings by Howorth (1982) and Harper (1989). The sandy beaches located just east of the port are very susceptible under El Niño westerly winds (Harper, 1989). This erosion demonstrates the negative impact of coastal structures in areas

where longshore sediment transport is dominant and in areas that are sensitive to the changing wind conditions associated with ENSO.

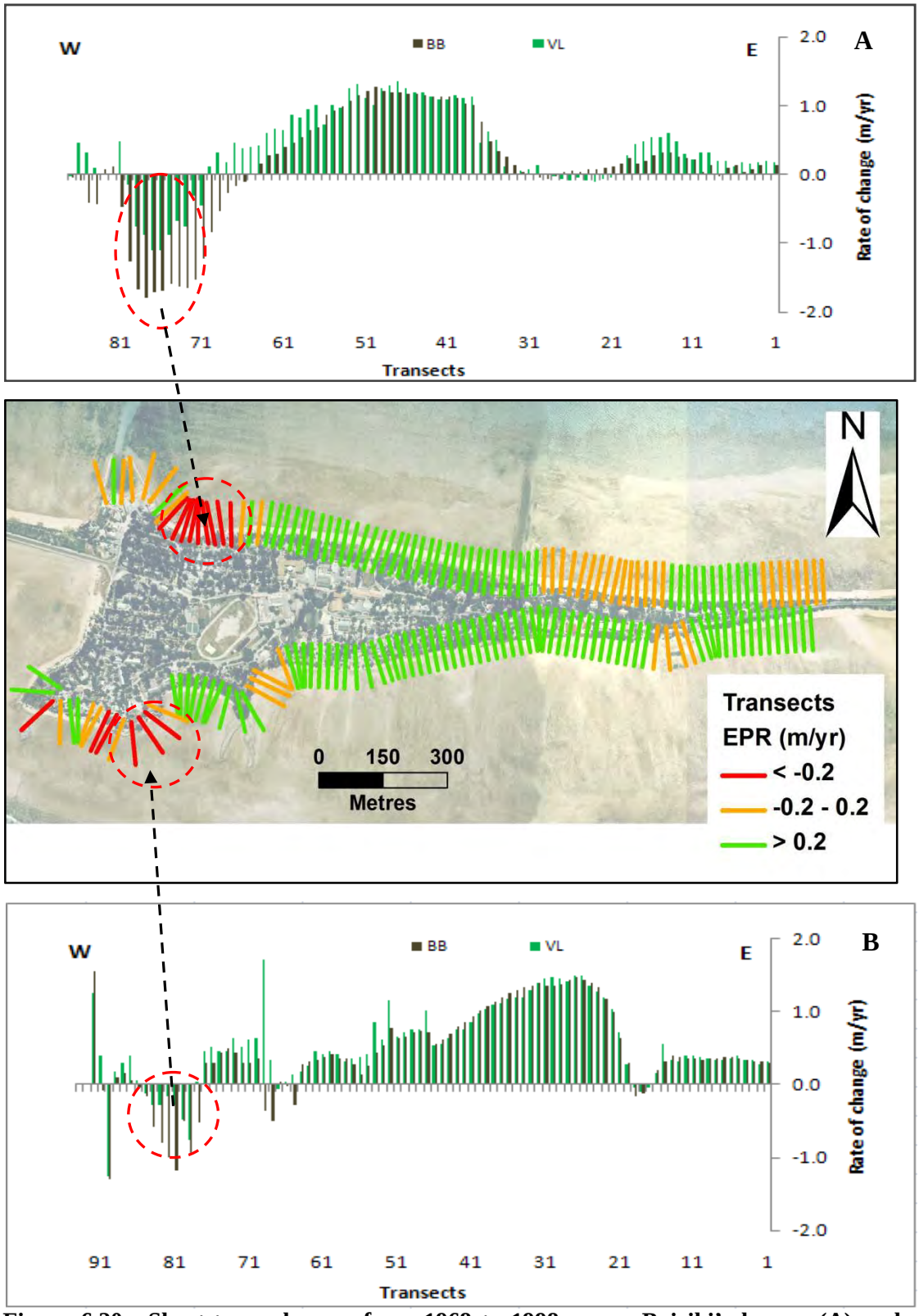

Figure 6.20. Short-term changes from 1968 to 1998 across Bairiki's lagoon (A) and ocean (B) shorelines. Red circles mark erosion occurring in areas that have been modified by humans. The middle panel shows the 30 years shoreline change on Bairiki using BB shoreline indicator.

Overall, building reclamations and seawalls have added more land to the reef island, especially on the ocean side as indicated by the high rates of accretion. The negative impact of this human activity is that protruding structures, such as the port in Bairiki, have blocked the longshore sediment transport to the east during El Niño periods, leading to acute erosion resulting in the loss of several houses (Solomon and Forbes, 1999; Webb, 2005; Biribo, 2008).

6.7 Rates and trend of shoreline change for 64 years (1943 – 2007)

Based on the 30 year shoreline change pattern, five reef islands were selected to determine long-term changes: Buariki, Taratai, Nea, Abairaranga and Bairiki. This involves a longer time scale of 64 years obtained from a time series of four shorelines: 1943, 1968, 1998 and 2007. The total coastline length investigated was 26.1 km involving 1233 transects. Table 6.11 summarises the results of the 64 years of shoreline change on the selected reef islands. The number of transects placed on the ocean and lagoon side of some reef islands differ from that used in the 30 years.

Table 6.11. Summary of 64 years of shoreline changes on selected reef island beaches.

ID	Reef island	Coastline	No	Overall	% of change			Status	Mean R^2
		Length (km)	of transects	Av. Rates (m/yr)	Accretion	Erosion	Stable		
Ocean Base of Beach									
1	Buariki	6	296	0.0	8	1	91	Stable	0.6
6	Taratai	4.1	201	0.1	7	2	91	Stable	0.4
41	Nea	0.5	11	0.0	0	0	100	Stable	0.5
53	Abairaranga	0.2	7	-0.2	0	0	100	Stable	0.7
58	Bairiki	1.8	81	0.4	93	0	7	Accretion	0.8
	Total	**14.7**	**596**						
Lagoon Base of Beach									
1	Buariki	7.4	344	0.2	36	4	60	Stable	0.6
6	Taratai	4.1	199	0.2	34	61	5	Stable	0.7
41	Nea	0.2	13	0.0	0	8	92	Stable	0.8
53	Abairaranga	0.1	5	-0.2	0	40	60	Stable	0.7
58	Bairiki	1.7	76	0.4	49	8	43	Accretion	0.7
	Total	**16.3**	**637**						

In the case of Bairiki, the number of transects placed on the ocean side has decreased from 92 to 81 as the shoreline in 1943 does not extend to the current shoreline in 2007 indicating that the eastern end of the reef island has accreted. The Linear Regression Rate (LRR) shows that the rates of shoreline change observed over 64 years are similar to the 30 year results for both North and South Tarawa. This supports the view that reef islands in North Tarawa have been stable over the 30 years (1968 to 1998) and that those in South Tarawa have been growing rapidly largely due to human influence. However, there are some anomalies such as those observed in Abaiaranga and Bairiki, South Tarawa. Abaiaranga's ocean beach shows that it has eroded over the 30 years but displays stability when analysed over the 64 years. In the case of Bairiki, its lagoon beach shows stability over the short-term but accretion over the long-term (Figure 6.21). For Abaiaranga, it is possible that this may be due to its small size, and the influence of ENSO reversing the longshore sediment transport during the period 1968 to 1998 leading to erosion. In the case of Bairiki, the long-term result shows accretion, indicating that natural coastal processes are influenced by human activities and ENSO.

This study has calculated R^2 to obtain a measure of how consistent the trends in erosion or accretion are. Overall the linear regression R^2 was predominantly greater than 0.6 for lagoon beaches with values up to 0.8 (Table 6.11). For instance, the lagoon beach of Nea is stable and has a high R^2 of 0.8, which suggests that stability governs the trend for the majority of the study period (Table 6.11). In the case of the ocean beaches, the lower mean R^2 value, below 0.6 for most ocean beaches, show that no one trend dominates. The only exception is Bairiki with a high mean R^2 value of 0.8 implying that accretion is dominant.

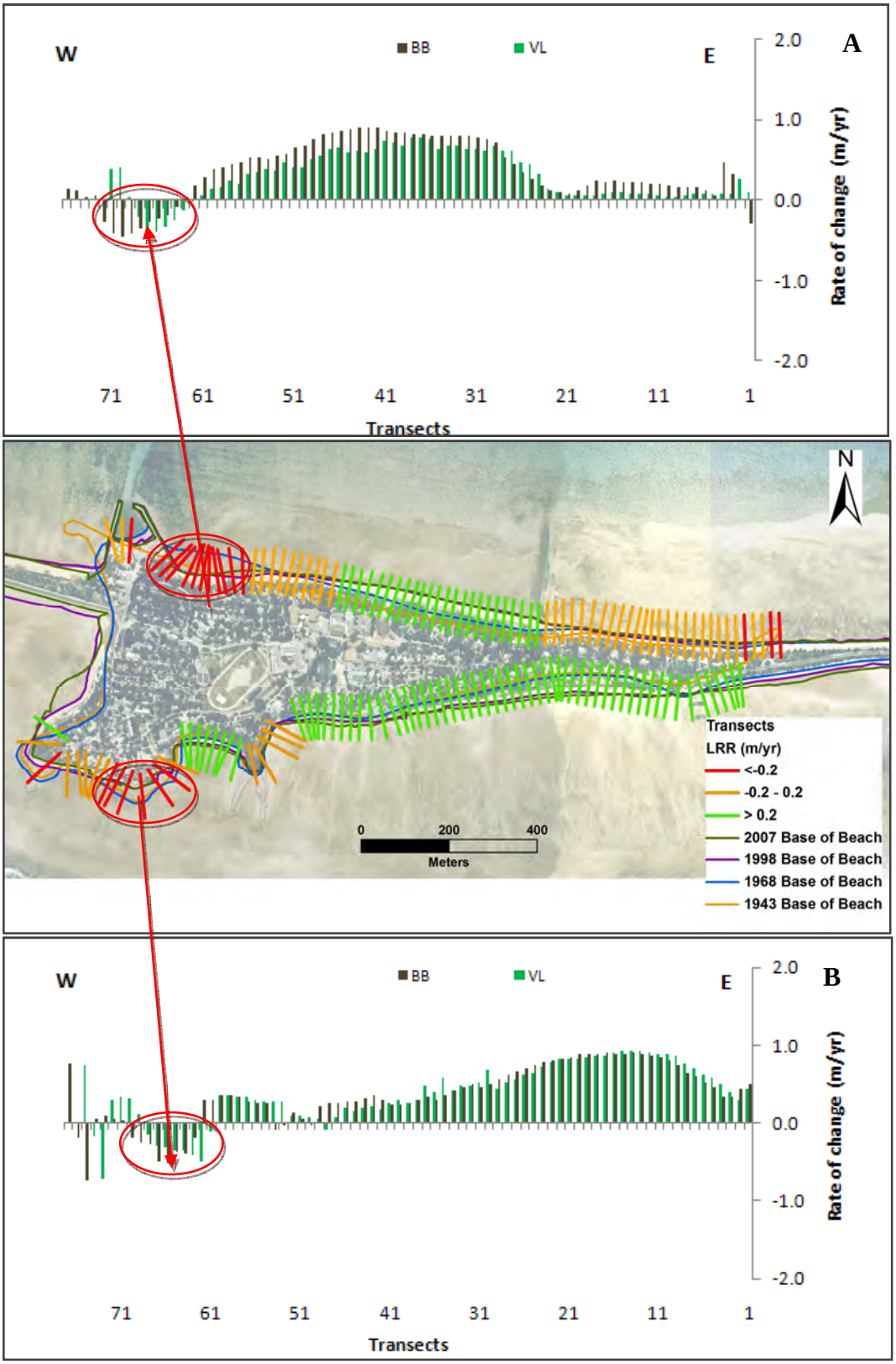

Figure 6.21. The long-term shoreline changes from 1943 – 2007 along Bairiki ocean (A) and lagoon (B) shores with BB shoreline indicator. Red transects mark eroding beaches, highlighted in green are accreting beaches. The middle panel shows the shoreline changes over 64 years for Bairiki using BB shoreline indicator.

The influence of ENSO is very important on the shoreline changes shown in the long-term results on the reef islands of South Tarawa. The time-series is limited in capturing the actual seasonal periods relating to ENSO, but the signal is evident indicating ENSO's important role on longshore sediment transport. The shoreline positions of Bairiki fluctuate with evidence of the 1998 shoreline receding in most places around the reef island. This recession in shoreline appears to be related to the reverse in longshore sediment transport from westward to eastward associated with the El Niño episodes that occurred during the early and late 1980's (Harper, 1989; Solomon and Forbes, 1999). On the lagoon side, time-series of shoreline positions show an eroded area just east of the Bairiki port. This may be due to the effect of the predominant longshore sediment transport to the east becoming blocked by the Bairiki port. This shows the negative influence of developments built out across the beach as they may interrupt or block longshore sediment transport resulting in down-drift areas experiencing erosion. This raises an important point, that this is not just a short-term issue but a long-term one, and will always occur during normal, El Niño or La Niña conditions.

The long-term shoreline change results of North Tarawa reef islands do not indicate longshore sediment transport as the predominant mode. To further investigate this, two areas spread across North Tarawa one on South Tarawa facing east were visited where a fish trap lies perpendicular to the shore. The three sites are Buariki (in the north), Tabiteuea (central), and the eastern end of Bonriki-Taborio reef island. Evidence shows that no sand is building up along the sides of these groyne-like structures (Figure 6.22). This suggests two things: one, that direct onshore transport is the predominant mode of sediment transport in North Tarawa, and two, El Niño is possibly not related to longshore sediment transport here.

Figure 6.22. Photos of fish traps located on the oceanside at different locations across North Tarawa. A: Buariki; B: Tabiteuea and; C: Bonriki-Taborio. No sediment is accumulating on either side of the feature to indicate evidence of longshore drift.

6.8 Discussion

The inference that reef islands are threatened by sea-level rise and land may disappear is due to evidence of erosion on reef islands. This may occur as prominent scarps on beaches, undercutting of vegetation and exposure of beach rocks that formed when the beach was stable. However, these trends are often cyclic, as in the case of Betio and Bairiki reef island, as shown by the bi-annual surveys carried out by SOPAC which indicate that these trends are associated with the fluctuations of the shorelines corresponding to the wind changes related to the inter-annual ENSO cycles (Solomon and Forbes, 1999).

Shoreline changes around reef islands of the Gilbert Group are subjected to short-term variations largely due to ENSO. A large body of evidence from SOPAC's coastal research work on South Tarawa and to some extent on some outer reef islands establishes these short-term variations, highlighting the important role that ENSO plays in longshore sediment transport (Harper, 1989; Byrne, 1991; Gillie, 1993; Gillie, 1994; Forbes and Hosoi, 1995; Solomon and Forbes, 1999). SOPAC's studies also indicate that the shorelines of South Tarawa reef islands are also largely influenced by anthropogenic factors (Harper, 1989; Byrne, 1991; Gillie, 1993; Forbes and Hosoi, 1995; Solomon and Forbes, 1999).

The shoreline changes around Tarawa Atoll show that it has substantially increased in area by 448.70 ha over the past three decades largely due to human activity on urban South Tarawa. This is clearly shown by the significant contribution of 409.58 ha from the six southern reef islands towards the 448.70 ha net increase of all reef islands on Tarawa Atoll and the major input of 363.50 ha from the reclamations in the southern section (Table 6.8). The reclamation in the eastern corner of Bonriki-Taborio reef island alone contributes a substantial 335 ha. The pressure for space in these highly populated urban reef islands appear to have largely contributed to the increase in size, even though these southern reef islands contribute a small proportion towards the sample population. Many studies support the findings that the increase in size of urban reef islands such as Betio is largely due to human factors (Howorth, 1982; Burne, 1983; Harper, 1989; Gillie, 1993). Even the land increase and

shoreline changes observed on urban Majuro, in the Marshall Islands are mainly related to human activity (Ford, 2012). Although the study by Webb and Kench (2010) did acknowledge that coastal processes around these urban reef islands were subjected to human activity, their conclusions gave the impression that the reef islands were growing as a result of natural processes. It is important to state that certain areas are affected by human activity when investigating changes. The reason is that impacts of such major or wide-spread activities may be significant to the changes observed there, especially so in urban areas. It may be possible to determine the contributions of anthropogenic influences when calculating the physical size of reclamations as has been done in this study. However, it may not be simple to determine their influence on the natural coastal processes, as in most cases they mask changes, making it difficult to discern what is natural or human influenced (Solomon and Forbes, 1999; Donner, 2012).

In North Tarawa, it was anticipated that the shoreline of reef islands would show little or no changes due to the low population density and pressures of development. The long-term results confirm that these reef islands have been stable over the past few decades indicating that they have been resilient. Relatively few areas experience accretion with rates >0.2 m/yr occurring in embayments, on sand spits and on beaches facing inter-island channels. These changes appear to be natural. A similar rate of accretion was measured for ocean shores of Maiana Atoll, Kiribati for the period 1969 to 2009 (Rankey, 2010). On the same atoll, Rankey (2010) observed obvious accretional changes in embayment and sand spits. However, not all accretional changes appeared to be natural, as accretion on lagoonal sandy beaches adjacent to causeways in North Tarawa is probably related to human activity similar to the accreting beaches close to the Nippon Causeway (Harper, 1989) and the Nanikai-Teaoraereke causeway in South Tarawa (Forbes and Biribo, 1996). Only some areas are affected by human activity, primarily those where causeways are built to create all tide accessibility between the reef islands.

The changes occurring on ocean and lagoon-facing beaches on North Tarawa differ from those results obtained in South Tarawa. This was anticipated, as North Tarawa is rural with little development whereas South Tarawa is urban and largely modified

due to development. In North Tarawa, with a lot of space on land for people to use, the need to build structures in areas close to the shore is low. Causeways are the only major developments that have taken place. In South Tarawa, with the pressures of high population densities, high average rates of accretion are observed on four beaches related to areas of development, suggesting that humans have contributed to these high rates of change. Other studies that have applied DSAS, such as one in Southern California, have also shown that high observed rates of shoreline accretion may be related to large scale engineering projects (Hapke *et al.*, 2009). Likewise, in other areas of Southern California, most of the erosional areas are linked with large coastal developments. For example, areas just south of a Newport Bay harbour where longshore sediment transport is blocked have long term erosion rates of -2.4 m/yr. Many reports on reef islands from the Marshall Islands, Tuvalu and Kiribati have shown that coastal developments such as seawalls, reclamations, causeways, groynes, sand mining and the removal of coastal vegetation have affected coastal areas by adding or removing land (Gillie, 1993; Gillie, 1994; Solomon and Forbes, 1999; Kench, 2005; Webb, 2006). In Oahu, Hawaii, seawalls on shorelines of adjoining beaches have led to beaches that tend to be narrower in width and appear to have eroded (Fletcher *et al.*, 1997).

The influence of El Niño is significant on the shorelines of South Tarawa where longshore sediment transport is predominant, however, in North Tarawa there is little or no evidence for longshore sediment transport. An understanding of these seasonal behaviours is very important in addressing changes on these vulnerable reef islands. Earlier studies also noted the effect of El Niño in reversing the direction of the normal westward sediment transport when investigating causes of erosion near the Bairiki jetty (Harper, 1989) and new central hospital located on the eastern end of Bonriki-Taborio reef island (Forbes and Hosoi, 1995). Prior understanding of this phenomenon's influence might have assisted with the planning of constructions, thus reducing the risk of erosion to assets within the vicinity as suggested by Forbes and Yoshitaka (1995). The same issue of erosion has been noted in Majuro, the Marshall Islands, where longshore sediment transport is evident (Ford, 2012). Urban areas are affected by coastal development and, through longshore sediment transport, this has had an influence on rural areas located further away. Another example is in the

major villages of Maiana and Aranuka atolls, Kiribati (Figure 2.2), where locals constructed groynes in an effort to prevent the shorelines from changing (Rankey, 2010). The groynes appear to have interrupted the predominant longshore sediment transport on these atolls, causing down-drift areas to erode. These examples imply that careful planning is required when constructing structures on shorelines in order to accommodate longshore sediment transport.

Development on South Tarawa is anticipated to continue and increase leading to more reclamations and seawalls. It is almost certain that these unplanned and increasing developments will cause widespread erosion as has been observed on many reef islands of the Pacific (Maragos, 1993; Kench and Cowell, 2002; Kench, 2005; Ford, 2012). These artificial structures will reduce the space for sediment deposition increasing the vulnerability of these shores should these structures fail. With less space for deposition, the beaches may not be replenished, with sediment deposited elsewhere, such as in channels or in the lagoon. It is expected that this issue will begin to occur in North Tarawa as more people move there rather than returning to the outer reef islands within the Gilbert Group. They will preferentially occupy those reef islands closest to South Tarawa after completing their service with Government, as they will still be within the reach of the urban area and its services that they have been used to. This move will increase the population density on these reef islands and may force people to build reclamations increasing the reef island size.

In summary, this study demonstrates that over the past decades during which there has been a gradual sea level rise, reef islands have increased in size largely due to anthropogenic factors. Natural coastal processes are largely influenced by human activities. This study has also shown that in areas of human activity, rates of accretion and erosion are increased, suggesting that they are influenced by human activities. Widespread erosion is the negative impact of anthropogenic activities such as disjointed reclamation structures on South Tarawa where longshore sediment transport is dominant and short-term variability is predominantly influenced by ENSO. This study shows that human activity and ENSO play a major role in the shoreline changes of Tarawa Atoll reef islands.

6.9 Limitations

Limitations of shoreline change analyses of reef islands revolve around the selection of an appropriate shoreline indicator. The dynamic nature of the shoreline, and the factors affecting it spatially and temporally, give rise to these errors and uncertainties. In general, the base of the beach on the lagoon side is the most difficult to detect. This is due to the gradual slope of the lagoon beach and the transition into the mud present on the lagoon reef flat. In other instances, the sunlight reflection back from the reef flat makes it hard to discern the foot of the beach. Such errors and uncertainties result from many factors such as quality of the aerial photograph or satellite imagery, image capture, geo-rectification, map resolution and seasonal changes related to ENSO conditions (Hennecke *et al.*, 2004). Great care and quality control was taken at each step when geo-rectifying these images, with particular care taken to address the distortion issues associated with the historical aerial photographs (Hanslow *et al.*, 1997). Other issues, such as the quality of the aerial photographs, could not be improved. For example, in the older photos from 1943, in areas where mangroves were present, the low resolution of the images made it difficult to distinguish the landward limit of the mangrove forest.

The lack of available aerial photography in the 30 year period between 1968 and 1998 made it difficult to identify shoreline responses related to ENSO events. However, when more than two time series of shorelines are used, it is possible to visually determine the short-term response of shorelines to events such as ENSO. This short-term behaviour is masked when LRR is applied. The linear regression calculation does not consider the change in trends, but focuses on achieving the slope of the line providing the overall rate of change (Thieler *et al.*, 2009). This may give misleading information; therefore it is important to understand the limitation of this statistical rate of shoreline change. When more than two shorelines are involved, the use of both LRR and explanation of the short-term behaviour within the shoreline data provides a better understanding of the rates and trends of shoreline change.

6.10 Summary

This chapter presents an atoll wide assessment of short-term area changes over a period of three decades and long-term changes over more than six decades. This study shows that the area of Tarawa Atoll has significantly increased by nearly 450 ha over the 30 year period studied, largely related to development on the urban reef islands of South Tarawa resulting from the pressures of increasing population density. A substantial increase of slightly more than 360 ha of the total 450 ha is directly associated with reclamations. The widespread coastal development on South Tarawa has masked the natural shoreline changes. Reef islands in North Tarawa, however, show stability or little change, which appears to be related to natural processes as these reef islands have low population densities and little development. Accretion and erosion changes are observed in localised areas such as embayments, beaches near closed channels, sand spits and beaches facing inter-island channels. The results of the shoreline changes on five selected reef islands from both North and South Tarawa over the longer time scale of 64 years were comparable to the 30 year results.

Shoreline changes along North and South Tarawa are affected by different factors. North Tarawa is largely influenced by natural factors, while in South Tarawa shoreline changes are almost certainly related to human activity influencing coastal processes and ENSO. Major developments, such as reclamations are related to the increases in land area. These appear to have contributed to the increased rates of accretion and wide-spread erosion due to the effect of disjointed reclamations around the reef islands blocking longshore sediment transport. Concerns are raised for the future of these reef islands, as evidence highlights that shorelines across South Tarawa are largely modified due to the concentration of development and population pressure. With increasing population pressure and development, more encroachment onto the active beach will occur resulting in greater interruption of longshore sediment transport and this may prevent sediment deposition on beaches thus increasing erosion issues and the susceptibility of reef islands to sea level rise. In addition, during El Niño, this may continue to negatively affect the coastal areas of South Tarawa causing coastal erosion, therefore, the sediment movements associated

with these seasonal variations such as ENSO need to be incorporated into management plans. North Tarawa's stable coastal area may also be affected by increasing population pressure when more people migrate to these rural areas.

The results in this chapter represent the best data on shoreline change for all reef islands of Tarawa Atoll. This serves as a platform for any future monitoring to be carried out on the atoll. Determination of shoreline change rates of these narrow low-lying reef islands will continue to be a challenge. Atoll scale monitoring is essential as well as the use of high-resolution imagery at regular intervals to capture the ENSO periods that influence shoreline change at intermediate temporal scales. In addition, it has been shown that the base of the beach shoreline indicator proves to be a robust measure of shoreline position on reef islands although it is not so good on lagoon shores.

The reef island dataset derived in this chapter will be used in the following chapter to discuss ways to increase the coastal resilience of reef islands.

7 CHAPTER SEVEN: DISCUSSIONS AND CONCLUSIONS

7.1 Introduction

The main objective of this thesis is to examine the morphological development of reef islands on Tarawa Atoll over different time scales. The three specific objectives of the study were to:

a) Examine the topography of reef islands and consider the implications of extreme sea levels; as well as calculate the first-order estimate of the sediment volume sequestered on the reef islands.
b) Establish the pattern of reef-island accretion and determine whether or not there is a supply of sediment that is still available to the reef islands.
c) Examine the historical changes that have occurred to reef island shorelines.

The aim of this chapter is to discuss the findings of Chapters 3 to 6 in order to understand the behaviour of reef islands over millennial and decadal time scales. This may provide greater insight into their future behaviour in response to anticipated sea-level rise. This chapter will be organised into seven sections:

a) Section 7.2 describes the evolution of reef islands over several millennia. In this section, the evolution of reef islands will be discussed by incorporating the findings of two chapters. One focused on the topography and total sediment volume of reef islands (Chapter 4). The second one investigated the morphological evolution of reef islands and the supply of skeletal sediment grains (Chapter 5).
b) Section 7.3 explores the present sediment supply to the reef islands by using inferences from the geological results and observations that live foraminifera are present on the ocean reef flats of North Tarawa although, they appear scarce on South Tarawa.
c) Section 7.4 discusses the implications for future coastal management. In this section the implications for future coastal management will be examined using the information gained in this thesis on the behaviour of reef islands over millennial (Chapter 5) and decadal time scales (Chapter 6). The inclusion of information on the behaviour of reef islands over the past decades, allows consideration of the impacts of humans on the present

sediment dynamics (Chapter 3 and 6), thus enabling a better understanding of the reef islands likely morphological response to anticipated sea-level rise.

d) Section 7.5 presents the conclusions. The focus of this section is to summarise the conclusions in order to address the main aim of this thesis. This will show the integration of science and natural resource management.
e) Section 7.6 discusses the limitations of the methods applied in this study.
f) Section 7.7 makes suggestions for future research.

7.2 Evolution of reef islands over several millennia

The total sediment that has been sequestered in the reef islands since the mid Holocene was investigated using Geographical Information Systems (Chapter 4). The total amount of sediment that has accumulated is estimated to be about 60,000,000 m^3. As the reef islands are likely to have commenced formation about 4,500 years BP based on radiocarbon dates of the oldest fossils (Chapter 5), the average long term rate of sand accumulation can be calculated by dividing the total volume of sediment by the time over which the reef islands have accumulated. The calculated rate of accumulation has been estimated to be approximately 13,000 m^3 per year for the whole atoll. This assumes that a constant supply of sediment for the reef islands has been available for transport onto reef islands over this time.

The topography of the reef islands as a result of the accumulation of sediment has been investigated using a digital terrain model (DTM) derived from photogrammetry. Chapter 4 shows that the morphology of 36 reef islands resembles that described by Woodroffe (2008). The morphology of most reef islands on Tarawa Atoll comprises an oceanward ridge that is generally 3 to 4 m above MSL and a lagoonward ridge that is only 1.5 to 2.0 m above MSL. Many reef islands have a low-lying central depression which has been excavated to form pits for the cultivation of taro. The distribution of elevation classes on the reef islands has been examined using a hypsometric approach. Predominantly the reef islands (n = 26) show an S-shaped form with a large proportion of the reef island low-lying. Ten reef islands, typically small in size, and uninhabited show little variability in elevation and are classified as platforms. Only two reef islands, the biggest in size, show a concave form, with a significant proportion being in the lowest elevation class. This implies that there

maybe a morphological adjustment between the processes responsible for the formation of these reef islands and their shape. In addition if modelled with extreme water levels, the concave forms are at greater risk from inundation and overwash compared to S-shaped and platform reef islands.

The evolution of reef islands was investigated by dating individual *Amphistegina* foraminifer fossils using radiocarbon dating by Accelerator Mass Spectrometry (AMS). In addition a program of paired AMS and amino-acid racemisation (AAR) dating was initiated to determine whether this technique could be used to supplement radiocarbon analysis. This has been used to examine fossils from other locations such as on the reef islands, lagoon beaches, ocean beaches, embayments and ends of the reef islands. The radiocarbon ages of foraminifera sampled from pits dug along a transect on each of the reef islands of Marenanuka, Tabiteuea and Notoue indicate that these three reef islands have undergone oceanward accretion (Chapter 5). The oldest radiocarbon ages found on Marenanuka and Tabiteuea indicate that the initial deposition of sediments at these two sites began approximately 4,500 yrs BP. These foraminiferal fossils are obtained from sites located closer to the lagoon side of the reef islands. The radiocarbon ages of these fossils are consistent with the radiocarbon ages of fossil materials from other reef islands around the Pacific and Indian Ocean (Woodroffe *et al.*, 1999; Woodroffe and Morrison, 2001; Dickinson, 2004; Kench *et al.*, 2005; Woodroffe, 2008; Kench *et al.*, 2012). This confirms that the reef islands of Tarawa Atoll commenced formation around 5,000 to 4,000 yrs BP.

The timing of deposition and the rates at which reef islands have formed appear to vary. The samples from Notoue differ from the other two reef islands as it had no fossils older than 1,500 yrs BP, however, it is highly likely that the area investigated on Notoue was not the central part of the reef island but an area that has developed later. The mode of reef-island development inferred from the radiocarbon ages of these three reef islands is consistent with the oceanward accretion pattern proposed by Woodroffe (2000) with the oldest ages located about three quarters of the width of the reef island, and the fossil ages becoming progressively younger towards the ocean side. The depositional pattern for Marenanuka suggests a slow oceanward and

lagoonward build out. Tabiteuea on the other hand has formed over a shorter period of approximately 1,000 years.

Most of the reef islands appear to have stopped growing. The AAR dates indicate a distinctive cluster of relatively old aged foraminifera obtained from the reef islands Tabiteuea and Notoue compared to the relatively younger foraminifera on their beaches. This implies that the reef islands currently occupy almost all of the accommodation space in which sediments can accumulate. However, localised accretion appears to be occurring in two places on reef islands: at the end of the reef islands and in embayments. For reef islands that are accreting at the ends, this can be seen by the presence of younger fossils with ages approximately modern (AD 1950). Embayments, occupying a small land area also have space for sediment deposition as indicated by the radiocarbon ages of fossils progressively getting younger towards the ocean side in an embayment on the northern section of Buariki.

The proportion of land above 3 m above MSL is less than 10% (Chapter 4). This is consistent with the range of elevations for other reef islands in the Pacific and Indian Ocean provided by Woodroffe (2008) indicating the similarity of reef islands in that they are generally low-lying. This evidence indicates that the majority of the reef islands on Tarawa Atoll are at risk to anticipated sea-level rise.

Chapter 4 investigated the risk of low-lying areas from inundation. The results showed that the risk largely depends on the topography of a reef island, in particular the elevation of the ocean and lagoon ridges. Low-lying areas on reef islands in North Tarawa are at less risk from wave impacts and inundation as they are protected from the waves by the generally high and broad ocean ridges. In South Tarawa, however, these low-lying areas on reef islands appear to be at greater risk to inundation as the ocean and lagoon ridges are generally low and narrow. This reaffirms the earlier findings on the significant role that these ridges play in protecting the low-lying areas from inundation (Solomon, 1997; Solomon and Forbes, 1999; He, 2001; Woodroffe, 2008). Reef islands in South Tarawa may face increasing risk with the rise in human activities reducing the elevation of the ridges. This will be further discussed in Section 7.3.

Another factor that influences the risk of inundation on reef islands is whether or not there is a direct connection to the ocean or lagoon (Chapter 4). This was highlighted in Funafuti, Tuvalu when a gap in a storm ridge allowed seawater to penetrate through and flood a well protected low-lying area located in the centre of the reef island (Yamano *et al.*, 2007). In South Tarawa, the reef islands of Betio, Bairiki and Bonriki-Taborio are forecast to be at increasing risk from inundation when modelled with extreme water levels. This led Solomon (1997) and He (2001) to propose that risks from inundation are primarily related to the elevation of ridges which needs to be maintained by sediment supply. This indicates the importance of sediment supply in maintaining the morphology of these ridges so that areas behind the ridge are at less risk from being flooded or inundated (Chapter 4). In South Tarawa, human activities have influenced or interrupted the sediment supply and this will be discussed in Section 7.3.

7.3 Present sediment dynamics

It is important to consider the present sediment supply to reef islands using the inferences from a) the geological results which imply that maximum accommodation space is nearly reached and; b) the observations that live foraminifera appear abundant in North Tarawa but scarce in South Tarawa, implying that sediment supply will differ for these two areas. As a result of these two inferences, the discussions will be divided into a) accommodation space; and b) sediment supply.

.

Accommodation space

The model developed by Barry *et al*. (2007) proposes that at a certain stage, reef islands will reach their maximum accommodation space whereby sediments cannot be sequestered on the reef islands. This is based on Barry's assumption that sediment sequestration depends on the morphological feedback between reef island morphology and fluid processes responsible for sediment distribution and transport. This section will examine evidence from this thesis that suggests that the reef islands of Tarawa Atoll have nearly reached their maximum accommodation space. This raises another question that will also be discussed, which is where the sediment will go to if the reef islands do reach maximum accommodation space.

Two lines of evidence show that most of the reef islands have nearly reached their maximum accommodation space (Chapter 5). This distinctive cluster of relatively old fossils suggests that the reef islands have stopped growing. The second line of evidence is that the stability of the shorelines in North Tarawa (Chapter 6) implies that most of the reef islands have nearly reached their maximum accommodation space, where little or no sediment can be further sequestered. This indicates that the main part of the reef island has reached the point at which it no longer can accrete sediment as there is no more accommodation space. However, this apparent stability could also be illusory, because the rate of accumulation may be scarcely detectable in view of the limitation of the method to detect shoreline changes, given the limits of uncertainty. The only places that are continuing to grow are the ends of the reef islands and embayments. Some areas were also experiencing erosion as shown by the shoreline changes, as a result of no more accommodation space. This level of detail at the ends of the reef islands and the embayments was not available for the model developed by Barry *et al*. (2008), therefore they did not consider that some areas are still undergoing accretion or erosion.

The results of this thesis support the view proposed by Barry *et al*. (2008), that a certain limit can be reached, where no more sediment can be sequestered on the reef islands. Based on two results of this thesis, it is proposed that the dynamic equilibrium of the reef islands in North Tarawa will be maintained unless the sediment supply and or the physical processes that control its transportation to the reef islands change. The first result shows that live foraminifera are found present on the reef flats indicating that the supply of modern foraminiferal sediment grains to the reef islands is highly likely. The second result shows that shorelines of reef islands in North Tarawa have been stable over the past 30 years.

This now raises the question that if maximum accommodation space is reached, where is sediment transported to, if it still being produced. Figure 7.1 shows sand shoals on the lagoon flats close to the inter-island channels which are still open in North Tarawa. The most extensive sediment shoal (apron) is located on the central part of North Tarawa where there are inter-island channels that are wider than most and through which sediment is still actively transported. The existence of this shoal suggests that sediment is transported from the ocean side through these inter-island

channels and deposited on the lagoon flats (Figure 7.1). On the other hand, this sand shoal also indicates that the sediment delivery to the lagoon flats has not been reduced by the narrow width of the reef flat in that area.

The extensive shoal located on the central part of North Tarawa as discussed above is likely to have developed due to a combination of factors. The first is that the reef flats in this area are low-lying compared to the other northern and southern areas, allowing wave-driven sediment transport to dominate. This leads to sediment from the ocean side being deposited as sand shoals on the lagoon flats. However, it was not possible to determine the reef flat elevation in this area as spot heights obtained from Schlencker Mapping Ltd for this area were few in number. The low number of spot heights showed that on average these areas are higher than other parts of Tarawa Atoll (Chapter 4). This may not be the case and more data is required to fully investigate these sand shoals and the surrounding reef flat. The second factor is that with reef islands that have nearly reached their maximum accommodation space, sediment that is not deposited on the ocean beaches may be moved here due to waves. This is similar to a situation in the Cocos (Keeling) Islands, where waves have entrained sediment through the channels developing sand shoals (Kench and McLean, 2004). The third factor is that as a result of the closure of the inter-island channels further north and south of this area, sediment can be transported here. The fourth factor is that it could also be due to the effect of the waves being diffracted once they come through the channels that the sediment is deposited as an extensive shoal (Kench, 1998; Kench and McLean, 2004; Kench and Brander, 2006). The last factor is based on evidence that there are a few signs if any of longshore sediment transport in North Tarawa (Chapter 6). In view of this, it is possible that areas that contribute to the sand shoal do not extend as far north as Buariki and as far south as Tabiteuea.

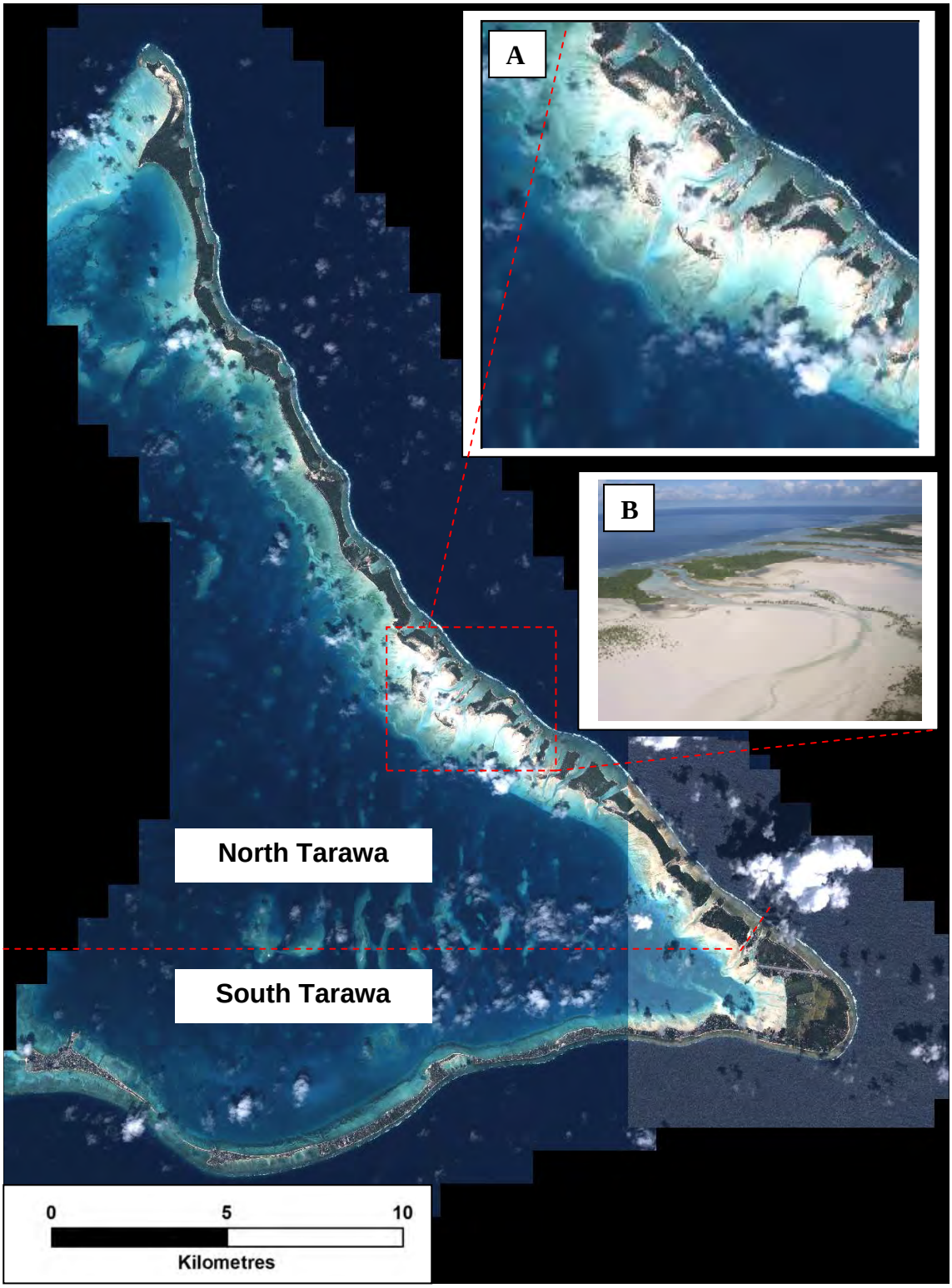

Figure 7.1. IKONOS satellite image showing an extensive sand apron on the lagoon flat near the islands in the central part of North Tarawa indicating net lagoonward movement of sediment via the inter-island channels. Insert A clearly shows the passages across the central part of North Tarawa where sediment is still being transported across to the lagoon side. The satellite image on the other hand shows that oceanward reef flats along Tarawa appear virtually clean of sediments. In South Tarawa, only the sheltered SE corner has extensive sediment flats. Insert B is an aerial photograph showing the reef islands in the central part of the North Tarawa showing the extensive shoals of sediment on the lagoon side. Source: Damalmian and Webb (2008).

The inference that sediment is deposited in locations other than the ocean-facing beaches is supported by results in Chapter 6 where it was shown that several areas on the lagoon side of reef islands have accreted over the past 30 years. Figure 7.2A shows that accretion has occurred on the southern parts of the reef islands close to the causeways on North Tarawa. The causeways were constructed in the early 1960's (Hydraulics Research Station, 1979) and, from that time, have prevented any movement of sediment from the ocean side to the lagoon side. The sediment present as shoals or extensive sand flats (Figure 7.1) around the inter-island channels appears to be building up on the sides of the causeways and the adjacent areas as there is no strong water flow from the channels to prevent it from depositing there. One example of this is Notoue, where both of the inter-island channels at the northern and southern ends of the reef island are blocked with solid causeways, preventing any hydraulic transportation of sediments from the ocean side to the lagoon side (Figure 7.2A). A similar situation is observed on South Tarawa with significant volumes of sediment present on the reef flat, which has accumulated over the past 20 years since the construction of the Nanikai-Teaoraereke Causeway (Forbes and Biribo, 1996). In Betio, the substantial accumulation of sediment beside the Nippon Causeway, constructed in 1987, is suggested to come from sediment present on the reef flat as mobile sand bars in between Betio and Bairiki (Forbes and Biribo, 1996). The wide channel between Betio and Bairiki has been significantly reduced by the massive Nippon Causeway resulting in sediment accumulating on the sides of the causeway. This has provided newly developed land, which through time has been stabilised by vegetation.

Chapter 6 demonstrates that on the lagoon side, the accreted areas are located along the length of the lagoon beach as well as the areas beside the causeways. However, it is difficult to determine the volume of accretion on lagoon beaches because the base of beach on the lagoon side is not as distinct as it is on the ocean-facing beaches. One example where this accretion is occurring is Notoue where there are no mangroves but just sand beaches accreting (Figure 7.2A). In Taratai this accretion is seen in areas where there are mangroves growing (Figure 7.2B). It is possible that this is related to the difficulty in mapping the 1968 base of the lagoon beach using low resolution aerial photography.

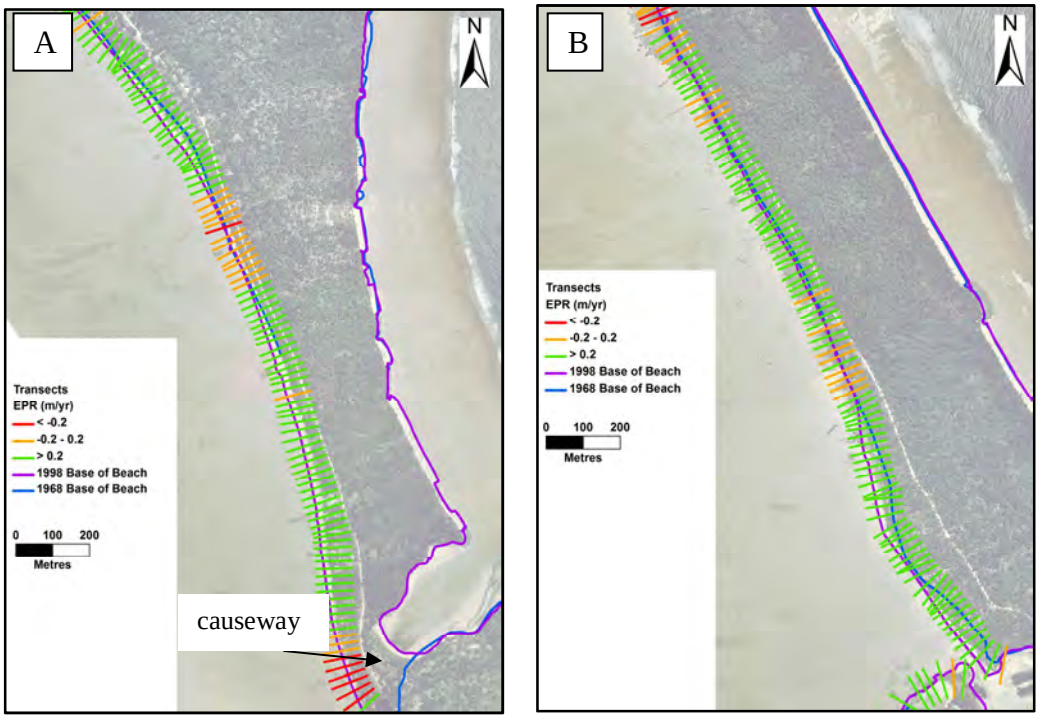

Figure 7.2. A. Notoue reef island showing the closed inter-island channel on the southern end, which blocks lagoonward transport. The lagoon shoreline change shows the southern and middle parts of the reef island are accreting. B. The middle part of the lagoon beach on Taratai which shows accretion, despite the causeways on both ends blocking lagoonward sediment transport from reaching these areas. These results are based on 30 year periods (1968 to 1998).

In South Tarawa, the shoreline changes on reef islands are largely due to anthropogenic influences as demonstrated by Chapter 6, which makes it very difficult to determine the natural changes and the accommodation space as they have been masked by human influences and ENSO.

Sediment supply

Live foraminifera are present in North Tarawa but they are scarce in South Tarawa (Chapter 5). Based on this information, it is therefore inferred that sediment supply is likely to continue in North Tarawa whereas in South Tarawa it is likely to be limited. Examining the factors responsible for these differences and the impact they have on reef-island stability will assist in forecasting future changes to these reef islands.

It was demonstrated in Chapter 6, that reef islands on North Tarawa are predominantly stable. Therefore it is inferred that the reef islands' state of dynamic

equilibrium has been maintained by sediment supply over the past 30 years despite sediment loss to the lagoon. As discussed in Chapter 3, removal of sediment from beaches appear to be relatively low as urbanisation is not focussed on North Tarawa, nor are there pressures of space, as population densities are low. A similar conclusion was found for Aranuka and Maiana atolls, Kiribati, which lie to the south of Tarawa Atoll as well as other atolls in Tuvalu which have stable shorelines in areas of low population (Rankey, 2010; Webb and Kench, 2010).

Chapter 6 demonstrates that shoreline changes in North Tarawa do occur, but only in some localised parts of reef islands, such as embayments (Figure 7.3A), sand spits (Figure 7.3B), beaches near closed channels, and beaches facing inter-island channels (Figure 7.3). These accretional changes imply that sediment supply still occurs. In the case of embayments, the radiocarbon ages of fossil foraminifera show a trend progressively becoming younger towards the ocean side, which indicates that this area is accreting (Chapter 5).

Chapter 5 shows that live foraminifera are present on ocean reef flats of North Tarawa but that they vary in abundance. They are even present in areas where population is high in Butaritari Atoll. Kiribati. Chapter 5 tests the views suggested by Ebrahim (1999) that environmental factors are affecting the health of these organisms as they were only observed on some ocean reef flats. The results of Chapter 6 show that the shorelines of reef islands in North Tarawa are predominantly stable. The low population density of these reef islands (Chapter 3) implies that sediment supply reaching the reef islands has not been largely affected and is likely to continue in the future unless environmental conditions change and human activity increases.

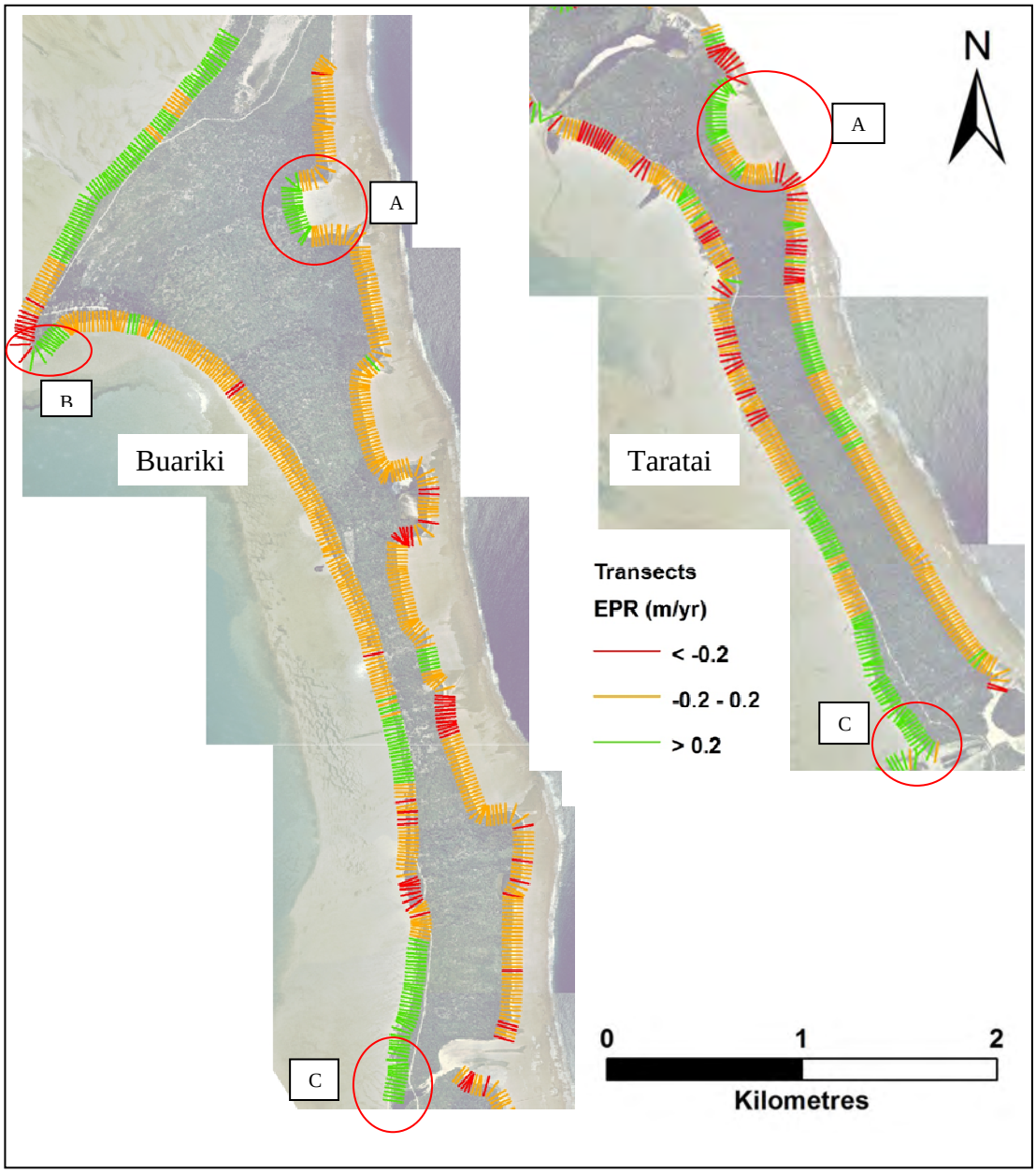

Figure 7.3. Examples of localised areas marked in red circles in Buariki and Taratai reef islands in North Tarawa that have accreted over the 30 year periods (1968 to 1998). A: Embayment; B: Sand spit; C: Beaches beside closed channels.

The inference that future long-term supply of sediment on South Tarawa will be reduced as indicated by the sightings of live but deformed foraminifera in Bonriki by Ebrahim (2000) was re-examined. Chapter 5 shows that live foraminifera are scarce along South Tarawa. This implies that human activities have affected the health of these organisms reaffirming Collen's (1995) and Ebrahim's (2000) views that sediment supply in South Tarawa will be low due to the low abundance of live foraminifera. The inference that sediment supply is low in South Tarawa is also supported by the relatively old ages of foraminifera on the beaches when compared

to North Tarawa beaches, however, the AAR method applied in this study is limited in the resolution to which numeric ages can be determined. The low sediment supply further implies that rapid growth of the reef islands over the past several decades does not seem to have occurred and this is in contrast to the rapid rates proposed by Webb and Kench (2010).

Reef islands in South Tarawa have grown substantially mainly due to human activities reaffirming the views of Howorth (1982), Burne (1983), Harper (1989), Gillie (1993) and Forbes and Yoshitaka (1995) (Chapter 6). High accretion rates are associated with reclamations which indicates that these changes are human-induced, supporting similar findings in Majuro, the Marshall Islands (Ford, 2012). This observation is in contrast to the high natural rates of accretion inferred by Webb and Kench (2010). In areas which have been largely modified, it is difficult to determine the natural changes as activities have masked them.

Chapter 6 establishes that shorelines have eroded in areas where humans have extended coastal structures onto beaches. Erosion rates of more than 2.0 m/yr appear to be occurring in areas down-drift of these extended coastal structures, such as Bairiki jetty which was also reported by Howorth (1985) and Harper (1985). This is especially predominant when longshore sediment transport is reversed during El Niño periods. Erosion adjacent to coastal structures indicates that structures block longshore sediment transport, preventing down-drift beaches being replenished with sediment. High rates of accretion and widespread erosion have been related to reclamations with varying sizes spread along South Tarawa, indicating that these activities also block longshore sediment transport and have more negative than positive impacts (Chapter 6). It is proposed that what has occurred in Majuro, Marshall Islands (Ford, 2012) will also occur in South Tarawa, i.e., areas where structures have not been built will be affected because the predominant mode of sediment transport is longshore sediment transport. With the anticipated increase in reclamation construction to meet the increasing population density, widespread erosion will become a more serious and chronic issue, as sediment transport will be greatly reduced with the varying reclamation designs encroaching onto the beaches.

It is of interest to compare the volume of sediment required to meet the annual aggregate demand with the volume that has naturally accreted. As discussed in Chapter 3, beach mining is a major activity on South Tarawa removing significant volumes of sediment to meet the growing construction needs. To compare the volumes of sediment involves several steps. The first step involves determining the total land area gained naturally over 30 years which is over 85 ha (Chapter 6). The second step is to calculate the rate of natural accretion over the 30 year period assuming that the rate is linear. To determine this involves, dividing the total land area of 85 ha by the number of years (30 years) to give a rate of 28, 000 m^2/yr. The third step entails determining the height or thickness of this area of sand (850,000 m^2) above the reef flat. To calculate this value of about 2 m can be achieved by dividing the total volume of sediment sequestered on the reef islands (60,000,000 m^3) (Chapter 4) with the total land area of the reef islands studied (29,000 m^2) (Chapter 3). The fourth step is to determine the volume of sand added per year. This volume of sand of about 56,000 m^3 added per year is calculated by multiplying the height of this area of sand (about 2 m) by the rate that it has been added naturally per year (28,000 m^2/yr). This amount of sand can be compared to the estimated annual aggregate demand of 82,500 m^3/yr (Geer Consulting Services, 2007) which shows that it takes more than a year for that volume of sediment to accumulate naturally. This reinforces that concept that beach mining is not a sustainable activity, requiring an urgent need to cease this activity and identify alternative sources to meet the growing demand for aggregates. If this is not addressed immediately, it will lead to widespread chronic erosion reducing the reef islands' resilience to anticipated sea-level rise.

Serious concerns are raised about the susceptibility of these reef islands, particularly on South Tarawa, as anthropogenic activities have threatened the health and production of foraminifera (pollution), blocked or interrupted the sediment transport pathways (causeways and reclamations) and removed enormous volumes of sediment (beach mining). In the immediate future, beaches of South Tarawa may not be able to cope as widespread erosion has already been observed (Forbes and Hosoi, 1995; Solomon and Forbes, 1999; Webb, 2005). With increasing development, human activities may exacerbate the current situation, placing these reef islands at great risk

to present high water levels and at even greater risk to anticipated sea-level rise, unless proper management plans are implemented.

7.4 Implications for coastal management

Based on the above discussion of sediment supply and the impacts of human activities on coastal areas, it is recommended that appropriate management plans aimed at increasing the resilience of reef islands are established immediately. These plans should incorporate three important factors: banning of beach mining, a long-term coastal awareness campaign, and stricter measures for construction of coastal structures. These factors are discussed below:

a) Beach mining should be banned immediately particularly in areas close proximity to settlements, as it is not a sustainable activity. Alternative options for aggregate supply should be explored that do not directly affect the beaches. These include purchasing aggregate from overseas, which has been done in the past (Geer Consulting Services, 2007), or supplying aggregate from the recently established state owned enterprise The Atinimarawa Company Ltd (ACL) (see Chapter 3) that plans to extract materials from the lagoon. The ACL needs to meet the local demands at a cheap price to stop locals from mining the beaches (Geer Consulting Services, 2007). One of the proposed options of this project is to encourage people who depend on the sales of aggregate to become retailers for the company (Leney, 2012)(Chapter 3). This is considered important as 38% of the households in Bonriki and Temaiku villages depend on aggregate sales as their main income. Doing this will ensure that these people do not lose their income, as well as stopping mining activities on the beaches (Peletikoti, 2007). The economic analysis shows that the amount of aggregates in the Vinstra shoal, located in the lagoon north of Betio is insufficient (see Chapter 3 for more details), meeting only half of the local demands. Therefore major developments are encouraged to source their materials from overseas, to enable the lagoon supply to be extended beyond the 50 year lifetime of the deposit (Geer Consulting Services, 2007). Other options may include using alternative construction materials such as prefabricated material, and constructing double storey buildings. The latter may also assist in reducing the construction of reclamations.

b) The approach to ban beach mining can only be successful if locals understand the important role that beaches and the associated ridges play in protecting reef islands from inundation. This requires a long-term awareness campaign that should commence soon and target all levels of the community, to ensure that people understand how critical it is to protect, and maintain the stability of the beaches.

c) Stricter measures for developing coastal structures must be established. Development of coastal structures should accommodate longshore sediment transport so that sediments can be deposited on the beaches. Structures such as solid causeways and groynes should be discouraged.

7.5 Conclusions

In response to the limited number of studies examining the morphological development of reef islands over different time scales, this study presents an atoll-wide assessment over millennial and decadal time scales of reef islands of Tarawa Atoll. The study has investigated the past behaviour of these reef islands by a) examining the topography of reef islands and considering the implications of extreme sea level, and calculating the total sediment volume sequestered on the reef islands; b) examining morphological evolution of reef islands and determining whether or not sediment supply is still available and; finally, c) examining historical shoreline changes.

Digital terrain analysis shows that a first-order sediment volume of about 60,000,000 m^3 has been sequestered on 36 reef islands of Tarawa Atoll over a period of 4,500 years. Investigation of the distribution of elevation across individual reef islands showed that reef islands are generally low-lying with more than 50% of the land area lying below 2.4 m above MSL and less than 10% above 3 m above MSL. Using the distribution of elevation, the reef islands can be classified into three hypsometric forms: S-shaped (n = 24), platform (n = 10) and concave (n = 2). Modelling using different tide and water levels generated using the coastal calculator showed that concave reef islands are at greater risk to rising sea level than S-shaped and platform reef islands as they have a greater proportion of low-lying areas.

General cross-island transects demonstrate two groups of reef islands; one group comprising of 25 reef islands with a prominent ocean ridge and a low-lying lagoon ridge separated by a central depression. An addition to this group is Betio, however, this reef island differs slightly from the other 25 showing less distinctive ocean and lagoon ridges. The second group of 10 reef islands do not have any central depressions and appear relatively flat. The low-lying central areas of reef islands are protected from extreme water levels by the ocean and lagoon ridges; however, in some situations these are not present. The factors influencing risks from extreme water levels depends on a) the direct connection of ocean and lagoon water levels to low-lying areas such as reclaimed lands on the southeastern corner of Bonriki-Taborio reef island and b) the width and low elevations of the ridges.

Examination of radiocarbon ages of individual foraminifera indicates that the reef islands are geologically young. The oldest radiocarbon ages of fossils were approximately 4,500 yrs BP. These samples were obtained from pits located about three quarters of the width of the reef islands of Tabiteuea and Marenanuka from the ocean side indicate the initiation of reef-island formation. The radiocarbon ages of fossils on both these reef islands become progressively younger towards the ocean side indicating similar oceanward accretion patterns. However, differences in fossil ages obtained from Tabiteuea and Marenanuka indicate different growth rates of the reef islands. Younger fossil ages obtained from the ends of reef islands, embayments and modern beaches show that these areas continued to receive young fossils up to modern age (AD 1950), indicating that the reef islands are still accreting.

Assessment of AAR ages of individual foraminifera demonstrates a broad range of relative ages. In decreasing order of relative age are a) pit samples; b) lagoon beach samples; c) ocean beach samples and d) live foraminifera. “Modern” beaches of Tarawa Atoll have mixed ages with South Tarawa beaches appearing very old. The presence of live foraminifera on ocean reef flats in North Tarawa indicates that sediment supply is likely to continue. In South Tarawa, the scarcity of live foraminifera on ocean reef flats and relatively old foraminifera appearing reworked on the ocean beaches show that sediment supply is limited.

The present sediment dynamics were investigated by comparing historical shoreline positions over the past 30 years, which demonstrated that shoreline responses of reef islands vary. One important finding is that the land area of Tarawa Atoll has increased significantly gaining more than 450 ha due to human influences in South Tarawa. Reclamations have been directly associated with this net increase contributing a substantial amount of more than 360 ha. High average rates of accretion and widespread erosion are related to disjointed reclamations spread along the shorelines of South Tarawa. Long-term shoreline changes over 60 years show that coastal structures extending across the length of beaches have blocked the eastward longshore sediment transport during El Niño periods. However, shoreline changes on rural North Tarawa show that the shorelines are predominantly stable, i.e., change is not detectable. Only some localised areas such as embayments, sand spits and beaches facing the inter-island channels have continued to accrete.

A major conclusion from this thesis is that by combining these different methods, the morphological development of reef islands can be studied at varying time scales enabling an understanding of their past behaviour.

7.6 Limitations of the methods

Although the strengths of the methods applied in this study have been discussed, there are also some weaknesses of the methods used. These include:

a) The DTM is limited in developing detailed cross-island transects requiring denser spot heights to be used. The TIN model developed from converting the contour to mass points is also restricted in determining the highest point on the reef island. An example is seen in the reef island Ambo-Taborio where the highest points on reef islands could not be captured but were averaged out as the spot height density was low. In both cases higher density data points are required, especially in areas of high elevations, so that they can be captured and modelled.

b) The AAR method, although calibrated against some paired AMS radiocarbon dating, was limited in providing numeric ages of fossils as it largely depends on the parabolic model that required more paired ages.
c) A limitation associated with detection of shoreline changes is that the accuracy of the method depends on which shoreline indicator is used on the aerial photographs or on the satellite imagery. With aerial photographs, it is difficult to discern the foot of the beach on the lagoon side due to the gradual transition between the base of the beach and the reef flat, where sediment is also present. In other instances, the glare from water over the reef flat prevents the detection of the shoreline.

7.7 Directions for future research

The morphological development approach applied in this study provides information by using a combination of methods. These methods examine the morphological evolution, distribution and variability of elevation across reef islands and the past shoreline changes that could be replicated in any reef island or atoll situation. The approach can also accommodate new information at greater spatial and temporal scale. The following are suggested ideas for future research.

Monitoring of shoreline changes on reef islands is very important as it provides an understanding of whether reef islands have grown or reduced in size, and the factors that influence such changes. In order to have data over a longer time period, it is essential to first locate any existing historical aerial photographs of the reef islands. New data can be acquired through high-resolution satellite imagery as they are becoming more readily available and relatively in-expensive. An alternative option would be to use recent technology such as LiDAR, which would increase the scale of mapping and the resolution of the data in terms of elevation. However, with high costs and large distances involved when working in the Pacific, it is proposed that several reef islands are mapped at the same time to reduce costs.

The additional benefit of LiDAR data is that it is able to provide detailed topographic information. This enables investigations of the elevations of reef islands to water

levels. For low-lying atoll nations where future sea-level rise is considered to be a crucial issue, elevation of a reef island is very important.

Another area of research would be to investigate the foraminiferal rates of production and the residence times of these organisms before they are deposited on the beaches. Another factor of importance is how well these foraminifera will cope with climate change effects such as increased temperature, salinity and acidity of seawater. Investigations on whether foraminifera could be re-established on affected areas; or whether cultured foraminifera could produce volumes of material to replenish areas where sediment supply is limited are also of interest especially as a lot of urban reef islands appear to have scarce live foraminifera present on their ocean reef flats. Such study would be of interest for the future sustainability of these reef islands.

REFERENCES

Abelson P. H. 1954. Organic constituents of fossils. *Carnegie Institution of Washington Yearbook* 53: 97-101.

Abuodha P. A. O. 2009. Application and evaluation of shoreline segmentation mapping approaches to assessing response to climate change on the Illawarra Coast, South East Australia. PhD. University of Wollongong. 10 April 2010, from http://ro.uow.edu.au/theses/852.286pp.

Abuodha P. A. O. and Woodroffe, C. D. 2010. Vulnerability assessment Coastal Zone Management. D. Green. London, United Kingdom, Thomas Telford Publishing

Alve E. and Bernhard, J. M. 1995. Vertical migratory response of benthic foraminifera to controlled oxygen concentrations in an experimental mesocosm. *Marine ecology. Progress series (Halstenbek)* 116, (1-3): 137-151.

Arnold J. R. and Libby, W. F. 1949. Age determinations by radiocarbon content, checks with samples of known age. *Science* 110: 678-680.

Arnold L. D. 1995. Conventional Radiocarbon Dating. Dating methods for Quaternary deposits. N. W. Rutter and N. R. Catto. Newfoundland, Geological Association of Canada: 117-123.

Asano D. 1942. Coral reefs in the South Seas Islands Tohuku Imperal University Geology and Paleo Institue, 1-9.

Australian Bureau of Meteorology and CSIRO 2011. Climate of the Pacific: Scientific Assessment and New Research, 9.

Bada J. L. 1985. Amino Acid Racemization Dating of Fossil Bones. *Annual Review of Earth and Planetary Sciences* 13, (1): 241-268.

Bada J. L. and Schroeder, R. A. 1972. Racemisation of isoleucine in calcareous marine sediments; kinetics and mechanism. *Earth Planet Science Letters*, (15): 1-11.

Bada J. L. and Schroeder, R. A. 1975. Amino acid racemization reactions and their geochemical implications. *Naturwissenschaften* 62, (2): 71-79.

Barry S. J., Cowell, P. J. and Woodroffe, C. D. 2007. A morphodynamic model of reef-island development on atolls. *Sedimentary Geology* 197, (1-2): 47-63.

Barry S. J., Cowell, P. J. and Woodroffe, C. D. 2008. Growth-limiting size of atoll-islets: Morphodynamics in nature. *Marine Geology* 247, (3-4): 159-177.

Bayliss-Smith T. P. 1988. The role of hurricanes in the development of reef islands, Ontong, Java Atoll, Solomon Islands. *The Geograhical Journal* 154, (3): 377-391.

Becker M., Meyssignac, B., Letetrel, C., Llovel, W., Cazenave, A. and Delcroix, T. 2012. Sea level variations at tropical Pacific islands since 1950. *Global and Planetary Change* 80-81, (0): 85-98.

Behrensmeyer A. K. and Kidwell, S. M. 1985. Taphonomy's contributions to paleobiology. *Paleobiology*. 11: 105-119.

Belasky P. 1996. Biogeography of Indo-Pacific larger foraminifera and scleractinian corals: A probalistic approach to estimating taxonomic diversity, faunal similarity and sampling bias. *Palaeogeography, Palaeoclimatology, Palaeoecology*, (122): 119-41.

Berkeley A., Perry, C. T. and Smithers, S. G. 2009. Taphonomic signatures and patterns of test degradation on tropical, intertidal benthic foraminifera. *Marine Micropaleontology* 73, (3-4): 148-163.

Bindoff N. L., Willebrand, J., Artale, V., Cazenave, A., Gregory, J., Gulev, S., Hanawa, K., Le Quéré, C., Levitus, S., Nojiri, Y., Shum, C. K., Talley, L. D. and Unnikrishnan, A. 2007. Observations: Oceanic Climate Change and Sea Level. In: Climate Change 2007: The Physical Science

Basis. Contribution of Working Group I to the Fourth Assessment Report of the Intergovernmental Panel on Climate Change Cambridge, United Kingdom and New York, NY, USA, 48.

Biribo N. 2008. Analyses of spatial and multi-temporal coastal changes of selected sites in Tarawa, Kiribati. Masters of Science in Marine Science. University of the South Pacific.239pp.

Biribo N. and Smith, R. 1994. Sand and gravel usage South Tarawa, Kiribati 1989-1993. *SOPAC Preliminary Report* Ministry of Environment and Natural Resources, Kiribati SOPAC Secretariat 75, Suva, 14.

Bloom A. L. 1970. Paludal Stratigraphy of Truk, Ponape, and Kusaie, Eastern Caroline Islands. *Geological Society of America Bulletin* 81, (7): 1895-1904.

Boak E., H. and Turner, I., L. 2005. Shoreline Definition and Detection: A Review. *Journal of Coastal Research* 21, (4): 688.

Bruun P. 1962. Sea-level rise as a cause of shore erosion. *Waterways and harbors division: Proceedings of the American Society of Civil Engineers* 26, (5): 2-15.

Bruun P. 1988. The Brunn Rule of erosion by sea-level rise: A discussion of large scale two and three dimensional usages. *Journal of Coastal Research* 4, (4): 627-648.

Bryan J. E. H. 1953. Checklist of atolls. *Atoll Research Bulletin* 19: 1-38.

Bureau of Meteorology 2007. Pacific Country Report. Sea Level and Climate: Their Present State, Kiribati, 35.

Bureau of Meteorology. 2010. "Monthly Southern Oscillation Index." Retrieved 12 June 2010, 2010, from ftp://ftp.bom.gov.au/anon/home/ncc/www/sco/soi/soiplaintext.html.

Bureau of Meteorology 2010. Pacific country report. Sea level and climate: Their present state, Kiribati Australia, 36.

Burgess S. M. 1987. Climate and weather of Western Kiribati New Zealand Meterological Service, Wellington, N.Z, 43.

Burne R. V. 1983. Origin and transportation of beach sand, Betio-Bairiki, Tarawa, Kiribati 24 July - 1 August, 1983 CCOP/SOPAC CCOP/SOPAC Technical Report CR0081, Suva, 79.

Burns W. C. G. 2000. The impact of climate chagne on Pacific island developing countries in the 21st century. Climate Change in the South Pacific: Impacts and Responses in Australia, New Zealand, and Small Island States. A. Gillespie and W. C. G. Burns. Dordrecht, Kluwer Academic: 233-251.

Burr G. S. and Scott, A. E. 2007. RADIOCARBON DATING | Causes of Temporal Variations. Encyclopedia of Quaternary Science. Oxford, Elsevier: 2931-2941.

Burrough P. A. and McDonnell, R. A. 1998. Spatial Analysis using continuous fields. Principles of geographical information systems, Oxford University Press: 183-194.

Byrne G. 1991. Sediment movement on Tarawa, Kiribati. Workshop on coastal processes in the South Pacific Island Nations, Lae, Papua New Guinea, 1-8 October 1987. D. Kear, R. Howorth and S. A. Suva, South Pacific Applied Geoscience Commission Technical Secretariat. Technical Bulletin 7: 155-159.

Byrne G., Gillie, R., Kaluwin, C. and Smith, A. 1994. Coastal Protection in the South Pacific South Pacific Applied Geoscience Commission, Suva, 43.

Callaghan D. P., Nielsen, P., Cartwright, N., Gourlay, M. R. and Baldock, T. E. 2006. Atoll lagoon flushing forced by waves. *Coastal Engineering* 53, (8): 691-704.

Cann J. H. and Murray-Wallace, C. V. 1986. Holocene distribution and amino acid racemisation of the benthic foraminifer Massilina milletti, northern Spencer Gulf, South Australia. *Alcheringa: An Australasian Journal of Palaeontology* 10, (1): 45 - 54.

Chow T. E. and Hodgson, M. E. 2008. Effects of lidar post-spacing and DEM resolution to mean slope estimation. *International Journal of Remote Sensing* 18, (2): 237-242.

Church J. A. 2006. A 20th century acceleration in global sea-level rise. *Geophysical research letters* 33, (1): L01602.

Church J. A., White, N. J., Coleman, R., Lambeck, K. and Mitrovica, J. X. 2004. Estimates of the Regional Distribution of Sea Level Rise over the 1950-2000 Period. *Journal of Climate* 17, (13): 2609.

Church J. A., White, N. J. and Hunter, J. R. 2006. Sea-level rise at tropical Pacific and Indian Ocean islands. *Global and Planetary Change* 53, (3): 155-168.

Clarke S. J. and Murray-Wallace, C. V. 2006. Mathematical expressions used in amino acid racemisation geochronology--A review. *Quaternary Geochronology* 1, (4): 261-278.

Cogley J. G. 2009. Geodetic and direct mass balance measurements: comparison and joint analysis. *Annals of Glaciology* 50: 96-100.

Collen J. D. 1995. Preliminary comment on visit to Funafuti, Majuro and Tarawa atolls, June - July, 1995 South Pacific Applied Geoscience Commission 81, Suva, Fiji, 14.

Collen J. D. 1996. Recolonisation of reef flats by larger foraminifera, Funafuti, Tuvalu. *Journal of Micropalaeontology* 15: 130.

Collen J. D. and Garton, D. W. 2004. Larger foraminifera and sedimentation around Fongafale Island, Funafuti Atoll, Tuvalu. *Coral Reefs* 23, (3): 445-454.

Collins M. J. and Riley, M. S. 2000. Amino acid racemisation in biominerals: the impact of protein degradation and loss. Perspectives in amino acid and protein geochemistry. A. J. Gooday, M. J. Collins, M. L. Fogel, S. A. Macko and J. Wehmiller. Oxford, Oxford University Press: 120-142.

Cook G. T., van der Plicht, J. and Scott, A. E. 2007. RADIOCARBON DATING | Conventional Method. Encyclopedia of Quaternary Science. Oxford, Elsevier: 2899-2911.

Cooper J. A. G. and Pilkey, O. H. 2004. Sea-level rise and shoreline retreat: time to abandon the Bruun Rule. *Global and Planetary Change* 43, (3-4): 157-171.

Crowell M., Leatherman, S. P. and Buckley, M. K. 1991. Historical shoreline change: Error analysis and mapping accuracy. *Journal of Coastal Research* 7, (3): 839-852.

Cushman J. A. 1959. Foraminifera and their classifcation and econonmic use, Cambridge, Massachusetts, Harvard University Press.

Damalmian H. 2008. Hydrodynamic Model of Tarawa Water Circulations and Applications Pacific Islands Applied Geoscience Commission EU/EDF ER0134, Suva, 39.

Damalmian H. and Webb, A. 2008. Inter-tidal channel flow in North Tarawa. *Reducing Vulnerability of Pacific ACP States* South Pacific Applied Geoscience Commission 136, Suva, 23.

Darwin C. 1842. The structure and distribution of coral reefs, London, Smith, Elder and Co. 214.

Davies D. J., Powell, E. N. and Stanton, R. J. J. 1989. Taphonomic signature as a function of environmental process: shells and shell beds in a hurricane-influenced inlet on the Texas coast. *Palaeogeography, Palaeoclimatology, Palaeoecology* 72: 317-356.

Davies D. J., Staff, G., M, Callender, W. R. and Powell, E. N. 1990. Description of a more quantitative approach to taphonomy and taphofacies analysis: all dead things are not created equal. 98, (6): 823-844.

Dawson E. Y. 1961. The reef rim of the reef. *Natural History* 70: 8-17.

Dickinson W. R. 2004. Impacts of eustasy and hydro-isostasy on the evolution and landforms of Pacific atolls. *Palaeogeography, Palaeoclimatology, Palaeoecology* 213, (3-4): 251-269.

Donahue D. J. 1995. Radiocarbon analysis by accelerator mass spectrometry. *International Journal of Mass Spectrometry and Ion Processes* 143: 235-245.

Donner S. D. 2012. Sea level rise and the ongoing battle of Tarawa. *EOS transactions American Geophysical Union* 93, (17): 169-176.

Donner S. D., Kirata, T. and Vieux, C. 2010. Recovery from the 2004 coral bleaching event in the Gilbert Islands, Kiribati. *Atoll Research Bulletin*, (587): 27.

Ebrahim M. 1999. Carbonate Sedimentation and Recent influence of Human Activity on Tarawa Atoll, Republic of Kiribati, South Pacific. Unpublished Phd. Victoria University.423pp.

Ebrahim M. 2000. Impact of anthropogenic environmental change on larger foraminifera. Environmental Micropaleontology: The application of microfossils to environmental geology. R. E. Martin. New York, Kluwer Academic/ Plenum Publishers. 15: 105-117.

Elrick C. and Kay, R. 2009. Mainstreaming of an Integrated Climate Change Adaptation Based Risk Diagnosis and Response Process into Government of Kiribati. P. I. Kiribati Adaptation Project. Perth, Coastal Zone Management Pty, Ltd. 67.

Emery K. O. and Tracey, J. I. L., H.S 1954. Geology of Bikini and nearby atolls, Marshall Islands. *United States Geological Survey Professional Paper* 260A: 1-265.

Falkland A. and Woodroffe, C. D. 1997. Geology and Hydrogeology of the Tarawa and Christmas Islands (Kiritimati), Kiribati, Central Pacific. Geology and hydrogeology of carbonate islands. H. L. Vacher and M. T. Quinn. Amsterdam, New York, Elsevier: 577-610.

Falkland A. C., Woodroffe, C. D., Vacher, H. L. and Terrence, M. Q. 2004. Chapter 19 Geology and hydrogeology of Tarawa and Christmas Island, Kiribati. Developments in Sedimentology, Elsevier. Volume 54: 577-610.

Falkner E. 1995. Aerial mapping: mapping and applications, London, Lewis publishers.

Fisher P. F. and Tate, N. J. 2006. Causes and consequences of error in digital elevation models. *Progress in physical geography* 30, (4): 467-489.

Fletcher C. H., Mullance, R. A. and Richmond, B. M. 1997. Beach loss along armoured shorelines on Oahu, Hawaiian Islands. *Journal of Coastal Research* 13, (1): 209-215.

Fletcher C. H., Rooney, J., Barbee, M., Lim, S. and Richmond, B. M. 2003. Mapping shoreline change using digital orthopothogrammetry on Maui, Hawaii. *Journal of Coastal Research* 38: 106-124.

Folk R. L. 1968. Petrology of Sedimentary Rocks, Texas, Hemphill.

Forbes D. L. and Biribo, N. 1996. Shore-zone sand and gravel resources of South Tarawa: a preliminary assessment of selected sites SOPAC SOPAC Technical Report TR235, Suva, 45.

Forbes D. L. and Hosoi, Y. 1995. Coastal erosion in South Tarawa, Kiribati South Pacific Applied Geoscience Commission Technical Report 225, Suva, 92.

Ford M. 2012. Shoreline changes on an urban atoll in the central Pacific Ocean: Majuro atoll, Marshall Islands. *Journal of Coastal Research* 28: 11.

Ford M., R 2010. Sedimentological Implications of durabitiy and physcial taphonomic processes on a fringing reef, Lizard Island, Australia. Doctor of Philosphy. University of Auckland.259pp.

Fujita K., Osawa, Y., Kayanne, H., Ide, Y. and Yamano, H. 2009. Distribution and sediment production of large benthic foraminifers on reef flats of the Majuro Atoll, Marshall Islands. *Coral Reefs* 28, (1): 29-45.

Geer Consulting Services 2007. Kiribati Technical Report: Economic analysis of aggregate mining on Tarawa. *Reducing Vulnerabilty of Pacific ACP States* South Pacific Applied Geoscience Commission 71, Suva, 112.

Gillie R. 1993. Historical changes of shoreline accretion and erosion Betio islet, South Tarawa, Kiribati South Pacific Applied Geoscience Commission 179, Suva, 21.

Gillie R. 1994. Coastal erosion problems in the Gilbert Islands Group, Republic of Kiribati: Phase II South Pacific Applied Geoscience Commission, Suva, 150.

Gillie R. 1997. Coastal processes and causes of coastal erosion on Pacific islands. Coastal and Environmental Geoscience Studies of the Southwest Pacific Islands. A. M. C. Sherwood. SOPAC Technical Bulletin: 11-23.

Goodfriend G. A. 1992. Rapid racemization of aspartic acid in mollusc shells and potential for dating over recent centuries. *Nature* 357, (6377): 399-401.

Goodfriend G. A. and Meyer, V. R. 1991. A comparative study of the kinetics of amino acid racemization/epimerization in fossil and modern mollusk shells. *Geochimica et Cosmochimica Acta* 55, (11): 3355-3367.

Goodfriend G. A. and Stanley, D. J. 1996. Reworking and discontinuities in Holocene sedimentation in the Nile Delta: documentation from amino acid racemization and stable isotopes in mollusk shells. *Marine Geology* 129, (3-4): 271-283.

Gordon N. D., McMahon, T. A., Finlayson, B. L., Gippel, C. J. and Nathan, R. J. 2004. Stream Hydrology: An introduction for ecologists. 2nd edn, West Sussex, John Wiley and Sons, Ltd. 429.

Gourlay M., J 1996. Wave set-up on coral reefs. 2.Set-up on reefs with various profiles. *Coastal Engineering* 28: 17-55.

Gourlay M., J 1997. Wave set-up on coral reefs: Some practical examples. Combined Australiasian Coastal Engineering and Ports Christchurch. 959-964.

Gourlay M., R 1988. Coral cays: Products of wave action and geological processes in a biogenic environment. Sixth International Coral Reef Symposium. Townsville. 491-496.

Grossman E. E., Richmond, B. M. and Fletcher III, C. H. 1998. The Holocene sea-level highstand in the equatorial Pacific: analysis of the insular paleosea-level database. *Coral Reefs* 17, (3): 309-327.

Guilcher A. 1988. Coral Reef Geomorphology, Chichester, Wiley.

Gupta B. K. S. 1999. Systematics of modern Foraminifera. Modern Foraminifera. B. K. S. Gupta. Cornwall, Kluwer Academic Publishers: 7-36.

Haberkorn G. 2007. Current Pacific population dynamics and recent trends, Noumea, South Pacific Commission.

Haberkorn G. 2008. Pacific Islands Population and Development: Facts, Fictions and follies. *New Zealand Population Review* 33, (34): 94-127.

Hallock P. 1981. Light dependance in Amphistegina. *Journal of Foraminiferal Research*, (11): 40-6.

Hallock P. 1981. Production of carbonate sediments by selected large benthic foraminifera on two Pacific coral reefs. *Journal of Sedimentary Petrology* 51, (2): 0467-0474.

Hallock P. 1999. Symbiont-bearing Foraminifera. Modern Foraminifera. B. Sen Gupta, Springer Netherlands: 123-139.

Hallock P. and Hansen, H. J. 1979. Depth adaptation in Amphistegina: change in lamellar thickness. *Bulletin of the Geological Society of Denmark* 27: 99.

Hansen H. J. 1999. Modern Foraminifera. Shell construction in modern calcareous foraminifera. B. K. S. Gupta. Netherlands, Kluwer Academic Publishers: 57-70.

Hanslow D. J. 2007. Beach erosion trend measurement: a comparison of trend indicators. . *Journal of Coastal Research* (Special Issue 50.).

Hanslow D. J., Clout, B., Evans, P. and Coates, B. 1997. Monitoring coastal change using photogrammetry. Proceedings of the Institute of Australian Geographers and New Zealand Geographical Society Second Joint Conference, Hobart, Australia. Department of Geography. The University of Waikato.

Hapke C. J. and Reid, D. 2007. National Assessment of Shoreline Change, Part 4: Historical Coastal Cliff Retreat along the California Coast U.S. Geological Survey Open-file Report 2007-1133., 57.

Hapke C. J., Reid, D. and Richmond, B. M. 2009. Rates and trends of coastal change in California and the regional behaviour of the beach and cliff system. *Journal of Coastal Research* 25, (3): 603-615.

Hapke C. J., Reid, D., Richmond, B. M., Ruggiero, P. and List, J. 2006. National assessment of shoreline change Part 3: Historical shoreline change and associated coastal land loss along sandy shorelines of the California coast U.S Geological Survey Open-File Report 2006-1219, 79.

Hare P. E. and Abelson, P. H. 1968. Racemization of amino acids in fossil shells. Year Book - Carnegie Institution of Washington. Washington, Carnegie Institution of Washington: 526-528.

Harper J. R. 1989. Evaluation of beach profile data from Betio and Bairiki, Republic of Kiribati, 1982-1988 CCOP/SOPAC Technical Report 94, Suva, 136.

Harris P., T, Heap, A., D, Marshall, J. F. and McCulloch, M. T. 2008. A new coral reef province in the Gulf of Carpentaria, Australia: Colonisation, growth and submergence during the early Holocene. *Marine Geology* 251: 85-97.

Harvey N. and Kench, P. S. 2003. Atoll island change and linkages to sea-level variations in Oceania. *Final activity report for APN Project 2002 - 16* University of Adelaide, Australia, 19.

Hay M. E. 1981. The Functional Morphology of Turf-Forming Seaweeds: Persistence in Stressful Marine Habitats. *Ecology* 62, (3): 739-750.

He C. 2001. Assessment of the vulnerability of Bairiki and Bikenibeu, South Tarawa Kiribati to accelerated sea-level rise South Pacific Applied Geoscience Commission Technical Report 322, Suva, 36.

Hearty P. J. and Aharon, P. 1988. Amino acid chronostratigraphy of late Quaternary coral reefs: Huon Peninsula, New Guinea, and the Great Barrier Reef, Australia. *Geology* 16, (7): 579-583.

Hearty P. J., O'Leary, M. J., Kaufman, D. S., Page, M. C. and Bright, J. 2004. Amino acid geochronology of individual foraminifer (*Pulleniatina obliquiloculata*) tests, north Queensland margin, Australia: A new approach to correlating and dating Quaternary tropical marine sediment cores. *Paleoceanography* 19, (PA4022).

Hengl T. and Evans, I. S. 2009. Mathematical and Digital Models of the land surface. Geomorphometry : concepts, software, applications. T. Hengl and H. Reuter, I. Amsterdam,Oxford Elsevier. 33: 31-63.

Hengl T. and Reuter, H., Eds. 2009. Geomorphometry: Concepts, Software, Applications. Amsterdam, Elesevier. 765.

Hennecke W. G., Greve, C. A., Cowell, P. J. and Thom, B. G. 2004. GIS-based coastal behaviour modelling and simulation of potential land and property loss: implications of sea-level rise at Collaroy/Narrabeen Beach, Sydney (Australia) *Coastal Management*, (32): 449-470.

Hinde G. J. 1904. Report on the materials from the borings at the Funafuti atoll: The atoll of Funafuti. *The Royal Society of London*: 186-361.

Hiroo O. 1993. Changes in the hypsometric curve through mountain building resulting from concurrent tectonics and denudation. *Geomorphology* 8, (4): 263-277.

Hohenegger J. 1994. Distribution of living larger foraminifera NW of Sesoko-Jima, Okinawa, Japan. *Marine Ecology*, (15): 291-334.

Hohenegger J. 2004. Depth coenoclines and environmental considerations of Western Pacific larger foraminifera. *Journal of Foraminiferal Research* 34, (1): 9-33.

Holmes D. W. 1979. Land reclamation and sea defences on Tarawa Atoll. H. R. Station. Wallington, England. 28.

Hopley D., Smithers, S. G. and Parnell, K. E. 2007. The geomorphology of the Great Barrier Reef, NewYork, Cambridge University Press.

Hottinger L. 1983. Processes determining the distribution of larger foraminifera in space and time. *Utrecht Micropaleontological Bulletin* 69, (30): 239-256.

Howorth R. 1982. Technical Report on Coastal Erosion in Kiribati; Visit to South Tarawa 22 January - 10 February, 1982 South Pacific Applied Geoscience Commission TR0022, Suva, 61.

Howorth R. 1983. Coastal erosion in Kiribati; South Tarawa CCOP/SOPAC Technical Report 31, Suva, Fiji.

Howorth R. 1985. Atlas of beach profiles monitored on Betio-Bairiki, Tarawa Atoll, Kiribati: January 1982 -July 1985 CCOPSOPAC Technical Report No 50, Suva, 46.

Howorth R., Cowan, H. and Carter, R. 1986. Coastal erosion potential South Tarawa, Kiribati. *South Pacific Marine Geological Notes* 3, (3): 29 - 32.

Howorth R. and Radke, B. 1991. Investigation of historical evidence for shoreline changes: Betio, Tarawa Atoll, Kiribati and Fongafale, Funafuti Atoll, Tuvalu. Workshop on Coastal Processes in the South Pacific Island Nations. Lae, Papua New Guinea. SOPAC Technical Bulletin 7: 91-98.

Hua Q., Smith, A. M., Jacobsen, G. E., Zoppi, U., Lawson, E. M., McGann, M. J. and Williams, A. A. 2001. Progress in radiocarbon target preparation at the ANTARES AMS Centre. *Radiocarbon* 43, (2a): 275-282.

Hydraulics Research Station 1979. Land reclamation and sea defences on Tarawa Atoll. H. R. Station. Wallington, England. 28.

IPCC 2007. Climate Change 2007: The Physical Science Basis. Contribution of Working Group I to the Fourth Assessment Report of the Intergovernmental Panel on Climate Change, Cambridge, United Kingdom and New York, NY, USA, 996.

Kaufman D. S. 2006. Temperature sensitivity of aspartic and glutamic acid racemization in the foraminifera *Pulleniatina*. *Quaternary Geochronology*, (1): 188-207.

Kaufman D. S. and Manley, W. F. 1998. A new procedure for determining DL amino acid ratios in fossils using reverse phase liquid chromatography. *Quaternary Science Reviews* 17, (11): 987-1000.

Kay R. 2008. Coordinated coastal hazard risk diagnosis and planning process. Workshop 2 Summary. Coastal Zone Management Pty Ltd.

Kelly D. J. 1994. The domestic waster on marine and groundwater quality in Tarawa Atoll, Republic of Kiribati Institute of Applied Science Environmental Report, University of the South Pacific Suva, 72.

Kench P. S. 1998. A currents of removal approach for interpreting carbonate sedimentary processes. *Marine Geology* 145, (3-4): 197-223.

Kench P. S. 2005. Coastal protection measures report: Government of Kiribati. Kiribati Adaptation Program: Preparation for Phase II project Kiribati Adaptation Program, Tarawa, 82.

Kench P. S. and Brander, R. W. 2006. Wave processes on coral reef flats: Implications for reef geomorphology using Australian Case studies. *Journal of Coastal Research* 22, (1): 209-223.

Kench P. S., Brander, R. W., Parnell, K. E. and McLean, R. F. 2006. Wave energy gradients across a Maldivian atoll: Implications for island geomorphology. *Geomorphology* 81, (1-2): 1-17.

Kench P. S. and Cowell, P. J. 2002. Erosion of low-lying reef islands. *Tiempo* 46: 6-12.

Kench P. S. and McLean, R. F. 2004. Hydrodynamics and sediment flux of hoa in an Indian Ocean atoll. *Earth Surface Processes and Landforms* 29, (8): 933-953.

Kench P. S., McLean, R. F., Brander, R. W., Nichol, S. L., Smithers, S. G., R., F. M., Parnell, K. E. and Aslan, M. 2006. Geological effects of tusnami on mid-ocean atoll islands: The Maldives before and after the Sumatran tsunami. *Geology* 34, (3): 177-180.

Kench P. S., McLean, R. F. and Nichol, S. L. 2005. New model of reef-island evolution: Maldives, Indian Ocean. *Geology* 33, (2): 145.

Kench P. S., Smithers, S. G. and McLean, R. F. 2012. Rapid reef island formation and stability over an emerging reef flat: Bewick Cay, northern Great Barrier Reef, Australia. *Geology* 40, (4): 347-350.

King K. and Neville, C. 1977. Isoleucine Epimerization for Dating Marine Sediments: Importance of Analyzing Monospecific Foraminiferal Samples. *Science* 195, (4284): 1333-1335.

Kinsey D. W. and Hopley, D. 1991. The significance of coral reefs as global carbon sinks in response to Greenhouse. *Palaeogeography, Palaeoclimatology, Palaeoecology* 89, (4): 363-377.

Kiribati Government and South Pacific Applied Geoscience Commission 2008. Environmentally Safe Aggregates for Tarawa (ESAT). M. o. F. a. M. R. Mineral Unit. Suva. 21.

Kolter 1992. Experimental Analysis of Abrasion and Dissolution Resistance of Modern Reef-Dwelling Foraminifera: Implications for the Preservation of Biogenic Carbonate. *Palaios* 7, (3): 244-276.

Kosnik M. A., Kaufman, D. S. and Hua, Q. 2008. Identifying outliers and assessing the accuracy of amino acid racemization measurements for geochronology: I. Age calibration curves. *Quaternary Geochronology* 3, (4): 308-327.

Kotler E., Martin, R. E. and Liddell, W. D. 1992. Experimental Analysis of Abrasion and Dissolution Resistance of Modern Reef-Dwelling Foraminifera: Implications for the Preservation of Biogenic Carbonate. *Palaios* 7, (3): 244-276.

Kowalewski M. 1996. Time-Averaging, Overcompleteness and the Geological Record. *The Journal of Geology* 104, (3): 317-326.

Kriausakul N. and Mitterer, R. M. 1978. Isoleucine eiperization in peptides and proteins: Kinetic factors and application to fossil proteins. *Science*, (201): 1011-1014.

Kvenvolden K., A and Peterson, E. 1976. Racemisation of amino acids in marine sediments determined by gas chromotography. *Geochimica et Cosmochimica Acta* 37: 2215-2225.

Ladd H. S., Ingerson, E., Townsend, R. C., Russell, M. and Stephenson, H. K. 1953. Drilling in Eniwetok atoll, Marshall islands. *Bulletin American Associates Petroleum Geology* 37: 2257-2280.

Ladd H. S., Jr, J. I. T., Wells, J. W. and Emery, K. O. 1950. Organic Growth and Sedimentation on an Atoll. *The Journal of Geology* 58, (4): 410-425.

Ladd H. S. and Tracey, J. I. 1948. Drilling on Bikini Atoll, Marshall Islands. *Science* 107, (2768): 51-55.

Lambeck K. 1993. Glacial rebound of the British Isles - II. A high resolution, high-precision model. *Geophysical Journal International* 115: 960-990.

Landerer F. W., Jungclaus, J. H. and Marotzke, J. 2007. Regional dynamic and steric sea level change in response to the IPCC-A1B scenario. *Journal of Physical Oceanography* 37: 296-312.

Langer M. R. and Hottinger, L. 2000. Biogeography of Selected "Larger" Foraminifera. *Micropaleontology* 46: 105-126.

Larsen A. R. and Drooger, C. W. 1977. Relative thickness of the tests in the *Amphistegina* species of the Gulf of Elat. *Utrecht Micropaleontological Bulletin* 30: 225-40.

Leney A. 2012. Analysis of the socio-economic impacts of the ESAT program, and mitigation measures being taken to minimise any adverse impacts on the community of South Tarawa, Bairiki, Tarawa, 15.

Leon J. 2010. Torres Strait reefs and carbonate production: A geospatial approach. Doctor of Philosophy. University of Wollongong.241pp.

Li Z. 1992. Variation of the accuracy of digital terrain model with sampling interval. *Photogrammetric Record*, (14): 113-128.

Li Z., Zhu, Q. and Gold, C. 2005. Digitial Terrain Modelling: Principles and Methodology, New York, CRC Press.

Libby W. F. 1955. Radiocarbon dating (2nd Ed), Chicago, Univeristy of Chicago Press.

Linick T. W., Damon, P. E., Donahue, D. J. and Jull, A. J. T. 1989. Accelerator Mass Spectrometry: The new revolution in radiocarbon dating. *Quaternary International* 1: 1-6.

Litter M., M 1973. The population and community structure of Hawaiian fringing-reef crustose Corallinaceae (Rhodophyta, Cryptonemiales). *Journal of Experimental Marine Biology and Ecology* II: 103-120.

Lobegeier M. K. 2002. Benthic foraminifera of the family Calcarinidae from Green Island reef, Great Barrier Reef Province. *Journal of Foraminiferal Research* 32, (3): 201-216.

Lomani E. and Tokalauvere, V. 2008. Federated States of Micronesia Report on Image Backdrop Production Training, Pohnpei South Pacific Applied Geoscience Commission EU-EDF SOPAC Report 120, Suva, 33.

Longley P. A., Goodchild, M. F., Maguire, D. J. and Rhind, D. Q. 2005. Geographic Information Systems and Science. 2nd edn, West Sussex, John Wiley and Sons, Ltd.

Loran A. T. 1994. The seawater and shellfish analyses in South Tarawa Atoll Research Program, Institute of Applied Science, University of the South Pacific Unpublished Report, Suva, 10.

Lovell E. 2000. Coral reef benthic surveys of Tarawa and Abaiang Atolls, Republic of Kiribati. *SOPAC Technical Report* South Pacific Applied Geoscience Commission, Suva, 88.

Lowe J. A. and Gregory, J. M. 2006. Understanding projections of sea level rise in a Hadley Centre coupled climate model. *Journal of Geophysical Research-Oceans* 111.

MacNeil F. S. 1954. The shape of atolls; an inheritance from subaerial erosion forms. *Am J Sci* 252, (7): 402-427.

MacNeil F. S. 1972. Physical and biological aspects of atolls in the northern Marshalls. First International Symposium of Corals and Coral Reefs, Mundapan Camp, India, Marine Biological Association of India.

Maragos J. E. 1993. Impact of coastal construction on coral reefs in the U.S. affiliated pacific Islands. *Coastal Management* 21, (4): 235-269.

Marshall J. F. and Davies, P. J. 1982. Internal Structure and Holocene Evolution of One Tree Reef, Southern Great Barrier Reef. *Coral Reefs*, (1): 21-28.

Marshall J. F. and Jacobson, G. 1985. Holocene growth of a mid-Pacific atoll: Tarawa, Kiribati. *Coral Reefs*, (4): 11-17.

Martin R. and Steinker, D. 1973. Evaluation of techniques for recognition of living foraminifera. *Compass* 50: 26-30.

Martin R. E., Harris, M. S. and Liddell, W. D. 1995. Taphonomy and time-averaging of foraminiferal assemblages in Holocene tidal flat sediments, Bahia la Choya, Sonora, Mexico (northern Gulf of California). *Marine Micropaleontology* 26, (1-4): 187-206.

Martin R. E. and Liddell, W. D. 1991. The taphonomy of foraminifera in modern carbonate environments: Implications for the formation of foraminiferal

assemblages. The processes of Fossilisation. S. K. Donovon. London, Belhaven Press: 170-193.
Masselink J. F. and Hughes, M. G. 2003. Introduction to Coastal Processes and Geomorphology, London, Hodder Headline Group.
Maximenko N., Niller, P., Rio, M. H., Melnichenko, O., Centurioni, L., Chambers, D., Ziotnicki, V. and Galperin, B. 2009. Mean dynamic topography of the ocean derived from satellite and drifting buoy data using three different techniques. *Journal of Atmospheric and Oceanic Technology* 26: 1910-1919.
Maxwell W. G. H., Day, R. W. and H., P. J. W. G. 1961. Carbonate Sedimentation on the Heron Island Reef, Great Barrier Reef. *Journal of sedimentary research* Vol. 31: 215.
McLean R. F. 2011. Atoll Islands (Motu). Encyclopedia of modern coral reefs: Structure, form and processes. D. Hopley. The Netherlands, Springer: 47-50.
McLean R. F. and Hoskings, P. L. 1991. Geomorphology of reef islands and atoll motu in Tuvalu. *South Pacific Journal of Natural Science* 11: 167-189.
McLean R. F. and Stoddart, D. R. 1978. Reef Island Sediments of the Northern Great Barrier Reef. *Philosophical Transactions of the Royal Society of London. Series A, Mathematical and Physical Sciences* 291, (1378): 101-117.
McLean R. F. and Woodroffe, C. D. 1994. Coral atolls. Coastal Evolution: Late Quaternary Shoreline Morphodynamics. R. W. G. Carter and C. D. Woodroffe. Cambridge, Cambridge University Press: 267-302.
Meehl G. A., Stocker, T. F., Collins, W. D., Friedlingstein, P., Gaye, A. T., Gregory, J. M., Kitoh, A., Knutti, R., Murphy, J. M., Noda, A., Raper, S. C. B., Watterson, I. G., J, W. A. and Zhao, Z.-C. 2007. Global Climate Projections. Climate Change 2007: The Physical Science Basis. Contribution of Working Group I to the Fourth Assessment Report of the Intergovernmental Panel on Climate Change S. Solomonet al. Cambridge University Press, Cambridge, United Kingdom and New York, NY, USA.: 98.
Miller G. H. and Brigham-Grette, J. 1989. Amino acid geochronology: Resolution and precision in carbonate fossils. *Quaternary International* 1: 111-128.
Miller G. H. and Hare, P. E. 1980. Amino acid geochronology: Integrity of the carbonate matrix and potential of molluscan fossils. Biochemistry of Amino Acids: Selected Papers. P. E. Hare, T. C. Hoeing and K. King. New York, Wiley: 415-451.
Mimura N., Nurse, L., McLean, R. F., Agard, J., Briguglio, L., Lefale, P., Payet, R. and Sem, G. 2007. Small islands. Climate Change 2007: Impacts, Adaptation and Vulnerability. Contribution of Working Group II to the Fourth Assessment Report of the Intergovernmental Panel on Climate Change. Fourth Assessment Report of the Intergovernmental Panel on Climate Change. M. L. Parry, O. F. Canziani, J. P. Palutikof, P. J. van der Linden and C. E. Hanson. Cambridge, UK, Cambridge University Press: 687-716.
Ministry of Finance 2007. 2005 Census of Population. M. o. Finance. Bairiki, Tarawa, Kiribati Government. 1: 159.
Ministry of Finance 2010. 2010 Census of Population. M. o. Finance. Bairiki.
Mitterer R. M. and Kriausakul, N. 1989. Calculation of amino acid racemization ages based on apparent parabolic kinetics. *Quaternary Science Reviews* 8, (4): 353-357.
Mook W. G. and Van der Plicht, J. 1999. Reporting 14C activities and concentrations. *Radiocarbon* 41, (227-239).

Moore L. J. 2000. Shoreline mapping techniques. *Journal of Coastal Research* 16: 111-124.

Morton R. A., Miller, H. L. and Moore, L. J. 2004. National assessment of shoreline change: Part 1 Historical shoreline changes and associated coastal land loss along the U.S.Gulf of Mexico U.S Geological Survey Open-File Report 2004-1043, 72.

Morton R. A. and Miller, T. L. 2005. National Assessment of Shoreline change - part 2 Historical shoreline changes and associated coastal land loss along the U.S. southeast Atlantic coast: U.S. Geological Survey Open-file Report 2005-1401.

Müller P. 1984. Isoleucine epimerization in Quaternary planktic foraminifera of sediment core GIK12519-2, Sierra Leone Rise.

Murray-Wallace C. V. 1995. Aminostratigraphy of Quaternary coastal sequences in southern Australia -- An overview. *Quaternary International* 26: 69-86.

Murray-Wallace C. V. 2000. Quaternary coastal aminostratigraphy: Australian data in a global context. Perspectives in amino acid and protein geochemistry. G. A. Goodfriend, M. J. Collins, M. L. Fogel, S. A. Macko and J. Wehmiller. Oxford, New York, Oxford University Press: 279-300.

Murray-Wallace C. V., Belperio, A. P., Gostin, V. A. and Cann, J. H. 1993. Amino acid racemization and radiocarbon dating of interstadial marine strata (oxygen isotope stage 3), Gulf St. Vincent, South Australia. *Marine Geology* 110, (1-2): 83-92.

Murray-Wallace C. V. and Bourman, R. P. 1990. Geological note: Direct radiocarbon calibration for amino acid racemization dating. *Australian Journal of Earth Sciences* 37, (3): 365 - 367.

Murray-Wallace C. V. and Colley, S. M. 1997. Amino acid racemisation and radiocarbon dating of contact period midden, Greenglade rockshelter, New South Wales. *Archaeology in Oceania* 32: 163-169.

Murray-Wallace C. V., Farland, M. A., Roy, P. S. and Sollar, A. 1996. Unravelling patterns of reworking in lowstand shelf deposits using amino acid racemisation and radiocarbon dating. *Quaternary Science Reviews* 15, (7): 685-697.

Murray-Wallace C. V., Ferland, M. A. and Roy, P. S. 2005. Further amino acid racemisation evidence for glacial age, multiple lowstand deposition on the New South Wales outer continental shelf, southeastern Australia. *Marine Geology* 214, (13): 235-250.

Murray-Wallace C. V. and Kimber, R. W. L. 1987. Evaluation of the amino acid racemization reaction in studies of Quaternary marine sediments in South Australia. *Australian Journal of Earth Sciences* 34, (3): 279 - 292.

Murray-Wallace C. V. and Kimber, R. W. L. 1989. Quaternary marine aminostratigraphy: Perth Basin, Western Australia. *Australian Journal of Earth Sciences: An International Geoscience Journal of the Geological Society of Australia* 36, (4): 553 - 568.

Murray J. 2006. Ecology and applications of benthic foraminifera, Cambridge, Cambridge University Press.

Murray J. W. 2000. Mortality, protoplasm decay rate and reliability of staining techniques to recognise 'living' foraminifera: a review. *Journal of Foraminiferal Research* 30, (1): 66-70.

Murray Wallace C. and Belperio, A. P. 1994. Identification of remanie fossils using amino acid racemisation. *Alcheringa: An Australasian Journal of Palaeontology* 18: 219-227.

Nelson A., Reuter, H., I, and Gessler, P. 2009. DEM production methods and sources. Geomorphometry concepts, software and applications. T. Hengl and H. Reuter, I. Amsterdam, Elsevier. 33: 65-85.

Neumann A. C. and Macintyre, I. 1985. Reef response to sea level rise: keep-up, catch-up or give-up. Proceedings of 5th International Coral Reef Congress.

Newell N. D. 1956. Geological reconnaissance of Rarioa (Kon tiki) Atoll, Tuamotu Archipelago. *Bulletin of the American Museum of Natural History* 109, (3): 311-327.

Nicholls R. J., Wong, P. P., Burkett, V. R., Codignotto, J. O., Hay, J. E., McLean, R. F., Ragoonaden, S. and Woodroffe, C. D. 2007. Coastal systems and low-lying areas. Climate Change 2007: Impacts, Adaptation and Vulnerability. Contribution of Working Group II to the Fourth Assessment Report of the Intergovernmental Panel on Climate Change. M. L. Parry, O. F. Canziani, J. P. Palutikof, P. J. van der Linden and C. E. Hanson. Cambridge, U.K, Cambridge University Press: 315-356.

Norton D. R. and Friedman, I. 1981. Ground-temperature measurements. *Other Information: Portions of document are illegible* USGS-PP-1203; Other: ON: DE83900376 United States10.2172/6741170Other: ON: DE83900376Mon May 14 08:40:51 EDT 2007GPO.DOEEEGTP; ERA-08-004798; EDB-83-003771English, 41.

Office of Te Beretitenti 2010. South Tarawa Coastal Condition Assessment Government of Kiribati, Tarawa, Kiribati, 56.

Office of the Beretitenti 2011. Coastal monitoring benchmark network, KAP - II FSP Improving the protection of public assets, 70.

Ohde S., Greaves, M., Matsuzawa, T., Buckley, H. A., van Woesik, R., Wilson, P. A., Pirazzoli, P., A. and Elderfield, H. 2002. The chronology of Funafuti Atoll: revisiting an old friend. *Proceedings of the Royal Society of London*, (A 458): 2289-2306.

Paulay G. 2000. Benthic ecology and biota of Tarawa Atoll lagoon: Influence of equatorial upwelling, circulation, and human harvest. *Atoll Research Bulletin* 487: 41.

Paulay G. and Kerr, A. 2001. Patterns of coral reef development on Tarawa Atoll (Kiribati). *Bulletin of Marine Science* 69, (3): 1191-1207.

Peletikoti N. 2007. Kiribati Technical Report: 1) Extent of Household Aggregate Mining in South Tarawa; and 2) Proposed Integrated Monitoring Framework for Tarawa Lagoon South Pacific Applied Geoscience Commission EU EDF8 SOPAC Project Report 72, Suva, 70.

Penkman K. E. H., Kaufman, D. S. and Collins, M. J. 2008. Closed-system behaviour of the intra-crystalline fraction of amino acids in mollusc shells. *Quaternary Geochronology* 3: 2-25.

Petchey F., Anderson, A., Zondervan, A., Ulm, S. and Hogg, A. 2008. New marine Delta R values for the South Pacific subtropical gyre region. *Radiocarbon* 50, (3): 373-397.

Powell E. N. and Davies, D. J. 1990. When Is an "Old" Shell Really Old? *The Journal of Geology* 98, (6): 823-844.

Purdy E. G. and Gischler, E. 2005. The transient nature of the empty bucket model of reef sedimentation. *Sedimentary Geology* 175, (1-4): 35-47.

Purdy E. G. and Winterer, E. L. 2001. Origin of atoll lagoons. *Geological Society of America Bulletin* 113, (7): 837-854.
Purdy E. G. and Winterer, E. L. 2006. Contradicting Barrier Reef relationships for Darwin's Evolution of reef types. *International Journal of Earth Sciences*, (95): 143-167.
Ramsay D., Stephens, S., Gorman, R., Oldman, J., Bell, R. and Damalmian, H. 2010. Sea levels, waves, run-up and overtopping N. I. o. W. a. A. R. Ltd. Hamilton. Kiribati Adaptation Programme. Phase II: Information for Climate Risk Management: 148.
Rankey E. C. 2011. Nature and stability of atoll island shorelines: Gilbert Island chain, Kiribati, equatorial Pacific. *Sedimentology* 58, (7): 1831-1859.
Rankey G. 2010. Stability of Atoll island shorelines: Republic of Kiribati University of Kansas, 46.
Rathburn A. E., Levin, L. A., Held, Z. and Lohmann, K. C. 2000. Benthic foraminifera associated with cold methane seeps on the northern California margin: Ecology and stable isotopic composition. *Marine Micropaleontology* 38, (3-4): 247-266.
Reuter H., I, Hengl, T., Gessler, P. and Sollie, P. 2009. Preparation of DEMs for geomorphometric analysis. Developments in Soil science, Elsevier.
Richmond B. M. 1990. Nearshore sediment distribution, South Tarawa, Kiribati CCOP/SOPAC Technical Report 91, Suva, 36.
Richmond B. M. 1992. Development of Atoll Islets in the Central Pacific. Seventh International Coral Reef Symposium, Guam.
Richmond B. M. 1993. Reconnaissance geology of the Gilbert Group, Western Kiribati South Pacific Applied Geoscience Commission, Suva, 64.
Rottger R. and Kruger, R. 1990. Observations on the biology of Calcarinidae (Foraminiferida). *Marine Biology* 106: 419-425.
Roy P. and Connell, J. 1991. Climatic change and the future of atoll states. *Journal of Coastal Research* 7, (4): 1057-1075
Roy P. S. 1991. Shell hash dating and mixing models for palimpsest marine sediments. *Radiocarbon* 33, (3).
Rutter N. W. and Blackwell, B. 1995. Amino acid racemisation dating. Dating methods for Quaternary deposits. N. W. Rutter and N. R. Catto. Canada, Geological Association of Canada: 125-166.
Samosorn B. 2006. Morphological changes of a small reef island on a platform reef. Doctor of Philosophy. University of Wollongong.280pp.
Schlencker Mapping. 2012. "Photogrammetry." Retrieved 20 April, 2012, 2012, from http://www.schmap.com.au/photogram.htm.
Schlencker Mapping Pty Ltd 1998. Report on GPS ground control survey, Tarawa Republic of Kiribati, Brisbane, 5.
Schlencker Mapping Pty Ltd 1998. Report on GPS ground control survey, Tarawa, Republic of Kiribati, Brisbane, 5.
Schofield J. C. 1977. Late Holocene sea level, Gilbert and Ellice Islands, West Central Pacific Ocean. *N.Z. Journal of Geology and Geophysics* 20, (3): 503-529.
Schroeder R. A. and Bada, J. L. 1976. A review of the geochemical applications of the amino acid racemization reaction. *Earth-Science Reviews* 12, (4): 347-391.
Sharma A. and Kruger, J. 2008. High resolution bathymetric survey in Kiribati. *EU EDF SOPAC Project Report* SOPAC 144, Suva, 66.

Shepard F. P. 1970. Lagoonal Topography of Caroline and Marshall Islands. *Geological Society of America Bulletin* 81, (7): 1905-1914.

Sheppard C., Dixon, D. J., Gourlay, M., Sheppard, A. and Payet, R. 2005. Coral mortality increases wave energy reaching shores protected by reef flats: Examples from the Seychelles. *Estuarine, Coastal and Shelf Science* 64, (2-3): 223-234.

Sloss C. R. 2005. Holocene sea-level change and the aminostratigraphy of wave-dominated barrier estuaries on the southeast cost of Australia. Doctor of Philosophy. University of Wollongong. from http://ro.uow.edu.au/theses/447.485pp.

Sloss C. R., Jones, B. G., McClennen, C. E., de Carli, J. and Price, D. M. 2006. The geomorphological evolution of a wave-dominated barrier estuary: Burrill Lake, New South Wales, Australia. *Sedimentary Geology* 187, (3-4): 229-249.

Sloss C. R., Murray-Wallace, C. V., Jones, B. G. and Wallin, T. 2004. Aspartic acid racemisation dating of mid-Holocene to recent estuarine sedimentation in New South Wales, Australia: a pilot study. *Marine Geology* 212, (1-4): 45-59.

Smith M. J. and Clark, C. D. 2005. Methods for the visualization of digital elevation models for landform mapping. *Earth Surface Processes and Landforms* 30, (7): 885-900.

Smith R. 1999. Study for numerical circulation model of Abaiang lagoon, Kiribati South Pacific Applied Geoscience Commission, Suva, 25.

Smith R. and Biribo, N. 1995. Marine Aggregate Resources Tarawa Lagoon, Kiribati including current meter studies at three localities South Pacific Applied Geoscience Commission, Suva, 41.

Solomon S. 1997. Assessment of the vulnerability of Betio (South Tarawa, Kiribati) to Accelerated sea level rise South Pacific Applied Geoscience Commission Technical Report 251, Suva, 66.

Solomon S. M. and Forbes, D. L. 1999. Coastal hazards and associated management issues on South Pacific Islands. *Ocean & Coastal Management* 42, (6-7): 523-554.

SOPAC 1993. Coastal protection in the South Pacific South Pacific Applied Geoscience Commission SOPAC Technical Report 190.

Statistics 2010. 2010 Census of Population. M. o. Finance. Bairiki.

Steers J. A. 1937. The Coral Islands and Associated Features of the Great Barrier Reefs. *The Geographical Journal* 89, (1): 1-28.

Stephens S. and Ramsey, D. 2008. Tarawa Survey Datums: Relationship between University of Hawaii Tide Gauge 0, Mean Sea Level and SEAFRAME Tide Gauge 0. Draft for discussion.

Stoddart D. R. 1969. Ecology and morphology of recent coral reefs. *Biological Review* 44: 433-498.

Stoddart D. R., McLean, R. F. and Hopley, D. 1978. Geomorphology of Reef Islands, Northern Great Barrier Reef. *Philosophical Transactions of the Royal Society of London. B, Biological Sciences* 284: 39-61.

Stoddart D. R. and Steers, J. A. 1977. The nature and origin of coral reef islands. Biology and Geology of Coral Reefs IV. O. A. Jones and R. Endean. London, Academic Press. Geology II: 59-105.

Strahler A. N. 1952. Hypsometric (Area-Altitude) analysis of erosional topography. *Geological Society of America Bulletin* 63, (11): 1117-1142.

Stuiver M. 1993. Extended 14C database and revised CALIB radiocarbon calibration program. *Radiocarbon* 35, (1): 215.
Stuiver M., Pearson, G. and Braziunas, T. 1986. Radiocarbon age calibration of marine samples back to 9000 cal yr BP. *Radiocarbon* 28, (2b): 980.
Stuiver M. and Reimer, P. J. 1986. A computer program for radiocarbon age calibration. *Radiocarbon* 28, (2b): 1022.
Stuiver M., Reimer, P. J. and Reimer, R. W. 2005. CALIB 5.0. [WWW program and documentation]. .
Stuvier M. and Polach, H. A. 1977. Discussion of reporting of ^{14}C data. *Radiocarbon* 19, (3): 355-363.
Summerfield M. A. 1991. Global Geomorphology; an introduction to the study of landforms, New York, Longman scientific and technical.
Suzuki T., Hasumi, H., Sakamoto, T. T., Nishimura, T., Abe-Ouchi, A., Segawa, T., Okada, N., Oka, A. and Emori, S. 2005. Projection of future sea level and its variability in a high-resolution climate model: Ocean processes and Greenland and Antarctic ice-melt contributions. *Geophysical Research Letters.* 32, (L19706).
Sykes G. A., Collins, M. J. and Walton, D. I. 1995. The significance of a geochemically isolated intracrystalline organic fraction within biominerals. *Organic Geochemistry* 23, (11-12): 1059-1065.
Tayama R. 1952. Coral reefs of the South Seas *Bulletin of the Hydrographic Department, Tokyo* 11: 1-292.
Thieler E. R., Himmelstoss, E. A., Zichichi, J. L. and Ergul, A. 2009. Digital Shoreline Analysis System (DSAS) version 4.0-An ArcGIS extension for calculating shoreline change U.S. Geological Survey Open-File Report 2008-1278, 79.
Thom B. G. and Chappell, J. 1975. Holocene sea levels relative to Australia. *Search* 6: 90-93.
Todd R. 1961. Foraminifera from Onotoa Atoll, Gilbert Islands. *United States Geological Survey Professional Paper*: 171-191.
Tracey J. I. 1972. Holocene emergent reefs in the central Pacific. American Quaternary Association Second Conference, AMQUA, University of Miami.
Tracey J. I., Ladd, H. S. and Hoffmeister, J. E. 1948. Reefs of Bikini, Marshall Islands. *Geological Society of America Bulletin* 59, (9): 861-878.
Trenberth K. E. 2001. El Nino Southern Oscillation (ENSO). Encyclopedia of Ocean Sciences. S. A. Thorpe and J. H. Steele. San Diego, Academia Press: 815-827.
Trumbore S. E. 2000. Radiocarbon geochronology. Quaternary Geochronology: Methods and applications. J. S. Noller, J. M. Sowers and W. R. Lettis. Washington, D.C, American Geophysical Union: 41-60.
Tucker M. E. and Wright, V. P. 1990. Carbonate sedimentology, London, Oxford, Blackwell Scientific Publications.
Turner R. K., Subak, S. and Adger, W. N. 1996. Pressures, trends, and impacts in coastal zones: Interactions between socioeconomic and natural systems. *Environmental Management* 20, (2): 159-173.
Velicogna I. 2009. Increasing rates of ice mass loss from the Greenland and Antarctic ice sheets revealed by GRACE. *Geophysical Research letters* 36.
Walters L. J. and Smith, C. M. 1994. Rapid rhizoid production in Halimeda discoidea decaisne (Chlorophyta, Caulerpales) fragments: a mechanism for survival

after separation from adult thalli. *Journal of Experimental Marine Biology and Ecology* 175, (1): 105-120.

Walton W. R. 1952. Techniques for recognition of living Foraminifera *Contributions to the Cushman Foundation for Foraminiferal Research* 3: 56-60.

Wang C. and Fiedler, P. C. 2006. ENSO variability and the eastern tropical Pacific: A review. *Progress In Oceanography* 69, (24): 239-266.

Webb A. 2005. An assessment of coastal processes, impacts, erosion mitigation options and beach mining. *EU EDF SOPAC Project Report* SOPAC, Suva, 47.

Webb A. 2005. Reducing Vulnerability of Pacific ACP States, Country Mission Report: Meetings with the Govt. of Kiribati, Kiribati European Union Programme Adviser and the World Bank's Kiribati Adaptation Project (KAP)-Coastal defence and aggregate supply on urban South Tarawa. *EU EDF SOPAC Project Report* SOPAC, Suva, 15.

Webb A. 2006. Tuvalu Technical Report - Coastal change analysis using multi-temporal image comparisons - Funafuti Atoll *EU EDF SOPAC Project Report* SOPAC, Suva, 19.

Webb A. and Kench, P. S. 2010. The dynamic response of reef islands to sea level rise: evidence from multi-decadal analysis of island change in the central pacific. *Global and Planetary Change* 72: 234-246.

Weber J. N. and Woodhead, P. M. J. 1972. Carbonate lagoon and beach sediments of Tarawa Atoll. *Atoll Research Bulletin* 157, (9): 31.

Wehimiller J. F. 1980. Intergeneric differences in apparent racemisation kinetics in molluscs and foraminifera: implications for models of diagenetic racemisation. Biogeochemistry of Amino Acids. P. E. Hare, T. C. Hoering and K. King. New York, Wiley: 341-355.

Wehmiller J., F and Miller, G. H. 2000. Aminostratigraphic dating methods in Quaternary geology. Quaternary geochronology:methods and applications. J. S. Noller, J. M. Sowers and W. R. Lettis. Washington, D.C, American Geophysical Union: 582.

Wehmiller J. F. 1977. Amino acid studies of the Del Mar, California, Midden Site: Apparent rate constants, ground temperature models and chronological implications. *Earth and Planetary Letters* 37: 184-196.

Wehmiller J. F., Himar, A., III, S., York, L. L. and Friedman, I. 2000. The thermal environment of fossils: Effective ground temperatures (1994-1999) at aminostratigraphic sites. Perspectives in Amino acid and protein geochemistry. G. A. Goodfriend, M. J. Collins, M. L. Fogel, S. A. Macko and J. F. Wehmiller. New York, Oxford University Press: 219-250.

Wehmiller J. F., York, L. L. and Bart, M. L. 1995. Amino acid racemization geochronology of reworked Quaternary mollusks on U.S. Atlantic coast beaches: implications for chronostratigraphy, taphonomy, and coastal sediment transport. *Marine Geology* 124, (1-4): 303-337.

Weins H. J. 1962. Atoll Environment and Ecology New Haven, Conn Yale University Press.

Whitehead D. R. and Jones, C. E. 1969. Small islands and the equilibrium theory of insular biogeography. *Evolution*, (23): 171-179.

Wiens H. J. 1962. Atoll Environment and Ecology New Haven, Conn Yale University Press.

Willgoose G. and Hancock, G. 1998. Revisiting the hypsometric curve as an indicator of form and processes in transport-limited catchment. *Earth Surface Processes and Landforms* 23: 611-623.
Woodroffe C. D. 2000. Reef-island sedimentation on Indo-Pacific atolls and platform reefs. 9th International Coral Reef Symposium, Bali, Indonesia.
Woodroffe C. D. 2003. Coasts: Form, process and evolution, New York, Cambridge University Press.
Woodroffe C. D. 2008. Reef-island topography and the vulnerability of atolls to sea-level rise. *Global and Planetary Change* 62, (1-2): 77-96.
Woodroffe C. D. and Biribo, N. 2011. Atolls. Encyclopedia of Modern Coral Reefs. D. Hopley, Springer: 51-71.
Woodroffe C. D., Mc Gregor, H. V., Lambeck, K., Smithers, S. G. and Fink, D. 2012. Mid-Pacific microatolls record sea-level stability over the past 5000 years. *Geology in press*.
Woodroffe C. D. and McLean, R. F. 1992. Kiribati vulnerability to accelerated sea-level rise: a preliminary study University of Wollongong and Australian Defence Force Academy Unpublished report to Australian Government, 76.
Woodroffe C. D. and McLean, R. F. 1998. Pleistocene morphology and Holocene emergence of Christmas (Kiritimati) Island, Pacific Ocean. *Coral Reefs* 17, (3): 235-248.
Woodroffe C. D., McLean, R. F., Smithers, S. G. and Lawson, E. M. 1999. Atoll reef-island formation and response to sea-level change: West Island, Cocos (Keeling) Islands. *Marine Geology* 160, (1-2): 85-104.
Woodroffe C. D. and Morrison, R. J. 2001. Reef-island accretion and soil development on Makin, Kiribati, central Pacific. *CATENA* 44, (4): 245-261.
Woodroffe C. D., Samosorn, B., Hua, Q. and Hart, D. E. 2007. Incremental accretion of a sandy reef island over the past 3000 years indicated by component-specific radiocarbon dating. *Geophysical Resource Letters.* 34, (3): L03602.
Wrytiki K. 1990. Review Article: Sea Level Rise: The facts and the future. *Pacific Science* 44, (1): 1-16.
Wyrtki K. and Mitchum, G. 1990. Interannual Differences of Geosat Altimeter Heights and Sea Level: The Importance of a Datum. *J. Geophys. Res.* 95, (C3): 2969-2975.
Xue C. 1996. Coastal erosion and management of Vaitupu Island, Tuvalu SOPAC Secretariat, Suva, 53.
Xue C. 2001. Coastal erosion and management of Majuro Atoll, Marshall Islands. *Journal of Coastal Research* 17, (4): 909 - 918.
Yabe H. 1942. Problems of corals reefs Tokoku Imperal University Geological and Paleo Insitute, 1-6.
Yamano H. 2007. The use of multi-temporal satellite images to estimate intertidal reef-flat topography. *Journal of Spatial Science* 52, (1): 73-79.
Yamano H., Kayanne, H. and Chikamori, M. 2005. An overview of the nature and dynamics of reef islands. *Global Environmental Research* 9, (1): 9-20.
Yamano H., Kayanne, H., Yamaguchi, T., Kuwahara, Y., Yokoki, H., Shimazaki, H. and Chikamori, M. 2007. Atoll island vulnerability to flooding and inundation revealed by historical reconstruction: Fongafale Islet, Funafuti Atoll, Tuvalu. *Global and Planetary Change* 57, (3-4): 407-416.
Yamano H., Miyajima, T. and Koike, I. 2000. Importance of foraminifera for the formation and maintenance of a coral sand cay: Green Island, Australia. *Coral Reefs* 19, (1): 51-58.

Yamano H., Shimazaki, H., Matsunaga, T., Ishoda, A., McClennen, C., Yokoki, H., Fujita, K., Osawa, Y. and Kayanne, H. 2006. Evaluation of various satellite sensors for waterline extraction in a coral reef environment: Majuro Atoll, Marshall Islands. *Geomorphology* 82, (3-4): 398-411.

Yamano H., Shimazaki, H., Murase, T., Itou, K., Sano, S., Suzuki, Y., Leenders, N., Forstreuter, W. and Kayanne, H. 2006. Construction of digital elevation models for atoll islands using digital photogrammetry. 7th International Symposium on GIS and Computer Cartography: GIS for the Coastal Zone. C. D. Woodroffe, E. M. Bruce, M. Puotinen and R. A. Furness. University of Wollongong, University of Wollongong, Australia. 165-175.

Yanalak M. and Baykal, O. 2003. Digital Elevation Model based volume calculations using topograhical data. *Journal of Surveying Engineering* 129, (2): 56-64.

Yang X. and Holder, T. 2000. Visual and Statistical Comparisons of Surface Modeling Techniques for Point-based Environmental Data. *Cartography and geographic information science* 27, (2): 165-176.

Yanko V., Arnold, A., J and Parker, W. C. 1999. Effects of marine pollution on benthic foraminifera. Modern Foraminifera. B. K. S. Gupta. London, Kluwer Academic Publishers: 217-235.

Yanko V., Kronfeld, J. and Flexer, A. 1994. Response of benthic Foraminifera to various pollution sources; implications for pollution monitoring. *Journal of Foraminiferal Research* 24, (1): 1-17.

Zann L. P. 1982. The marine ecology of Betio Island, Tarawa Atoll, Republic of Kiribati CCOP/SOPAC Suva, 23.

Zann L. P. and Bolton, L. 1985. The distribution, abundance and ecology of the blue coral Heliopora coerulea (Pallas) in the Pacific. *Coral Reefs* 4, (2): 125-134.

APPENDIX A-1. REEF ISLAND DISTRIBUTION OF ELEVATIONS AND VOLUMES

MSL(m)	Above SEAFRAME (m)	Buariki	SA (m^2)	V= (SA +SA)/2 x0.1(m^3)	SA(%)
-0.5	1.119	0.7	3147500	314750	100.0
-0.4	1.219	0.8	3147500	314750	100.0
-0.3	1.319	0.9	3147500	314748	100.0
-0.2	1.419	1	3147466	314726	100.0
-0.1	1.519	1.1	3147056	314639	100.0
0	1.619	1.2	3145722	314472	100.0
0.1	1.719	1.3	3143725	314041	100.0
0.2	1.819	1.4	3137086	311875	100.0
0.3	1.919	1.5	3100422	301911	99.0
0.4	2.019	1.6	2937789	283574	93.0
0.5	2.119	1.7	2733694	266475	87.0
0.6	2.219	1.8	2595801	253635	82.0
0.7	2.319	1.9	2476905	242564	79.0
0.8	2.419	2	2374366	232165	75.0
0.9	2.519	2.1	2268937	221382	72.0
1	2.619	2.2	2158708	209796	69.0
1.1	2.719	2.3	2037204	196603	65.0
1.2	2.819	2.4	1894860	182574	60.0
1.3	2.919	2.5	1756622	167583	56.0
1.4	3.019	2.6	1595046	151561	51.0
1.5	3.119	2.7	1436176	134029	46.0
1.6	3.219	2.8	1244408	116330	40.0
1.7	3.319	2.9	1082201	102157	34.0
1.8	3.419	3	960937	91534	31.0
1.9	3.519	3.1	869736	82953	28.0
2	3.619	3.2	789317	74366	25.0
2.1	3.719	3.3	697995	64558	22.0
2.2	3.819	3.4	593160	54832	19.0
2.3	3.919	3.5	503476	46337	16.0
2.4	4.019	3.6	423265	38502	13.0
2.5	4.119	3.7	346769	32307	11.0
2.6	4.219	3.8	299367	28140	10.0
2.7	4.319	3.9	263439	24734	8.0
2.8	4.419	4	231244	21360	7.0
2.9	4.519	4.1	195961	17412	6.0
3	4.619	4.2	152287	12712	5.0
3.1	4.719	4.3	101945	8153	3.0
3.2	4.819	4.4	61122	4345	2.0
3.3	4.919	4.5	25785	1781	1.0
3.4	5.019	4.6	9826	848	0.3
3.5	5.119	4.7	7143	592	0.2
3.6	5.219	4.8	4698	470	0.1
3.7	5.319	4.9	4698	314	0.1

3.8	5.419	5	1578	102	0.1
3.9	5.519	5.1	465	27	0.0
4	5.619	5.2	79	4	0.0
4.1	5.719	5.3	0	0	0.0
		Total		**6,182,723.46**	

MSL(m)	Above SEAFRAME (m)	Nuatabu	SA (m^2)	V= (SA +SA)/2 x0.1(m^3)	SA(%)
-0.5	1.119	0.7	530583	53032	100.0
-0.4	1.219	0.8	530052	52974	100.0
-0.3	1.319	0.9	529436	52909	100.0
-0.2	1.419	1	528750	52841	100.0
-0.1	1.519	1.1	528061	52773	100.0
0	1.619	1.2	527390	52706	99.0
0.1	1.719	1.3	526737	52642	99.0
0.2	1.819	1.4	526101	52578	99.0
0.3	1.919	1.5	525452	52505	99.0
0.4	2.019	1.6	524643	52405	99.0
0.5	2.119	1.7	523460	52234	99.0
0.6	2.219	1.8	521212	51946	98.0
0.7	2.319	1.9	517699	51590	98.0
0.8	2.419	2	514098	51211	97.0
0.9	2.519	2.1	510121	50693	96.0
1	2.619	2.2	503744	49962	95.0
1.1	2.719	2.3	495498	48886	93.0
1.2	2.819	2.4	482217	47418	91.0
1.3	2.919	2.5	466133	45744	88.0
1.4	3.019	2.6	448742	43802	85.0
1.5	3.119	2.7	427306	41322	81.0
1.6	3.219	2.8	399129	38213	75.0
1.7	3.319	2.9	365132	35020	69.0
1.8	3.419	3	335260	31912	63.0
1.9	3.519	3.1	302975	28806	57.0
2	3.619	3.2	273148	25597	51.0
2.1	3.719	3.3	238788	21945	45.0
2.2	3.819	3.4	200118	17274	38.0
2.3	3.919	3.5	145361	12120	27.0
2.4	4.019	3.6	97044	7960	18.0
2.5	4.119	3.7	62148	4652	12.0
2.6	4.219	3.8	30892	2551	6.0
2.7	4.319	3.9	20136	1722	4.0
2.8	4.419	4	14305	1149	3.0
2.9	4.519	4.1	8668	687	2.0
3	4.619	4.2	5069	380	1.0
3.1	4.719	4.3	2523	170	0.5
3.2	4.819	4.4	869	48	0.2
3.3	4.919	4.5	100	5	0.0
3.4	5.019	4.6	0	0	0.0
		Total		**1,292,381**	

MSL(m)	Above SEAFRAME (m)	Tebangaroi	SA (m^2)	V= (SA +SA)/2 x0.1(m^3)	SA(%)
-0.5	1.119	0.7	527500	52750	100.0
-0.4	1.219	0.8	527500	52750	100.0
-0.3	1.319	0.9	527500	52750	100.0
-0.2	1.419	1	527500	52750	100.0
-0.1	1.519	1.1	527500	52750	100.0
0	1.619	1.2	527500	52750	100.0
0.1	1.719	1.3	527500	52750	100.0
0.2	1.819	1.4	527500	52750	100.0
0.3	1.919	1.5	527500	52750	100.0
0.4	2.019	1.6	527500	52750	100.0
0.5	2.119	1.7	527500	52750	100.0
0.6	2.219	1.8	527500	52749	100.0
0.7	2.319	1.9	527477	52739	100.0
0.8	2.419	2	527304	52713	100.0
0.9	2.519	2.1	526954	52660	100.0
1	2.619	2.2	526256	52448	100.0
1.1	2.719	2.3	522714	51758	99.0
1.2	2.819	2.4	512454	50441	97.0
1.3	2.919	2.5	496373	48842	94.0
1.4	3.019	2.6	480461	46787	91.0
1.5	3.119	2.7	455276	43742	86.0
1.6	3.219	2.8	419559	40273	80.0
1.7	3.319	2.9	385911	37159	73.0
1.8	3.419	3	357272	34059	68.0
1.9	3.519	3.1	323908	30393	61.0
2	3.619	3.2	283952	26343	54.0
2.1	3.719	3.3	242903	21964	46.0
2.2	3.819	3.4	196376	16949	37.0
2.3	3.919	3.5	142601	11598	27.0
2.4	4.019	3.6	89364	6265	17.0
2.5	4.119	3.7	35931	3054	7.0
2.6	4.219	3.8	25154	2215	5.0
2.7	4.319	3.9	19140	1531	4.0
2.8	4.419	4	11477	842	2.0
2.9	4.519	4.1	5363	346	1.0
3	4.619	4.2	1563	86	0.3
3.1	4.719	4.3	162	8	0.0
3.2	4.819	4.4	0	0	0.0
		Total		**1,318,216**	

MSL(m)	Above SEAFRAME(m)	Taratai	SA (m^2)	V= (SA +SA)/2 x0.1(m^3)	SA(%)
-0.5	1.119	0.7	1470000	147000	100.0
-0.4	1.219	0.8	1470000	147000	100.0
-0.3	1.319	0.9	1470000	147000	100.0
-0.2	1.419	1	1470000	147000	100.0
-0.1	1.519	1.1	1470000	147000	100.0
0	1.619	1.2	1470000	147000	100.0
0.1	1.719	1.3	1470000	147000	100.0
0.2	1.819	1.4	1470000	147000	100.0
0.3	1.919	1.5	1469992	146994	100.0
0.4	2.019	1.6	1469893	146939	100.0
0.5	2.119	1.7	1468882	146636	100.0
0.6	2.219	1.8	1463834	145920	100.0
0.7	2.319	1.9	1454561	144801	99.0
0.8	2.419	2	1441460	143318	98.0
0.9	2.519	2.1	1424891	141602	97.0
1	2.619	2.2	1407152	139687	96.0
1.1	2.719	2.3	1386594	136784	94.0
1.2	2.819	2.4	1349078	132942	92.0
1.3	2.919	2.5	1309770	128089	89.0
1.4	3.019	2.6	1252007	121170	85.0
1.5	3.119	2.7	1171399	112646	80.0
1.6	3.219	2.8	1081512	104053	74.0
1.7	3.319	2.9	999545	95480	68.0
1.8	3.419	3	910048	85304	62.0
1.9	3.519	3.1	796030	72857	54.0
2	3.619	3.2	661116	59671	45.0
2.1	3.719	3.3	532302	48750	36.0
2.2	3.819	3.4	442698	40109	30.0
2.3	3.919	3.5	359488	31930	24.0
2.4	4.019	3.6	279119	24453	19.0
2.5	4.119	3.7	209939	17784	14.0
2.6	4.219	3.8	145750	11468	10.0
2.7	4.319	3.9	83612	7114	6.0
2.8	4.419	4	58658	4865	4.0
2.9	4.519	4.1	38638	3206	3.0
3	4.619	4.2	25487	2162	2.0
3.1	4.719	4.3	17753	1521	1.0
3.2	4.819	4.4	12665	1080	1.0
3.3	4.919	4.5	8931	729	1.0
3.4	5.019	4.6	5641	451	0.4
3.5	5.119	4.7	3387	188	0.2
3.6	5.219	4.8	371	19	0.0
3.7	5.319	4.9	0	0	0.0
		Total		**3,576,720**	

MSL(m)	Above SEAFRAME (m)	7	SA (m^2)	V= (SA +SA)/2 x0.1(m^3)	SA(%)
-0.5	1.119	0.7	20000	2000	100.0
-0.4	1.219	0.8	20000	2000	100.0
-0.3	1.319	0.9	20000	2000	100.0
-0.2	1.419	1	20000	2000	100.0
-0.1	1.519	1.1	20000	2000	100.0
0	1.619	1.2	20000	2000	100.0
0.1	1.719	1.3	20000	2000	100.0
0.2	1.819	1.4	20000	2000	100.0
0.3	1.919	1.5	20000	2000	100.0
0.4	2.019	1.6	20000	2000	100.0
0.5	2.119	1.7	20000	2000	100.0
0.6	2.219	1.8	20000	2000	100.0
0.7	2.319	1.9	20000	2000	100.0
0.8	2.419	2	20000	2000	100.0
0.9	2.519	2.1	20000	2000	100.0
1	2.619	2.2	20000	2000	100.0
1.1	2.719	2.3	20000	2000	100.0
1.2	2.819	2.4	20000	2000	100.0
1.3	2.919	2.5	20000	2000	100.0
1.4	3.019	2.6	20000	2000	100.0
1.5	3.119	2.7	20000	1997	100.0
1.6	3.219	2.8	19949	1755	100.0
1.7	3.319	2.9	15141	1192	76.0
1.8	3.419	3	8695	662	43.0
1.9	3.519	3.1	4553	228	23.0
2	3.619	3.2	0	0	0.0
		Total		**45,834**	

MSL (m)	Above SEAFRAME (m)	Notoue	SA (m^2)	V= (SA +SA)/2 x0.1(m^3)	SA (%)
-0.5	1.119	0.7	942500	94250	100.0
-0.4	1.219	0.8	942500	94250	100.0
-0.3	1.319	0.9	942500	94250	100.0
-0.2	1.419	1	942500	94250	100.0
-0.1	1.519	1.1	942500	94250	100.0
0	1.619	1.2	942500	94250	100.0
0.1	1.719	1.3	942500	94250	100.0
0.2	1.819	1.4	942500	94250	100.0
0.3	1.919	1.5	942500	94250	100.0
0.4	2.019	1.6	942500	94250	100.0
0.5	2.119	1.7	942500	94250	100.0
0.6	2.219	1.8	942500	94250	100.0
0.7	2.319	1.9	942500	94250	100.0
0.8	2.419	2	942500	94250	100.0
0.9	2.519	2.1	942500	94249	100.0
1	2.619	2.2	942486	94245	100.0
1.1	2.719	2.3	942421	94236	100.0
1.2	2.819	2.4	942303	94220	100.0
1.3	2.919	2.5	942091	93926	100.0
1.4	3.019	2.6	936428	92833	99.0
1.5	3.119	2.7	920235	90650	98.0
1.6	3.219	2.8	892766	86531	95.0
1.7	3.319	2.9	837857	81297	89.0
1.8	3.419	3	788084	75907	84.0
1.9	3.519	3.1	730058	70006	77.0
2	3.619	3.2	670070	64669	71.0
2.1	3.719	3.3	623303	59554	66.0
2.2	3.819	3.4	567782	52389	60.0
2.3	3.919	3.5	479991	43313	51.0
2.4	4.019	3.6	386274	33450	41.0
2.5	4.119	3.7	282730	24127	30.0
2.6	4.219	3.8	199818	17011	21.0
2.7	4.319	3.9	140403	12290	15.0
2.8	4.419	4	105402	9407	11.0
2.9	4.519	4.1	82732	7204	9.0
3	4.619	4.2	61352	5363	7.0
3.1	4.719	4.3	45907	3918	5.0
3.2	4.819	4.4	32449	2624	3.0
3.3	4.919	4.5	20031	1554	2.0
3.4	5.019	4.6	11047	898	1.0
3.5	5.119	4.7	6914	561	1.0
3.6	5.219	4.8	4310	298	0.5
3.7	5.319	4.9	1657	98	0.2
3.8	5.419	5	293	15	0.0
3.9	5.519	5.1	0	0	0.0
		Total		**2,626,344**	

MSL(m)	Above SEAFRAME (m)	Abaokoro	SA (m^2)	V= (SA +SA)/2 x0.1(m^3)	SA(%)
-0.5	1.119	0.7	207500	20750	100.0
-0.4	1.219	0.8	207500	20750	100.0
-0.3	1.319	0.9	207500	20750	100.0
-0.2	1.419	1	207500	20750	100.0
-0.1	1.519	1.1	207500	20750	100.0
0.0	1.619	1.2	207500	20750	100.0
0.1	1.719	1.3	207500	20750	100.0
0.2	1.819	1.4	207500	20750	100.0
0.3	1.919	1.5	207500	20750	100.0
0.4	2.019	1.6	207500	20750	100.0
0.5	2.119	1.7	207500	20750	100.0
0.6	2.219	1.8	207500	20750	100.0
0.7	2.319	1.9	207500	20750	100.0
0.8	2.419	2	207500	20750	100.0
0.9	2.519	2.1	207500	20750	100.0
1.0	2.619	2.2	207500	20750	100.0
1.1	2.719	2.3	207500	20750	100.0
1.2	2.819	2.4	207500	20750	100.0
1.3	2.919	2.5	207500	20750	100.0
1.4	3.019	2.6	207500	20750	100.0
1.5	3.119	2.7	207500	20750	100.0
1.6	3.219	2.8	207500	20750	100.0
1.7	3.319	2.9	207500	20747	100.0
1.8	3.419	3	207434	20696	100.0
1.9	3.519	3.1	206487	20429	100.0
2.0	3.619	3.2	202089	19806	97.0
2.1	3.719	3.3	194027	18887	94.0
2.2	3.819	3.4	183721	16810	89.0
2.3	3.919	3.5	152481	13921	73.0
2.4	4.019	3.6	125944	10238	61.0
2.5	4.119	3.7	78816	5784	38.0
2.6	4.219	3.8	36862	3157	18.0
2.7	4.319	3.9	26275	1978	13.0
2.8	4.419	4	13286	1152	6.0
2.9	4.519	4.1	9749	865	5.0
3.0	4.619	4.2	7545	671	4.0
3.1	4.719	4.3	5884	484	3.0
3.2	4.819	4.4	3801	235	2.0
3.3	4.919	4.5	905	60	0.4
3.4	5.019	4.6	287	15	0.1
3.5	5.119	4.7	15	1	0.0
3.6	5.219	4.8	0	0	0.0
			Total	**612,436**	

MSL (m)	Above SEAFRAME (m)	10	SA (m^2)	V= (SA +SA)/2 x0.1(m^3)	SA (%)
-0.5	1.119	0.7	35000	3500	100
-0.4	1.219	0.8	35000	3500	100
-0.3	1.319	0.9	35000	3500	100
-0.2	1.419	1	35000	3500	100
-0.1	1.519	1.1	35000	3500	100
0	1.619	1.2	35000	3500	100
0.1	1.719	1.3	35000	3500	100
0.2	1.819	1.4	35000	3500	100
0.3	1.919	1.5	35000	3500	100
0.4	2.019	1.6	35000	3500	100
0.5	2.119	1.7	35000	3500	100
0.6	2.219	1.8	35000	3500	100
0.7	2.319	1.9	35000	3500	100
0.8	2.419	2	35000	3500	100
0.9	2.519	2.1	35000	3500	100
1	2.619	2.2	35000	3500	100
1.1	2.719	2.3	35000	3500	100
1.2	2.819	2.4	35000	3500	100
1.3	2.919	2.5	35000	3500	100
1.4	3.019	2.6	35000	3500	100
1.5	3.119	2.7	35000	3491	100
1.6	3.219	2.8	34818	3420	99.0
1.7	3.319	2.9	33581	3225	96.0
1.8	3.419	3	30926	2743	88.0
1.9	3.519	3.1	23943	2215	68.0
2	3.619	3.2	20357	1895	58.0
2.1	3.719	3.3	17542	1624	50.0
2.2	3.819	3.4	14935	1369	43.0
2.3	3.919	3.5	12442	1029	36.0
2.4	4.019	3.6	8141	541	23.0
2.5	4.119	3.7	2683	147	8.0
2.6	4.219	3.8	263	13	1.0
2.7	4.319	3.9	0	0	0.0
			Total	**91,713**	

MSL (m)	Above SEAFRAME(m)	Marenanuka	SA (m^2)	V= (SA +SA)/2 x0.1(m^3)	SA (%)
-0.5	1.119	0.7	825000	82500	100.0
-0.4	1.219	0.8	825000	82500	100.0
-0.3	1.319	0.9	825000	82500	100.0
-0.2	1.419	1	825000	82500	100.0
-0.1	1.519	1.1	825000	82500	100.0
0	1.619	1.2	825000	82498	100.0
0.1	1.719	1.3	824952	82495	100.0
0.2	1.819	1.4	824952	82471	100.0
0.3	1.919	1.5	824467	82425	100.0
0.4	2.019	1.6	824028	82374	100.0
0.5	2.119	1.7	823459	82311	100.0
0.6	2.219	1.8	822759	82231	100.0
0.7	2.319	1.9	821856	82121	100.0
0.8	2.419	2	820572	81969	99.0
0.9	2.519	2.1	818811	81704	99.0
1	2.619	2.2	815276	81327	99.0
1.1	2.719	2.3	811270	80543	98.0
1.2	2.819	2.4	799585	78975	97.0
1.3	2.919	2.5	779907	76753	95.0
1.4	3.019	2.6	755149	74004	92.0
1.5	3.119	2.7	724932	70851	88.0
1.6	3.219	2.8	692088	67328	84.0
1.7	3.319	2.9	654478	63581	79.0
1.8	3.419	3	617133	59746	75.0
1.9	3.519	3.1	577787	55247	70.0
2	3.619	3.2	527153	49520	64.0
2.1	3.719	3.3	463246	42618	56.0
2.2	3.819	3.4	389120	35740	47.0
2.3	3.919	3.5	325686	29085	39.0
2.4	4.019	3.6	256009	21552	31.0
2.5	4.119	3.7	175036	14835	21.0
2.6	4.219	3.8	121662	10824	15.0
2.7	4.319	3.9	94810	8603	11.0
2.8	4.419	4	77251	6926	9.0
2.9	4.519	4.1	61265	5298	7.0
3	4.619	4.2	44696	3837	5.0
3.1	4.719	4.3	32046	2816	4.0
3.2	4.819	4.4	24277	2198	3.0
3.3	4.919	4.5	19674	1732	2.0
3.4	5.019	4.6	14975	1250	2.0
3.5	5.119	4.7	10015	805	1.0
3.6	5.219	4.8	6093	484	1.0
3.7	5.319	4.9	3588	243	0.4
3.8	5.419	5	1268	63	0.2
3.9	5.519	5.1	0	0	0.0
			Total	**2,181,883**	

MSL (m)	Above SEAFRAME (m)	Tabonibara	SA (m^2)	V= (SA +SA)/2 x0.1(m^3)	SA (%)
-0.5	1.119	0.7	262500	26250	100.0
-0.4	1.219	0.8	262500	26250	100.0
-0.3	1.319	0.9	262500	26250	100.0
-0.2	1.419	1	262500	26250	100.0
-0.1	1.519	1.1	262500	26250	100.0
0	1.619	1.2	262500	26250	100.0
0.1	1.719	1.3	262500	26250	100.0
0.2	1.819	1.4	262500	26250	100.0
0.3	1.919	1.5	262500	26250	100.0
0.4	2.019	1.6	262500	26250	100.0
0.5	2.119	1.7	262500	26250	100.0
0.6	2.219	1.8	262500	26250	100.0
0.7	2.319	1.9	262500	26250	100.0
0.8	2.419	2	262500	26250	100.0
0.9	2.519	2.1	262500	26250	100.0
1	2.619	2.2	262500	26250	100.0
1.1	2.719	2.3	262500	26250	100.0
1.2	2.819	2.4	262500	26250	100.0
1.3	2.919	2.5	262500	26250	100.0
1.4	3.019	2.6	262500	26250	100.0
1.5	3.119	2.7	262500	26243	100.0
1.6	3.219	2.8	262355	26223	100.0
1.7	3.319	2.9	262114	26166	100.0
1.8	3.419	3	261208	25969	100.0
1.9	3.519	3.1	258179	25684	98.0
2	3.619	3.2	255507	25341	97.0
2.1	3.719	3.3	251310	24790	96.0
2.2	3.819	3.4	244486	23886	93.0
2.3	3.919	3.5	233235	21931	89.0
2.4	4.019	3.6	205376	19072	78.0
2.5	4.119	3.7	176054	15777	67.0
2.6	4.219	3.8	139485	12162	53.0
2.7	4.319	3.9	103746	8937	40.0
2.8	4.419	4	74995	5853	29.0
2.9	4.519	4.1	42057	3383	16.0
3	4.619	4.2	25609	2141	10.0
3.1	4.719	4.3	17207	1406	7.0
3.2	4.819	4.4	10912	768	4.0
3.3	4.919	4.5	4454	346	2.0
3.4	5.019	4.6	2473	182	1.0
3.5	5.119	4.7	1176	65	0.4
3.6	5.219	4.8	120	6	0.0
3.7	5.319	4.9	0	0	0.0
			Total	**821,331**	

MSL (m)	Above SEAFRAME (m)	13	SA (m^2)	V= (SA +SA)/2 x0.1(m^3)	SA (%)
-0.5	1.119	0.7	5000	500	100.0
-0.4	1.219	0.8	5000	500	100.0
-0.3	1.319	0.9	5000	500	100.0
-0.2	1.419	1	5000	500	100.0
-0.1	1.519	1.1	5000	500	100.0
0	1.619	1.2	5000	500	100.0
0.1	1.719	1.3	5000	500	100.0
0.2	1.819	1.4	5000	500	100.0
0.3	1.919	1.5	5000	500	100.0
0.4	2.019	1.6	5000	500	100.0
0.5	2.119	1.7	5000	500	100.0
0.6	2.219	1.8	5000	500	100.0
0.7	2.319	1.9	5000	500	100.0
0.8	2.419	2	5000	500	100.0
0.9	2.519	2.1	5000	500	100.0
1	2.619	2.2	5000	500	100.0
1.1	2.719	2.3	5000	500	100.0
1.2	2.819	2.4	5000	500	100.0
1.3	2.919	2.5	5000	500	100.0
1.4	3.019	2.6	5000	500	100.0
1.5	3.119	2.7	5000	500	100.0
1.6	3.219	2.8	5000	500	100.0
1.7	3.319	2.9	5000	500	100.0
1.8	3.419	3	5000	500	100.0
1.9	3.519	3.1	5000	500	100.0
2	3.619	3.2	5000	500	100.0
2.1	3.719	3.3	5000	500	100.0
2.2	3.819	3.4	5000	495	100.0
2.3	3.919	3.5	4892	436	98.0
2.4	4.019	3.6	3831	310	77.0
2.5	4.119	3.7	2377	149	48.0
2.6	4.219	3.8	603	30	12.0
2.7	4.319	3.9	0	0	0.0
			Total	**14,920**	

MSL(m)	Above SEAFRAME (m)	14	SA (m^2)	V= (SA +SA)/2 x0.1(m^3)	SA(%)
-0.5	1.119	0.7	70000	7000	100.0
-0.4	1.219	0.8	70000	7000	100.0
-0.3	1.319	0.9	70000	7000	100.0
-0.2	1.419	1	70000	7000	100.0
-0.1	1.519	1.1	70000	7000	100.0
0	1.619	1.2	70000	7000	100.0
0.1	1.719	1.3	70000	7000	100.0
0.2	1.819	1.4	70000	7000	100.0
0.3	1.919	1.5	70000	7000	100.0
0.4	2.019	1.6	70000	7000	100.0
0.5	2.119	1.7	70000	7000	100.0
0.6	2.219	1.8	70000	7000	100.0
0.7	2.319	1.9	70000	6999	100.0
0.8	2.419	2	69986	6995	100.0
0.9	2.519	2.1	69914	6985	100.0
1	2.619	2.2	69782	6969	100.0
1.1	2.719	2.3	69590	6951	99.0
1.2	2.819	2.4	69440	6921	99.0
1.3	2.919	2.5	68972	6853	99.0
1.4	3.019	2.6	68087	6728	97.0
1.5	3.119	2.7	66465	6494	95.0
1.6	3.219	2.8	63425	6046	91.0
1.7	3.319	2.9	57496	5274	82.0
1.8	3.419	3	47983	4269	69.0
1.9	3.519	3.1	37402	3064	53.0
2	3.619	3.2	23874	1778	34.0
2.1	3.719	3.3	11679	903	17.0
2.2	3.819	3.4	6371	533	9.0
2.3	3.919	3.5	4298	349	6.0
2.4	4.019	3.6	2687	237	4.0
2.5	4.119	3.7	2056	185	3.0
2.6	4.219	3.8	1642	143	2.0
2.7	4.319	3.9	1227	102	2.0
2.8	4.419	4	812	61	1.0
2.9	4.519	4.1	400	21	0.6
3	4.619	4.2	26	1	0.0
3.1	4.719	4.3	0	0	0.0
			Total	**168,862**	

MSL(m)	Above SEAFRAME(m)	17	SA (m^2)	V= (SA +SA)/2 x0.1(m^3)	SA(%)
-0.5	1.119	0.7	90000	9000	100.0
-0.4	1.219	0.8	90000	9000	100.0
-0.3	1.319	0.9	90000	9000	100.0
-0.2	1.419	1	90000	9000	100.0
-0.1	1.519	1.1	90000	9000	100.0
0	1.619	1.2	90000	9000	100.0
0.1	1.719	1.3	90000	9000	100.0
0.2	1.819	1.4	90000	9000	100.0
0.3	1.919	1.5	90000	9000	100.0
0.4	2.019	1.6	90000	9000	100.0
0.5	2.119	1.7	90000	9000	100.0
0.6	2.219	1.8	90000	9000	100.0
0.7	2.319	1.9	90000	9000	100.0
0.8	2.419	2	90000	9000	100.0
0.9	2.519	2.1	90000	9000	100.0
1	2.619	2.2	90000	9000	100.0
1.1	2.719	2.3	90000	9000	100.0
1.2	2.819	2.4	90000	9000	100.0
1.3	2.919	2.5	90000	9000	100.0
1.4	3.019	2.6	90000	9000	100.0
1.5	3.119	2.7	90000	9000	100.0
1.6	3.219	2.8	89994	8991	100.0
1.7	3.319	2.9	89830	8962	100.0
1.8	3.419	3	89411	8871	99.0
1.9	3.519	3.1	88004	8600	98.0
2	3.619	3.2	83991	8062	93.0
2.1	3.719	3.3	77252	7042	86.0
2.2	3.819	3.4	63583	5551	71.0
2.3	3.919	3.5	47441	3715	53.0
2.4	4.019	3.6	26852	2303	30.0
2.5	4.119	3.7	19211	1671	21.0
2.6	4.219	3.8	14214	1167	16.0
2.7	4.319	3.9	9135	774	10.0
2.8	4.419	4	6352	531	7.0
2.9	4.519	4.1	4263	347	5.0
3	4.619	4.2	2675	210	3.0
3.1	4.719	4.3	1518	108	2.0
3.2	4.819	4.4	652	36	1.0
3.3	4.919	4.5	59	3	0.0
3.4	5.019	4.6	0	0	0.0
			Total	**255,944**	

MSL(m)	Above SEAFRAME(m)	19	SA (m^2)	V= (SA +SA)/2 x0.1(m^3)	SA(%)
-0.5	1.119	0.7	30000	3000	100.0
-0.4	1.219	0.8	30000	3000	100.0
-0.3	1.319	0.9	30000	3000	100.0
-0.2	1.419	1	30000	3000	100.0
-0.1	1.519	1.1	30000	3000	100.0
0	1.619	1.2	30000	3000	100.0
0.1	1.719	1.3	30000	3000	100.0
0.2	1.819	1.4	30000	3000	100.0
0.3	1.919	1.5	30000	3000	100.0
0.4	2.019	1.6	30000	3000	100.0
0.5	2.119	1.7	30000	3000	100.0
0.6	2.219	1.8	30000	3000	100.0
0.7	2.319	1.9	30000	3000	100.0
0.8	2.419	2	30000	3000	100.0
0.9	2.519	2.1	30000	3000	100.0
1	2.619	2.2	30000	3000	100.0
1.1	2.719	2.3	30000	3000	100.0
1.2	2.819	2.4	30000	3000	100.0
1.3	2.919	2.5	30000	3000	100.0
1.4	3.019	2.6	30000	3000	100.0
1.5	3.119	2.7	30000	3000	100.0
1.6	3.219	2.8	30000	3000	100.0
1.7	3.319	2.9	30000	3000	100.0
1.8	3.419	3	30000	3000	100.0
1.9	3.519	3.1	30000	3000	100.0
2	3.619	3.2	30000	2993	100.0
2.1	3.719	3.3	29865	2949	100.0
2.2	3.819	3.4	29108	2581	97.0
2.3	3.919	3.5	22520	1569	75.0
2.4	4.019	3.6	8858	458	30.0
2.5	4.119	3.7	306	15	1.0
2.6	4.219	3.8	0	0	0.0
			Total	**85,566**	

MSL(m)	Above SEAFRAME(m)	24	SA (m^2)	V= (SA +SA)/2 x0.1(m^3)	SA(%)
-0.5	1.119	0.7	15000	1500	100.0
-0.4	1.219	0.8	15000	1500	100.0
-0.3	1.319	0.9	15000	1500	100.0
-0.2	1.419	1	15000	1500	100.0
-0.1	1.519	1.1	15000	1500	100.0
0	1.619	1.2	15000	1500	100.0
0.1	1.719	1.3	15000	1500	100.0
0.2	1.819	1.4	15000	1500	100.0
0.3	1.919	1.5	15000	1500	100.0
0.4	2.019	1.6	15000	1500	100.0
0.5	2.119	1.7	15000	1500	100.0
0.6	2.219	1.8	15000	1500	100.0
0.7	2.319	1.9	15000	1500	100.0
0.8	2.419	2	15000	1500	100.0
0.9	2.519	2.1	15000	1500	100.0
1	2.619	2.2	15000	1500	100.0
1.1	2.719	2.3	15000	1500	100.0
1.2	2.819	2.4	15000	1500	100.0
1.3	2.919	2.5	15000	1500	100.0
1.4	3.019	2.6	15000	1500	100.0
1.5	3.119	2.7	15000	1500	100.0
1.6	3.219	2.8	15000	1500	100.0
1.7	3.319	2.9	14997	1494	100.0
1.8	3.419	3	14888	1475	99.0
1.9	3.519	3.1	14616	1440	97.0
2	3.619	3.2	14182	1392	95.0
2.1	3.719	3.3	13649	1332	91.0
2.2	3.819	3.4	12993	1099	87.0
2.3	3.919	3.5	8979	719	60.0
2.4	4.019	3.6	5405	452	36.0
2.5	4.119	3.7	3641	288	24.0
2.6	4.219	3.8	2121	157	14.0
2.7	4.319	3.9	1019	62	7.0
2.8	4.419	4	229	11	2.0
2.9	4.519	4.1	0	0	0.0
			Total	**42,922**	

MSL(m)	Above SEAFRAME(m)	26	SA (m^2)	V= (SA +SA)/2 x0.1(m^3)	SA(%)
-0.5	1.119	0.7	5000	500	100.0
-0.4	1.219	0.8	5000	500	100.0
-0.3	1.319	0.9	5000	500	100.0
-0.2	1.419	1	5000	500	100.0
-0.1	1.519	1.1	5000	500	100.0
0	1.619	1.2	5000	500	100.0
0.1	1.719	1.3	5000	500	100.0
0.2	1.819	1.4	5000	500	100.0
0.3	1.919	1.5	5000	500	100.0
0.4	2.019	1.6	5000	500	100.0
0.5	2.119	1.7	5000	500	100.0
0.6	2.219	1.8	5000	500	100.0
0.7	2.319	1.9	5000	500	100.0
0.8	2.419	2	5000	500	100..
0.9	2.519	2.1	5000	500	100.0
1	2.619	2.2	5000	500	100.0
1.1	2.719	2.3	5000	500	100.0
1.2	2.819	2.4	5000	500	100.0.
1.3	2.919	2.5	5000	500	100.0
1.4	3.019	2.6	5000	500	100.0
1.5	3.119	2.7	5000	500	100.0
1.6	3.219	2.8	5000	500	100.0
1.7	3.319	2.9	5000	500	100.0
1.8	3.419	3	5000	500	100.0
1.9	3.519	3.1	5000	500	100.0
2	3.619	3.2	5000	500	100.0
2.1	3.719	3.3	5000	500	100.0
2.2	3.819	3.4	5000	498	100.0
2.3	3.919	3.5	4959	453	99.0
2.4	4.019	3.6	4099	359	82.0
2.5	4.119	3.7	3087	236	62.0
2.6	4.219	3.8	1629	81	33.0
2.7	4.319	3.9	0	0	0.0
			Total	**15,127**	

MSL(m)	Above SEAFRAME(m)	Kairiki	SA (m^2)	V= (SA +SA)/2 x0.1(m^3)	SA(%)
-0.5	1.119	0.7	187500	18750	100.0
-0.4	1.219	0.8	187500	18750	100.0
-0.3	1.319	0.9	187500	18750	100.0
-0.2	1.419	1	187500	18750	100.0
-0.1	1.519	1.1	187500	18750	100.0
0	1.619	1.2	187500	18750	100.0
0.1	1.719	1.3	187500	18750	100.0
0.2	1.819	1.4	187500	18750	100.0
0.3	1.919	1.5	187500	18750	100.0
0.4	2.019	1.6	187500	18750	100.0
0.5	2.119	1.7	187500	18750	100.0
0.6	2.219	1.8	187500	18750	100.0
0.7	2.319	1.9	187500	18750	100.0
0.8	2.419	2	187500	18750	100.0
0.9	2.519	2.1	187500	18750	100.0
1	2.619	2.2	187500	18750	100.0
1.1	2.719	2.3	187500	18750	100.0
1.2	2.819	2.4	187500	18750	100.0
1.3	2.919	2.5	187500	18750	100.0
1.4	3.019	2.6	187500	18750	100.0
1.5	3.119	2.7	187500	18703	100.0
1.6	3.219	2.8	186550	18519	99.
1.7	3.319	2.9	183820	18298	98.0
1.8	3.419	3	182131	18110	97.0
1.9	3.519	3.1	180072	17886	96.0
2	3.619	3.2	177649	17505	95.0
2.1	3.719	3.3	172452	16684	92.0
2.2	3.819	3.4	161228	15235	86.0
2.3	3.919	3.5	143473	13080	77.0
2.4	4.019	3.6	118127	10589	63.0
2.5	4.119	3.7	93653	8204	50.0
2.6	4.219	3.8	70418	5702	38.0
2.7	4.319	3.9	43624	3773	23.0
2.8	4.419	4	31840	2629	17.0
2.9	4.519	4.1	20730	1692	11.0
3	4.619	4.2	13100	1078	7.0
3.1	4.719	4.3	8460	642	5.0
3.2	4.819	4.4	4386	290	2.0
3.3	4.919	4.5	1412	72	1.0
3.4	4.219	4.6	37	2	0.0
			Total	**563,691**	

MSL(m)	Above SEAFRAME		Kainaba	SA (m^2)	V= (SA +SA)/2 x0.1(m^3)	SA(%)
-0.5	1.119	0.7	0.7	187500	18750	100.0
-0.4	1.219	0.8	0.8	187500	18750	100.0
-0.3	1.319	0.9	0.9	187500	18750	100.0
-0.2	1.419	1	1	187500	18750	100.0
-0.1	1.519	1.1	1.1	187500	18750	100.0
0	1.619	1.2	1.2	187500	18750	100.0
0.1	1.719	1.3	1.3	187500	18750	100.0
0.2	1.819	1.4	1.4	187500	18750	100.0
0.3	1.919	1.5	1.5	187500	18750	100.0
0.4	2.019	1.6	1.6	187500	18750	100.0
0.5	2.119	1.7	1.7	187500	18750	100.0
0.6	2.219	1.8	1.8	187500	18750	100.0
0.7	2.319	1.9	1.9	187500	18750	100.0
0.8	2.419	2	2	187500	18750	100.0
0.9	2.519	2.1	2.1	187500	18750	100.0
1	2.619	2.2	2.2	187500	18750	100.0
1.1	2.719	2.3	2.3	187500	18750	100.0
1.2	2.819	2.4	2.4	187500	18750	100.0
1.3	2.919	2.5	2.5	187500	18750	100.0
1.4	3.019	2.6	2.6	187500	18750	100.0
1.5	3.119	2.7	2.7	187499	18749	100.0
1.6	3.219	2.8	2.8	187488	18748	100.0
1.7	3.319	2.9	2.9	187464	18743	100.0
1.8	3.419	3	3	187390	18721	100.0
1.9	3.519	3.1	3.1	187030	18669	100.0
2	3.619	3.2	3.2	186342	18584	99.0
2.1	3.719	3.3	3.3	185328	18448	99.0
2.2	3.819	3.4	3.4	183624	18272	98.0
2.3	3.919	3.5	3.5	181811	17967	97.0
2.4	4.019	3.6	3.6	177523	17383	95.0
2.5	4.119	3.7	3.7	170130	16485	91.0
2.6	4.219	3.8	3.8	159562	15386	85.0
2.7	4.319	3.9	3.9	148152	14117	79.0
2.8	4.419	4	4	134192	12625	72.0
2.9	4.519	4.1	4.1	118300	10621	63.0
3	4.219	4.2	4.2	94118	8051	50.0
3.1	4.319	4.3	4.3	66895	5608	36.0
3.2	4.419	4.4	4.4	45268	3540	24.0
3.3	4.519	4.5	4.5	25533	1767	14.0
3.4	4.619	4.6	4.6	9811	808	5.0
3.5	4.719	4.7	4.7	6340	531	3.0
3.6	4.819	4.8	4.8	4280	214	2.0
3.7	4.919	4.9	4.9	0	0	0.0
			Total		**649,033**	

MSL(m)	Above SEAFRAME	29	SA (m^2)	V= (SA +SA)/2 x0.1(m^3)	SA(%)
-0.5	-0.518	0.7	5000	500	100.0
-0.4	-0.418	0.8	5000	500	100.0
-0.3	-0.318	0.9	5000	500	100.0
-0.2	-0.218	1	5000	500	100.0
-0.1	-0.118	1.1	5000	500	100.0
0	-0.018	1.2	5000	500	100.0
0.1	0.082	1.3	5000	500	100.0
0.2	0.182	1.4	5000	500	100.0
0.3	0.282	1.5	5000	500	100.0
0.4	0.382	1.6	5000	500	100.0
0.5	0.482	1.7	5000	500	100.0
0.6	0.582	1.8	5000	500	100.0
0.7	0.682	1.9	5000	500	100.0
0.8	0.782	2	5000	500	100.0
0.9	0.882	2.1	5000	500	100.0
1	0.982	2.2	5000	500	100.0
1.1	1.082	2.3	5000	500	100.0
1.2	1.182	2.4	5000	500	100.0
1.3	1.282	2.5	5000	500	100.0
1.4	1.382	2.6	5000	500	100.0
1.5	1.482	2.7	5000	500	100.0
1.6	1.582	2.8	5000	500	100.0
1.7	1.682	2.9	5000	500	100.0
1.8	1.782	3	5000	500	100.0
1.9	1.882	3.1	5000	500	100.0
2	1.982	3.2	5000	500	100.0
2.1	2.082	3.3	5000	500	100.0
2.2	2.182	3.4	4999	495	100.0
2.3	2.282	3.5	4898	448	98.0
2.4	2.382	3.6	4067	358	81.0
2.5	2.482	3.7	3098	271	62.0
2.6	2.582	3.8	2322	197	46.0
2.7	2.682	3.9	1609	110	32.0
2.8	2.782	4	581	32	12.0
2.9	2.882	4.1	54	3	1.0
3	2.982	4.2	0	0	0.0
		Total		**15,413**	

MSL(m)	Above SEAFRAME(m)	Bikenubati	SA (m^2)	V= (SA +SA)/2 x0.1(m^3)	SA(%)
-0.5	-0.518	0.7	65000	6500	100.0
-0.4	-0.418	0.8	65000	6500	100.0
-0.3	-0.318	0.9	65000	6500	100.0
-0.2	-0.218	1	65000	6500	100.0
-0.1	-0.118	1.1	65000	6500	100.0
0	-0.018	1.2	65000	6500	100.0
0.1	0.082	1.3	65000	6500	100.0
0.2	0.182	1.4	65000	6500	100.0
0.3	0.282	1.5	65000	6500	100.0
0.4	0.382	1.6	65000	6500	100.0
0.5	0.482	1.7	65000	6500	100.0
0.6	0.582	1.8	65000	6500	100.0
0.7	0.682	1.9	65000	6500	100.0
0.8	0.782	2	65000	6500	100.0
0.9	0.882	2.1	65000	6500	100.0
1	0.982	2.2	65000	6500	100.0
1.1	1.082	2.3	65000	6500	100.0
1.2	1.182	2.4	65000	6500	100.0
1.3	1.282	2.5	65000	6500	100.0
1.4	1.382	2.6	65000	6500	100.0
1.5	1.482	2.7	65000	6500	100.0
1.6	1.582	2.8	65000	6500	100.0
1.7	1.682	2.9	65000	6500	100.0
1.8	1.782	3	65000	6500	100.0
1.9	1.882	3.1	65000	6500	100.0
2	1.982	3.2	65000	6500	100.0
2.1	2.082	3.3	65000	6499	100.0
2.2	2.182	3.4	64974	6165	100.0
2.3	2.282	3.5	58321	5399	90.0
2.4	2.382	3.6	49655	4606	76.0
2.5	2.482	3.7	42457	3779	65.0
2.6	2.582	3.8	33119	2861	51.0
2.7	2.682	3.9	24105	2051	37.0
2.8	2.782	4	16914	1441	26.0
2.9	2.882	4.1	11903	994	18.0
3	2.982	4.2	7985	593	12.0
3.1	3.082	4.3	3885	264	6.0
3.2	3.182	4.4	1393	98	2.0
3.3	3.282	4.5	563	36	1.0
3.4	3.382	4.6	156	8	0.2
3.5	3.482	4.7	2	0	0.0
3.6	3.582	4.8	0	0	0.0
		Total		**203,793**	

MSL(m)	Above SEAFRAME (m)	Nea	SA (m^2)	V= (SA +SA)/2 x0.1(m^3)	SA (%)
-0.5	-0.518	0.7	82500	8250	100.0
-0.4	-0.418	0.8	82500	8250	100.0
-0.3	-0.318	0.9	82500	8250	100.0
-0.2	-0.218	1	82500	8250	100.0
-0.1	-0.118	1.1	82500	8250	100.0.
0	-0.018	1.2	82500	8250	100.0
0.1	0.082	1.3	82500	8250	100.0
0.2	0.182	1.4	82500	8250	100.0
0.3	0.282	1.5	82500	8250	100.0
0.4	0.382	1.6	82500	8250	100.0
0.5	0.482	1.7	82500	8250	100.0
0.6	0.582	1.8	82500	8250	100.0
0.7	0.682	1.9	82500	8250	100.0
0.8	0.782	2	82500	8250	100.0
0.9	0.882	2.1	82500	8235	100.0
1	0.982	2.2	82206	8195	100.0
1.1	1.082	2.3	81687	8130	99.0
1.2	1.182	2.4	80908	8039	98.0
1.3	1.282	2.5	79870	7910	97.0
1.4	1.382	2.6	78338	7703	95.0
1.5	1.482	2.7	75725	7109	92.0
1.6	1.582	2.8	66447	6433	81.0
1.7	1.682	2.9	62205	6005	75.0
1.8	1.782	3	57891	5362	70.0
1.9	1.882	3.1	49357	4386	60.0
2	1.982	3.2	38371	3254	47.0
2.1	2.082	3.3	26706	2289	32.0
2.2	2.182	3.4	19067	1534	23.0
2.3	2.282	3.5	11603	1160	14.0
2.4	2.382	3.6	11603	995	14.0
2.5	2.482	3.7	8290	631	10.0
2.6	2.582	3.8	4321	283	5.0
2.7	2.682	3.9	1331	67	2.0
2.8	2.782	4	0	0	0.0
		Total		**203,218**	

MSL (m)	Above SEAFRAME (m)	Biketawa	SA (m^2)	V= (SA +SA)/2 x0.1(m^3)	SA (%)
-0.5	-0.518	0.7	35000	3500	100.0
-0.4	-0.418	0.8	35000	3500	100.0
-0.3	-0.318	0.9	35000	3500	100.0
-0.2	-0.218	1	35000	3500	100.0
-0.1	-0.118	1.1	35000	3500	100.0
0	-0.018	1.2	35000	3500	100.0
0.1	0.082	1.3	35000	3500	100.0
0.2	0.182	1.4	35000	3500	100.0
0.3	0.282	1.5	35000	3500	100.0
0.4	0.382	1.6	35000	3500	100.0
0.5	0.482	1.7	35000	3500	100.0
0.6	0.582	1.8	35000	3500	100.0
0.7	0.682	1.9	35000	3500	100.0
0.8	0.782	2	35000	3500	100.0
0.9	0.882	2.1	35000	3500	100.0
1	0.982	2.2	35000	3500	100.0
1.1	1.082	2.3	35000	3500	100.0
1.2	1.182	2.4	35000	3500	100.0
1.3	1.282	2.5	35000	3500	100.0
1.4	1.382	2.6	35000	3500	100.0
1.5	1.482	2.7	35000	3500	100.0
1.6	1.582	2.8	35000	3500	100.0
1.7	1.682	2.9	35000	3500	100.0
1.8	1.782	3	35000	3500	100.0
1.9	1.882	3.1	35000	3492	100.0
2	1.982	3.2	34844	3345	100.0
2.1	2.082	3.3	32048	2942	92.0
2.2	2.182	3.4	26790	2526	77.0
2.3	2.282	3.5	23730	2199	68.0
2.4	2.382	3.6	20240	1779	58.0
2.5	2.482	3.7	15339	778	44.0
2.6	2.582	3.8	230	12	1.0
2.7	2.682	3.9	0	0	0.0
		Total		**101,072**	

MSL(m)	Above SEAFRAME	Nabeina	SA (m^2)	V= (SA +SA)/2 x0.1(m^3)	SA(%)
-0.5	-0.518	0.7	260000	26000	100.0
-0.4	-0.418	0.8	260000	26000	100.0
-0.3	-0.318	0.9	260000	26000	100.0
-0.2	-0.218	1	260000	26000	100.0
-0.1	-0.118	1.1	260000	26000	100.0
0	-0.018	1.2	260000	26000	100.0
0.1	0.082	1.3	260000	26000	100.0
0.2	0.182	1.4	260000	26000	100.0
0.3	0.282	1.5	260000	26000	100.0
0.4	0.382	1.6	260000	26000	100.0
0.5	0.482	1.7	260000	26000	100.0
0.6	0.582	1.8	260000	26000	100.0
0.7	0.682	1.9	260000	26000	100.0
0.8	0.782	2	260000	26000	100.0
0.9	0.882	2.1	260000	26000	100.0
1	0.982	2.2	260000	26000	100.0
1.1	1.082	2.3	260000	26000	100.0
1.2	1.182	2.4	260000	26000	100.0
1.3	1.282	2.5	260000	26000	100.0
1.4	1.382	2.6	260000	26000	100.0
1.5	1.482	2.7	260000	26000	100.0
1.6	1.582	2.8	260000	26000	100.0
1.7	1.682	2.9	260000	25986	100.0
1.8	1.782	3	259719	25800	100.0
1.9	1.882	3.1	256272	25293	99.0
2	1.982	3.2	249590	24640	96.0
2.1	2.082	3.3	243209	23829	94.0
2.2	2.182	3.4	233379	22724	90.0
2.3	2.282	3.5	221102	21359	85.0
2.4	2.382	3.6	206081	19901	79.0
2.5	2.482	3.7	191938	18547	74.0
2.6	2.582	3.8	179000	15410	69.0
2.7	2.682	3.9	129192	10268	50.0
2.8	2.782	4	76174	6556	29.0
2.9	2.882	4.1	54953	4696	21.0
3	2.982	4.2	38957	3371	15.0
3.1	3.082	4.3	28465	2477	11.0
3.2	3.182	4.4	21070	1847	8.0
3.3	3.282	4.5	15868	1322	6.0
3.4	3.382	4.6	10566	829	4.0
3.5	3.482	4.7	6014	410	2.0
3.6	3.582	4.8	2187	152	1.0
3.7	3.682	4.9	847	56	0.3
3.8	3.782	5	271	14	0.1
3.9	3.882	5.1	14	1	0.0
4	3.982	5.2	0	0	0.0
		Total		**827,487**	

MSL (m)	Above SEAFRAME (m)	Tabiang	SA (m^2)	V= (SA +SA)/2 x0.1(m^3)	SA (%)
-0.5	-0.518	0.7	642500	64250	100.0
-0.4	-0.418	0.8	642500	64250	100.0
-0.3	-0.318	0.9	642500	64250	100.0
-0.2	-0.218	1	642500	64250	100.0
-0.1	-0.118	1.1	642500	64250	100.0
0	-0.018	1.2	642500	64250	100.0
0.1	0.082	1.3	642500	64250	100.0
0.2	0.182	1.4	642500	64250	100.0
0.3	0.282	1.5	642500	64250	100.0
0.4	0.382	1.6	642500	64250	100.0
0.5	0.482	1.7	642500	64250	100.0
0.6	0.582	1.8	642500	64250	100.0
0.7	0.682	1.9	642500	64250	100.0
0.8	0.782	2	642500	64250	100.0
0.9	0.882	2.1	642500	64250	100.0
1	0.982	2.2	642490	64245	100.0
1.1	1.082	2.3	642413	64208	100.0
1.2	1.182	2.4	641755	64124	100.0
1.3	1.282	2.5	640728	63932	100.0
1.4	1.382	2.6	637921	63523	99.0
1.5	1.482	2.7	632530	62877	98.0
1.6	1.582	2.8	625003	62062	97.0
1.7	1.682	2.9	616244	61016	96.0
1.8	1.782	3	604069	59783	94.0
1.9	1.882	3.1	591596	58467	92.0
2	1.982	3.2	577745	56580	90.0
2.1	2.082	3.3	553852	53375	86.0
2.2	2.182	3.4	513655	48152	80.0
2.3	2.282	3.5	449384	41014	70.0
2.4	2.382	3.6	370894	33996	58.0
2.5	2.482	3.7	309032	28844	48.0
2.6	2.582	3.8	267854	24308	42.0
2.7	2.682	3.9	218315	19249	34.0
2.8	2.782	4	166659	14936	26.0
2.9	2.882	4.1	132057	11414	21.0
3	2.982	4.2	96221	7948	15.0
3.1	3.082	4.3	62734	4805	10.0
3.2	3.182	4.4	33362	2215	5.0
3.3	3.282	4.5	10932	818	2.0
3.4	3.382	4.6	5421	338	1.0
3.5	3.482	4.7	1337	67	0.0
3.6	3.582	4.8	0	0	0.0
		Total		**1,936,045**	

MSL(m)	Above SEAFRAME (m)	44	SA (m^2)	V= (SA +SA)/2 x0.1(m^3)	SA (%)
-0.5	-0.518	0.7	227500	22750	100
-0.4	-0.418	0.8	227500	22750	100
-0.3	-0.318	0.9	227500	22750	100
-0.2	-0.218	1	227500	22750	100
-0.1	-0.118	1.1	227500	22750	100
0	-0.018	1.2	227500	22750	100
0.1	0.082	1.3	227500	22750	100
0.2	0.182	1.4	227500	22750	100
0.3	0.282	1.5	227500	22750	100
0.4	0.382	1.6	227500	22750	100
0.5	0.482	1.7	227500	22750	100
0.6	0.582	1.8	227500	22750	100
0.7	0.682	1.9	227500	22750	100
0.8	0.782	2	227500	22750	100
0.9	0.882	2.1	227500	22750	100
1	0.982	2.2	227500	22750	100
1.1	1.082	2.3	227500	22750	100
1.2	1.182	2.4	227500	22750	100
1.3	1.282	2.5	227500	22750	100
1.4	1.382	2.6	227500	22750	100
1.5	1.482	2.7	227500	22750	100
1.6	1.582	2.8	227500	22750	100
1.7	1.682	2.9	227500	22750	100
1.8	1.782	3	227500	22741	100
1.9	1.882	3.1	227311	22485	100
2	1.982	3.2	222395	21579	98
2.1	2.082	3.3	209194	19780	92
2.2	2.182	3.4	186413	17576	82
2.3	2.282	3.5	165104	15235	73
2.4	2.382	3.6	139592	12312	61
2.5	2.482	3.7	106649	8856	47
2.6	2.582	3.8	70461	5094	31
2.7	2.682	3.9	31417	1946	14
2.8	2.782	4	7510	410	3
2.9	2.882	4.1	688	34	0
3	2.982	4.2	0	0	0
		Total		**671,298**	

MSL (m)	Above SEAFRAME (m)	Tabiteuea	SA (m^2)	V= (SA +SA)/2 x0.1(m^3)	SA(%)
-0.5	-0.518	0.7	812500	81250	100.0
-0.4	-0.418	0.8	812500	81250	100.0
-0.3	-0.318	0.9	812500	81250	100.0
-0.2	-0.218	1	812500	81250	100.0
-0.1	-0.118	1.1	812500	81250	100.0
0	-0.018	1.2	812500	81250	100.0
0.1	0.082	1.3	812500	81250	100.0
0.2	0.182	1.4	812500	81250	100.0
0.3	0.282	1.5	812500	81250	100.0
0.4	0.382	1.6	812500	81250	100.0
0.5	0.482	1.7	812500	81250	100.0
0.6	0.582	1.8	812500	81250	100.0
0.7	0.682	1.9	812500	81250	100.0
0.8	0.782	2	812500	81250	100.0
0.9	0.882	2.1	812500	81250	100.0
1	0.982	2.2	812500	81246	100.0
1.1	1.082	2.3	812415	81189	100.0
1.2	1.182	2.4	811365	81025	100.0
1.3	1.282	2.5	809139	80741	100.0
1.4	1.382	2.6	805690	80345	99.0
1.5	1.482	2.7	801203	79829	99.0
1.6	1.582	2.8	795385	79187	98.0
1.7	1.682	2.9	788354	78403	97.0
1.8	1.782	3	779705	76850	96.0
1.9	1.882	3.1	757298	73761	93.0
2	1.982	3.2	717917	69283	88.0
2.1	2.082	3.3	667751	64840	82.0
2.2	2.182	3.4	629048	60201	77.0
2.3	2.282	3.5	574974	53291	71.0
2.4	2.382	3.6	490847	43662	60.0
2.5	2.482	3.7	382399	33651	47.0
2.6	2.582	3.8	290611	26596	36.0
2.7	2.682	3.9	241310	22028	30.0
2.8	2.782	4	199250	17873	25.0
2.9	2.882	4.1	158202	13754	19.0
3	2.982	4.2	116872	10086	14.0
3.1	3.082	4.3	84848	7159	10.0
3.2	3.182	4.4	58331	4891	7.0
3.3	3.282	4.5	39498	3294	5.0
3.4	3.382	4.6	26389	2155	3.0
3.5	3.482	4.7	16717	1320	2.0
3.6	3.582	4.8	9686	677	1.0
3.7	3.682	4.9	3847	240	0.5
3.8	3.782	5	947	56	0.1
3.9	3.882	5.1	181	9	0.0
4	3.982	5.2	4	0	0.0
4.1	4.082	5.3	0	0	0.0
		Total		**2,446,393**	

MSL(m)	Above SEAFRAME	Abatao	SA (m^2)	V= (SA +SA)/2 x0.1(m^3)	SA(%)
-0.5	-0.518	0.7	649919	64989	100.0
-0.4	-0.418	0.8	649868	64985	100.0
-0.3	-0.318	0.9	649840	64978	100.0
-0.2	-0.218	1	649727	64968	100.0
-0.1	-0.118	1.1	649638	64959	100.0
0	-0.018	1.2	649536	64948	100.0
0.1	0.082	1.3	649422	64936	100.0
0.2	0.182	1.4	649295	64923	100.0
0.3	0.282	1.5	649156	64908	100.0
0.4	0.382	1.6	649003	64892	100.0
0.5	0.482	1.7	648839	64875	100.0
0.6	0.582	1.8	648662	64857	100.0
0.7	0.682	1.9	648472	64837	100.0
0.8	0.782	2	648270	64816	100.0
0.9	0.882	2.1	648055	64794	100.0
1	0.982	2.2	647818	64762	100.0
1.1	1.082	2.3	647418	64711	100.0
1.2	1.182	2.4	646802	64149	100.0
1.3	1.282	2.5	636183	62529	98.0
1.4	1.382	2.6	614387	59868	95.0
1.5	1.482	2.7	582979	57406	90.0
1.6	1.582	2.8	565148	55647	87.0
1.7	1.682	2.9	547790	53683	84.0
1.8	1.782	3	525871	51108	81.0
1.9	1.882	3.1	496299	47798	76.0
2	1.982	3.2	459668	43587	71.0
2.1	2.082	3.3	412067	38382	63.0
2.2	2.182	3.4	355571	31553	55.0
2.3	2.282	3.5	275492	22933	42.0
2.4	2.382	3.6	183171	14039	28.0
2.5	2.482	3.7	97603	7629	15.0
2.6	2.582	3.8	54986	4201	8.0
2.7	2.682	3.9	29038	2063	4.0
2.8	2.782	4	12228	893	2.0
2.9	2.882	4.1	5642	387	1.0
3	2.982	4.2	2093	133	0.3
3.1	3.082	4.3	559	28	0.1
3.2	3.182	4.4	0	0	0.0
		Total		**1,721,155**	

MSL(m)	Above SEAFRAME	Buota	SA (m^2)	V= (SA +SA)/2 x0.1(m^3)	S(%)
-0.5	-0.518	0.7	707500	70750	100.0
-0.4	-0.418	0.8	707500	70750	100.0
-0.3	-0.318	0.9	707500	70750	100.0
-0.2	-0.218	1	707500	70750	100.0
-0.1	-0.118	1.1	707500	70750	100.0
0	-0.018	1.2	707500	70750	100.0
0.1	0.082	1.3	707500	70750	100.0
0.2	0.182	1.4	707500	70750	100.0
0.3	0.282	1.5	707500	70750	100.0
0.4	0.382	1.6	707500	70750	100.0
0.5	0.482	1.7	707500	70750	100.0
0.6	0.582	1.8	707500	70750	100.0
0.7	0.682	1.9	707500	70750	100.0
0.8	0.782	2	707500	70750	100.0
0.9	0.882	2.1	707500	70750	100.0
1	0.982	2.2	707500	70750	100.0
1.1	1.082	2.3	707499	70679	100.0
1.2	1.182	2.4	706074	70293	100.0
1.3	1.282	2.5	699786	69540	99.0
1.4	1.382	2.6	691015	68094	98.0
1.5	1.482	2.7	670860	65950	95.0
1.6	1.582	2.8	648150	63196	92.0
1.7	1.682	2.9	615778	60056	87.0
1.8	1.782	3	585348	56676	83.0
1.9	1.882	3.1	548178	52636	77.0
2	1.982	3.2	504539	47827	71.0
2.1	2.082	3.3	452010	42223	64.0
2.2	2.182	3.4	392457	36749	55.0
2.3	2.282	3.5	342532	32307	48.0
2.4	2.382	3.6	303605	28724	43.0
2.5	2.482	3.7	270872	25633	38.0
2.6	2.582	3.8	241781	23027	34.0
2.7	2.682	3.9	218755	20763	31.0
2.8	2.782	4	196511	18673	28.0
2.9	2.882	4.1	176955	16789	25.0
3	2.982	4.2	158824	14863	22.0
3.1	3.082	4.3	138446	13061	20.0
3.2	3.182	4.4	122774	11317	17.0
3.3	3.282	4.5	103559	9054	15.0
3.4	3.382	4.6	77531	6859	11.0
3.5	3.482	4.7	59656	5137	8.0
3.6	3.582	4.8	43091	3640	6.0
3.7	3.682	4.9	29699	2577	4.0
3.8	3.782	5	21850	1783	3.0
3.9	3.882	5.1	13816	713	2.0
4	3.982	5.2	449	22	0.1
4.1	4.082	5.3	0	0	0.0
		Total		**2,070,865**	

MSL(m)	Above SEAFRAME	Tanaea	SA (m^2)	V= (SA +SA)/2 x0.1(m^3)	SA(%)
-0.5	-0.518	0.7	45000	4500	100.0
-0.4	-0.418	0.8	45000	4500	100.0
-0.3	-0.318	0.9	45000	4500	100.0
-0.2	-0.218	1	45000	4500	100.0
-0.1	-0.118	1.1	45000	4500	100.0
0	-0.018	1.2	45000	4500	100.0
0.1	0.082	1.3	45000	4500	100.0
0.2	0.182	1.4	45000	4500	100.0
0.3	0.282	1.5	45000	4500	100.0
0.4	0.382	1.6	45000	4500	100.0
0.5	0.482	1.7	45000	4500	100.0
0.6	0.582	1.8	45000	4500	100.0
0.7	0.682	1.9	45000	4500	100.0
0.8	0.782	2	45000	4500	100.0
0.9	0.882	2.1	45000	4500	100.0
1	0.982	2.2	45000	4500	100.0
1.1	1.082	2.3	45000	4498	100.0
1.2	1.182	2.4	44955	4477	100.0
1.3	1.282	2.5	44579	4433	99.0
1.4	1.382	2.6	44079	4377	98.0
1.5	1.482	2.7	43471	4311	97.0
1.6	1.582	2.8	42746	4232	95.0
1.7	1.682	2.9	41890	4139	93.0
1.8	1.782	3	40894	4032	91.0
1.9	1.882	3.1	39743	3902	88.0
2	1.982	3.2	38293	3746	85.0
2.1	2.082	3.3	36620	3565	81.0
2.2	2.182	3.4	34687	3340	77.0
2.3	2.282	3.5	32105	2960	71.0
2.4	2.382	3.6	27104	2048	60.0
2.5	2.482	3.7	13853	888	31.0
2.6	2.582	3.8	3901	291	9.0
2.7	2.682	3.9	1910	129	4.0
2.8	2.782	4	679	39	2.0
2.9	2.882	4.1	91	5	0.0
3	2.982	4.2	0	0	0.0
		Total		**127,410**	

MSL	Above SEAFRAME	Bonriki-Taborio	SA (m^2)	V= (SA +SA)/2 x0.1(m^3)	SA%
-0.5	-0.518	0.7	7392500	739250	100.0
-0.4	-0.418	0.8	7392500	739250	100.0
-0.3	-0.318	0.9	7392500	739250	100.0
-0.2	-0.218	1	7392500	739250	100.0
-0.1	-0.118	1.1	7392500	739250	100.0
0	-0.018	1.2	7392500	739250	100.0
0.1	0.082	1.3	7392498	739250	100.0
0.2	0.182	1.4	7392498	739247	100.0
0.3	0.282	1.5	7392444	739213	100.0
0.4	0.382	1.6	7391820	739056	100.0
0.5	0.482	1.7	7389292	738774	100.0
0.6	0.582	1.8	7386180	738430	100.0
0.7	0.682	1.9	7382419	737628	100.0
0.8	0.782	2	7370134	735790	100.0
0.9	0.882	2.1	7345671	730809	99.0
1	0.982	2.2	7270517	716342	98.0
1.1	1.082	2.3	7056329	687641	95.0
1.2	1.182	2.4	6696497	640155	91.0
1.3	1.282	2.5	6106610	582824	83.0
1.4	1.382	2.6	5549878	531571	75.0
1.5	1.482	2.7	5081540	487701	69.0
1.6	1.582	2.8	4672483	449863	63.0
1.7	1.682	2.9	4324786	414422	59.0
1.8	1.782	3	3963650	375579	54.0
1.9	1.882	3.1	3547935	334041	48.0
2	1.982	3.2	3132895	293391	42.0
2.1	2.082	3.3	2734922	254249	37.0
2.2	2.182	3.4	2350060	215664	32.0
2.3	2.282	3.5	1963225	178208	27.0
2.4	2.382	3.6	1600932	143014	22.0
2.5	2.482	3.7	1259353	111233	17.0
2.6	2.582	3.8	965299	85722	13.0
2.7	2.682	3.9	749146	66725	10.0
2.8	2.782	4	585354	52371	8.0
2.9	2.882	4.1	462073	41311	6.0
3	2.982	4.2	364146	32578	5.0
3.1	3.082	4.3	287405	24766	4.0
3.2	3.182	4.4	207913	17716	3.0
3.3	3.282	4.5	146401	12191	2.0
3.4	3.382	4.6	97415	7820	1.0
3.5	3.482	4.7	58987	4679	1.0
3.6	3.582	4.8	34597	2761	0.5
3.7	3.682	4.9	20615	1642	0.3
3.8	3.782	5	12227	972	0.2
3.9	3.882	5.1	7207	456	0.1
4	3.982	5.2	1917	124	0.0
4.1	4.082	5.3	567	33	0.0
4.2	4.182	5.4	87	5	0.0
4.3	4.282	5.5	16	1	0.0
4.4	4.382	5.6	0	0	0.0
		Total		**1,7841,469**	

MSL(m)	Above SEAFRAME	Abairaranga	SA (m^2)	V= (SA +SA)/2 x0.1(m^3)	SA(%)
-0.5	-0.518	0.7	2500	250	100.0
-0.4	-0.418	0.8	2500	250	100.0
-0.3	-0.318	0.9	2500	250	100.0
-0.2	-0.218	1	2500	250	100.0
-0.1	-0.118	1.1	2500	250	100.0
0	-0.018	1.2	2500	250	100.0
0.1	0.082	1.3	2500	250	100.0
0.2	0.182	1.4	2500	250	100.0
0.3	0.282	1.5	2500	250	100.0
0.4	0.382	1.6	2500	250	100.0
0.5	0.482	1.7	2500	250	100.0
0.6	0.582	1.8	2500	250	100.0
0.7	0.682	1.9	2500	250	100.0
0.8	0.782	2	2500	250	100.0
0.9	0.882	2.1	2500	250	100.0
1	0.982	2.2	2500	250	100.0
1.1	1.082	2.3	2500	250	100.0
1.2	1.182	2.4	2500	250	100.0
1.3	1.282	2.5	2500	250	100.0
1.4	1.382	2.6	2500	250	100.0
1.5	1.482	2.7	2500	250	100.0
1.6	1.582	2.8	2500	250	100.0
1.7	1.682	2.9	2500	250	100.0
1.8	1.782	3	2500	250	100.0
1.9	1.882	3.1	2500	250	100.0
2	1.982	3.2	2500	250	100.0
2.1	2.082	3.3	2500	250	100.0
2.2	2.182	3.4	2500	125	100.0
2.3	2.282	3.5	0	0	100.0
2.4	2.382	3.6	0.0	0	0.0
		Total		**6,875**	

MSL(m)	Above SEAFRAME	Abaokoro	SA (m^2)	V= (SA +SA)/2 x0.1(m^3)	SA(%)
-0.5	-0.518	0.7	10000	1000	100.0
-0.4	-0.418	0.8	10000	1000	100.0
-0.3	-0.318	0.9	10000	1000	100.0
-0.2	-0.218	1	10000	1000	100.0
-0.1	-0.118	1.1	10000	1000	100.0
0	-0.018	1.2	10000	1000	100.0
0.1	0.082	1.3	10000	1000	100.0
0.2	0.182	1.4	10000	1000	100.0
0.3	0.282	1.5	10000	1000	100.0
0.4	0.382	1.6	10000	1000	100.0
0.5	0.482	1.7	10000	1000	100.0
0.6	0.582	1.8	10000	1000	100.0
0.7	0.682	1.9	10000	1000	100.0
0.8	0.782	2	10000	1000	100.0
0.9	0.882	2.1	10000	1000	100.0
1	0.982	2.2	10000	1000	100.0
1.1	1.082	2.3	10000	1000	100.0
1.2	1.182	2.4	10000	1000	100.0
1.3	1.282	2.5	10000	1000	100.0
1.4	1.382	2.6	10000	1000	100.0
1.5	1.482	2.7	10000	996	100.0
1.6	1.582	2.8	9910.2	973	99.1
1.7	1.682	2.9	9545.4	922	95.5
1.8	1.782	3	8899.9	844	89.0
1.9	1.882	3.1	7973.7	737	79.7
2	1.982	3.2	6766.9	581	67.7
2.1	2.082	3.3	4849.6	334	48.5
2.2	2.182	3.4	1833.9	96	18.3
2.3	2.282	3.5	83.5	4	0.8
2.4	2.382	3.6	0.0	0	0.0
		Total		**25,486**	

MSL (m)	Above SEAFRAME	Ambo-Teaoraereke	SA (m^2)	V= (SA +SA)/2 x 0.1 (m^3)	SA (%)
-0.5	-0.518	0.7	1297500	129750	100.0
-0.4	-0.418	0.8	1297500	129750	100.0
-0.3	-0.318	0.9	1297500	129750	100.0
-0.2	-0.218	1	1297500	129750	100.0
-0.1	-0.118	1.1	1297500	129750	100.0
0	-0.018	1.2	1297500	129750	100.0
0.1	0.082	1.3	1297500	129750	100.0
0.2	0.182	1.4	1297500	129750	100.0
0.3	0.282	1.5	1297500	129750	100.0
0.4	0.382	1.6	1297500	129750	100.0
0.5	0.482	1.7	1297500	129750	100.0
0.6	0.582	1.8	1297500	129750	100.0
0.7	0.682	1.9	1297500	129750	100.0
0.8	0.782	2	1297498	129749	100.0
0.9	0.882	2.1	1297478	129746	100.0
1	0.982	2.2	1297433	129740	100.0
1.1	1.082	2.3	1297359	129728	100.0
1.2	1.182	2.4	1297202	129683	100.0
1.3	1.282	2.5	1296467	129247	100.0
1.4	1.382	2.6	1288483	127602	99.0
1.5	1.482	2.7	1263548	123682	97.0
1.6	1.582	2.8	1210088	119107	93.0
1.7	1.682	2.9	1172051	115149	90.0
1.8	1.782	3	1130924	110290	87.0
1.9	1.882	3.1	1074877	104130	83.0
2	1.982	3.2	1007715	97480	78.0
2.1	2.082	3.3	941889	90497	73.0
2.2	2.182	3.4	868043	83139	67.0
2.3	2.282	3.5	794743	75571	61.0
2.4	2.382	3.6	716676	68140	55.0
2.5	2.482	3.7	646118	60116	50.0
2.6	2.582	3.8	556199	50560	43.0
2.7	2.682	3.9	455003	39822	35.0
2.8	2.782	4	341434	29558	26.0
2.9	2.882	4.1	249729	20947	19.0
3	2.982	4.2	169208	13819	13.0
3.1	3.082	4.3	107172	8873	8.0
3.2	3.182	4.4	70293	5334	5.0
3.3	3.282	4.5	36388	2588	3.0
3.4	3.382	4.6	15370	1174	1.0
3.5	3.482	4.7	8103	605	1.0
3.6	3.582	4.8	4006	303	0.3
3.7	3.682	4.9	2049	150	0.2
3.8	3.782	5	943	71	0.1
3.9	3.882	5.1	482	37	0.0
4	3.982	5.2	260	19	0.0
4.1	4.082	5.3	118	8	0.0
4.2	4.182	5.4	35	2	0.0
4.3	4.282	5.5	2	0	0.0
4.4	4.382	5.6	0	0	0.0
		Total		**3,813,413**	

MSL(m)	Above SEAFRAME	Nanikai	SA (m^2)	V= (SA +SA)/2 x0.1(m^3)	SA(%)
-0.5	-0.518	0.7	45000	4500	100.0
-0.4	-0.418	0.8	45000	4500	100.0
-0.3	-0.318	0.9	45000	4500	100.0
-0.2	-0.218	1	45000	4500	103.0
-0.1	-0.118	1.1	45000	4500	100.0
0	-0.018	1.2	45000	4500	100.0
0.1	0.082	1.3	45000	4500	100.0
0.2	0.182	1.4	45000	4500	100.0
0.3	0.282	1.5	45000	4500	100.0
0.4	0.382	1.6	45000	4500	100.0
0.5	0.482	1.7	44999	4499	100.0
0.6	0.582	1.8	44976	4495	100.0
0.7	0.682	1.9	44923	4488	100.0
0.8	0.782	2	44841	4479	100.0
0.9	0.882	2.1	44730	4466	99.0
1	0.982	2.2	44589	4450	99.0
1.1	1.082	2.3	44419	4432	99.0
1.2	1.182	2.4	44219	4410	98.0
1.3	1.282	2.5	43982	4375	98.0
1.4	1.382	2.6	43515	4299	97.0
1.5	1.482	2.7	42470	4162	94.0
1.6	1.582	2.8	40761	3935	91.0
1.7	1.682	2.9	37948	3620	84.0
1.8	1.782	3	34462	3247	77.0
1.9	1.882	3.1	30477	2772	68.0
2	1.982	3.2	24967	2192	55.0
2.1	2.082	3.3	18874	1558	42.0
2.2	2.182	3.4	12279	921	27.0
2.3	2.282	3.5	6133	382	14.0
2.4	2.382	3.6	1507	104	3.0
2.5	2.482	3.7	582	32	1.0
2.6	2.582	3.8	62	3	0.0
2.7	2.682	3.9	0	0	0.0
		Total		**112,322**	

MSL(m)	Above SEAFRAME	Bairiki	SA (m^2)	V= (SA +SA)/2 x0.1(m^3)	SA(%)
-0.5	-0.518	0.7	352500	35250	100.0
-0.4	-0.418	0.8	352500	35250	100.0
-0.3	-0.318	0.9	352500	35250	100.0
-0.2	-0.218	1	352500	35250	100.0
-0.1	-0.118	1.1	352499	35249	100.0
0	-0.018	1.2	352489	35248	100.0
0.1	0.082	1.3	352472	35247	100.0
0.2	0.182	1.4	352472	35243	100.0
0.3	0.282	1.5	352386	35230	100.0
0.4	0.382	1.6	352212	35207	100.0
0.5	0.482	1.7	351919	35169	100.0
0.6	0.582	1.8	351470	35116	100.0
0.7	0.682	1.9	350848	35045	100.0
0.8	0.782	2	350052	34955	99.0
0.9	0.882	2.1	349055	34857	99.0
1	0.982	2.2	348090	34764	99.0
1.1	1.082	2.3	347195	34676	99.0
1.2	1.182	2.4	346319	34584	98.0
1.3	1.282	2.5	345360	34479	98.0
1.4	1.382	2.6	344222	34347	98.0
1.5	1.482	2.7	342725	34166	97.0
1.6	1.582	2.8	340600	33914	97.0
1.7	1.682	2.9	337686	33549	96.0
1.8	1.782	3	333295	33021	95.0
1.9	1.882	3.1	327120	32301	93.0
2	1.982	3.2	318897	31403	90.0
2.1	2.082	3.3	309158	30307	88.0
2.2	2.182	3.4	296983	28690	84.0
2.3	2.282	3.5	276822	25189	79.0
2.4	2.382	3.6	226964	19490	64.0
2.5	2.482	3.7	162839	16120	46.0
2.6	2.582	3.8	159562	10590	45.0
2.7	2.682	3.9	52238	3980	15.0
2.8	2.782	4	27370	1818	8.0
2.9	2.882	4.1	8980	676	3.0
3	2.982	4.2	4543	375	1.0
3.1	3.082	4.3	2947	272	1.0
3.2	3.182	4.4	2500	162	1.0
3.3	3.282	4.5	742	37	0.0
3.4	3.382	4.6	0	0	0.0
		Total		**1,036,478**	

MSL(m)	Above SEAFRAME	Betio	SA (m^2)	V= (SA +SA)/2 x0.1(m^3)	SA (%)
-0.5	-0.518	0.7	1270000	127000	100.0
-0.4	-0.418	0.8	1270000	127000	100.0
-0.3	-0.318	0.9	1270000	127000	100.0
-0.2	-0.218	1	1270000	127000	100.0
-0.1	-0.118	1.1	1270000	127000	100.0
0	-0.018	1.2	1270000	127000	100.0
0.1	0.082	1.3	1270000	127000	100.0
0.2	0.182	1.4	1270000	127000	100.0
0.3	0.282	1.5	1270000	127000	100.0
0.4	0.382	1.6	1270000	127000	100.0
0.5	0.482	1.7	1270000	127000	100.0
0.6	0.582	1.8	1270000	127000	100.0
0.7	0.682	1.9	1270000	127000	100.0
0.8	0.782	2	1270000	127000	100.0
0.9	0.882	2.1	1270000	127000	100.0
1	0.982	2.2	1270000	127000	100.0
1.1	1.082	2.3	1270000	127000	100.0
1.2	1.182	2.4	1270000	127000	100.0
1.3	1.282	2.5	1270000	127000	100.0
1.4	1.382	2.6	1270000	127000	100.0
1.5	1.482	2.7	1270000	127000	100.0
1.6	1.582	2.8	1270000	126920	100.0
1.7	1.682	2.9	1268406	126640	100.0
1.8	1.782	3	1264386	125950	100.0
1.9	1.882	3.1	1254610	124903	99.0
2	1.982	3.2	1243457	123345	98.0
2.1	2.082	3.3	1223447	120212	96.0
2.2	2.182	3.4	1180785	112879	93.0
2.3	2.282	3.5	1076793	101412	85.0
2.4	2.382	3.6	951443	85468	75.0
2.5	2.482	3.7	757909	65027	60.0
2.6	2.582	3.8	542627	45247	43.0
2.7	2.682	3.9	362304	28422	29.0
2.8	2.782	4	206136	14884	16.0
2.9	2.882	4.1	91553	5809	7.0
3	2.982	4.2	24635	1409	2.0
3.1	3.082	4.3	3544	269	0.3
3.2	3.182	4.4	1835	130	0.1
3.3	3.282	4.5	764	46	0.1
3.4	3.382	4.6	151	8	0.0
3.5	3.482	4.7	0	0	0.0
		Total		**3,875,979**	

APPENDIX A-2. REEF ISLAND HYPSOMETRIC FORMS WITH GENERATED EXTREME SEA LEVEL FROM COASTAL CALCULATOR

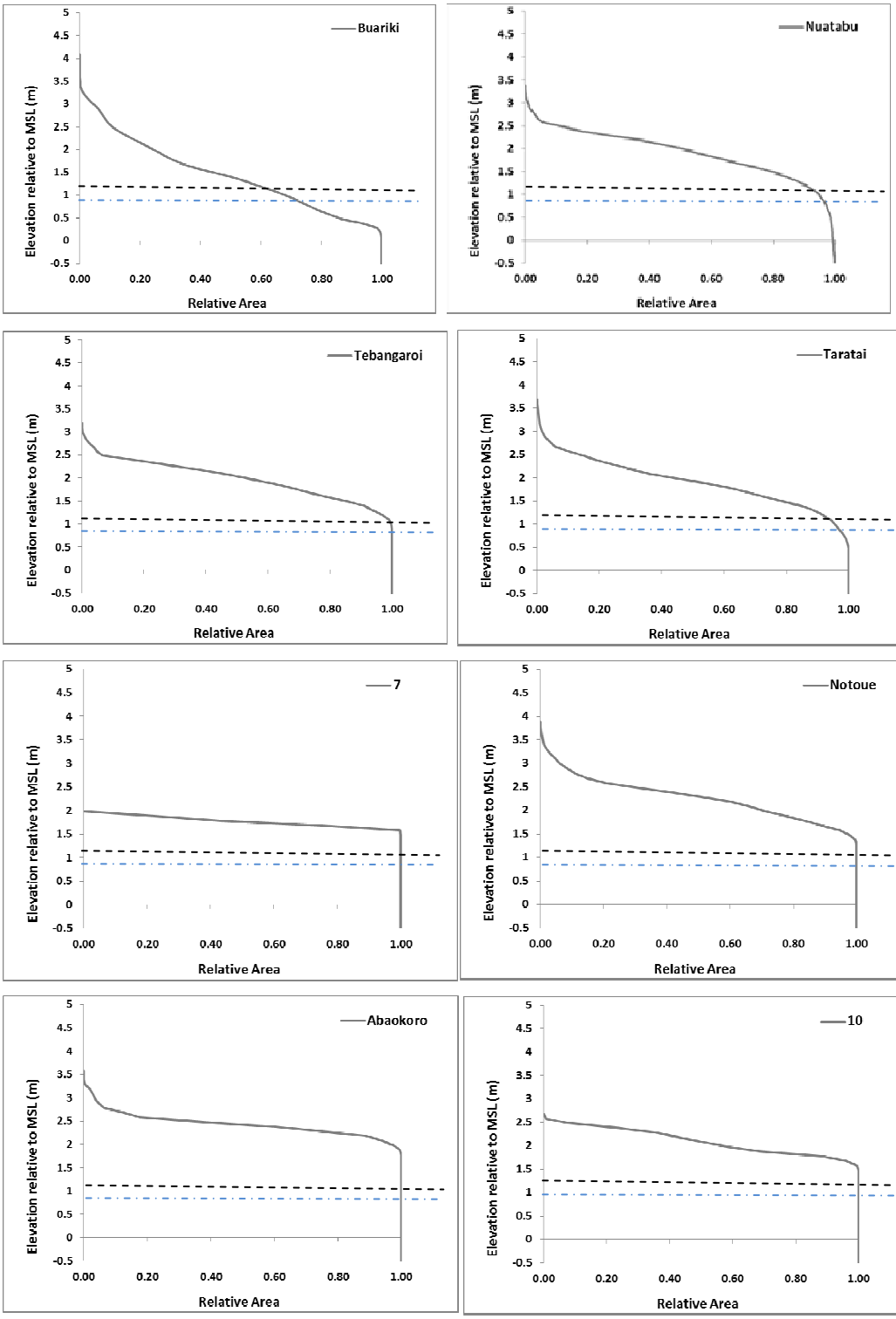

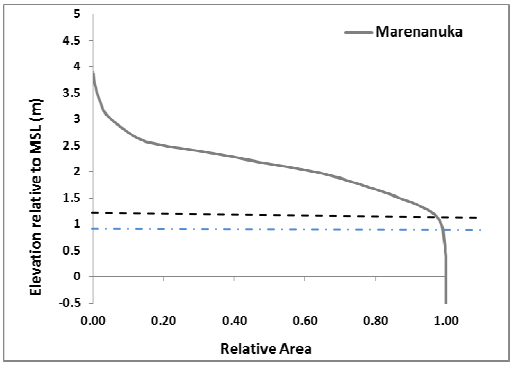

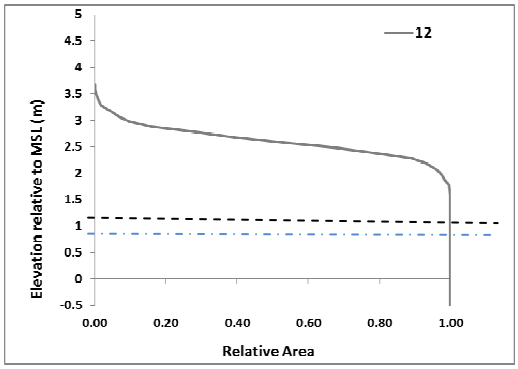

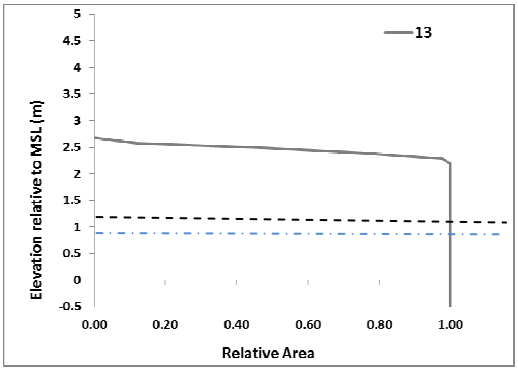

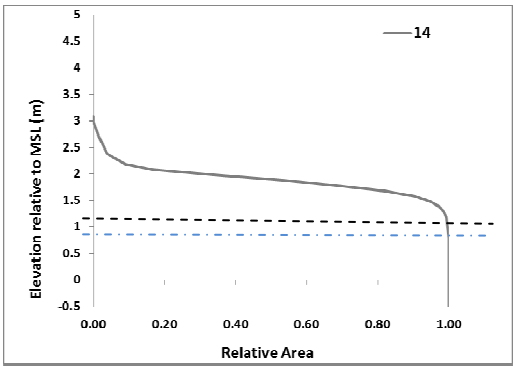

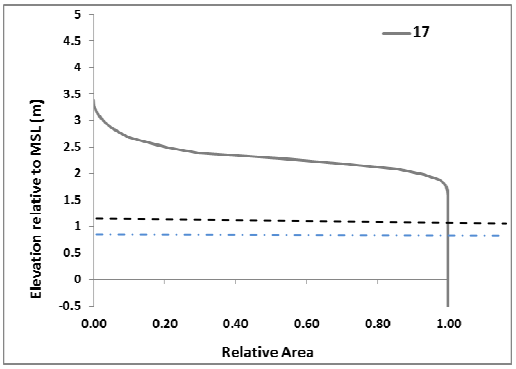

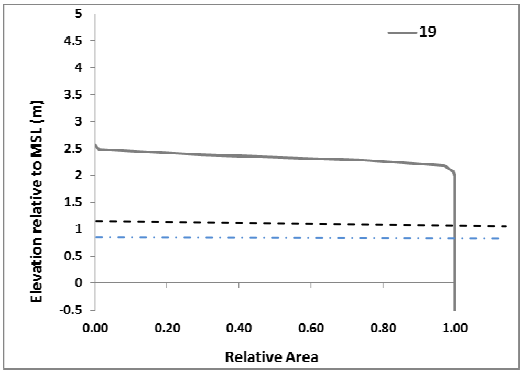

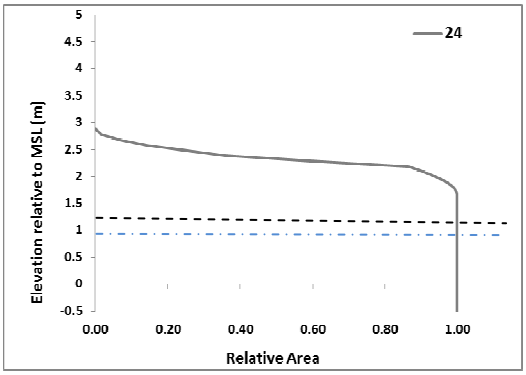

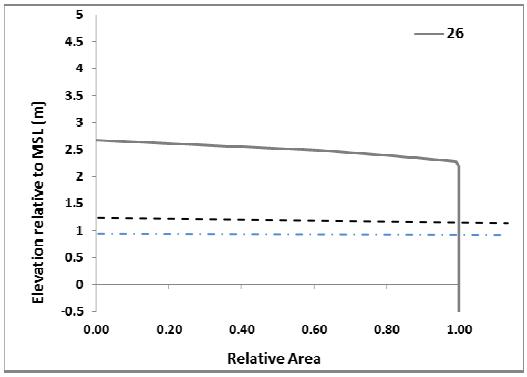

KEYS MHWSP ---------- MHWS

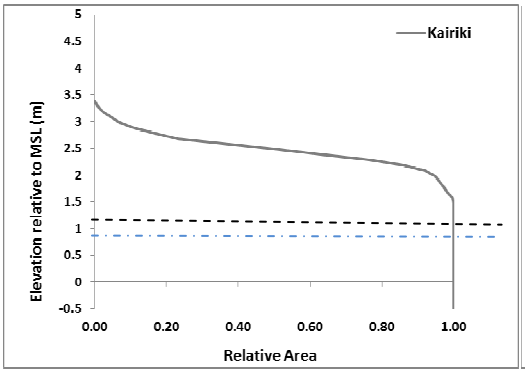

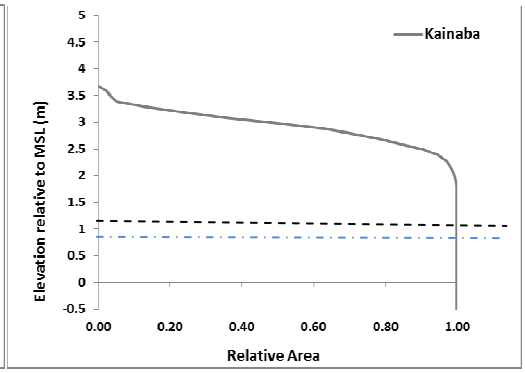

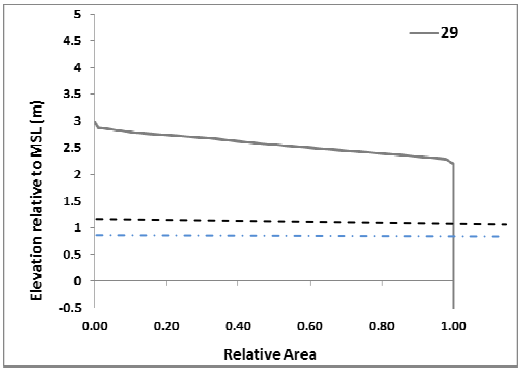

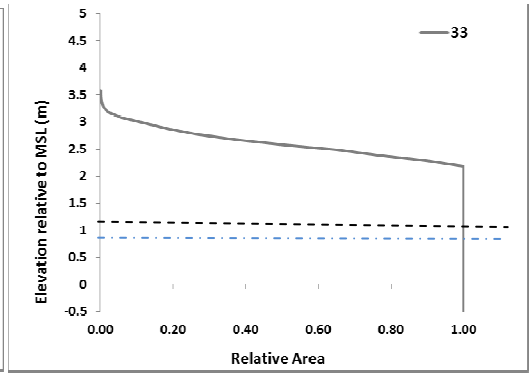

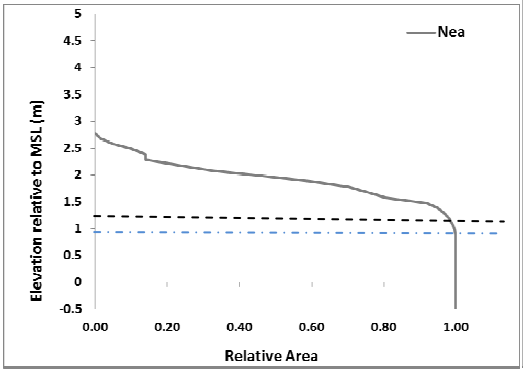

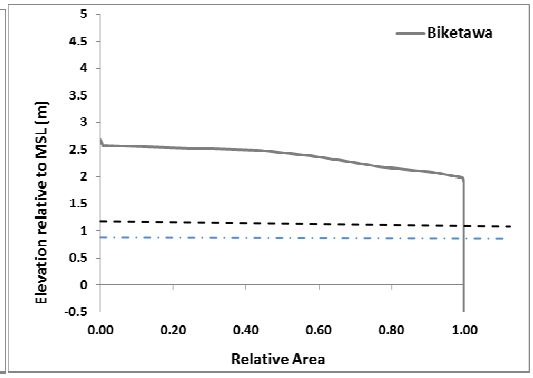

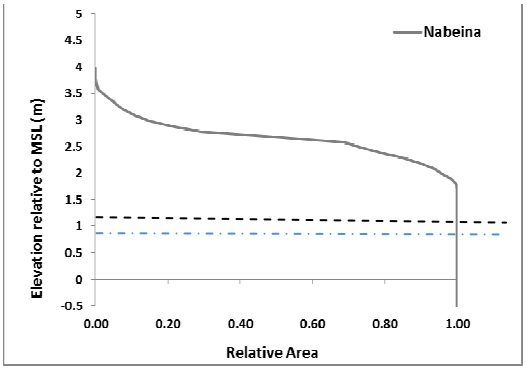

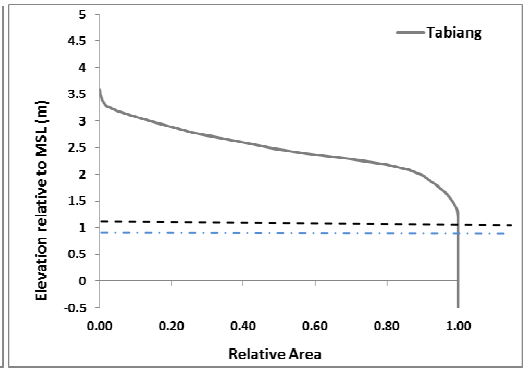

KEYS MHWSP ---------- MHWS

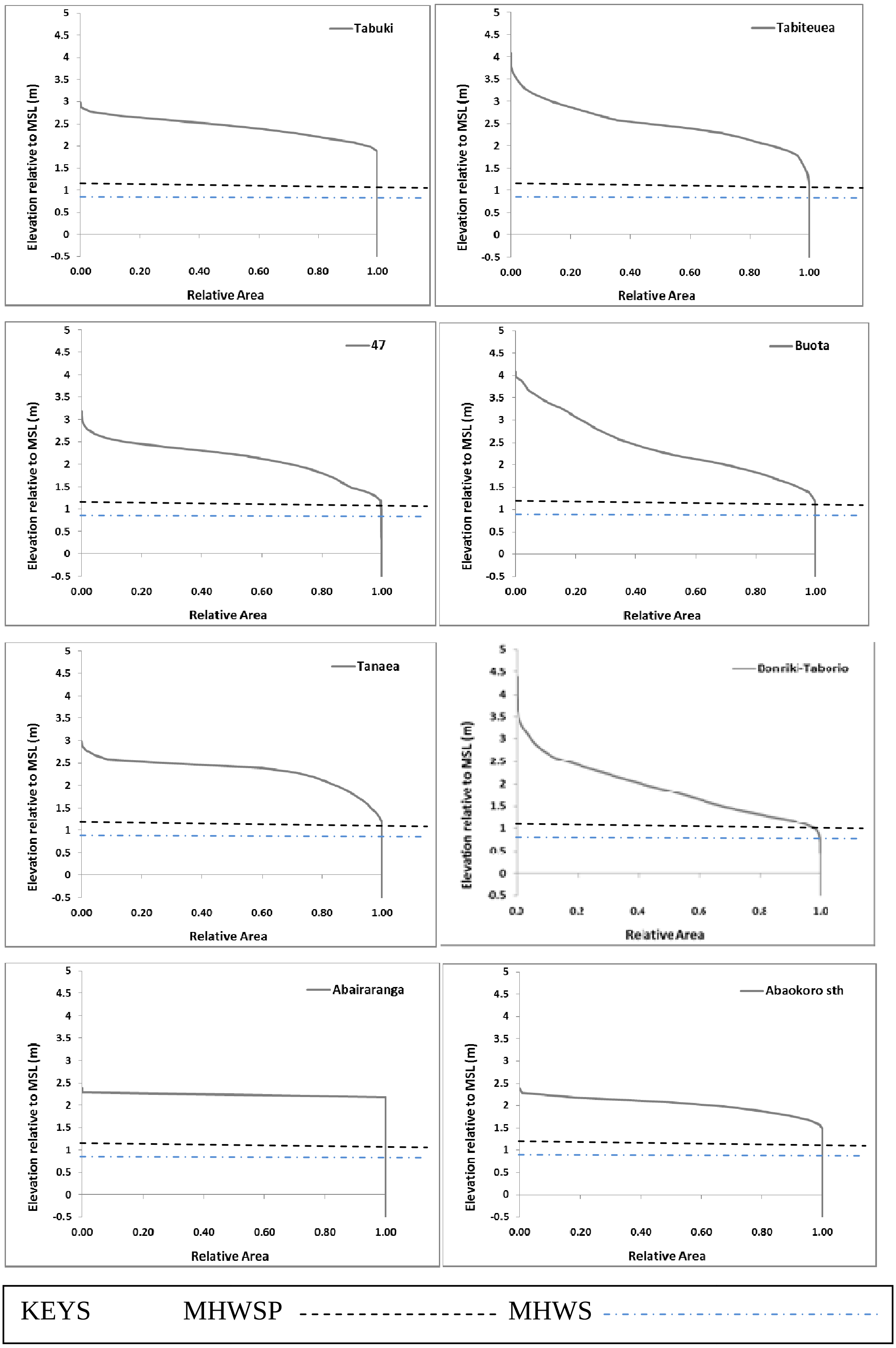
Tabuki
Tabiteuea
47
Buota
Tanaea
Bonriki-Taborio
Abairaranga
Abaokoro sth
Elevation relative to MSL (m)
Relative Area
5
4.5
4
3.5
3
2.5
2
1.5
1
0.5
0
-0.5
0.00
0.20
0.40
0.60
0.80
1.00
KEYS
MHWSP
MHWS

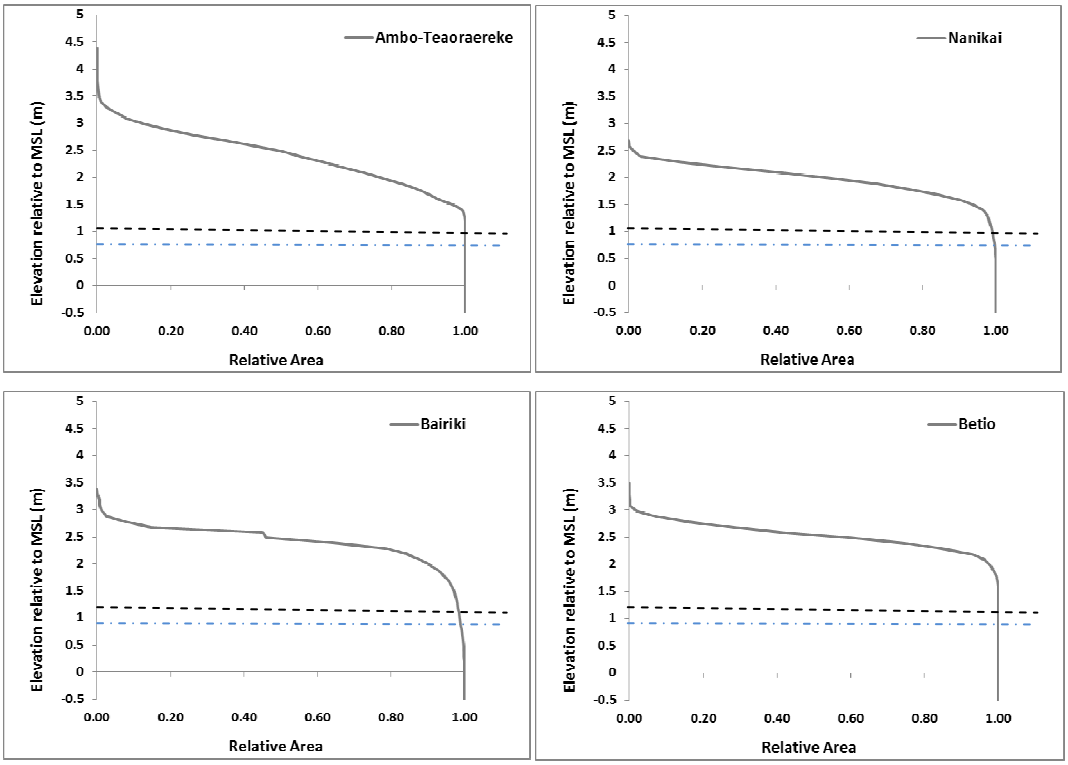

KEYS MHWSP ---------- MHWS

APPENDIX B-1. TAPHONOMIC INDICATORS UTILISED TO SELECT FORAMINIFERA SAMPLES

General Taphonomy for Foraminifera		
Taphonomic Indicator	**Grade**	**Description**
Completeness	0	Live Foraminifera, complete
	1	> 90% complete (able to identify to species level)
	2	< 90% complete, identifiable to species level
	3	<90% complete, identifiable to genus level
	4	<90% complete, unidentifiable to genus level
Corrasion dissolution, abrasion, and re-crystallisation	0	none, maybe transparent
	1	translucent, generally beginning of dissolution
	2	white surfaces, none to slight abrasion, retains structural strength
	3	white pores enlarged, strong abrasion of sculpture, minor delamination, and/or minor pitting, minor loss of structural strength
	4	chalky, sculpture gone, strong delamination, substantial integrity, internal structure of foraminifer invisible
Discolouration	0	none, strong original colour present or transparent
	1	slight fading of original colour, or translucent
	2	very strong fading of original colour, nearly totally white
	3	white, no original colour visible anywhere
	4	lightly discoloured e.g. light brown, light grey, light orange
	5	strongly discoloured e.g. black, dark grey
Lustre	0	original pearly lustre
	1	faded slightly, yet retains gloss, or oily state
	2	earthy, faded and no gloss
	3	chalky, no lustre
Fractures	0	None
	1	fractures present
Bioerosion	0	None
	1	single small hole
	2	single large hole
	3	multiple holes
	4	large multiple holes

APPENDIX B-2. RAW DATA FOR THE EXTENT OF AMINO ACID RACEMISATION OF *AMPHISTEGINA* FORAMINIFERA OBTAINED FROM DIFFERENT PIT AND BEACH SAMPLES

	Site Code	Asp	Glu	Serine	Alanine	Valine	Pheny	A/I	Leucine
		Area	area	area	area	area	area	area	area
Tabiteuea	7732A	0.37	0.14	0.06	0.27	0.17	0.04	0.24	0.19
Pit 1	7732B	0.44	0.21	0.23	0.36	0.20	0.23	0.25	0.18
	7732C	0.51	0.27	0.44	0.47	0.26	0.40	0.25	0.26
	7732D	0.53	0.29	0.51	0.50	0.30	0.54	0.32	0.30
	7732E	0.47	0.26	0.39	0.50	0.31	0.44	0.35	0.31
	7732F	0.49	0.27	0.38	0.44	0.25	0.48	0.30	0.26
	7732G	0.42	0.23	0.02	0.36	0.21	0.30	0.22	0.22
	7732H	0.52	0.28	0.37	0.49	0.29	0.54	0.36	0.30
	7732J	0.51	0.28	0.45	0.49	0.28	0.54	0.35	0.29
	7732K	0.47	0.22	0.35	0.37	0.22	0.39	0.27	0.23
	Ave	**0.47**	**0.24**	**0.32**	**0.43**	**0.25**	**0.39**	**0.29**	**0.25**
	Std dev.	**0.05**	**0.05**	**0.16**	**0.08**	**0.05**	**0.16**	**0.05**	**0.05**
	CV	**0.11**	**0.19**	**0.51**	**0.19**	**0.19**	**0.41**	**0.18**	**0.19**
Tabiteuea	7733A	0.31	0.14	0.08	0.28	0.17	0.12	0.25	0.20
Pit 2	7733A	0.36	0.16	0.09	0.30	0.19	0.10	0.34	0.23
	7733B	0.51	0.27	0.50	0.47	0.28	0.23	0.53	0.29
	7733C	0.46	0.25	0.42	0.42	0.24	0.43	0.26	0.25
	7733D	0.44	0.21	0.23	0.35	0.41	0.26	0.58	0.28
	7733E	0.49	0.25	0.46	0.42	0.25	0.46	0.31	0.24
	7733G	0.47	0.22	0.43	0.36	0.20	0.38	0.21	0.21
	7733H	0.47	0.21	0.44	0.35	0.20	0.36	0.23	0.20
	7733I	0.47	0.25	0.41	0.41	0.24	0.41	0.28	0.24
	7733J	0.50	0.26	0.00	0.00	0.00	0.00	0.00	0.00
	7733K	0.49	0.25	0.44	0.43	0.25	0.46	0.28	0.25
	Ave	**0.45**	**0.22**	**0.35**	**0.38**	**0.24**	**0.32**	**0.33**	**0.24**
	Std dev.	**0.06**	**0.04**	**0.16**	**0.06**	**0.07**	**0.14**	**0.13**	**0.03**
	CV	**0.14**	**0.19**	**0.45**	**0.16**	**0.28**	**0.42**	**0.39**	**0.13**
	Site Code	**Asp**	**Glu**	**Serine**	**Alanine**	**Valine**	**Phenye**	**A/I**	**Leucine**
Tabiteuea		Area	area	area	area	area	area	area	area
Pit 3	7734A	0.42	0.19	0.16	0.36	0.23	0.23	0.33	0.27
		0.36	0.15	0.10	0.30	0.21	0.17	0.10	0.23
	7734B	0.43	0.19	0.19	0.36	0.21	0.33	0.21	0.19
	7734C	0.46	0.22	0.27	0.39	0.25	0.43	0.34	0.22
	7734D	0.46	0.22	0.41	0.34	0.19	0.33	0.18	0.20
	7734E	0.47	0.23	0.46	0.38	0.24	0.41	0.26	0.24
	7734G	0.46	0.22	0.41	0.35	0.22	0.41	0.26	0.22
	7734H	0.46	0.23	0.39	0.38	0.25	0.36	0.27	0.23
	7734I	0.45	0.20	0.46	0.33	0.23	0.36	0.26	0.19
	7734K	0.46	0.22	0.37	0.34	0.20	0.38	0.26	0.21
	Aver	**0.44**	**0.21**	**0.32**	**0.35**	**0.22**	**0.34**	**0.25**	**0.22**
	Std dev.	**0.03**	**0.03**	**0.13**	**0.03**	**0.02**	**0.08**	**0.07**	**0.02**
	CV	**0.07**	**0.12**	**0.41**	**0.08**	**0.09**	**0.24**	**0.28**	**0.11**

Tabiteuea	7735A	0.39	0.16	0.05	0.33	0.23	0.10	0.38	0.25
Pit 4	7735A	0.48	0.32	0.29	0.45	0.00	0.00	0.00	0.00
	7735B	0.48	0.30	0.39	0.44	0.26	0.41	0.30	0.27
	7735C	0.48	0.25	0.39	0.41	0.25	0.40	0.21	0.24
	7735F	0.46	0.24	0.30	0.37	0.21	0.34	0.23	0.22
	7735G	0.49	0.25	0.33	0.42	0.25	0.43	0.27	0.23
	7735H	0.44	0.23	0.37	0.35	0.20	0.01	0.23	0.20
	7735I	0.46	0.24	0.35	0.35	0.19	0.32	0.21	0.21
	7735J	0.48	0.25	0.37	0.38	0.21	0.34	0.21	0.21
	7735K	0.47	0.25	0.33	0.38	0.23	0.34	0.25	0.22
	Aver	**0.46**	**0.25**	**0.32**	**0.39**	**0.23**	**0.30**	**0.26**	**0.23**
	Std dev.	**0.03**	**0.04**	**0.10**	**0.04**	**0.02**	**0.14**	**0.06**	**0.02**
	CV	**0.06**	**0.17**	**0.31**	**0.11**	**0.11**	**0.49**	**0.22**	**0.10**
	Site Code	**Asp**	**Glu**	**Serine**	**Alanine**	**valine**	**Phenyl**	**A/l**	**Leucine**
		Area	**area**	**area**	**area**	**area**	**area**	**area**	**area**
Tabiteuea	7736A	0.32	0.12	0.05	0.27	0.16	0.07	0.26	0.14
Pit 5	7736A	0.52	0.27	0.17	0.52	0.00	0.00	0.00	0.00
	7736B	0.43	0.22	0.32	0.33	0.20	0.33	0.22	0.19
	7736C	0.47	0.29	0.35	0.45	0.30	0.41	0.30	0.26
	7736D	0.50	0.25	0.41	0.44	0.28	0.53	0.31	0.27
	7736E	0.43	0.24	0.23	0.38	0.23	0.36	0.27	0.21
	7736F	0.43	0.22	0.32	0.39	0.23	0.35	0.25	0.21
	7736G	0.44	0.23	0.27	0.36	0.20	0.30	0.18	0.19
	7736H	0.35	0.17	0.14	0.29	0.18	0.25	0.21	0.15
	7736I	0.39	0.21	0.15	0.35	0.23	0.26	0.28	0.17
	7736J	0.44	0.21	0.25	0.34	0.19	0.00	0.21	0.19
	0.00	0.00	0.00	0.00	0.00	0.00	0.00	0.00	0.00
	Aver	**0.43**	**0.22**	**0.24**	**0.37**	**0.22**	**0.29**	**0.25**	**0.20**
	Std dev.	**0.06**	**0.05**	**0.11**	**0.07**	**0.04**	**0.15**	**0.04**	**0.04**
	CV	**0.14**	**0.21**	**0.44**	**0.19**	**0.20**	**0.54**	**0.17**	**0.21**
Tabiteuea	7737A	0.41	0.18	0.07	0.40	0.33	0.17	0.62	0.40
Pit 6	7737A	0.40	0.18	0.07	0.37	0.33	0.13	0.63	0.40
	7737B	0.47	0.26	0.38	0.42	0.22	0.34	0.16	0.21
	7737C	0.44	0.24	0.27	0.36	0.23	0.32	0.22	0.20
	7737D	0.41	0.26	0.35	0.42	0.39	0.40	0.45	0.28
	7737E	0.43	0.23	0.28	0.39	0.28	0.43	0.31	0.21
	7737F	0.33	0.19	0.17	0.26	0.15	0.22	0.19	0.13
	7737G	0.42	0.20	0.30	0.33	0.19	0.31	0.22	0.17
	7737H	0.47	0.24	0.39	0.44	0.27	0.46	0.29	0.26
	7737I	0.45	0.22	0.33	0.39	0.23	0.39	0.25	0.22
	7737J	0.39	0.20	0.21	0.33	0.29	0.36	0.36	0.19
	Ave	**0.42**	**0.22**	**0.26**	**0.37**	**0.26**	**0.32**	**0.33**	**0.24**
	Std dev.	**0.04**	**0.03**	**0.11**	**0.05**	**0.07**	**0.11**	**0.16**	**0.09**
	CV	**0.09**	**0.14**	**0.44**	**0.14**	**0.26**	**0.33**	**0.49**	**0.36**

	Site code	Asp	Glut	Serine	Alanine	Valine	Phenyl	A/I	Lecuine
		area	area	area	area	area	area	area	area
Notoue	7744B	0.32	0.15	0.38	0.19	0.12	0.22	0.12	0.11
Pit 1	7744C	0.32	0.13	0.36	0.18	0.11	0.20	0.11	0.11
	7744D	0.29	0.11	0.30	0.14	0.07	0.12	0.12	0.08
	7744E	0.32	0.14	0.37	0.19	0.10	0.18	0.01	0.11
	7744F	0.32	0.14	0.33	0.18	0.10	0.19	0.13	0.11
	7744G	0.31	0.13	0.38	0.18	0.11	0.18	0.12	0.10
	7744H	0.31	0.13	0.42	0.20	0.13	0.23	0.18	0.10
	7744I	0.33	0.14	0.37	0.19	0.10	0.20	0.11	0.11
	7744J	0.28	0.12	0.23	0.18	0.10	0.15	0.11	0.10
	Average	**0.31**	**0.13**	**0.35**	**0.18**	**0.10**	**0.19**	**0.11**	**0.10**
	Std dev.	**0.02**	**0.01**	**0.06**	**0.02**	**0.02**	**0.04**	**0.04**	**0.01**
	CV	**0.05**	**0.08**	**0.16**	**0.10**	**0.16**	**0.19**	**0.39**	**0.11**
Notoue	7745D	0.33	0.14	0.21	0.23	0.12			
Pit 2	7745E	0.29	0.10	0.22	0.16	0.09	0.16	0.11	0.10
	7745F	0.37	0.16	0.42	0.22	0.12	0.22	0.14	0.11
	7745G	0.32	0.13	0.37	0.19	0.10	0.17	0.15	0.10
	7745H	0.35	0.14	0.34	0.19	0.11	0.20	0.12	0.12
	7745I	0.31	0.12	0.29	0.16	0.09	0.18	0.11	0.10
	7745J	0.33	0.14	0.38	0.20	0.11	0.18	0.16	0.11
	7745K	0.31	0.12	0.34	0.16	0.09	0.15	0.10	0.10
	Ave	**0.33**	**0.13**	**0.32**	**0.19**	**0.10**	**0.18**	**0.13**	**0.10**
	Std dev.	**0.03**	**0.02**	**0.08**	**0.03**	**0.01**	**0.02**	**0.02**	**0.01**
	CV	**0.08**	**0.12**	**0.24**	**0.14**	**0.11**	**0.14**	**0.19**	**0.09**
Notoue	7746B	0.31	0.13	0.28	0.16	0.10	0.17	0.12	0.11
Pit 3	7746C	0.29	0.11	0.22	0.15	0.08	0.14	0.09	0.09
	7746D	0.29	0.19	0.13	0.18	0.10	0.14	0.09	0.10
	7746E	0.35	0.15	0.27	0.21	0.12	0.20	0.13	0.13
	7746G	0.32	0.12	0.29	0.17	0.11	0.21	0.12	0.11
	7746K	0.40	0.21	0.38	0.32	0.15	0.27	0.16	0.13
	Ave	**0.33**	**0.15**	**0.26**	**0.20**	**0.11**	**0.19**	**0.12**	**0.11**
	Std dev.	**0.04**	**0.04**	**0.08**	**0.06**	**0.02**	**0.05**	**0.02**	**0.02**
	CV	**0.13**	**0.27**	**0.32**	**0.31**	**0.20**	**0.27**	**0.21**	**0.14**

Notoue	Site code	Aspartic	Glutamic	Serine	Alanine	Valine	Phenylalanine	A/I	Lecuine
Pit 4	7747B	0.37	0.15	0.38	0.22	0.13	0.24	0.14	0.13
	7747C	0.36	0.22	0.29	0.24				
	7747D	0.39	0.28	0.44	0.32	0.21	0.31	0.12	0.19
	7747E	0.37	0.18	0.46	0.26	0.26	0.31	0.18	0.17
	7747F	0.34	0.14	0.34	0.22	0.12	0.19	0.13	0.12
	7747G	0.35	0.13	0.32	0.19	0.12	0.23	0.14	0.12
	7747I	0.36	0.13	0.31	0.18	0.10	0.19	0.13	0.12
	7747J	0.34	0.13	0.38	0.20	0.11	0.19	0.13	0.12
	7747K	0.32	0.01	0.37	0.19	0.11	0.19	0.13	0.10
	Ave	**0.35**	**0.15**	**0.37**	**0.23**	**0.14**	**0.23**	**0.14**	**0.13**
	Std dev.	**0.02**	**0.07**	**0.06**	**0.04**	**0.06**	**0.05**	**0.02**	**0.03**
	CV	**0.05**	**0.49**	**0.16**	**0.20**	**0.40**	**0.23**	**0.13**	**0.21**

Tabiteuea Ocean	Site code	Aspartic	Glutamic	Serine	Alanine	Valine	Phenylalanine	A/I	Lecuine
		area	**area**	**area**	**area**	**area**	**area**	**area**	**area**
	7731A	0.156	0.065	0.170	0.063	0.034	0.070	0.009	0.050
	7731B	0.232	0.111	0.332	0.133	0.055	0.103	0.090	0.066
	7731C	0.227	0.105	0.230	0.128	0.052	0.099	0.067	0.068
	7731D	0.125	0.057	0.187	0.051	0.028	0.043	0.041	0.030
	7731E	0.270	0.167	0.310	0.187	0.100	0.158	0.123	0.114
	7731F	0.181	0.073	0.181	0.075	0.035	0.077	0.013	0.053
	7731G	0.270	0.170	0.299	0.199	0.164	0.239	0.222	0.137
	7731H	0.185	0.089	0.220	0.109	0.048	0.069	0.056	0.059
	7731K	0.145	0.066	0.224	0.077	0.036	0.086	0.056	0.046
	7731L	0.245	0.125	0.293	0.147	0.072	0.121	0.067	0.090
	7731M	0.188	0.087	0.261	0.110	0.051	0.109	0.007	0.058
	7731N	0.186	0.091	0.227	0.104	0.050	0.005	0.010	0.063
	7731O	0.254	0.106	0.288	0.156	0.067	0.011	0.082	0.066
	7731P	0.169	0.084	0.320	0.101	0.034	0.080	0.032	0.042
	7731R	0.133	0.059	0.190	0.066	0.031	0.005	0.013	0.038
	7731S	0.226	0.105	0.317	0.125	0.061	0.005	0.054	0.062
	7731T	0.181	0.094	0.279	0.088	0.036	0.071	0.033	0.056
	7731U	0.351	0.158	0.329	0.236	0.140	0.014	0.179	0.120
	7731V	0.379	0.175	0.355	0.240	0.143	0.024	0.148	0.122
	7731W	0.249	0.116	0.335	0.140	0.076	0.021	0.090	0.078
	7731X	0.169	0.085	0.273	0.103	0.051	0.117	0.033	0.080
	7731Y	0.234	0.118	0.305	0.141	0.141	0.063	0.004	0.063
	Ave	**0.216**	**0.105**	**0.269**	**0.126**	**0.068**	**0.072**	**0.065**	**0.071**
	Std dev.	**0.06**	**0.04**	**0.06**	**0.05**	**0.04**	**0.06**	**0.06**	**0.03**
	CV	**29.97%**	**34.09%**	**21.04%**	**41.53%**	**61.07%**	**79.57%**	**90.21%**	**40.69%**

Tabiteuea Lagoon	Site code	Aspartic	Glutamic	Serine	Alanine	Valine	Phenylalanine	A/I	Lecuine
		area	area	area	area	area	area	area	area
	7738A	0.285	0.157	0.113	0.243	0.158	0.009	0.157	0.118
	7738D	0.287	0.152	0.287	0.186	0.118	0.174	0.100	0.091
	7738E	0.362	0.182	0.318	0.286	0.179	0.347	0.203	0.162
	7738F	0.306	0.169	0.260	0.227	0.139	0.213	0.142	0.119
	7738G	0.277	0.136	0.316	0.172	0.086	0.010	0.079	0.091
	7738H	0.314	0.161	0.254	0.237	0.132	0.215	0.140	0.125
	7738I	0.326	0.200	0.186	0.303	0.192	0.009	0.190	0.179
	7738J	0.198	0.097	0.194	0.123	0.059	0.098	0.052	0.058
	7738K	0.325	0.193	0.181	0.303	0.195	0.021	0.236	0.163
	7738M	0.267	0.157	0.116	0.223	0.143	0.011	0.170	0.116
	7738N	0.231	0.126	0.227	0.177	0.095	0.182	0.098	0.097
	7738O	0.207	0.123	0.148	0.161	0.086	0.006	0.094	0.082
	7738Q	0.254	0.137	0.302	0.155	0.091	0.097	0.075	0.074
	7738S	0.360	0.201	0.267	0.336	0.189	0.261	0.181	0.167
	7738T	0.268	0.170	0.183	0.273	0.151	0.214	0.196	0.140
	7738U	0.245	0.162	0.169	0.259	0.159	0.018	0.163	0.132
	7738W	0.236	0.128	0.206	0.183	0.151	0.146	0.104	0.089
	7738X	0.245	0.121	0.260	0.150	0.073	0.131	0.080	0.076
	7738Y	0.218	0.109	0.208	0.117	0.063	0.126	0.021	0.063
	Average	**0.274**	**0.152**	**0.221**	**0.217**	**0.129**	**0.120**	**0.131**	**0.113**
	Std dev.	**0.05**	**0.03**	**0.06**	**0.06**	**0.04**	**0.10**	**0.06**	**0.04**
	CV	**17.66%**	**19.99%**	**28.59%**	**29.98%**	**34.67%**	**84.95%**	**44.50%**	**32.83%**

Notoue Ocean	Site code	Aspartic	Glutamic	Serine	Alanine	Valine	Phenylalanine	A/I	Lecuine
		area	area	area	area	area	area	area	area
	7743A	0.084	0.038	0.088	0.038	0.037	0.004	0.040	0.003
	7743B	0.090	0.045	0.047	0.044	0.040	0.003	0.035	0.002
	7743C	0.080	0.036	0.077	0.034	0.040	0.002	0.020	0.027
	7743D	0.061	0.033	0.056	0.029	0.025	0.037	0.017	0.014
	7743E	0.071	0.081	0.143	0.066	0.132	0.108	0.316	0.076
	7743F	0.097	0.043	0.126	0.040	0.060	0.006	0.035	0.024
	7743G	0.082	0.039	0.055	0.038	0.036	0.004	0.026	0.037
	7743H	0.287	0.142	0.340	0.181	0.088	0.149	0.109	0.085
	7743I	0.068	0.093	0.109	0.091	0.077	0.051	0.046	0.018
	7743J	0.087	0.046	0.062	0.038	0.023	0.042	0.059	0.028
	7743K	0.071	0.036	0.061	0.036	0.032	0.002	0.014	0.032
	7743M	0.085	0.051	0.064	0.039	0.021	0.034	0.019	0.028
	7743N	0.082	0.055	0.082	0.036	0.031	0.030	0.061	0.021
	7743O	0.091	0.037	0.143	0.037	0.016	0.035	0.010	0.020
	7743P	0.074	0.038	0.062	0.031	0.031	0.043	0.012	0.034
	7743Q	0.088	0.041	0.098	0.035	0.043	0.051	0.036	0.027
	7743R	0.078	0.041	0.066	0.036	0.020	0.034	0.070	0.021
	7743S	0.095	0.002	0.094	0.046	0.033	0.044	0.023	0.039
	7743T	0.085	0.038	0.090	0.035	0.022	0.040	0.082	0.020
	7743U	0.093	0.052	0.066	0.045	0.036	0.036	0.017	0.037
	7743V	0.090	0.044	0.111	0.037	0.026	0.037	0.015	0.028
	7743W	0.092	0.047	0.108	0.042	0.020	0.037	0.028	0.023
	7743X	0.102	0.040	0.123	0.032	0.023	0.035	0.132	0.017
	7743Y	0.070	0.031	0.070	0.002	0.046	0.032	0.049	0.021
	Average	**0.092**	**0.048**	**0.098**	**0.045**	**0.040**	**0.037**	**0.053**	**0.028**
	Std dev.	**0.04**	**0.03**	**0.06**	**0.03**	**0.03**	**0.03**	**0.07**	**0.02**
	CV	**48.76%**	**56.83%**	**61.93%**	**75.15%**	**69.04%**	**87.56%**	**126.33%**	**61.69%**

Notoue Lagoon	Site code	Aspartic	Glutamic	Serine	Alanine	Valine	Phenylalanine	A/I	Lecuine
		area	area	area	area	area	area	area	area
	7748A	0.279	0.177	0.111	0.276	0.155	0.015	0.185	0.145
	7748B	0.197	0.160	0.087	0.215	0.109	0.077	0.162	0.129
	7748C	0.283	0.162	0.134	0.248	0.132	0.004	0.177	0.143
	7748D	0.305	0.199	0.197	0.301	0.285	0.265	0.279	0.167
	7748F	0.208	0.148	0.283	0.199	0.122	0.199	0.127	0.100
	7748G	0.274	0.118	0.375	0.136	0.071	0.139	0.082	0.067
	7748H	0.319	0.192	0.212	0.286	0.204	0.265	0.195	0.130
	7748J	0.288	0.153	0.226	0.199	0.124	0.174	0.130	0.117
	7748K	0.131	0.096	0.126	0.082	0.046	0.066	0.044	0.044
	7748L	0.348	0.201	0.263	0.324	0.207	0.294	0.196	0.154
	7748M	0.136	0.055	0.023	0.101	0.064	0.062	0.059	0.051
	7748N	0.149	0.063	0.113	0.085	0.042	0.004	0.035	0.051
	7748O	0.265	0.126	0.108	0.204	0.131	0.171	0.126	0.110
	7748P	0.216	0.134	0.115	0.177	0.115	0.005	0.119	0.090
	7748R	0.274	0.159	0.132	0.213	0.159	0.161	0.141	0.110
	7748T	0.286	0.164	0.247	0.206	0.112	0.162	0.147	0.106
	7748U	0.248	0.157	0.284	0.210	0.123	0.207	0.140	0.099
	7748V	0.311	0.194	0.205	0.306	0.187	0.225	0.227	0.153
	7748W	0.277	0.163	0.157	0.252	0.162	0.173	0.170	0.132
	7748X	0.197	0.107	0.157	0.144	0.082	0.130	0.093	0.000
	7748Y	0.239	0.121	0.183	0.165	0.090	0.148	0.098	0.082
	Average	**0.249**	**0.145**	**0.178**	**0.206**	**0.130**	**0.140**	**0.140**	**0.104**
	Std dev.	**0.06**	**0.04**	**0.08**	**0.07**	**0.06**	**0.09**	**0.06**	**0.04**
	CV	**24.41%**	**28.29%**	**46.18%**	**34.42%**	**45.27%**	**63.92%**	**43.25%**	**41.17%**

Buota Lagoon	**Site code**	**Aspartic**	**Glutamic**	**Serine**	**Alanine**	**Valine**	**Phenylalanine**	**A/I**	**Lecuine**
		area	**area**	**area**	**area**	**area**	**area**	**area**	**area**
	7750B	0.420	0.248	0.286	0.415	0.223	0.338	0.237	0.201
	7750D	0.316	0.214	0.287	0.340	0.312	0.204	0.311	0.191
	7750M	0.259	0.122	0.334	0.151	0.085	0.143	0.102	0.080
	7750N	0.439	0.315	0.437	0.510	0.479	0.424	0.612	0.347
	7750O	0.247	0.124	0.313	0.161	0.078	0.089	0.082	0.082
	7750P	0.345	0.170	0.360	0.265	0.145	0.277	0.177	0.141
	7750Q	0.359	0.273	0.372	0.428	0.428	0.546	0.557	0.319
	7750S	0.315	0.193	0.284	0.302	0.238	0.179	0.263	0.159
	7750U	0.220	0.125	0.341	0.152	0.102	0.158	0.126	0.069
	7750W	0.233	0.134	0.218	0.173	0.097	0.151	0.108	0.083
	7750X	0.395	0.244	0.283	0.413	0.241	0.380	0.277	0.214
	Average	**0.323**	**0.197**	**0.320**	**0.301**	**0.221**	**0.263**	**0.259**	**0.171**
	Std dev.	**0.08**	**0.07**	**0.06**	**0.13**	**0.14**	**0.14**	**0.18**	**0.10**
	CV	**23.72%**	**34.38%**	**18.25%**	**43.18%**	**62.88%**	**54.42%**	**69.01%**	**55.77%**

Bonriki Ocean	Site code	Aspartic	Glutamic	Serine	Alanine	Valine	Phenylalanine	A/I	Lecuine
		area	area	area	area	area	area	area	area
	7751B	0.204	0.108	0.4	0.133	0.108	0.119	0.097	
	7751F	0.08	0.078	0.168	0.114	0.184	0.458	0.458	0.243
	7751J	0.1	0.046	0.139	0.047	0.024	0.041	0.013	0.029
	7751L	0.206	0.132	0.371	0.166	0.075	0.144	0.018	0.086
	7751N	0.203	0.151	0.379	0.157	0.116	0.179	0.098	0.076
	7751P	0.219	0.093	0.276	0.119	0.056	0.109	0.079	0.063
	7751R	0.227	0.122	0.228	0.168	0.072	0.087	0.075	0.085
	7751V	0.193	0.076	0.175	0.102	0.041	0.074	0.050	0.048
	7751W	0.182	0.124	0.290	0.151	0.140	0.236	0.278	0.086
	7751Y	0.193	0.100	0.219	0.102	0.058	0.083	0.060	0.059
	Average	**0.181**	**0.103**	**0.265**	**0.126**	**0.087**	**0.153**	**0.123**	**0.086**
	Std dev.	**0.05**	**0.03**	**0.09**	**0.04**	**0.05**	**0.12**	**0.14**	**0.06**
	CV	**28%**	**30%**	**36%**	**30%**	**56%**	**79%**	**113%**	**72%**

Teaoraereke Ocean	Site code	Aspartic	Glutamic	Serine	Alanine	Valine	Phenylalanine	A/I	Lecuine
		area	area	area	area	area	area	area	area
	7739B	0.161	0.084	0.237	0.081	0.044	0.093	0.034	0.046
	7739C	0.35	0.172	0.328	0.259	0.159	0.264	0.02	0.142
	7739D	0.309	0.159	0.215	0.248	0.145	0.218	0.004	0.133
	7739G	0.294	0.15	0.248	0.22	0.117	0.193	0.111	0.112
	7739I	0.341	0.172	0.325	0.295	0.165	0.3	0.171	0.157
	7739K	0.236	0.128	0.16	0.156	0.082	0.128	0.093	0.08
	7739L	0.287	0.221	0.365	0.359	0.385	0.376	0.444	0.263
	7739N	0.311	0.177	0.265	0.265	0.18	0.233	0.242	0.145
	7739O	0.23	0.259	0.436	0.261	0.299	0.234	0.27	0.18
	7739Q	0.314	0.159	0.222	0.215	0.154	0.282	0.031	0.135
	7739R	0.224	0.213	0.415	0.214	0.209	0.218	0.241	0.148
	7739U	0.206	0.087	0.259	0.107	0.056	0.091	0.073	0.058
	7739V	0.270	0.125	0.281	0.179	0.103	0.175	0.099	0.094
	7739W	0.288	0.164	0.254	0.262	0.142	0.181	0.170	0.132
	7739X	0.138	0.088	0.208	0.088	0.073	0.068	0.034	0.029
	7739Y	0.154	0.076	0.234	0.076	0.035	0.06	0.036	0.038
	Average	**0.257**	**0.152**	**0.278**	**0.205**	**0.147**	**0.195**	**0.130**	**0.118**
	Std dev.	**0.07**	**0.05**	**0.08**	**0.08**	**0.09**	**0.09**	**0.12**	**0.06**
	CV	**26%**	**35%**	**27%**	**41%**	**63%**	**46%**	**93%**	**51%**

Teaoraereke Lagoon	Site code	Aspartic	Glutamic	Serine	Alanine	Valine	Phenylalanine	A/I	Lecuine
		area	area	area	area	area	area	area	area
	7740A	0.362	0.214	0.223	0.395	0.255	0.432	0.004	0.242
	7740C	0.359	0.204	0.215	0.335	0.185	0.331	0.014	0.2
	7740D	0.39	0.225	0.224	0.431	0.252	0.414	0.275	0.263
	7740E	0.35	0.204	0.18	0.329	0.167	0.272	0.198	0.167
	7740F	0.399	0.217	0.224	0.408	0.218	0.371	0.253	0.222
	7740G	0.346	0.216	0.226	0.372	0.213	0.32	0.207	0.214
	7740H	0.347	0.201	0.245	0.316	0.187	0.292	0.195	0.172
	7740I	0.272	0.18	0.161	0.278	0.148	0.241	0.008	0.163
	7740J	0.368	0.249	0.29	0.403	0.323	0.603	0.523	0.254
	7740K	0.332	0.187	0.254	0.306	0.18	0.315	0.183	0.18
	7740N	0.354	0.206	0.219	0.31	0.189	0.308	0.194	0.182
	7740O	0.34	0.201	0.205	0.343	0.202	0.32	0.037	0.199
	7740P	0.303	0.185	0.179	0.326	0.180	0.282	0.196	0.182
	7740Q	0.293	0.182	0.216	0.320	0.171	0.281	0.040	0.181
	7740S	0.297	0.183	0.186	0.288	0.198	0.213	0.173	0.140
	7740V	0.300	0.196	0.190	0.336	0.204	0.282	0.190	0.191
	7740X	0.323	0.204	0.193	0.322	0.222	0.319	0.242	0.177
	7740Y	0.334	0.198	0.196	0.301	0.194	0.293	0.189	0.173
	Average	**0.337**	**0.203**	**0.213**	**0.340**	**0.205**	**0.327**	**0.173**	**0.195**
	Std dev.	**0.034**	**0.017**	**0.031**	**0.044**	**0.040**	**0.087**	**0.125**	**0.033**
	CV	**10%**	**9%**	**15%**	**13%**	**20%**	**27%**	**72%**	**17%**

Bairiki Lagoon	Site code	Aspartic	Glutamic		Serine		Alanine		Valine
		height	height	area	height	area	height	area	height
	7749I	0.274	0.144	0.269	0.203	0.109	0.16	0.133	0.107
	7749J	0.238	0.123	0.254	0.161	0.086	0.121	0.097	0.08
	7749M	0.243	0.121	0.224	0.158	0.083	0.134	0.094	0.086
	7749N	0.216	0.119	0.201	0.14	0.078	0.108	0.08	0.074
	7749O	0.184	0.231	0.475	0.219	0.217	0.23	0.642	0.142
	7749P	0.247	0.129	0.179	0.181	0.096	0.130	0.124	0.091
	7749Q	0.313	0.221	0.410	0.320	0.314	0.349	0.460	0.248
	7749S	0.184	0.180	0.364	0.200	0.174	0.211	0.167	0.112
	7749T	0.384	0.157	0.187	0.194	0.097	0.166	0.146	0.148
	7749U	0.286	0.150	0.187	0.221	0.131	0.180	0.155	0.117
	7749W	0.288	0.152	0.190	0.228	0.118	0.166	0.131	0.107
	Average	**0.260**	**0.157**	**0.267**	**0.202**	**0.137**	**0.178**	**0.203**	**0.119**
	Std dev.	**0.06**	**0.04**	**0.10**	**0.05**	**0.07**	**0.07**	**0.18**	**0.05**
	CV	**23%**	**25%**	**39%**	**24%**	**53%**	**38%**	**88%**	**41%**

APPENDIX C-1. THIRTY YEARS OF OCEAN SHORELINE CHANGES ON NORTH TARAWA REEF ISLANDS USING VL

ID	Name	Length (km)	No of transects	Average Rates (m/yr) (±0.2)	Accretion (%)	Erosion (%)	Stable (%)	Status
Vegetation Line								
1	Buariki	6.3	296	0.0	8	2	90	Stable
2	Nuatabu	1.8	87	0.1	3	0	97	Stable
3		0.1	3	-0.1	0	0	100	Stable
5	Tebangaroi	1.5	76	0.1	8	1	91	Stable
6	Taratai	4.1	201	0.1	10	5	85	Stable
8	Notoue	2.3	111	0.0	6	2	92	Stable
9	Abaokoro	0.1	41	0.0	0	5	95	Stable
10		0.4	18	0.0	0	0	100	Stable
11	Marenanuka	1.7	57	0.1	7	0	93	Stable
16		0.2	15	0.0	0	7	93	Stable
24		0.2	13	0.0	0	0	100	Stable
25		0.1	6	-0.2	17	66	17	Stable
27	Kairiki	1.2	56	0.1	27	7	66	Stable
28	Kainaba	0.9	42	0.1	11	0	88	Stable
29		0.2	8	0.0	0	0	100	Stable
33	Bikenubati	0.5	21	0.0	14	0	86	Stable
38		0.1	6	0.3	60	0	40	Accretion
41	Nea	0.2	9	0.1	0	0	100	Stable
42	Biketawa	0.4	23	0.6	67	19	24	Accretion
43	Nabeina	0.5	25	-0.1	0	0	100	Stable
44	Tabiang	1.2	59	0.1	8	0	92	Stable
45	Tabuki	0.7	29	-0.1	0	4	96	Stable
46	Tabiteuea	2.2	101	0.0	0	0	100	Stable
47	Abatao	1.7	74	0.0	3	0	97	Stable
49	Buota	1.5	63	-0.1	5	11	84	Stable
50	Tanaea	0.3	20	-0.1	5	35	60	Stable
26	**Total**	**30.4**	**1481**					

APPENDIX C-2. THIRTY YEARS OF LAGOON SHORELINE CHANGES ON NORTH TARAWA REEF ISLANDS USING VL

ID	Name	Length (km)	No of transects	Average Rates (m/yr) (±0.2)	Accretion (%)	Erosion (%)	Stable (%)	Status
Vegetation Line								
1	Buariki	7.4	360	0.2	34	5	61	Stable
2	Nuatabu	1.6	74	0.0	28	41	31	Stable
5	Tebangaroi	1.5	71	0.5	68	11	21	Accretion
6	Taratai	4.1	200	0.2	30	9	61	Stable
8	Notoue	3.3	145	0.5	64	3	33	Accretion
9	Abaokoro	0.5	28	0.6	93	0	7	Accretion
11	Marenanuka	2.6	125	0.5	56	9	35	Accretion
17		0.4	18	0.0	6	6	88	Stable
24		0.1	3	0.1	67	33	0	Accretion
25		0.1	4	0.1	0	0	100	Stable
27	Kairiki	0.7	30	0.2	30	3	67	Stable
29		0.1	10	-0.1	10	30	60	Stable
28	Kainaba	1.0	54	-0.1	6	24	70	Stable
33	Bikenubati	0.1	21	0.0	0	14	86	Stable
41	Nea	0.2	13	0.2	8	8	85	Stable
42	Biketawa	0.5	24	-0.1	29	46	25	Erosion
43	Nabeina	0.4	25	0.1	56	4	40	Accretion
44	Tabiang	1.7	74	-0.1	7	26	67	Stable
45	Tabuki	1.0	51	-0.1	2	24	74	Stable
46	Tabiteuea	2.8	142	0.0	29	31	29	Stable
47	Abatao	1.7	85	0.0	15	7	78	Stable
49	Buota	1.1	57	0.0	7	26	67	Stable
50	Tanaea	0.1	4	0.1	0	25	75	Stable
23	**Total**	**0.2**	**1628**					

APPENDIX C-3. THIRTY YEARS OF OCEAN AND LAGOON SHORELINE CHANGES ON SOUTH TARAWA REEF ISLANDS USING VL

ID	Name	Length (km)	No of transects	Average Rates (m/yr) (±0.2)	Accretion (%)	Erosion (%)	Stable (%)	Status
Ocean								
52	Bonriki-Taborio	3.6	853	-0.1	4	17	79	Stable
53	Abairaranga	0.2	5	0.3	60	0	40	Accretion
55	Abaokoro-South Tarawa	0.2	6	0.6	100	0	0	Accretion
56	Ambo-Teaoraereke	5.2	293	0.1	26	10	64	Stable
57	Nanikai	1.2	53	0.1	30	23	47	Stable
58	Bairiki	2.6	92	0.5	79	7	14	Accretion
59	Betio	4.3	159	0.4	56	8	36	Accretion
7	**Total**	**17.3**	**1504**					
Lagoon								
52	Bonriki-Taborio	10.7	639	0.1	22	12	66	Stable
53	Abairaranga	0.2	5	-0.3	0	60	40	Erosion
55	Abaokoro-South Tarawa	0.1	5	0.0	0	20	80	Stable
56	Ambo-Teaoraereke	5.3	273	0.3	54	12	34	Accretion
57	Nanikai	1.0	56	-0.3	0	50	50	Erosion
58	Bairiki	1.7	87	0.4	54	10	36	Accretion
59	Betio	3.6	180	0.6	94	6		Accretion
7	**Total**	**22.6**	**1282**					

APPENDIX C-4. SIXTY-FOUR YEARS OF OCEAN AND LAGOON SHORELINE CHANGES ON SOUTH TARAWA REEF ISLANDS USING VL

ID	Reef island	Coastline	No	Overall	% of change			Status	Mean R^2
		Length (km)	of transects	Av. Rates (m/yr)	Accretion	Erosion	Stable		
Ocean Base of Beach									
1	Buariki	6.0	296	0.0	8	0	92	Stable	0.6
6	Taratai	4.1	201	0.0	5	0	95	Stable	0.4
41	Nea	0.5	11	0.0	0	0	100	Stable	0.3
53	Abairaranga	0.2	7	0.0	0	0	100	Stable	0.0
58	Bairiki	1.8	75	0.4	71	9	20	Accretion	0.8
	Total	**14.7**	**596**						
Lagoon Base of Beach									
1	Buariki	7.4	344	0.2	35	2	63	Stable	0.6
6	Taratai	4.1	199	0.3	42	3	55	Stable	0.7
41	Nea	0.2	13	0.0	0	8	92	Stable	0.4
53	Abairaranga	0.1	5	-0.2	0	40	60	Stable	0.5
58	Bairiki	1.7	70	0.3	51	6	43	Accretion	0.6
	Total	**16.3**	**637**						